MATERIALS AND MOLECULAR RESEARCH DIVISION

Annual Report 1982

May 1983

Lawrence Berkeley Laboratory
University of California
Berkeley, California 94720

Prepared for the U.S. Department of Energy under Contract DE-AC03-76SF00098

DISCLAIMER

LBL-15150

MATERIALS AND MOLECULAR RESEARCH DIVISION

Annual Report 1982

May 1983

Alan W. Searcy, Division Head
Rolf H. Muller, Asst. Division Head for Research
Conway V. Peterson, Asst. Division Head for Administration

Lawrence Berkeley Laboratory
University of California
Berkeley, California 94720

I
Materials
Sciences

II
Chemical
Sciences

III
Nuclear
Sciences

IV
Fossil
Energy

V
Advanced Isotope
Separation Technology

VI
Energy
Storage

VII
Magnetic
Fusion Energy

VIII
Nuclear Waste
Management

IX
Work for
Others

X
Appendices

Contents

GENERAL INTRODUCTION xxiii

I. MATERIALS SCIENCES
A. Metallurgy and Ceramics
1. Structure of Materials

a. Structure and Properties of Transformation Interfaces
Ronald Gronsky, Investigator

1. Grain Boundaries in Body-Centered Cubic Metals 1
2. Grain Boundaries and Interfaces in Semiconductors 2
3. Transformation Interfaces in Aluminum Alloys 2

1982 Publications and Reports 3

b. Microstructure, Properties, Alloy Design: Inorganic Materials
Gareth Thomas, Investigator

A. Alloy Design: Medium Carbon Steels

1. Characterization of the Effects of Laser Heat-Treatment Upon the Microstructure and Mechanical Properties of Fe/3Cr/2Mn/0.5Mo/0.3C 4
2. Mechanical Properties and Microstructure of Lower Bainite in a 0.3%C-3%Cr-2%Mn Steel 5
3. The Nature and Origin of Sliding Wear Debris from Steels 5
4. Fundamentals of Abrasive Wear 6

B. Alloy Design: Low-Carbon Dual Phase Steels

1. Design of High Strength Dual-Phase Steel Wire 6

C. Magnetic Materials

1. EM Study of CaO Segregation at the Grain Boundaries in $(Mn,Zn)Fe_2O_4$ 7
2. Development of the Cellular Microstructure in the $SmCo_{7.4}$-Type Magnets 8
3. Electron Microscopy of Mn-Al Magnets 8
4. Annealing of High Permeability $(Mn,Zn)Fe_2O_4$ 9

1982 Publications and Reports 9

c. Solid State Phase Transformation Mechanisms
Kenneth H. Westmacott, Investigator

1. Precipitation in the Pt-C System 11
2. Ledge Structure and Precipitate Growth in Al-Cu 11
3. The Relationship Between Invariant Line Strain and Precipitate Needle Growth 11
4. Mo_2C Precipitate Structure and Morphology in Molybdenum 12
5. Work in Progress 13

1982 Publications and Reports 13

d. National Center for Electron Microscopy
Gareth Thomas, Ronald Gronsky, and
Kenneth H. Westmacott, Investigators

1. 1.5 MeV High Voltage Electron Microscope 14
2. Atomic Resolution Microscope 19
3. Periodic Extension in Optical Diffraction Analysis 20
4. Real Space Image Simulation in High Resolution Microscopy 20
5. Characterization of AlN Ceramics Containing Long Period Polytypoids 21

1982 Publications and Reports 21

e. In-Situ Investigations of Gas-Solid Reactions by Electron Microscopy
James W. Evans and Kenneth H. Westmacott, Investigators

1. The Microstructure and Reactivity of Metal Oxides 22

1982 Publications and Reports 24

f. Local Atomic Configurations in Solid Solutions
Didier de Fontaine, Investigator

1. Long-Period Superstructures 25
2. TTT Diagrams 25

1982 Publications and Reports 26

2. Mechanical Properties

a. Theoretical Problems in Alloy Design
John W. Morris, Jr., Investigator

1. The Linear Elastic Theory of Phase Transformations in Solids 27
2. Dislocation Motion at Low Temperature 27
3. Microstructural Sources of the Ductile-To-Brittle Transition in Steel 28
4. The Coupling Between Magnetic- and Deformation-Induced Martensite in Metastable Austenitic Steels 29
5. Mössbauer Spectrometry 29
6. The Metallurgy of Fe-Mn Steels 29
7. High Temperature Embrittlement of an Iron-Based Superalloy 30
8. Microstructure Control During Welding of Ferritic Steels 30
9. Superalloy Welding 30
10. The Use of Heat Treatment to Improve the Critical Current of Bronze-Process Multifilamentary Superconducting Wire 31
11. The Influence of Magnesium Additions on the Properties of Multifilamentary Nb_3Sn Superconducting Wire 31

1982 Publications and Reports 32

b. Mechanical Properties of Ceramics
Anthony G. Evans, Investigator

High Temperature Failure

1. High Temperature Failure Initiation in Liquid Phase Sintered Materials 34
2. A Damage Model of Creep Crack Growth in Polycrystals 34
3. High Crack Growth in Polycrystalline Alumina 35
4. The Influence of Inhomogeneities on High Temperature Failure in Ceramics 35

Sintering

1. Microstructure Evolution During Sintering: The Role of Evaporation/Condensation 36

2. An Experimental Assessment of Pore Breakaway During Sintering 36
3. Initial Stage Sintering with Coupled Grain Boundary and Surface Diffusion 37

1982 Publications and Reports 37

c. Environmentally Affected Crack Growth in Engineering Materials
Robert O. Ritchie, Investigator

1. On the Load Ratio Dependence of Fatigue Thresholds 39
2. Influence of Viscous Environments on Fatigue Crack Growth 40
3. Fatigue Resistant Microstructures in Dual-Phase Steels 40
4. Mechanisms of Fatigue Crack Growth Under Variable Amplitude Loading 40

1982 Publications and Reports 40

3. Physical Properties

a. Interfaces and Ceramic Microstructures
Joseph A. Pask, Investigator

1. Wetting and Reactions in the Lead Borosilicate Glass-Precious Metal Systems 43
2. The Silica-Alumina System 43

1982 Publications and Reports 44

b. High Temperature Reactions
Alan W. Searcy, Investigator

1. The Equilibrium Shapes of Crystals and of Cavities in Crystals 45
2. Effects of Particle Size and Powder Bed Size on Calcite Decomposition Rates 45
3. Possible Metastability of MgO Resulting From the Decomposition of $Mg(OH)_2$ 46
4. Confirmation of Bimodal Pore Size Distribution in CaO from Calcite Decomposition 47
5. Gas Flow Through Porous Barriers: The O_2-Pt, CO-Pt Systems 47

1982 Publications and Reports 48

c. Structure-Property Relationships in Semiconductor Materials
Jack Washburn, Investigator

1. The Mechanism of Degradation of Cu_2S-CdS Solar Cells as Revealed by High Resolution Electron Microscopy 49
2. An Application of High Resolution Lattice Imaging Electron Microscopy to a Study of the Mechanism of the Crystalline to Amorphous Transformation 49
3. Effect of Recoil Implanted Oxygen on the Development of Secondary Defects in MOS Test Wafers 50
4. In-Situ Observations of MeV Electron Beam Induced Crystal Growth into an Amorphous Layer in Silicon 50
5. Effect of Temperature and Displacement Damage on the Growth of Amorphous Layers in Silicon 50
6. A Model for Redistribution of Phosphorus During Annealing of High Dose Ion Implanted Silicon 51
7. Diffraction Extinction Conditions for Silicon and Other Materials with Diamond Glide Planes 51

1982 Publications and Reports 52

d. Chemical Properties and Processing of Refractory Ceramics
Lutgard C. De Jonghe, Investigator

1. Processing of Ceramics 53
2. Structure and Nonstoichiometry of Calcium Aluminates 53
3. Work in Progress 55

1982 Publications and Reports 55

e. Structure and Electrical Properties of Composite Materials
Robert H. Bragg, Investigator

1. Density of Heat-Treated GC 56
2. Pore Growth in Glassy Carbon 57
3. Work in Progress 57

1982 Publications and Reports 57

f. High Temperature Oxidation and Corrosion of Materials
David P. Whittle, Investigator

1. Mechanism of Peg Growth and Influence on Scale Adhesion 58
2. Microstructure and Growth of Protective Cr_2O_3 and Al_2O_3 Scales at High Temperature 59
3. The Influence of Alloy Microstructure on Al_2O_3 Peg Morphologies in CoCrAl Alloys and Coatings 60
4. Sulfur Diffusion in Oxide Grain Boundaries 60
5. The Effects of SO_2 and SO_3 on the Na_2SO_4 Induced Corrosion of Nickel 61
6. Effects of Chlorides on Na_2SO_4-Induced Hot Corrosion of MCrAl 61
7. Multiphase Diffusional Growth During Aluminizing 62
8. High Temperature Oxidation of Ni-Co Alloy 62

1982 Publications and Reports 63

g. Ceramic Interfaces
Andreas M. Glaeser, Investigator

1. Grain Boundary Mobility Measurements in MgO-Doped Al_2O_3 64

1982 Publications and Reports 65

4. Engineering Materials

a. Abrasive, Erosive, and Sliding Wear of Materials
Iain Finnie, Investigator

1. Sliding Wear of Dissimilar Metals 66
2. Abrasive Wear 66
3. An Overview of Wear 66

1982 Publications and Reports 67

b. Erosion-Corrosion Wear Program
Alan V. Levy, Investigator

1. Measurement and Numerical Modeling of Two Phase Flow 68
2. Measurements of Air Flow in a Curved Pipe Using Laser-Doppler Velocimetry 68
3. Particle Flow Characteristics Determination in Gas and Liquid-Solid Particle Streams 68

1982 Publications and Reports 69

c. Erosion of Brittle Solids
Anthony G. Evans, Investigator

1. The Mechanical Behavior of Brittle Coatings and Layers 70
2. Measurements of Dynamic Hardness by a Controlled Impact Technique 71

1982 Publications and Reports 71

d. Chemical Degradation of Refractories
David P. Whittle, Investigator

1. High Temperature Degradation of Refractories in Mixed Gas Environments 72

5. Experimental Research

a. Far Infrared Spectroscopy
Paul L. Richards, Investigator

1. Infrared Emission Spectroscopy of CO on Ni 73
2. Low Temperature Infrared Absorption Spectroscopy of CO on Ni 74
3. Far Infrared Optical Properties of an Organic Superconductor 74
4. Work in Progress 74

1982 Publications and Reports 75

b. Experimental Solid State Physics and Quantum Electronics
Yuen-Ron Shen, Investigator

1. Spectroscopy of Molecular Monolayers by Resonant Second-Harmonic Generation 77
2. Transient Four-Wave Mixing and Coherent Transient Optical Phenomena 78
3. Nonlinear Wave Interaction Involving Surface Polaritons 79
4. Surface-Enhanced Second-Harmonic Generation and Raman Scattering 79

1982 Publications and Reports 79

c. Excitations in Solids
Carson D. Jeffries, Investigator

1. Period Doubling and Universal Chaotic Behavior in P-N Junctions in Silicon 82
2. Intermittency Route to Chaos 83
3. Period Doubling and Chaos in Spin Wave Instabilities in Yttrium Iron Garnet 83

1982 Publications and Reports 84

d. Time-Resolved Spectroscopies in Solids
Peter Y. Yu, Investigator

1. Nonequilibrium Phonon Spectroscopy in GaAs 85
2. Lifetime of Ortho-Exciton and Ortho- to Para-Exciton Conversion in Cu_2O 85

1982 Publications and Reports 85

e. Superconductivity, Superconducting Devices, and 1/f Noise
John Clarke, Investigator

1. Chaos in Josephson Junctions 87
2. Measurements of Current Noise in DC SQUIDs 88

3. Correlation Lengths in Magnetotellurics 88

1982 Publications and Reports 89

6. Theoretical Research

a. Theoretical Studies of the Electronic Properties of Solid Surfaces
Leo M. Falicov, Investigator

1. Magnetic and Electronic Properties of Ni Films, Surfaces, and Interfaces 91
2. Thermodynamic Properties of Li Intercalated and Disordered Layer Compounds 92

1982 Publications and Reports 92

b. Theoretical Solid State Physics
Marvin L. Cohen, Investigator

1. Solid Surfaces 94
2. Crystal Structure 94
3. Lattice Dynamics 94
4. Electronic Structure 95
5. Work in Progress 95

1982 Publications and Reports 95

7. Chemical Structure

a. Low Temperature Properties of Materials
Norman E. Phillips, Investigator

1. Absolute Temperature Determinations in the mK Region 97
2. The Specific Heat of ^{3}He in the Fermi Liquid Region 97
3. Low-Temperature Specific Heat of Potassium 98
4. Observation of the Spin Glass-Paramagnet Phase Boundary 98

1982 Publications and Reports 98

b. Electrochemical Processes
Charles W. Tobias, Investigator

1. Anodic Processes in Propylene Carbonate 100
2. Work in Progress 101

1982 Publications and Reports 101

8. High Temperature and Surface Chemistry

a. High Temperature Thermodynamics
Leo Brewer, Investigator

1. Use of Gaseous-Condensed Phase Equilibration to Determine Thermodynamic Quantities for Very Stable Transition Metal Alloys 103
2. High Temperature EMF Measurements 104

1982 Publications and Reports 104

b. Chemistry and Materials Problems in Energy Production Technologies
D. R. Olander, Investigator

1. The UO_2 - Zircaloy Chemical Interaction 106
2. Investigation of Iron-Chlorine Reaction by Modulated Molecular Beam Mass Spectrometry 107

3. A Thermodynamic Assessment of In-Reactor Iodine SCC of Zircaloy 107
4. Multiphoton Laser Ionization Mass Spectrometry of CsI and I 107
5. The Kinetics of Gas/Solid/Liquid Reactions by Modulated Molecular Beam Mass Spectrometry 108

1982 Publications and Reports 108

c. Plasma Enhanced Deposition of Thin Films
Dennis W. Hess, Investigator

1. Plasma-Deposited Titanium Oxide Photoanodes 110
2. Structure and Photoelectrochemical Properties of Plasma-Deposited Iron Oxide Films 110

1982 Publications and Reports 110

d. Electrochemical Phase Boundaries
Rolf H. Muller, Investigator

1. Nucleation of Pb Electrodeposits on Ag and Cu 112
2. Effect of Rhodamine-B on Pb Electrodeposition on Ag and Cu 112
3. Self-Compensating Spectroscopic Ellipsometer 113
4. Work in Progress . . . . . .

1982 Publications and Reports 113

e. Solid State and Surface Reactions
Gabor A. Somorjai, Investigator

Surface Structure and Chemisorption by Low Energy Electron Diffraction and Electron Spectroscopy

1. A LEED Crystallography Study of the (2x2)-C_2H_3 Structure Obtained After Ethylene Adsorption on Rh(111) 115
2. Evidence for the Formation of Stable Alkylidyne Structures From C_3 and C_4 Unsaturated Hydrocarbons Adsorbed on the Pt(111) Single Crystal Surface 115
3. Force-Field Calculations of the Packing Energy of Monolayers of C_3 and C_4 Hydrocarbon Molecules Adsorbed on Single Crystal Metal Surfaces 115
4. Vibrational Studies of Alkene Decomposition on the Rh(111) Surface 116
5. A Covalent Model for the Bonding of Adsorbed Hydrocarbon Fragments on the (111) Face of Platinum 116
6. The Adsorption of Benzene and Naphthalene on the Rh(111) Surface: A LEED, AES, and TDS Study 116
7. Vibrational Spectroscopy Using HREELS of Benzene Adsorbed on the Rh(111) Crystal Surface 116
8. The Structure of Graphitic Carbon on Pt(111) 117
9. The Coadsorption of Potassium and CO on the Pt(111) Crystal Surface: A TDS, HREELS, and UPS Study 117
10. The Interaction of Potassium with π-Electron Orbital Containing Molecules on Pt(111) 117
11. The Characterization of Pt/Cu Alloy and Epitaxial Surfaces 117
12. A New Model for CO Ordering at High Coverages on Low Index Metal Surfaces: A Correlation Between LEED, HREELS, and IRS. CO Adsorbed on fcc (100) Surfaces 118
13. LEED Intensity Analysis of the (1 x 5) Reconstruction of Ir(100) 118
14. The Adsorption and Binding of Thiophene, Butene, and H_2S on the Basal Plane of MoS_2 Single Crystals 118
15. LEED and AES Study of Zirconium Overlayers on the Pt(100) Crystal Face 118

Studies of Catalyzed Surface Reactions

1. Ammonia Synthesis Catalyzed by Rhenium 119

2. Interaction of CO, CO_2, and D_2 with Rhodium Oxide: Its Reduction and Catalytic Stability 119
3. Deuterium Isotope Effects for Hydrocarbon Reactions Catalyzed Over Platinum Single Crystal Surfaces 119
4. Studies of Sulfur Monolayers on Mo(100) and Its Effects on Adsorbate Binding 119
5. The Effect of Potassium on the Catalyzed Reactions of n-Hexane Over Pt(111) and Pt-[6(111)x(111)] Single Crystal Surfaces 119
6. Dehydrogenation of Cyclohexane Catalyzed by Bimetallic Au-Pt Single Crystal Surfaces 120
7. Energy Redistribution Among Internal States of Nitric Oxide Molecules Upon Scattering From Pt(111) Crystal Surface 120

1982 Publications and Reports 120

f. Nuclear Magnetic Resonance
Alexander Pines, Investigator

1. Broadband Population Inversion 124
2. Time-Resolved Optical Nuclear Polarization 124
3. Zero Field NMR 124
4. Anisotropic Diffusion in Oriented Systems 125
5. High Resolution NMR of Feldspars and Zeolites 125
6. Theory of Spin Diffusion in Solids 125
7. Time-Resolved CIDNP and Magnetic Isotope Effect 125
8. Molecular Conformation in Liquid Crystals 125
9. Excitation of High N-Quantum Transitions 126

1982 Publications and Reports 126

II. CHEMICAL SCIENCES
A. Fundamental Interactions
1. Photochemical and Radiation Sciences

a. Photon-Assisted Surface Reactions, Materials, and Mechanisms
Gabor A. Somorjai, Investigator

1. Photocatalytic Production of Hydrogen from Water by a p- and n-Type Polycrystalline Iron Oxide Assembly 129
2. The Preparation and Selected Properties of Mg-Doped p-Type Iron Oxide as a Photocathode for the Photoelectrolysis of Water Using Visible Light 129
3. Work in Progress 129

1982 Publications and Reports 130

b. Photochemistry of Materials in the Stratosphere
Harold S. Johnston, Investigator

1. The Reaction of Chlorine Atoms with Nitric Acid Vapor 131
2. Temperature-Dependent Ultraviolet Absorption Spectrum of Di-Nitrogen Pentoxide 131
3. Work in Progress 132

1982 Publications and Reports 132

2. Chemical Physics

a. Energy Transfer and Structural Studies of Molecules on Surfaces
Charles B. Harris, Investigator

1. Enhanced Photochemistry on Metal Surfaces 133
2. Electronic Energy Transfer to Semiconductor Surfaces 133
3. Vibrational Coherence and Picosecond Studies in Liquids 134

1982 Publications and Reports 134

b. Molecular Beam Spectroscopy
John S. Winn, Investigator

1. Dissociation Mechanisms of Metal Carbonyls 136
2. Supersonic Molecular Beam Relaxation Mechanisms 136

1982 Publications and Reports 137

c. Selective Photochemistry
C. Bradley Moore, Investigator

1. Absolute Rate Constants for the Removal of CH_2 ($^1A_1$). 138
2. High Vibrational Overtone Photochemistry 139

1982 Publications and Reports 140

d. Physical Chemistry with Emphasis on Thermodynamic Properties
Kenneth S. Pitzer, Investigator

1. Relativistic Ab Initio Molecular Structure Calculations Including Configuration Interaction with Application to Six States of TlH 141
2. Electron Structure Calculations Including CI for Ten Low Lying States of Pb_2 and Sn_2. Partition Function and Dissociation Energy of Sn_2 141
3. Nuclear Spin Statistics of Cubane and Icosahedral Borohydride Ions 142

1982 Publications and Reports 142

e. Molecular Interactions
William A. Lester, Jr., Investigator

1. Theoretical Study of Elementary Reactions in Combustion Processes 144
2. Theory of Polyatomic Photodissociation 145
3. Fixed-Node Quantum Monte Carlo for Molecules 146
4. Work in Progress 146

1982 Publications and Reports 146

f. Theory of Atomic and Molecular Collision Processes
William H. Miller, Investigator

1. Dynamical Models for Polyatomic Reaction Dynamics 148
2. Dynamical Effects of Reaction Path Symmetry; Mode-Specificity in the Unimolecular Dissociation of Formaldehyde 148

1982 Publications and Reports 149

g. Photoelectron Spectroscopy
David A. Shirley, Investigator

1. Direct Surface Structure Determination with Photoelectron Diffraction 151
2. High Resolution Fourier Analysis with Auto-Regressive Linear Prediction 151
3. Normal Photoelectron Diffraction of O/Cu(001): A Surface Structural Determination 152
4. The Two-Dimensional Valence Electronic Structure of a Monolayer of Ag on Cu(001) 152
5. The Evolution to Three-Dimensional Valence Band Structure in Ag Overlayers on Cu(001) 153
6. High Resolution Angle-Resolved Photoemission Study of the Valence Band Structure of Ag(111) 154

7. Construction of a High Resolution Electron Energy Loss Spectrometer 154
8. Threshold Measurements of the K-Shell Photoelectron Satellites in Ne and Ar 155
9. Photoelectron Measurements of the Mercury 4f, 5p, and 5d Subshells 155
10. Photoionization of Helium to $He^+(n=2)$: Autoionization and Final-State Symmetry 156
11. Photoelectron Angular Distributions of the N_2O Outer Valence Orbitals in the 19-31 eV Photon Energy Range 156
12. Rotationally Resolved Photoelectron Angular Distributions for H_2^+ (v'=0) at λ = 584 Å and 736 Å 157
13. Rotational Relaxation in Supersonic Beams of Hydrogen by High Resolution Photoelectron Spectroscopy 157

1982 Publications and Reports 158

h. Crossed Molecular Beams
Yuan T. Lee, Investigator

1. $O(^1D)$ + HD Reactive Scattering 160
2. Photoexcitation Studies of Substituted Cycloheptatrienes 160
3. Photochemistry of Glyoxal 161
4. Elastic Scattering of ArXe and KrXe 162
5. Photodissociation of Large Water Clusters 162
6. Infrared Multiphoton Dissociation of C_2F_5CL and C_2F_5Br 162
7. Molecular Beam Studies of Vibrational Predissociation of $(C_2H_4)_2$ and $(NH_3)_2$ Using a Pulsed CO_2 Laser 163

1982 Publications and Reports 163

i. Potential Energy Surfaces for Chemical Reactions
Henry F. Schaefer III, Investigator

1. Terminal vs Bridge Bonding of Methylene to Metal Systems Al_2CH_2 as a Model System 166
2. The Weakly Exothermic Rearrangement of Methoxy Radical ($CH_3O\cdot$) to the Hydroxymethyl Radical ($CH_2OH\cdot$) 167
3. Cyclic D_{6h} Hexaazabenzene--A Relative Minimum on the N_6 Potential Energy Hypersurface 167

1982 Publications and Reports 168

3. Atomic Physics

a. Atomic Physics
Richard Marrus, Investigator

1. Parity Violation in Atoms 170
2. One Percent Measurement of the Lifetime of the $2\ ^2S_{1/2}$ State of Hydrogenlike Argon (Z = 18) 170
3. Electron Capture by Low-Energy Multicharged Neon Ions 171

1982 Publications and Reports 171

4. Chemical Energy

a. Formation of Oxyacids of Sulfur from SO_2
Robert E. Connick, Investigator

1. The Rate and Mechanism of Exchange of Oxygens Between Bisulfite Ion and Water 172
2. Rates of Substitution Reactions on Metal Ions 172

1982 Publications and Reports 172

b. Catalytic Hydrogenation of CO: Catalysis on Well-Characterized Surfaces
Gabor A. Somorjai, Investigator
and
Catalysis by Supported Metals
Alexis T. Bell, Investigator

1. The Hydrogenation of CO Over Rhodium Foil, and Rhodium Compounds, $FeRhO_3$ and Na_2RhO_3 173
2. The Effects of Additives on the Fe and Re Catalyzed CO Hydrogenation Reactions 173
3. The Production of Methanol from CO and H_2 Over Thorium Oxide Catalyst Surfaces 174
4. Characterization of Carbon Deposits Formed During CO Hydrogenation Over Ruthenium 174
5. The Influence of Metal-Support Interactions on the Synthesis of Methanol Over Palladium 174

1982 Publications and Reports 174

c. Organometallic Chemistry of Coal Conversion
K. Peter Vollhardt, Investigator

1. Biscarbyne Clusters as Homogeneous Analogs of Fischer-Tropsch Intermediates on Surfaces 176
2. Transition Metal Mediated Thermal Extrusion of Sulfur Dioxide from Thiophene-1,1 Dioxides 176
3. Work in Progress 177

1982 Publications and Reports 177

d. Synthetic and Physical Chemistry
William L. Jolly, Investigator

1. An X-Ray Photoelectron Spectroscopic Study of the σ- and π-Allyl Groups 179
2. An X-Ray Photoelectron Spectroscopic Study of the Bonding in (Alkylidyne) Tricobalt Nonacarbonyl Complexes and Related Compounds 179
3. An X-Ray Photoelectron Spectroscopy Study of Transition Metal μ-Methylene Complexes and Related Compounds 179
4. Justification of the Approximation That Shifts in Nonbonding Valence Orbital Ionization Potential are Eight-Tenths of Shifts in Core Binding Energy 179
5. Work in Progress 180

1982 Publications and Reports 180

e. Chemistry and Morphology of Coal Liquefaction
Heinz Heinemann, Investigator, with Alexis T. Bell, James W. Evans, Richard H. Fish, Alan V. Levy, Eugene E. Petersen, Gabor A. Somorjai, Theodore Vermeulen, and K. Peter Vollhardt, Investigators

[See Fossil Energy Section]

f. Electrochemical Systems
John Newman, Investigator

1. Mathematical Modeling and Optimization of Liquid-Junction Photovoltaic Cells 181
2. Electrochemical Removal of Mercury from Contaminated Brine Solutions 182

1982 Publications and Reports 182

g. Surface Chemistry--Application of Coordination Principles
Earl L. Muetterties, Investigator

1982 Publications and Reports 183

h. High-Energy Oxiders and Delocalized-Electron Solids
Neil Bartlett, Investigator

1. An Electrochemically Reversible Intercalation of Graphite by Fluorine in the Presence of Hydrogen Fluoride 185
2. A Thermodynamic Threshold for the Intercalation of Graphite by Hexafluorospecies MF_6^- 186
3. Intercalation of Graphite by Silicon Tetrafluoride and Fluorine to Yield a Second-Stage Salt $C_{24}SiF_5$ 186

1982 Publications and Reports 187

i. Transition Metal Catalyzed Conversion of CO, NO, H_2, and Organic Molecules to Fuels and Petrochemicals
Robert G. Bergman, Investigator

1. Activation of C-H Bonds in Saturated Hydrocarbons on Photolysis of $(\eta^5\text{-}C_5Me_5)(PMe_3)IrH_2$. Relative Rates of Reaction of the Intermediate with Different Types of C-H Bonds, and Functionalization of the Metal-Bound Alkyl Groups 188
2. Work in Progress 189

1982 Publications and Reports 189

5. Chemical Engineering Sciences

a. High-Pressure Phase Equilibria in Hydrocarbon-Water (Brine) Systems
John M. Prausnitz, Investigator

1. Experimental High-Pressure Vapor-Liquid Equilibrium 191
2. Modeling of High-Pressure Phase Equilibria 191

1982 Publications and Reports 192

III. NUCLEAR SCIENCES
A. Low-Energy Nuclear Science
1. Heavy Element Chemistry

a. Actinide Chemistry
Norman M. Edelstein, Richard A. Andersen, Neil Bartlett, John G. Conway, Kenneth N. Raymond, Glenn T. Seaborg, Andrew Streitwieser, Jr., David H. Templeton, and Alan Zalkin, Investigators

Specific Sequestering Agents for the Actinides

1. Lipophilic Enterobactin Analogues. Terminally N-Alkylated Spermine/Spermidine Catecholcarboxamides 195
2. Ferric Ion Sequestering Agents. Selectivity of Sulfonated Poly(Catechoylamides) for Ferric Ion 196
3. Gallium and Indium Imaging Agents 197
4. Synthesis and Structural Chemistry of Tetrakis(Thiohydroxamato) Hafnium(IV) in $Hf(CH_3C_6H_4(S)N(O)CH_3)_4 \cdot C_2H_5OH$. 197

Synthetic and Structure Studies of Actinides and Other Compounds

1. Organouranium Complexes of Pyrazole and Pyrazolate. Synthesis and X-Ray Structures of $U(C_5Me_5)_2Cl_2(C_3H_4N_2)$, $U(C_5Me_5)_2Cl(C_3H_4N_2)$, and $U(C_5Me_5)(C_3H_3H_2)_2$ 198

2. Synthesis and Crystal Structures of the Tetrakis(Methy-Trihydroborato) Compounds of Zirconium(IV), Thorium (IV), Uranium(IV) and Neptunium(IV) 198
3. Tertiary Phosphine Complexes of the f-Block Metals; Preparation of Pentamethylcyclopentadienyl-tertiary Phosphine Complexes of Ytterbium (II and III) and Europium (II). The Crystal Structure of $Yb(Me_5C_5)_2Cl(Me_2PCH_2PMe_2)$. 199
4. Preparation and Crystal Structure of Bis[Bis(Pentamethyl-cyclopentadienyl)Ytterbrium(III)]un Decacarbonylferrate, $[(Me_5C_5)_2Yb]_2[Fe_3(CO)_{11}]$: A Compound with Four Isocarbonyl (Fe-CO-Yb) Interactions 200
5. Tertiary Phosphine Complexes of the f-Block Metals: Crystal Structure of $Yb[N(SiMe_3)_2]_2$ $[Me_2PCH_2CH_2PMe_2]$: Evidence for a Ytterbium-γ-Carbon Interaction 201
6. Stereochemistry of Bis(Carboxylato)Bis (Chloro)Bis(Tertiary Phosphine) Dimolybdenum Complexes; Crystal and Molecular Structure of Two Isomers of $(Me_3CCO_2)_2Cl_2(PEt_3)_2Mo_2$ 201
7. Anomalous Scattering by Praseodymium, Samarium and Gadolinium and Structures of Ethylenediaminetetra-acetate Salts 202
8. Dipotassiumo Bis-([8]Annulene)Ytterbium(II) and Bis-([8]Annulene)-Calcium 203

Physical and Spectroscopic Properties

1. Optical Spectroscopy and Electron Paramagnetic Resonance of Pa^{4+} in $ThBr_4$ and $ThCl_4$ Crystals 203
2. Fourier Transform Spectrometry Observations of the Actinides 204

1982 Publications and Reports 205

IV. FOSSIL ENERGY

a. Electrode Surface Chemistry
Phillip N. Ross, Jr., Investigator

1. High Coverage States of Oxygen on Pt(001) and (111) 209
2. Adsorptive and Catalytic Properties of Zirconium Overlayers on Pt(001) 210
3. Adsorptive and Catalytic Properties of Polycrystalline Pt_3Ti 210

1982 Publications and Reports 211

b. Studies of Materials Erosion/Wear in Coal Conversion Systems
Alan V. Levy, Investigator

1. The High Temperature Erosion of Ductile Alloys 212
2. Methods for Characterization of Erosion by Gas-Entrained Solid Particles 212
3. Effect of Particle Velocity on the Platelet Mechanism of Erosion 213
4. Erosion of Boride Coatings 213
5. Erosion-Corrosion of Steels in a Burner Duct Test Device 214
6. Erosion of Metals in Liquid Slurries 215
7. Corrosion of Metals in Oil Shale Retorts 216

1982 Publications and Reports 216

c. Chemistry and Morphology of Coal Liquefaction
Heinz Heinemann, Investigator, with Alexis T. Bell, James W. Evans, Richard H. Fish, Alan V. Levy, Eugene E. Petersen, Gabor A. Somorjai, Theodore Vermeulen, and K. Peter Vollhardt, Investigators

Introduction 217

Task 1: Selective Synthesis of Gasoline Range Components from Synthesis Gas
A. T. Bell, Investigator, with R. Dictor and J. Canella 217

Task 2: Electron Microscope Studies
J. W. Evans, Investigator, with D. J. Coates 218

Task 3: Catalyzed Low Temperature Hydrogenation of Coal
G. A. Somorjai, Investigator, with A. Cabrera and R. Casanova 218

Task 4: Selective Hydrogenation, Hydrogenolysis, and Alkylation of Coal and Coal Related Liquids by Organometallic Systems
K. P. C. Vollhardt, Investigator 219

Task 5: Chemistry of Coal Solubilization
R. H. Fish and T. Vermeulen, Investigators, with
A. D. Thormodsen 221

Task 6: Coal Conversion Catalysts: Deactivation Studies
A. V. Levy and E. E. Petersen, Investigators, with
M. West and M. C. Smith 221

1982 Publications and Reports 222

d. Materials Characterization in Fossil Fuel Combustion Products
Donald H. Boone and Alan V. Levy, Investigators

1. Erosion of SiC Hard Coating Materials 224
2. Erosion of Ceramic Thermal Barrier Coatings 224

1982 Publications and Reports 225

e. Solution Thermodynamics of Sulfites and Sulfite Oxidation Mechanisms
Leo Brewer and Robert E. Connick, Investigators

1. The Mechanism of Oxidation Bisulfite Ion by Oxygen 226

1982 Publications and Reports 226

f. Process Chemicals Parameters in Aqueous Sulfur Dioxide Removal by Lime/Limestone Scrubbers
C. Beat Meyer and Robert E. Connick, Investigators

1. The Thermal Decomposition of Aqueous Tri- and Tetrathionate 227
2. The Structure of Dithionite Ion 227

1982 Publications and Reports 227

V. ADVANCED ISOTOPE SEPARATION TECHNOLOGY
A. Applications and Assessments of Advanced Techniques

a. Isotope Separation by Laser Photochemistry
C. Bradley Moore, Investigator

1. Determination of Arrhenius Parameters for Unimolecular Reactions of Chloroalkanes by IR Laser Pyrolysis 229

1982 Publications and Reports 230

VI. ENERGY STORAGE
Electrochemical Energy Storage
James W. Evans, Rolf H. Muller, John Newman,
Philip N. Ross, and Charles W. Tobias, Investigators

a. Surface Morphology of Metals in Electrodeposition
Charles W. Tobias, Investigator

1. Limiting Currents and the Effect of Hydrodynamic Flow on the Morphology of Zinc Deposits 231
2. Modeling of Current Distribution with Active-Passive Kinetics 232

b. Metal Couples in Nonaqueous Electrolytes
Charles W. Tobias, Investigator

1. Solubility of Potassium Salts in Selected Organic Solvents 233

c. Engineering Analysis of Electrolytic Gas Evolution
Charles W. Tobias, Investigator

1. Studies of Bubble Dynamics with the Mosaic Electrode and an Improved Data Acquisition System 234

1982 Publications and Reports 234

d. Surface Layers on Battery Materials
Rolf H. Muller, Investigator

1. Impedance and Ellipsometer Measurements of Surface Layers on Lithium 236
2. Work in Progress 236

1982 Publications and Reports 237

e. Electrode Kinetics and Electrocatalysis
Philip N. Ross, Jr., Investigator

1. Low Energy Electron Diffraction (LEED) Characterization of Metal Electrode Surfaces 238
2. Diffusion Controlled Multi-Sweep Cyclic Voltammetry for a Reversible Deposition Reaction Occurring on Rotating Disk and Stationary Electrodes 239

1982 Publications and Reports 240

f. Electrical and Electrochemical Behavior of Particulate Electrodes
James W. Evans, Investigator

1. Development and Testing of the Mathematical Model for the Hall-Héroult Cell 242
2. Work in Progress 243

1982 Publications and Reports 243

g. Electrochemical Properties of Solid Electrolytes
Lutgard C. De Jonghe, Investigator

1. Impurities and Solid Electrolyte Failure 244
2. Grain Boundaries and Solid Electrolyte Degradation 244

1982 Publications and Reports 245

h. Analysis and Simulation of Electrochemical Systems
John Newman, Investigator

1. Work in Progress 246

1982 Publications and Reports 247

VII. MAGNETIC FUSION ENERGY

a. Structural Materials and Weldments for High Field Superconducting Magnets
John W. Morris, Jr., Investigator

1. The Magneto-Mechanical Cryogenic Research Facility (MMCR) 249
2. Magnetic Field Effects on Mechanical Properties of Stainless Steels 250
3. Austenitic Fe-Mn Cryogenic Steels 250

1982 Publications and Reports 250

VIII. NUCLEAR WASTE MANAGEMENT

a. Thermodynamic Properties of Chemical Species in Nuclear Waste
Norman M. Edelstein, Investigator

1. Voltammetric Studies of the NpO_2^+ Carbonate Systems 251
2. The Solubilities of Crystalline Neodymium and Americium Trihydroxide 251
3. Hydrolysis and Hydrolytic Precipitation Reactions for NpO_2^+, Nd^{3+}, and Cm^{3+} 253

1982 Publications and Reports 254

IX. WORK FOR OTHERS

1. National Aeronautics and Space Administration (NASA)

a. Theoretical Studies of Formyl Radical Formation in Selected Combustion Reactions
William A. Lester, Jr., Investigator

1. Work in Progress 255

2. Office of Naval Research

a. Structure and Performance of Al_2O_3
Donald H. Boone and Alan V. Levy, Investigators

1. Platinum Modified Alumina Coatings 256

b. Electron-Phonon Coupling and the Properties of Thin Films and Inhomogeneous Superconductors
Vladimir Z. Kresin, Investigator

1. Systems Containing Thin Films 257
2. Josephson Tunneling and Proximity Effect 257
3. Work in Progress 258

1982 Publications and Reports 258

3. Electric Power Research Institute (EPRI)

a. Phase Equilibria for Fixed Bed Gasification Products, Byproducts, and Water
John M. Prausnitz, Investigator

1. Measurement of Phase Equilibria 259
2. Theoretical Methods for Correlation of Phase Equilibria 259

1982 Publications and Reports 260

b. Inhibitive Salts for Reducing High Temperature Oxidation and Spallation
David P. Whittle, Investigator

1. Oxidation of Ni-Cr and Co-Cr Alloys Coated with Reactive Element Salts 261

c. Investigate New Fuel Cell Electrolyte and Electrode Concepts
Philip N. Ross, Jr., Investigator

1. The Effect of $H_2PO_4^-$ Anion of the Kinetics of Oxygen Reduction on Pt 262

1982 Publications and Reports 263

d. Improved Beta-Alumina Electrolytes for Advanced Storage Batteries
Lutgard C. De Jonghe, Investigator

1. Degradation of Sodium Beta"-Alumina: Effect of Microstructure 264

1982 Publications and Reports 265

X. APPENDICES

Appendix A. Materials and Molecular Research Division Personnel

Scientific Staff 267
Support Staff 278

Appendix B. MMRD Committees 279

Appendix C. List of Seminars 281

Appendix D. Index of Investigators 287

General Introduction

Overshadowing all else that happened in MMRD in 1982 were the deaths in mid-career of two very distinguished investigators. David P. Whittle, who was a Staff Senior Scientist with MMRD and Professor in Residence in the Department of Materials Science and Mineral Engineering of UCB, died on July 23, 1982, and Bruce H. Mahan, Professor of Chemistry at UCB and Faculty Senior Scientist in MMRD, died on October 12, 1982.

Several other staff changes occurred during the year. John S. Winn of the UCB Department of Chemistry and investigator with MMRD left to become Associate Professor of Chemistry at Dartmouth College in Hanover, New Hampshire. Richard A. Andersen an Associate Professor of the UCB Department of Chemistry is now an MMRD investigator doing synthetic actinide and organo-actinide chemistry, and Richard J. Saykally an Assistant Professor of that department is now also an investigator with the Division doing chemical physics. Professor Iain Finnie, Chairman of the Department of Mechanical Engineering has become an MMRD investigator in the area of abrasive, erosive and sliding wear of materials. Eugene Haller Professor in the UCB Department of Materials Science and Mineral Engineering and Scientific Program Director of the National Center for Advanced Materials, at LBL, has become an MMRD investigator in electronic materials.

At the end of 1982, there were affiliated with MMRD eight staff senior scientists, 50 University of California Berkeley faculty investigators, 39 staff scientists, 126 postdoctorals and other temporary scientific personnel, 353 graduate students, and a support staff of 75 technical, administrative and clerical personnel--for a total of 651. During the calendar year, 343 journal articles and LBL reports were published by members of MMRD. Students associated with MMRD were awarded 55 Ph.D. and 29 M.S. degrees.

The success of MMRD in basic research and in graduate student training were among the key factors that persuaded the Department of Energy and the Office of the President that Director Shirley's proposal for a National Center for Advanced Materials (NCAM) is built on a solid foundation. The entire MMRD staff share in the honor conveyed to LBL by the inclusion of NCAM as a major new initiative in the President's Budget in January 1983 for proposed funding in FY 1984.

Awards, honors, and appointments received by MMRD personnel in 1982:

- Four investigators, John Clarke, John M. Prausnitz, David A. Shirley, and Gabor A. Somorjai were elected Fellows of the American Association for the Advancement of Science.
- Robert G. Bergman received a Sherman Fairchild Distinguished Scholarship in residence at the California Institute of Technology.
- Michael Cima (Graduate Student with Leo Brewer) received a scholarship from the Achievement Rewards for College Scientists (ARCS) Foundation.
- Iain Finnie received the 1982 Nadai Award from the American Society of Mechanical Engineers for outstanding and continuing contributions in advancing the knowledge on erosive wear and strength of materials, in furthering high temperature design analysis, and in the teaching of engineering materials technology.
- Andreas M. Glaeser received a Junior Faculty Fellowship at UCB, and was elected Arco Junior Faculty Fellow.
- Heinz Heinemann was honored at the "Advances in Catalytic Chemistry II" symposium for his research and consulting achievements in catalysis and fossil fuel processing.
- Harold S. Johnston received a certificate of Commendation from the Federal Aviation Administration of the Department of Transportation for his help in fostering a better understanding of the effects of aircraft exhaust emissions on the upper atmosphere.
- Eduardo Kamenetzky (Graduate Student with Ronald Gronsky), won a Presidential Scholarship to present his paper, "The Accommodation of a Change in Grain Boundary Plane in Molybdenum," at the national meeting of the Electron Microscopy Society of America.
- Carl Lampert was elected next General Editor of the International Journal, Solar Energy Materials, published by North-Holland, Amsterdam.
- Yuan T. Lee was one of five United States scientists to receive the 1981 Ernest O. Lawrence Memorial Award for his distinguished contributions in the field of energy.
- C. Bradley Moore was a Visiting Fellow of the Joint Institute for Laboratory Astrophysics.
- William H. Miller was named Alexander von Humbolt U.S. Senior Scientist, 1981-1982.
- Earl L. Muetterties was the Centennary Lecturer, Royal Chemical Society, United Kingdom.

- Joseph A. Pask was elected to full membership in the International Institute for the Science of Sintering. He also received an Alumni Honor Award for Distinguished Service in Engineering from the College of Engineering, University of Illinois at Urbana-Champaign; and received the 1982 "Teacher of the Year" Award from the Committee of the Confucius Commemorative Day Ceremony for outstanding achievement in the field of education, and for dedicated service rendered to the Chinese community.

- Alexander Pines and his student Warren S. Warren received the 1982 J. T. Baker/American Chemical Society Nobel Laureate Signature Award for Graduate Education in Chemistry. Pines was also named R. W. Vaughan Plenary Lecturer for the 24th Rocky Mountain Conference, and received the Louis A. Strait Award from the Northern California Society for Spectroscopy.

- John M. Prausnitz was the Union Carbide Lecturer at the State University of New York (Buffalo), and van Winkle Lecturer at the University of Texas (Austin).

- Paul L. Richards received an Alexander von Humbolt Senior Scientist Award.

- Robert O. Ritchie and Subramanian Suresh were co-winners for the 1982 DOE/BES Materials Sciences Division Award for Outstanding Scientific Accomplishment in Metallurgy and Ceramics for work on "Modelling the Role of Microstructure and Environment in Influencing Fatigue Crack Propagation in Metals." Ritchie was also awarded an Alcoa Foundation Fellowship.

- Henry F. Schaefer, III, was the Lester P. Kuhn Memorial Lecturer, Johns Hopkins University.

- Glenn T. Seaborg was named President of the International Organization for Chemical Sciences in Development (IOCD). He was appointed by U.S. Education Secretary Bell to a new National Commission on Excellence in Education (NCEE); was elected President of the International Platform Association; was elected honorary member of the Swedish Royal Society for his contribution to the development of humanity; and was named Interim Director of the Lawrence Hall of Science.

- Gabor A. Somorjai was named by the National Academy of Sciences as Distinguished Scholar for an Exchange Visit to China. He also delivered the Kilpatrick Lecture at Chicago Institute of Technology; and was the Dow Lecturer at Michigan State University.

- Subramanian Suresh (Postdoctoral with Robert O. Ritchie) was the winner of the Robert Lansing Hardy Gold Medal from AIME for most promising young metallurgist.

- Gareth Thomas and Mehmet Sarikaya were awarded the 1981 Prize for Physical Sciences by the Electron Microscopy Society of America. Thomas was also elected a member of the National Academy of Engineering; was elected Chairman of the Board of Governors of Acta Metallurgica, Inc., and elected Fellow of the University of Wales, Cardiff.

- Charles W. Tobias was the first recipient of the Electrochemistry Society's Henry B. Linford Award for Distinguished Teaching.

- David P. Whittle, Kenneth A. Gaugler, and Haroun N. Hindam received the following awards from the 1982 IMS/ASM International Metallographic Exhibit held in Orlando, Florida: Judged 1st in Class No. 7, Pretty Microstructures: "Mystery Towers"; judged 2nd in Class No. 6, Electron Microscopy-Scanning: "Short Circuit Diffusion in Al_2O_3 Scales"; and awarded honorable mention in No. 6, Electron Microscopy-Scanning: "Continuous Internal Al_2O_3 Precipitates."

MMRD's National Center for Electron Microscopy (NCEM) is continuing to develop close to schedule. The new Atomic Resolution Microscope (ARM) was delivered in December 1982 and its assembly has been impressively rapid. Present progress indicates that acceptance tests for this unique instrument will be completed by June 1983. During its 9 months of operation, the 1.5 MeV High Voltage Electron Microscope (HVEM) has been used by more than 40 different scientists coming from a broad spectrum of disciplines. Usage is divided almost equally between LBL/UCB and outside microscopists, and the ratio of physical to biological science use is about 5:1. The Steering Committee which monitors the facility operation and assesses proposals to use the instruments has a new member, Professor John Hren, University of Florida, Gainesville, and another member with high resolution expertise will be added soon. Completion of the ARM Support Laboratory has been delayed by the stormy winter, but full occupancy is expected in July. NCEM/MMRD is hosting the 7th International Conference on HVEM, August 17-19, 1983, and a dedication ceremony for the Center is planned for September 1983.

The MMRD Annual Review of the 1982 Programs was held on February 28 and March 1, 1983. Dr. Harold W. Paxton, Vice President for Research, U.S. Steel Corporation, served as chairman of the Review Committee. Other members were: Dr. Richard Bernstein, Senior Vice President, Occidental Research Corporation; Professor Michel Boudart, Department of Chemical Engineering, Stanford University; Professor Richard Bradt, Department of Materials Sciences, Pennsylvania State University; Dr. George W. Parshall, E. I. Du Pont de Nemours and Company; and Dr. James C. Phillips, Bell Laboratories.

This year an outside Review Committee joined the Department of Energy, Division of Chemical

Sciences Program Managers on February 23-25, 1983, to review about one-half of our programs in Chemical Sciences. These Committee members were: John Pople, Department of Chemistry, Carnegie-Mellon University; Henry Taube, Department of Chemistry, Stanford University; and John Yates, Department of Chemistry, University of Pittsburg, who served as Committee chairman.

Alan W. Searcy
Division Head

I Materials Sciences

A. Metallurgy and Ceramics

1. Structure of Materials

a. Structure and Properties of Transformation Interfaces*

Ronald Gronsky, Investigator

Introduction. Transformation interfaces include homophase boundaries, heterophase boundaries, and "free" surfaces at which solid state reactions are either initiated or propagated. The goal of this research program is to determine the atomic configurations of such interfaces and to establish the relationship between their detailed structure and interfacial properties (mobility, diffusivity, reactivity, conductivity, ductility) since these strongly influence, if not completely dominate, the overall performance of materials.

Experiments are carried out chiefly by transmission electron microscopy, including energy dispersive x ray and electron energy loss spectroscopies; results are correlated with theoretical predictions of interfacial structure and high spatial resolution image simulations.

1. GRAIN BOUNDARIES IN BODY-CENTERED CUBIC METALS†

E. A. Kamenetzky, J. M. Penisson, and R. Gronsky

The body-centered cubic metals are a technologically important class of materials, encompassing most ferrous alloys as well as refractories. Their properties are also particularly sensitive to grain boundary structure, and this fundamental research effort is initially aimed at providing direct experimental data on the atomic structure and deformation characteristics of grain boundaries in bcc systems. The results reported here have been obtained using specimens of molybdenum, prepared under ultrahigh vacuum to avoid grain boundary segregation.

Attention has been paid to the mechanisms by which deformation of bcc structures can be accommodated at the grain boundary as determined by diffraction contrast imaging methods in the TEM. It has been found that a dominant mode of accommodation is the decomposition of matrix slip dislocations into defects of extended core volume within the grain boundary plane. One observation in particular takes the form

$$\frac{a}{2}[11\bar{1}] \longrightarrow 3\,\frac{a}{82}\,[1\ \bar{1}\ \bar{11}] + \frac{a}{41}\,[19\ 22\ 4]$$

at a $\Sigma = 41$ boundary. Such decomposition products are observed to remain localized at the boundary and their Burgers vectors correspond to those predicted for the DSC lattice at this misorientation.

Grain boundaries of lower Σ value frequently exhibited faceting as a response to deformation, where the change in grain boundary plane was accompanied by a change in dislocation structure. Evidence was also obtained of the emission of dislocations onto adjacent {110} planes with remnant decomposition products trapped at the boundary plane. These mechanisms play a critical role in either promoting or inhibiting the continuation of plastic flow across grain boundaries.

Atomic resolution images were also obtained of a $\Sigma = 41$ boundary oriented along its [001] tilt axis. These micrographs show clearly that the grain boundary accommodates discrete dislocations separated by a nearly perfect (but visibly deformed) bcc crystal (Fig. 1.1). The boundary

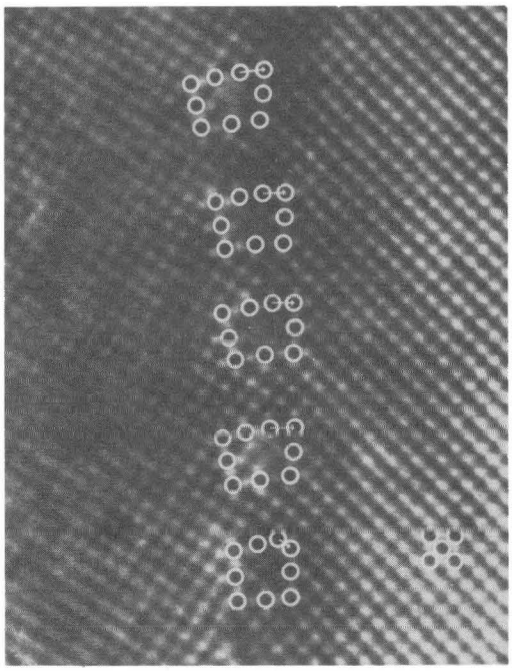

Fig. 1.1. Atomic resolution image of a $\Sigma = 41$ boundary in molybdenum. Atom positions in the unit cell projection of perfect bcc structure are circled in the lower right. At the boundary plane, the dislocations are located by their Burgers circuits. Recorded on a JEOL JEM 200CX with ultrahigh resolution goniometer, 500,000X, 4-sec exposure time. (XBB 827-5910)

*This work was supported by the Director, Office of Energy Research, Office of Basic Energy Sciences, Materials Sciences Division of the U.S. Department of Energy under Contract No. DE-AC03-76SF00098.

dislocations are of two types, b_1 = a [100], which are predicted by O-lattice theory for the symmetrical boundary, and b_2 = a/2[111], which accommodate the deviation from the symmetrical (910) position and are responsible for the observed boundary faceting. Detailed analysis of core atom positions is under way using computer simulation of atomic structure and imaging.

* * *

†A full account of this subprogram is published in LBL-14528, LBL-13822, LBL-14029, LBL-14613, and LBl-14702.

2. GRAIN BOUNDARIES AND INTERFACES IN SEMICONDUCTORS†

C. S. Murty, J. H. Rose, T. D. Sands, J. Washburn, and R. Gronsky

The interfaces studied here include grain boundaries in polycrystalline silicon, the crystalline/amorphous interface in ion-implanted silicon, and transformation interfaces between phases in copper sulfide.

Grain boundaries in fine-grained polycrystalline Si have been observed to greatly affect carrier mobility at low to moderate dopant levels either because these boundaries can induce defect states in the bandgap which capture majority carriers or because these boundaries may exhibit dopant segregation which results in electrical neutrality. The latter effect was directly observed in LPCVD Si doped with 0.6 at.% P and annealed in the 650 to 800°C range. Using a 10 nm electron probe at 100 kV, the amount of P at various grain boundaries was quantitatively evaluated by TEM/STEM analysis. To a detection limit of 0.2 at.% P, the occurrence of P segregation was found to depend strongly upon boundary structure; the energy of segregation varied between 5 and 10 kcal/mole.

In lattice-resolution studies of As-implanted Si, evidence points to the conclusion that the implantation-induced, crystalline-to-amorphous transformation is rarely "homogeneous" in character. Partially damaged crystals exhibit isolated amorphous and crystalline regions which co-exist with sharp interfaces, an interpretation which is supported by computer simulations.

High resolution imaging of the copper sulfide system has revealed detail on the mechanisms of the transformation from the chalcocite (Cu_2S) to djurleite ($Cu_{1.97-1.94}S$) phases. Results suggest that the djurleite structure can be derived from the low chalcocite structure by the clustering of Cu vacancies into $Cu_{20}S_{16}$ groups which simultaneously order into the periodic framework of djurleite. By all indications, the chalcocite-djurleite interface is both abrupt and fully coherent.

* * *

†Detailed reports of this subprogram appear in LBL-14703, LBL-13746, LBL-14165, LBL-14614, LBL-15063, LBL-14873, and LBl-14923.

3. TRANSFORMATION INTERFACES IN ALUMINUM ALLOYS†

J. Howe, G. Tamayo, and R. Gronsky

An examination of the structural characteristics of G.P. zones in an Al-4.2 at.% Ag alloy was carried out by high resolution electron microscopy to specifically test the proposed models of Ag-rich clusters. The results (see Fig. 3.1) clearly show that: (1) the zones have relatively large planar facets along {111} yielding an octahedral shape, and (2) there is no ordering within the zones. Furthermore, the images show no detectable distortion in lattice spacing through the zones, although in some cases there is evidence of unit-cell-height interfacial ledges at the zone-matrix interface.

In a separate study, it was found that substitution of aluminum for chromium and nickel in iron-base alloys can be made with little or no loss of favorable microstructures and properties characteristic of stainless steels. Microchemical analysis showed that the added Al is effective in forming a passivating oxide, with some occurrence of DO_3 ordered particles in the matrix. The most effective strengthening mechanism still appears to be the precipitation hardening resulting from M_6C carbides, with Zr and Ce inclusions responsible for enhanced oxidation resistance.

* * *

†Research results from the subprogram are fully published in LBL-14164, LBl-15278, and LBL-15434.

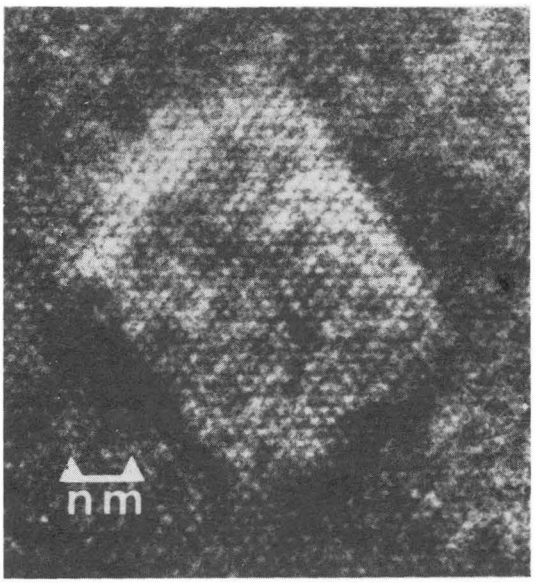

Fig. 3.1. High resolution electron micrograph of a G.P. zone in an Al-4.2 at.% Ag alloy. All {111} atomic planes are imaged, showing full octahedral zone shape. Recorded on a JEOL JEM 200 CX with ultrahigh resolution goniometer, 300,000X, 2.8-sec exposure time. (XBB 827-6377)

1982 PUBLICATIONS AND REPORTS

Refereed Journals

1. R. Gronsky, "Structure of Surfaces and Interfaces," in Proc. 10th Int. Cong. Elec. Micros., J. B. LePoole et al. (eds.), Deutsche Gesellschaft für Elektronmikroskopie, Hamburg, Vol. 2, 1982, p. 325; LBL-14528.

2. J. H. Rose and R. Gronsky, "A Scanning Transmission Electron Microscopy Microanalytical Study of Phosphorus Segregation at Grain Boundaries in Thin-Film Silicon," Appl. Phys. Lett. 41, 993 (1982); LBL-14703.

3. J. M. Penisson, R. Gronsky, and J. B. Brosse, "High Resolution Study of a Σ = 41 Grain Boundary in Molybdenum," Scripta Met. 16, 1239 (1982); LBL-13822.

4. T. D. Sands, J.Washburn, and R. Gronsky, "High Resolution Observations of Copper Vacancy Ordering in Chalcocite (Cu_2S) and the Transformation to Djurleite ($Cu_{1.97-1.94}S$)," Phys. Stat. Sol. (a) 72, 551 (1982); LBL-13746.

5. P. Ling, R. Gronsky, and J. Washburn, "Electron Diffraction Analysis of Microtwin Structures in Regrown (111) Silicon," in Proc. 40th Ann. Meeting Elec. Micros. Soc. Am., G. W. Bailey (ed.), Claitor's, 1982, p. 460; LBL-14165.

6. R. Gronsky, "A High Resolution Study of G. P. Zones in Aluminum-4.2 at.% Silver," in Proc. 40th Ann. Meeting Elec. Micros. Soc. Am., G. W. Bailey (ed.), Claitor's, 1982, p. 722; LBL-14164.

7. E. Kamenetzky, "The Accommodation of a Change in Grain Boundary Plane in Molybdenum," in Proc. 40th Ann. Meeting Elec. Micros. Soc. Am., G. W. Bailey (ed.), Claitor's, 1982, p. 722; LBL-14029.

Other Publications

1. L. E. Tanner, A. R. Pelton, and R. Gronsky, "The Characterization of Pretransformation Morphologies: Periodic Strain Modulations," in Proc. ICOMAT-82, J. de Physique, in press.

LBL Reports

1. E. A. Kamenetzky, "The Mechanisms of Accommodation of Deformation at Grain Boundaries in BCC Materials," M. S. thesis, LBL-14613.

2. J. H. Rose, "A STEM X-Ray Microanalytical Study of Phosphorus Segregation to Grain Boundaries in Thin-Film Silicon," M. S. thesis, LBL-14614.

3. E. A. Kamenetzky and R. Gronsky, "The Mechanisms of Accommodation of Deformation at Grain Boundaries in BCC Metals," LBL-14702.

4. J. Washburn, C. S. Murty, D. Sadana, P. Byrne, R. Gronsky, N. Cheung, and R. Kilaas, "The Crystalline-to-Amorphous Transformation in Silicon," LBL-14873.

5. C. S. Murty, "Crystalline to Amorphous Transformation in Silicon," Ph.D. thesis, LBL-14923.

6. T. D. Sands, R. Gronsky, and J. Washburn, "High Resolution Study of the Chalcocite (Cu_2S)-Djurleite ($Cu_{1.969}S$) Transformation in $Cu_{2-x}S$ Thin Films," LBL-15063.

7. J. Howe, "Relief Etching for SEM and TEM Characterization of Sub-Micron Precipitates in Aluminum Alloys," LBL-15278.

8. G. Tamayo, "Microstructure, Transformations and Properties of Oxidation-Resistant, Iron-Base, Aluminum-Modified Alloys," M. S. thesis, LBL-15434.

Invited Talks

1. R. Gronsky, "High Resolution Imaging of Interfaces in Close-Packed Structures," ASU Workshop on Imaging and Microanalysis with High Spatial Resolution, Castle Hot Springs, Arizona, January 5-9, 1982.

2. R. Gronsky, "Typical Problems in Imaging and Microanalysis with High Spatial Resolution," ASU Winter school, Castle Hot Springs, Arizona, January 11-15, 1982.

3. R. Gronsky, "Interfacial Structure and Segregation," Department of Metallurgical and Materials Engineering, University of Pittsburgh, Pittsburgh, Pennsylvania, May 13, 1982.

4. R. Gronsky, "Analytical Electron Microscopy of Grain Boundary Segregation," Hitachi Workshop, Mountain View, California, May 22, 1982.

5. J. Howe, "High Resolution Electron Microscopy and its Application to the Study of Precipitate Plate Growth," Department of Materials Science and Engineering, Carnegie-Mellon University, Pittsburgh, Pennsylvania, August 26, 1982.

6. R. Gronsky, "Atomic Structure of Interfaces: Direct Imaging," Department of Materials Science and Engineering Seminar, U. C. Berkeley, September 30, 1982.

7. R. Gronsky, "High Resolution Imaging of Interfaces," Joint Meeting of Northern California Society of Electron Microscopy and Microbeam Analysis Society, U. C. Davis, October 7, 1982.

8. R. Gronsky, "Microchemical Analysis of Interfaces in Materials," Students' Night, ASM Golden Gate Chapter, Berkeley, Novermber 1, 1982.

9. R. Gronsky, "Electron Analytical Instruments," ASM Golden Gate Chapter Education Seminar, Berkeley, November 6, 1982.

b. Microstructure, Properties, Alloy Design: Inorganic Materials*

Gareth Thomas, Investigator

INTRODUCTION

A. Alloy Design of Steels. Strength, toughness and ductility are undoubtedly the most important properties specified for structural steels, unless the application involves aggressive environments. The major difficulty in optimizing these properties comes from the fact that strength is usually inversely related to toughness and ductility; the increase in the former is achieved at the expense of the latter and vice versa. This is true in the majority of cases when relatively inexpensive alloying and processing are sought for a practical alloy development.

Thus alloy design programs utilize the concept of two-phase steels as a means of optimizing these mutually exclusive properties. The underlying principle here is to obtain, by heat treatment, composites wherein the advantages of one phase are optimized while the less desirable features of this phase are simultaneously mitigated by the presence of the other constituent phase. The size, distribution, shape and volume fraction of the second phase critically control the mechanical behaviour of the dual phase systems. As a consequence, these structures offer a degree of metallurgical flexibility that is absent in single phase structures or in many precipitation strengthened systems, for attaining optimum sets of mechanical properties.

Examples are given below of martensite/austenite (~2-5%) mixtures designed for optimum combinations of high strength toughness and wear properties in medium carbon steels, e.g., for mining, ordnance, and agricultural applications and of martensite/ferrite (~80%) structure for high strength, good formability and improved low temperature ductility in low carbon steels, for applications to sheet, line pipe rods and wires.

B. Magnetic Materials. Research on magnetic materials is concentrated on three main areas: (1) (Mn, Zn) ferrites, (2) rare earth-cobalt magnets, and (3) Mn-Al-C permanent magnets. Summaries of published results are given below.

*This work was supported by the Director, Office of Energy Research, Office of Basic Energy Sciences, Materials Sciences Division of the U.S. Department of Energy under Contract No. DE-AC03-76SF00098.

A. Alloy Design: Medium Carbon Steels

1. CHARACTERIZATION OF THE EFFECTS OF LASER HEAT-TREATMENT UPON THE MICROSTRUCTURE AND MECHANICAL PROPERTIES OF Fe/3Cr/2Mn/0.5Mo/0.3C

J. J. Rayment, W. J. Salesky,† and X. M. Meng‡

Recently, high powered lasers have been used to locally heat-treat a variety of engineering alloys[1,2] in an attempt to produce a surface that has undergone rapid heating and cooling and, as a result, has refined induced by the rapid heating/cooling cycle.

Fig. 1.1 shows the amount of wear as a function of different laser processing parameters for an experiment set up to examine and continuously measure the relative sliding wear resistance of some laser heat-treated specimens. All the laser heat-treated specimens wear significantly less than those conventionally heat-treated (1100°C austenitization for 1 hour and oil quenched). Moreover, specimens that were processed in an adjacent pass geometry at a laser traverse velocity of 0.35 in./sec showed less than half the wear experienced by the conventionally heat-treated material.[3]

* * *

†Present Address: Smith Tool, P. O. Box C-19511, Irvine, CA.
‡Present Address: Wuhan Research Institute of Materials Protection, Wuhan, China.

1. D. S. Gnanamuthu, "Applications of Lasers in Materials Processing," Am. Soc. for Metals (1979).
2. F. D. Seaman and D. S. Gnanamuthu, Metals Progress 8, 67 (1975).
3. W. J. Salesky, Ph. D. thesis, University of California, Berkeley, Nov. 1982, LBL-15164.

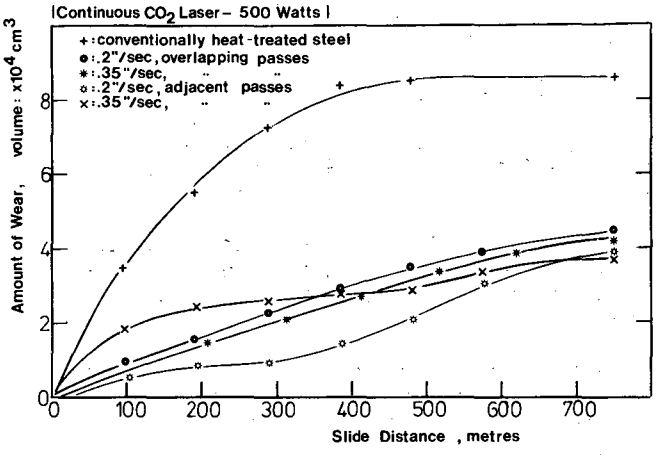

Fig. 1.1. Amount of wear as a function of sliding distance for conventional and laser heat-treated Fe/3Cr/2Mn/.5Mo/.3C. (XBL 826-10345)

2. MECHANICAL PROPERTIES AND MICROSTRUCTURE OF LOWER BAINITE IN A 0.3%C-3%Cr-2% Mn STEEL

Hiroyuki Tokushige† and G. Thomas

A metallographic study of isothermally transformed lower bainite in a 0.3C-3Cr-2Mn steel has been carried out, and the results correlated with mechanical properties[1] microstructure as well as higher hardness and an increased wear resistance. Unfortunately, too little research has been carried out into the characterization of the effects of laser heat-treatment upon the microstructure and subsequent mechanical properties of the heat-treated material.

In an effort to bridge this gap, a project has been undertaken in which a continuous wave CO_2 laser has been used at two power levels, three different pass geometries and at four different traverse velocities, to examine the effects of these parameters on (1) the microstructures of the heat-affected zone (HAZ), the tempered zone adjacent to the HAZ, and the regions in which overlapping of laser passes has occurred, (2) the microstructures of the different regions mentioned in (1), and (3) the sliding wear resistance. The alloy chosen for examination was Fe/3Cr/2Mn/0.5Mo/0.3C, an alloy developed through the alloy design program, and one that has already been shown to have not only a good strength/toughness combination, but also good wear resistance (both sliding and abrasive). Laser heat-treating produces a surface layer ~300-450 μm deep, depending on the laser traverse velocity. This heat-treated layer has a microhardness of 600-650 VHN, significantly harder than the matrix hardness of ~450 VHN. This increase in hardness is the result of a refinement in grain-size (from a matrix value of ~250 μm down to ~30 μm), as well as the high level of residual compressive stress present in the HAZs.

Depending on the isothermal holding time at 360°C, the microstructure changed considerably. After 10-min holding, the microstructure, although predominantly martensitic, was found to contain regions of lower bainite. Retained austenite was observed not only at the martensite interlath boundaries, but also at the boundaries between lower bainitic ferrite laths. These laths contained the characteristic unidirectional carbides (Figs. 2.1a and b). However, when the microstructure became mostly lower bainitic, i.e., after 1-hour holding, no retained austenite was observed. Instead, there were interlath carbides decorating bainitic ferrite laths in addition to unidirectional intralath carbides (Figs. 2.1c and d). In this condition both strength and toughness were considerably lower than those of the as-quenched martensite.

It appears that retained austenite transformed to elongated carbides during the prolonged isothermal holding. Thus with long-time holding, bainite has a very similar structure to that of martensite tempered in the range between 300 and 400°C,[2] and its low toughness is essentially a consequence of tempered martensite embrittlement.[3]

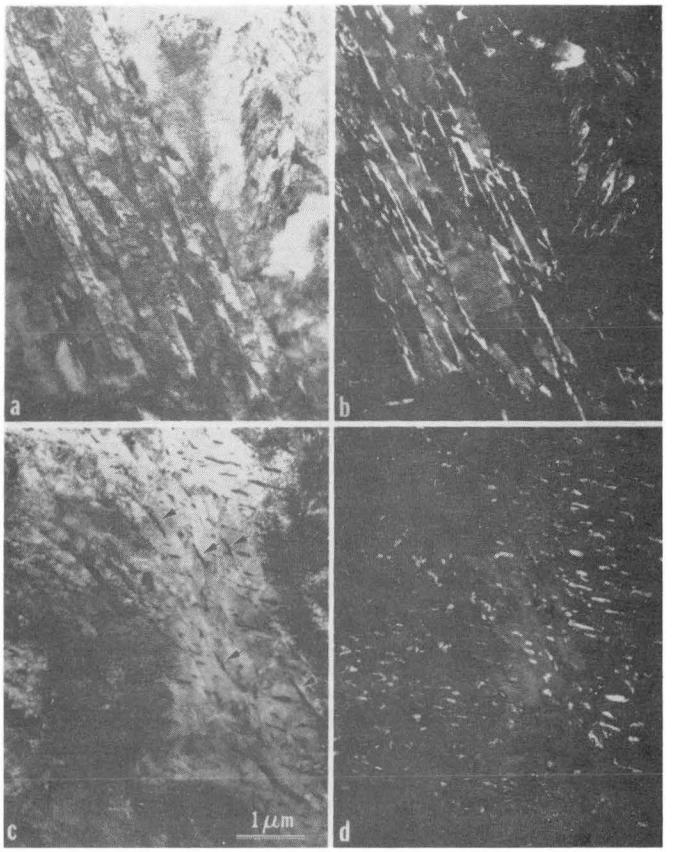

Fig. 2.1. Transmission electron micrographs of the lower bainite isothermally transformed at 360°C. (a) BF after 10 min of isothermal holding, (b) DF image of retained austenite in the same condition, (c) BF after 1 hour of isothermal holding (arrows indicate interlath carbides), (d) DF image of carbides in the same condition. (XBB 8212-10841)

* * *

†Ph.D. thesis research in progress.

1. H. Tokushige, MMRD Annual Report 1981, LBL-13840.
2. M. Sarikaya, A. K. Jhingan, and G. Thomas, Winchell Symposium, ASM-AIME, Oct. 1981, in press.
3. G. Thomas, Met Trans. 9A, 439-450 (1978).

3. THE NATURE AND ORIGIN OF SLIDING WEAR DEBRIS FROM STEELS†

W. J. Salesky,‡ R. M. Fisher,§ R. O. Ritchie, and G. Thomas

The mechanism of wear-particle formation during unlubricated sliding wear of several carbon and alloy steels has been investigated by scanning (SEM) and transmission electron microscopy (TEM). A detailed study by SEM of individual debris particles has revealed that they are plate-like and typically 200 to 400 nm in thickness. The thinner particles are generally iron oxides except for tests conducted at low temperatures or in inert

atmospheres when predominantly metallic particles result. Using SEM automatic image analysis, the mean debris particle width was determined to be 1 to 2 μm. Examination of cross sections from bulk specimens by TEM revealed a fine dislocation cell structure typical of large strain deformation to a depth of 10 to 50 μm, depending on the material and load. The subsurface cell dimensions and bending of pearlite colonies indicate that the shear strain near the surface is at least 5. In many instances, a 200 to 300 nm wide zone of lower dislocation density, indicative of recovery, was noted immediately below the surface. Some cracks formed along dislocation cell walls at the boundary of the recovered zone; others were associated with decohesion of particle interfaces or subgrain triple points. Some oxidation then occurs during separation of the platelet from the parent material as a consequence of the highly pyrophoric nature of thin metal flakes.

* * *

†Accepted for International Conf. Wear, Reston, VA, April 1983.
‡W. J. Salesky, "On the Fundamental of Sliding Wear in Steel," Ph.D. thesis, University of California, Berkeley, Nov. 1982, LBL-15164.
§Present Address: U. S. Steel, Research Center, Monroeville, PA.

4. FUNDAMENTALS OF ABRASIVE WEAR

Chi Kong Kwok† and G. Thomas

Abrasive wear can be taken as a set of microscopic inelastic deformation and fracture processes involving crack initiation and propagation near the surface. Extensive plastic deformation can be accommodated due to the hydrostatic nature of loading.

Results as shown in Fig. 4.1 provide a comprehensive understanding of abrasion. Extrusion-type plastic flow of material is observed in Fig. 4.1a with maximum strain occurring at the foremost region of material flow. A very steep strain gradient is established, and the extent of deformation is decreased rapidly away from the worn surface. The depth of deformation is very shallow (< 5 μm from the surface). Very high true strain is involved in abrasion and is estimated to be > 500% at the surface.[1,2]

Wear particles were collected from wear tests, and a typical result is shown in Fig. 4.1b. Comparison of Figs. 4.1a and b indicated that the crack appears to initiate at the region of highest strain and propagate along the direction parallel to the worn surface. Very fine dislocation cells on the order of 250-Å diameter are found at the surface (Fig. 4.1c).

* * *

†Ph.D. thesis research in progress.

1. J. H. Dantenberg and J. H. Zaat, Wear 23, 9 1973.
2. W. J. Salesky, LBL-15164.

B. Alloy Design: Low-Carbon Dual Phase Steels

1. DESIGN OF HIGH STRENGTH DUAL-PHASE STEEL WIRE

A. Nakagawa† and G. Thomas

Conventional high strength wire is produced by cold-drawing a high carbon pearlitic steel to large strains with several intermediate annealing or patenting heat treatments. Dual-phase steels show great promise as a starting material for cold-drawing into high strength wire because of their high strain-hardening rates and the ductility possible with the second phase, lath martensite. Moreover, dual-phase steels do not need intermediate patenting treatments and instead can

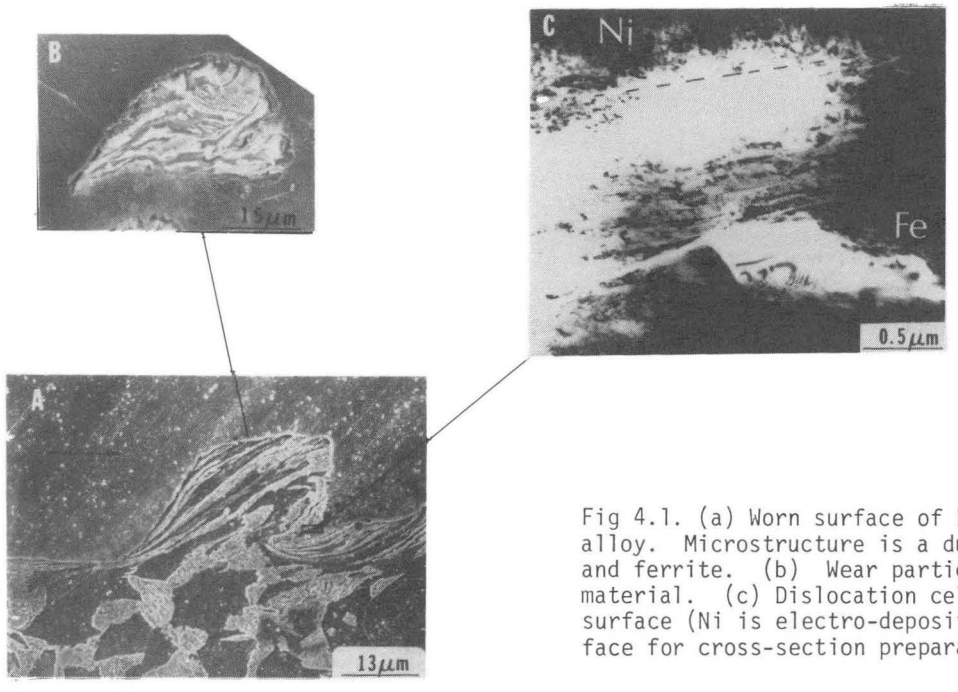

Fig 4.1. (a) Worn surface of Fe/1.2 Mn/0.6Si/0.1C alloy. Microstructure is a duplex of martensite and ferrite. (b) Wear particles of the same material. (c) Dislocation cell structure at the surface (Ni is electro-deposited on the worn surface for cross-section preparation.
(XBB 820-10906)

be drawn in one continuous, multipass cold-drawing operation. This is shown in Fig. 1.1, which is a schematic of the drawing procedure for both dual-phase steels and pearlitic wire. Note that three patenting treatments are required for pearlitic wire (dashed line) to produce tire cord, whereas only an initial heat treatment is required in the dual-phase steel case (solid line). This results in a reduction in the complexity of the operation as well as production cost and energy consumption.

Results have shown that cold-drawn dual-phase steels can exceed the tensile strength requirement of 270 ksi and torsion test requirement of 58 twists in an 8 in. length for automobile tire bead wire.

* * *

†Ph.D. thesis research in progress.
Patents applied for.

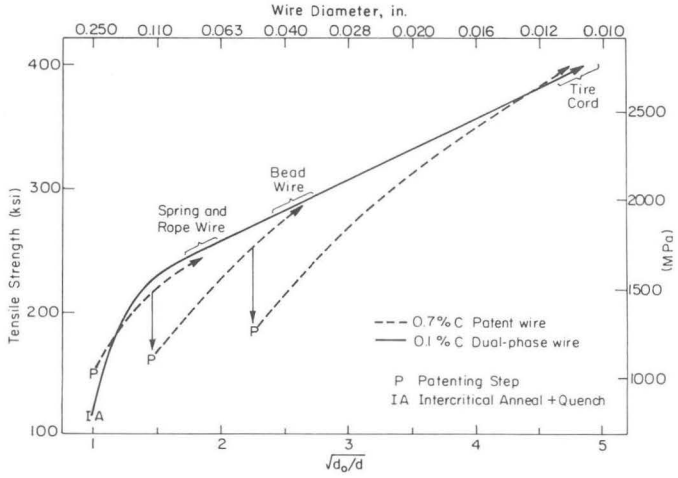

Fig. 1.1. Comparison of the drawing schedule and work hardening for dual-phase steel and patented pearlitic wire. (XBL 8210-6760)

C. Magnetic Materials

1. EM STUDY OF CaO SEGREGATION AT THE GRAIN BOUNDARIES IN $(Mn,Zn)Fe_2O_4$†‡

I-Nan Lin,§ R. K. Mishra, and G. Thomas

Electron diffraction and microscopy studies supplemented by electron spectroscopic techniques such as Auger electron spectroscopy and energy dispersive x-ray spectroscopy were used to characterize the nature of grain boundary segregation in commercial grade $(Mn,Zn)Fe_2O_4$ samples containing small quantities of CaO. Chemical analyses by AES and EDAX show an enrichment of Ca near the grain boundary region. Convergent beam electron diffraction experiments show that the crystal symmetry of the spinel structure is distorted in the vicinity of the grain boundary (Fig. 1.1). In-situ heating experiments in HVEM show the existence of a disordered phase at the sintering temperature. Lorentz microscopy in TEM shows the interaction of magnetic domain walls with grain boundaries.

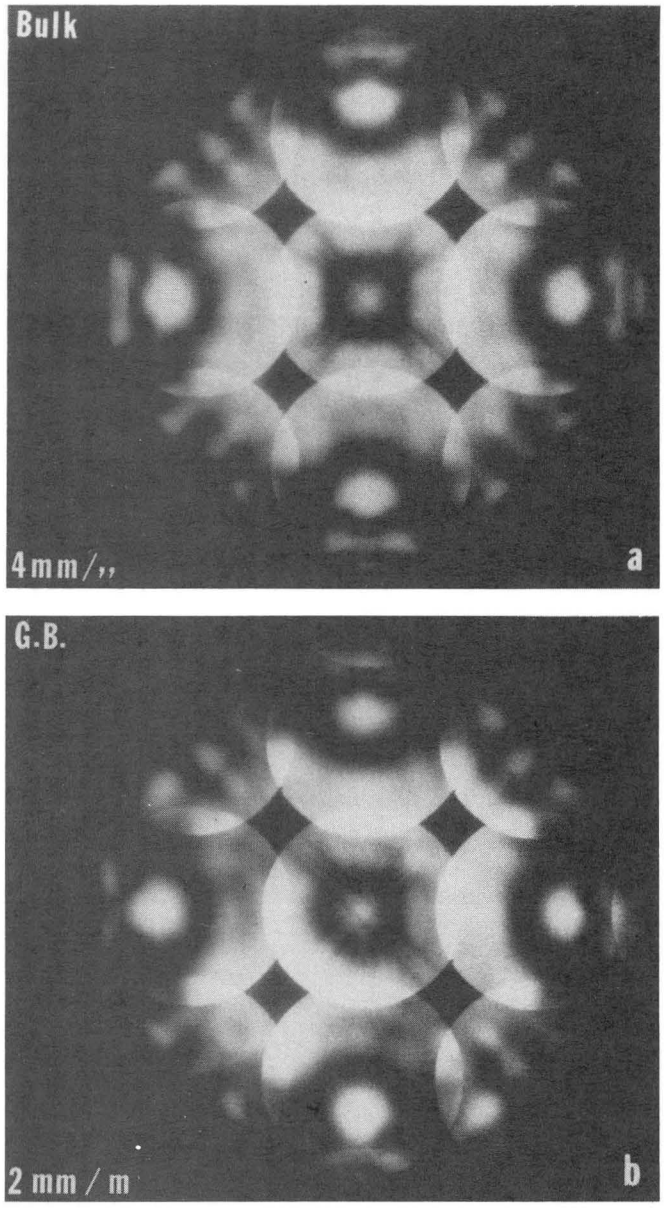

Fig. 1.1. CBD patterns of $(Mn,Zn)Fe_2O_4$ with electron beams incident along [001] zone axis and electron probe placed at (a) interior of the grain and (b) region near grain boundary respectively. The symmetry of the Holz lines in the central disk and the intensity distribution of the surrounding disks have lower symmetry in the region near grain boundaries. (XBB 817-7040)

In low loss Mn,Zn-ferrites, CaO is added to form a high resistivity layer along grain boundaries so that the electrical resistivity of the materials increases significantly. There exist two different views on the formation of this high resistivity layer, namely, (1) the formation of an amorphous phase containing CaO at the sintering temperature and (2) grain boundary oxidation as a result of Ca segregation during cooling of the sample from high temperature. A recent study of CaO-doped Mn,Zn-ferrites showing an amorphous intergranular phase favors the former model. In the present study, further experiments were done

to ascertain whether CaO enrichment at the grain boundary region occurs during sintering or during cooling. The distribution of Ca on the fractured surface of $(Mn,Zn)Fe_2O_4$ in as-sintered and annealed samples was studied using Auger electron microscopy. In the as-sintered samples, Ca was detected only at intergranular fractured surfaces and not on the intergranular regions. If these samples were heated at 1300°C and then quenched or cooled slowly, the Ca distribution on the fracture surface did not become homogeneous. If the Ca dissolved into the grains at 1300°C and resegregated upon cooling, Ca must be distributed uniformly on the fracture surface in slowly cooled samples. On the other hand, if the intergranular amorphous phase containing Ca only melted upon heating but still continued to stay in the liquid state, Ca distribution must remain unchanged irrespective of whether the sample is quenched or slowly cooled. Thus it is concluded that Ca segregation at grain boundaries occurs during liquid phase sintering at high temperature. Although the solubility of CaO in $(Mn,Zn)Fe_2O_4$ decreases with temperature, the segregation of Ca during cooling is not the dominant process by which grain boundaries are enriched with Ca in $(Mn,Zn)Fe_2O_4$.

* * *

†In press, J. Applied Physics, 1983.
‡Abstracts of LBL-14892 and LBL-14797.
§I.-Nan Lin, "Microstructure and Magnetic Properties of Mn,Zn Ferrites," Ph.D. thesis, University of California, Berkeley, Dec. 1982, LBL-15434.

2. DEVELOPMENT OF THE CELLULAR MICROSTRUCTURE IN THE $SmCo_{7.4}$-TYPE MAGNETS†

L. Rabenberg,‡ R. K. Mishra and G. Thomas

Permanent magnets with energy products in excess of 33 MGOe and iH_c over 13 kOe have become a reality in the $Sm(Co, Cu, Fe, Zr)_{7.4}$ alloy system. Typically these magnets have a cellular microstructure consisting of Sm_2Co_{17} (2:17) cells surrounded by $SmCo_5$ (1:5) cell walls. The role of heat treatment in the development of this microstructure and also in the chemical partitioning of various alloying elements has been established. The kinetics of the growth of the 2:17 and 1:5 phases have been examined.

In our recent work, $Sm\ (Co, Cu, Fe, Zr)_{7.4}$ alloys, annealed at 1160 - 1200°C and quenched, are shown to consist of a heavily faulted hexagonal structure that provides ample sites for easy nucleation of the $SmCo_5$ phase. It is argued that the development of the cellular microstructure consisting of twinned rhombohedral Sm_2Co_{17} cells and hexagonal $SmCo_5$ cell boundaries on pyramid planes occurs by diffusionless transformation of the hexagonal Sm_2Co_{17} phase to the rhombohedral Sm_2Co_{17} phase and subsequent diffusional growth of the $SmCo_5$ phase. The addition of Zr favours the formation of a third phase with rhombohedral symmetry, and all these features are shown in the lattice fringe image of Fig. 2.1.

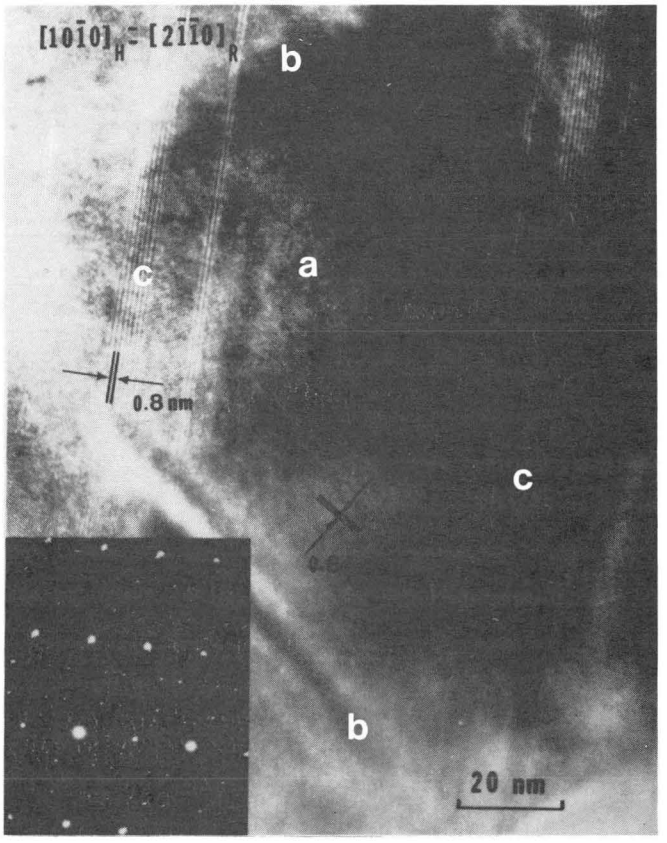

Fig. 2.1. Lattice fringe image and selected area diffraction pattern (inset) from a $Sm_2(Co,Fe,Zr,Cu)_{17}$ alloy showing (a) twin variants of 2:17 phase (chevron pattern), (b) 1:5 type cell boundary phase, and (c) z phase with rhombohedral symmetry.
(XBB 8111-10172A)

* * *

†Brief version of LBL-13395.
‡Ph.D. thesis research in progress.

3. ELECTRON MICROSCOPY OF Mn-Al MAGNETS†

J. S. Gau,‡ R. K. Mishra, and G. Thomas

Warm extruded Mn-Al-C alloys containing 0.8% Ni have been shown to have the highest $(BH)_{max}$ values among the Mn-Al magnets. The microstructure of these magnets were studied using transmission electron microscopy and diffraction. It is seen that the grain size of Ni containing alloys is much finer (0.5-1 μm diameter) than the magnets without Ni. The grains contain no antiphase boundaries (APB) although the crystal structure of the grains is the ordered $L1_0$ structure characteristics of the phase. The material is heavily deformed with grains highly twinned or dislocated. Individual grains containing more than one variant of the {111} <112> deformation twins were seen. It is argued that addition of Ni to the Mn-Al-C alloy helps in the deformation process. The small grain size and the large number of twins are responsible for the absence of the antiphase boundaries.

Careful tilting experiments coupled with convergent beam electron diffraction and high resolution imaging experiments failed to show any kind of precipitation. Lorentz electron microscopy showed that the twins act as pinning sites for the magnetic domain walls unlike the APBs that are nucleation sites. These observations are correlated with the deformation process and the phase transformation in the alloy.

* * *

†Presented at the International Magnetic Society Meeting in Montreal, July 20-23, 1982. Submitted to IEEE Trans. Magnetics.
‡Ph.D. thesis research in progress.

4. ANNEALING OF HIGH PERMEABILITY $(Mn,Zn)Fe_2O_4$†

R. K. Mishra and G. Thomas

The effect of control-atmosphere annealing on properties of high permeability MnZn-ferrite was studied. The results show that the electrical resistivity can be increased dramatically due to annealing without adversely affecting initial permeability. A processing scheme is suggested for producing additive-free $(Mn,Zn)Fe_2O_4$ of high permeability and high resistivity.

* * *

†Research in progress.

1982 PUBLICATIONS AND REPORTS

Refereed Journals

1. L. Rabenberg, R. K. Mishra, and G. Thomas, "Microstructure of Precipitation-Hardened SmCo Permanent Magnets," J. Appl. Phys. 53, 2389 (1982); LBL-13395.

2. H. Mori, H. Fujita, R. Sinclair, and G. Thomas, "Electron Irradiation Induced Crystalline Amorphous Transitions in Ni-Ti Alloys," Scripta Met. 16, 589 (1982).

3. J. S. Gau, J. Y. Koo, A. Nakagawa, and G. Thomas, "Microstructure and Properties of Dual Phase Steels Containing Fine Precipitates," Fundamentals of Dual Phase Steels AIME 47 (1982), LBL-12177.

4. G. Thomas, C. Ahn, and J. Weiss, "Characterization of Y-Si-Al-O-N Glass and Crystallization," J. Am. Ceram. Soc. 65, 185, (1982); LBL-13942.

5. C. Y. Kung and J. J. Rayment, "An Examination of the Validity of Existing Formulae for the Calculation of M_S Temperature," Met. Trans. 13A, 328 (1982); LBL-13191.

6. M. Sarikaya, B. G. Steinberg, and G. Thomas, "Optimization of Fe/Cr/C Base Structural Steels for Improved Strength and Toughness," Met. Trans. 13A, 2227 (1982); LBL-11421.

7. M. M. Disko, O. L. Krivanek, and Peter Rez, "Orientation-Dependent Extended Fine Structure in Electron Energy Loss Spectra," Phys. Rev. B 25, (1982).

LBL Reports

1. I-Nan Lin, R. K. Mishra, and G. Thomas, "Electron Microscopy Study of the Structure and Composition of Grain Boundaries in $(Mn, Zn)Fe_2O_4$," Proceedings of Advances in Materials Characterization, in press, LBL-14892.

2. W. J. Salesky, R. M. Fisher, R. O. Ritchie, and G. Thomas, "Nature and Origin of Sliding Wear Debris From Steels," Proceedings of International Conference on Wear Materials, April 11-14, 1983, in press, LBL-15059.

3. C. Hayzelden, J. J. Rayment, and B. Cantor, "Rapid Solidification Microstructure in Austenitic Fe-Ni Alloys," Acta Met., in press, LBL-14812.

4. M. Sarikaya, "Crystallography of Lath Martensite and Stabilization of Retained Austenite," Ph.D. thesis, LBL-15111.

5. N. J. Kim, A. J. Yang, and G. Thomas, "Microstructure-Properties of Directly Quenched Nb Containing Low Carbon Steel," submitted to Met. Trans., LBL-14469.

6. C. K. S. Kwok, "Two Body, Dry Abrasive Wear of Fe/Cr/C Experimental Alloys-Relationship Between Microstructure and Mechanical Properties," M.S. thesis, LBL-13393.

7. J. A. Wasynczuk, "The Effect of Microstructure on Fatigue Crack Growth in Duplex Ferrite-Martensite Steels," LBL-15110.

8. W. J. Salesky, "On Fundamentals of Sliding Wear in Steel," Ph.D. thesis, LBL-15164.

9. A. Pelton, "Interstitial Phase Precipitation in Iron Base Alloys: A Comparative Study," Ph.D. thesis, LBL-14643.

10. J. H. Rose, "A STEM X-ray Microanalytical Study of Phosphorous Segregation to Grain Boundaries in Thin-Film Silicon," M. S. thesis, LBL-14614.

11. E. A. Kamentzky, "The Mechanisms of Accommodation of Deformation at Grain Boundaries in BCC Materials," LBL-14613.

12. C. C. Ahn and G. Thomas, "Microstructure and Grain Boundary Composition of Hot Pressed Silicon Nitride with Yttria and Alumina," J. Am. Ceram. Soc., in press, LBL-14627.

13. J.-M. Lang, "A TEM Characterization of Mo_2C Precipitates in Molybdenum," M. S. thesis, LBL-14295.

14. M. H. Harmer, R. K. Mishra, and G. Thomas, "Electron Microscopy of Annealed $(Ni,Zn,Co)Fe_2O_4$," J. Am. Ceram. Soc., in press, LBL-11223.

15. G. Van Tendeloo, K. T. Faber, and G. Thomas, "Characterization of Long Period Polytypoids in AlN Ceramics," J. Mat. Sci., in press, LBL-14566.

Other Publications

1. G. Thomas, M. Sarikaya, G. D. W. Smith, and S. J. Barnard, "Microstructural Basis of Alloy Design for High Strength, Tough Structural Steels," Proceedings of Advances in the Physical Metallurgy and Application of Steels 28A, Institute of Metals, paper 29, 1982, LBL-13048.

2. G. Thomas, Y. Fujiyoshi, and N. Uyeda, "Structure Imaging of 21R Polytype in Be-Si-N Ceramics," Proceedings of the 10th International Congress on Electron Microscopy, Hamburg, August 17-24, 21, 1982.

3. G. Van Tendeloo and G. Thomas, "High Resolution Electron Microscopy of Sintered AlN," Proceedings of 40th Annual EMSA Meeting, Baton Rogue, LA, G. W. Bailey (Ed.), 546, 1982.

4. M. Sarikaya and G. Thomas, "Solute Element Partitioning and Austenite Stabilization in Steels," International Conference on Solid-Solid Phase Transformations, Pittsburgh, PA, Aug. 1981, published in 1982, LBL-13099.

5. J. J. Rayment and G. Thomas, "Transmission Electron Microscopy of RSP Fe/Cr/Mn/Mo/C Alloy," Proceedings of MRS Symposium on Rapidly Solidified Materials, Boston, MA, Nov. 1981, LBL-13672, March 1982.

6. M. Sarikaya and P. Rez, "The Thickness Dependence of Energy Loss Spectra," Proceedings of 40th Annual EMSA Meeting, Claitors, Baton Rouge, LA, G. W. Bailey (Ed.), 436, 1982, LBL-14191.

7. M. Sarikaya and G. Thomas, "Lath Martensites in Low Carbon Steels," Proceedings of International Conference on Martensitic Transformation Leuven, Belgium, Aug. 1982, in press, LBL-14506.

8. M. Sarikaya and G. Thomas, "Lath Martensites in Carbon Steels--Are They Bainitic?" International Conference on Solid-Solid Phase Transformations, Pittsburgh, PA, Aug. 1981, in press, LBL-13098.

Invited Talks

1. J. J. Rayment, "Laser Surface Hardening of Steels," Society of Manufacturing Engineers Seminar on Laser Innovations in Manufacturing Technology," Palo Alto, April 1982.

2. G. Thomas, "Fundamentals of Dual Phase Steels," 11th Annual TMS-AIME Meeting, Dallas, February 22-26, 1982.

3. G. Thomas, "Electron Microscopy Diffraction and Spectroscopy--The Modern Approach to Characterizing Solids," University of California, Irvine, Physics Department, January 8, 1982.

4. G. Thomas, "Atomic Resolution Microscopy and Spectroscopy," Third Conference on Electron Microscopy, Taipei, Taiwan, Republic of China, April 1982.

5. G. Thomas, "The Role of Microstructural Analysis in Materials Science and Engineering," Keynote address at official opening of Engineering School, National Sun-Yat-Sen University, Kaohsiung, Republic of China, April 1982.

6. G. Thomas, "Alloy Design of Structural Steels," Fourth Industrial Liaison Program Meeting, Berkeley, CA, March 3, 1982.

7. G. Thomas, "The Future of High Voltage Electron Microscopy," All-Institute Keynote Speaker at South African Institute of Physics Conference, Stellenbosch, Republic of South Africa, July 13-16, 1982.

8. G. Thomas, "Nitrogen Ceramics," Keynote Speaker, South African Institute of Chemistry Conference, Pretoria, Republic of South Africa, July 19-22, 1982.

9. G. Thomas, "Design of Strong Ductile, Duples Low Alloy Steels," Keynote Paper at I.U.P.A.P. Conference on Recent Developments in Specialty Steels and Hard Materials, Pretoria, Republic of South Africa, November 1982.

c. Solid State Phase Transformation Mechanisms*

Kenneth H. Westmacott, Investigator

Introduction. New perspectives and concepts continue to emerge from fundamental transmission electron microscope studies of the crystallography of precipitation processes. The developing crystallographic theory based on the results identifies and correlates the fundamental deformation processes that must occur to allow a product phase to form. Unlike other approaches that consider only the final state, this approach concentrates on understanding the basic mechanisms whereby the final state is achieved. A major goal of this research is to isolate the principal factors governing the transformations in order to enhance the possibilities for alloy design from first principles.

The articles that follow summarize recent results for diverse alloy systems selected to illuminate two important parameters already identified, the type of transformation strain and its associated volume change. Four cases have been treated in detail: (1) invariant plane strain (IPS) with large positive volume change, Pt-C; (2) IPS with small negative volume change, θ' in Al-Cu; (3) invariant line strain (ILS) with no volume change, Cu-Cr and Fe-Cu; and (4) ILS with positive volume change, Mo-C.

1. PRECIPITATION IN THE Pt-C SYSTEM†

Michael J. Witcomb, Ulrich Dahmen, and Kenneth H. Westmacott

In the Pt-C alloy system, plate-shaped precipitates form with IPS and an associated volume change of +50%; it therefore proved ideal for studying the role of vacancies in the transformation. A major part of this work has now been completed and reported in a series of three papers. To summarize the main conclusions:

(1) The dilute supersaturated fcc Pt-C interstitial solid solution undergoes a precipitation sequence completely analogous to the Al-4Cu substitutional system. Moreover, the previously unknown carbide structure which forms, Pt_2C, is isomorphous with θ' Al_2Cu.

(2) The indispensable role of lattice vacancies for initiating the reaction via the co-precipitation process was demonstrated.

(3) The recently developed concept of coherency[1] was extended to the mechanisms of precipitate growth, systematically incorporating lattice defects.

(4) The fundamental connection between crystal lattice defects and the accommodation of misfitting precipitates in the parent matrix became apparent.

* * *

†Brief version of LBL-14775, LBL-14776, and LBL-14777.

1. G. B. Olson and M. Cohen, Acta. Met. 27, 1907 (1979).

2. LEDGE STRUCTURE AND PRECIPITATE GROWTH IN Al-Cu †

Ulrich Dahmen and Kenneth H. Westmacott

Extension of the precipitate growth model established for Pt-C to the substitutional Al-4 w/o Cu system (IPS with -4% misfit) has resulted in a greatly improved understanding of the nucleation and growth of the θ' phase from the supersaturated solid solution.

After recognizing a simple lattice correspondence for the transformation, the basic conservative and non-conservative growth units were identified. By adding these basic building blocks in combinations which minimized both the precipitate shape and volume change, a growth thickness sequence in perfect agreement with that observed experimentally was found. Precipitate growth occurs by the expansion of partial dislocation loops bounding ledges. Different combinations of shear and prismatic loops correspond to different ledge heights and growth units. Another attractive feature of the proposed model is that misfit accommodation on the broad faces of the precipitate is also naturally incorporated. In addition, the experimentally observed structural role of excess vacancies in initiating the θ" to θ' transformation is now understood.

* * *

†Brief version of LBL-14687.

3. THE RELATIONSHIP BETWEEN INVARIANT LINE STRAIN AND PRECIPITATE NEEDLE GROWTH†

Ulrich Dahmen, Patrick Ferguson, and Kenneth H. Westmacott

A different type of structural transformation (ILS without volume change) is exemplified in the alloy systems Cu-Cr and Fe-Cu which develop needle-shaped precipitates.

The growth direction of a precipitate needle was shown earlier[1] to originate from an invariant line along its axis. This condition limits coherent needle growth to directions that lie on cones with semi-angles defined by the lattice parameter ratio of the parent and product phases.

*This work was supported by the Director, Office of Energy Research, Office of Basic Energy Sciences, Materials Sciences Division of the U.S. Department of Energy under Contract No. DE-AC03-76SF00098.

Since, during continued growth the needles lose coherency by the nucleation and growth of shear loops, the crystallography of the available shear systems places a further restriction on the permissible growth directions. These principles, developed in agreement with an fcc/bcc alloy system (Cu-Cr),[2] are now being tested by observations of precipitate needles in a bcc/fcc (Fe-Cu) system representing the structural inverse of the fcc/bcc Cu-Cr.

Figure 3.1a shows a typical area of quenched and aged Fe-2 w/o Cu foils containing semicoherent needles of fcc Cu in a bcc ferrite matrix. The random appearance of the needle axis directions is deceptive and results from the distribution of 24 variants of a single crystallographic type of needle.

In Fig. 3.1b the orientation relationship of a Cu needle is shown to agree with the predicted Kurdjumov-Sachs relationship. The corresponding needle lies in the $(111)_{fcc}$ $(110)_{bcc}$ common close packed planes.

These results demonstrate that the relief of shear stresses, developed during coherent needle growth, by shear loop nucleation controls the growth process.

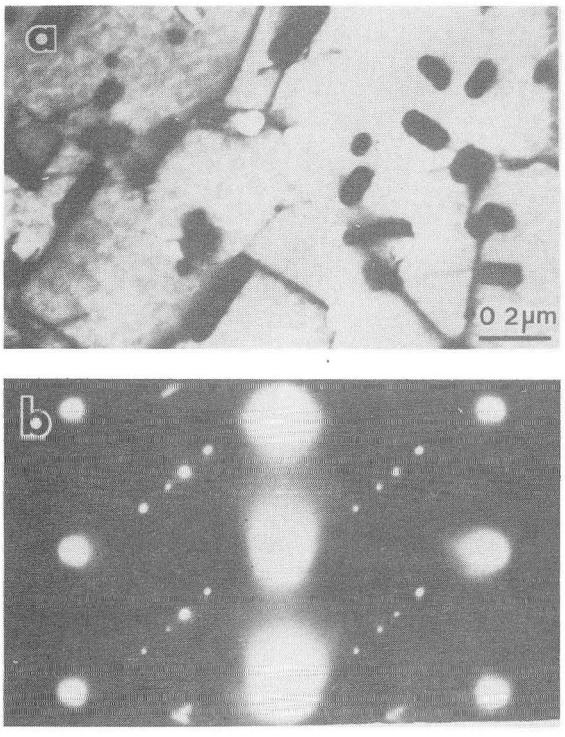

Fig. 3.1. Fe-2 w/o Cu alloy quenched from 850°C and aged 18 h at 750°C showing semicoherent fcc Cu needles; (a) needle distribution with connecting dislocations, (b) selected area diffraction from a single precipitate showing Kurdjumov-Sachs orientation relationship. (XBB 831-224)

* * *

†Brief version of LBL-13336.

1. U. Dahmen and K. H. Westmacott, Proc. Int. Conf. on Solid-Solid Phase Transformations, Pittsburgh, PA (1981), in press.
2. G. C. Weatherly, P. Humble, and D. Borland, Acta. Met. 27, 1815 (1979).

4. Mo_2C PRECIPITATE STRUCTURE AND MORPHOLOGY IN MOLYBDENUM†

J.-M. Lang, Ulrich Dahmen, and Kenneth H. Westmacott

Mo-C represents a class of alloy system in which the transformation is characterized by an ILS with +17% volume change. In spite of its plate-shaped morphology, the Mo_2C carbide phase cannot grow by a ledge mechanism because the invariant plane strain condition necessary for such growth is not fulfilled. However, the stresses that develop during plate growth as a result of the invariant line transformation strain can be relieved by shear loop propagation. In contrast to the IPS case, the loops are inclined to the habit plane. Striated structures observed in the interface of large carbide precipitates in Mo (see Fig. 4.1) can be interpreted successfully on this basis. The more complex precipitate structure and morphology reflect greater restrictions on the available deformation processes and the incomplete plastic accommodation of the more general transformation strains.

* * *

†Brief version of LBL-14295 and LBL-14970.

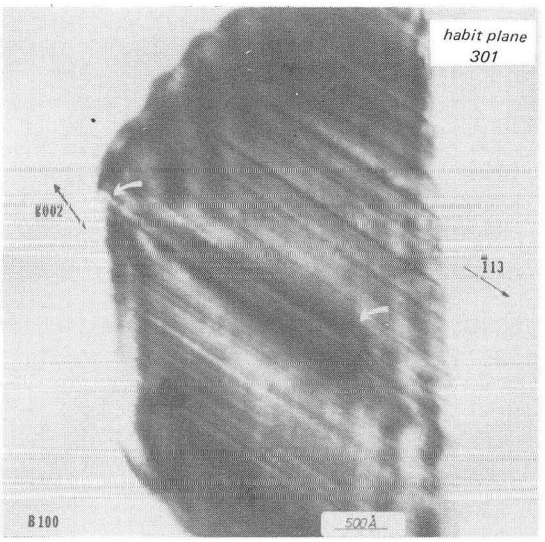

Fig. 4.1. Mo_2C precipitate on a (301) habit plane in Mo, seen in [100] beam direction. The straight lines in the precipitate/matrix interface lie along the $[\bar{1}13]$ invariant line direction. (XBB 823-2109)

5. WORK IN PROGRESS

The present emphasis is on the systematic development of the crystallographic theory for the case of coherent precipitates to incorporate elastic anisotropy and the effect of coherency loss on precipitate morphologies. This advance is expected to allow prediction of the morphology, orientation relationship, and growth paths of precipitates.

In the experimental program, the established principles are being tested further and also applied to more complex alloy systems such as bcc/hcp, fcc/dc, and bcc/orthorhombic.

1982 PUBLICATIONS AND REPORTS

Refereed Journals

1. U. Dahmen, "Orientation Relationships in Precipitation Systems," Acta Met. 30, 63 (1982), LBL-12147.

2. P.Regnier, N. Q. Lam, and K. H. Westmacott, "Defect Clustering Induced by Secondary Collisions in Pt(C) Alloys During HVEM Irradiation," Scripta Met. 16, 643 (1982).

3. M. J. Witcomb, "A Method of Alignment for Convergent Beam Diffraction in TEM Mode for a JEM-100C Electron Microscope," Ultramicroscopy 7, 343 (1982).

4. K. H. Westmacott and U. Dahmen, "Loss of Coherency of Precipitates in Al-Si: An HVEM Study," 40th Ann. Proc. Electron Microscopy Soc. Am., Washington, D.C., 1982, G. W. Bailey (ed.); LBL-14180.

5. J. M. Lang, "Invariant Line and Loss of Coherency in Mo(C) System," 40th Ann. Proc. Electron Microscopy Soc. Am., Washington, D.C., 1982, G. W. Bailey (ed.); LBL-14014.

LBL Reports

1. M. J. Witcomb, U. Dahmen, and K. H. Westmacott, "A Study of Precipitation in Interstitial Alloys: II. A New Metastable Carbide Phase in Platinum," LBL-14775.

2. U. Dahmen, M. J. Witcomb, and K. H. Westmacott, "A Study of Precipitation in Interstitial Alloys: III. Coherent and Semi-Coherent Growth Mechanisms," LBL-14776.

3. K. H. Westmacott, M. J. Witcomb, and U. Dahmen, "A Study of Precipitation in Interstitial Alloys: IV. The Precipitation Sequence in Pt-C," LBL-14777.

4. U. Dahmen and K. H. Westmacott, "Ledge Structure and the Mechanisms of Precipitate Growth in Al-Cu," LBL-14687.

5. A. Pelton, "Interstitial Phase Precipitation in Iron-Base Alloys: A Comparative Study," Ph.D. thesis, LBL-14643.

6. J. M. Lang, "A TEM Characterization of Mo_2C Precipitates in Molybdenum," M.S. thesis, LBL-14295.

7. J. M. Lang, U. Dahmen, and K. H. Westmacott, "The Origin of Mo_2C Precipitate Morphology in Molybdenum," LBL-14970.

Other Publications

1. U. Dahmen and K. H. Westmacott, "A Novel Method for Analyzing Phase Transformations from Diffraction Patterns," 10th Int. Cong. on Elec. Micros., Hamburg, August 1982.

2. J.-Y. Laval, K. H. Westmacott, and M. C. Amamra, "Characterization and Structure of Intergranular Glassy Phases in Ceramics," submitted to 5th Int. Conf., The Physics of Non-Crystalline Solids, Univ. of Montpellier, France, July 5-9, 1982.

Invited Talks

1. K. H. Westmacott, "Applications of HVEM in Materials Science," Exxon Research and Development, Linden, NJ, May 21, 1982.

d. National Center for Electron Microscopy*

Gareth Thomas, Ronald Gronsky, and Kenneth H. Westmacott, Investigators

Introduction. The National Center for Electron Microscopy (NCEM) aims to provide state-of-the-art facilities for electron-optical characterization of materials and to develop techniques of imaging, interpretation, and microanalysis.

The very high cost of modern instruments dictates time-sharing centers where facilities, support, and staff are all available. The present NCEM facilities consist of a 650-kV Hitachi (1969) and a new 1.5-MeV Kratos microscope largely for in-situ work, a 1-MeV atomic resolution microscope (ARM), which was delivered in January 1983, and commercial support instruments (JEOL 200 CX, Siemens 102 and a JEOL 200 CX analytical microscope). One of the principles of the facility is that while a microscope is normally dedicated to a single purpose, certain projects will use many, if not all, of these microscopes. Hence, considerable outlay is needed for equipment and staffing.

It is anticipated that the facility will be fully operational by May 1983. The Seventh International Conference on High Voltage Electron Microscopy will be held at Berkeley on August 16-19, 1983.

The Center is guided by a Steering Committee whose present non-LBL members are: Drs. M. Simnad (General Atomic Company), W. L. Bell (General Electric Company), D. G. Howitt (U.C. Davis), J. J. Hren (University of Florida),J. C. H. Spence (Arizona State University), and A. Taylor (Argonne National Laboratory).

1. 1.5 MeV HIGH VOLTAGE ELECTRON MICROSCOPE

K. H. Westmacott

The HVEM was accepted on March 19, 1982 when all instrument performance specifications had been met or exceeded. Since that time, in spite of a high-voltage instability problem that developed and was difficult to diagnose, work on all 40 of the original research proposals has been carried out (Table 1.1). Modifications to the original accelerator design which are being made to correct problems with the long-term voltage stability have, however, impinged on the experimental running time.

A wide variety of experiments are being conducted on the microscope, with users coming from universities, industry, and government laboratories (Table 1.1). The present use ratio of LBL/UCB to other laboratories is almost exactly unity, and the ratio of physical to biological science use is ~8:1.

Many experimentalists have taken advantage of the various tilting, heating, cooling, and environmental control stages to perform dynamic in-situ studies, and these functions have been enhanced by the acquisition of a videocamera/image intensifier and magnetic tape recorder.

Brief summaries of some typical examples of research in progress are given in the following table.

*This work was supported by the Director, Office of Energy Research, Office of Basic Energy Sciences, Materials Sciences Division of the U.S. Department of Energy under Contract No. DE-AC03-76SF00098.

Table 1.1. HVEM Research Proposals.

Principal Investigator	Affiliation	Title
R. L. Hines	Northwestern University	Electron Phase Microscopy
R. Glaeser	UCB, Biophysics/Donner	"... for electron diffraction and EM image work on thin crystals of proteins and nuclei acids."
T. L. Hayes	UCB, Biophysics/Donner	"... studying the phagocytic process involved in the uptake of coal combustion particulates (fly ash) by pulmonary macrophase cells."
R. Sinclair	Stanford University, Materials Science	To study the relationship of atomic modes of deformation to mechanical properties such as hardness and toughness in tool carbides
R. Sinclair	Stanford University, Materials Science	Investigation of $BaTiO_3$-Based Dielectrics
R. Sinclair	Stanford University, Materials Science	High Resolution Multi-Beam Lattice Imaging of Defects in Compound Semiconductors
H. R. Wenk	UCB, Geology and Geophysics/LBL	Dislocation Properties of Silicate Garnets
R. Gronsky	NCEM/LBL	High Resolution Imaging at 1.5 MeV
D. G. Howitt	UC Davis, Mechanical Engineering	In-situ studies of the kinetics of transformations in nuclear waste glasses[a]
D. G. Howitt	UC Davis, Mechanical Engineering	In-situ environmental studies of the leaching behavior in nuclear waste glasses[a]
T. F. Budinger	UCB, Electrical Engineering and Computer Science/Donner	Blood Brain Permeability Studies
T. F. Budinger	UCB, Electrical Engineering and Computer Science/Donner	Platelet Architecture and Responses to Physical Insults
T. F. Budinger	UCB, Electrical Engineering and Computer Science/Donner	Leukemic White Blood Cell Architecture
J. Steeds	University of Bristol, Physics (England)	Zone axis critical voltages of layer structured materials
L. Eyring	Arizona State University, Chemistry	In-situ studies of phase reactions in PrO
K. H. Westmacott	NCEM/LBL	The mechanism of carbon precipitation in platinum
K. H. Westmacott	NCEM/LBL	Dynamic hot-stage studies of precipitation development in interstitial and substitutional alloys
K. H. Westmacott	NCEM/LBL	Dynamic studies of changes in interface structure during the overgrowth of oxide films on metal substrates
J. W. Evans and K. H. Westmacott	UCB, Materials Science and Mineral Engineering/LBL NCEM/LBL	In-situ reduction studies of NiO and related materials
A. G. Evans	UCB, Materials Science and Mineral Engineering/NCEM/LBL	High temperature deformation of ceramics

[a]Environmental Cell of the High Voltage Electron Microscope.

(Continued)

Table 1.1. (Continued)

Principal Investigator	Affiliation	Title
J. L. Brimhall	Battelle Pacific Northwest Laboratories	Bombarding a $Mo_{50}Ni_{50}$ alloy to determine if high energy electrons can render the material amorphous
J. L. Brimhall	Battelle Pacific Northwest Laboratories	Bombarding $Mo_{50}Ni_{50}$ alloys made amorphous by sputter deposition by high energy electrons at elevated temperatures to determine if the irradiation enhances the crystallization reaction.
W. Stacy	Philips Research Laboratories	Transistor Pipes[b]
D. R. Clarke	Rockwell International Science Center	Dissolution Mechanisms of Nuclear Waste Ceramics[a]
J. R. Porter	USC/Materials Science	Direct Observation of the Reduction of Pure and Doped Zinc Ferrite by In-Situ High Voltage Electron Microscopy[a,b]
G. J. Thomas and J. C. Hamilton	Sandia Laboratories	In-situ oxidation studies on stainless steel[a]
T. Lechtenberg	General Atomic Corporation	In-situ observation of deformation and crack-nucleation of embrittled 12Cr-1Mo steel[b]
G. W. Owen	UCB, Biophysics/Donner	...3D reconstruction of extended cellular processes (axons, fibers, etc.) from serial sections of epon-embedded tissue[b]
H. S. Gill	Hewlett-Packard Laboratories	High resolution microscopy on Co-X/Cr bilayer thin/thick film composite
J. Walton	LLNL/Biomedical Research	HVEM of skeletal muscle mitochondria[b] (work completed)
G. Thomas and K. Krishnan	UCB, Materials Science and Mineral Engineering NCEM/LBL NCEM/LBL	Study of the space group of epitaxially grown garnet films
V. Jayaram and R. Sinclair	Stanford University Materials Science	...to study WC-Co samples that have been deformed by micro-indentations[b]
S. L. Shinde and R. Sinclair	Stanford University, Materials Science	Deformation studies of (W,Ti)C
W. J. Salesky, J. J. Rayment, and G. Thomas	NCEM/LBL, MMRD	Investigation into the micromechanisms of wear
D. K. Sadana	LBL, MMRD	TEM investigations of high energy ion implanted Si and GaAs
C. S. Murty and R. Gronsky	NCEM/LBL	Crystalline to Amorphous Transformation in Silicon
D. R. Cole	UCB/Biochemistry	Structural studies of metaphase chromosomes
J. J. Rayment	LBL/MMRD	Laser Surface Hardening of Steels
A. Pelton	Stanford University, Materials Science	Amorphitization of TiNi
R. H. Steinberg	UCSF, Physiology	Cytoskeleton of the pigment epithelium and photo receptors of the vertebrate retina

[a]Environmental Cell of the High Voltage Electron Microscope.

[b]Non-DOE Support.

Crystallization of Amorphous Metals

J. L. Brimhall†

The HVEM is being used to study the effects of electron irradiation on the crystallization of amorphous materials. The results are compared with earlier work using heavy ion irradiation.

Figure 1.1 shows a region of a partially crystallized amorphous Fe-Cr-Ni-W alloy after irradiation with 1.5 MeV electrons at 530°C for 30 minutes. A slightly accelerated crystallization rate was observed in the irradiated region. This behavior is in marked contrast to the ion-irradiation results, in which a large decrease in crystallization temperature and the development of an Fe-Cr-WX phase was observed.

Radiation-Induced Amorphitization

A. R. Pelton‡

Further studies were conducted on electron-irradiation-induced amorphitization of Ni-Ti intermetallic compounds. Several experimental parameters were investigated, and it was shown that the crystalline-to-amorphous transition occurs by atomic displacements. For example, it is now apparent that in the austenite phase (B2 crystal structure) the process is a function of electron energy, dose rate, and crystal thickness, but not of crystal orientation. Figure 1.2 shows

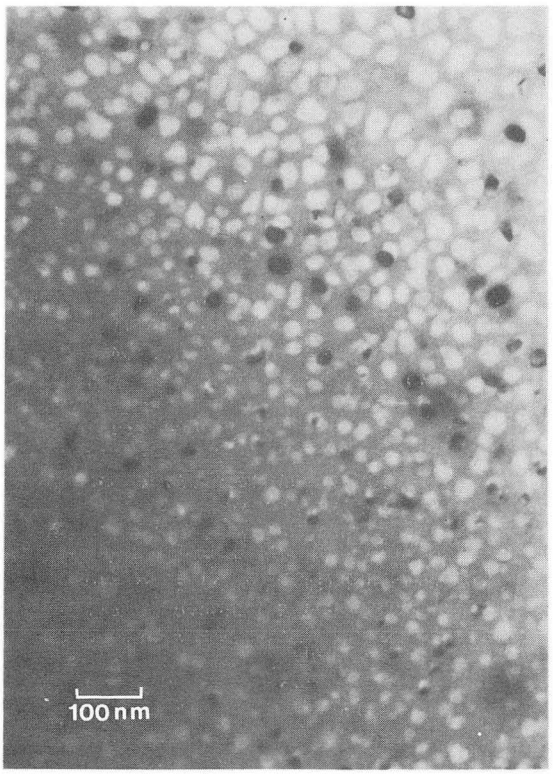

Fig. 1.1. Light and dark crystalline regions in an Fe-Cr-Ni-W amorphous alloy following irradiation with 1500 kV electrons at 530°C for 30 minutes.
(XBB 831-237)

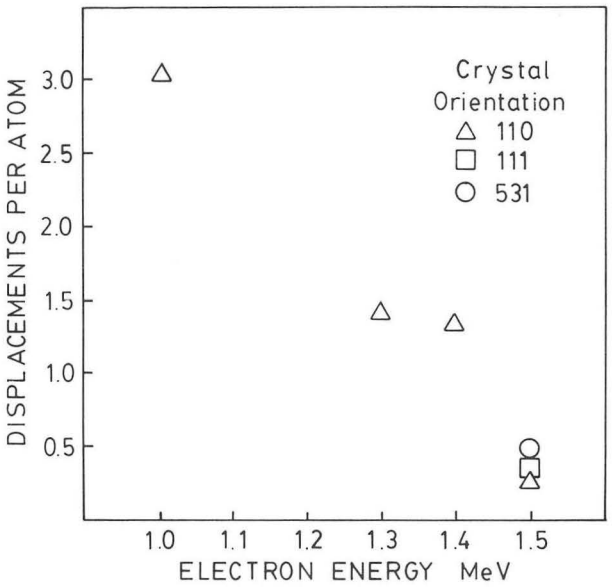

Fig. 1.2. Plot showing the variation of electron dose with energy for the onset of amorphitization in a Ni-Ti alloy as a function of crystal orientation relative to the electron beam.
(XBL 831-7574)

the relationship between electron energy and the number of displacements per atom required for the onset of amorphitization for three orientations. It was also determined that the B2 structure does not disorder prior to becoming amorphous. The martensitic phase, however, readily detwins and transforms to austenite when irradiated. These observations agree well with recent results from Ni^+ irradiations, although much greater electron doses (~10^{22} electrons/cm^2) are required than for ion bombardment (~10^{16} ions/cm^2).

Radiation Damage in Silicate Glasses

D. G. Howitt,§ J. F. DeNatale,§ D. K. McElfresh§

In an interesting application of the environmental cell of the HVEM, the behavior of glasses during exposure to both electron irradiation and leaching environments is being studied. Leaching rates and changes in the glass microstructure can be studied directly as a function of such variables as temperature, partial pressure, irradiation dose rate, and fluence and glass composition. It is found that in certain temperature ranges silicate glasses form oxygen-stabilized voids and undergo amorphous-amorphous and crystalline-amorphous decomposition.

An example of the microstructural features observed after exposing a silicate glass to water vapor and an electron beam in the HVEM environmental cell is seen in Figure 1.3. The selective dissolution or leaching of the glass components is attributed to attack following radiolytic decomposition of the water vapor by the electron beam.

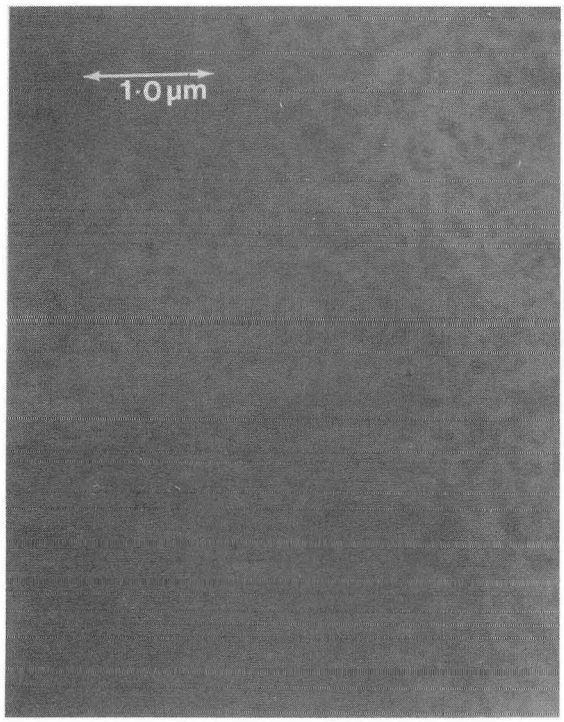

Fig. 1.3. Selective dissolution of the surfaces of a silicate glass during combined exposure to water vapor and high energy electrons in the HVEM. (XBB 831-238)

In-Situ Studies of Precipitation in the Fe-N System

P. Ferguson, U. Dahmen, and K. H. Westmacott

HVEM has been shown to be a powerful tool in in-situ precipitation studies in many age-hardening alloys. Studies are being conducted on nitrogen-ferrite, a system in which the intermediate precipitate b.c. tetragonal α'' - $Fe_{16}N_2$ forms on {100} matrix planes as discs thin in the c direction. The α'' structure consists of eight body-centered cubic ferrite unit cells distorted by ordered nitrogen atoms occupying two of the 16 octahedral interstices whose tetrad axes are parallel with one of the cube directions, i.e., the c edge. At temperatures >250°C, α'' transforms rapidly to the equilibrium precipitate γ'-Fe_4N, which has an f.c.c. arrangement of metal atoms with a single nitrogen atom occupying an ordered position in the central octahedral interstice. Fe_4N often precipitates as "V"-section double platelets and has the orientation relationship with the parent ferrite $(112)_{\gamma'} \parallel (210)_f$; $[110]_{\gamma'} \parallel [001]_f$. The α''-$Fe_{16}N_2$ structure can be regarded as a distorted γ' in which alternate nitrogen atoms are missing and which fits with the ferrite matrix with a Baker-Nutting orientation relationship $(001)_f \parallel (001)Fe_4N_{0.5}$; $[110]_f \parallel [100]Fe_4N_{0.5}$; it seems therefore that γ'-Fe_4N can be nucleated from α'' by nitrogen enrichment. This hypothesis was tested by heating at 285°C an Fe-0.08 wt% N thin foil that initially contained stress-oriented α''-$Fe_{16}N_2$ precipitates. It is clearly seen in Fig. 1.4 that

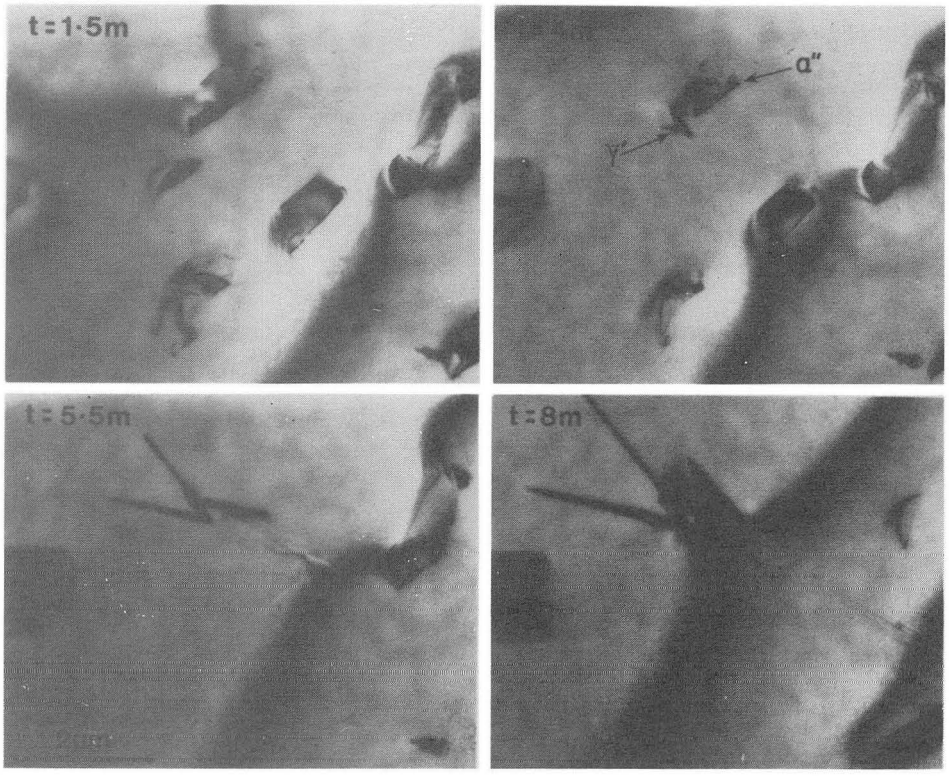

Fig. 1.4. In-situ aging study, on an Fe-0.08 wt% N alloy in the HVEM operating at 500 kV. the sequence of micrographs show the nucleation and growth of γ'-Fe_4N from dissolving α''-precipitate. Beam direction near to [001]. (XBB 831-315)

after 4 minutes, a V-shaped γ' particle is nucleated at a shrinking α'' precipitate. The γ' particle, once formed, readily grows with a complex double-"V" morphology as the surrounding α'' precipitates dissolve. The particle marked A is the broad face of a γ' platelet growing from an adjacent region. This observation of γ' nucleation at α'' particles has been found in other in-situ experiments and confirms the aforementioned mechanism by which $Fe_{16}N_2$ transforms to Fe_4N.

* * *

†Battelle-Pacific Northwest Laboratories.
‡Stanford University.
§UC Davis.

2. ATOMIC RESOLUTION MICROSCOPE

R. Gronsky

Final factory certification of the Atomic Resolution Microscope (ARM) was given on November 19, 1982 at JEOL, Ltd., Tokyo, Japan. By then, the microscope had either met or exceeded all factory performance tests, including a convincing demonstration of resolution (Fig. 2.1). This is an impressive result, since the factory is not equipped with a vibration isolation system; in fact, no resolution test was specified for the factory site because of potential problems with mechanical instabilities.

Other performance data include a voltage stability of 8×10^{-7} volts per minute and ripple of 7×10^{-7} volts at top accelerating potential (1 MeV). The vacuum in both the specimen stage area of the column and the accelerating tube was in the mid 10^{-8} torr range. The most critical design feature of the new instrument, its biaxial tilt-lift stage, also yielded outstanding results (Fig. 2.2).

Installation in the ARM building began on January 10, 1983. The microscope should be ready for initial tests of its electrical system by mid-February 1983.

The ARM Support Laboratory (ASL) is also under construction, with a projected completion date in May 1983. This addition to Building 72 will house support microscopes, specimen preparation equipment, and image analysis hardware.

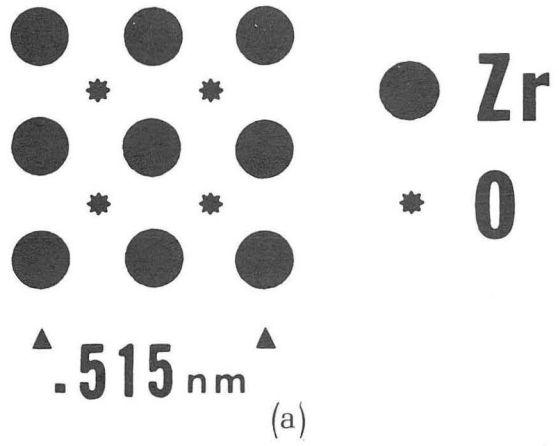

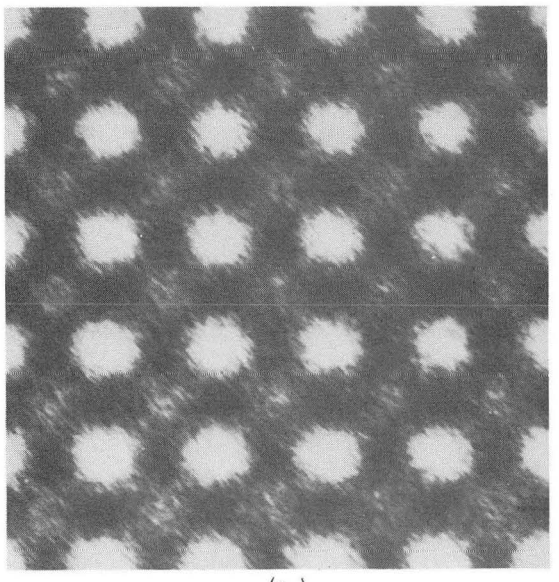

Fig. 2.1. (a) Structural model and (b) atomic resolution image of zirconia ZrO_2, illustrating the factory resolution performance of the ARM.
[(a) XBL 828-10954; (b) XBB 828-6828]

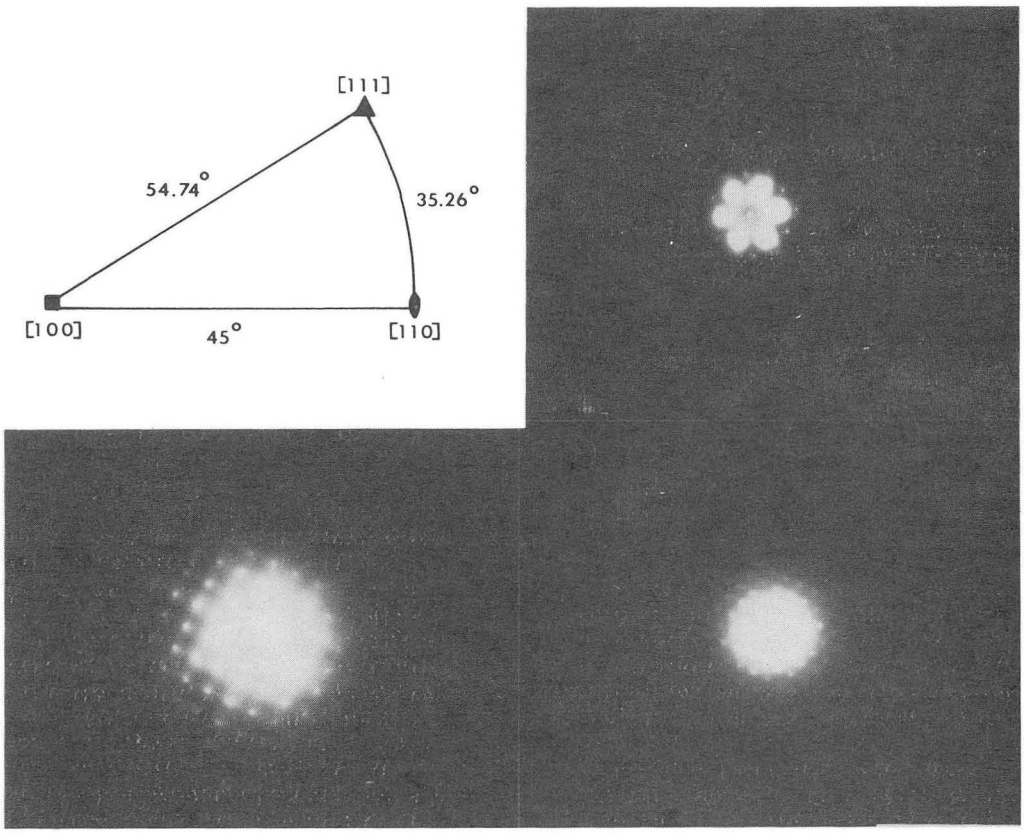

Fig. 2.2. Tilting experiment designed to test the range of the new double-tilt-lift goniometer stage in the ARM. The entire unit triangle of the Si specimen was accessible with no interruptions. (XBB 828-6831)

3. PERIODIC EXTENSION IN OPTICAL DIFFRACTION ANALYSIS†

R. Gronsky and C. S. Murty

Although optical diffractograms are usually used in high resolution electron microscopy to determine instrumental performance, they can also be used to advantage in the analysis of fine microstructural detail. In optical microdiffraction, a field-limiting aperture in the optical bench system selectively obtains diffraction spectra of specific segments of high resolution negatives, for a considerable increase in spatial resolution. Unfortunately, diffraction effects from the sampling aperture itself often interfere with the interpretation of results.

In this work, a method to overcome these difficulties has been developed. It is based upon a periodic extension of the small region from which a microdiffraction pattern is desired, making the problem a much simpler deconvolution of the desired pattern and that of the periodic array.

With proper care to avoid emulsion grain effects (due to high printing enlargement ratios), this method was successfully applied to the study of small amorphous zones (~50Å diameter) in a crystalline Si matrix. Information was obtained on the nature of these amorphous zones during a transformation sequence from their periodically reinforced scattering patterns.

* * *

†Condensed version of LBL-14163.

4. REAL SPACE IMAGE SIMULATION IN HIGH RESOLUTION MICROSCOPY†

R. Kilaas and R. Gronsky

The Atomic Resolution Microscopy project urgently needs reliable computer simulation of atomic resolution images so that they can be correctly interpreted. Although most image calculation programs are based upon dynamical multi-slice formulations, a new method has emerged, which promises an even more dramatic reduction in calculation time. The present work examines the domain of validity of this new technique, termed here the Real Space (RSP) method.

The RSP method treats the interaction of the electron beam with the specimen by using an expansion of the propagator $\exp(\varepsilon\Delta)$ to second order in ε. Its usefulness therefore depends upon the errors introduced by this truncation, and computations were performed using both RSP and fast Fourier transform (FFT) algorithms for the same specimen (copper) and imaging conditions.

The RSP method gives results similar to the conventional FFT calculation when care is taken to include enough reflections. To keep within the

domain of validity of the RSP method, it might be necessary to reduce slice thickness as the number of reflections increases as needed to maintain $\lambda \varepsilon g^{a}_{max} < 1/2$. If this condition is not satisfied, the RSP method will begin to diverge because of a near-exponential growth of higher order reflections. Nevertheless, for the same number of reflections, the RSP method offers a significant saving in computer time, which is of major importance for larger calculations.

* * *

†Condensed version of LBL-15345.

5. CHARACTERIZATION OF AlN CERAMICS CONTAINING LONG PERIOD POLYTYPOIDS†

G. Van Tendeloo‡§ and G. Thomas

Two AlN-SiO_2 materials have been investigated by means of very high resolution electron microscopy carried out in the JEOL 200 CX instrument. Three new long period polytypes, close to the 2H hexagonal AlN structure, have been identified by high resolution electron microscopy, namely 33R, (Fig. 5.1), 24H, and 39R. These polytypoids are built on the same stacking principle as those in the previously observed shorter polytypes in the AlN system.

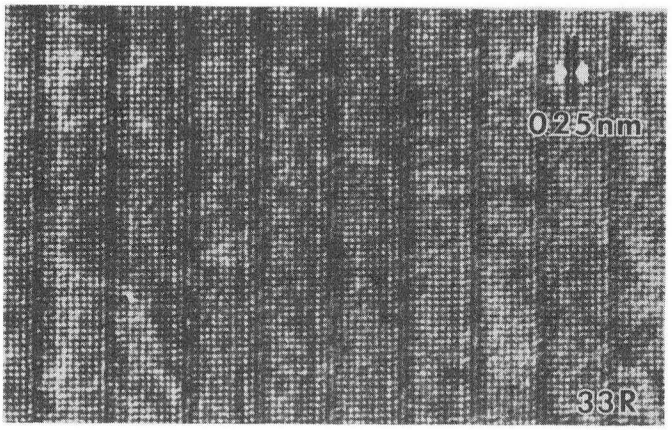

Fig. 5.1. Example of 2.5 Å point-to-point resolution of the 33R polytypoid. The bright dots correspond to the carbon sites. (XBB 824-3421)

* * *

†J. Materials Science (in press).
‡On leave from RUCA, University of Antwerp, Groenenborgerlaan, Belgium.
§Partial financial support form the National Science Foundation.

1982 PUBLICATIONS AND REPORTS

Refereed Journals

1. R. Gronsky and C. S. Murty, "Periodic Extension in Optical Diffraction Analysis," in Proceedings of the 40th Annual Meeting of the Electron Microscopy Society of America, edited by G. W. Bailey (Claitors, Baton Rouge, 1982), p. 428, LBL-14163.

2. K. H. Westmacott, "Life Beyond 1 MeV," Prakt. Met. 19, 474 (1982).

3. G. Van Tendeloo and G. Thomas, "High Resolution TEM of Sintered AlN," in Proceedings of the 40th Annual Meeting of the Electron Microscopy Society of America, edited by G. W. Bailey (Claitors, Baton Rouge, 1982), p. 546.

4. G. Thomas, Y. Fujiyoshi, and N. Uyeda, "Structure Imaging of the 21R Polytypoid in Be-Si-N Ceramics," in Electron Microscopy 1982, 10th International Congress, Deutsche Gesellschaft für Elektronik, Vol. 2, 21, 1982.

LBL Reports

1. G. Van Tendeloo, K. T. Faber, and G. Thomas, "Characterization of AlN Ceramics Containing Long Period Polytypoids," J. Mat. Sci., in press, LBL-14566.

2. R. Kilaas and R. Gronsky, "Real Space Image Simulation in High Resolution Electron Microscopy," LBL-15345.

Invited Talks

1. K. H. Westmacott, "The Berkeley High Voltage Electron Microscopy Facility," Microbeam Analysis Society of Northern California, Sunol, March 5, 1982.

2. K. H. Westmacott, "Argonne National Laboratory HVEM Summer Institute Lecture--Kinetics II, Argonne, IL, July 22, 1982, LBL-14720.

e. In-Situ Investigations of Gas-Solid Reactions by Electron Microscopy*

James W. Evans and Kenneth H. Westmacott, Investigators

Introduction. There is considerable evidence in the literature that there is a link between the defect structure of a solid and the kinetics of the reaction with a liquid or gas. However, there has been little examination of the nature of this link, presumably because of the difficulty of simultaneously reacting the solid and characterizing its microstructure. Such simultaneous measurements are necessary in view of the propensity for a microstructure to change between the time of its characterization and any reaction experiments that are subsequent, rather than simultaneous. This difficulty has recently been overcome with the use of an "environmental cell" in a high voltage transmission electron microscope, which permits observation of the microstructure as the solid reacts.

1. THE MICROSTRUCTURE AND REACTIVITY OF METAL OXIDES

J. W. Evans, D. J. Coates,† and K. H. Westmacott

Reductions of NiO and iron oxide in an environmental cell in a 650 kV Hitachi transmission electron microscope have been studied. The reduction of NiO by H_2 is interesting in that there is much evidence that the reaction is significantly affected by the microstructure. Prior work at Berkeley has indicated that cracks provide sites for nucleation of the Ni phase formed by reaction. Experiments in the environmental cell suggest that antiferromagnetic domain boundaries also provide nucleation sites. This would be consistent with the macroscopic observations, made by other workers, that there is a change in activation energy for reaction at the Néel temperature (~520 K). However, the evidence linking the antiferromagnetic domain boundaries to Ni nucleation is not certain. A double tilt stage is required to properly image the boundaries, and the environmental cell is only equipped with a single tilt stage.

Figure 1.1 shows two regions of a NiO single crystal that have been reduced at approximately 570 K for 90 minutes in a 50 torr, 5% H_2 95% Ar mixture. The white areas are pores formed by reduction; gray and black areas are Ni of varying thickness; the small amount of remaining nickel oxide in these samples is not evident in these pictures. Diffraction patterns are inset, and it is remarkable that, even with the extensive reduction and development of porosity evident in these figures, epitaxy is retained between the unreacted NiO and the nickel formed by reduction. This is evident from the absence of "powder" rings in the diffraction pattern and the presence of double diffraction spots.

Fig. 1.2 shows NiO that was reduced in situ, subjected to further ion beam thinning, and examined in the microscope (without further reduction). It is clear that the porosity of the Ni produced by reaction extends right up to the interface between the Ni and NiO. This result was to be expected since the pores provide the route for the ready diffusion of hydrogen to this interface and of water vapor away from it.

Figure 1.3 shows a wüstite (FeO) sample prior to reduction (left) and after exposure to a 50 torr, 10% H_2, 90% Ar mixture at 784 K for 14 minutes (right). Fe nuclei are evident across the surface of the wüstite and particularly at the edge of the sample. The powder rings of the diffraction pattern correspond to Fe, and it is clear that the iron nuclei are not epitaxial with the host oxide, in contrast to the case in nickel oxide reduction.

* * *

†Present address: METTEK, Santa Ana, CA 92705.

*This work was supported by the Director, Office of Energy Research, Office of Basic Energy Sciences, Materials Sciences Division of the U.S. Department of Energy under Contract No. DE-AC03-76SF00098.

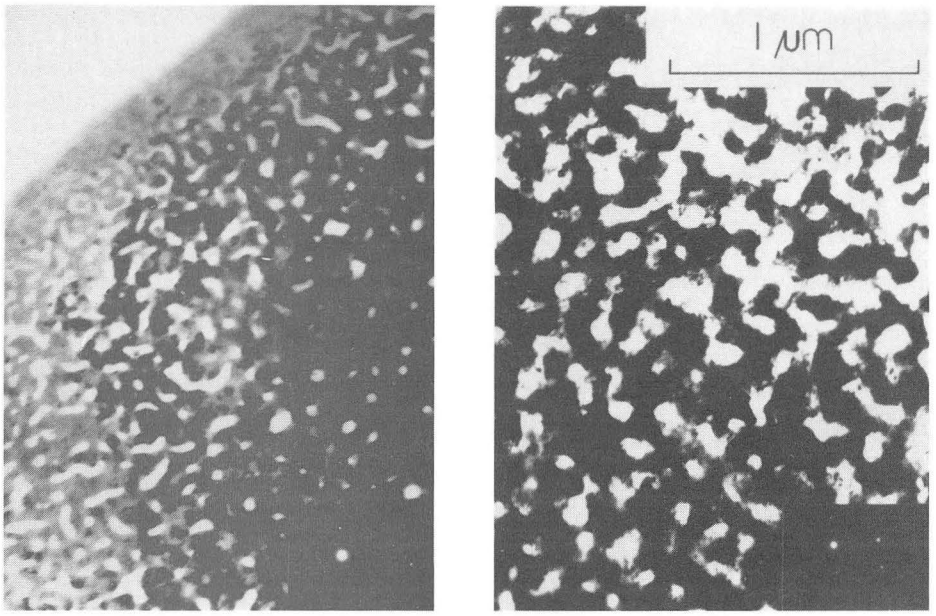

Fig. 1.1. Two regions of a nickel oxide single crystal that have been extensively reduced to nickel. Electron diffraction patterns inset. (XBB 821-714)

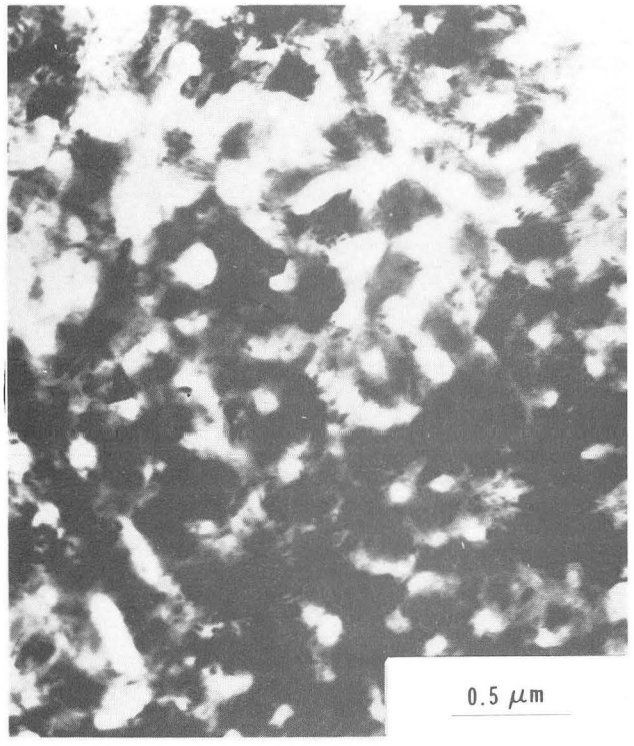

Fig. 1.2. Nickel oxide specimen that has been ion beam thinned after partial reduction. Pores in the nickel extend to the nickel-nickel oxide interface. (XBB 831-790)

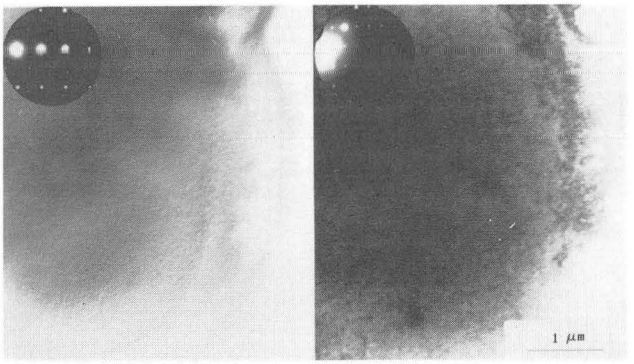

Fig. 1.3. Ferrous oxide sample before (left) and after (right) partial reduction. Diffraction pattern of partly reduced sample inset. (XBB 831-791)

1982 PUBLICATIONS AND REPORTS

Refereed Journals

†1. I. Masterson and J. W. Evans, "Fluidized Bed Electrowinning of Copper; Experiments Using 150 Amp and 1,000 Amp Cells and Some Mathematical Modelling," Met. Trans. 13B, 3 (1982).

‡2. M. Dubrovsky and J. W. Evans, "An Investigation of Fluidized Bed Electrowinning of Cobalt Using 50 and 1,000 Amp Cells, " Met. Trans. 13B, 293 (1982).

§3. M. H. Abbasi and J. W. Evans, "Monte Carlo Simulation of Radiant Transport through an Adiabatic Packed Bed or Porous Solid," AIChE J. 28, 853 (1982).

¶4. J. N. Barbier, P. Cremer, J. W. Evans, and Y. R. Fautrelle, "Simulation Numérique des Fours Chauffés par Induction," J. de Mécanique, Théorique et Appliquée 1, 533 (1982).

5. D. J. Coates, J. W. Evans, and S. S. Pollack, "Identification of the Origin of TiO_2 Deposits on a Hydrodesulfurisation Catalyst," Fuel 61, 1245 (1982), LBL 13244.

6. D. J. Coates, J. W. Evans and K. H. Westmacott, "Defects in Antiferromagnetic Nickel Oxide," J. of Materials Sci. 17, 3281 (1982).

7. J. A. Little and K. H. Westmacott, "The Origin of Unusual Dislocation Structures Observed in Ion-Thinned Nickel Oxide," Metallography 15, 259 (1982).

Other Publications

1. J. W. Evans, "Physical Chemistry of High Temperature Technology," AIChE J. 28, 868 (1982), book review.

LBL Reports

1. S. D. Lympany and J. W. Evans, "The Hall-Héroult Cell: Some Design Alternatives Examined by a Mathematical Model," Met. Trans., in press, LBL-14386.

2. S. D. Lympany and J. W. Evans, "An Improved Mathematical Model for Melt Flow in Induction Furnaces and Comparison with Experimental Data," Met. Trans., in press, LBL-15170.

3. D. J. Coates, A. L. Cabrera, J. W. Evans, H. Heinemann, and G. A. Somorjai, "An Electron Microscopy Study of the Low Temperature Catalyzed Steam Gasification of Graphite," J. of Catal., in press, LBL-14463.

Invited Talks

1. D. J. Coates, K. H. Westmacott, and J. W. Evans, "The Effect of Microstructure on the Reduction of Nickel Oxide," AIME Annual Meeting, Las Vegas, Nevada, February 1982.

2. M. Dubrovsky, J. W. Evans, and T. Huh, "Fluidized Bed Electrowinning of Metals at Moderate Electrical Energy Consumption Rates," AIME Annual Meeting, Las Vegas, Nevada, February 1982.

3. Y. Nakano, M. Abbasi, and J. W. Evans, "A New Predictive Technique for the Diffusion of Gases in Porous Solid," International Symposium on the Physical Chemistry of Iron and Steelmaking," Conference of Metallurgists, Toronto, Canada, August 1982.

4. S. D. Lympany, R. Moreau, and J. W. Evans, "Magnetohydrodynamic Effects in Aluminum Reduction Cells," Proc. Int. Union of Theoretical and Applied Mechanics Symp., Cambridge, England, September 1982.

5. S. D. Lympany, D. Ziegler, and J. W. Evans, "Simulation of Electrolyte Flows and Mass Transport in Electrometallurgy," AIChE Annual Meeting, Los Angeles, November 1982.

* * *

†Supported by the Office of Surface Mining, Department of the Interior.
‡Supported by the National Science Foundation.
§Supported by intramural funds, University of California.
¶Supported by the Institut de Mécanique, Grenoble, France.

f. Local Atomic Configurations in Solid Solutions*

Didier de Fontaine, Investigator

Introduction. This research is aimed at understanding basic atomic mechanism leading to observed microstructures of certain metallic alloys. In particular, work begun after October 1981 has been focused on two topics: (1) a theoretical study of very regular long-period superstructures observed in some ordered alloys and (2) a theoretical study of the kinetics of phase transformations responsible for the change of shape from a "C-curve" to an "S-curve" in transformation-temperature-time (TTT) diagrams of eutectoid carbon steels upon alloying with ternary substitutional elements. Both of these theoretical studies will be followed by experimental investigations aimed at confirming (or infirming) the models and at suggesting new directions for further basic research and possible applications.

1. LONG-PERIOD SUPERSTRUCTURES

Joseph Kulik and Didier de Fontaine

Early attempts at explaining the occurrence of long-period superstructures were based entirely on energy considerations: for example, much was made of the lowering of energy resulting from the creation of new Brillouin Zone boundaries near the Fermi surface.[1] The experimental fact that long-period superstructures often disappeared at low temperatures flatly contradicted the predictions of such models, however.

Recently, new statistical mechanical theories have shown long periods in magnetic structures to be caused by the interplay of atomic interactions and configurational entropy effects. In particular, Fisher and Selke (FS)[2] have performed a very detailed low temperature expansion of the free energy of an Ising ferromagnet with axial nearest and next-nearest competing ($J_1 > 0$, $J_2 < 0$) interactions (ANNNI Model), in vanishing applied field. The present study is aimed at extending the FS results to the antiferromagnetic case (isomorphic to the ordered alloy case), i.e., with J_0, J_1, and J_2 all negative.

Results to second order of the low temperature expansion are shown in the phase diagram of Fig. 1.1. The multicritical point is found at T = 0 K and $\kappa = J_2/J_1 = 1/2$. Phase boundaries between ordered structures are indicated; <1> denotes the simple antiferromagnetic (or ordered structure); <2> denotes two identical ordered layers followed by two others in antiphase relation with respect to the first two. Symbols <21> and <221> denote ordered structures consisting of double and single layers in an obvious extension of the notation.

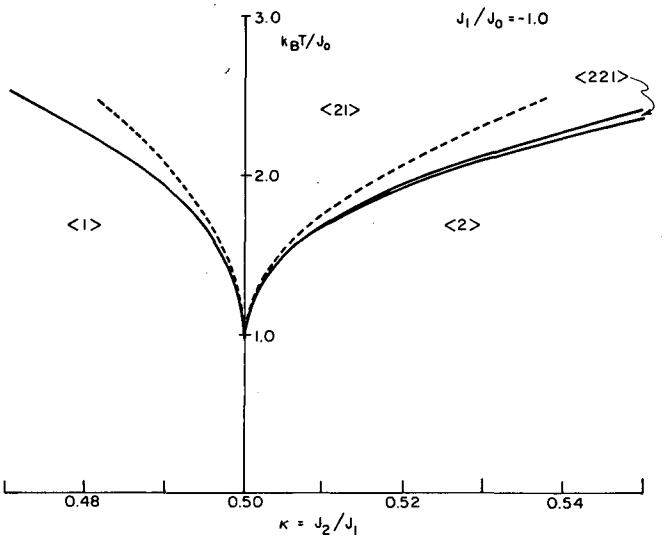

Fig. 1.1. Phase diagram of the axial-next-nearest-neighbor-Ising model (ANNNI) in the antiferromagnetic case. Dashed and full lines represent phase boundaries calculated to first and second order, respectively, in the low temperature expansion. (XBL 8212-6981)

Analysis taken to higher orders show that the <221> phase field will further break up into distinct phase regions, all of structure-type $<2^n1>$. As an example, a $<2^41>$ superstructure of the predicted type was observed experimentally[3] in Ag_3Mg. The analysis further shows that long-period superstructures disappear at low enough temperatures, in agreement with experimental findings.

***

1. H. Sato and I. Toth, in Alloying Behavior and Effects in Concentrated Solutions, Metall. Soc. Conf., Vol. 29, Gordon and Breach, NY, 1965, p. 295-419.
2. M. E. Fisher and W. Selke, Phil. Trans. Roy. Soc. 302, 1 (1981).
3. R. Portier and D. Gratias, Acta Cryst. A36, 190 (1980).

2. TTT DIAGRAMS

Osamu Dairiki, Etienne Colas, and Didier de Fontaine

Of fundamental importance in heat treating of industrial alloys, steels in particular, is the determination of their so-called TTT diagrams. There is little hope of ever deriving such kinetic diagrams directly from first principles, but it would be of considerable interest to discover what are the most important physical parameters that influence the shape of the TTT curves, and in what way. The limited objective here proposed is to discover how a ternary (substitutional)

*This work was supported by the Director, Office of Energy Research, Office of Basic Energy Sciences, Materials Sciences Division of the U.S. Department of Energy under Contract No. DE-AC03-76SF00098.

addition will affect the C-curve of a simple eutectoid carbon steel, in particular, under what circumstances (alloying element, concentration, ...) a "bay" will develop in the C-curve to produce a characteristic S-shape.

A very simple mathematical model has been developed for S-shaped TTT curves. The model is based on classical nucleation-and-growth theory applied to two austenite decomposition processes: a high temperature one producing pearlite and a low temperature one producing bainite. Complete partitioning of the ternary element between precipitating phases was assumed for the high temperature mechanism and zero partitioning was assumed for the low temperature mechanism.

Calculated TTT "start" and "end" curves are shown in Fig. 2.1; model parameters were chosen so as to simulate experimentally determined S-curves of a near-eutectoid Fe-C-Cr steel. The present model is still very primitive; it is being modified so as to allow variable partitioning, to be determined, at each temperature, by optimizing overall growth kinetics. Also, a more realistic evaluation of parameters is being developed.

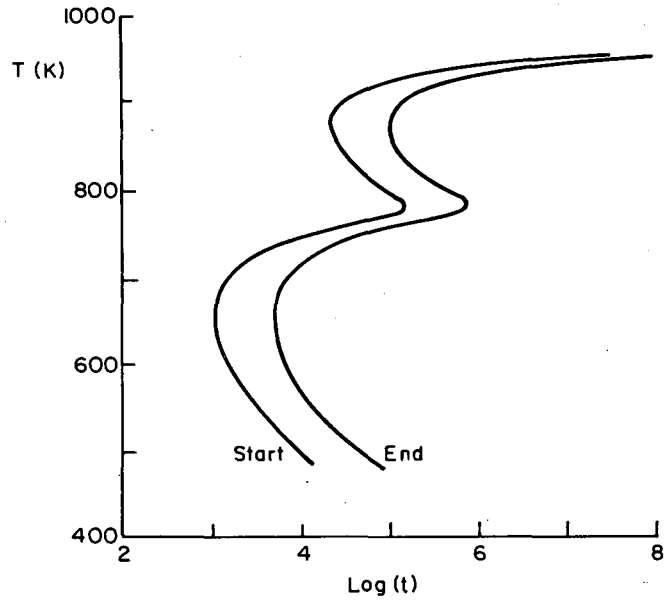

Fig. 2.1. TTT curves calculated according to a simple nucleation-and-growth model with parameters chosen so as to resemble S-curves of Fe-C-Cr near-eutectoid steels. (XBL 8212-6982)

1982 PUBLICATIONS AND REPORTS

Refereed Journals

†1. J. M. Sanchez, D. Gratias, and D. de Fontaine, "Special Point-Ordering in General Crystal Structures," Acta Cryst. A 38, 214 (1982).

†2. J. M. Sanchez and D. de Fontaine, "Ising Model Phase Diagram Calculations in the fcc Lattice with First- and Second-Neighbor Interactions," Phys. Rev. B 25, 1759 (1982).

‡3. A. R. Forouhi, B. Sleaford, V. Perez-Mendez, D. de Fontaine, and J. Fodor, "Small-Angle X-ray Scattering System with Position-Sensitive Detector," IEEE Trans. Nucl. Sci. 29, 275 (1982).

†4. D. Gratias, J. M. Sanchez, and D. de Fontaine, "Application of Group Theory of the Calculation of the Configurational Entropy in the Cluster Variation Method," Physica A 113, 315 (1982).

†5. J. M. Sanchez, D. de Fontaine, and W. Teitler, "Comparison of Approximate Methods for the Study of Antiferromagnetism in the fcc Lattice," Phys. Rev. B 26, (1982).

Other Publications

†1. D. de Fontaine, "Studies of the Thermodynamics of Ordering by the Cluster Variation Method," Proc. International Conference on Solid-Solid Phase Transformation, American Society for Metals, Metals Park, Ohio, 1982.

††2. D. de Fontaine, "Compositional Instabilities," in Il Nuovo Cimento Course on Mechanical and Thermal Behaviour of Metallic Materials, G. Caglioti and A. Ferro Milone, Eds., Enrico Fermi School of Physics, 1982.

3. D. de Fontaine, "Le Francais Scientifique," La Recherche 13, 812 (1982), in French.

Invited Talks

1. D. de Fontaine, "Kinetic Paths in Metallurgical Phase Transformations," Workshop on Kinetics of Phase Changes, Institute for Theoretical Physics, Santa Barbara, California, March 1-5, 1982.

2. D. de Fontaine, "In Phase with Phase Diagrams," Northern California AIME Student Meeting, University of California, Berkeley, California, March 21, 1982.

3. D. de Fontaine, "Coherent Phase Diagrams in the Cluster Variation Approximation," Alloy Workshop, Los Alamos National Laboratory, New Mexico, September 9, 1982 and Alloy Phase Diagram Symposium, Materials Research Society Annual Meeting, Boston, Massachusetts, November 2, 1982.

4. D. de Fontaine, "First-Principles Phase Diagram Calculations, a Possibility?" ALCOA Research Laboratory, Pittsburgh, Pennsylvania, October 13, 1982.

* * *

†This work was supported in part by ARO(D) under Contract No. P-DAAG29-80-K-0044.
‡This work was supported in part by NSF under Contract No. 79-20405a03.

2. Mechanical Properties

a. Theoretical Problems in Alloy Design*

John W. Morris, Jr., Investigator

Introduction. The purpose of this research project is to advance the science of alloy design through appropriate fundamental research and through the systematic development of new materials that have exceptional engineering properties. The current alloy development projects fall in three areas: new structural steels, particularly those intended for use at cryogenic temperature, weld filler metals and welding procedures for high strength structural steels, and superconducting wire for high field magnets. The supporting fundamental research includes theoretical studies of the microstructure, processing and mechanical properties of materials, and experimental research in materials characterization and analysis.

1. THE LINEAR ELASTIC THEORY OF PHASE TRANSFORMATIONS IN SOLIDS

J. W. Morris, Jr. and Y.-C. Shih

It has been known since the classic work of Eshelby and Khatchaturyan that the theory of linear elasticity can be used to explain many of the most important features of structural phase transformations in solids. Recent research has shown that the theory yields predictive, quantitative results as well. The present research was undertaken to explore its applicability to precipitation reactions.

The theory was cast in the most appropriate form[1] and solved in the thin-plate limit to obtain general relations for the internal strain and preferred habit of a coherent, tetragonal precipitate in a cubic matrix.[2] The theory proved widely applicable, but failed in the specific case of the $Fe_{16}N_2$ precipitate in iron. Further work[3] showed that theory and experiment are in agreement if the finite thickness of the nitride is taken into account, and that the theory then resolves discrepancies in the reported lattice constants of the nitride.

The analysis of the nitride habit was continued during the past year. The habit plane shift predicted by the theory was observed experimentally.[4] Further theoretical computations showed that the habit plane shift should be accompanied by a change in both the constrained lattice parameters and the apparent symmetry of the nitride.[5] Both predictions agree with the experimental data. Research in progress indicates that the theoretical results can be extended to other combinations of precipitate and matrix symmetry.

* * *

1. J. W. Morris, Jr., A. G. Khatchaturyan, and Sheree H. Wen, Phase Transformations in Solids, in press, LBL-9800.
2. S. H. Wen, E. Kostlan, M. Hong, A. G. Khatchaturyan, and J. W. Morris, Jr., Acta Met. 29, 1247 (1981); LBL-10262.
3. M. Hong, D. E. Wedge, and J. W. Morris, Jr., LBL-12973.
4. Y. C. Shih and J. W. Morris., Jr., Proc. EMSA, 1982, p. 382; Y. C. Shih, M.S. thesis, LBL-14284.
5. M. Hong, D. E. Wedge, and J. W. Morris, Jr., LBL-12973 Rev.

2. DISLOCATION MOTION AT LOW TEMPERATURE†

T. Mohri and J. W. Morris, Jr.

A number of recent reports suggest peculiarities in the motion of dislocations at very low temperature. The reports are controversial, but imply that the unusual behavior is associated with changes in the damping force on the dislocation and with interactions between the moving dislocation and applied magnetic fields. There is little relevant theory to guide the analysis of either effect.

The free electron gas model was used to estimate the electron damping force on a moving dislocation in a normal state. The estimate was checked by computing the contribution of the moving dislocation to the electrical resistivity. The values obtained show reasonable agreement with experimental results, and do not suggest anomalies in the dislocation motion. The calculations were extended to estimate the coupling between a moving dislocation and an applied magnetic field. The results indicate that the coupling is negligible.

On the basis of these results we conclude that the low temperature anomalies in plastic flow are either experimental artifacts or are caused by factors other than the electromagnetic properties of single dislocations.

*This work was supported by the Director, Office of Energy Research, Office of Basic Energy Sciences, Materials Sciences Division of the U.S. Department of Energy under Contract No. DE-AC03-76SF00098.

* * *

†Abstracted from LBL-12223.

3. MICROSTRUCTURAL SOURCES OF THE DUCTILE-TO-BRITTLE TRANSITION IN STEEL

G. Fior, H. J. Kim, P. Johnson-Walls, and J. W. Morris, Jr.

A typical structural steel undergoes a dramatic loss in toughness when it is cooled below its ductile-to-brittle transition temperature (T_B). As the name implies, the transition is marked by a change in the fracture mode, from ductile rupture to brittle fracture by transgranular cleavage or intergranular separation. To design steel microstructures that insure a low value of T_B, it is essential to identify the microstructural mechanisms that lead to the transition. Two classes of theory exist. The first emphasizes changes in the flow properties of the steel and suggests that the transition is caused by changes in the mode of ductile rupture. The second, which has been used in our own prior work, holds that the transition occurs because of the intrusion of the brittle fracture mode.

The two interpretations of the transition can be tested against the geometry of the fracture surface. A change in the mode of ductile rupture should alter the type and shape of the rupture dimples that dot the fracture surface, while the intrusion of brittle fracture should appear as a simple increase in the area fraction of brittle fracture. The fracture surface of quenched 5.5Ni steel was studied as a function of the temperature of fracture, using stereo fractography and quantitative stereological techniques to characterize the fracture features.[1] Some of the central results are plotted in Fig. 3.1. They show a clear intrusion of brittle fracture against a background of ductile rupture that is remarkably constant in its morphology.

The demonstration that the ductile-to-brittle transition occurs through of the intrusion of the brittle mode, at least in the class of steels represented by 5.5Ni, supports the alloy design approach previously taken in this group: to lower T_B by decreasing the microstructural dimension of cleavage fracture.[2] The same approach is applicable to ferritic weldments in low temperature steels, as work completed during the past year has shown.[3] Research is currently under way to generalize the stereological results to other alloy systems and to identify more precisely the microstructural features that effectively inhibit cleavage fracture.

* * *

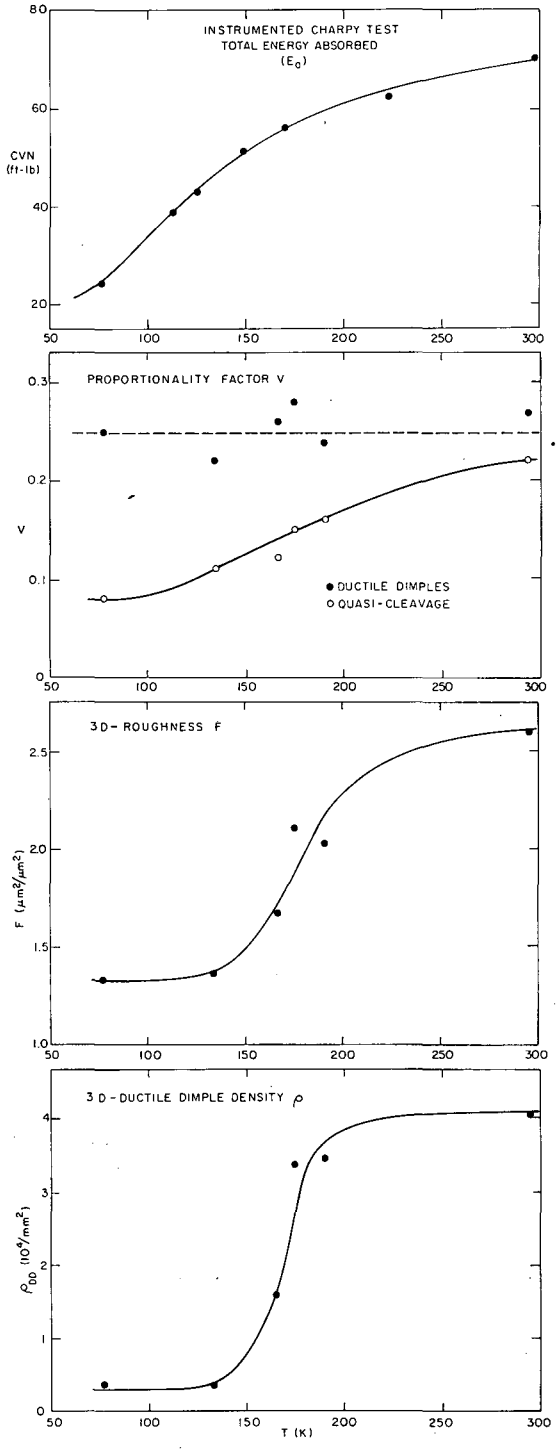

Fig. 3.1. The Charpy impact energy of 5.5Ni steel is plotted as a function of temperature and compared to three stereological measures of the fracture surface: the aspect ratio, V, of the ductile dimples and cleavage features; the surface roughness; and the area fraction or density of dimples. The figure shows that the geometry of ductile rupture remains constant while the ductile fraction decreases on passing through T_B. (XBL 8110-6898A)

1. G. O. Fior, M. S. thesis, LBL-1475.
2. S. Jin et al., Met. Trans. 6A, 1569 (1975); C. K. Syn et al., Met. Trans. 7A, 1827 (1976); M. Niikura and J. W. Morris, Jr., Met. Trans 11A, 1531 (1980), LBL-9798; J. I. Kim and J. W. Morris, Jr., LBL-9956.
3. H. J. Kim, H. K. Shin, and J. W. Morris, Jr., Proceedings of the International Cryogenic Materials Conference, Kobe, Japan, edited by K. Tachikawa and A. Clark, Butterworths, London, England, 1982, p. 129-133; LBL-14175.

4. THE COUPLING BETWEEN MAGNETIC- AND DEFORMATION-INDUCED MARTENSITE IN METASTABLE AUSTENITIC STEELS

B. Fultz, G. M. Chang, and J. W. Morris, Jr.

The martensitic transformation in steels is promoted by high magnetic fields and by plastic strain in ways that are only partly understood. Both types of loading increase the thermodynamic driving force for the martensitic transformation, at least in isolated regions within the material, and may influence martensite nucleation as well. It is not known whether the two effects are additive or reinforcing. Their coupling may have engineering significance, since the austenitic steels that are most commonly used in the structures of high field superconducting magnets are metastable at the 4 K service temperature.

Two experimental devices were set up to study deformation-induced martensitic transformations in high magnetic fields. The first employs a pulsed magnet to apply magnetic pulses of strength up to 16 T to a specimen that is prestrained in a bolt loading fixture. The second utilizes a large-bore superconducting magnet to impose steady fields of up to 8.5 T on test specimens in a universal cryogenic testing machine (the MMCR facility). These devices are being used to investigate the martensitic transformation in the metastable austenitic steels 304L and 304LN, and the transformation of precipitated austenite in tempered 9Ni steel.

The initial results[1] show that the strain and the field do reinforce. The degree of transformation is measurably increased when prestrained 304L or 304LN is subjected to repeated 16 T pulses at 77 K. The flow stress, elongation, and ultimate tensile strengths of the two steels at 77 K are altered when they are tested in an 8 T field. Further tests and detailed metallographic studies are in progress.

* * *

1. J. W. Morris, Jr. and B. Fultz, Proceedings of the International Cryogenic Materials Conference, Kobe, Japan, edited by K. Tachikawa and A. Clark, Butterworths, London, England, 1982, p. 343, LBL-15518; B. Fultz, G. M. Chang, and J. W. Morris, Jr., LBL-15324.

5. MÖSSBAUER SPECTROMETRY

B. Fultz

The Mössbauer effect measures the local magnetic field at a nucleus and is hence useful for distinguishing the paramagnetic austenite phase of iron from the ferromagnetic ferrite or martensite phase. The Mössbauer spectra also contains chemical information, since the field at a nucleus is influenced by its environment. It follows that the Mössbauer effect can be a useful tool in the characterization and analysis of steel.

Some years ago a Mössbauer laboratory was established here and the effect was used to measure the fraction of austenite in bulk alloy steels and on fracture surfaces.[1] Further experimental development and theoretical work[2] made it possible to use Mössbauer spectrometry in an increasingly quantitative way. The technique was then used to study chemical segregation during the tempering of ferritic Fe-Ni steel.

Research completed during the past year[3] yields new information on the segregation of alloying species to austenite during the intercritical tempering of 9Ni steel. Ni, Mn, Cr, and Si were found to gather in the austenite. The addition of ternary solutes to the Fe-9Ni binary altered both the rate of austenite formation and its thermal stability. The austenite phase boundary was displaced toward lower Ni concentrations by several of the solutes. The solute concentration in the austenite is strongly influenced by the diffusivity of the solute relative to Ni. A corollary research effort advanced the quantitative theory of backscatter Mössbauer spectroscopy.[4]

* * *

1. B. Fultz, M. S. thesis, LBL-7671.
2. B. Fultz and J. W. Morris, Jr., Nucl. Instrum. Meth. 188, 97 (1981); LBL-11022.
3. B. Fultz, Ph. D. thesis, LBL-13588.
4. B. Fultz and J. W. Morris, Jr., in press, LBL-15433.

6. THE METALLURGY OF Fe-Mn STEELS

H. J. Lee and J. W. Morris, Jr.

The element Mn resembles Ni in many of its metallurgical effects on alloy steel. It is, however, a less costly alloying element, and has distinct influences on the properties of steel that can be useful in alloy design. The Fe-Mn system is not nearly so well researched as the Fe-Ni and Fe-Cr systems. Many of its most interesting and potentially useful properties remain poorly understood.

The inherent intergranular fracture mode in Fe-(10-12)Mn alloys is particularly interesting. Intergranular fracture apparently intrudes because of the difficulty of transgranular cleavage through the blocky martensite substructure of these alloys. It was shown some years ago[1] that the intergranular mode disappears after the addition of a small amount of boron, causing a spectacular decrease in T_B. The optimum grain boundary composition of boron was, however, unclear, as was the reason for the restoration of the intergranular fracture mode after tempering.

Auger spectroscopic studies completed during the past year[2] show that the optimum grain boundary concentration of boron is near 3 at.% and suggest, surprisingly, that the common beneficial surfactants Mg and Zr have a negligible influence on intergranular fracture. Tempering at 450°C causes an enrichment of the prior austen-

ite grain boundary to 32-38 at.% Mn, depending on the boron concentration. This enrichment is presumably responsible for the embrittlement. It also causes the eventual precipitation of a grain boundary austenite phase that alters the fracture behavior. Work is continuing on other aspects of the metallurgy of Fe-Mn steels.

* * *

1. S. K. Hwang and J. W. Morris, Jr., Met Trans. 10A,. 545 (1979).
2. H. J. Lee, Ph. D. thesis, LBL-14747.

7. HIGH TEMPERATURE EMBRITTLEMENT OF AN IRON-BASED SUPERALLOY

G. Hu† and J. W. Morris, Jr.

Research for the Electric Power Research Institute on new alloys for generator retaining rings resulted in the design of a new iron-based superalloy that combined exceptional strength, toughness, and hydrogen resistance at ambient temperature.[1] The alloy is a forged and double-aged superalloy of composition Fe-34.5Ni-5Cr-3Ti-3Ta-0.5Al-1.0Mo-0.3V-0.01B. Given its composition and mechanical properties, the alloy may be useful at elevated temperature. Its high temperature properties were explored both to test them and to obtain fundamental data on the behavior of high strength Fe-based superalloys.

It was found that the alloy retained high strength at 650°C in air, but was brittle if it had been solution annealed prior to aging. The fracture was intergranular due to the combination of grain boundary oxidation and cellular precipitation of a laves phase. An alternate heat treatment was designed to suppress laves phase formation. The modified alloy had good ductility at 650°C in vacuum, but remained brittle in air. Metallographic analysis showed that the alloy is self-embrittling. Surface oxidation during testing induces intergranular precipitation of the laves phase.

* * *

†Present address: Department of Metallurgy, Jiao Tong University, Shanghai, China.
1. K. M. Chang and J. W. Morris, Jr., ASTM STP, 792, in press.

8. MICROSTRUCTURE CONTROL DURING WELDING OF FERRITIC STEELS

H. J. Kim, H. Shin, and J. W. Morris, Jr.

The fracture toughness of a welded plate is often lower than that of the base metal because of the impurities introduced during welding and the coarse microstructure of the weld deposit and heat affected zone. For this reason ferritic low temperature steels are often welded with high-alloy austenitic filler metals, sacrificing strength and economy to achieve toughness.

A promising alternative approach is to use a multipass gas tungsten arc (GTA) welding process as a metallurgical treatment to maintain purity and to control the microstructure. Each successive weld pass serves to temper the material previously laid down. The technique can be made to work extremely well[1] and has been commercialized in Japan, but its metallurgical details are still not understood in the depth needed to exploit its full potential.

Research completed during the past year[2] identified the mechanism of toughening in 9Ni steel welded with ferritic filler metal. The 9Ni base plate is toughened by a distribution of precipitated austenite phase. The multipass GTA-welded plate is tough in both the weld metal and heat affected zone, but, surpisingly, has little or no austenite in either region. Rapid thermal cycles are imposed by the successive weld passes. A cycle to above 700°C refines the microstructure by destroying the alignment between martensite laths, hence lowering T_B. A subsequent cycle to 500-600°C getters carbon into fine lath boundary carbides that raise the toughness in the ductile mode. The results are being used in research on the manufacture of cryogenic components by weld buildup.

* * *

1. H. J. Kim and J. W. Morris, Jr., LBL-13046.
2. H. J. Kim, H. K. Shin, and J. W. Morris, Jr., LBL-14175; H. J. Kim, Ph. D. thesis, LBL-14748.

9. SUPERALLOY WELDING

M. Strum, L. Summers, and J. W. Morris, Jr.

Precipitation hardened alloys such as Fe-based superalloys must usually be welded prior to aging. However, the microstructure of the weld differs from that of the base metal and may hence have a different aging response, causing a strength mismatch in the aged condition.

This phenomenon has been investigated in the iron-based superalloys A286 and JBK-75, a modified form of A286 that is more resistant to weld cracking. After welding, both alloys were aged at 700°C to precipitate the Ni_3Ti hardening phase. The aging kinetics and hardness were monitored in both the weld and base plate, and their differences were correlated to the chemistry and microstructure of the weld.

The results[1] show that precipitation occurs more rapidly in the weld than in the base plate. However, the base plate reaches and maintains higher hardness for all aging times. The results are explained by the segregation of titanium to the interdendritic regions of the weld metal. Rapid precipitation occurs between the dendrites, but the hardened regions are dispersed and hence do not establish a high overall strength. Matching weld and base metal properties could be achieved by interposing a solution anneal before aging. The details of these processes are still under investigation.

* * *

1. M. J. Strum, M. S. thesis, LBL-14750.

10. THE USE OF HEAT TREATMENT TO IMPROVE THE CRITICAL CURRENT OF BRONZE-PROCESS MULTIFILAMENTARY SUPERCONDUCTING WIRE†

I. W. Wu, D. Dietderich, J. Holthuis, W. Hassenzahl,‡ and J. W. Morris, Jr.

The most common route to high field Nb_3Sn superconducting wire is the "internal bronze" process. In this method niobium rods are inserted into a Cu-Sn bronze billet and drawn into a fine, multifilamentary wire. The wire is then heat treated to form the A15 superconducting phase of the niobium bronze interface. The critical current that can be carried by the wire at given values of the temperature and the applied magnetic field is a sensitive function of the composition and microstructure of the A15 layer. It increases if the A15 phase is made more nearly stoichiometric or if its grain size is made smaller. However, the distribution of composition and grain size in the A15 phase within a multifilamentary wire is not well known.

The present project was undertaken to characterize the microstructure of a prototype commercial Nb_3Sn superconducting wire as a function of the time and temperature of the reaction heat treatment and to determine the relation between the microstructure and the critical current. A commercial, 2869 filament wire was procured, heat treated in the temperature range 650-800°C, and tested to establish its critical current as a function of applied magnetic field at 4 K. Work done during the previous year[1] showed that the critical current is largely controlled by the properties of a central, fine-grained layer in the A15 phase. The combination of grain size and stoichiometry is best if the reaction is done at intermediate temperature, and can be improved further by properly designed double-aging treatments, with a concomitant improvement in the critical current.

More recent research has concentrated on the details of the microstructure and mechanisms that control it.[2] The grain size and volume fraction of the fine-grained sublayer of the A15 phase were determined quantitatively as a function of the temperature of heat treatment. The mechanism of formation of the fine-grained layer was found to involve the polygonization of dislocations into cell walls (Fig. 10.1). The composition profile within the layer was found by STEM analysis. The double aging treatments were shown to yield a higher volume fraction of fine-grained material with a flatter, and more nearly stoichiometric composition profile. Given these results, it was decided to seek chemical additives that might supplement heat treatment to create an A15 phase that is still more uniformly grain-refined.

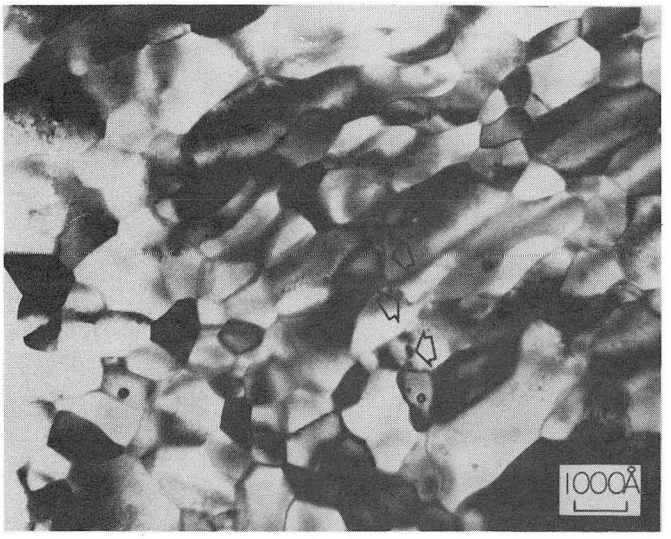

Fig. 10.1. A transmission electron micrograph of the interface between the columnar and fine-grained sublayers of an Nb_3Sn reacted layer. The process of dislocation accumulation into boundaries is visible. (XBB 824-4087)

* * *

†Supported in part by the Division of High Energy Physics, U. S. Department of Energy through the Accelerator and Fusion Research Division, LBL.
‡Accelerator and Fusion Research Division, LBL.
1. M. Hong, I. W. Wu, and J. W. Morris, Jr., Advances in Cryogenic Materials, Vol. 28, Plenum Press, New York, 1982, p. 435; LBL-13013.
2. I. W. Wu, M. Hong, W. Hassenzahl, and J. W. Morris, Jr., Proceedings of the International Cryogenic Conference, Kobe, Japan, edited by K. Tachikawa and A. Clark, Butterworths, London, England, 1982, p. 388; LBL-14177.

11. THE INFLUENCE OF MAGNESIUM ADDITIONS ON THE PROPERTIES OF MULTIFILAMENTARY Nb_3Sn SUPERCONDUCTING WIRE†

I. W. Wu, D. Dietderich, J. Holthuis, J. Glazer, W. Hassenzahl,‡ and J. W. Morris, Jr.

Work by Tachikawa and co-workers[1] showed that the addition of Mg to the bronze matrix prior to the formation of bronze-process Nb_3Sn tape causes a significant increase in the critical superconducting current density at 6.5 T, and that this increase is associated with an apparent decrease in the A15 grain size. Research was undertaken here to determine whether a similar improvement would follow the addition of Mg to multifilamentary Nb_3Sn wires and to identify the microstructural and mechanistic sources of any beneficial effort.

To accomplish this, multifilamentary wires were drawn in the laboratory. They contained 133

filaments of pure Nb embedded in bronze with various concentrations of Sn and Mg. Their critical current densities were measured as a function of bronze composition, heat treatment, and transverse magnetic field at 4.2 K. The reacted A15 layers were subsequently examined using a variety of microscopic and microanalytic techniques.

The work is incomplete, but the results obtained to date[2] seem sufficient to justify three major conclusions: (1) Magnesium additions to the bronze increase the attainable critical current at all fields tested (8-15 T). The increase is large enough to be of technological interest (Fig. 11.1). (2) The magnesium segregates almost completely to the Nb_3Sn layer during the reaction. The Mg resides predominantly within the A15 matrix; it is not a strong surfactant in Nb_3Sn. (3) The most obvious effect of the Mg addition is to retard grain coarsening during growth of the A15 layer, yielding a uniformly fine-grained product. This effect accounts for much, if not most of the improvement in J_c. Preliminary results also suggest that Mg decreases the A15 grain size and improves the Sn distribution through the reacted layer. It is not clear what, if any,effect Mg has on the inherent superconducting properties of Nb_3Sn.

* * *

†Supported in part by the Division of High Energy Physics, U. S. Department of Energy through the Accelerator and Fusion Research Division, LBL.
‡Accelerator and Fusion Research Division, LBL.
1. K. Tachikawa et al., Adv. Cryr. Eng. 26, 375 (1980).
2. I. W. Wu et al., in press, LBL-15336.

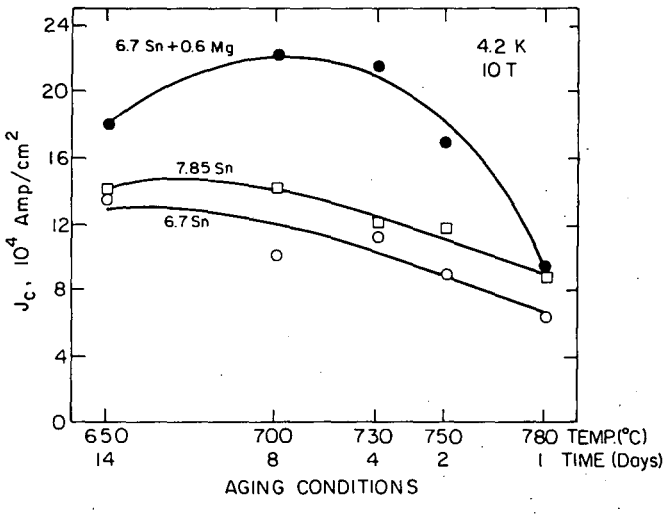

Fig. 11.1. Plot of the critical superconducting current vs the aging temperature for bronze-process multifilamentary Nb_3Sn wires with varied Sn and Mg content in the bronze. The data were taken in a 10 T field at 4 K and show the increase associated with the Mg addition. (XBL 8211-6901)

1982 PUBLICATIONS AND REPORTS

Refereed Journals

1. D. E. Williams and J. W. Morris, Jr., "Weldability of Grain-Refined Fe-12Ni-0.25Ti Steel for Cryogenic Use," Welding J. Suppl., May, p. 133-138, 1982; LBL-11777.

2. J. M. Hong, J. Holthuis, I. W. Wu, and J. W. Morris, Jr., "Developmental Studies on Powder Processed Nb_3Al Superconducting Wire," Advances in Cryogenic Materials, Vol. 28, Plenum Press, New York, 1982, p. 435-444; LBL-13013.

3. M. Hong, I. W. Wu, and J. W. Morris, Jr., "An Investigation on the Critical Current Densities in Bronze-Process Nb_3Sn," Advances in Cryogenic Materials, Vol. 28, Plenum Press, New York, 1982, p. 435-44; LBL-13015.

4. J. J. Kim, C. K. Syn, and J. W. Morris, Jr., "Ferritic Weldment of Ferritic Ni Steels for Low Temperature Use," Advances in Cryogenic Materials, Vol. 28, Plenum Press, New York, 1982, p. 878-882; LBL-13017.

5. Y. C. Shih and J. W. Morris, Jr., "The Habit Plane Shift and the Morphology of α" Precipitate in α-Fe," 40th Ann. Proc. Elect. Micro. Soc. Am., 1981, p. 728-729; LBL-14159.

LBL Reports

1. H. J. Lee and J. W. Morris, Jr., "High Resolution Scanning Auger Microscopic Investigation of Intrergranular Fracture in As-Quenched Fe-12Mn," Met. Trans., in press, LBL-11629.

2. T. Mohri, "Calculations of the Electron Damping Force on Moving Edge Dislocations," Ph.D. thesis, LBL-12223.

3. K. M. Chang and J. W. Morris, Jr., "Research Toward New Alloys for Generator Retaining Rings," Proc. Micro. Conf., in press, LBL-13467.

4. B. Fultz, "A Mössbauer Spectrometry Study of Fe-Ni-X Steel," Ph.D. thesis, LBL-13588.

5. H. J. Kim, H. K. Shin and J. W. Morris, Jr., "The Influence of Rapid Thermal Cycles in Multi-Pass Welding of Heat-Affected Zone Properties of Ferritic Cryogenic Steels," Proceedings of the International Cryogenic Materials Conference, Kobe, Japan, May 11-14, 1982, Butterworths, England, p. 129-133, LBL-14175.

6. I. W. Wu, M. Hong, W. Hassenzahl, and J. W. Morris, Jr., "The Influence of Heat Treatment on the Structure and Properties of Bronze-Process Multifilamentary Nb_3Sn Superconducting Wire," Proceedings of the International Cryogenic Conference, 1982, p. 388-391, LBL-14177.

7. Y. C. Shih, "The Observation of the Habit Plane Shift and the Habit Plane Shift and the Morphology of α" Nitride ($Fe_{16}N_2$) Precipitate in α-Fe," M. S. thesis, LBL-14284.

8. H. J. Lee, "The Study of Intergranular Embrittlement in Fe-12Mn Alloys," Ph. D. thesis, LBL-14747.

9. H. J. Kim, "Development of Ferritic Weldments for Grain Refined Ferritic Steels for 4.2 K Service," Ph. D. thesis, LBL-14748.

10. J. M. Hong, "Powder Metallurgy Processed A15 Nb_3Al Superconducting Wires," M. S. thesis, LBL-14749.

11. M. J. Strum, "Effects of Welding of Weldment Mechanical Performance in Two Austenitic Steels," M. S. thesis, LBL-14750.

12. G. O. Fior, "Quantitative Analysis of Fracture Modes in Cryogenic 6Ni Steel by Stereo SEM Technique," M. S. thesis, LBL-14751.

13. I. W. Wu, D. R. Dietderich, J. T. Holthuis, W. V. Hassenzahl, and J. W. Morris, Jr., "The Influence of Magnesium Addition to the Bronze on the Critical Current of Bronze-Processed Multifilamentary Nb_3Sn," Proc., IEEE, in press, LBL-15336.

14. J. W. Morris, Jr., "Cryogenic Steels," in Encyclopedia of Materials Science and Engineering, in press, LBL-15408.

15. B. Fultz and J. W. Morris, Jr., "The Thickness Distortion of ^{57}Fe Backscatter Mössbauer Spectra: II. Effects of Secondary Resonant Absorptions," in press, LBL-15433.

16. J. W. Morris and B. Fultz, "Effects of Magnetic Fields on Martensitic Transformations and Mechanical Properties of Stainless Steels at Low Temperatures," Nucl. Instrum. Meth., in press, LBL-15518.

Other Publications

1. J. I. Kim, C. K. Syn, and J. W. Morris, Jr., "Microstructural Sources of Toughness in QLT-Treated 5.5Ni Cryogenic Steel," Met. Trans., in press, ONR Technical Report No. 11.

2. J. I. Kim and J. W. Morris, Jr., "A Microstructural Analysis of the QLT Treatment of Ferritic Fe-Ni Cryogenic Steels," Proceedings of the International Cryogenic Materials Conference, Kobe, Japan, May 11-14, 1982, Butterworths, England, p. 315-355, ONR Technical Report No. 12.

b. Mechanical Properties of Ceramics*

Anthony G. Evans, Investigator

Introduction. The current research activity is devoted to studies of both high temperature deformation and failure, and microstructure development during sintering. High temperature deformation and failure addresses the response of refractory materials to stress. Research in this area is devoted to the generation of a self-consistent scientific comprehension of the mechanisms of deformation and failure, using both experimental and theoretical techniques. The ultimate objective of this study is the development of a scheme for predicting high temperature mechanical failure.

The development of microstructure during sintering has a direct influence upon the defect structure in the material and hence, upon the mechanical strength. Much of the microstructure evolution occurs during the final stage of sintering. Research in this area is devoted primarily to a study of microstructural changes occurring during this stage, using a combination of theory and experiment. Particular emphasis is devoted both to the pore/grain boundary separation phenomenon and to the concomitant coarsening and pore shrinkage processes.

High Temperature Failure

1. HIGH TEMPERATURE FAILURE INITIATION IN LIQUID PHASE SINTERED MATERIALS†

J. E. Marion, M. D. Drory, A. G. Evans, and D. R. Clarke

The nucleation and growth of damage in liquid phase sintered ceramics under stress at high temperatures has been examined both theoretically and experimentally. Damage, consisting of holes and cavities, has been observed by transmission electron microscopy. The damage has been correlated using theoretical analysis. The process of hole nucleation has been analyzed by considering viscous flow in the amorphous phase channels. Hole growth has been analyzed by considering the coupled influence of viscous flow and solution/reprecipitation. Viscous flow permits the existence of a pressure gradient in the amorphous phase, which then establishes the chemical potential gradient required for the solution/reprecipitation mechanism of atom transport. Consequently, the atoms of the solid phase can be transmitted through the liquid and allow the cavities to enlarge. It is demonstrated that solution/reprecipitation is the rate controlling damage mechanism, at most stress levels of interest. Hence, the processes of solution under local compression, as dictated by the dissolution rate constant, and of atom transport through the amorphous phase, as determined by the solubility of the solid phase and the thickness of the liquid layer, are of central importance to the failure of these materials. Further studies of these phenomena, including the influence of the second phase volume concentration and disposition and of its viscosity/diffusivity, are in progress.

***

†Brief version of LBL-14266.

2. A DAMAGE MODEL OF CREEP CRACK GROWTH IN POLYCRYSTALS†

M. D. Thouless, C. H. Hsueh, W. Blumenthal, and A. G. Evans

The slow growth of cracks, formed by damage coalescence, constitutes an important component of the net failure time at elevated temperatures. The growth occurs by the nucleation and growth of cavities in a damage zone ahead of the crack (Fig. 2.1). The damage ahead of the crack modifies the crack tip stress field and thus exerts an important influence on the crack growth rate. A crack growth model that incorporates the stress modifying influence on the damage has been developed. The model allows crack advance when the cavities on the grain facet ahead of the crack attain a critical size. Grain boundary sliding

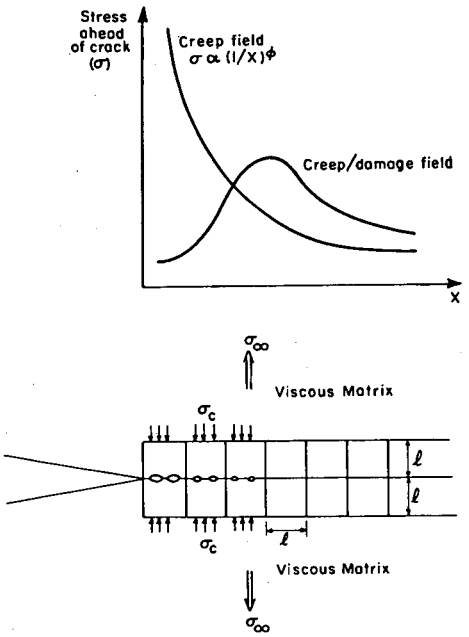

Fig. 2.1. A schematic indicating the existence of a damage zone ahead of a crack and of the stress field modification induced by the damage. (XBL 831-5067)

*This work was supported by the Director, Office of Energy Research, Office of Basic Energy Sciences, Materials Sciences Division of the U.S. Department of Energy under Contract No. DE-AC03-76SF00098.

within the damage zone is also permitted. Numerical solutions for the crack growth rate indicate that the crack velocity in ceramics depends on the stress intensity factor, the grain size, the number of grain facets in the damage zone, the characteristic cavity spacing, and the creep rate of the material. Specifically, the crack growth rate increases with decrease in grain size and cavity spacing and increases with increase in the damage zone size and creep rate. Comparisons of the model with experimental results for polycrystalline Al_2O_3 reveal good consistency. The primary influential variable that presently defies fundamental understanding is the cavity spacing. This spacing has no obvious microstructural association and evidently requires further study. However, it is important to appreciate the strong dependence of the crack growth rate on the creep rate of the material, by virtue of its effect on the stress amplitude at the crack tip. Hence, creep resistant materials should also be resistant to high temperature crack growth.

***

†Brief version of LBL-15348.

3. HIGH CRACK GROWTH IN POLYCRYSTALLINE ALUMINA†

W. Blumenthal and A. G. Evans

The behavior of cracks under stress at high temperature has been studied in a fine grained, polycrystalline Al_2O_3. Small, brittle cracks introduced by indentation subject to stress intensities, K, less than the critical vlue K_c have been shown to exhibit two types of response. At $K \gtrsim 0.5\ K_c$, the cracks blunt without significant growth (Fig. 3.1a) and are thus innocuous with regard to mechanical reliability. The blunting involves the creation of damage within shear lobes at the sides of the crack and damage coalescence from this region with the crack surface. At higher crack driving forces, crack growth occurs by the nucleation and growth of damage in a small zone ahead of the crack. The damage consists primarily of cavities on two grain interfaces (Fig. 3.1b) that coalesce with the crack tip, causing incremental crack advance. These observations provide the basis for a model of crack growth above the threshold (Thouless, Hsueh, Blumenthal, and Evans).

The behavior of small cracks formed by inhomogeneous damage coalescence (Fig. 3.1a) has also been investigated. These cracks appear to move at appreciably lower crack driving forces than the deliberately introduced cracks, even though the crack morphology appears to be similar. The motion of these small cracks will require further study because they appear to exert a major influence on the failure time (Johnson and Evans).

***

†Brief version of LBL-15452.

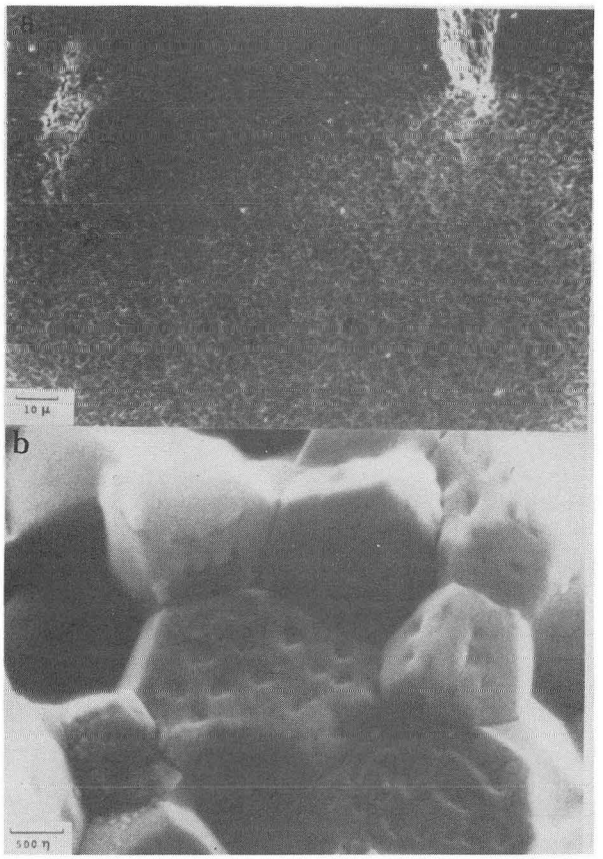

Fig. 3.1. Scanning electron micrographs of cracks exposed to creep strains. (a) the crack blunting that occurs at low crack driving force and (b) the cavitation damage formed on grain facets in the damage zone. (XBB 831-174)

4. THE INFLUENCE OF INHOMOGENEITIES ON HIGH TEMPERATURE FAILURE IN CERAMICS†

S. M. Johnson and A. G. Evans

The stress dependence of the failure time has been measured at high temperatures (1400°C) in a fine-grained alumina. The failure time, t_f, varied with stress, σ, as $t_f \propto \sigma^{-5}$. Observations of the material in interrupted tests revealed the nucleation of cracks at microstructural heterogeneities during the early stages of the failure process. The failure thus appears to be dominated by the crack propagation time. The crack initiating heterogeneities are characterized by material regions that exhibit rapid grain boundary grooving at the test temperature. This behavior suggests the presence of local impurity concentrations that produce premature crack nucleation. Observations of the fracture surfaces indicate the existence of cavities on two grain interfaces. Measurements of the spacing between these cavities suggest that the spacing decreases as the stress increases. This observation is consistent with the notion that cavities nucleate during grain boundary sliding transients. Analysis of crack

growth rates based on crack growth data (Blumenthal and Evans) confirmed that the failure times were crack propagation controlled.

***

†Brief version of LBL-15451.

Sintering

1. MICROSTRUCTURE EVOLUTION DURING SINTERING: THE ROLE OF EVAPORATION/CONDENSATION†

C. H. Hsueh and A. G. Evans

The movement of pores with grain boundaries during final stage sintering can occur either by surface diffusion or by evaporation/condensation. A comparison of pore motion by these two mechanisms revealed that the evaporation/condensation mechanism dominates at pore sizes in excess of a critical value determined primarily by the ratio of the surface diffusion parameter to the equilibrium vapor pressure.

At pore sizes in excess of this critical value, the important final stage sintering phenomena of pore breakaway and pore drag have been analyzed. The pore breakaway process has been shown to occur, independently of the pore size, when the ratio of the grain boundary mobility to the equilibrium vapor pressure exceeds a relatively low critical value. Hence, pore breakaway, when evaporation/condensation controlled pore motion prevails, and the consequent inhibition of complete densification can only be averted by imposing very stringent conditions on the final stage sintering schedule. Microstructure control is thus contingent upon the avoidance of the evaporation/condensation mechanism, by starting with sufficiently fine powders that the resulting pores are small enough to allow their motion to be surface diffusion controlled. Control of grain growth, e.g., by solute drag, is also needed to restrict the formation of large pores that then move by evaporation/condensation.

Finally, pore drag and the associated grain size, pore size trajectories, have been analyzed (Fig. 1.1). This study indicates that fully dense materials are only attainable when the ratio of the grain boundary diffusion parameter to the product of the equilibrium vapor pressure and the square of the grain size exceeds a minimum value. Again, therefore, fine powders are critical.

***

†Brief version of LBL-14110.

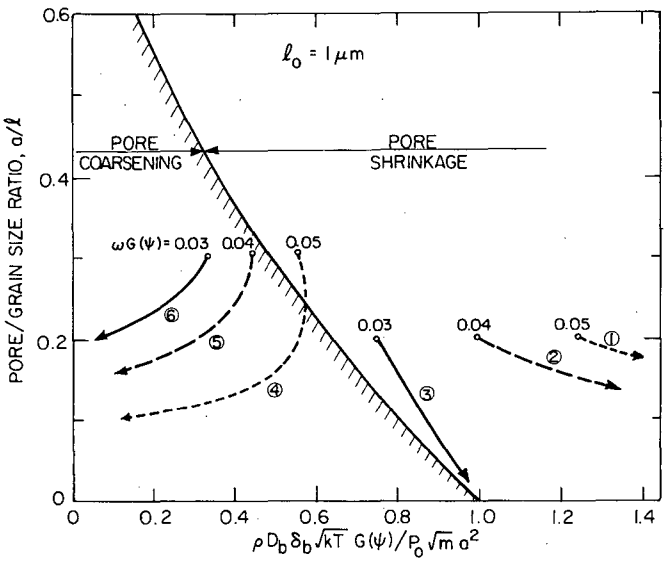

Fig. 1.1. Sintering trajectories predicted for conditions of pore motion by evaporation/condensation and pore shrinkage by grain boundary diffusion. (XBL 823-5469)

2. AN EXPERIMENTAL ASSESSMENT OF PORE BREAKAWAY DURING SINTERING†

M. Sakarcan, C. H. Hsueh, and A. G. Evans

Intergranular and grain boundary pores have been observed in MgO during the final stages of sintering. Measurement of the shapes of pores attached to grain boundaries, subject to distortion (Fig. 2.1), have been used to estimate the ratio of the grain boundary mobility to surface diffusivity for the material using a theory developed during the preceding year. This estimate has then been used to predict the critical pore size for the separation of pores from two grain interfaces, again using a theoretical analysis completed during the preceding year. This prediction has been compared with the median size of the intergranular, separated pores (Fig. 2.1) measured in the material in the final stage. The prediction (0.3 μm) is within less than a factor of two (0.3 to 0.6 μm) of the median pore sizes determined experimentally. It is thus concluded that the presently developed theoretical description of pore, grain boundary separation provides an adequate basis for the understanding of the role of separation on microstructure development during final stage sintering. The dominant role of the grain boundary mobility to the surface diffusivity ratio in the separation process highlights the need to obtain a fundamental understanding of the associated

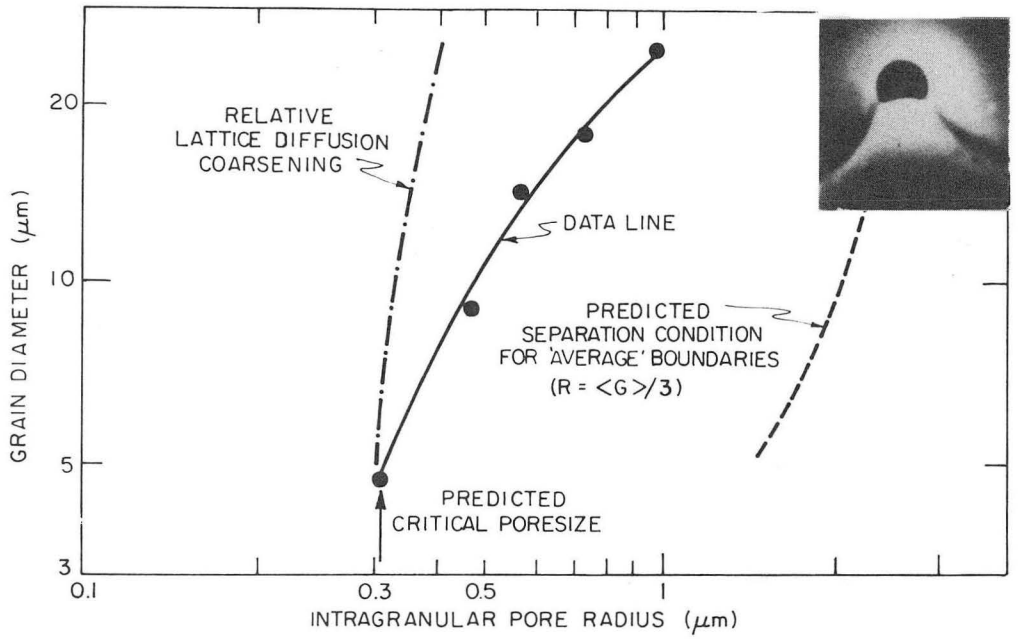

Fig. 2.1. Comparison of predicted and measured critical pore sizes for the separation of pores from grain boundaries. Also shown is a distorted pore/grain boundary used to evaluate the kinetic parameter. (XBB 831-236)

atom transport mechanisms and their dependence on additives and impurities. Techniques for measuring these parameters, in situ, on the appropriate microstructural scale, are of paramount importance.

***

†Brief version of LBL-14334.

3. INITIAL STAGE SINTERING WITH COUPLED GRAIN BOUNDARY AND SURFACE DIFFUSION†

C. H. Hsueh and A. G. Evans

Initial stage sintering of fine powders occurs by coupled grain boundary and surface diffusion, in series. Yet, the series process has never been analyzed. The rates of shrinkage and neck growth that obtain for various ratios of the boundary to the surface diffusivity have thus been calculated, numerically, for the sintering of rows of spheres, using a finite difference scheme. The scheme allows for a flux of atoms out of the grain boundary and a flux along the surface, dictated by the ratio of the surface to boundary diffusivity and the surface curvatures. A continuous transition from surface diffusion dominance to grain boundary diffusion control is predicted, with the surface adjusting rapidly to accommodate the grain boundary flux, even when the surface diffusivity is small. The results obtained for both large and small values of the diffusivity ratio have been compared with analytic approximations for the separate mass transport processes. Certain of these approximations have been found to agree relatively well with the numerical solution. This agreement has been shown to permit the judicious choice of approximations suitable for the analysis of the more complex sintering problems pertinent to actual powder compacts, such as the sintering of multiple arrays of ellipsoidal particles.

***

†Brief version of LBL-15450.

1982 PUBLICATIONS AND REPORTS

Refereed Journals

1. C. H. Hsueh, A. G. Evans, and M. Spears, "Microstructure Developmnt During Final Stage Sintering: I. Pore/Grain Boundary Separation," Acta Met. 30, 1269 (1982); LBL-12619 1/2.

2. M. Spears and A. G. Evans, "Microstructure Development During Final Stage Sintering: II. Grain and Pore Coarsening," Acta Met. 30, 1281 (1982); LBL-12619 2/2.

3. A. G. Evans, "The Structural Reliabilty of Ceramics: A Processing Dependent Phenomenon," J. Am. Ceram. Soc. 65(3), 127 (1982); LBL-12208.

4. C. H. Hsueh and A. G. Evans, "Microstructure Evolution During Sintering: The Role of Evaporation/Condensation," Acta Met. 31, 189 (1982).

Other Publications

1. A. G. Evans, "The High Temperature Failure of Ceramics," in Recent Advances in Creep and Fracture of Engineering Materials and Structures,

edited by B. Wilshire and D. Owen, Pineridge, 1982, p. 53; LBL-13839.

LBL Reports

1. M. Sakarcan, C. H. Hsueh, and A. G. Evans, "An Experimental Assessment of Pore Breakaway During Sintering," J. Am. Ceram. Soc., in press, LBL 14334.

2. S. Johnson, "The Role of Micrstructural Inhomogeneities on High Temperature Failure," Ph.D. thesis, LBL-14588.

3. M. D. Thouless, "Propagation of Creep Cracks by Cavitation in Fine Grained Materials," M.S. thesis, LBL-14915.

4. M. Sakarcan, "Experimental Observations of Pore Breakaway from Two Grain Junctions," M.S. thesis, LBL-13686.

5. J. E. Marion, A. G. Evans, M. D. Drory, and D. R. Clarke, "High Temperature Failure Initiation in Liquid Phase Sintered Materials," LBL-14266.

6. M. D. Huang and A. G. Evans, "The Strain Energy of Twinned Martensite: Applications to ZrO_2," LBL-15087.

Invited Talks

1. A. G. Evans and W. Blumenthal, "High Temperature Crack Nucleation and Propagation," American Ceramic Society, Cincinnati, Ohio, May 1982.

2. S. M. Johnson and A. G. Evans, "Probabilistic Aspects of High Temperature Failure," American Ceramic Society, Cincinnati, Ohio, May 1982.

3. A. G. Evans, "High Temperature Failure in Ceramics," Gordon Conference, Plymouth, New Hampshire August 1982.

4. A. G. Evans, "Reliability of Brittle Materials," Shell Laboratory, Houston, Texas, October 1982.

5. A. G. Evans, "High Temperature Failure Mechanisms, Massachusetts Institute of Technology, Cambridge, Massachusetts, November 1982.

6. C. H. Hsueh and A. G. Evans, "Neck Growth During Sintering," Pacific Coast Regional Meeting, American Ceramic Society, Seattle, Washington, October 1982.

7. J. E. Marion and A. G. Evans, "High Temperature Failure Initiation in Ceramics Containing an Intergranular Phase," Pacific Coast Regional Meeting, American Ceramic Society, Seattle, Washington, October 1982.

8. W. Blumenthal and A. G. Evans, "The Growth of Cracks During Creep in Alumina," Pacific Coast Regional Meeting, American Ceramic Society, Seattle, Washington, October 1982.

9. M. Drory and A. G. Evans, "A 3-Dimensional Ellipsoidal Pore Growth Model," Pacific Coast Regional Meeting, American Ceramic Society, Seattle, Washington, October 1982.

10. C. Ostertag and A. G. Evans," Dominant Diffusion Processes by Initial Stage Sintering of Al_2O_3," Pacific Coast Regional Meeting, American Ceramic Society, Seattle, Washington, October 1982.

c. Environmentally Affected Crack Growth in Engineering Materials*

Robert O. Ritchie, Investigator

Introduction. The objective of this program is to examine mechanical and microstructural factors involved in the micromechanisms of environmentally influenced fatigue crack growth. Models have been developed for the premature closure of cracks at ultralow growth rates approaching the threshold stress intensity ΔK_0 for no crack growth, where the driving force for crack extension is limited by the wedging action of corrosion debris and rough fracture morphologies (oxide-induced and roughness-induced crack closure, respectively, Fig. 1). In the past year, such concepts have been used to interpret fatigue under variable amplitude loading and crack growth behavior in aqueous and viscous environments, and to develop new fatigue resistant microstructures.

1. ON THE LOAD RATIO DEPENDENCE OF FATIGUE THRESHOLDS†

S. Suresh and R. O. Ritchie

A study was made of the influence of load ratio R on fatigue crack propagation and threshold (ΔK_0) behavior in 2-1/4Cr-1Mo steel tested in distilled water, moist air, and dry hydrogen gas. The dependence of ΔK_0 on load ratio was found to be far less marked in aqueous compared to gaseous environments, where ΔK_0 decreased sharply with increasing R. Based on Auger measurements of crack face oxidation and crack closure measurements using ultrasonics, such results were attributed to oxide-induced closure. Significant

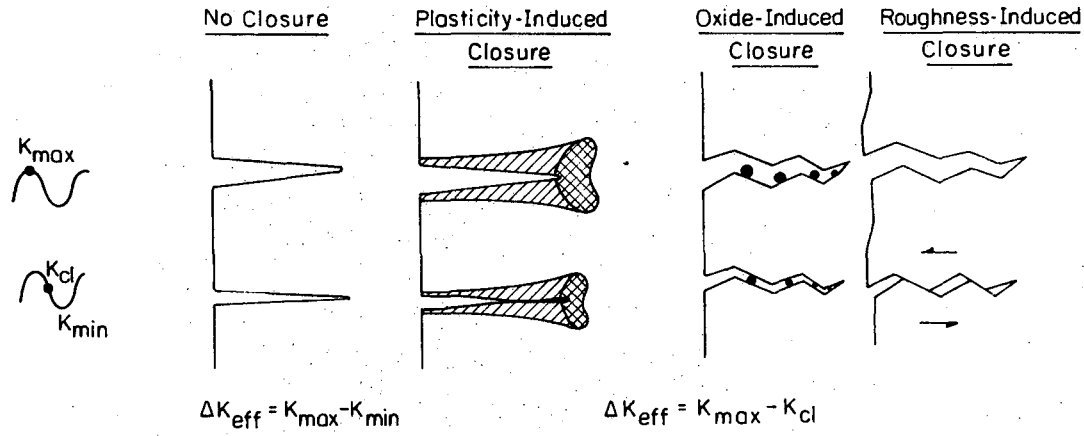

Fig. 1. Schematic illustration of mechanisms of fatigue crack closure relevant to growth rate behavior at near-threshold levels. ΔK_{eff} is the effective stress intensity range (i.e., local near-tip crack driving force), given by the difference between the maximum stress intensity (K_{max}) and the stress intensity at closure of the crack (K_{cl}). For closure to be effective, K_{cl} must exceed the minimum stress intensity in the cycle (K_{min}). (XBL 823-8161)

*This work was supported by the Director, Office of Energy Research, Office of Basic Energy Sciences, Materials Sciences Division of the U.S. Department of Energy under Contract No. DE-AC03-76SF00098.

corrosion deposits and hence closure are only developed at low load ratios in the gaseous environments because of "fretting oxidation" induced by mechanical closure. In the more oxidizing water environments, crack face oxide debris form at all load ratios because of thermal mechanisms which make closure, and hence ΔK_o values, much less dependent upon the load ratio.

* * *

†Brief version of LBL-14280 Rev.

2. INFLUENCE OF VISCOUS ENVIRONMENTS ON FATIGUE CRACK GROWTH†

J.-L. Tzou, S. Suresh, and R. O. Ritchie

The influence of viscous environments (dehumidified silicone and paraffin oils) has been examined for fatigue crack growth in A542-3 steel. Above ~10^{-5} mm/cycle, crack growth rates in oil were an order of magnitude slower than in either moist air or dry hydrogen gas. Conversely, below ~10^{-6} mm/cycle in the near-threshold regime, growth rates were an order of magnitude faster in oil. Such contrasting behavior was attributed to three competing mechanisms specific to oil environments, namely (a) suppression of moisture-induced hydrogen embrittlement, (b) minimization of crack flank oxidation and hence oxide-induced closure at near-threshold levels, and (c) development of enhanced closure from the hydrodynamic wedge effect of a viscous medium within the crack.

* * *

†Brief version of LBL-15780.

3. FATIGUE RESISTANT MICROSTRUCTURES IN DUAL-PHASE STEELS

V. Dutta, S. Suresh, and R. O. Ritchie

The incentive was to develop a ferritic-martensitic microstructure in a Fe/2Si/0.1C steel with superior resistance to near-threshold fatigue by promoting crack path meandering and consequent roughness-induced crack closure. Three microstructures (yield strength 600 MPa) were examined, namely, (a) a fine fibrous martensite in a ferrite matrix (obtained by intermediate quenching), (b) a coarse martensite with continuous ferrite (obtained by step quenching), and (c) a fine globular martensite along ferrite boundaries (obtained by intercritical annealing). It was found that the threshold ΔK_o was significantly higher (at $R = 0.05$) in the step-quenched and intercritical annealed structures (16.7 and 19.4 $MPa\sqrt{m}$, respectively) compared to the intermediate quenched structure (ΔK_o = 10.6 $MPa\sqrt{m}$), as a direct consequence of the rougher crack path in the former two microstructures.

4. MECHANISMS OF FATIGUE CRACK GROWTH UNDER VARIABLE AMPLITUDE LOADING†

S. Suresh and R. O. Ritchie

New mechanistic interpretations for fatigue crack growth retardation because of load excursions were developed based on a microroughness induced closure model. Analyses for the reductions in effective driving force for crack advance following overloads were based on mechanisms of crack blunting, branching and closure, compressive stresses, and fracture morphology. It was argued that retarded crack growth is effectively governed by micromechanisms of near-threshold crack growth, thus permitting quantitative estimates of the local effective driving force to be computed.

* * *

†Brief version of LBL-14482.

1982 PUBLICATIONS AND REPORTS

Refereed Journals

1. R. O. Ritchie and S. Suresh, "Some Considerations on Fatigue Crack Closure at Near-Threshold Stress Intensities Due to Fracture Surface Morphology," Met. Trans. 13A, 937 (1982); LBL-13836.

2. S. Suresh and R. O. Ritchie, "Mechanistic Dissimilarities Between Environmentally Influenced Fatigue Crack Propagation at Near-Threshold and Higher Growth Rates in Lower Strength Steels," Metal Science 16, 529 (1982); LBL-13585.

3. S. Suresh and R. O. Ritchie, "A Geometric Model for Fatigue Crack Closure Induced by Fracture Surface Roughness," Met. Trans. 13A, 1627 (1982); LBL-13837.

†4. R. O. Ritchie, F. A. McClintock, H. Nayeb-Hashemi, and M. A. Ritter, "Mode III Fatigue Crack Propagation in Low Alloy Steels," Met. Trans. 13A, 101 (1982).

†5. M. A. Ritter and R. O. Ritchie, "On the Calibration, Optimization and Use of D.C. Electrical Potential Methods for Monitoring Mode III Crack Growth in Torsionally-Loaded Samples," Fatigue Eng. Mater. Struct. 5, 91 (1982).

†6. H. Nayeb-Hashemi, F. A. McClintock, and R. O. Ritchie, "Effects of Friction and High Torque on Fatigue Crack Propagation in Mode III," Met. Trans. 13A, 2197 (1982).

‡7. M. Kurkela, G. Frankel, R. M. Latanision, S. Suresh, and R. O. Ritchie, "Influence of Plastic Deformation on Hydrogen Transport in 2-1/4Cr-1Mo Steel," Scripta Met. 16, 455 (1982).

§8. J. F. McCarver and R. O. Ritchie, "Fatigue Crack Propagation Thresholds for Long and Short Cracks in René 95 Nickel-Base Superalloys," Mat. Sci. Eng. 55, 63 (1982); LBL-13453.

9. A. K. Vasudévan and S. Suresh, "Influence of Corrosion Deposits on Near-Threshold Fatigue Crack Growth Behavior in 2XXX and 7XXX Series Aluminum Alloys," Met. Trans. 13A, 2271 (1982).

10. S. Suresh, "Crack Growth Retardation due to Micro-Roughness: A Mechanism for Overload Effects in Fatigue," Scripta Met. 16, 995 (1982); LBL-14483.

11. S. Suresh and S. Bahadur, "Evaluation of Polymers as Lubricants in the Extrusion of Aluminum," J. Lubrication Tech., Trans. ASME 104, 552 (1982).

12. S. Suresh, I. G. Palmer, and R. E. Lewis, "Effects of Environment on Fatigue Crack Growth Behavior of 2021 Aluminum Alloy," Fatigue Eng. Mater. Struct. 5 133 (1982).

LBL Reports

1. S. Suresh and R. O. Ritchie, "On the Influence of Environment on the Load Ratio Dependence of Fatigue Thresholds in Pressure Vessel Steel," LBL-14280 Rev.

2. S. Suresh and R. O. Ritchie, "A Model for the Contribution to Plasticity-Induced Fatigue Crack Closure from Residual Compressive Stresses," LBL-14405.

3. J. A. Wasynczuk, R. O. Ritchie, and G. Thomas, "Effects of Microstructure on Fatigue Crack Growth in Duplex Ferrite-Martensite Steels," LBL-14891.

4. W. J. Salesky, R. M. Fisher, R. O. Ritchie, and G. Thomas, "The Nature and Origin of Sliding Wear Debris from Steels," LBL-15059.

5. S. Suresh, "Micromechanisms of Fatigue Crack Growth Retardation Following Overloads," LBL-14482.

Other Publications

‡1. R. O. Ritchie and S. Suresh, "Effects of Crack Flank Oxide Debris and Fracture Surface Roughness on Near-Threshold Corrosion Fatigue," in Atomistics of Fracture, edited by R. M. Latanision and J. Pickens, Plenum Press, New York, 1982.

2. R. O. Ritchie, S. Suresh, and P. K. Liaw, "A Comparison of Environmentally Influenced Near-Threshold Fatigue Crack Growth Behavior in High and Lower Strength Steels at Conventional Frequencies," in Ultrasonic Fatigue, edited by J. M. Wells, O. Buck, L. D. Roth, and J. K. Tien, TMS-AIME, Warrendale, Pennsylvania, 1982, p. 443; LBL-13571.

‡3. S. Suresh, G. F. Zamiski, and R. O. Ritchie, "Fatigue Crack Propagation Behavior of 2-1/4Cr-1Mo Steels for Thick Wall Pressure Vessels," in Application of 2-1/4Cr-1Mo Steels for Thick Wall Pressure Vessels, ASTM Special Technical Publication 755, ASTM, Philadelphia, Pennsylvania, 1982, p. 49.

Invited Talks

1. S. Suresh and R. O. Ritchie, "On the Load Ratio Dependence of Near-Threshold Corrosion Fatigue Growth," 111th Annual Meeting of AIME, Dallas, Texas, February 1982.

2. M. Kurkela, S. Suresh, R. M. Latanision, and R. O. Ritchie, "Effects of Plastic Deformation on Hydrogen Permeation," 111th Annual Meeting of AIME, Dallas, Texas, February 1982.

3. R. O. Ritchie, "Non-Linear Fracture Mechanics: Uses and Limitations," Sandia National Laboratories, Livermore, California, April 1982.

4. R. O. Ritchie, "Influence of Material Microstructure on Fatigue and Fracture," San Jose State University, San Jose, California, May 1982.

5. R. O. Ritchie, "Fatigue Crack Propagation in Mode III," Rockwell International Science Center, Thousand Oaks, California, May 1982.

6. R. O. Ritchie, "Environmental Effects on Fatigue Crack Propagation," Rockwell International Fatigue Symposium, Science Center, Thousand Oaks, California, May 1982.

7. P. K. Liaw and R. O. Ritchie, "Influence of Gaseous Environment on Near-Threshold Crack Growth Behavior in Steels," International Congress on Technology and Technology Exchange, Pittsburgh, Pennsylvania, May 1982.

8. R. O. Ritchie, "Microstructural Modelling for the Prediction of Fracture Toughness," Exxon Research and Engineering Company, Linden, New Jersey, June 1982.

9. R. O. Ritchie, "Application of Fracture Mechanics to Fatigue Crack Propagation," University of California Extension Program, Berkeley, California, June 1982 and Exxon Education Center, Florham Park, New Jersey, December 1982.

10. R. O. Ritchie, "Physical Basis for Fracture Toughness," University of California Extension Program, Berkeley, California, June 1982.

11. R. O. Ritchie, "Elastic-Plastic Fracture Mechanics," U.S. Steel, Monroeville, Pennsylvania, July 1982.

12. R. O. Ritchie and S. Suresh, "Mechanics and Physics of the Growth of Short Cracks," plenary lecture to 55th Specialists Meeting of AGARD Structural and Materials Panel, Toronto, Canada, September 1982.

13. R. O. Ritchie, "Crack Closure Mechanisms During Near-Threshold Fatigue Crack Growth," Cockburn Engineering Center, University of Toronto, Canada, September 1982.

14. S. Suresh and R. O. Ritchie, "A Geometric Model for Fracture Surface Induced Crack Closure," TMS-AIME Fall Meeting, St. Louis, Missouri, October 1982.

15. R. O. Ritchie, F. A. McClintock, and H. Nayeb-Hashemi, "Mode III Fatigue under Combined Loading," TMS-AIME Fall Meeting, St. Louis, Missouri, October 1982.

16. R. O. Ritchie, "New Mechanisms of Corrosion Fatigue," General Motors Research Laboratories, Warren, Missouri, October 1982.

17. R. O. Ritchie, "Metal Fatigue: Ways of Slowing Down the Growth of Fatigue Cracks," ASM Fall 1982 Educational Seminar, University of California, Berkeley, California, October 1982.

18. R. O. Ritchie, "Analytical Framework for Linear Elastic Fracture Mechanics Methods," Exxon Education Center, Florham Park, New Jersey, December 1982.

19. R. O. Ritchie, "Brittle Fracture Mechanisms and Phenomenology," Exxon Education Center, Florham Park, New Jersey, December 1982.

20. R. O. Ritchie, "Short Fatigue Cracks," Westinghouse Research and Development Center, Pittsburgh, Pennsylvania, December 1982.

21. R. O. Ritchie, "Role of Oxide-Induced Crack Closure in Corrosion Fatigue," invited presentation to ASTM E24.04.05 Task Group on Fatigue Crack Growth Rate Testing in Aqueous Environments, San Francisco, California, December 1982.

22. R. O. Ritchie and S. Suresh, "Fatigue Crack Growth of Short Cracks: Limitations Based on Microstructural Considerations," invited presentation to ASTM E24.04.06 Task Group on the Growth of Short Cracks, San Francisco, California, December 1982.

23. R. O. Ritchie, F. A. McClintock, and H. Nayeb-Hashemi, "Mode III Fatigue Crack Growth under Combined Torsional and Axial Loading," International Symposium on Biaxial/Multiaxial Fatigue, San Francisco, California, December 1982.

24. S. Suresh, "Plane Strain Closure Phenomena," Southwest Research Institute, San Antonio, Texas, February 1982.

25. S. Suresh, "Influence of Oxide Deposits on Fatigue Thresholds," University of Houston, Texas, February 1982.

26. S. Suresh, "Fatigue Crack Closure: New Mechanistic Interpretations and Implications," University of Southern California, Los Angeles, California, May 1982.

27. S. Suresh, "Micromechanisms of Crack Growth Retardation Following Overloads, Parts I & II," TMS-AIME Fall Meeting, St. Louis, Missouri, October 1982.

* * *

†Work supported in part by the Division of Energy Conservation, U.S. Department of Energy under Contract No. EX-76-A-01-2295, TO 51.
‡Work supported in part at MIT by the Office of Basic Energy Sciences of the U.S. Department of Energy under Contract No. DE-AC02-79ER10389.
§Work supported in part by National Science Foundation through the Center for Materials Science and Engineering, MIT, under Contract No. DMR-78-24185.

3. Physical Properties

a. Interfaces and Ceramic Microstructures*

Joseph A. Pask, Investigator

Introduction. The purpose of this work is to advance basic understanding of the nature of interfaces (primarily those between dissimilar materials, e.g., metals and ceramics), particularly in terms of bonding and adherence. This understanding is critical in the development of composites, protective coatings, glass/ceramic to metal seals, and in the reduction of corrosion at interfaces. The work involves studies of thermodynamics and kinetics of reactions at interfaces and of wetting and spreading of liquids.

Another objective in this work is to advance the understanding of the factors that play roles in the development of desired microstructures in ceramic materials, with and without a liquid phase. This understanding depends on a knowledge of the interfacial phenomenon from a thermodynamics point of view and of the mass transport mechanisms during sintering.

1. WETTING AND REACTIONS IN THE LEAD BOROSILICATE GLASS-PRECIOUS METAL SYSTEMS†

V. K. Nagesh, A. P. Tomsia, and J. A. Pask

Sessile drop experiments of lead borosilicate glass on Ag, Au, and Pt were performed in air, vacuum, and helium at 700°C.

The glass spread on Ag in the presence of oxygen, and very strong adherence developed. The driving force for spreading was provided by the reduction of interfacial energy caused by a reaction between Ag oxide formed on the Ag surface and SiO_2 in the glass. A low contact angle (2-12°C) was observed for vacuum conditions and good adherence developed. The adherence was due to the saturation of the interface with Ag oxide as a result of a redox reaction between PbO in the glass and the Ag, indicated by a loss of Pb from the glass. In 1 atom helium, adherence was poor because of the absence of the redox reaction, caused by suppression of any Pb vapor evolution that would be formed; this absence also effects an increase in γ_{SL} (solid-liquid interfacial energy) and the contact angle (5-48°).

With Au, the contact angle was 18° and good adherence was observed in air because of the dissolution of the Au oxide layer on the Au surface by the glass at the interface. In vacuum, the adherence was poor because of the absence of an Au oxide layer. The contact angle was lower (7°) due to a higher γ_{SV} (surface energy of Au) resulting from the absence of adsorbed oxygen on Au.

In air, glass had a contact angle of 2-3° and adhered strongly to Pt because of the dissolution of a Pt oxide layer on the Pt surface. In vacuum adherence was poor due to absence of adsorbed oxygen. The contact angle, however, varied from 58 to 73° depending on the absence or presence of adsorbed carbon on the surface; adsorbed carbonaceous material reduces γ_{SV}.

Oxygen is chemisorbed on Ag, Au, and Pt in air. Although the surface oxides do not grow in thickness, the amounts are sufficient to saturate the glass at the interface since the solubilities of the precious metal oxides in glass are very low; also, interfacial saturation is sufficiently maintained, since diffusion gradients are small because of the low oxide concentrations.

* * *

†Brief version of LBL-15614.

2. THE SILICA-ALUMINA SYSTEM†

J. A. Pask

This system is one of the more important systems in ceramic oxide materials technology, but considerable confusion still exists in the nature of the phase equilibrium diagram. It has been indicated that difficulties are due to the fact that alumino-silicate liquids can be readily supercooled and supersaturated. A liquid that, on cooling, would normally precipitate the crystal α-Al_2O_3 can be easily supercooled in the absence of nuclei of α-Al_2O_3 before the mullite crystallizes. Mullite growing under these conditions is capable of accommodating larger amounts of Al_2O_3, i.e., it has a larger solid solution range. Mullite grown isothermally by chemically interdiffusion has a narrower solid solution range. Procedures in the preparation of specimens in this system are thus critical and misinterpretations of experimental data have occurred in published papers. Stable and metastable phase equilibria have been identified in the α Al_2O_3-SiO_2 system.

* * *

†Brief version of LBL-14678.

*This work was supported by the Director, Office of Energy Research, Office of Basic Energy Sciences, Materials Sciences Division of the U.S. Department of Energy under Contract No. DE-AC03-76SF00098.

1982 PUBLICATIONS AND REPORTS

Refereed Journals

1. S. M. Johnson, J. S. Moya, and J. A. Pask, "Influence of Impurities on High-Temperature Reactions of Kaolinite," J. Am. Ceram. Soc., 65, 31-35 (1982); LBL-11949.

2. M. D. Sacks and J. A. Pask, "Sintering of Mullite-Containing Materials: I. Effect of Composition," J. Am. Ceram. Soc. 65, 65-70 (1982); LBL-11857-1/2.

3. M. D. Sacks and J. A. Pask, "Sintering of Mullite-Containing Materials: II. Effect of Agglomeration," J. Am. Ceram. Soc. 65, 70-77 (1982); LBL-11857-2/2.

4. I. Nurishi and J. A. Pask, "Sintering of α Al_2O_3-Amorphous Silica Compacts," Ceramics International 8, 57-59 (1982); LBL-12457.

5. A. P. Tomsia, Z. Feipeng, and J. A. Pask, "Wetting Behavior in the Iron-Silver System," Acta Met. 30, 1203-1208 (1982); LBL-13390.

6. S. T. Tso and J. A. Pask, "Reaction of Glasses with Hydrofluoric Acid Solution," J. Am. Ceram. Soc., 65, 360-362 (1982); LBL-12800.

7. S. T. Tso and J. A. Pask, "Reaction of Silicate Glasses and Mullite with Hydrogen Gas," J. Am. Ceram. Soc. 65, 383-387 (1982), 457-460; LBL-12882.

8. S. M. Johnson and J. A. Pask, "Role of Impurities on Formation of Mullite from Kaolinite and Al_2O_3-SiO_2 Mixtures," Bull. Am. Ceram. Soc. 61, 838-842 (1982); LBL-13062.

9. S. T. Tso and J. A. Pask, "Reaction of Fused Silica with Hydrogen Gas," J. Am. Ceram. Soc. 65, 457-460 (1982).

LBL Reports

1. D. J. Miller, "Liquid Phase Densification of Titanium Carbide-Nickel Composites," Ph.D. thesis, LBL-13580.

2. A. P. Tomsia, F. Zhang, and J. A. Pask, "Wetting and Reactions in Glass/Non-Precious Metal Alloy Systems," LBL-13847.

3. K. Wada, A. P. Tomsia, and J. A. Pask, "Kinetics of Glass/Metal Reactions," LBL-13848.

4. P. L. Flaitz, "Some Aspects of Liquid Phase Sintering of Alumina," Ph.D. thesis, LBL-13849.

5. J. A. Pask, "Current Understanding of Stable and Metastable Phase Equilibria and Reactions in the SiO_2-α Al_2O_3 System," LBL-14678.

6. W. M. Kriven and J. A. Pask, "Solid Solution Range and Microstructures of Melt-Grown Mullite," LBL-14679.

7. V. K. Nagesh and J. A. Pask, "Wetting of Nickel by Silver," LBL-15023.

b. High Temperature Reactions*

Alan W. Searcy, Investigator

Introduction. The first of the following articles initiates a series of theoretical and experimental papers planned on surface thermodynamics and related topics of adsorption-vapor equilibrium and of the kinetics of surface processes. The article explores the assumption that the most stable forms of small crystals or cavities are the forms for which the $\Sigma n_i G_i$ is a minimum, where n_i is the number of atoms with excess free energies G_i by virtue of being near a surface. This model predicts forms of crystals that are sometimes more stable than those governed by the Wulff relation. This relation, $\sigma_i/h_i = \sigma_j/h_j \ldots$, where σ_i is the surface tension of a stable face at a distance h_i from a common center, has been accepted as governing crystal and cavity shapes for 80 years. The new relation recognizes that spherical crystals need not have isotropic specific-surface-free energies and permits better understanding of the kinetics of surface-shape changes and of the persistence of metastable shapes. The remaining articles describe recent studies directed toward the long-range objectives of generating reliable experimental data for decomposition reactions and formulating a coherent theoretical framework for analyzing the kinetics and thermodynamics of such reactions and of the physical properties, thermodynamics, and kinetics of the solid products of decomposition reactions.

1. THE EQUILIBRIUM SHAPES OF CRYSTALS AND OF CAVITIES IN CRYSTALS†

Alan W. Searcy

It has been believed that a proof of Gibbs'[1] rules out rounded equilibrium surfaces for particles or cavities in particles, unless the surface tensions (or specific surface free energies) in the rounded surfaces are essentially isotropic. It has also been believed that an inescapable corollary of Gibbs' proof is that equilibrium surfaces must obey the relation deduced by Wulff,[2] $\sigma_i/h_i = \sigma_j/h_j = \ldots$, where σ_i is a surface tension and h_i is the distance of the surface from a common center.

In this article, surface free energies are assumed to be the sum of the excess free energies of bonding of molecules in or near the surface, and the stable form of a crystal or cavity is assumed to be the form that makes the sum of these excess free energies a minimum.

When only plane surfaces are allowed, this model predicts the same shapes for crystals as the relation of Wulff. The model predicts rounding of edges and corners of kinds that are not allowed by the Wulff relation and predicts that quasispherical equilibrium crystals can have anisotropic surface-free energies. The model appears to be consistent with experimental observations, and it provides a useful framework for analysis of whether unstable crystal or cavity shapes will evolve into stable or metastable forms. Some crystals and cavities that have been assumed to have equilibrium shapes instead have metastable shapes.

* * *

†Brief version of LBL-14716, to appear in J. Solid State Chem.

1. J. W. Gibbs, The Collected Works. Vol. 1: Thermodynamics, Longmans, Green, New York, 1931, p. 320.
2. G. Wulff, Z. Krist. 34, 449 (1901).

2. EFFECTS OF PARTICLE SIZE AND POWDER BED SIZE ON CALCITE DECOMPOSITION RATES†

Mun Gyu Kim, Alan W. Searcy, and Dario Beruto

The kinetics of endothermic decomposition reactions of the type AB(s) = A(s) + B(g) have been so poorly understood that reviewers have often described them as reversible, yet analyzed them in terms of kinetic models that implicitly assume complete irreversibility. Beruto and Searcy[1] proved that decomposition of calcite single crystals is highly irreversible; the rate of CO_2 escape is only ~10^{-5} times the rate possible for a reversible reaction.[2] But calcite powder beds give unexpected apparent equilibrium pressures only ~10^{-4} times the thermodynamic equilibrium pressure for the reaction. This study was undertaken to determine the influences of particle size, sample size, and particle packing densities on decomposition rates. No detailed systematic study of these questions had been previously reported.

High-purity, natural-calcite single crystals were cut and separated into sized fractions with particles in the range 74-90 μm, 0.5-0.6 mm, 1.0-1.4 mm, and 4 mm average cross sections. Samples of ~3 μm, 5-10 μm, and 10-20 μm average cross sections were separated from commercial calcite powders by means of an ultrasonic fine sieve. Regardless of particle size, the powders had rhombohedral shapes, which implies that the individual particles were single crystals. Sam-

*This work was supported by the Director, Office of Energy Research, Office of Basic Energy Sciences, Materials Sciences Division of the U.S. Department of Energy under Contract No. DE-AC03-76SF00098.

ples of various particle sizes were decomposed at 610°C or 670°C in vacuum in alumina cells. For calcite of >0.5 mm cross section, weight losses were directly proportional to sample heights from 2.5 mm to 14.4 mm: Decomposition of these beds of large crystals is irreversible, as found for single crystals.[1] In contrast, the flux-per-unit cross sectional area of the exposed powder bed surface was independent of sample height and packing density (Fig. 2.1). For these powder beds, near-equilibrium pressures are established when the CO_2 flux from the bed is ~10^{-4} times that for true equilibrium. Neither XRD studies nor TEM studies show products of calcite decomposition other than normal CaO. It is suggested nonetheless that the CO_2 pressure in the bed may be characteristic of an equilibrium between $CaCO_3$ and an unstable $CaO(CaCO_3)_x$ phase which decomposes irreversibly when its layer thickness is only a few nm. TEM experiments in controlled CO_2 atmospheres could test this hypothesis.

* * *

†Brief version of LBL-15236.

1. D. Beruto and A. W. Searcy, J. Chem. Soc. Faraday Trans. I 70, 215 (1979).
2. G. F. Knutsen, A. W. Searcy, and D. Beruto, J. Am. Ceram. Soc. 65, 219 (1982).

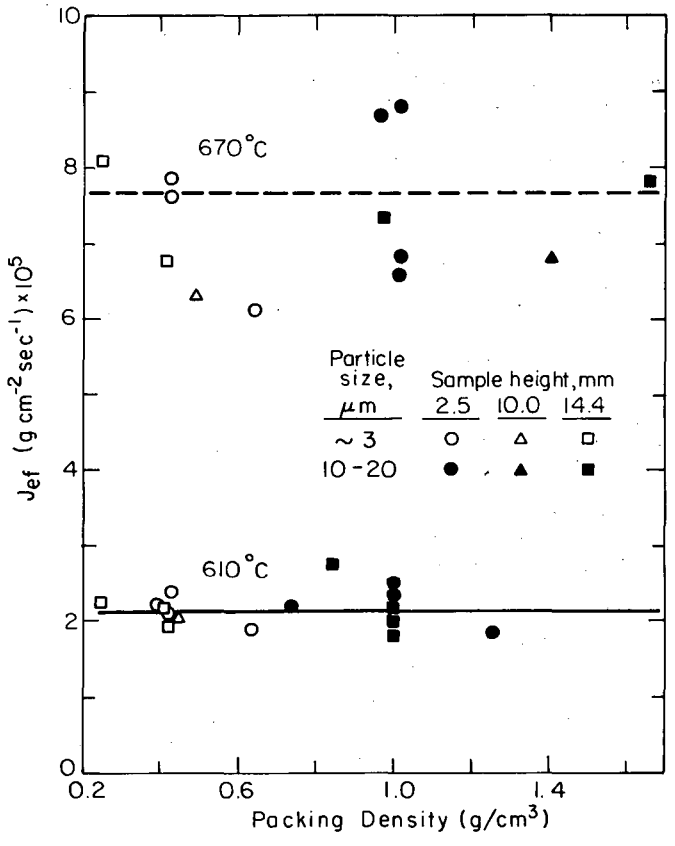

Fig. 2.1. J_{ef} vs packing density with a constant distance (=1 cm) between the top of sample cell and the top of sample, where J_{ef} is the weight loss per unit cross-section area of sample cell per unit time. (XBL 825-5764)

3. POSSIBLE METASTABILITY OF MgO RESULTING FROM THE DECOMPOSITION OF $Mg(OH)_2$ †

Thomas A. Reis, David J. Meschi, and Alan W. Searcy

Measurements of the equilibrium H_2O decomposition pressure for the reaction $Mg(OH)_2(s) = MgO(s) + H_2O(g)$ were made by Giauque and Archibald[1] at 463 and 485 K using a static manometric technique, and later by Kay and Gregory[2] in the same temperature range by means of a kinetic Knudsen cell method. The pressures measured by Kay and Gregory were only ~10^{-4} times those of Giauque and Archibald. Theoretically, possible explanations for the discrepancy are that vacuum decomposition yields MgO of (surprisingly) high surface free energy or a metastable solid, either a metastable form of MgO or an $MgO_xMg(OH)_2$ phase where $x > 0$. Such a metastable product would have to have a heat of formation ~48 KJ/mole of MgO present higher than that of normal MgO. X-ray studies show no evidence of a product other than normal MgO.[3] We report here calorimetric measurements designed to test for metastable product formation.

Samples of $Mg(OH)_2$ were prepared in the same manner as that used by Giauque and Archibald[1] and then decomposed to varying degrees in vacuo at ~300°C, some in open crucibles, most in Knudsen cells under conditions like those of Kay and Gregory. Products were then dissolved in 1M HCl and the heats of solution measured. The heat of solution of any residual undecomposed $Mg(OH)_2$ was subtracted from the measured values to give the heats of solution of the MgO products.

Figure 3.1 is a plot of the results in which the molar enthalpy of solution of the MgO is plotted against the mole fraction of MgO in the sample. To represent the equilibrium form of MgO, we used samples annealed at 1000°C for 10 hr or more. The dashed line represents the value for this standard material. Although there is considerable scatter in the data, the deviations from the dashed line appear to be random and amount to 12 kJ mole^{-1} at most; much less than the ~48 kJ mole^{-1} required by the hypothesis.

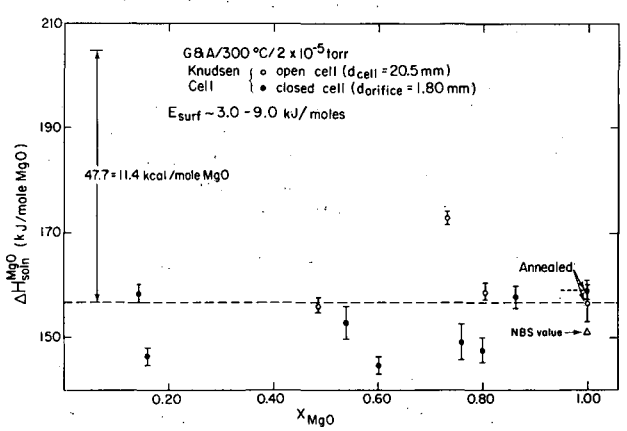

Fig. 3.1. Enthalpies of solution of MgO as a function of the mole fraction of MgO in the sample. (XBL 823-2078)

Any metastable solid product must be a transient phase present in quantities too small to be detected either by x-ray diffraction measurements or by these calorimetric measurements. A TEM search for a transient phase is planned.

* * *

†Brief version of LBL-15725.

1. W. F. Giauque and R. C. Archibald, J. Am. Chem. Soc. 56, 561 (1937).
2. E. Kay and N. W. Gregory, J. Phys. Chem. 62, 1079 (1958).
3. T. A. Reis, D. J. Meschi, and A. W. Searcy, MMRD Annual Report for 1978, LBL-8580, p. 114.

4. CONFIRMATION OF BIMODAL PORE SIZE DISTRIBUTION IN CaO FROM CALCITE DECOMPOSITION†

Dario Beruto, Luigi Barco, and Alan W. Searcy

In the 1981 Annual Report we reported that surface areas and pore volumes in the CaO compacts formed by decomposing a calcite single crystal in steps, with measurements made on the same sample at liquid N_2 temperatures before it was reheated for an additional fractional decomposition of the calcite present. These data supported the suggestion of Powell and Searcy[1] that a duplex pore structure is formed, but the surface areas of the CaO when decomposition was complete was only ~90 m^2/g, compared to ~120 m^2/g expected from Powell and Searcy's results. The discrepancy is shown here to be a consequence of thermal cycling between the decomposition temperature and liquid N_2 temperature. The volume of >0.1 μm pores, which had been calculated by difference, has been confirmed by means of mercury porisimetry.

The uppermost line of Fig. 4.1 is the theoretical pore volume calculated from the sample mass and its external dimensions as a function of extent of reaction. The points marked a and b are the total volumes calculated from N_2 condensation in pores too small for Hg porisimetry measurements and from Hg porisimetry measurements in pores too large for N_2 condensation measurements. The lowest line shows the N_2 condensation data. Agreement of points a and b with the theoretical curve confirms the duplex pore structure. The middle curve shows that the specific surface area of CaO is independent of extent of reaction (in disagreement with results reported from other laboratories), and the specific surface areas found are ~120 m^2/g, as reported by Powell and Searcy.

* * *

†Brief version of LBL-13882 Rev.

1. E. K. Powell and A. W. Searcy, J. Am. Ceram. Soc. 65, C42 (1982); LBL-11207.

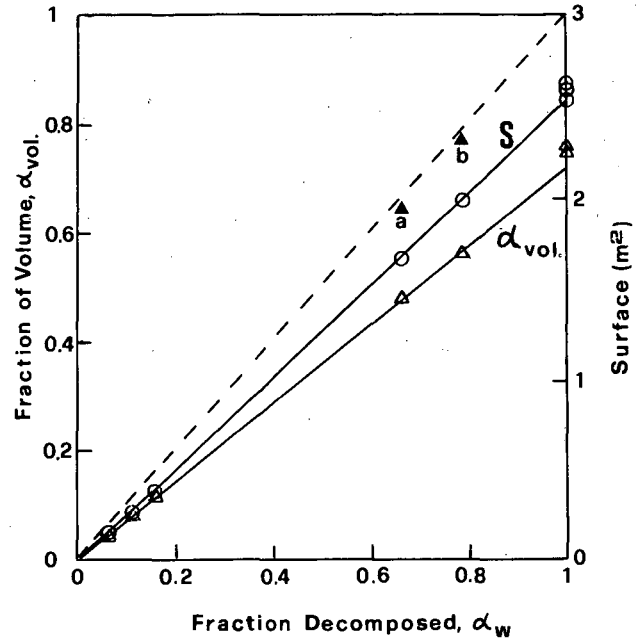

Fig. 4.1. Volume of <0.1 μm pores, Δ's, sum of large and small pore volumes ▲'s, and total surface areas o's, as functions of fraction of CaO formed by $CaCO_3$ single crystal decomposition in vacuum. (XBL 832-8442)

5. GAS FLOW THROUGH POROUS BARRIERS: THE O_2-Pt, CO-Pt SYSTEMS†

Jeffrey N. Farnsworth and Alan W. Searcy

For gases that show physical adsorption on surfaces of porous barriers, surface diffusion has been found to contribute measurably to barrier permeation only if temperatures are low, usually less than room temperature, and if pore dimensions are <0.1 μm. But recently Jacobson and Searcy[1] showed that surface diffusion makes measurable contributions to transport of LiF, NaF, and NaCl vapors through alumina. This study was undertaken to determine if gases that chemisorb with energies comparable to those of the alkali halide vapors, as measured by $\Delta H_{ads}/RT$, where ΔH_{ads} is the enthalpy of adsorption, would also show high surface diffusion fluxes on porous Pt metal barriers.

A manifold system contained pressure monitoring devices, allowed access for the gases studied, and also served as a reservoir. A valved mullite tube connected the manifold system to the platinum porous barrier, which was mounted in a vacuum furnace. Fluxes through the barrier were calculated from the recorded pressure drop with time.

For a particular gas, the flux measured (J) may be compared with the flux of a standard gas,

such as helium (J_k), in which Knudsen flow is the only transport mechanism. A ratio J/J_k provides a measure of the importance of surface diffusion. The quantity J/J_k is plotted vs $\Delta H_{ads}/RT$ (Fig. 5.1) for the systems in this and the alkali halide-alumina study.[1] In the range of $\Delta H_{ads}/RT$ values for which the alkali halide-alumina systems show significant surface diffusion, the O_2-Pt, CO-Pt systems do not. The importance of surface diffusion relative to vapor phase diffusion varies with radius^{-1}. The studies with ~5 μm pores in platinum permit the conclusion that diffusion of O_2 and CO on Pt is less important than that of NaF or LiF on alumina. The data show that surface diffusion depends on the kinds of chemisorption bonds.

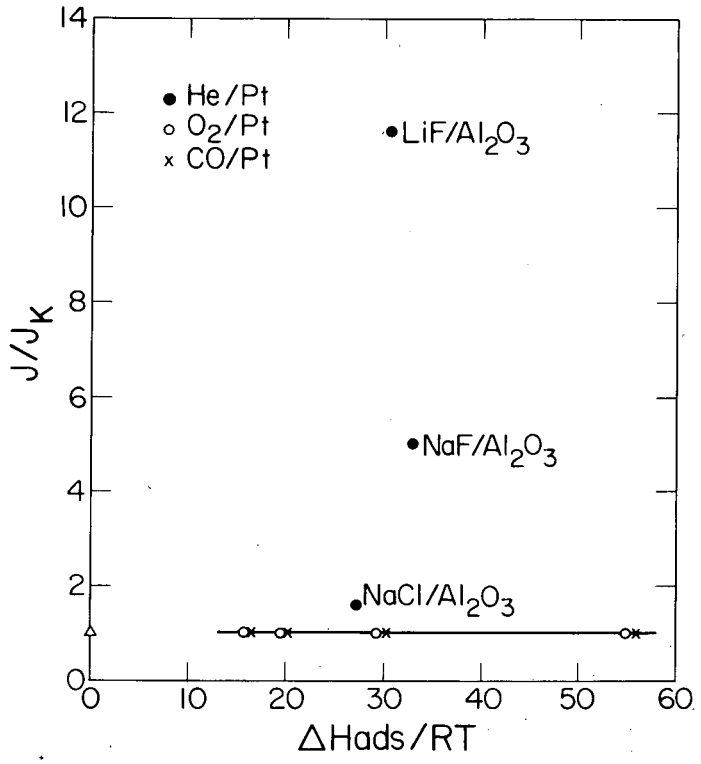

Fig. 5.1. Surface diffusion as a function of the normalized heat of adsorption for gas/solid systems. (XBL 832-1193)

* * *

†Brief version of LBL-15724.

1. N. S. Jacobson, "The Diffusion of Gases in Capillaries," Ph.D. thesis, LBL-13227.

1982 PUBLICATIONS AND REPORTS

Refereed Journals

1. G. F. Knutsen, A. W. Searcy, and D. Beruto, "Effects of LiCl on the Rate of Calcite Decomposition," J. Am. Ceram. Soc. 65(4), 219-222 (1982); LBL-12043.

2. E. K. Powell and A. W. Searcy, "Surface Areas and Morphologies of CaO Produced by Decomposition of Large $CaCO_3$ Crystals in Vacuum," J. Am. Ceram. Soc. 65(3), C42-C44 (1982); LBL-11207 Rev.

3. A. W. Searcy and D. J. Meschi, "Electronic Ceramics in High-Temperature Environments, J. Am. Ceram. Soc. 65(4), 216-218 (1982); LBL-11821.

LBL Reports

1. S. L. Roche, "Thermal Decomposition of Magnesium and Calcium Sulfates," Ph.D. thesis, LBL-14303.

2. D. J. Meschi and A. W. Searcy, "Catalysis of $MgSO_4$ Decomposition by Fe_2O_3," LBL-14393.

3. A. W. Searcy, "The Equilibrium Shapes of Crystals and of Cavities in Crystals," to be published in J. Solid State Chem., LBL-14716.

†4. D. Beruto, L. Barco, and A. W. Searcy, "Rearrangement of Porous CaO Aggregates During Calcite Decomposition in Vacuum," LBL-14901.

5. M. G. Kim, "Effects of Particle Size on Calcite Decomposition," M.S. thesis, LBL-15236.

* * *

†Supported in part by the Division of Materials Sciences, Office of Basic Energy Sciences, U.S. Department of Energy and in part by the Italy-U.S. Exchange Program of CNR (Italy) and NSF.

c. Structure-Property Relationships in Semiconductor Materials*

Jack Washburn, Investigator

Introduction. The aim of the program is to undertake basic research leading to a more complete understanding of the structure-sensitive electrical properties of semiconductor materials. An attempt is made to choose topics for investigation that have a relation to state-of-the art technology and to carry on joint research with the semiconductor industry where possible.

The current activity of the program is in three major areas:

1. Applications of high resolution lattice imaging electron microscopy to the study of interfaces,
2. Effects of ion damage in silicon and gallium arsenide, and
3. Improvement of experimental and analytical techniques for the characterization of defects in semiconductors.

Some of the individual research topics briefly described in this report can be related to more than one of the major areas.

1. THE MECHANISM OF DEGRADATION OF Cu_2S-CdS SOLAR CELLS AS REVEALED BY HIGH RESOLUTION ELECTRON MICROSCOPY†

T. Sands, R. Gronsky, and J. Washburn

The major factor preventing the production of inexpensive and efficient Cu_2S-CdS thin film solar cells is the inherent instability of the p-type copper sulfide layer. This layer can act as an efficient adsorber-emitter only if the predominant phase is chalcocite (Cu_2S). A small amount of copper loss because of non-optimum formation conditions, in-service oxidation, or electromigration under load results in the formation of djurleite ($Cu_{1.97}S$) and a corresponding reduction in cell efficiency. This study addresses the problem of determining the microscopic mechanism of the chalcocite-djurleite transformation so that methods to produce more stable layers for device configurations may be systematically explored.

High resolution transmission electron microscopy (HRTEM) of copper sulfide thin films has revealed the formation and growth characteristics of coherent djurleite domains in chalcocite during aging in air at room temperature. Specifically, chalcocite/djurleite interfaces are abrupt and tend to lie in planes which minimize the lattice mismatch between the two phases (see Fig. 1.1). A model for the transformation involving the clustering of copper vacancies into

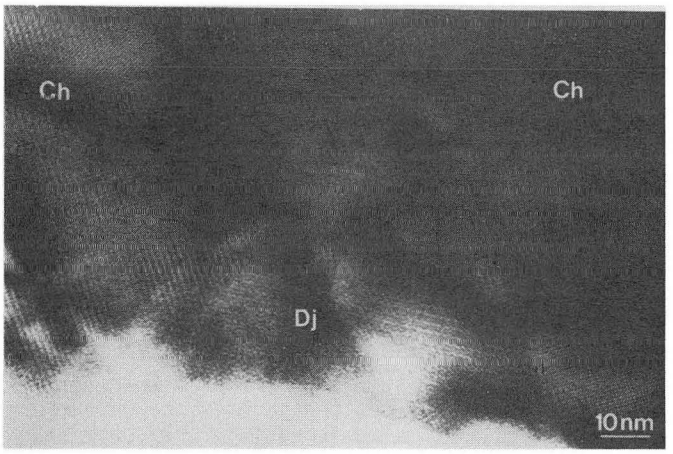

Fig. 1.1. HRTEM image of a djurleite domain formed in a basal chalcocite film after aging in air at room temperature for four days. (XBB 829-7601)

$Cu_{20}S_{12}$ four-vacancy clusters has been developed. These clusters order simultaneously into the superstructure of djurleite, leaving the common h.c.p. sulfur lattice intact.

* * *

†Extended abstract of LBL-15063; also presented at the Sixteenth IEEE Photovoltaic Specialists Conference, San Diego, CA, September 1982; in press.

2. AN APPLICATION OF HIGH RESOLUTION LATTICE IMAGING ELECTRON MICROSCOPY TO A STUDY OF THE MECHANISM OF THE CRYSTALLINE TO AMORPHOUS TRANSFORMATION†

J. Washburn, C. Murty, and R. Gronsky

The mechanism of the crystal to amorphous transformation during ion damage in silicon has been investigated using high resolution lattice imaging electron microscopy. It was found that sharp interfaces exist between amorphous and crystalline regions in partially amorphous silicon. Simulated lattice fringe images for increasing Frenkel pair concentrations were generated which suggest that a sharp change in lattice fringe visibility implies a sharp change in structure.

There is enough evidence from conventional transmission electron microscopy that amorphous silicon, even restricting consideration to those structures produced by radiation damage, is in reality a class of materials with structures ranging from something like the idealized random network models to something considerably less random. It is likely that the mechanism of formation of "amorphous" silicon may be significantly different at low and high temperature.

*This work was supported by the Director, Office of Energy Research, Office of Basic Energy Sciences, Materials Sciences Division of the U.S. Department of Energy Under Contract No. DE-AC03-76SF00098.

* * *

†Brief version of LBL-14873.

3. EFFECT OF RECOIL IMPLANTED OXYGEN ON THE DEVELOPMENT OF SECONDARY DEFECTS IN MOS TEST WAFERS†

N. R. Wu, P. Ling, D. K. Sadana, J. Washburn, and M. I. Current‡

The growth or annihilation of secondary defects can be profoundly affected by surrounding impurity complexes and the annealing ambient. When high dose implantations are done through screen-oxides into Si, high concentrations ($>10^{21}$ cm^{-3}) of recoil implanted oxygen are also incorporated into the amorphous regions. Subsequent annealing of such amorphous layers have been shown to cause the formation of numerous Si-O complexes dispersed throughout the implanted depth that interact with the secondary defects to inhibit their growth.

The experimental program was designed to relate to the general processing conditions of an all-implanted MOS device fabrication technology. The implantation was carried out into (100) Si wafers with As ion beams of 4 to 12 mA for doses 4 to 7 x 10^{15} cm^{-2} at 100 or 120 keV followed by annealing at 1,000°C for 30 minutes in N_2 or O_2 or their combination. The TEM results from the above wafers revealed that interstitial dislocation loops of irregular shape were present beneath the surface in two discrete layers. It was found that annealing out of the loops is accelerated in the presence of O_2 in the annealing atmosphere. This finding is in contradiction to many previous papers, in which the injection of Si interstitials from the advancing SiO_2/Si interface into the bulk has been proposed. Under these conditions, the loops should grow rather than shrink as observed in the present study.

* * *

†Brief version of LBL-15491.
‡Now at Trilogy, Cupertino, CA.

4. IN-SITU OBSERVATIONS OF MeV ELECTRON BEAM INDUCED CRYSTAL GROWTH INTO AN AMORPHOUS LAYER IN SILICON†

J. Washburn and D. K. Sadana

Deep buried amorphous layers were created in (100) Si by 11 MeV As implantation. The effect of 1.2 MeV electron irradiation at the upper and lower interfaces of the buried layer was investigated on thin cross-section specimens prepared for transmission electron microscopy. It was found that amorphous zones shrink at both interfaces; however, the effect was most pronounced at the near-surface interface where amorphous zones would have been expected to be surrounded by crystalline material over a wider region. The experiment was repeated at high and low beam current in order to estimate the effect of beam heating. The result was almost the same for the two beam currents for comparable total electron fluence which shows that the shrinkage of amorphous zones was not because of specimen heating. Previous experience also suggests that the rise in temperature of the specimen could not have approached the 450°C necessary to get thermal regrowth of amorphous regions.

The experiment suggests that the formation of amorphous material during ion damage can involve a competition between two processes:

1) formation of new amorphous zones, and

2) shrinkage of amorphous zones that are still surrounded by crystalline material.

At low temperatures (<RT), the first process is dominant and the ion implanted material eventually becomes 100% amorphous. However, at higher temperatures the second process becomes important, and it is increasingly difficult to produce amorphous layers in silicon.

* * *

†Brief version of LBL-15487.

5. EFFECT OF TEMPERATURE AND DISPLACEMENT DAMAGE ON THE GROWTH OF AMORPHOUS LAYERS IN SILICON†

D. K. Sadana, J. Washburn, P. F. Byrne,‡ and N. W. Cheung‡

One of the undesirable effects of ion implantation is the temperature rise of semiconductor wafers during the implantation. This rise is caused by dissipation of kinetic energy of the ion beam before coming to rest in the wafer. If the wafer being implanted with beam currents of greater than several hundred μA has a poor thermal contact with its mounts in the implantation chamber, nonuniform heating of the wafer results. The effect of implantation temperature on the formation of amorphous layers in Si during ion implantation has therefore been systematically investigated by transmission electron microscopy (Fig. 5.1). The mechanisms of in-situ annealing suggested by J. Washburn et al.[1] have been further clarified. In order to investigate the effect of displacement damage on in-situ annealing, the sample of Fig. 5.1a was subsequently implanted at higher temperature (RT-400°C). It was found that at 200°C or above isolated small amorphous zones (<50 Å diameter) embedded in the crystalline matrix near the two amorphous/crystalline interfaces dissolved into the crystal, but the width of the 100% amorphous layer was not appreciably affected by further implantation at up to 200°C.

It is suggested that small amorphous zones surrounded by crystalline material can undergo radiation induced shrinkage at temperatures $\geq$100°C where elementary point defects are mobile.

* * *

†Brief version of LBL-15489.
‡Dept. of Electrical Engineering, U. C. Berkeley.
1. J. Washburn et al., LBL-14873; Nucl. Instrum. Meth., in press.

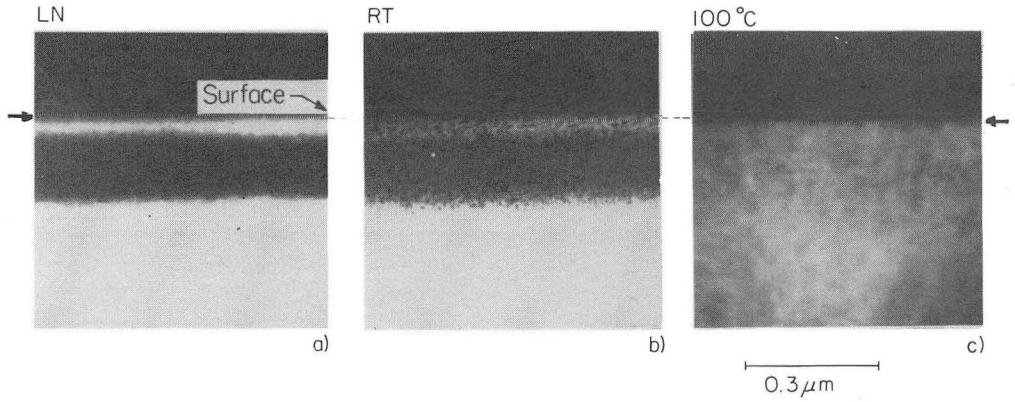

Fig. 5.1. The effect of implantation temperature on the formation of an amorphous layer in P implanted (111) Si. Dose: 3 x 10^{14} cm^{-2}; Energy: 120 keV; implantation temperature: a) LN, b) RT, and c) 100°C. (XBB 820-9449A)

6. A MODEL FOR REDISTRIBUTION OF PHOSPHORUS DURING ANNEALING OF HIGH DOSE ION IMPLANTED SILICON†

D. K. Sadana and J. Washburn

One of the reasons for widespread usage of arsenic as the n-type dopant in most implanted silicon devices despite its relatively low electrical activity at high doses is that it has predicable redistribution behavior on post implantation annealing. On the other hand, phosphorus doping can produce higher electrical activity, but its redistribution behavior on annealing is anomalous. In the present investigation, ion implantation of phosphorous into silicon has been investigated by cross-sectional transmission electron microscopy and secondary ion mass spectrometry.

In the case of high dose (>10^{15} cm^{-2}) implantation, in which the implanted region becomes amorphous and extends to the surface, it has been observed that the P atoms in the initially amorphous region do not redistribute on subsequent annealing while the P atoms below the initial amorphous crystalline interface diffuse rapidly into the Si substrate. The carrier concentration profiles from the annealed samples were found to follow the atomic profiles almost exactly over the depth range extending from the surface to where the original amorphous/crystalline interface existed. However, in the deeper regions, the electrical activity was found to be dependent on the annealing temperature. The different behavior of phosphorus in the initially amorphous and crystalline regions has been explained by a model which assumes that during recrystallization, the moving amorphous/crystalline interface incorporates both impurity as well as silicon atoms on substitutional sites. The P atoms in the deeper regions are believed to redistribute via an interstitial diffusion mechanism at low temperatures ($\leq$750°C) and eventually occupy substitutional sites at higher temperatures ($\geq$800°C).

* * *

†Brief version of LBL-15488.

7. DIFFRACTION EXTINCTION CONDITIONS FOR SILICON AND OTHER MATERIALS WITH DIAMOND GLIDE PLANES†

P. Ling, R. Caron, and J. Washburn

Although {200} Bragg reflections are kinematically forbidden in diamond cubic and spinel (i.e., Fd3m) structures, they often appear in electron diffraction patterns because of dynamical effects. In <100> and <012> diffraction patterns {200} spots cannot arise from multiple diffraction within the zeroth Laue zone. Our analysis shows that these spots can arise from double diffraction which must involve both higher and lower order Laue zones. We call this higher-lower Laue zone pair-double diffraction (HLLZPDD).

We derived the dynamical extinction conditions for these Fd3m structures using the method developed by Gjønnes and Moodie.[1] We showed that for the Fd3m diamond glide plane perpendicular to the x-y plane and passing through (0,1/8,0), structure factors are related by F (h,k,l) = i (h + k + l) F (h,k,l). For the four-fold screw axis perpendicular to the x-y plane and passing through (0,1/4,0), the relation is F (h,k,l) + i (h + k + l) F(k,h,l). In electron diffraction patterns, these spots often appear even when the extinction conditions are met. This is because of the non-parallel nature of the incident electron beam.

Reasons are given for spinel crystals having stronger {200} reflections than diamond cubic crystals in <001> diffraction patterns. Firstly, spinel has a denser reciprocal space than diamond cubic, so there are more possibilities for diffraction, contributing more dynamical intensity to {200} spots. Secondly, among allowed reflections, a greater portion of spinel reflections can contribute to HLLZPDD which results in {200} spots.

* * *

†Brief version of LBL-15490.

1. J. Gjønnes and A. F. Moodie, Acta Cryst. 19, 65 (1965).

1982 PUBLICATIONS AND REPORTS

Refereed Journals

1. T. D. Sands, J. Washburn, and R. Gronsky, "High Resolution Observations of Copper Vacancy Ordering in Chalcocite (Cu_2S) and the Transformation to Djurleite ($Cu_{1.97}$ to $Cu_{1.94}$ S)," Phys. Stat. Sol. (a) 72, 551 (1982); LBL-13746.

2. D. K. Sadana, J. Washburn, and G. R. Booker, "Recrystallization of Buried Amorphous Layers in P^+ Implanted Si and Associated Electrical Behavior," Phil. Mag. B 46, 611 (1982); LBL-14889.

3. D. K. Sadana, J. Washburn, T. Zee, and R. G. Wilson, "Effect of O on Cr Redistribution in Ion Implanted GaAs," J. Appl. Phys. 53, 6413 (1982); LBL-13527.

4. P. F. Byrne, N. W. Cheung, and D. K. Sadana, "Mega-Volt Arsenic Implantation into Si," Thin Solid Films 95, 363 (1982).

5. M. Maenpaa, T. F. Kuech, M-A. Nicolet, S. S. Lau and D. K. Sadana, "The Heteroepitaxy of Ge on Si: A comparison of Chemical Vapor and Vacuum Deposited Layers," J. Appl. Phys. 53, 1076 (1982).

6. M. Maenpaa, L. S. Hung, S. S. Lau and D. K. Sadana, "Epitaxial Reordering of Ion-Irradiated $NiSi_2$ Layers," Thin Solid Films 87, 277 (1982).

7. P. F. Byrne, N. W. Cheung and D. K. Sadana, "11 MeV As Implantation into Si," Appl. Phys. Lett. 41, 537 (1982).

LBL Reports

1. M. Current and D. K. Sadana, "Materials Characterization for Ion Implantation," VLSI Electronics: Microstructure Science, Vol. 6, Chapter 7, edited by N. G. Einspruch and G. L. Larrabee, Academic Press, in press, LBL-15014.

2. T. D. Sands, R. Gronsky, and J. Washburn, "High Resolution Study of the Chalcocite (Cu_2S)-Djurleite ($Cu_{1.97}S$) Transformation in $Cu_{2-x}S$ Thin Films," presented at the Sixteenth IEEE Photovoltaic Specialists Conference, San Diego, CA, September 1982, in press, LBL-15063.

3. D. K. Sadana, "Cross-Sectional Transmission Electron Microscopy of Semiconductors," 18th University Series on Ceramic Science Advances in Materials Characterization, Alfred University, New York, August 16-18, 1982, in press, LBL-15085.

4. C. S. Murty, "Crystalline to Amorphous Transformation in Silicon," Ph.D. thesis, LBL-14923.

5. J. Washburn, C. Murty, D. K. Sadana, P. Byrne, R. Gronsky, N. Cheung, and R. Kilaas, "The Crystalline to Amorphous Transformation," Nucl. Instrum. Meth., in press, LBL-14873.

6. D. K. Sadana, N. R. Wu, J. Washburn, M. I. Current, A. Morgan, D. Reed, and M. Maenpaa, "The Effect of Recoiled O on Damage Regrowth and Electrical Properties of Through-Oxide Implanted Si," Nucl. Instrum. Meth., in press, LBL-15086.

7. D. K. Sadana, J. Washburn, and C. W. Magee, "Substitutional Placement of Phosphorus in Ion Implanted Silicon by Recrystallizing Amorphous Crystalline Interface," J. Appl. Phys., in press, LBL-15488.

8. D. K. Sadana, J. Washburn, P. F. Byrne, and N. W. Cheung, "Damage and In Situ Annealing During Ion Implantation," Defects in Semiconductors (Materials Research Society Symposium), Vol. 4, in press, LBL-15489.

Invited Talks

1. D. K. Sadana, "Profiling of Ion Implanted Semiconductor Surfaces by TEM, RBS, SIMS and Electrical Measurements," Microelectronics Center of North Carolina, Research Triangle Park, Raleigh, North Carolina, December 7, 1982.

2. D. K. Sadana, "Structural, Electrical and Compositional Characterization of Interfaces in Ion Implanted and Processed Semiconductors," presented at the Naval Research Labs., Washington, D.C., November 5, 1982.

3. D. K. Sadana, "Ion Implanted Generated Microdefects and Their Electrical Properties," National Semiconductor, Santa Clara, CA, June 4, 1982.

4. D. K. Sadana, "Materials Characterization for Ion Implantation," U.C. Extension Course, Hyatt Rickey Hotel, Palo Alto, CA, April 20, 1982.

5. D. K. Sadana, "Recrystallization of Amorphous Layers in Ion Implanted Si and GaAs and Associated Electrical Effects," University of Southern California, Los Angeles, CA, March 12, 1982.

d. Chemical Properties and Processing of Refractory Ceramics*

Lutgard C. De Jonghe, Investigator

1. PROCESSING OF CERAMICS

Lutgard C. De Jonghe

Many ceramics and refractories are prepared by the sintering of component oxides. A variety of chemical reactions and microstructural developments occurs during the densification of such mixed powders, including the transient or permanent formation of compounds and liquids. These reactions may significantly affect the densification rates and the microstructural developments of the ceramic body.

The first step in studying such reactions has been the study of the densification of a simple pseudo-binary system: MgF_2 + CaF_2. This system exhibits a eutectic at 918°C and does not form compounds. Dialotometric measurements and examination of microstructures of power mixtures containing up to 5 wt% CaF_2 showed that CaF_2 significantly enhanced densification of MgF_2 well below the eutectic temperature. This result could be attributed to an increase in the solid state grain boundary transport rate, caused by the presence of small amounts of calcium fluoride.[1] The significant increase in solid state grain boundary transport rates below the eutectic temperature of a binary system should be a general phenomenon that could be usefully exploited in ceramic processing, since it could lead to enhanced densification without the abnormal grain growth caused by the presence of active liquid phases.

The system under investigation at present is CaO-Al_2O_3. Enhanced pre-eutectic densification rates, around 1350°C, are not observed in the system, but they are observed in, e.g., Cu_2O-Al_2O_3. The decrease of the densification rates of Al_2O_3 caused by CaO are thought to be due to rapid and extensive formation of very stable, intergranular compounds such as $CaO{\cdot}(Al_2O_3)_6$. The reactions between CaO and Al_2O_3 are described below in more detail.

* * *

1. S. C. Hu and L. C. De Jonghe, LBL-12849, April 1982.

2. STRUCTURE AND NONSTOICHIOMETRY OF CALCIUM ALUMINATES†

Herbert Schmid and Lutgard C. De Jonghe

Calcium aluminates form the basis of many refractory and high temperature cements. The phase relationships in this system have been studied by several investigators; the most recent phase diagrams now include C_3A, CA, CA_2, and CA_6(C = CaO; A = Al_2O_3).

In the present work, ceramic alloys were prepared by reacting dense, polycrystalline alumina with a liquid of approximately eutectic composition, at 1530°C, for about 4 hours. The reaction zone was then examined by transmission electron microscopy and by x-ray microanalysis in an analytical transmission electron microscope. The foils show planar defects in the CA_6 phase similar to those found in sodium beta and beta aluminas.[1] The observed planar defects are syntactic intergrowths whose structure could be described by the formalism developed by Braun.[3] Planar defects were found on (OO.1) planes (Fig. 2.1). The lattice fringe images of faulted areas exhibit variations in spacings where the faults occur. In large CA_6 grains, syntactic intergrowth regions could be found with a periodicity significantly larger than that of the CA_6 matrix. Non-periodic arrays of syntact intergrowths were also found (Fig. 2.2).

Toward the boundaries of some large grains, irregularities in the fringe images could be found. Examples of the various types of irregularities are shown in Fig. 2.3. They include irregular intergrowths, Fig. 2.3a; gradual disappearance of fringe contrast, Fig. 2.3b and 2.3c; or switching to a different fringe spacing, Fig. 2.3c. Micro-x-ray analysis revealed that these fringe irregularities were linked to a decrease in the CaO contents.

The observation indicated that the crystallography of CA_x compounds may be described in a manner analogous to that of the barium hexaferrites.[2]

* * *

†Brief version of LBL-14291.

1. L. C. De Jonghe, J. Mat. Sci. 12, 497 (1977).
2. P. B. Braun, Philips Res. Rep. 12, 491 (1957).

*This work was supported by the Director, Office of Energy Research, Office of Basic Energy Sciences, Materials Sciences Division of the U.S. Department of Energy under Contract No. DE-AC03-76SF00098.

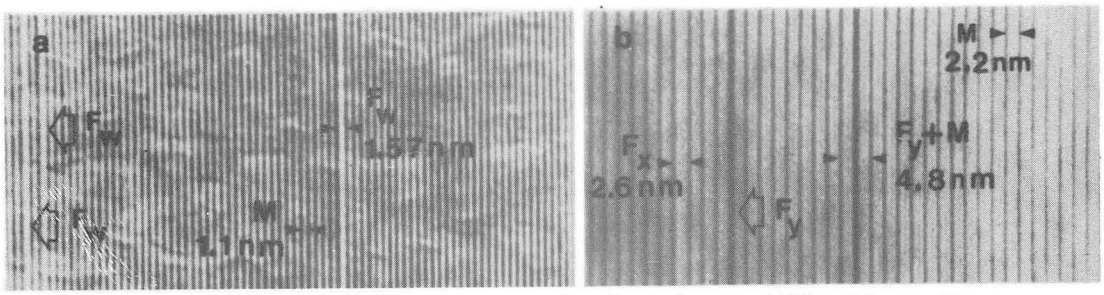

Fig. 2.1. Lattice fringe images and selected area diffraction pattern of faulted CA_6. (a) BF image showing 00.2 fringes of the CA_6 phase, and F_W intergrowths. (b) BF image showing 00.1 fringes of the CA_6 phase with F_x and F_y intergrowths. (XBB 824-3406)

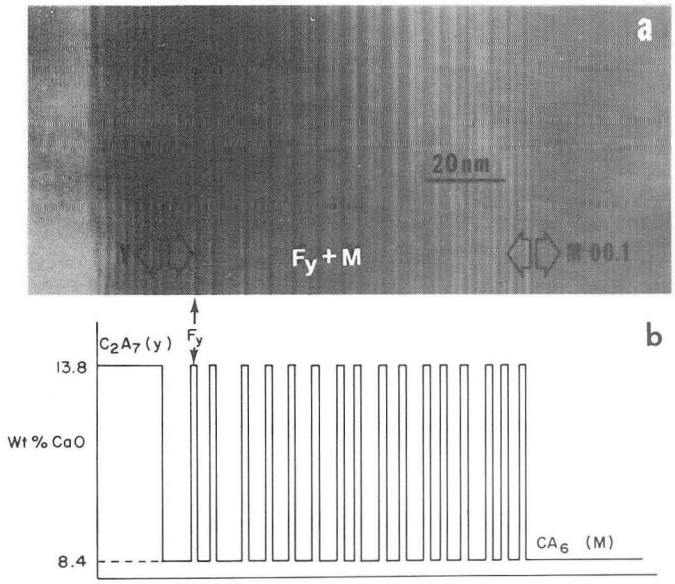

Fig. 2.2. (a) Non-periodic F_y intergrowth forming a transition zone between the M(CA_6) and the Y(C_2A_7) phase. (b) Schematic representation of the local CaO content in the Y-M transition zone imaged in (a). (XBB 824-3978)

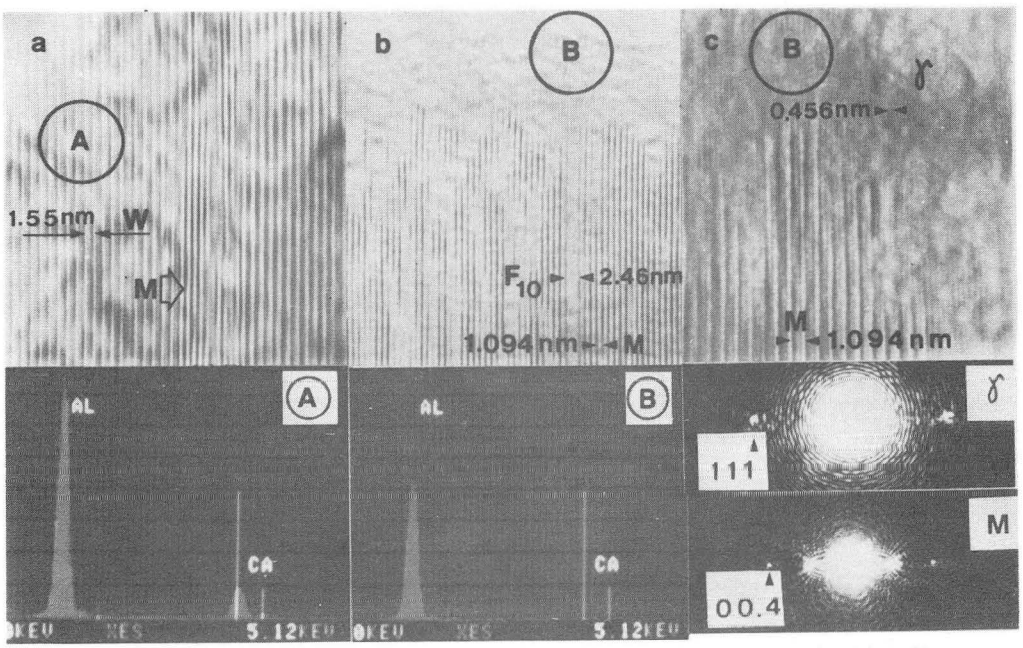

Fig. 2.3. (a) Irregular lattice fringe images due to terminating M intergrowths in a W matrix. The energy-dispersive x-ray spectra of the marked regions are also shown. (b) Terminating F_{2n} intergrowths in a transition zone between a CA_6 and CaO-free region. (c) Transition of M phase to γ alumina. (XBB 824-3398)

3. WORK IN PROGRESS

Whisker Growth During CO/CO_2 Reduction of Iron-Bearing Oxides

Mei Chang and Lutgard C. De Jonghe

When iron-bearing oxides such as cobalt ferrite are reduced with CO/CO_2 mixtures, profuse formation of metallic whiskers may be observed. It is found that the whisker diameter is determined by the overall reaction rate and can be changed to a larger or smaller diameter by changing the total gas pressure during the reduction. This indicated that the whisker morphology is a consequence of the difficulty of removing oxygen from under the advancing metal oxide interface. This difficulty is related to the rate at which CO is converted to CO_2 at the whisker base. This conversion is dependent on the presence of impurities that may catalyze or inhibit the CO to CO_2 reaction. A model is under development that takes into account interface oxygen diffusion and $CO-CO_2$ conversion catalysis to predict the morphology of the reduction product.

1982 PUBLICATIONS AND REPORTS

LBL Reports

1. H. Schmid and L. C. De Jonghe, "Structure and Non-Stoichiometry of Calcium Aluminates," LBL-94291.

2. S. C. Hu and L. C. De Jonghe, "Pre-Eutectic Densification in MgF_2-CaF_2," LBL-12849.

Invited Talks

1. L. C. De Jonghe, "Densification in MgF_2-CaF_2," Fifth International Meeting on Modern Ceramic Technologies, Lignano, Italy, June 1982.

e. Structure and Electrical Properties of Composite Materials*

Robert H. Bragg, Investigator

Introduction. The purpose of this work is to understand how the properties of hard carbons and soft carbons are related to their structure. The latter become physically soft when heated above about 2000°C; whereas the former, typified by glassy carbon (GC), are little affected by heating above 3000°C. Soft carbons are fairly well understood, but basic knowledge concerning hard carbons is scant. In this work GC is used as a model hard carbon because it is obtained as chemically pure (i.e., elemental carbon) monolithic solid suitable for a wide variety of measurements of physical properties. Results to date show that GC is composed of laths or ribbons of turbostratic graphite-like carbon layers that enclose a closed pore volume of about 30%. Whereas soft carbons are semimetallic conductors, GC has electrical properties like those of amorphous semiconductors. At low measurement temperatures, in material heated below 2000°C, there is evidence of one-dimensional electrical conduction.

1. DENSITY OF HEAT-TREATED GC†

Bhola N. Mehrotra and Robert H. Bragg

Polycrystalline carbons swell irreversibly about 1% when heated above their processing temperature, but in GC it reaches 15% for samples heated to 2750°C. It is important to understand this swelling in carbons because it can be deleterious in structural applications. It may be caused by internal gas pressures,[1] but a thermal stress mechanism has also been proposed.[2] Measurements of density, weight, length, and volume changes were made on samples heated in inert atmosphere in the range 1000-2700°C for three hours. Density changes caused by hydrostatic compression up to 1550 MPa (225,000 psi) were also measured.

Results: density decreases are mostly due to volume increases; dimensional changes (Fig. 1.1--open circles) are macroscopically isotropic and are not reversed by hydrostatic pressures. In-situ measurements (Fig. 1.2) show that during initial heating relief of residual stresses occurs, irreversible dilation occurs above 1000°C, and the upper cooling curve is followed thereafter in thermal cycling. This interpretation predicts the closed circles in Fig. 1.1. A detailed analysis shows that some swelling is caused by gas pressures, but most of it is because of thermal stress.

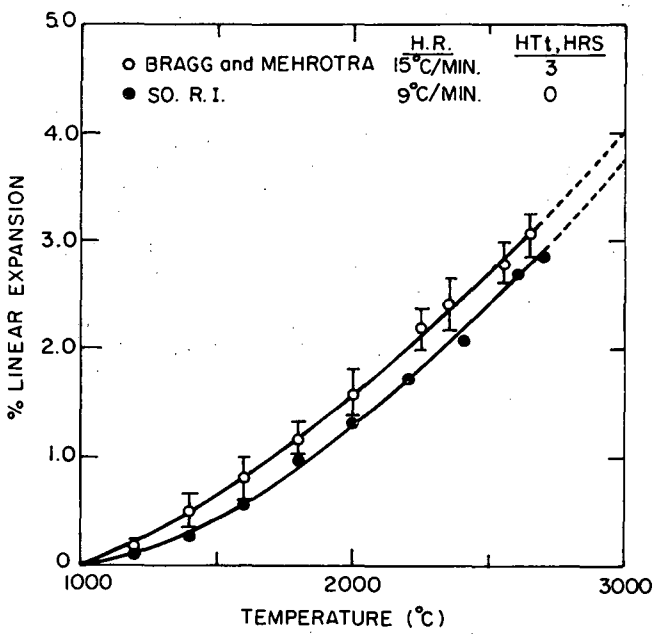

Fig. 1.1. Comparison of average linear dilation of GC with values calculated from in-situ measurements. (XBL 827-6012)

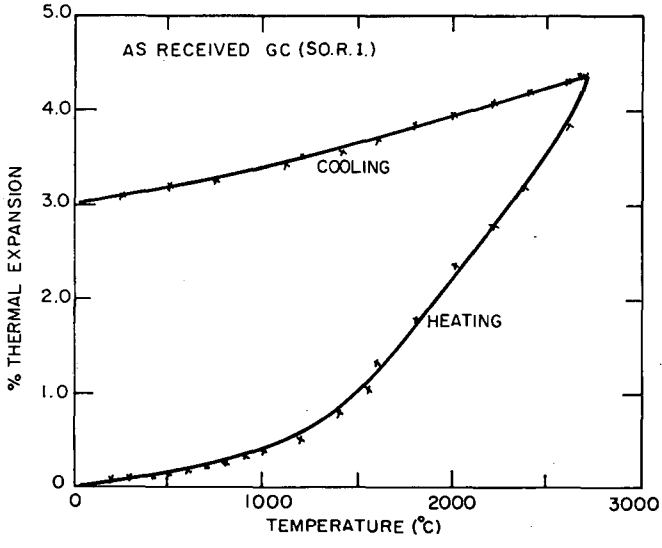

Fig. 1.2. In-situ thermal expansion measurements on GC. Room temperature to 2700°C and return. (XBL 827-6011)

* * *

†Brief version of LBL-15072, to be published in J. Mat. Sci.

1. D. B. Fischbach and M. E. Rorabaugh, High Temperature and High Pressure 9, 199 (1977).
2. R. H. Bragg and S. Bose, "Thermally Induced Density Changes in Glassy Carbon," 14th Biennial Carbon Conference, University Park, Pennsylvania, June 1970, p. 189.

*This work was supported by the Director, Office of Energy Research, Office of Basic Energy Sciences, Materials Sciences Division of the U. S. Department of Energy under Contract No. DE-AC03-76SF00098.

2. PORE GROWTH IN GLASSY CARBON†

Jeffrey Hoyt and Robert H. Bragg

During heat treatment of GC the specific surface area, S/V, decreases with an activation energy of about 60 ± 10 kcal/mole.[1] Most of the change is in S; thus, the internal pore structure of GC is coarsening. Another parameter to characterize pores is the radius of gyration, R_g, a dimension analogous to the quantity in classical mechanics of physical bodies, but with electron density replacing mass. Its geometrical interpretation can be very ambiguous,[2] but a kinetic study of R_g can reveal changes in average pore size, and possibly in pore size distribution.

Samples of GC were heated in pure argon or helium at 1600, 1800, 2100, and 2500°C for times ranging from 1 up to 48 hr. SAXS measurements were made using crystal monochromated CuK_α radiation in an apparatus employing linear position sensitive x-ray detection. The data were fitted to an expression in which R_g is related to the temperature and a diffusion coefficient D.

The results show the expected $t^{1/3}$ dependence of R_g. The average R_g increases with HTT with an activation energy of 51 ± 9 kcal/mole, compared with the value of 60 ± 10 kcal/mole determined from S/V kinetics.[1] These results lend strong support to the hypothesis that the vacancy migration is the mechanism that governs the coarsening of the pore structure.

* * *

†Brief version of LBL-14580.

1. S. Bose and R. H. Bragg, Carbon 19, 289 (1981).
2. A. Guinier and G. Fournet, Small Angle Scattering of X-rays, Wiley, London (1955).

3. WORK IN PROGRESS

D. Baker is preparing three papers for publication based on his Ph.D. dissertation, and also concentrating on one-dimensionality and other anomalous aspects of electrical properties in GC. A collaboration has been initiated with Drs. James Rhyne and Jack Rush, Reactor Radiation Division, National Bureau of Standards, to obtain neutron diffraction patterns of GC samples. Efforts to determine the amount and bonding of hydrogen in GC were initiated in 1981 via a second collaboration, with Professor Cary Maciel at the Regional Center for Nuclear Magnetic Resonance at Colorado State University, but the results thus far have not been interpretable. Very recently, a third collaboration has been initiated with Dr. J. D. Jorgensen, Neutron Scattering Group, Material Science and Technology Division at Argonne National Laboratory, to obtain measurements of total neutron scattering cross section of GC where the sensitivity for hydrogen is very large. Kinetic studies of the loss of hydrogen from GC are envisaged. Both L. G. Henry and B. N. Mehrotra are involved in this work. A. Pearson is doing a computer simulation of the effect of crystallite size on radial distribution functions. The principal investigator will be on sababatical leave during January-June 1983. About three months will be spent at CNRS, University of Bordeaux, to do work on magnetic susceptibility of GC.

1982 PUBLICATIONS AND REPORTS

Other Publications

1. R. H. Bragg, "Is Graphitization the Result of a Thermal Decomposition Reaction," 35th Pacific Coast Regional Meeting, American Ceramic Society, Seattle, Washington, October 26-28, 1982.

2. D. F. Baker and R. H. Bragg, "Electrical Conductivity in Glassy Carbon," 35th Pacific Coast Regional Meeting, American Ceramic Society, Seattle, Washington, October 26-28, 1982.

3. L. G. Henry and R. H. Bragg, "The Measurement of Specific Surface Area and Pore Size in Some Ceramic Materials Using a Modified General Electric (GE) Diffractometer," 35th Pacific Coast Regional Meeting, American Ceramic Society, Seattle, Washington, October 26-28, 1982.

4. J. J. Hoyt and R. H. Bragg, "A Study of Pore Growth in Glassy Carbon Using Small Angle X-ray Scattering," 35th Pacific Coast Regional Meeting, American Ceramic Society, Seattle, Washington, October 26-28, 1982.

5. B. N. Mehrotra and R. H. Bragg, "Volume Expansion and Weight Loss in Heat-Treated Glasslike Carbon (GC)," 35th Pacific Coast Regional Meeting, American Ceramic Society, Seattle, Washington, October 26-28, 1982.

LBL Reports

1. J. Hoyt, "A Study of Pore Growth in Glassy Carbon Using Small Angle X-Ray Scattering," M. S. thesis, LBL-14580.

2. B. N. Mehrotra, R. H. Bragg, and A. S. Rao, "Effect of Heat Treatment Temperature (HTT) on Density, Weight, and Volume of Glasslike Carbon (GC)," LBL-15072, submitted to J. Mat. Sci.

3. L. G. Henry and R. H. Bragg, "Comparative Determination of the Incoherent Scattering in Amorphous Materials," LBL-15611.

4. D. F. Baker and R. H. Bragg, "One-Dimensionality in Glassy Carbon," LBL-15445, submitted to Phys. Rev. Lett.

Invited Talks

1. D. F. Baker and R. H. Bragg, "Electrical Properties of Glassy Carbon," International Symposium on Carbon: New Processing and Applications, Toyohashi, Japan, November 1-4, 1982, Extended Abstracts 2B08, p. 208, LBL-14938.

f. High Temperature Oxidation and Corrosion of Materials *

David P. Whittle, Investigator †

Introduction. The principal aim of this program is to establish mechanisms of materials degradation in environments associated with the combustion of fossil fuels and relating these mechanisms to fundamental thermodynamic, kinetic, and metallurgical variables. A recent major achievement has been to establish the mechanism by which certain active additions to heat-resisting alloys improve the adherence of the protective scales. This is reported in article 1.

Sulfur is a critical impurity present in almost all fossil fuels. Its presence in the gaseous products of combustion can result in accelerated degradation of alloys. Article 4 demonstrates the rapid diffusion of sulfur species down oxide grain boundaries at rates much higher than previously reported. Articles 5 and 6 are concerned with the sulfur-induced hot corrosion which is due to the formation of molten deposits on alloy surfaces.

Multiphase diffusional growth during aluminizing, a thermochemical process by which Al is diffused into the surface of a material to improve high temperature oxidation resistance, is described in article 7. Finally, mathematical models have been developed to predict and interpret the concentration profiles developed when Ni-Co alloys are oxidized to produce a single phase oxide; these are described in article 8.

1. MECHANISM OF PEG GROWTH AND INFLUENCE ON SCALE ADHESION ‡

Horoun M. Hindam and David P. Whittle

It has been known, for many years, that minor additions of oxygen active elements (e.g., Ca, Sc, Y, Zr, Ce, Hf, etc.) or their oxide dispersions improve the scaling properties of alloys. While there is no general consensus to explain the cause of this phenomenon, the evidence suggests that this improvement is because of the development of inwardly growing oxide pegs, which mechanically key the scale to the substrate. Detailed observations of different peg morphologies are used to define the conditions and mechanisms of growth.

Following standard preparation, samples were oxidized in static air at 1200°C. Specimen characterization included optical and scanning electron microscopy, x-ray diffraction, and electron probe microanalysis. A deep etching technique, based on partial dissolution of the alloy, was employed to examine peg morphologies.

Two distinct types of peg were identified based on morphological and growth criteria:

Class I. The growth of this peg type was observed on alloys forming external NiO scales containing small additions of oxygen active elements and is illustrated in Fig. 1.1a. Growth is controlled by solute and/or oxygen diffusion in the alloy. It can be interpreted by classical internal oxidation theory.[1]

Class II. The growth of this peg type was observed in Al_2O_3-forming alloys (Fe-10% Al) with small additions of Hf and is illustrated in Fig. 1.1b. Its development can be rationalized by short circuit diffusion in an host scale.

* * *

‡Brief version of LBL-15039.

1. J. H. Swisher, "Oxidation of Metals and Alloys," edited by D. L. Douglass, American Society for Metals, Metals Park, Ohio, 1971, p. 235.

*This work was supported by the Director, Office of Energy Research, Office of Basic Energy Sciences, Materials Sciences Division of the U. S. Department of Energy under Contract No. DE-AC03-76SF00098.

†Dr. Whittle died in July 1982. This report has been prepared by Dr. Stephen Smith. Since Dr. Whittle's death, Dr. J. Stringer of the Electric Power Research Institute has been acting as technical advisor, pending the appointment of a full-time successor.

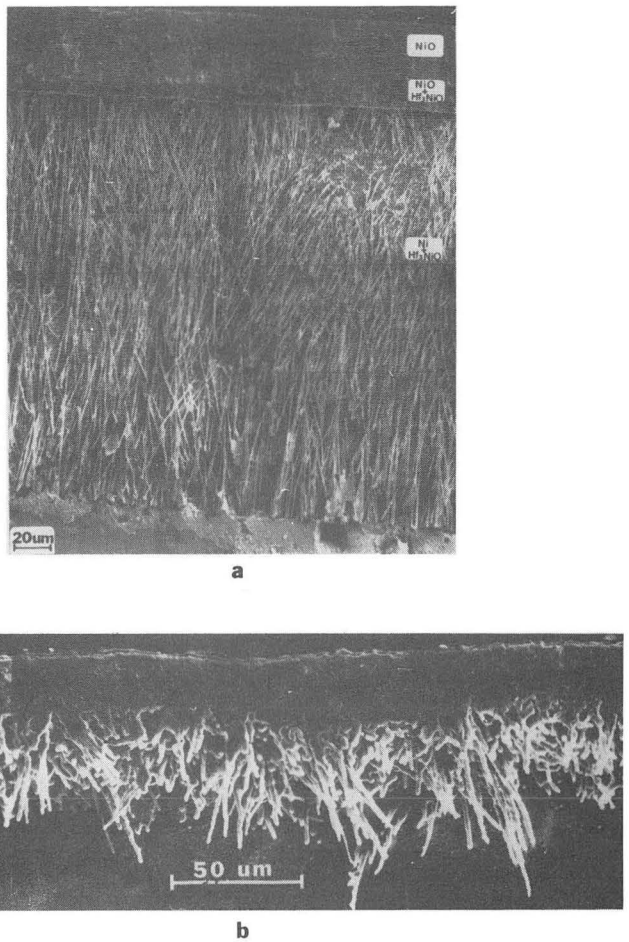

Fig. 1.1. Oxide peg morphologies: (a) Ni-2Hf alloy and (b) Fe-10Al-1Hf alloy. (XBB 831-996)

2. MICROSTRUCTURE AND GROWTH OF PROTECTIVE Cr_2O_3 AND Al_2O_3 SCALES AT HIGH TEMPERATURE[‡]

David P. Whittle and Haroun M. Hindam

Current understanding of the complex interrelationships between growth kinetics, scale microstructure, and scale adhesion for Cr_2O_3 and Al_2O_3 protective scales has been critically reviewed.

A close interaction between the above parameters was demonstrated, although this is probably not of major importance in terms of the growth rate of the protective oxide. This is especially true in the case of Al_2O_3, since growth at the fastest observed rate does not correspond to a major loss in material in many instances. The spread of growth rates observed for Cr_2O_3 scale does encompass unacceptedly high rates (Fig. 2.1).

Breakdown of the protective scale, especially by mechanical spallation, is critically dependent on the details of the microstructure, and the ability of active element or oxide dispersion additions to modify this is of clear technological importance. However, without a clear understanding of the mechanism, it is unlikely that the maximum benefit of these effects can be achieved. The work described in the later part of this review points to the right direction.

* * *

[‡]Brief version of LBL-14296.

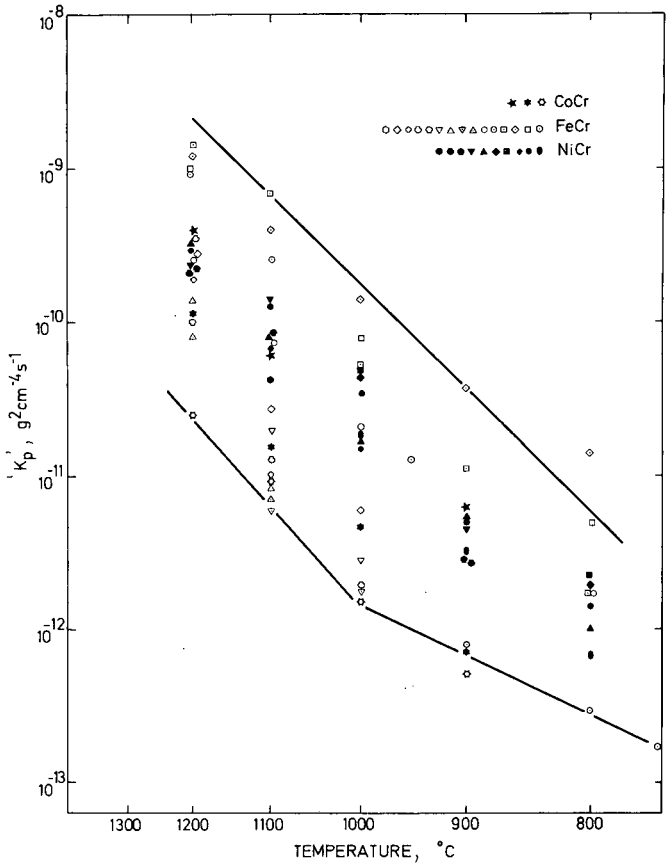

Fig. 2.1. Summary of reported parabolic rate constants for the growth of Cr_2O_3 on binary Cr-containing alloys. (XBL 821-7735)

3. THE INFLUENCE OF ALLOY MICROSTRUCTURE ON Al_2O_3 PEG MORPHOLOGIES IN CoCrAl ALLOYS AND COATINGS‡

Rajendra D. Pendse and David P. Whittle

A comparative study of Al_2O_3-peg morphologies in oxidized Co-10Cr-11Al-1Hf as-cast and heat-treated alloys was carried out with a view to examine the role of alloy/coating microstructure in the pegging process. The fundamental aspects of selective oxidation have been developed in several earlier papers.[1]

The Y-containing alloys exhibited internal Al_2O_3 formation in two distinct zones. An upper zone of relatively short branched pegs directly connected to the scale and a lower zone of morphologically different sheaths developing along, and associated with, the microstructurally segregated yttride phase (Co_3Y) at α-β boundaries. The peg morphology in the Hf-alloys, which form no segregated Hf-containing phase, is not associated with the alloy phase boundaries, and no sheaths were found.

These observations in conjunction with previous observations of sheaths in vapor-deposited coatings are considered as evidence of an indirect influence of microstructure on the pegging process. A zone depleted of the β-phase was observed below the scale in all oxidized alloys. Simple observations and calculations were made with a view to elucidate the pegging mechanism; however, these are not entirely conclusive and additional work was suggested.

* * *

‡Brief version of LBL-14668.

1. See for example, D. P. Whittle, "High Temperature Corrosion of Aerospace Alloys," AGARD Conference Proceedings No. 120, p. 174-199, 1972.

4. SULFUR DIFFUSION IN OXIDE GRAIN BOUNDARIES‡

Frank C. Yang and David P. Whittle

As part of a study examining sulfur transport in oxides, we have fully oxidized iron coupons and then exposed them to an H_2-10% H_2S mixture at 870°C for 1 min.

Figure 4.1 shows the impact fracture cross section of the scale. The left side of the micrograph shows a region of intergranular fracture, whereas the right side shows a transgranular fracture area. Figures 4.1b and c are Auger electron maps of the same area. Consideration of these pictures clearly shows that sulfur is present only along the grain boundaries of the scale and is rapidly removed via argon sputtering into the grain. Even in this very short exposure, sulfur penetrated completely through the 1-mm-thick sample.

These results indicate an effective diffusion coefficient of at least 10^{-4} cm^2 sec^{-1}. This is considerably higher than reported for the diffusion of sulfur in wustite. Whether the value implied by the present results represent grain boundary diffusion or gaseous transport through fine pores at the oxide grain boundaries remains in question.

* * *

‡Brief version of LBL-14594.

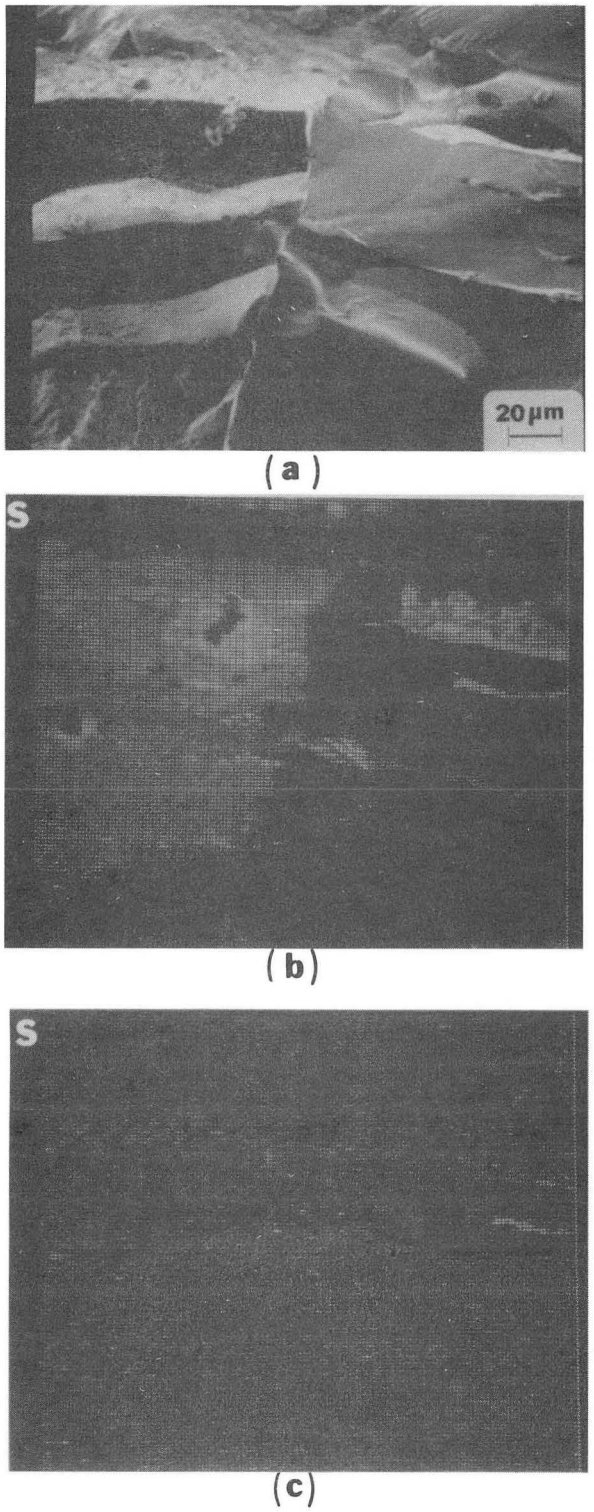

Fig. 4.1. Fracture reaction through iron oxide exposed to H_2 - 10% H_2S for 1 min at 870°C, showing sulfur penetration through the grain boundaries. (a) Image, (b) sulfur map, and (c) sulfur map after 5 min argon ion sputtering. (XBB 831-994)

5. THE EFFECTS OF SO_2 and SO_3 ON THE Na_2SO_4 INDUCED CORROSION OF NICKEL[‡]

Ajaya K. Misra and David P. Whittle

Hot corrosion in gas turbines operating in marine environments is attributed to the deposition of Na_2SO_4 on the blade and vane surfaces. The temperature of operation and SO_3 concentration in the turbine atmosphere determine the corrosion behavior of the component. The effects of SO_2 and SO_3 in the environment on the hot corrosion of Ni in the temperature range 750 to 950°C have been studied.

Below the melting point of Na_2SO_4 (880°C), rapid corrosion takes place by the formation of a Na_2SO_4-$NiSO_4$ melt that penetrates the oxide layer and reaches the metal surface where further dissolution takes place. At temperatures above the melting point of Na_2SO_4, degradation occurs because of a dissolution reprecipitation mechanism.

In all cases the final corrosion product is dependent upon, and varies with, the SO_2 content in the atmosphere. (It is probable that the significant species in the atmosphere was SO_3, but this was not directly measured.) At low SO_2 concentrations at low temperatures, an intermixed oxide and sulfide scale with a layer of sulfide at the scale/metal interface are formed. Increasing the PSO_2 content results in the formation of a thick intermixed oxide-sulfide layer above a NiO layer; once again sulfide is found at the scale-metal interface.

* * *

[‡]Brief version of LBL-14597.

6. EFFECTS OF CHLORIDES ON Na_2SO_4-INDUCED HOT CORROSION OF MCrAl[‡]

Ajaya K. Misra and David P. Whittle

Chloride-containing species are often present in a typical gas turbine atmosphere. The major species are NaCl and HCl.[1] The effects of HCl and a Na_2SO_4-NaCl deposit on the hot corrosion of Ni and Co base alloys in the temperature range 750-850°C have been studied.

In this investigation, the corrosion experiments are carried out under very severe conditions at the level of HCl and the amount of Na_2SO_4-NaCl deposit are much higher than would occur under actual turbine operating conditions. The results do indicate the role of the chloride-containing species in the degradation of the alloys tested.

* * *

[‡]Brief version of LBL-14388.

1. F. J. Kohl, C. A. Stearns, and G. C. Fryburg, in Metal-Slag Gas Reactions and Processes, edited by Z. A. Foroulis and W. W. Smeltzer, Electrochemical Society, Princeton, NJ, 1975, p. 649.

7. MULTIPHASE DIFFUSIONAL GROWTH DURING ALUMINIZING‡

Hilary C. Akuezue and David P. Whittle

Aluminizing is a thermochemical process by which Al is diffused into the surface of a material to improve, for instance, its high temperature oxidation resistance. An aluminized sample, on exposure to high temperature oxidizing environments, forms a protective Al_2O_3 scale.

Six aluminizing packs with different Fe-50 w/o Al/Pure Al ratios were used to aluminize Fe-20 Cr samples at 850,900,950, and 1000°C. Mass change vs time curves were determined at all temperatures. The Al and Cr profiles as a function of depth were determined using electron probe microanalysis on polished cross sections.

Figure 7.1 shows etched cross sections of specimens aluminized in various packs for 5 hr at 900°C. This suggests that pack Al compositions affect the distribution of the aggregates and the relative depth of the consequent two-layered diffusion zone and determines the interface morphology. Near the terminal composition, the diffusion path runs parallel to the Al line of the corresponding ternary phase equilibrium diagram, but near the $\alpha\delta/\alpha\delta Fe+\beta_2$ line the diffusion paths run parallel to the Cr line. This work is part of an overall effort to use diffusion data and kinetic data from aluminizing as well as phase equilibria in the design of diffusional coatings for high temperature corrosion protection.

* * *

‡Brief version of LBL-15058.

8. HIGH TEMPERATURE OXIDATION OF Ni-Co ALLOY

Peggy Y. Hou and David P. Whittle

Ni and Co form a near ideal solid solution over their entire composition range above 900°C. The objectives of this project is to use this relatively simple system to gain a quantitative understanding of binary alloy oxidation.

Ni Co alloys in the composition range 1-80% Co are being studied in high- and low-oxygen activity atmospheres. Kinetic data are measured thermogravimetrically, and diffusion profiles are obtained using electron probe microanalysis. Theoretical calculations make use of the transport equations originally proposed by Wagner.[1] Diffusion in the alloy is considered negligible when oxidation occurs in high oxygen activity atmospheres. However, cation transport in the scale as well as diffusion in the alloy must be considered for oxidation in low-oxygen activity atmospheres. Cation diffusion in the scale is solved using a total defect model developed by Whittle et al.[2]

Theoretical calculations of Co concentration profiles in the scales oxidized under 1 atm O_2 show good agreement with experimentally measured data (Fig. 8.1). However, oxidation in the low-oxygen activity environments, resulted in measured profiles that deviated from those predicted using this model. This is probably because of inward anion transport leading to internal oxidation becoming more prevalent in low P_{O_2} atmospheres, a factor not considered in the model.

* * *

1. C. Wagner, Corrosion Science 9, 91 (1969).
2. D. P. Whittle, F. Gesmundo, and F. Viani, Oxid. Met. 16, 1-2, 81 (1981).

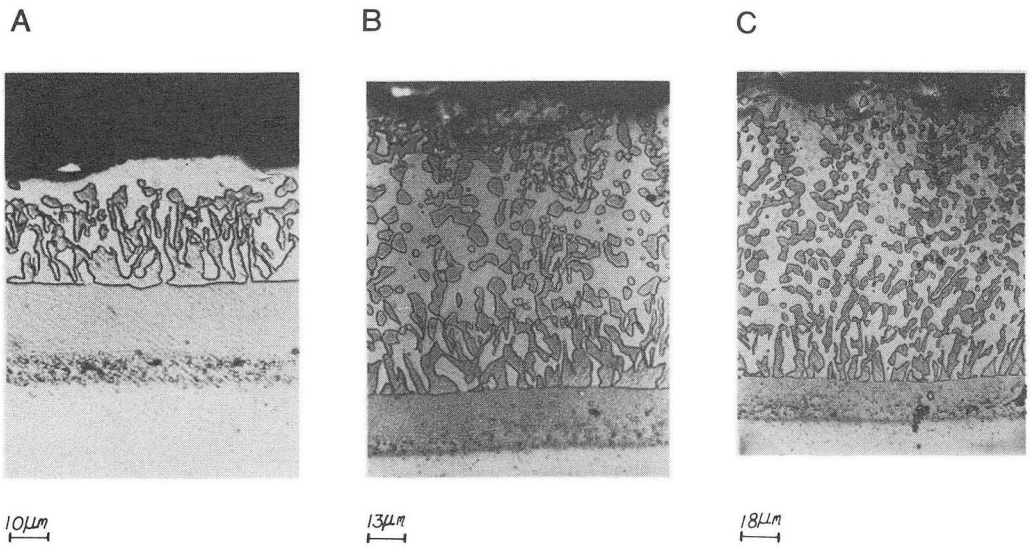

Fig. 7.1. Cross sections of Fe-20Cr samples aluminized in various parts for 5 hr at 900°C. (XBB 820-10998)

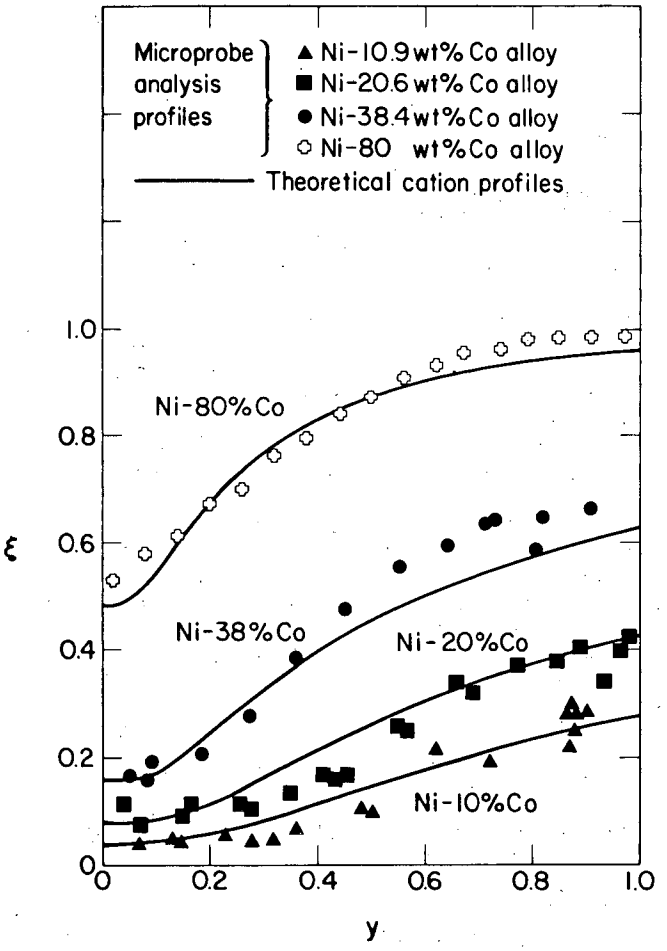

Fig. 8.1. Comparison at theoretical and experimental Co profiles in (Ni,Co)O scales. Oxidized at 1000°C in 1 atm O_X. (XBL 832-8037)

1982 PUBLICATIONS AND REPORTS

Refereed Journals

1. H. Hindam and D. P. Whittle, "Corrosion Behavior of Cr_2O_3 Former Alloys in $H_2/H_2S/H_2O$ Atmospheres," Corros.-NACE 38, 32 (1982).

2. H. Hindam and D. P. Whittle, "Peg Formation by Short-Circuit Diffusion in Al_2O_3 Scales Containing Oxide Dispersions," J. Electrochem. Soc. 129, 1147 (1982).

3. A. K. Misra, D. P. Whittle, and W. L. Worrel, "Thermodynamics of Molten Sulfate Mixtures," J. Electrochem. Soc. 9, 8 (1982).

LBL Reports

1. D. P. Whittle and H. Hindam, "Microstructure and Growth of Protective Cr_2O_3 and Al_2O_3 Scales at High Temperatures," LBL-14296.

2. H. Hindam and D. P. Whittle, "High Temperature Internal Oxidation of Dilute Ni-Al Alloys," LBL-14389.

3. H. Hindam and D. P. Whittle, "Evidence for the Growth Mechanisms of Cr_2O_3 at Low Oxygen Potentials," LBL-14834.

4. H. Hindam and D. P. Whittle, "Microstructure, Adhesion and Growth Kinetics of Protective Scales on Metal and Alloys," LBL-15004.

5. H. Hindam and D. P. Whittle, "Mechanism of Peg Growth and Influence on Scale Adhesion," LBL-15039.

6. A. K. Misra and D. P. Whittle, "Effect of Chlorides on Na_2SO_4 - Induced Hot Corrosion of MCrAl's," LBL-14388.

7. F. C. Yang and D. P. Whittle, "Sulfur Diffusion in Oxide Grain Boundaries," LBL-14594.

8. A. K. Misra and D. P. Whittle, "The Effects of SO_2 on the Na_2SO_4 - Induced Corrosion of Nickel," LBL-14597.

9. H. C. Akuezue and D. P. Whittle, "Surface Al Composition During Pack Aluminizing--A Quantitative Model," LBL-15058.

Invited Talks

1. D. P. Whittle and H. Hindam, Conference on Corrosion-Erosion-Wear of Materials in Emerging Fossils Energy Systems, Berkeley, California, January 1982.

2. H. Hindam and D. P. Whittle, "Characterization, Amelioration and Mechanism of Scale Adhesion to Metallic Substrates Subjected to Agressive Environments," Canadian Metal Chemistry Conference, Kingston, Ontario, June 1982.

3. H. Hindam and D. P. Whittle, "Mechanism of Peg Growth and Influence on Scale Adhesion," Japanese Institute for Metals, Third International Symposium on High Temperature Corrosion of Metals, Tokyo, Japan, November 1982.

g. Ceramic Interfaces*

Andreas M. Glaeser, Investigator

Introduction. Numerous properties of ceramics are strongly dependent upon the nature of the microstructure. Consequently, successful fabrication of ceramics that meet design requirements necessitates that the microstructural characteristics (grain size, density, pore size, etc.) developed during processing and the stability of the microstructure during subsequent use be understood and controlled. The grain size and other microstructural characteristics are directly or indirectly affected by the rate of grain boundary motion. Thus control of microstructural evolution during processing and degradation during use requires that the grain boundary migration rate be controlled. The focus of this program is to further our understanding of the factors that influence or control the nature of the boundary migration process.

The grain boundary migration rate in a material can be characterized in terms of a parameter known as the boundary mobility, defined as the boundary velocity per unit driving force. The grain boundary mobility is affected by interactions between the grain boundary and solutes, pores, precipitates, etc. Although reported boundary mobilities for a specific material may differ by orders of magnitude at a particular temperature, the nature of the interactions responsible for these differences, and consequently their effects on microstructure development, are poorly understood. The development of an experimental technique[1] to permit these interactions to be isolated for high temperature oxides has made possible an investigation of the migration behavior of individual grain boundaries in theoretically dense MgO-doped Al_2O_3.

* * *

1. A. M. Glaeser and J. C. Chen, J. Am. Ceram. Soc. 65 (7), (1982).

1. GRAIN BOUNDARY MOBILITY MEASUREMENTS IN MgO-DOPED Al_2O_3†

Andreas M. Glaeser

When undoped Al_2O_3 is processed by conventional powder processing techniques, a porous, and often coarse grained material is produced. In contrast, small additions of MgO permit preparation of fine grain size, theoretically dense material having superior optical and mechanical properties. At present, the mechanism by which MgO additions modify the course of microstructural evolution is still a subject of controversy. One explanation is that (MgO) solute-boundary interactions reduce the grain boundary mobility (relative to that in undoped material), and consequently produce conditions favoring pore-grain boundary attachment and complete densification. The alternate explanation suggests that MgO additions enhance the pore mobility (relative to that in undoped material), thus promoting pore-grain boundary attachment and permitting theoretical density to be reached. Resolution of this controversy would constitute an important first step in the development of a scientific basis for testing and selecting appropriate additives for other ceramic systems.

In order to determine the effects of MgO additions on pore and boundary mobilities, the solute-boundary interaction and pore-boundary interaction (in doped and undoped material) must be isolated and characterized. In the present work, a small coarse-grained region is introduced into an otherwise pore-free fine-grained MgO-doped Al_2O_3 sample by means of a laser melting technique. Coarse grains produced in this way, as well as those which develop naturally in the material, are subject to a larger driving force than the average sized matrix grains and thus coarsen at a substantially higher rate, consuming the surrounding matrix. Grain boundary migration can be characterized by monitoring the growth rates of the coarse grains. Systematic variation of a single microstructural characteristic (such as the grain size, solute content, or volume fraction porosity), permits the effect of driving force, solutes, or pores on boundary migration rates to be determined. To date, work has focused on investigation of the solute-boundary interaction.

The growth rates of laser-introduced abnormal coarse grains, naturally occurring coarse grains, and in some cases those of the finer matrix grains in MgO doped Al_2O_3 have been measured at temperatures from 1600-1900°C (Table 1.1). The growth rates of both types of coarse grains were generally spatially nonuniform, maximum and minimum mobilities differing by more than an order of magnitude; minimum growth rates and hence boundary mobilities were often too low to be measurable. A few cases of uniform boundary migration were observed; these occurred more frequently as the anneal temperature increased. The maximum mobilities and other aspects of the migration behavior of the two types of coarse grains were similar (Table 1.1) over the entire temperature range investigated. The maximum observed mobilites in this study exceed those reported in previous studies conducted on porous doped material and are comparable to those observed in porous undoped Al_2O_3. One possible interpretation of this result is that the maximum mobilities observed do not reflect a Mg-boundary interaction, i.e., that these boundaries have broken away from the segregated solute cloud. The observation that the maximum mobilities of coarse grains exceed that of the "average" matrix grains is

*This work was supported by the Director, Office of Energy Research, Office of Basic Energy Sciences, Materials Sciences Division of the U. S. Department of Energy under Contract No. DE-AC03-76SF00098.

Table 1.1. Summary of Calculated Grain Mobilities.

Temp (°C)	M_{max} laser nucleated (cm^3/dyne sec)	M_{max} naturally nucleated	$\overline{M}$ (from grain growth rate)
1600	3.0×10^{13}	2.5×10^{-13}	2.0×10^{-14}
1700	8.6×10^{-13}	1.2×10^{-12}	(not yet measured)
1800	2.3×10^{-12}	3.8×10^{-12}	1.7×10^{-13}
1900	1.4×10^{-11}	6.2×10^{-12}	(not yet measured)

consistent with this hypothesis and furthermore suggests that boundary breakaway may be the event that catalyzes abnormal grain growth. Synthesis of samples with varying MgO content is in progress; measurements of the concentration dependence of both the maximum and average mobility should test the validity of the proposed interpretation of the data.

* * *

†Brief version of LBL-15406 and J. C. Chen and A. M. Glaeser, "Grain Boundary Mobility Measurements in MgO Doped Al_3O_3," 35th Pacific Coast Regional Meeting, American Ceramic Society, Seattle, Washington, October 26-29, 1982.

1982 PUBLICATIONS AND REPORTS

Refereed Journals

1. A. M. Glaeser and J. C. Chen, "Technique for Measuring Grain Boundary Mobility: Application to MgO-Doped Al_2O_3," J. Am. Ceram.Soc. 65 (7), C97 (1982); LBL-13800.

Invited Talks

1. A. M. Glaeser, R. M. Cannon, and M. F. Yan, "Effect of Solutes on Grain Boundary Migration," Annual Meeting of American Ceramic Society, International Symposium on Grain Boundaries and Interfaces in Ceramics, Cincinnati, Ohio, May 2-5, 1982.

2. A. M. Glaeser and J. C. Chen, "Technique for Measuring Grain Boundary Mobility in Ceramics," 35th Pacific Coast Regional Meeting, American Ceramic Society, Seattle, Washington, October 26-29, 1982.

3. J. C. Chen and A. M. Glaeser, "Grain Boundary Mobility Measurements in MgO Doped Al_2O_3," 35th Pacific Coast Regional Meeting, American Ceramic Society, Seattle, Washington, October 26-29, 1982.

4. Engineering Materials

a. Abrasive, Erosive, and Sliding Wear of Materials*

Iain Finnie, Investigator

Introduction. The damage done by wear has been estimated to represent about 6% of our gross national product. By contrast, about 0.02% of the national research dollar is invested in wear research.[1] As a result, progress in understanding wear has developed much less rapidly than in other areas of science and engineering. Most of our current knowledge of wear is based on empirical tests that simulate the behavior of specific components. This type of information is of little value in understanding the basic mechanisms of wear or in predicting the wear to be expected in new applications. For this reason the purpose of the present work is to obtain a more detailed understanding of wear mechanisms. In the period covered by this report, attention has been given to the sliding wear of dissimilar metals, abrasive wear of metals, and the preparation of an overview to summarize the economic importance of wear, its various categories and the extent of our current knowledge.

* * *

1. E. Rabinowicz, Mech. Eng. 104, 62 (1983).†

1. SLIDING WEAR OF DISSIMILAR METALS

Iain Finnie, Susan Chevez, and Remy Glardon

The traditional explanation of sliding wear, which was based on adhesion of contacting asperities, has been questioned in recent years. Our work in the past year confirmed that the accumulation of subsurface plastic deformation followed by crack initiation and propagation is the primary mechanism of material removal in this type of wear.

Our research has followed two routes. One has involved the detailed investigation for five alloys of the macroscopic and microscopic aspects of the surface and subsurface features of the damage produced by sliding wear. At the same time we have been developing a test to simulate sliding wear with a larger scale mechanical test. This involves loading specimens in combined compression and shear with alternating loads.

Preliminary indications are that the simple mechanical test provides considerable insight into the processes involved in sliding wear. A model of sliding wear has been developed, but critical tests have still to be made to confirm some of the assumptions involved.

* * *

†Brief version of R. Glardon and I. Finnie, ASME J. Eng. Mat. Technol. 105, 36 (1983) and R. Glardon and I. Finnie. ASME J. Eng. Mat. Technol. 105, 31 (1983).

2. ABRASIVE WEAR†

Iain Finnie and S. Soemantri

Abrasive wear continues to be the predominant wear problem in industry. The choice of materials for abrasive wear resistance is inadequately understood. A major problem is that different types of abrasive wear may occur in service with different material properties governing wear resistance in these different regimes.

During the past year we have studied different types of abrasive wear tests at ambient and elevated temperature. Limitations of several test techniques have been observed, and the role of many variables has been studied. In particular, the role of temperature in several types of abrasive wear tests has been investigated.

Conventional theories of abrasive wear have been shown to be inadequate for explaining experimental results. Our attempts to produce a more general approach are drawing on experience also with erosive wear and hopefully will lead to an approach that unifies the erosive and abrasive wear phenomenon.

* * *

†Brief version of A. Misra and I. Finnie, ASME J. Eng. Mat. Technol. 104, 94 (1982).

3. AN OVERVIEW OF WEAR

I. Finnie and A. McGee

Because of the general neglect of wear research alluded to in the introduction, it was thought worthwhile to prepare a general review. This covers the economic importance of wear, the classification of wear into its different categories, and a brief summary of the state of knowledge on different aspects of wear.

Our approach is to draw literature on the economic importance of wear from various sources and to attempt our own classification of wear into different categories. There is a danger in oversimplification when subdividing any field, yet one

*This work was supported by the Director, Office of Energy Research, Office of Basic Energy Sciences, Materials Sciences Division of the U. S. Department of Energy under Contract No. DE-AC03-76SF00098.

has to compartmentalize wear in order to develop analyses of individual mechanisms. In reviewing different areas of wear, our emphasis has been on unsolved problems and areas that are poorly understood.

The final report which is now in preparation is based on preliminary versions[1] delivered as seminars or invited papers. It is hoped that it will stimulate additional research in the field of wear.

* * *

1. I. Finnie, Mechanisms of Wear, Proceedings of the First International Conference on Production Engineering, Design and Control, Alexandria, Egypt, December 1980.

1982 PUBLICATIONS AND REPORTS

Refereed Journals

1. A. Misra and I. Finnie, "A Review of the Abrasive Wear of Metals," ASME J. Eng. Mat. Technol. 104, 94 (1982).

b. Erosion-Corrosion Wear Program*

Alan V. Levy, Investigator

1. MEASUREMENT AND NUMERICAL MODELING OF TWO PHASE FLOW†

Joseph Humphrey, Farzad Pourahmadi, Michel Arnal, and Alan Levy

The purpose of this research is to develop and apply a numerical model that will predict the behavior of two phase flows composed of fluids with solid particulates in suspension. A model has been developed that is based on the continuum hypothesis for both phases. It applies to both laminar and turbulent flows and has been used to predict erosion in curved channels.

Figure 1.1 shows predictions of erosive wear in a curved duct (3-D flow) predicted with the 2-D model. Agreement with measured erosion is good in regions of the flow where 3-D effects are weak. The 2-D limitation is among the restrictions being removed, as is the assumption of a dilute particulate phase and fast particle response time. Curved channel-flow, erosive-wear maps have also been predicted which permit a relative evaluation of erosion through particle impingement as a function of the flow Reynolds number, particle response time, and bend angle of the curved channel. The experimental results in the literature that show large reductions in the turbulent kinetic energy of a turbulent two phase flow through viscous interaction effects were successfully predicted by the current model.

* * *

†Brief version of LBL-13808.

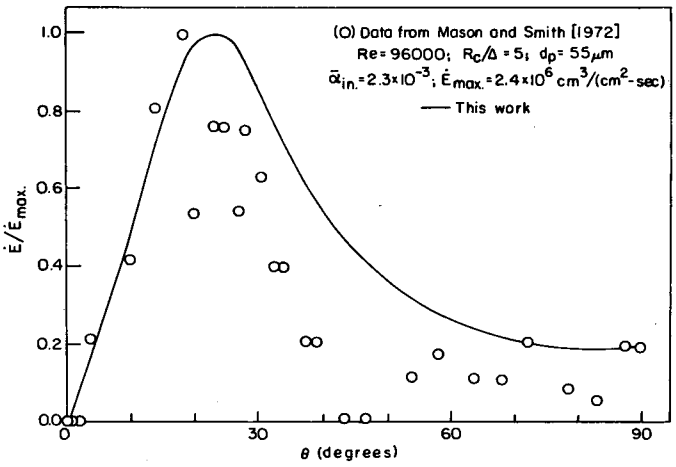

Fig. 1.1. Predicted and experimental erosion rates. (XBL 824-2158)

*This work was supported by the Director, Office of Energy Research, Office of Basic Energy Sciences, Materials Sciences Division of the U.S. Department of Energy under Contract No. DE-AC03-76SF00098.

2. MEASUREMENTS OF AIR FLOW IN A CURVED PIPE USING LASER-DOPPLER VELOCIMETRY

Maurice Holt, Jolen Flores, and Peter J. Turi

Before meaningful two-phase, gas-solid particle flow experiments can be conducted in the fluid mechanics test facility developed to study erosive flows simulating conditions in coal corrosion equipment, single-phase, air-flow experiments must be conducted. The computer driven Laser Dopper Velocimetry (LDV) system was used to study the flow of air near the entry section of a 90° circular bend in a duct of 50 mm x 50 mm square cross section.

Data were collected in equally spaced-cross planes in the bend, separated by angular intervals of 15°. Every data plane contained nine columns made up of 24 to 26 points each. Within a given cross section, the probe volume was brought within 2 mm of the wall for observation. Radial and axial velocity components were measured in 10 planes normal to the curved duct wall. In each of these, velocity profiles were obtained at nine stations spanning the duct, extending from the vertical center plane to a parallel plane 1 mm from the wall. The stations were spaced at equal distance of 6 mm. Vector velocity diagrams showing the evolution of the flow between entry and the 90° station are displaced successive vertical planes. This information is the basis for the determination of the flow behavior of particles entrained in gases that simulate the erodent streams in coal conversion processes.

* * *

†Brief version of LBL-15659.

3. PARTICLE FLOW CHARACTERISTICS DETERMINATION IN GAS AND LIQUID-SOLID PARTICLE STREAMS†

Peter Turi, Jolen Flores, Ionnis Kliafas, and Maurice Holt

The rates of erosion of metal and ceramic containment surfaces in energy conversion and utilization systems are dependent upon the velocity, impingement angle, and solids loading of the carrier fluid. These variables are functions of the fluid mechanics in the various geometries of components in the systems. In order to determine the nature of the fluid flow in two-phase systems, a complex text facility is required.

A Laser Doppler Velocimetry (LDV) system was assembled to make measurements on the flow of air through a 90° bend in a square duct. Measurements were facilitated through the use of a computer controlled, X-Y-Z traversing table upon which the laser optical components were fastened. Doppler signals were received and processed by the LDV frequency counter. These signals were then reduced to mean velocities after undergoing a sta-

tistical analysis in a data acquisition software package designed for this system. The system was modified to overcome various problems determined in its shakedown period. It will be utilized for several years to study the behavior of 2 and 3 phase fluid systems in various chemical process system containment geometries.

* * *

†Brief version of LBL-15660.

1982 PUBLICATIONS AND REPORTS

Refereed Journals

1. W. Yeung and M. Holt, "Boundary Layer Control in Pipes through Strong Injection," ZAMM 62, 391 (1982).

Other Publications

1. J. Humphrey, F. Pouramahdi, and A. Levy, "Prediction of Erosive Wear by Solid Particles in a Turbulent Curved Flow," Proceedings of 7th Annual Conference on Coal Conversion and Utilization, DOE-EPRI-GRI, Gaithersburg, Maryland, November 1982.

2. M. Holt, J. Flores, and P. Turi, "Measurements of Air Flow in a Curved Pipe Using Laser-Doppler Velocimetry," Proceedings of International Symposium on Applications of Laser Doppler Anemometry to Fluid Mechanics, Lisbon, Portugal, July 5-7, 1982.

3. P. Turi, "A Laser Dopper Velocimetry System Designed for Two-Phase Flows," Pub-3027.

LBL Reports

1. F. Pouramahdi, "Turbulence Modeling of Single- and Two-Phase Curved Channel Flows," Ph.D. thesis, LBL-13808.

2. J. Humphrey, M. Chang, and M. Krodan, "Developing Turbulent Flow in a 180° Bend and Down Stream Tangent of Square Cross Sections," LBL-14844.

Invited Talks

1. J. Humphrey, "Predicting Erosive Wear by Solid Particles in Solid Gas/Solid Liquid Flows," Argonne National Laboratory, Argonne, Illinois, November 1982.

2. J. Humphrey, "Curved Duct Turbulent Flow and Erosive Wear by Solid Particulates," General Electric Company, Schenectady, New York, November 1982.

c. Erosion of Brittle Solids*

Anthony G. Evans, Investigator

Introduction. The intent of the program is to develop a fundamental comprehension of the erosion and erosion/corrosion of brittle surfaces, with emphasis on high temperature material removal. The study involves the observation and analysis of the impact damage and erosion mechanisms pertinent to homogeneous ceramics and glasses and to oxide films on metallic and ceramic alloys. The relatively comprehensive understanding of material removal by lateral cracking--used to predict the dependence of the ambient temperature erosion of brittle materials on the fracture toughness, hardness and elastic modulus--provides an established background for the study. An extension to the cracking along interfaces that occurs in oxidative or corrosive environments is also being explored, as a basis for understanding erosion/corrosion problems.

Previous studies of surface damage in ceramics have identified a fracture threshold that dictates a transition from a modest to a rapid material removal rate. The dependence of this fracture threshold on material properties has yet to be adequately elucidated. Threshold studies constitute a major theme of the current program.

1. THE MECHANICAL BEHAVIOR OF BRITTLE COATINGS AND LAYERS†

A. G. Evans, G. C. Crumley, and E. Demaray

The cracking and spalling of brittle coatings and layers on inorganic substrates have been evaluated. It is demonstrated that residually compressed coatings are susceptible to elastic buckling in the presence of an interface separation and that the buckled configuration yields a stress intensification capable of crack growth and eventual spalling. A critical dimensionless parameter for crack growth and spalling has thereby been identified. The parameter depends on the residual compression in the coating, the coating thickness and the toughness of the interface. Attempts have been made to compare the predicted behavior with experimental observations of spalling, as required to interpret the effects of temperature variation on the mechanical integrity of the coatings and on their erosion resistance, both processes being dependent on brittle cracking and spalling of the coating. The experimental studies have been conducted on a NiCrAl alloy coated with ZrO_2. Mechanical studies have shown that the mechanical behavior of the system is limited by the properties of the ZrO_2 or Al_2O_3 layer in the as-formed state, because cracks propagate preferentially through the ZrO_2 or Al_2O_3 (Fig. 1.1a). However, void formation at the Al_2O_3, alloy interface during oxygen exposure, is shown to appreciably reduce the interface toughness below that of the ZrO_2 or Al_2O_3 (Fig. 1.1b), resulting in premature spalling at this interface during either temperature excursions or projectile impact. Void formation at the interface and the effects of rare earth additions are presently being investigated, with special emphasis on the effects of residual stress at the interface on void nucleation (cf creep cavitation).

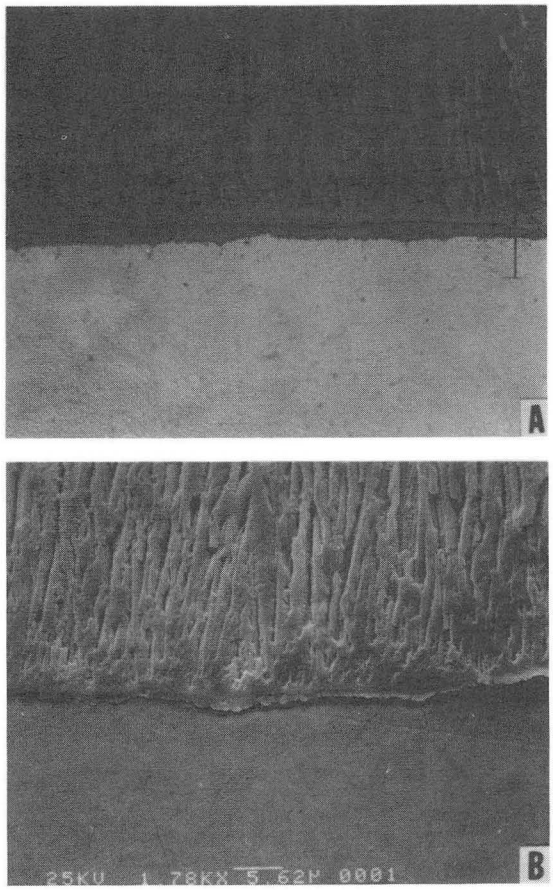

Fig. 1.1 Scanning electron micrographs of crack propagation in oxide layers on NiCrAl superalloy. (a) cracking through the Al_2O_3 and ZrO_2 layers and (b) cracking at the Al_2O_3/superalloy interface because of void formation at the interface.
(XBB 831-225)

***

†Brief version of LBL-15474.

*This work was supported by the Director, Office of Energy Research, Office of Basic Energy Sciences, Materials Sciences Division of the U.S. Department of Energy under Contract No. DE-AC03-76SF00098.

2. MEASUREMENTS OF DYNAMIC HARDNESS BY A CONTROLLED IMPACT TECHNIQUE†

D. B. Marshall, A. G. Evans, and Z. Nisenholz

The magnitude of the impact induced residual stress field that governs crack initiation and growth under erosive conditions is strongly influenced by the dynamic hardness. A simple technique for measuring the dynamic hardness has been devised, based on the response to impact by a sapphire rod, with a pyramidal profile machined into the impact surface. The size of the hardness impression has been related to the dynamic hardness, through the impact velocity, the projectile mass, etc. Application of this technique to ZnS has revealed that the hardness, for loading times in the range 1 to 10 μs, is more than twice the static hardness. The increase in hardness has been independently confirmed from measurements of the plastic zone size and of the residual depth of the surface impression. The higher hardness also accounts for the substantial increase in crack size measured dynamically for the equivalent impression size (Fig. 2.1a). In fact, the dynamic hardness provides a quantitative prediction of the enhanced impact induced cracking, in very close agreement with the change observed on ZnS (Fig. 2.1b). Extension of the technique to brittle coatings will assist in the interpretation of their susceptibility to impact damage and erosion.

***

†Brief version of LBL-15339.

1982 PUBLICATIONS AND REPORTS

LBL Reports

1. A. G. Evans, G. C. Crumley, and E. Demeray, "The Mechanical Behavior of Brittle Coatings and Layers," LBL-15474.

2. D. B. Marshall, A. G. Evans, and Z. Nisenholz, "Measurement of Dynamic Hardness by a Controlled Impact Technique," LBL-15339.

Invited Talks

1. G. Crumley and A. G. Evans, "The Adherence of ZrO_2 Thermal Barrier Coatings," Pacific Coast Regional Meeting, American Ceramic Society, Seattle, Washington, October 1982.

2. D. B. Marshall, Z. Nisenholz, and A. G. Evans, "Controlled Impact Damage in ZnS," Pacific Coast Regional Meeting, American Ceramic Society, Seattle, Washington, October 1982.

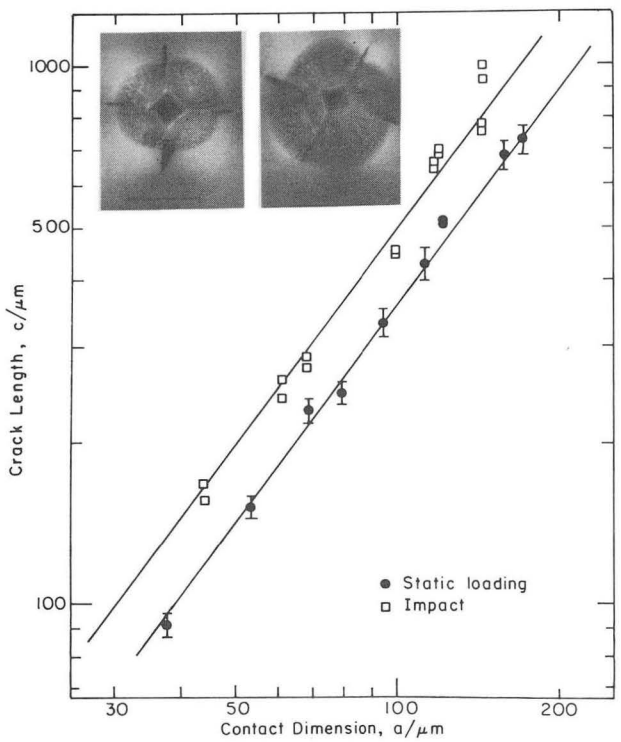

Fig. 2.1. Hardness measurements and cracking induced by indentation. (a) optical micrographs comparing quasistatic and dynamic indentation damage and (b) the variation in indentation cracking for quasistatic and dynamic conditions, based on the rate induced change in hardness.
(XBB 820-9210A)

d. Chemical Degradation of Refractories*

David P. Whittle, Investigator†

Introduction. The energy technologies that are most likely to be developed intensely in the next few decades relate to the use of coal; they are coal combustion, liquefaction, and gasification. In the reaction chambers of most of these systems, ceramic materials are exposed to extremely aggressive environments. Temperatures up to 1500°C, corrosive gases under high pressure, and slag severely limit the materials that can be used.

The objective of this program is to establish the scientific principles of chemical interactions under conditions relevant to advanced coal technology systems.

1. HIGH TEMPERATURE DEGRADATION OF REFRACTORIES IN MIXED GAS ENVIRONMENTS ‡

Stephen Smith and David P. Whittle

To permit high temperature operation of coal technology systems, the reaction chamber must be refractory lined to insulate the external metal pressure vessel thermally, to protect it from chemical attack, and to minimize heat losses. Two systems of lining design are presently used. One is a layer of dense-alumina-castable refractory (calcium-aluminate-bonded alumina) at the hot face, with a layer of less dense, high alumina castable between it and the pressure vessel wall. An alternative design uses dense alumina blocks, in which calcium oxide is present as a common impurity. The purpose of this work is to investigate the behavior of the Al_2O_3-CaO refractory system in gaseous atmospheres representative of those present in coal conversion systems.

Initially, it was proposed to study the behavior of pure Al_2O_3, pure CaO and Al_2O_3 up to 10% CaO refractory specimens in H_2-H_2O-H_2S gas mixtures of controlled oxygen, and sulfur fugacities at 1200°C. The test environments used were very aggressive compared with actual coal conversion atmospheres. Reference to the appropriate phase stability diagram indicates that CaO should be unstable and CaS would be expected to form.

Following 250-hr exposure, pure Al_2O_3 and Al_2O_3 up to 10% CaO specimens were found not to be susceptible to sulfur attack. Pure CaO specimens were attacked by sulfur species and resulted in the formation of a dense CaS layer approximately 40 μm thick at the specimen surface. In a recently published paper by Tak and Young,[1] it was reported that calcium-aluminate-bonding phases are prone to sulfur attack in H_2-H_2S gas mixtures (with an unknown oxygen potential) at temperatures up to 1,000°C. Recent experiment here confirms this behavior (Fig. 1.1). It is proposed to try and establish the kinetic boundary on the thermodynamic phase stability diagram and determine at what particular oxygen potential sulfur attack becomes a problem.

* * *

‡Brief version of LBL-15523.

1. J. B. Tak and D. J. Young, Ceramic Bulletin 61, 7 (1982).

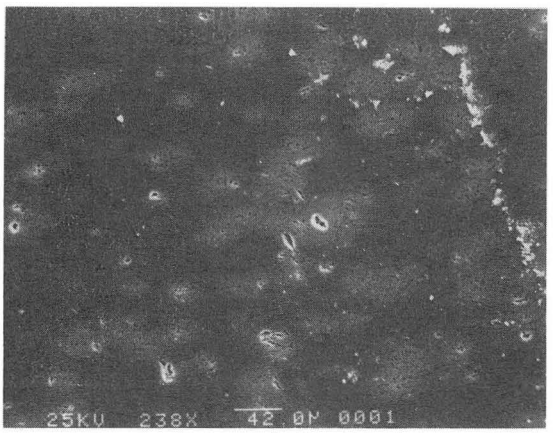

a

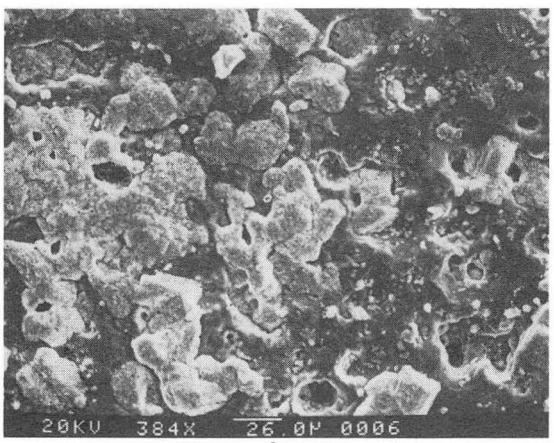

b

Fig. 1.1. Scanning electron micrograph of Al_2O_3 - 10% CaO specimens. (a) Unexposed and (b) exposed to H_2 - 2% H_2S at 1200°C for 250 hr.
(XBB 831-995)

*This work was supported by the Director, Office of Energy Research, Office of Basic Energy Sciences, Materials Sciences Division of the U.S. Department of Energy under Contract No. DE-AC03-76SF00098.

†Dr. Whittle died in July 1982. This report has been prepared by Dr. Stephen Smith. Since Dr. Whittle's death, Dr. J. Stringer of the Electric Power Research Institute has been acting as technical advisor, pending the appointment of a full-time successor.

5. Experimental Research

a. Far Infrared Spectroscopy*

Paul L. Richards, Investigator

Introduction. The objective of our research is to use the infrared and near-millimeter wavelength range of the electromagnetic spectrum as a probe to do experiments that are selected for their technical novelty and potential for revealing new physics.

We are developing new measurement techniques, including sensitive infrared detectors for use in experiments in which the background photon level is low. The Ge:Ga photoconductors, the composite bolometers, and the superconducting diode photon detectors developed by our group are now the most sensitive existing infrared and near-millimeter detectors over the wavelength range from 30 μm to 8 mm.

We are now using sensitive infrared technology to measure the spectra of one-dimensional conductors, of molecules chemisorbed on metal surfaces, of dust clouds in our galaxy, and of the 3 K blackbody radiation that fills the universe.

1. INFRARED EMISSION SPECTROSCOPY OF CO ON Ni†

Shirley Chiang, Roger G. Tobin, and Paul L. Richards

Vibrational spectroscopy yields valuable information about the structure and bonding of molecules to surfaces. We have developed the technique of infrared emission spectroscopy for use over the broad range of frequencies from 300 to 3000 cm^{-1} (with a resolution of 1 to 15 cm^{-1}) in order to permit the study of the linewidths of vibrational spectra of chemisorbed molecules. Conventional reflection-absorption spectroscopy from highly reflective metal samples requires the observation of the small surface absorption signal on top of the large background of the bulk reflection. Our infrared emission technique has the advantage that we observe the small surface emission signal on top of the much smaller background resulting from the bulk emission.

In order to observe the thermal radiation from a room temperature, single-crystal sample, we cool the environment around the sample to ~80 K and cool our grating spectrometer to ~5 K. We obtain high sensitivity by using an extremely low noise Si:Sb photoconductive detector, which is limited by statistical fluctuations in the photon stream, even at the very low photon backgrounds that occur in the cold environment. The sample is mounted in an ultrahigh vacuum system equipped with surface preparation and characterization facilities. With this system, we can routinely measure emission from as little as 0.05 L CO on Ni, with a line center signal-to-noise ratio of 4 in one second of integration.

We have observed thermally emitted infrared radiation from the carbon-oxygen stretching vibration of CO on a crystal of Ni that was cut at about 8° from a (100) surface. The spectra of Ni with increasing amounts of CO on the surface are shown in Fig. 1.1, normalized to room temperature blackbody emission. We observe two prominent emission bands due to the C-O stretching vibration. The strongest band, due to terminally bonded molecules, falls in the range 2010-2035 cm^{-1} and has a width of about 35 cm^{-1}. A weaker band from bridge-bonded molecules, with a width of 60-80 cm^{-1}, is observed in the range 1850-1930 cm^{-1}. The peak frequencies shift continuously

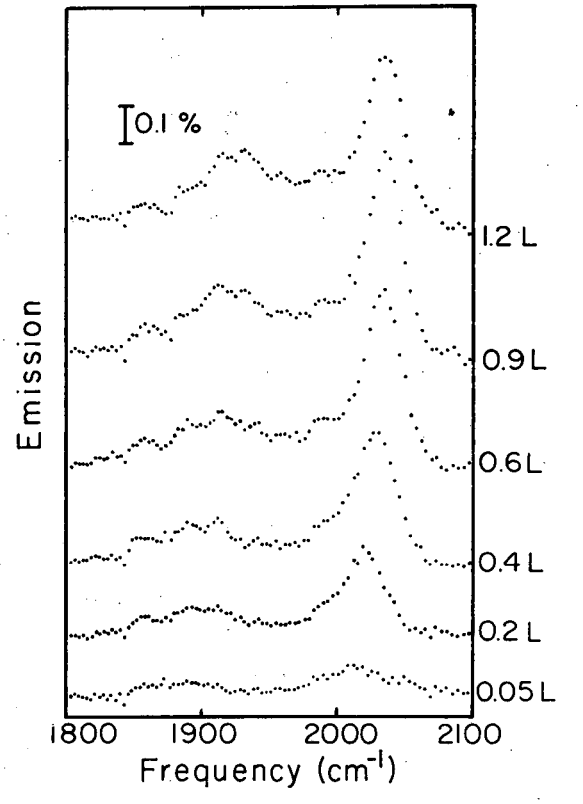

Fig. 1.1. Observed infrared emission spectra from Ni(100)8° stepped surface as a function of frequency for CO exposures from 0.05 L to 1.2 L. The vertical bar indicated 0.1% absolute emissivity. The instrumental resolution was 15 cm^{-1}. (XBL 828-6354)

*This work was supported by the Director, Office of Energy Research, Office of Basic Energy Sciences, Materials Sciences Division of the U. S. Department of Energy under Contract No. DE-AC03-76SF00098.

upward with increasing exposure, reaching a total shift of 25 cm^{-1} for the on-top site and 35 cm^{-1} for the bridge site at saturation. Development of this instrument is being continued and attempts are being made to observe the C-metal stretch absorption.

* * *

†Brief version of LBL-14552.

2. LOW TEMPERATURE INFRARED ABSORPTION SPECTROSCOPY OF CO ON Ni†

Harry J. Levinson,‡ Roger G. Tobin, and Paul L. Richards

The infrared absorption spectrometer developed in our group is a sensitive probe of the vibrational structure of molecules adsorbed on metal films at low temperatures. A sensitive thermometer measures the sample temperature change, as infrared radiation from a rapid-scan Fourier spectrometer is absorbed. The sample is in ultrahigh vacuum. It is held at 1.5 K during the measurements, but it can be heated to ~50 K to study temperature-dependent effects. This low temperature regime is of particular interest for studies of chemisorption kinetics and molecular surface diffusion.

We have investigated in detail the adsorption of CO on evaporated nickel films at 1.5 K and at 40 K, as a function of surface coverage. In contrast to published reports, we have found no evidence for a physisorbed precursor state. Substantial surface diffusion occurs when the sample is heated to 40 K, but some regions are apparently unaffected. In addition, we observed an unexplained splitting of the infrared band due to molecules bonded to a single nickel atom, at high CO coverages.

* * *

†Brief version of LBL-14556.
‡Advanced Micro Devices, Sunnyvale, CA.

3. FAR INFRARED OPTICAL PROPERTIES OF AN ORGANIC SUPERCONDUCTOR

William A. Challener, Paul L. Richards, and Richard L. Greene†

The charge transfer compound $(TMTSF)_2\ ClO_4$ is the first organic compound to be synthesized that becomes superconducting at ambient pressure. The nature of the highly conducting state above $T_c \approx 1$ K is a matter of controversy. One hypothesis suggests that quasi-one-dimensional superconducting fluctuations exist in this material up to 40 K. If this is true, a pseudogap of about 3.8 MeV or 30 cm^{-1} should exist in the electronic density of states that might produce an observable feature in the far infrared optical properties of this material. We have made both reflectance and transmittance measurements from 5 to 40 cm^{-1} as a function of temperature, magnetic field, and x-ray induced defect density to search for such an effect.

At temperatures below 60 K, reflectance peaks have been observed at 7 and 29 cm^{-1} (Fig. 3.1). The 29 cm^{-1} peak is very sensitive to radiation-induced defects and is insensitive to magnetic fields up to 40 kG at 4.4 K. In contrast to reports by others, our results suggest that these features are not related to a superconductive pseudogap.

* * *

†IBM Research Laboratories, San Jose, CA.

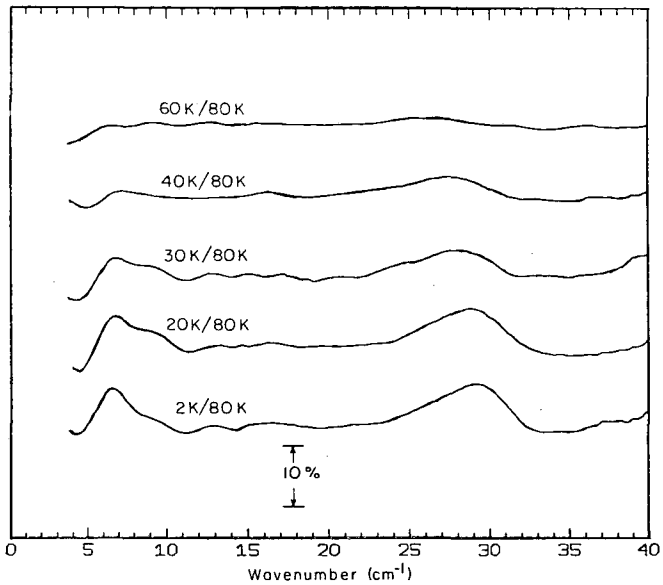

Fig. 3.1. Reflectance of $(TMTSF)_2\ ClO_4$ as a function of temperature. (XBL 831-5046)

4. WORK IN PROGRESS

Studies of hole transport in Ge:Ga are being pursued to understand the semiconductor physics that underlies the performance of technologically important far infrared detectors. Current-voltage curves and the Hall effect are being measured as a function of temperature, photon flux, and electric field. Many important detector properties depend on the sensitivity of the hole lifetime to these parameters. Detectors have been produced with noise performance at very low photon backgrounds equal to the (BLIP) limit set by the fluctuations in the arrival of background photons.

The far infrared properties of the quasi-one-dimensional charge density wave (CDW) compound, $NbSe_3$, are being measured. Reflectivity data show a plasma edge, phonon modes made infrared active by the CDW transition, and a possible CDW energy gap.

A new experiment is being prepared to measure the spectrum of the cosmic microwave background

radiation. It will be different in most respects from our previous experiment. It is designed to test the apparent deviations from a blackbody spectrum.

A balloon experiment designed to survey the sky for far infrared sources was successfully flown in 1982. Data were obtained over 2/3 of the northern sky at seven wavelengths between 20 μm and 2 mm. A preliminary catalog is being prepared of hundreds of far infrared sources, many of which were not previously known.

Calculations are being carried out to see if synchrotron radiation is a useful source for infrared spectroscopy. When diffraction effects are included, it appears that the time average brilliance of a source such as the proposed Advanced Light Source will be very useful for wavelengths longer than 10 μ. Fast pulses will be useful for measurements of relaxation times.

1982 PUBLICATIONS AND REPORTS

Refereed Journals

†1. A. D. Smith and P. L. Richards, "Analytic Solutions to SIS Quantum Mixer Theory," J. Appl. Phys. 53(5), 3806 (1982).

2. P. L. Richards, "Spectrum of the Microwave Background Radiation," Phil. Trans. R. Soc. Lond. A 307, 77 (1982); LBL-14311.

3. W. R. McGrath and P. L. Richards, "A Convenient Low Temperature Heat Sink for Electrical Leads," Rev. Sci. Instrum. 53(5), 709 (1982); LBL-13764.

†4. P. L. Richards, "Superconducting Microwave Devices Reach Fundamental Quantum Limits," Phys. B1 38, 215 (1982).

Other Publications

1. M. R. Hueschen, E. E. Haller, and P. L. Richards, "Lifetime and Mobility in Ge:Ga Far Infrared Photoconductors," Bull. Am. Phys. Soc. 27, 391 (1982); LBL-13761.

2. W. A. Challener and P. L. Richards, "Far Infrared Optical Properties of $NbSe_3$," Bull. Am. Phys. Soc. 27, 283 (1982); LBL-13762.

3. S. Chiang, R. G. Tobin, and P. L. Richards, "Infrared Emission Spectroscopy from Surfaces," Bull. Am. Phys. Soc. 27, 345 (1982); LBL-13763.

†4. P. L. Richards and L. T. Greenberg, "Infrared Detectors fow Low-Background Astronomy: Incoherent and Coherent Devices from One Micrometer to One Millimeter," Infrared and Millimeter Waves, Vol. 6, edited by Kenneth J. Button, Academic Press, 1982, p. 149-207.

†5. P. L. Richards, "Superconducting Detectors and Mixers for Near-Millimeter Wavelengths," McGraw Hill Yearbook of Science and Technology 1982-1983, p. 438-439.

†6. A. D. Smith, W. R. McGrath, P. L. Richards, D. E. Prober, and P. Santhanam, "SIS Quasiparticle Tunnel Junctions as Microwave Mixers and Direct Detectors," Bull. Am. Phys. Soc. 27, 266 (1982).

†7. W. R. McGrath, A. D. Smith, P. L. Richards, R. E. Harris, and F. L. Lloyd, "Noise Measurements in SIS Quasiparticle Array Mixers," Bull. Am. Phys. Soc. 27, 266 (1982).

LBL Reports

1. S. Chiang, R. G. Tobin, and P. L. Richards, "Infrared Emission Spectroscopy of Co on Ni," to be published in a special issue of J. of Electron Spectroscopy and Related Phenomena, LBL-14552.

2. H. J. Levinson, R. G. Tobin, and P. L. Richards, "Infrared Spectra of CO Adsorbed at Low Temperatures on Ni," to be published in a special issue of the Journal of Electron Spectroscopy and Related Phenomena, LBL-14556.

3. M. R. Hueschen, E. E. Haller, and P. L. Richards, "Ge:Ga Photoconductors: Development and Ideal Performance," to be published in the Proceedings of the Seventh International Conference on I-R and mm Waves, LBL-14998.

4. W. A. Challener, P. L. Richards, and R. L. Greene, "Far Infrared Optical Properties of $TMTSF_2\ ClO_4$," to be published in the Proceedings of the International Conference on Low Dimensional Conductors and Superconductors, LBL-15279.

5. P. L. Richards, "Infrared Measurements of Molecules Chemisorbed on Metal Surfaces," to be published in the proceedings of the Symposium on Photoprocesses on Solid Surfaces, LBL-15337.

6. S. Chiang, R. G. Tobin, and P. L. Richards, "Infrared Emission Spectroscopy of CO on Ni(100)," to be published in the Bull. Am. Phys. Soc., LBL-15379.

7. W. A. Challener, P. L. Richards, and R. L. Greene, "Far Infrared Optical Properties of $(TMTSF)_2\ ClO_4$," to be published in the Bull. Am. Phys. Soc., LBL-15380.

‡8. J. L. Bonomo, J. B. Peterson, P. L. Richards, and T. Timusk, "Calibration of a Photometer for Measurement of the Cosmic Microwave Background," to be published in the Proc. of the International School of Physics, "Enrico Fermi," Vol. LXXXVI, LBL-14739.

Invited Talks by P. L. Richards

Talk I, "Infrared Measurements of the Spectrum of the Cosmic Blackbody Radiation," given at:

1. Physics Colloquium, University of Regensburg, W. Germany, February 8, 1982.

2. Seminar, Cambridge University, England, March 9, 1982.

3. Seminar, Rheinisch-Westfälische Technische Hochschule Aachen, W. Germany, May 6, 1982.

4. Seminar, Phsikalisches Institut University of Tübingen, W. Germany, May 19, 1982.

5. Seminar, Istituto di Fisica Superiore, Università di Firenze, and CNR-Istituto di Ricera sulle Onde Elettromagnetiche, Florence, Italy, May 31, 1982.

6. Physics Colloquium, University of St. Andrews, Scotland, May 28, 1982.

7. Seminar, E.T.H., Zurich Switzerland, June 10, 1982.

8. Colloquim, Max Planck Institut für Festkörperforschung, Stuttgart, West Germany, June 15, 1982.

9. Seminar, Laboratoire Infrarouge Lointain, Université de Nancy, France, June 18, 1982.

10. Colloquium, Max Planck Institut fur Physik und Astrophysik, Garching, West Germany, June 25, 1982.

11. Seminar, Academy of Sciences, Space Research Institute, Moscow, U.S.S.R., June 30, 1982.

12. General Colloquium, Technical University of Munich, Garching, W. Germany, July 5, 1982.

13. Lecture, International School of Physics "Enrico Fermi," Varenna, Italy, July 16 and 18, 1982.

Talk II, "Superconducting Microwave Devices Reach Fundamental Quantum Limits," given at:

1. Low Temperature Seminar, Oxford University, England, March 4, 1982.

2. Seminar Queen Mary College, University of London, England, March 5, 1982.

3. Seminar Max Planck Institut fur Radio-astronomie, Bonn, W. Germany, February 4, 1982.

4. Plenary Talk, German Physical Society, Münster, W. Germany, March 31, 1982.

5. Seminar, Bell Laboratories, Murray Hill, New Jersey, April 20, 1982.

6. Seminar, Physikalisches Institut, University of Stuttgart, W. Germany, May 4, 1982.

7. Seminar, Observatoire de Paris, Meudon, France, May 14, 1982.

8. Solid State Colloquim, Cambridge University, England, May 26, 1982.

9. Seminar, Max Planck Institut für Festkörperforschung, Stuttgart, W. Germany, June 9, 1982.

10. Seminar, Laboratoire Infrarouge Lointain, Université de Nancy 1, France, June 18, 1982.

11. Seminar, Academy of Sciences, Space Research Institute, Moscow, U.S.S.R., June 30, 1982.

12. Solid State Colloquium, University of Hamburg, Hamburg, W. Germany, July 8, 1982.

13. Lecture, International School of Physics "Enrico Fermi," Varenna, Italy, July 19, 1982.

Talk III, "Detectors of Far Infrared and mm Waves," given at:

1. Seminar, Istituto di Fisica Superiore, Università di Firenze and CNR-Istituto di Ricercà sulle Onde Electromagnetiche, Florence, Italy, June 1, 1982.

2. Seminar, Academy of Sciences, Space Research Institute, Moscow, U.S.S.R., June 30, 1982.

Talk IV, "Spectrum of the Microwave Background Radiation," given at:

1. Royal Society Discussion Meeting. The Big Bang and Element Creation, London, England, March 11, 1982.

2. U.C. Santa Barbara, Theoretical Physics Institute, Colloquium, September 22, 1982.

3. XI Texas Symposium on Relativistic Astrophysics, Austin, Texas,, December 12-16, 1982.

Talk V, "Progress in Far Infrared Bolometer Research," given at:

1. Workshop on the Scientific Importance of Submillimeter Observations, E.S.A., Noordwijk, The Netherlands, May 10-12, 1982.

* * *

†Supported also by the Office of Naval Research.
‡Supported also by NASA.

b. Experimental Solid State Physics and Quantum Electronics*

Yuen-Ron Shen, Investigator

1. SPECTROSCOPY OF MOLECULAR MONOLAYERS BY RESONANT SECOND-HARMONIC GENERATION†

Tony F. Heinz, Chenson K. Chen, Daniel Ricard, and Y. Ron Shen

Second-order nonlinear optical processes are forbidden in media with inversion symmetry. The surface atomic or molecular layers, on the other hand, are always asymmetric, and their contribution to the second-order processes can often dominate over that of the bulk. Therefore, second-order nonlinear optical effects from the surface can be used as sensitive probes for surface studies. That the nonlinear optical technique has indeed the sensitivity to detect a submonolayer of adsorbed molecules has been demonstrated in our earlier investigations.

To show that the nonlinear optical technique can actually be applied to surface studies, an experiment has recently been carried out in our laboratory using surface second-harmonic (SH) generation to study a submonolayer of dye molecules adsorbed on a fused quartz substrate. Samples of rhodamine 110 and rhodamine 6G with an average surface coverage of 5×10^{13} molecules/cm^2 were prepared by the spinning technique. A dye laser pumped by a Q-switched Nd^{3+}-doped yttrium aluminum garnet laser provided tunable pulses approximately 10 ns duration, 1 cm^{-1} linewidth, and 1 mJ energy. The output of the dye laser, focused to an area of 10^{-3} cm^2, fell on the sample at an angle of 45°. The reflected SH light, which amounted to ~10^4 photons per pulse for the peak signal, was detected by a photomultiplier and a gated integrator after it passed through low frequency blocking filters and a monochromator.

Figure 1.1 displays the observed SH spectra for the monolayer samples in the region of the $S_0 \rightarrow S_2$ electronic transition. The resonant SHG process is described in Fig. 1.2, which also shows the transition energies of the relevant states for the two dyes.

The SH signal was found to be independent of the rotation of the sample about its surface normal, indicating a fully isotropic distribution of the molecules in the surface plane. The polarization dependence of the SH output suggests a molecular orientation in which the y'-axis of the molecule (see Fig. 1.2) is in the surface plane, and the z'-axis is tilted 34° from the surface normal.

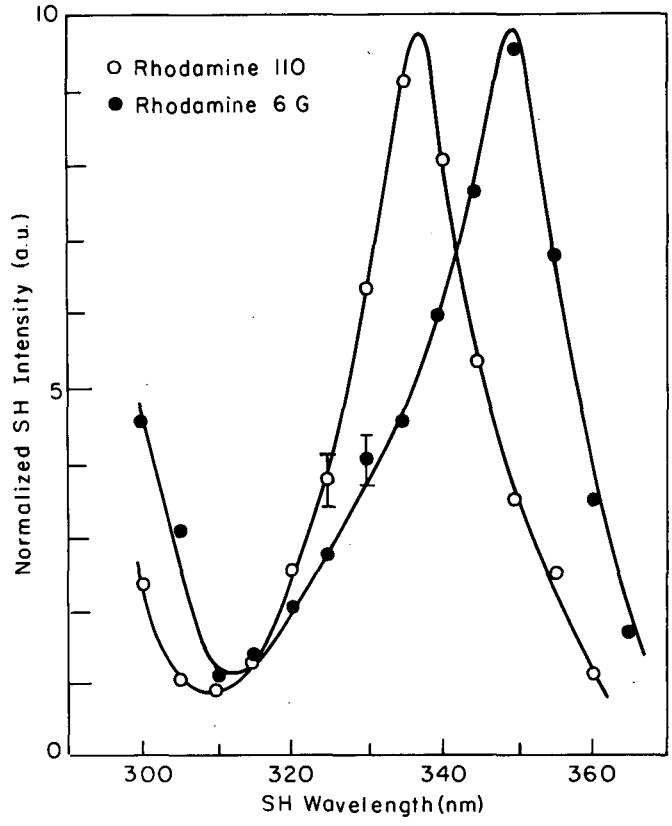

Fig. 1.1. Normalized SH intensity for p-polarized excitation of monolayer samples of rhodamine 110 and rhodamine 6G on fused silica as a function of the SH wavelength in the region of the $S_0 \rightarrow S_2$ transition. (XBL 8110-6773)

* * *

†Brief version of Phys. Rev. Lett. 48, 478 (1982); LBL-13667.

*This work was supported by the Director, Office of Energy Research, Office of Basic Energy Sciences, Materials Sciences Division of the U.S. Department of Energy under Contract No. DE-AC03-76SF00098.

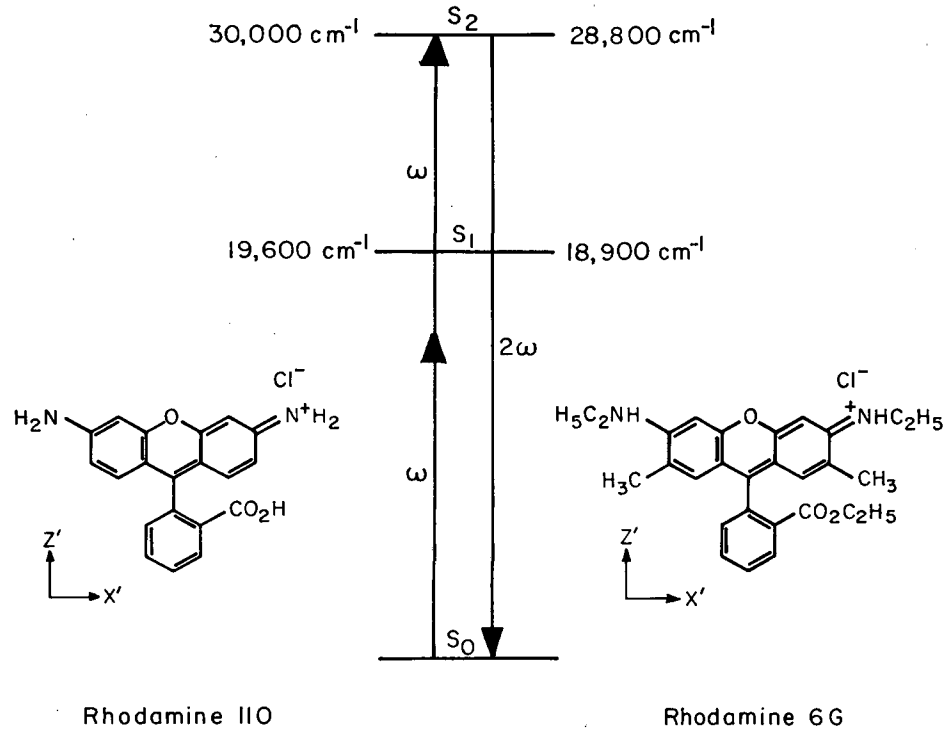

Rhodamine 110 Rhodamine 6G

Fig. 1.2. Energy-level diagrams for rhodamine 110 and rhodamine 6G with the line centers for the linear absorption of the dyes dissolved in ethanol given in units of inverse centimeters. The structure of the dyes and the molecular axes referred to in the text are indicated. (XBL 8111-12843)

2. TRANSIENT FOUR-WAVE MIXING AND COHERENT TRANSIENT OPTICAL PHENOMENA†

Peixian Ye and Y. Ron Shen

Four-wave mixing has recently become one of the most interesting and thoroughly investigated nonlinear optical effects. It is a process that is allowed in all media, and has therefore found numerous important applications. The inherent resonant enhancement feature allows the process to be exploited as a new spectroscopic technique. For example, with the appropriate experimental arrangement, four-wave mixing can be used to obtain Doppler-free spectra or spectra with reduced inhomogeneous broadening, to study transitions between excited states, to measure longitudinal and transverse relaxation times, etc. The systematic study of four-wave mixing has so far been restricted to the steady-state case. With time as an additional variable, transient four-wave mixing offers more possibilities.

A general formalism has been developed by us to describe transient four-wave mixing. The results of such processes in two-, three-, and four-level systems are derived. They are found to be directly connected with some well-known coherent transient effects. In general, transient four-wave mixing deals with the situation where three input pulses of either the same or different frequencies excite a medium successively in a given order. The amplitude and temporal character of the radiative output (the fourth wave) shows a time variation depending on the time sequence and separation of the input pulses. By choosing the input frequencies to excite the medium resonantly or near-resonantly, coherent superpositions of states and populations can be created. Thus, experiments on transient four-wave mixing can be used not only to study the particular time-ordered four-wave mixing process itself, but also to obtain the various relaxation rates in the medium.

Transient four-wave mixing can be considered as a special class of phenomena among all of the possible coherent transient optical effects. Included in this class are the various known cases of photon echoes, such as trilevel echoes, stimulated echoes, and backward echoes. Although these echo phenomena are usually discussed in terms of the vector model of excitation in a nonperturbative approach, in the limit in which no pump saturation occurs, they can be treated as transient four-wave mixing processes. On the other hand, transient four-wave mixing is more general and predicts coherent transient effects other than the photon-echos phenomena. It covers, for example, the cases of free-induction decay, transient coherent Raman scattering, and transient optical-field-induced effects. A systematic study starting from a general formalism allows a thorough investigation of all possible cases of transient four-wave mixing.

* * *

†Brief version of Phys. Rev. A 25, 2183 (1982); LBL-13462.

3. NONLINEAR WAVE INTERACTION INVOLVING SURFACE POLARITONS†

Y. Ron Shen and Francesco DeMartini

Nonlinear optical studies involving surface polaritons have attracted increasing attention recently. Because the surface polaritons are localized to a thin surface layer near an interface, nonlinear optical effects involving surface polaritons have a surface-specific nature. In fact, surface nonlinear optics with all of the interacting waves being surface polaritons are also possible. With tunable laser excitation, new techniques of surface nonlinear optical spectroscopy can be devised and applications to surface science can be envisioned.

We have developed a general formalism to describe the surface polaritons. It is shown that surface polaritons can exist in a multilayer system. The theory of linear excitation of surface polaritons is given. It is then extended to the case of nonlinear optical excitation with the nonlinear polarization acting as the driving source. The interaction of surface polaritons with bulk waves and the interaction between surface polaritons are treated from a unified point of view. The generation of surface polaritons by optical mixing of bulk waves can be considered as a special case of nonlinear optical reflection from a surface. The same formalism can be used to describe the generation of bulk and surface waves by optical mixing of surface polaritons or surface polaritons with bulk waves.

* * *

†Brief version of LBL-11358.

4. SURFACE-ENHANCED SECOND-HARMONIC GENERATION AND RAMAN SCATTERING

Chenson K. Chen, Tony F. Heinz, Daniel Ricard, and Y. Ron Shen

The phenomenon of surface-enhanced Raman scattering has attracted and continues to attract considerable attention. An appreciable enhancement in the effective Raman scattering cross section has been manifested by a wide range of molecular adsorbates on surfaces of various metals at solid/liquid, solid/vacuum, and even at solid/solid interfaces. It has come to be accepted that the macroscopic electrodynamics of the surface plays a significant role in SERS: the presence of the roughened metal can produce a local field strength at the interface which greatly exceeds that of the applied field. This mechanism of local field enhancement should affect all surface optical processes. The second harmonic generation (SHG) process is of particular interest since it is forbidden in the bulk of a centrosymmetric medium, and has, consequently, an intrinsic surface sensitivity.

We have elaborated the theory of local-field enhancement in a general fashion. By extending the notion of a correction to the molecular polarizability from macroscopic local fields to microscopic ones, we can describe directly the amplification of the incident and radiated field induced by the presence of the surface. The surface enhancement of any particular process can then be readily calculated.

On the experimental side, while both surface-enhanced Raman scattering the SHG have been observed, they have not been simultaneously measured and correlated with the different phases of oxidation-reduction cycles in an electrochemical cell. The Raman and second-harmonic signals from a silver electrode were monitored during cycling in pure electrolytes (K_2SO_4 or KCl) and during cycling with cyanide ions also present. In the latter case, a rich surface chemistry resulted. The rather different responses of the two optical probes could be interpreted with the aid of voltammograms indicating the onset of various reactions. Using a simple geometric model, predictions are made of the macroscopic local-field enhancements for SHG and Raman scattering. Experimental values for both processes with identical excitation of a given sample can then be compared. For the chosen pump radiation, the second-harmonic nonlinearity proves to be dominated by that of the silver itself. For this case, the macroscopic local-field corrections should completely account for the surface enhancement. From the experimental Raman scattering power, we can then estimate the residual enhancement of the Raman cross section associated with microscopic local fields and the direct molecule-metal interaction.

* * *

†Brief version of LBL-14840.

1982 PUBLICATIONS AND REPORTS

Refereed Journals

1. H. W. K. Tom, C. K. Chen, A. R. B. de Castro, and Y. R. Shen, "Effect of Extended Surface Plasmons on Surface Enhanced Raman Scattering," Solid State Commun. 41, 259 (1982); LBL-13027.

2. Peixian Ye and Y. R. Shen, "Transient Four-Wave Mixing and Coherent Transient Optical Phenomena," Phys. Rev. A. 25, 2183 (1982); LBL-13462.

†3. S. D. Durbin, S. M. Arakelian, and Y. R. Shen, "Strong Optical Diffraction in a Nematic Liquid Crystal with High Nonlinearity," Optics Lett. 7, 145 (1982).

4. T. F. Heinz, C. K. Chen, D. Ricard, and Y. R. Shen, "Spectroscopy of Molecular Monolayers by Resonant Second-Harmonic Generation," Phys. Rev. Lett. 48, 478 (1982); LBL-13667.

5. M. F. Vernon, D. J. Krajnovich, H. S. Kwok, J. M. Lisy, Y. R. Shen, and Y. T. Lee, "Infrared Vibrational Predissociation Spectroscopy of Water Clusters by the Crossed-Molecular Beam Technique," J. Chem. Phys. 77, 47 (1982).

†6. R. Hsu and Y. R. Shen, "Effects of Self-Induced Ellipse Rotation and Self-Focusing in a Q-Switched Laser Cavity," Appl. Optics 21, 2608 (1982).

LBL Reports

1. A. Jacobson, "Coherent Rayleigh-Brillouin Spectroscopy," Ph. D. thesis, LBL-14373.

2. D. Krajnovich, F. Huisken, Z. Zhang, Y. R. Shen, and Y. T. Lee, "Competition Between Atomic and Molecular Chlorine Elimination in the Infrared Multiphoton Dissociation of Cf_2Cl_2," LBL-14478.

3. C. K. Chen, T. F. Heinz, D. Ricard, and Y. R. Shen, "Surface-Enhanced Second-Harmonic Generation and Raman Scattering," LBL-14840.

4. T. F. Heinz, "Nonlinear Optics of Surfaces and Adsorbates," Ph. D. thesis, LBL-15255.

5. R. Hsu, "Nonlinear Effects of Materials in Laser Cavities," Ph. D. thesis, LBL-11519.

6. M. F. Vernon, J. M. Lisy, D. J. Krajnovich, A. Tramer, H. S. Kwok, Y. R. Shen, and Y. T. Lee, "Vibrational Predissociation Spectra and Dynamics of Small Molecular Clusters of H_2O and HF," LBL-13740.

Other Publications

1. D. Krajnovich, Z. Zhang, F. Huisken, Y. R. Shen, and Y. T. Lee, "The Effects of Reagent Translational and Vibrational Energy on the Dynamics of Endothermic Reactions," in Physics of Electronic and Atomic Collisions, edited by S. Datz, North Holland, NY, 1982, p. 733; LBL-12982.

2. Y. R. Shen, "Nonlinear Optical Techniques for Surface Studies," in Novel Materials and Techniques in Condensed Matter, edited by G. W. Crabtree and P. Vashishta, North Holland, NY, 1982, p. 193; LBL-13365.

3. T. F. Heinz, C. K. Chen, D. Ricard, and Y. R. Shen, "Optical Second-Harmonic Spectroscopy of Molecular Monolayers," Bull. Am. Phys. Soc. 27, 77 (1982); LBL-13715 Abs.

†4. S. D. Durbin, M-M. Cheung, S. M. Arakelian, and Y. R. Shen, "Quantitative Studies of Some Highly Nonlinear Optical Effects in Nematic Liquid Crystals," Bull. Am. Phys. Soc. 27, 328 (1982).

5. C. K. Chen, T. F. Heinz, D. Ricard, and Y. R. Shen, "Correlation of Surface Enhanced Second Harmonic Generation and Raman Scattering of Molecules Adsorbed to a Silver Surface," Bull. Am. Phys. Soc. 27, 377 (1982), LBL-13717 Abs.

6. G. T. Boyd, Z. H. Yu, and Y. R. Shen, "Multiphoton-Induced Luminescence from Roughened Metal Surfaces," Bull. Am. Phys. Soc. 27, 377 (1982), LBL-13718 Abs.

7. C. K. Chen, T. F. Heinz, D. Ricard, and Y. R. Shen, "Nonlinear Optical Study of Interfaces," Proceedings of the International Conference on Lasers '81, New Orleans, Dec. 14-18, 1981, STS Press, McLean, VA, 1982, p. 61; LBL-13878.

8. Y. R. Shen, "Recent Advances in Optical Bistability," Nature 299, 779 (1982); LBL-14971.

9. Y. R. Shen and F. DeMartini, "Nonlinear Wave Interaction Involving Surface Polaritons," in Surface Polaritons, edited by V. M. Agranovitch and D. L. Mills, North Holland, NY, 1982, p. 629; LBL-11358.

†10. S. D. Durbin, S. M. Arakelian, M. M. Cheung, and Y. R. Shen, "Nonlinear Optical Effects in a Nematic Liquid Crystal Resulting from Laser-Induced Refractive Indices," Appl. Phys. B 28, 145 (1982).

11. T. F. Heinz, C. K. Chen, D. Ricard, and Y. R. Shen, "Nonlinear Optical Detection of Adsorbed Monolayers and Monolayers Spectroscopy," Appl. Phys. B 28, 229 (1982); LBL-13829 Abs.

Invited Talks

1. J. M. Lisy, M. F. Vernon, H. S. Kwok, A. Tramer, D. J. Krajnovich, Y. R. Shen, and Y. T. Lee, "Vibrational Predissociation Dynamics and Spectroscopy of Small Molecular Clusters," Faraday Discussion #73, Van der Waals Molecules, St. Catherine's College, Oxford, England, April 5-7, 1982.

2. M. F. Vernon, J. M. Lisy, D. J. Krajnovich, A. Tramer, H. S. Kwok, Y. R. Shen, and Y. T. Lee, "Vibrational Predissociation Spectra and Dynamics of Small Molecular Clusters of H_2O and HF," Faraday Discussion #73, Van der Waals Molecules, St. Catherine's College, Oxford, England, April 5-7, 1982.

3. T. F. Heinz, C. K. Chen, D. Ricard, and Y. R. Shen, "Nonlinear Optical Detection of Adsorbed Monolayers and Monolayer Spectroscopy," XII International Quantum Electronics Conference, Munich, W. Germany, June 22-23, 1982.

†4. S. D. Durbin, S. M. Arakelian, M. M. Cheung, and Y. R. Shen, "Nonlinear Optical Effects in a Nematic Liquid Crystal Resulting from Laser-Induced Refractive Indices," XII International Quantum Electronics Conference, Munich, W. Germany, June 22-23, 1982.

†5. S. D. Durbin, S. M. Arakelian, M. M. Cheung, and Y. R. Shen, "Highly Nonlinear Optical Effects in Liquid Crystals," International Workshop on Optical Phase Conjugation and Instabilities, Cargese, Corsica, September 20-24, 1982.

†6. S. D. Durbin, Y. R. Shen, and S. M. Arakelian, "Strong Dynamical Self-Diffraction Effects in a Nematic Liquid Crystal: Experimental Investigation," XI National Conference on Coherent and Nonlinear Optics, Yerevan, USSR, November 22-25, 1982.

7. Y. R. Shen, "Nonlinear Optical Studies of Adsorbed Monolayers," Optical Society Meeting, Tuscon, Arizona, October 18, 1982.

8. Y. R. Shen, "Surface Nonlinear Optics," U. C. Davis, Colloquium, November 9, 1982.

†9. Y. R. Shen, "Highly Nonlinear Optical Effects in Liquid Crystals," Quantum Electronics Seminar, Stanford University, November 22, 1982.

10. Y. R. Shen, "Recent Advances in Nonlinear Optics," Lawrence Livermore Laboratory Colloquium, November 23, 1982.

11. Y. R. Shen, "Applications of Nonlinear Optics to Surface Studies," Toronto University Colloquium, December 7, 1982.

12. Y. R. Shen, "Applications of Nonlinear Optics to Material Studies," Condensed Matter Physics Meeting, Beijing, China, December 28, 1982-January 3, 1983.

13. Y. R. Shen, "Lasers and Surface Science," seminar at Ecole Polytechnique, Palaiseau, France, September 12-18, 1982.

14. Y. R. Shen, "Nonlinear Optical Effects in Liquid Crystals," seminar at Ecole Polytechnique, Palaiseau, France, September 12-18, 1982.

15. Y. R. Shen, "Lasers and Surface Science," Technische Universitat, Wien, Austria, June 21, 1982.

16. Y. R. Shen, "Study of Molecular Adsorption at an Interface," Oak Ridge National Laboratory, Oak Ridge, Tennessee, May 5-7, 1982.

17. Y. R. Shen, "Surface Studies by Nonlinear Optical Techniques," Lockheed Missiles and Space Co., Inc., Palo Alto, California, May 13, 1982.

* * *

†Research supported by the National Science Foundation under Grant DMR81-17366.

c. Excitations in Solids*

Carson D. Jeffries, Investigator

Introduction. There exists a large class of nonlinear dissipative systems with very complex behavior. One is faced with the problem of formulating and, if possible, answering new types of questions which are independent of detailed knowledge of system dynamics. This is what is done in the renormalization group formulation of critical phenomena; the questions and answers become universal in a certain sense. An analogous universal viewpoint has recently been developed for dealing with systems which display recognizable patterns as they are driven harder, to points of instability and onset of a pseudorandom or so-called chaotic state. Examples are: onset of turbulence in fluids; noisy electrical, mechanical, and chemical oscillators; and "solid state turbulence," such as plasma instabilities in semiconductors, spin wave instabilities, acoustic and electro-acoustic instabilities, and piezo and ferroelectric instabilities. Many of these systems display qualitatively similar routes to chaos. The goal of this research is a detailed experimental study of solid state turbulence and an analysis based on present theoretical models of the dynamical structure of chaotic behavior. This has applications to materials and processes of technological importance.

1. PERIOD DOUBLING AND UNIVERSAL CHAOTIC BEHAVIOR IN P-N JUNCTIONS IN SILICON†

Carson Jeffries, Jose Perez, and James Testa

A period doubling route to chaos has been proposed by Feigenbaum and others. This route may be approximately modeled by a simple recursion relation, or map, such as the logistic equation $x_{n+1} = \lambda x_n(1-x_n)$, where λ is the driving parameter. The bifurcation diagram, Fig. 1.1, plots the iterated value $\{x_n\}$ vs λ. As λ is increased, $\{x_n\}$ displays a sequence of pitchfork bifurcations at λ_n, with period doubling by 2^n, converging geometrically like $(\lambda_c - \lambda_n) \propto \delta^{-n}$, to the onset of chaos at λ_c, where $\{x_n\}$ becomes aperiodic. In the chaotic regime, noise bands merge and narrow periodic windows emerge in a specific order and pattern. This model is made quantitative by computed values of some universal numbers (as $n \to \infty$): convergence rate δ, pitchfork ratio α, power spectral ratio R, wide band noise scaling factor β, and noise sensitivity factor κ.

To make a quantitative test of the model, data were taken on a p-n silicon junction driven resonantly by a sinusoidal voltage $V_0(t)$. By sampling and displaying the successive peak values of the diode current I, the bifurcation diagram of

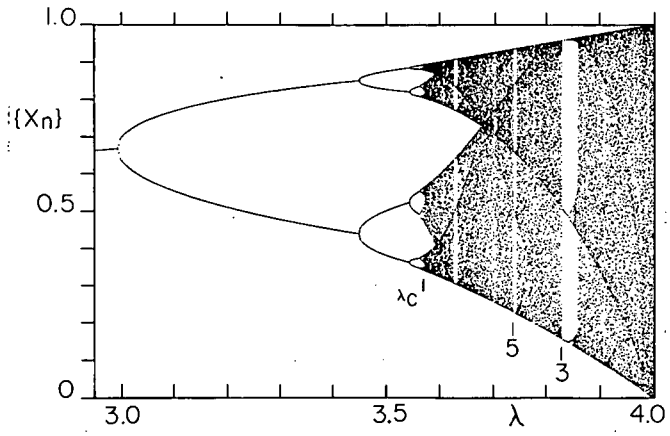

Fig. 1.1. Computed values of the dynamical variable x vs the driving parameter λ for the quadratic logistic difference equation. (XBL 823-8500)

Fig. 1.2 was obtained, in surprisingly good agreement with theory, Fig. 1.1: bifurcation, onset of chaos, band merging, and periodic windows are all observed.

More detailed measurements on power spectra and effects of additive noise provide a direct comparison between measured and theoretical values for five universal numbers in Table 1.1.

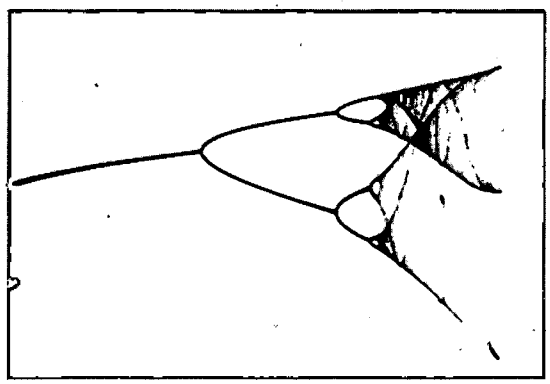

Fig. 1.2. Measured values of the peak current I (vertical) vs the driving voltage V_0 for a p-n junction. This bifurcation diagram shows the features of the model, Fig. 1.1. (XBB 828-7406)

*This work was supported by the Director, Office of Energy Research, Office of Basic Energy Sciences, Materials Sciences Division of the U. S. Department of Energy under Contract No. DE-AC03-76SF00098.

Table 1.1 Comparison--Theory and Experiment.

	Universal Number	Measured Value
Bifurcation ratio	$\delta = 4.669$[a]	4.26 ± 0.5
Pitchfork ratio	$\alpha = 2.502$[a]	2.43 ± 0.1
Power spectral ratio	R = 13.2 db[b]	13 ± 2 db
Noise sensitivity factor	$\beta = 6.619$ [c]	6.5 ± 0.5
Wide band noise	$\beta = 3.237$[d]	3.26 ± 0.4

[a]Feigenbaum.
[b]Nauenberg and Rudnick.
[c]Crutchfield, Nauenberg, and Rudnick.
[d]Huberman and Zisook.

These are the most detailed measurements to be reported for a real physical system; they strongly suggest a universal period doubling route for the p-n junction under the operating conditions used. For other operating conditions, e.g., a much larger driving voltage, more complex behavior is observed, characteristic of a higher dimensional map.

* * *

†Brief version of Phys. Rev. Lett. 48, 714 (1982) and Phys. Rev. B 26, 3460 (1982).

2. INTERMITTENCY ROUTE TO CHAOS

Carson Jeffries and Jose Perez

Another route to chaos has been proposed by Manneville and Pomeau, which is characterized by a periodic (laminar) phase randomly interrupted by bursts of aperiodic behavior. This occurs near a tangent bifurcation, e.g., near the period 3 window in Fig. 1.1 of the preceding article as the driving parameter λ is reduced by a small amount ϵ from the threshold value for the periodic window. Theory predicts that the average laminar length $\langle \ell \rangle \propto \epsilon^{-0.5}$. In the window itself intermittency may be induced by adding a random noise voltage of standard deviation g; the predicted scaling behavior is $\langle \ell \rangle \propto g^{-0.666}$. The probability distribution $P(\ell)$ is also predicted.

Using the same driven p-n junction as in the preceding article, we observe the intermittency in the threshold of the period 5 window. Using real-time analysis of the diode voltage with window comparators and additional logic circuitry to detect the beginning and ending of a laminar train allowed a quantitative measurement of the average length $\langle \ell \rangle$. The data yield $\langle \ell \rangle \propto \epsilon^{-(0.45 \pm 0.005)}$ and $\langle \ell \rangle \propto g^{-(0.65 \pm 0.005)}$.

This is the first experiment to quantitatively measure the scaling behavior of $\langle \ell \rangle$, and it is found to be in agreement with expectations except for very small values of ϵ where some significant deviation is found. Possible causes are being examined.

* * *

†Brief version of Phys. Rev. A 26, 2117 (1982).

3. PERIOD DOUBLING AND CHAOS IN SPIN WAVE INSTABILITIES IN YTTRIUM IRON GARNET†

George Gibson and Carson Jeffries

It has been known previously that ferromagnetic resonance in a sphere displays the so-called Suhl instability because of coupling of the uniform precession mode with spin wave modes. Although Suhl writes "...the situation bears a certain resemblance to the turbulent state in fluid dynamics...," the behavior was not fully understood.

A reexamination of this phenomenon has been done for YIG spheres at f = 1.2 GHz. Autooscillations at 16 kHz were observed corresponding to standing spin wave modes. As the rf driving field was increased, we observed threshold values for period doubling, onset of chaos, intermittency, periodic windows, and hysteresis. The behavior is considerably more complex than found in p-n junctions but less complex than found in fluids. It is clear that one or more distinct routes to chaos are being followed. For some cases the Poincaré return map has a close resemblance to that predicted from the two-dimensional quadratic Henon map in the limit where the map is nearly area preserving. This corresponds to a system which has relatively low loss, which would be the case for a weak coupling of the spin waves with the crystal lattice.

This is an interesting system, again displaying aspects of universal chaotic behavior, somewhat like a "spin-liquid" but with very low viscosity. Further studies of magnetic instabilities are under way.

* * *

†Brief version of LBL-15202.

1982 PUBLICATIONS AND REPORTS

Refereed Journals

1. James Testa, Jose Perez, and Carson Jeffries, "Evidence for Universal Chaotic Behavior of a Driven Nonlinear Oscillator," Phys. Rev. Lett. 48, 714 (182); LBL-13884.

2. Jose Perez and Carson Jeffries, "Effects of Additive Noise on a Nonlinear Oscillator Exhibiting Period Doubling and Chaotic Behavior," Phys. Rev. B 26, 3460 (1982); LBL-14208.

3. Carson Jeffries and Jose Perez, "Observation of a Pomeau-Manneville Intermittent Route to Chaos in a Nonlinear Oscillator," Phys. Rev. A 26, 2117 (1982).

4. James Testa, Jose Perez, and Carson Jeffries, "Testa, Perez, and Jeffries Respond," Phys. Rev. Lett. 49, 1055 (1982); LBL-15082.

5. Jose Perez and Carson Jeffries, "Direct Observation of a Tangent Bifurcation in a Nonlinear Oscillator," Phys. Lett. 92A, 82 (1982); LBL-14633.

6. S. M. Kelso, "The Strain-Confined Electron-Hole Liquid in Ge: Density Variations and Compressibility," Phys. Rev. B 26, 591 (1982); LBL-13911.

7. S. M. Kelso, "Energy- and Stress-Dependent Hole Masses in Germanium and Silicon," Phys. Rev. B 25, 1116 (1982); LBL-12854.

8. S. M. Kelso, "Calculation of Properties of the Electron Hole Liquid in Uniaxially Stressed Ge and Si," Phys. Rev. B 25, 763 (1982); LBL-13387.

9. J. C. Culbertson and J. E. Furneaux, "Density Dependence of an Electron-Hole Liquid Correlation Factor in Ge: Experiment," Phys. Rev. Lett. 49, 1528 (1982); LBL-14424.

Other Publications

1. Carson Jeffries, "Routes to Chaos," Physics News in 1982, American Institute of Physics (New York), in press.

2. J. E. Furneaux, J. C. Culbertson, E. E. Haller, "A Mechanism for Electron-Hole Droplet Pinning in Ge," BAPS 27, 320 (1982).

3. J. C. Culbertson and J. E. Furneaux, "Density Dependence of the Electron-Hole Liquid Enhancement Factor in Ge," BAPS 27, 321 (1982); LBL-13688.

4. E. J. Pakulis and C. D. Jeffries, "Electric Detection of Magnetic Resonance at Dislocations in Ge," BAPS 27, 144 (1982); LBL-13631.

5. C. D. Jeffries, "Observation of Periodic Windows in the Chaotic Regime of a Nonlinear Semiconductor Oscillator," presented at the Conference on Dynamics Days, University of California, San Diego, Jan. 5-7, 1982.

LBL Reports

1. Carson Jeffries and Jose Perez, "Direct Observation of Crises of the Chaotic Attractor in a Nonlinear Oscillator," Phys. Rev. A, in press, LBL-14653.

2. James Testa and G. A. Held, "Period Doubling, Bifurcations, Chaos, and Periodic Windows of the Cubic Map," LBL-14559.

3. James Testa, Jose Perez, and Carson Jeffries, "Evidence for Bifurcation and Universal Chaotic Behavior in Nonlinear Semiconducting Devices," LBL-13719.

4. E. J. Pakulis, E. E. Haller, and C. D. Jeffries, "EPR of the Lithium Ion-Dangling Bond Complex in Germanium Containing Dislocations," Sol. State Comm., in press, LBL-14836.

5. E. J. Pakulis, "Electrically Detected Electron Paramagnetic Resonance in Germanium Single Crystals," submitted to J. Mag. Res., LBL-14802.

6. E. J. Pakulis, "EPR at Dislocations in Germanium," Ph.D. thesis, LBL-14664.

7. George Gibson and Carson Jeffries, "Observation of Period Doubling and Chaos in Spin Wave Instabilities in Yttrium Iron Garnet," LBL-15202.

Invited Talks

Colloquia given by Carson Jeffries on various aspects of universal chaotic behavior in solids:

University of California, Santa Cruz, Physics Colloquium, February 4, 1982.

Institute of Theoretical Physics Colloquium, Univ. of Calif., Santa Barbara, February 18, 1982.

Xerox Palo Alto Research Laboratory Colloquium, April 23, 1982.

Stanford University, Dept. of Chemical Engineering Colloquium, April 28, 1982.

Stanford University, Div. of Applied Physics Seminar, October 21, 1982.

Harvard University, Physics Dept. Colloquium, October 25, 1982.

Bell Telephone Labs, Murray Hill, Seminar, October 26, 1982.

University of Illinois, Urbana, Nonlinear Dynamics Seminar, October 27, 1982.

University of Illinois, Urbana, Physics Colloquium, October 28, 1982.

Purdue University, Physics Seminar, October 29, 1982.

d. Time-Resolved Spectroscopies in Solids*

Peter Y. Yu, Investigator

1. NONEQUILIBRIUM PHONON SPECTROSCOPY IN GaAs†

C. L. Collins and P. Y. Yu

It is well known that hot electrons in GaAs will relax extremely rapidly (in ~0.1 psec) by emission of longitudinal optical (LO) photons. On the other hand, the LO phonon lifetime is ~10 psec at low temperature. These facts suggest that if one excites hot carriers in GaAs with a picosecond laser pulse, a transient nonequilibrium LO phonon population lasting for ~10 psec can be excited. We have studied this nonequilibrium LO phonon population, using Raman scattering with a picosecond laser pulse. In the experiment a GaAs sample is excited by a train of picosecond dye laser pulses. If the kinetic energy of the photoexcited hot carrier is much larger than the LO phonon energy, one expects that several LO photons can be emitted by one hot carrier so we predict that N_q, the number of LO phonons excited, should increase with the excitation photon energy. This prediction is verified by the experimental result in Fig. 1.1, where the solid circles are the experimental points and the curve is calculated using the empirical pseudopotential band structure of GaAs obtained by Professor M. L. Cohen and co-workers. The interesting feature in Fig. 1.1 is the abrupt drop in the phonon occupation number for photon energy ≥ 2.1 eV. Our theory explains this decrease as due to scattering of the hot carriers from the Γ-valley to the X-valleys. Furthermore, we find the Γ-X intervalley deformation potential in GaAs to be 1.1 x 10^9 eV/cm. Previously this deformation potential had been estimated only indirectly from Gunn oscillations in GaAs. Our technique is much more direct and precise than the Gunn effect in determining the intervalley scattering rates and the energy of the X minima. Extension of this work to study other semiconductors is in progress now.

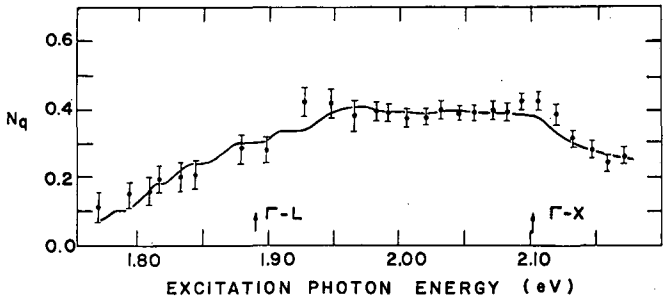

Fig. 1.1. LO phonon population N_q in GaAs plotted as a function of excitation photon energy. The solid circles are experimental points while the solid curve is the result of a model calculation. The arrows labeled as Γ-L and Γ-X represents, respectively, the photon energies for the onset of Γ to L and Γ to X-intervalley scatterings according to pseudopotential band structure calculation. (XBL 831-7973)

* * *

†Brief version of LBL-14992.

2. LIFETIME OF ORTHO-EXCITON AND ORTHO-TO PARA-EXCITON CONVERSION IN Cu_2O†

J. S. Weiner, N. Caswell,‡ and P. Y. Yu

Cu_2O is a classical semiconductor for studying properties of excitons, which are bound states of electrons and holes and are often thought of as analogues of positronium in a solid. In Cu_2O as many as 13 Rydberg states of its exciton have been observed in absorption. Optical dipole transitions to the lowest 1s state of the exciton in Cu_2O is forbidden by parity, so it is expected that the lifetime of this state in Cu_2O should be very long (>1 μsec). However, previous attempts to measure its lifetime with nanosecond-long laser pulses have not been successful.

We have utilized a modelocked picosecond dye laser in conjunction with a delayed coincidence photon counting system to determine the lifetime of the 1s excitons in Cu_2O. We found that the triplet state of the 1s exciton (known as the ortho-exciton) has a lifetime of $\leq$2.5 nsec which is limited by its decay into the para-exciton (singlet state of the 1s exciton). The para-exciton lifetime is determined by recombination at impurities so it can vary between $\lesssim$10 nsec and 13 μsec. The conversion of ortho-excitons to para-excitons is found to be dependent on temperature as $T^{3/2}$. A comparison with existing theories shows that none of them can account for this $T^{3/2}$ dependence.

* * *

†This work was supported in part by the Director, Office of Energy Research, Office of Basic Energy Science, Materials Sciences Division of the U. S. Department of Energy under Contract No. DE-AC03-76SF00098 and the National Science Grant No. DMR79-19463.

‡Present address: IBM T. J. Watson Research Center, Yorktown Heights, NY 10598.

1982 PUBLICATIONS AND REPORTS

Refereed Journals

1. N. Caswell and P. Y. Yu, "Physical Origin of the Anomalous Temperature Dependence of the 1s Yellow Exciton Luminescence Intensity in Cu_2O," Phys. Rev. B. 25, 5519 (1982).

*This work was supported by the Director, Office of Energy Research, Office of Basic Energy Sciences, Materials Sciences Division of the U.S. Department of Energy under Contract No. DE-AC03-76SF00098.

LBL Reports

1. C. L. Collins and P. Y. Yu, "Nonequilibrium Phonon Spectroscopy: A New Technique for Studying Intervalley Scattering in Semiconductors," LBL-14992.

2. J. S. Weiner, N. Caswell, P. Y. Yu, and A. Mysyrowicz, "Orthoto Para-Exciton Conversion in Cu_2O: A Subnanosecond Time Resolved Photoluminescence Study," LBL-15350.

Other Publications

1. N. Caswell and P. Y. Yu, "Physical Model for the Temperature Dependence of the Cu_2O Yellow Exciton Luminescence Intensity," Bull. Am. Phys. Soc. 27, 175 (1982).

2. J. S. Weiner and P. Y. Yu, "Lifetime of Photoexcited Carriers in Pure GaAs, GaAs:Cr, and GaAs:O," Bull. Am. Phys. Soc. 27, 335 (1982), LBL-13757.

Invited Talks

1. P. Y. Yu, "Some Picosecond Laser Experiments in GaAs," Quantum Electronics Seminar, Dept. of Electrical Engineering of Computer Science, UC-Berkeley, April 14, 1982.

2. P. Y. Yu, "Picosecond Laser Spectroscopies in Semiconductors," Cavendish Laboratory, Cambridge, August 26, 1982.

e. Superconductivity, Superconducting Devices, and 1/f Noise*

John Clarke, Investigator

1. CHAOS IN JOSEPHSON JUNCTIONS†

R. F. Miracky, R. H. Koch, and J. Clarke

There has been increased interest over the past several years in the properties of nonlinear differential equations and physical systems described by such equations. Under appropriate circumstances, such systems exhibit chaos, a special, aperiodic solution to the governing equations that appears experimentally as broad band noise. However, most physical systems are too complicated to be represented by models suitable for analytical or numerical methods. The Josephson junction is a notable exception and is thus an excellent system for studies of chaotic behavior.

We have studied Josephson tunnel junctions fabricated to exhibit chaotic behavior. Each junction is shunted with its self-capacitance and an external resistance with substantial self-inductance. The equation of motion of this system, when biased with a constant current, is third order and nonlinear in the phase difference across the junction and is therefore expected to exhibit chaos. We have modeled this system using analog and digital computers, with parameters chosen to approximate those of the tunnel junctions.

Experiments performed on these junctions reveal two phenomena. First, the current-voltage characteristics exhibit stable regions of negative resistance. Second, measurements of the low frequency voltage noise as a function of bias current show excessively noisy intervals, usually in the vicinity of the negative resistance regions, separated by low-noise regions. We have identified this excess noise as arising from two different mechanisms: chaos, characterized by noise temperatures T_N of about 10^3 K; and switching between subharmonic modes, with $T_N \gtrsim 10^6$ K. Representative voltage spectral densities from the analog are given in Fig. 1.1a and b. In Fig. 1.1a, which represents a chaotic region, the low frequency noise has a temperature of about 800 K, independent of whether or not thermal noise is present in the shunt resistor. Figure 1.1b shows the spectral density of the noise in a switching regime, with a noise temperature of over 10^5 K when thermal noise equivalent to about 3 K is present in the resistor. When this thermal noise is removed, the switching ceases, and the noise from the simulator becomes too low to be measured. Figure 1.1c shows the spectral density of the high frequency noise from a real junction and shows clearly the two metastable subharmonic modes between which the junction switches, producing a low frequency noise of over 10^6 K.

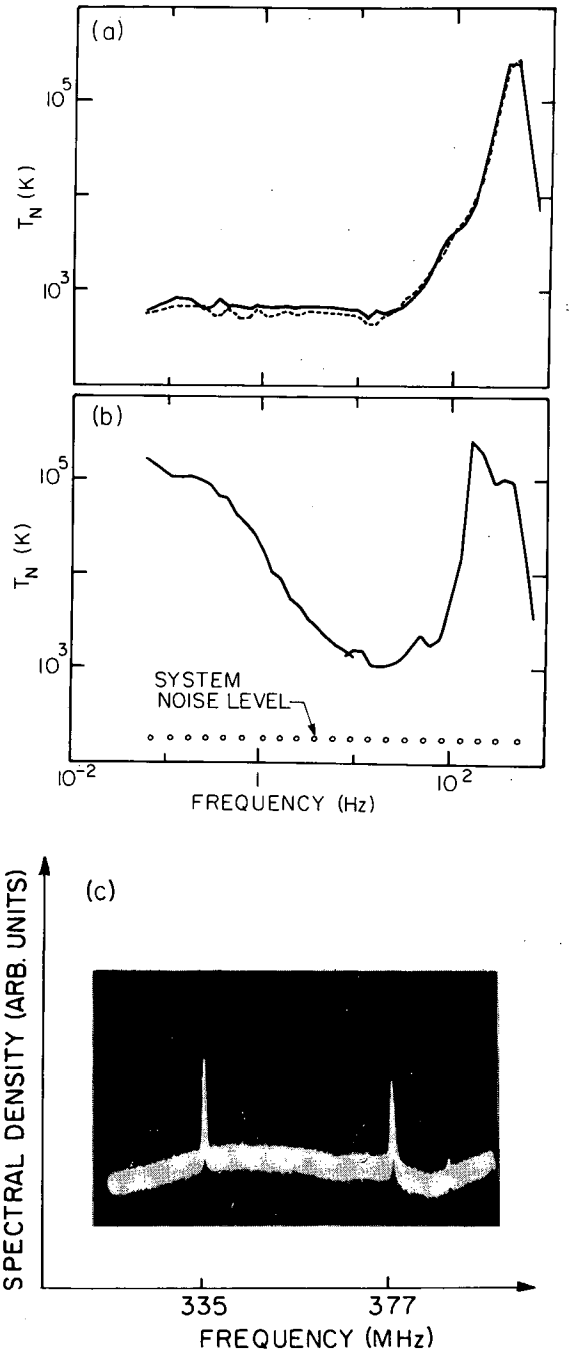

Fig. 1.1. Spectral density of voltage noise from analog in (a) chaotic regime and (b) switching regime with (____) and without (---) 3 K thermal noise in shunt resistor. (c) shows two subharmonic modes in real junction between which the system switches to produce large levels of low frequency noise. (XBB 820-9646A)

* * *

*This work was supported by the Director, Office of Energy Research, Office of Basic Energy Sciences, Materials Sciences Division of the U.S. Department of Energy under Contract No. DE-AC03-76SF00098.

†Brief version of LBL-15221.

2. MEASUREMENTS OF CURRENT NOISE IN DC SQUIDs†

J. M. Martinis and J. Clarke

To calculate the noise temperature of a voltage amplifier involving a dc superconducting quantum interference device (SQUID) one needs to know the flux-to-voltage transfer function, $V_\Phi \equiv \partial V/\partial\Phi$, the spectral density of the voltage noise across the SQUID, $S_V(f)$, the spectral density of the current noise in the SQUID loop, $S_J(f)$, and the cross-spectral density of these two noises, $S_{VJ}(f)$. Here, V is the voltage across the SQUID, Φ is the applied magnetic flux, and f is the frequency, assumed to be much less than the Josephson frequency. At frequencies above the 1/f noise region, the noise terms arise from Johnson noise in the resistive shunts of the junctions and have white spectral densities. The terms $S_J(f)$ and $S_{VJ}(f)$ have not been measured previously; we here report results of such measurements and compare them with the predictions of an analog simulator.

The SQUID were fabricated from thin films in a planar configuration, tightly coupled to a 50-turn superconducting spiral input coil. The shunt resistance of the SQUID on which noise measurements were made was two orders of magnitude lower than usual so as to enhance the magnitude of the current noise. The coil of this SQUID was coupled to the coil of a second SQUID, which was then used to measure the current noise. The voltage across the first SQUID was measured with a cooled resonant tank circuit coupled to a low noise preamplifier, and the cross correlation between the current and voltage noises was measured with a spectrum analyzer. An analog simulation of the SQUID was also fabricated and used to predict the performance of the real SQUID.

The results are shown in Fig. 2.1, where the measured values of $|V_\Phi|/(I_0R/\Phi_0)$, γ_V, γ_J, and γ_{VJ} are plotted vs Φ/Φ_0. The results are in good agreement with the predictions of the analog simulator. From these measurements, we can calculate the noise temperature of the SQUID used as an amplifier with a tuned input circuit and find $T_N \approx 10^{-6}(f/1\ \text{Hz})$ K. The corresponding value for a SQUID with the usual values of the shunt resistors is about $10^{-8}(f/1\ \text{Hz})$ K.

* * *

†Brief version of LBL-15313.

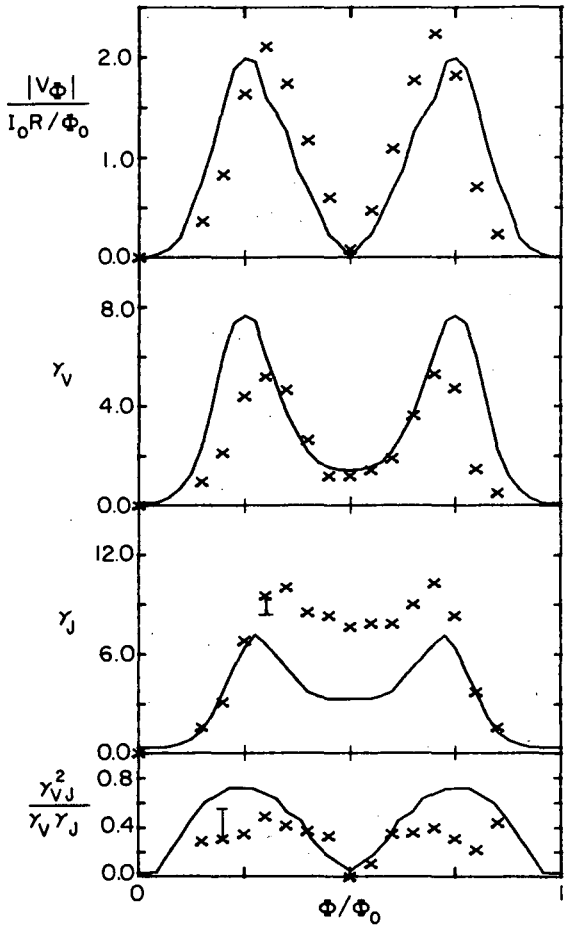

Fig. 2.1. $|V_\Phi|$, γ_V, γ_J and γ_{VJ} for real SQUID (x) and analog SQUID (___) with the same parameters. (Φ_0 is the flux quantum, I_0 and R are the critical current and resistance of each junction, and the γ's are the dimensionless spectral densities of the noises normalized to the Johnson noise in the resistive shunts.)
(XBL 831-5084)

3. CORRELATION LENGTHS IN MAGNETOTELLURICS†

W. M. Goubau, P. Maxton, and J. Clarke

In the magnetotelluric method, one determines the impedance tensor of the ground, $\underset{\approx}{Z}(\omega)$, by simultaneously measuring the orthogonal horizontal components of the fluctuating magnetic and elec-

tric fields $\vec{H}(\omega)$ and $\vec{E}(\omega)$. These fluctuations are generated in the magnetosphere and propagate to the earth's surface approximately as plane waves. The magnetic field fluctuations can be measured with SQUID magnetometers, while the electric field fluctuations are measured by means of buried electrodes. The method is widely used in geophysical prospecting for geothermal sources, oil deposits, and other natural resources. A significant advance in the technique was the introduction by this group of the remote reference technique in which the two horizontal components of the magnetic field are measured by a second, remote magnetometer. The signals are telemetered to the base station and used to lock-in detect the magnetotelluric signals. This technique has resulted in a major improvement in the quality of magnetotelluric data. However, the minimum necessary separation of the base and remote stations has never been established--separations of 5 km or more are typically used--and the purpose of this investigation was to establish this length.

The site chosen was near Mount Hamilton, California. A base station consisting of a two-axis SQUID magnetometer and buried electrodes was established, as was a remote reference SQUID magnetometer, with telemetry to the base station. A third SQUID magnetometer was then used as a local reference; its separation from the base magnetometer was varied between 2 and 400 m. Signals from the local reference were transmitted to the base station via coaxial cables. Data from the buried electrodes and three magnetometers were collected simultaneously. The impedance tensor was then calculated using the remote reference, the local reference, and using the least squares technique on data from the base magnetometer alone (i.e., auto-reference).

The results are shown in Fig. 3.1, where the apparent resistivity in a particular direction is plotted vs period for each of the three methods and for three separations between the base and local reference. We see immediately that the remote and local reference methods yield substantially higher quality data than the auto-reference. The discrepancies between the local and remote references are small but significant at the 2 and 100 m separations, and have disappeared by the time the separation has been increased to 200 m. This result has important consequencies for surveying, implying that the magnetic fields from stations only (say) 1 km apart can be used as reference signals. Thus, remote referenced data can be collected at two nearby sites simultaneously, without the need for a relatively distant reference magnetometer, thereby doubling the rate at which an area can be surveyed.

* * *

†Brief version of LBL-15484.

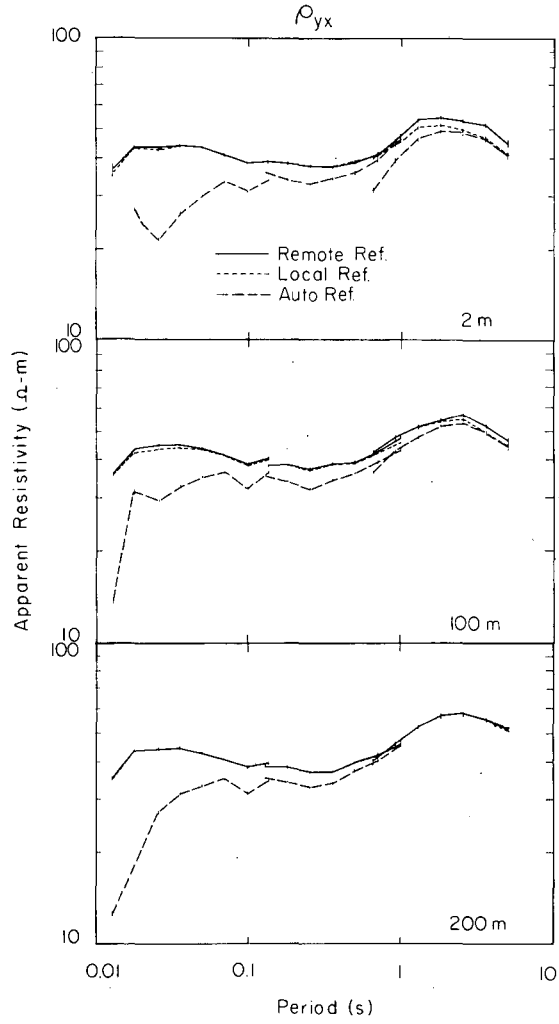

Fig. 3.1. Apparent resistivity vs period using remote, local, and auto-reference techniques for three separations of the base magnetometer and the local reference magnetometer. (XBL 831-5085)

1982 PUBLICATIONS AND REPORTS

Refereed Journals

1. T. D. Gamble, W. M. Goubau, R. Miracky, and J. Clarke, "Magnetotelluric Regional Strike," Geophys. 27, 932 (1982); LBL-10846.

2. D. J. Van Harlingen, R. H. Koch, and J. Clarke, "Superconducting Quantum Interference Device with Very Low Magnetic Flux Noise Energy," Appl. Phys. Lett. 41, 197 (1982); LBL-13668.

3. R. H. Koch, D. J. Van Harlingen, and J. Clarke, "Measurements of Quantum Noise in Resistively Shunted Josephson Junctions," Phys. Rev. B 26, 74 (1982); LBL-13326.

4. R. H. Koch, D. J. Van Harlingen, and J. Clarke, "Observation of Quantum Noise in a Resistively Shunted Josephson Junction," Physica B and C 109 & 110, 2055 (1982); LBL-13748.

Other Publications

1. J. Clarke and P. L. Richards, "Quantum Noise in Superconducting Tunnel Junctions," Physics News in 1981, p. 37.

2. J. Clarke, "Superconducting Devices," in Concise Encyclopedia of Sciences and Technology, edited by R. G. Lerner and G. L. Trigg, Addison-Wesley, Reading, Massachusetts, 1982, p. 263; LBL-12135.

3. R. H. Koch, J. M. Martinis, and J. Clarke, "Measurements of Chaotic Noise in Current-Biased Josephson Junctions Shunted with a Resistance and an Inductance in Series," Bull. Am. Phys. Soc. 27, 266 (1982); LBL-13750 Abs.

4. D. Seligson and J. Clarke, "Phonon-Induced Enhancement of the Energy Gap and Critical Current of Superconducting Aluminum Films," Bull. Am. Phys. Soc. 27, 252 (1982); LBL-13749 Abs.

5. J. Clarke, "SQUID," McGraw-Hill Encyclopedia of Sciences and Technology, 1982, p. 28; LBL-12136.

6. J. Clarke, "Superconducting Devices," McGraw-Hill Encyclopedia of Sciences and Technology, 1982, p. 339; LBL-12136.

7. W. M. Goubau, N. E. Goldstein, and J. Clarke, "Magnetotelluric Studies at the Cerro Prieto Geothermal Field," Proceedings of the 3rd Symposium on the Cerro Prieto Geothermal Field, Baja California, Mexico, March 24-26, 1981, p. 357; LBL-11967, published in 1982.

LBL Reports

1. J. Clarke, "Fundamental Limits on SQUID Technology," LBL-14972.

2. R. H. Koch, J. Clarke, W. M. Goubau, J. M. Martinis, C. M. Pegrum, and D. J. Van Harlingen, "Flicker (1/f) Noise in Tunnel Junction DC SQUIDs," LBL-14973.

3. J. Clarke, "Geophysical Applications of SQUIDs," LBL-15312.

4. J. M. Martinis and J. Clarke, "Measurements of Current Noise in DC SQUIDs," LBL-15313.

5. R. H. Koch, J. Clarke, J. M. Martinis, W. M. Goubau, C. M. Pegrum, and D. J. Van Harlingen, "Investigation of 1/f Noise in Tunnel Junction DC SQUIDs," LBL-15314.

Invited Talks

1. J. Clarke, "Quantum Noise in Josephson Junctions and SQUIDs," Department of Applied Science, Stanford University, November 5, 1981.

2. J. Clarke, "Quantum Noise in Josephson Junctions and SQUIDs," Institute for Theoretical Physics, University of California, Santa Barbara, November 18, 1981.

3. R. H. Koch and J. Clarke, "Chaotic Noise Observed in Current-Biased Josephson Junctions Shunted with a Resistance in Series with an Inductance," Dynamic Days, La Jolla Institute, La Jolla, California, January 5-7, 1982.

4. D. Seligson and J. Clarke, "Phonon-Induced Enhancement of the Energy Gap and Critical Current of Superconducting Aluminum Films," 1982 March Meeting of the American Physical Society, Dallas, Texas.

5. R. H. Koch, J. M. Martinis, and J. Clarke, "Measurements of Chaotic Noise in Current-Biased Josephson Junctions Shunted with a Resistance and an Inductance in Series," 1982 March Meeting of the American Physical Society, Dallas, Texas.

6. J. Clarke, "SQUIDs and Geophysics," Physics Division Colloquium, Los Alamos Scientific Laboratory, Los Alamos, New Mexico, May 6, 1982.

7. J. Clarke, "SQUIDs," Low Energy Physics, Quarks, SQUIDs, and the Cosmos Conference, University of California, Davis, California, May 16, 1982.

8. J. Clarke, "Applications of SQUIDs," NATO Summer School on Superionic Conductors, Erice, Sicily, July 10, 1982.

9. J. Clarke, "The Limits of SQUID Technology I," NATO Summer School on Advances in Superconductivity, Erice, Sicily, July 12, 1982.

10. J. Clarke, "The Limits of SQUID Technology II," NATO Summer School on Advances in Superconductivity, Erice, Sicily, July 13, 1982.

11. J. Clarke, "Experiments on Chaos in Josephson Junctions," Gordon Conference in Quantum Solids and Fluids, Plymouth, New Hampshire, July 19, 1982.

12. J. Clarke, "Chaos in Josephson Junctions," Bell Laboratories, Murray Hill, New Jersey, July 26, 1982.

13. J. Clarke, "Quantum Noise in Josephson Junctions and SQUIDs," Oak Ridge National Laboratory, Oak Ridge, Tennessee, November 29, 1982.

14. J. Clarke, "Geophysical Applications of SQUIDs," 1982 Applied Superconductivity Conference, Knoxville, Tennessee, November 30 - December 3, 1982.

15. J. M. Martinis and J. Clarke, "Measurements of Current Noise in DC SQUIDs," 1982 Applied Superconductivity Conference, Knoxville, Tennessee, November 30 - December 3, 1982.

16. R. H. Koch, J. Clarke, J. M. Martinis, W. M. Goubau, C. M. Pegrum, and D. J. Van Harlingen, "Investigation of 1/f Noise in Tunnel Junction DC SQUIDs," 1982 Applied Superconductivity Conference, Knoxville, Tennessee, November 30 - December 3, 1982.

6. Theoretical Research

a. Theoretical Studies of the Electronic Properties of Solid Surfaces*

Leo M. Falicov, Investigator

Introduction. The purpose of this program is to study properties of solid surfaces. In particular the interest is in determining: (a) structural properties of surfaces, namely, the organization and arrangement of atomic constituents at equilibrium; (b) constitutional properties of the surface, in particular the segregation properties of alloys at the surface as a function of crystal structure, surface orientation, nominal chemical composition and temperature; (c) electronic structure of surfaces, in particular electron states and electron densities in the neighborhood of the surface; (d) vibronic properties of surfaces; (e) magnetic properties of surface, both in magnetic solids (ferromagnetic and antiferromagnetic) or in nonmagnetic solids that may develop a magnetic surface layer; and (f) chemical--in particular the catalytic--properties of solids as they are related to basic physical properties (a)-(e).

A variety of theoretical techniques and models to focus on the various properties (band-structure models, many-body electron physics, numerical relaxation techniques) are developed, but the emphasis is on physical aspects and their implication to experiments rather than techniques per se.

1. MAGNETIC AND ELECTRONIC PROPERTIES OF Ni FILMS, SURFACES, AND INTERFACES

L. M. Falicov and Jerry D. Tersoff

The problem of magnetism on Ni surfaces, Ni interfaces, and overlayers of Ni on a variety of other nonmagnetic metals has been an open problem for a long time. Reports of "dead layers," i.e., layers which are nonmagnetic, have been abundant in the literature. This seems to indicate that the surface of Ni contains up to two atomic layers in which the magnetism is quenched. The reports, however, are not consistent with one another, and the various experiments have been done by measuring the total magnetization of relatively thin films of Ni deposits on a variety of mostly poorly characterized substrates. Recent experiments, however, as well as a few first-principle calculations, seem to indicate that the surface layer of pure Ni metals is either fully magnetic, has its magnetism only very slightly reduced, or even has a small enhancement of its magnetization.

The purpose of this research was to investigate these apparently contradictory results and to resolve the controversy. In a series of papers[1] self-consistent calculations of the electronic structure and the magnetization of Ni, NiCu interfaces, Ni overlayers on Cu, and in general Ni overlayers have been carried out.

It is found that magnetization is suppressed in the Ni-Cu or Ni-simple metal interfaces, but enhanced in either the Ni surface or in isolated Ni thin films. The net effect of this competition is that a Ni monolayer is substantially magnetic on Cu(100) but paramagnetic (or nearly so) on Cu(111). Film magnetization is found to be very sensitive to substrate composition. For substrates which couple strongly to the Ni film, ferromagnetism first appears at about three atomic layer Ni, in quantitative agreement with experiments based on Al and Pb-Bi substrates. The crucial mechanism acting to suppress Ni magnetization is sp-d hybridization. Figure 1.1 shows the magnetization at the various atomic layers of Ni overlayers of various thicknesses on any metal that couples strongly to the Ni electrons. The results are striking and in good agreement with experiment: Overlayers of up to two atom thickness are "dead." Overlayers thicker than two atoms are fully magnetic, with the magnetization enhanced at the free surface and completely quenched at the interface.

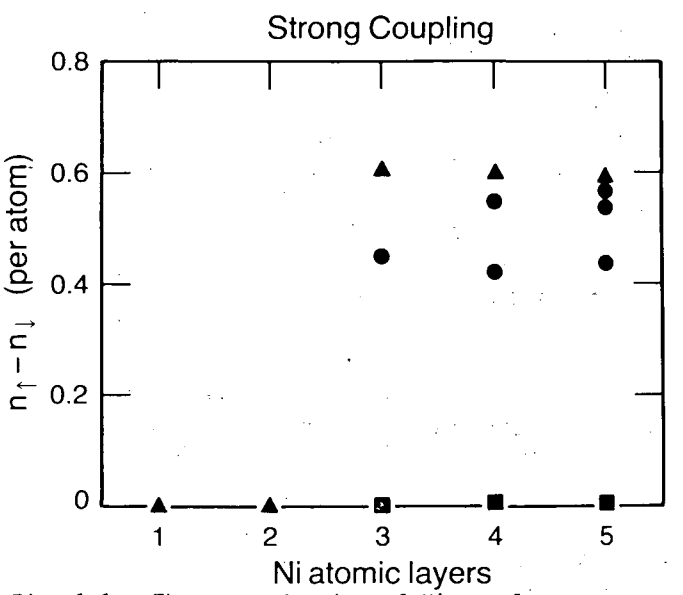

Fig. 1.1. The magnetization of Ni overlayers on a strongly coupled metallic substrate. The abscissa indicates the thickness (in atoms) of the Ni overlayer. The ordinate is the magnetization of each atomic layer. Triangles correspond to the surface (free) layer, squares are the interface layer, and circles correspond to layers in between. (XBL 832-8068)

*This work was supported by the Director, Office of Energy Research, Office of Basic Energy Sciences, Materials Sciences Division of the U.S. Department of Energy under Contract No. DE-AC03-76SF00098.

* * *

1. L. M. Falicov and J. Tersoff, Phys. Rev. B 25, 2959 (1982); Phys. Rev. B 26, 469 (1982); Phys. Rev. B 26, 6186 (1982).

2. THERMODYNAMIC PROPERTIES OF Li INTERCALATED AND DISORDERED LAYER COMPOUNDS

L. M. Falicov and R. Osório

The electrochemical properties of Li intercalation in $Ta_yTi_{1-y}S_2$ have been the subject of intensive experimental studies. The structure in the "incremental capacity" is difficult to understand and shows signs of strong correlation between the Li ions themselves, and between the position of the Li ions and the composition of the disordered structure.

We have completed a mean-field approximation calculation[1] applied to a triangular-lattice gas model with three different randomly distributed sites and nearest-neighbor interaction between the gas particles. This represents well the system under consideration. Ground-state diagrams show various sequences of ordered phases. Finite temperature results show minima in the "incremental capacity" curves because of nearly complete filling of sites of a given chemical type. The model is good for those alloys where the experimental results suggest a disordered distribution of Li atoms.

* * *

1. L. M. Falicov and R. Osório, J. Chem. Phys. 77, 6218 (1982).

1982 PUBLICATIONS AND REPORTS

Refereed Journals

†1. M. Kiwi, T. H. Lin, and L. M. Falicov, "Antiferromagnetism, Projected Density of States and the Bogoliubov Transformation for Bosons," Phys. Rev. B 25, 432 (1982).

2. R. Osório and L. M. Falicov, "Cluster-Variation Method for the Triangular Lattice Gas," J. Phys. Chem. Solids 43, 73 (1982); LBL-11474 and LBL-11475.

†3. L. M. Falicov and B. Joós, "Potential of a Positive Test Charge in Germanium: Application to Hydrogen," Phil. Mag. 45, 255 (1982).

†4. M. Robbins and L. M. Falicov, "Electronic Theory of Ordering and Segregation in Binary Alloys: Application to Simple Metals," Phys. Rev. B 25, 2343 (1982).

5. J. Tersoff and L. M. Falicov, "Interface Magnetization: Cu Films on Ni(100)," Phys. Rev. B 25, 2959 (1982); LBL-13624.

†6. J. L. Morán-López and L. M. Falicov, "Theory of Hydrogen Chemisorption," J. Vac. Sci. Technol. 20, 831 (1982).

7. J. Tersoff and L. M. Falicov, "Calculation of Magnetization in Ordered Ni-Cu Alloys," Phys. Rev. B 25, 4937 (1982); LBL-13625.

†8. J. Testa and L. M. Falicov, "Two-Band Model of Itinerant Magnetism," Am. J. Phys. 50, 647 (1982).

9. J. Tersoff and L. M. Falicov, "Presence and Absence of Magnetism in Thin Ni Films," Phys. Rev. B 26, 459 (1982); LBL-13958.

10. J. Tersoff and L. M. Falicov, "sp↔d Charge Transfer at Transition- and Noble-Metal Surfaces: A Reply," Phys. Rev. B 26, 1058 (1982); LBL-14363.

†11. J. L. Morán-López and L. M. Falicov, "Self-Consistent Model of Hydrogen Chemisorption on Ferromagnetic Transition Metals," Phys. Rev. B 26, 2560 (1982).

12. J. Tersoff and L. M. Falicov, "Magnetic and Electronic Properties of Ni Films, Surfaces, and Interfaces," Phys. Rev. B 26, 6186 (1982); LBL-14507.

13. R. Osório and L. M. Falicov, "Effect of Disorder on the Li Intercalation Properties of $Li_xTa_yTi_{1-y}S_2$: A Mean-Field Theory, J. Chem. Phys. 77, 6218 (1982); LBL-14816.

†14. M. J. Pinto and B. Koiller, "Optical Properties of Crystals with Impurities," J. Phys. C 15, 7229 (1982).

LBL Reports

1. J. Tersoff, "Electronic, Magnetic and Chemical Properties of Films, Surfaces and Alloys," Ph.D. thesis, LBL-14484.

2. R. Osório, "The Two-Dimensional Triangular Lattice and Its Application to Lithium Intercalated Layered Compounds," Ph.D. thesis, LBL-14815.

Other Publications

1. L. M. Falicov, "Spin Waves at Surfaces and Steps in Ferromagnets and Antiferromagnets," in Excitations in Disordered Systems, edited by M. F. Thorpe, Plenum Press, New York, 1982, p. 489.

2. J. L. Morán-López and L. M. Falicov, "Magnetic Excitations at the Surface of Alloys with Magnetic Components," in Excitations in Disordered Systems, edited by M. F. Thorpe, Plenum Press, New York, 1982, p. 501.

†3. L. M. Falicov and M. Robbins, "Theory of Ordering and Segregation in Binary Alloys: Application to Alkali and Noble Metals," in Excitations in Disordered Systems, edited by M. F. Thorpe, Plenum Press, New York, 1982, p. 613.

†4. L. M. Falicov, "Summary: Disordered Systems in Perspective," in Excitations in Disordered Systems, edited by M. F. Thorpe, Plenum Press, New York, 1982, p. 677.

5. J. Tersoff and L. M. Falicov, "Calculations of Magnetization in Ni- on Cu- and Cu-on-Ni Film Systems," Bull. Am. Phys. Soc. 27, 153 (1982).

†6. M. Robbins and L. M. Falicov, "Total Energies and Short-Range Order in Transition-Metal Alloys," Bull. Am. Phys. Soc. 27, 186 (1982).

7. L. M. Falicov and J. Tersoff, "Calculations of Magnetization in Artificial Ordered Ni-Cu Alloys," Bull. Am. Phys. Soc. 27, 214 (1982).

Invited Talks

1. L. M. Falicov, "Electronic, Chemical and Magnetic Properties of Metallic Overlayers," Materials and Molecular Research Division Annual Review Symposium, Lawrence Berkeley Laboratory, February 8, 1982.

2. L. M. Falicov, "Theory of Hydrogen Chemisorption on Ferromagnetic Transition Metals," International Symposium on the Electronic Structure and Properties of Hydrogen in Metals, Richmond, Virginia, March 6, 1982.

3. L. M. Falicov, "Electrical, Magnetic and Chemical Properties of Ni Overlayers," Seminaire de Physique des Solides, L.M.S.E.S., France, July 2, 1982.

4. L. M. Falicov, "Electronic, Magnetic, and Chemical Properties of Nickel Overlayers," Seminar at General Motors Research Laboratories, Warren, Michigan, July 22, 1982.

5. J. L. Morán-López and L. M. Falicov, "Theory of Surface Effects in Binary Alloys," Symposium on Alloys Phase Diagrams, Materials Research Society Meeting, Boston, Massachusetts, November 1, 1982.

6. M. O. Robbins and L. M. Falicov, "Electronic Energy and Short-Range Order in Binary Alloys," Symposium on Alloys Phase Diagrams, Materials Research Society Meeting, Boston, Massachusetts, November 1, 1982.

* * *

†Work supported in part by the National Science Foundation through Grant DMR81-06494.

b. Theoretical Solid State Physics*

Marvin L. Cohen, Investigator

Introduction. In addition to developing general theories and techniques for studying the properties of solids, solid state theorists are now able to calculate the properties of real materials. The necessary ingredients are quantum mechanics, a theory of how electrons interact with each other and with atomic ions in a crystal, and a technique for computing properties that can be measured. In the description below, specific applications to solid surfaces, crystal structure, lattice dynamics, and electronic structure are described. Much of the work is based on the use of a pseudopotential to represent the interaction between the electrons and ions, and a method for computing the total energy of the solid.

1. SOLID SURFACES†

John E. Northrup and Marvin L. Cohen

One of the most important problems in surface physics is the determination of the structure of Si(111). This surface is the most studied surface in science. However, a detailed description of its atomic arrangement and electronic structure is still lacking.

An attempt to calculate the atomic positions and electronic structure was made. To compute the surface atomic arrangement, the forces on all the atoms were calculated as a function of the positions of the atoms. By moving atoms near the surface in the direction of the residual forces found, a minimum energy configuration could be obtained. It was necessary to include the effects of spin in these calculations.

The results were two-fold: for a 1 x 1 geometry it was found that the lowest energy structure is spin polarized; for a 2 x 1 geometry the lowest energy structure was found to be similar to a chain model proposed by Pandey. The 1 x 1 structure is stable against buckling distortions and is antiferromagnetic. The 2 x 1 configuration has lower energy, and the calculated electronic structure agrees well with the corresponding angle-resolved photoemission experimental results.

* * *

†Brief version of Phys. Rev. Lett. 47, 1910 (1981), J. Vac. Sci. Technol. 21, 333 (1982), and Phys. Rev. Lett. 49, 1349 (1982).

*This work was supported by the Director, Office of Energy Research, Office of Basic Energy Sciences, Materials Sciences Division of the U.S. Department of Energy under Contract No. DE-AC03-76SF00098 and also by the National Science Foundation Grant No. DMR7822465.

2. CRYSTAL STRUCTURE†

M. Y. Chou, S. Froyen, Pui K. Lam, M. T. Yin, and Marvin L. Cohen

For the first time, it has become possible to calculate accurately the crystal structure of solids. The first examples of successes for this method involve the semiconductors Si and Ge. The current extensions are to diamond, beryllium, and compound semiconductors.

The method involved in these calculations consists of an evaluation of the total energy of a solid in an assumed configuration. The total energy is then compared for various structures, and a minimum energy structure is assumed to correspond to the actual structure. One limitation of this method is that it requires a subset of likely structures as input. The only other input to the calculation is the atomic number.

The results for the materials investigated are consistent with experiment. Lattice constants, bulk moduli, cohesive energies, and other properties are computed. A major focus of this research is the prediction of stable structures at high pressure. A significant amount of effort was made to compute high-pressure forms of III-V semiconductors. Although the experimental results are sparse, there is some agreement for the structure and transition pressure between theory and experiment. This work is being expanded with the hope that high-pressure structures will be predicted successfully.

* * *

†Brief version of Phys. Rev. B 24, 6121 (1981), Solid State Comm. 42, 861 (1982), Solid State Comm. 43, 447 (1982), and Phys. Rev. B 26, 5668 (1982).

3. LATTICE DYNAMICS†

Pui K. Lam, M. T. Yin, and Marvin L. Cohen

In the past the calculation of the vibrational structure of solids often involved the use of empirical parameters. Recently an ab initio approach was developed which is an outgrowth of the total energy formalism discussed above. The method involves a calculation of the total energy for an undistorted crystal and for a crystal containing a frozen-in distortion corresponding to a phonon. A comparison of these two cases yields the energy of the phonon or lattice vibration of interest.

The applications of this method have been made to Si, Ge, and Al. At first it was only possible to calculate the lattice vibrational frequencies at specific wavevectors in the Brillouin zone. A recent development involves the computation of

force constants determined by computing the forces on atoms arising from the displacement of a plane of atoms. This method allows the calculation of the frequency of the lattice vibration as a function of wavevector along a symmetry line in the Brillouin zone.

The applications to Si, Ge, and Al have been successful. In addition to yielding the frequencies of the vibrations, the pressure coefficients of the vibrational modes have also been determined. This ab initio approach requires only the atomic mass, atomic number, and crystal structure.

* * *

†Brief version of Phys. Rev. B 25, 4317 (1982), Phys. Rev. B 25, 6139 (1982), Solid State Comm. 43, 391 (1982), and Phys. Rev. B 26, 3259 (1982).

4. ELECTRONIC STRUCTURE†

M. Y. Chou, Pui K. Lam, J. E. Northrup, M. T. Yin, and Marvin L. Cohen

Once the crystal structure of a material or its surface has been determined, it is possible using modern electronic structure techniques to compute the behavior of the electrons in the crystal. In particular, the electronic band structure, density of states, and charge density can be evaluated. These functions are useful in determining the electronic properties of materials.

The calculations were applied both to ideal materials and solids with defects (i.e., dislocations). In general, the results yield good agreement with experiment, and the calculations often indicate new theoretical solutions and problems. For example, the calculation of the Compton profile of Be gave excellent agreement with experiment; however, a small directionally independent difference between the measured and calculated spectra remained. This difference was substantially reduced by incorporating correlation effects. The application of electronic structure theory leads to improvements of the pseudopotential itself and the underlying theory involved in its applications.

* * *

†Brief version of Phys. Rev. B 24, 7210 (1981); Phys. Rev. Lett. 49, 1452 (1982).

5. WORK IN PROGRESS

The above research will be extended to include other materials. In particular, more ionic crystals will be investigated. Some calculations on the electronic structure of alloys of semiconductors are in progress. Compton effect calculations for graphite are also in progress.

1982 PUBLICATIONS AND REPORTS

Refereed Journals

1. John E. Northrup, Marvin L. Cohen, J. R. Chelikowsky, J. Spence, and A. Olsen, "Electronic Structure of the Unreconstructed 30° Partial Dislocation in Silicon," Phys. Rev. B 24, 4623 (1981).

2. M. T. Yin and Marvin L. Cohen, "Ground-state Properties of Diamond," Phys. Rev. B 24, 6121 (1981).

3. John E. Northrup, J. Ihm, and Marvin L. Cohen, "Spin Polarization and Atomic Geometry of the Si(111) Surface," Phys. Rev. Lett. 47, 1910 (1981).

4. A. K. McMahan, M. T. Yin, and Marvin L. Cohen, "Comparison of Methods for the Calculation of Phase Stability in Silicon," Phys. Rev. B 24, 7210 (1981).

5. Marvin L. Cohen and J. R. Chelikowsky, "Pseudopotentials for Semiconductors," in Handbook on Semiconductors, Vol. 1, edited by W. Paul, North-Holland, Amsterdam, 1982, p. 219.

6. Marvin L. Cohen, V. Heine, and J. C. Phillips, "The Quantum Mechanics of Materials," Scientific American 246, 66 (1982).

7. M. T. Yin and Marvin L. Cohen, "Ab Initio Calculation of the Phonon Dispersion Relation: Application to Si," Phys. Rev. B 25, 4317 (1982).

8. Pui K. Lam and Marvin L. Cohen, "Ab Initio Calculation of Phonon Frequencies of Al," Phys. Rev. B 25, 6139 (1982).

9. M. Y. Chou, Pui K. Lam, and Marvin L. Cohen, "Ab Initio Calculation of the Static Structural Properties of Be," Solid State Comm. 42, 861 (1982).

10. M. T. Yin and Marvin L. Cohen, "Theory of Ab Initio Pseudopotential Calculations," Phys. Rev. B 25, 7403 (1982).

11. M. T. Yin and Marvin L. Cohen, "Calculation of the Lattice Dynamical Properties of Ge," Solid State Comm. 43, 391 (1982).

12. S. Froyen and Marvin L. Cohen, "High Pressure Phase of III-V Semiconductors: A Microscopic Theory," Solid State Comm. 43, 447 (1982).

13. John E. Northrup and Marvin L. Cohen, "Electronic Structure of the π-bonded Chain Model and the Nonbuckled Antiferromagnetic Insulator Model for the Si(111) Surface," J. Vac. Sci. Technol. 21, 333 (1982).

14. Steven G. Louie, S. Froyen, and Marvin L. Cohen, "Nonlinear Ionic Pseudopotentials in Spin-density-functional Calculations," Phys. Rev. B 26, 1738 (1982).

15. M. T. Yin and Marvin L. Cohen, "Theory of Lattice-dynamical Properties of Solids: Application to Si and Ge," Phys. Rev. B 26, 3259 (1982).

16. J. C. Phillips and Marvin L. Cohen, "Molecular Models of Giant Photocontractive Evaporated Chalcogenide Films," Phys. Rev. B 26, 3510 (1982).

17. John E. Northrup and Marvin L. Cohen, "Reconstruction Mechanism and Surface State Dispersion for Si(111)-2x1," Phys. Rev. Lett. 49, 1349 (1982).

18. M. Y. Chou, Pui K. Lam, Marvin L. Cohen, G. Loupias, J. Chomilier, and J. Petiau, "Compton Profile of Beryllium," Phys. Rev. Lett. 49, 1452 (1982).

19. Marvin L. Cohen and T. Geballe, "Novel Superconducting Materials and Mechanisms," in Superconductivity in d- and f-Band Metals, edited by W. Buckel and W. Weber, Kernforschungszentrum Karlsruhe GmbH, Karlsruhe, 1982, p. 619.

20. Marvin L. Cohen, "Pseudopotentials and Total Energy Calculations," Physica Scripta T1, 5 (1982).

21. M. T. Yin and Marvin L. Cohen, "Theory of Static Structural Properties, Crystal Stability, and Phase Transformations: Application to Si and Ge," Phys. Rev. B 26, 5668 (1982).

Other Publications

1. Marvin L. Cohen, "Calculations of Properties of Materials," submitted to Encyclopedia of Material Science and Engineering.

2. Marvin L. Cohen, "Semiconductor," Funk and Wagnall's Encyclopedia, in press.

3. John E. Northrup and Marvin L. Cohen, "Pseudopotential Total Energy Calculations for Si(111)-(1x1) and Si(111)-(2x1)," The 16th International Conference on the Physics of Semiconductors, Montpellier, France, in press.

4. S. Froyen and Marvin L. Cohen, "Static and Structural Properties of III-V Zincblende Semiconductors," The 16th International Conference on the Physics of Semiconductors, Montpellier, France, in press.

5. Pui K. Lam and Marvin L. Cohen, "Calculation of High Pressure Phases of Al," in press.

Invited Talks

1. Marvin L. Cohen, "Pseudopotentials and Solid State Physics," Department of Physics, University of Oregon, February 11, 1982.

2. Marvin L. Cohen, "Surfaces and Interfaces," Department of Physics, University of Oregon, February 12, 1982.

3. Marvin L. Cohen, "Pseudopotentials and Total Energy Calculations," invited opening plenary paper, European Physical Society, Manchester, England, March 22, 1982.

4. Marvin L. Cohen, "Pseudopotential Calculations for Real Materials," Department of Physics, Virginia Polytechnic Institute and State University, Blacksburg, VA, April 29, 1982.

5. Marvin L. Cohen, "Electrons on Solid Surfaces and Interfaces," Department of Physics, Virginia Polytechnic Institute and State University, Blacksburg, VA, April 30, 1982.

6. Marvin L. Cohen, "Quantum Mechanical Structure Calculations Using Pseudopotentials," invited opening paper, CALPHAD XI Conference, Argonne National Laboratory, Argonne, IL, May 17, 1982.

7. Marvin L. Cohen, "Pseudopotentials: Past, Present, and Future," combined Physics Colloquium for the University of Heidelberg, the University of Karlsruhe, and the Kernforschungszentrum Karlsruhe, Karlsruhe, Germany, June 25, 1982; Max Planck Institute, Stuttgart, Germany, July 1, 1982; Department of Physics, University of Chicago, IL, October 14, 1982; Department of Physics, University of Wisconsin, Madison, WI, October 15, 1982.

8. Marvin L. Cohen, "Novel Superconducting Materials and Mechanisms," invited closing paper, International Conference on Superconductivity in d- and f-Band Metals, Karlsruhe, Germany, June 30, 1982.

9. Marvin L. Cohen, "Pseudopotential Total Energy Calculations for Si(111)-(1x1) and Si(111)-(2x1)," 16th International Conference on the Physics of Semiconductors, Montpellier, France, September 7, 1982.

10. Marvin L. Cohen, "Static and Structural Properties of III-V Zincblende Semiconductors," 16th International Conference on the Physics of Semiconductors, Montpellier, France, September 10, 1982.

11. Marvin L. Cohen, "Predicting the Bulk and Surface Structure of Solids," Department of Chemistry, University of Hawaii, December 23, 1982.

7. Chemical Structure

a. Low-Temperature Properties of Materials*

Norman E. Phillips, Investigator

Introduction. This program contributes to an understanding of the properties of materials by providing experimental data, usually on low-temperature specific heats, for comparison with models or microscopic theories. Specific heat measurements can be made under pressure and in high magnetic fields. Since the accuracy of heat capacity data is critically dependent on the accuracy of temperature measurements, the maintenance and improvement of a laboratory temperature scale for the region 1 mK to 30 K are important parts of the program.

1. ABSOLUTE TEMPERATURE DETERMINATIONS IN THE mK REGION†

W. E. Fogle, E. W. Hornung, M. C. Mayberry, and Norman E. Phillips

Thermometers that measure absolute temperatures in the mK region are generally not useful as working thermometers. For example, noise and nuclear orientation (NO) thermometers require long measuring times for good accuracy. In certain important applications cerium magnesium nitrate (CMN) susceptibility thermometers are excellent working thermometers but their accuracy is limited by the uncertainty in Δ ($\approx 0 \pm 1$ mK) in the expression for the susceptibility, $\chi = \text{const.}/(T - \Delta)$. The value of Δ cannot be obtained with sufficient accuracy at temperatures above 2 K, where the absolute temperature has been relatively well defined by classical methods, and it has been a subject of controversy for over 10 years.

The value of Δ was determined by comparing a ^{60}Co in Co NO thermometer with several CMN thermometers in the mK region. Values of temperature were derived from the γ-ray intensities in two directions, thus exploiting an infrequently used but important capability of the NO technique to provide an internal check on the accuracy of the results.

For several thermometers using stoichiometric CMN, $\Delta = 1.05 \pm 0.10$ mK. Evidence was obtained that both excess water of hydration and an effect associated with superconducting coils and flux-trapping tubes can lower the value of Δ. The results have interesting implications for mK temperature measurements in general and for the properties of ^{3}He in particular.

*This work was supported by the Director, Office of Energy Research, Office of Basic Energy Sciences, Materials Sciences Division of the U.S. Department of Energy under Contract No. DE-AC03-76SF00098.

* * *

†Based on LBL-13790 and LBL-14399.

2. THE SPECIFIC HEAT OF ^{3}He IN THE FERMI LIQUID REGION†

M. C. Mayberry, E. W. Hornung, and Norman E. Phillips

Because the interactions between ^{3}He atoms are the same as those that produce superfluidity in ^{4}He but the statistics are the same as those of the conduction electrons in metallic superconductors, the properties of liquid ^{3}He provide a unique opportunity to test theories of many-body systems in general and of superconductivity in particular. The values of Fermi liquid parameters that can be derived from the Fermi liquid specific heat are of fundamental importance to these tests, but the specific heat data reported to date differ by up to 40% in magnitude and have qualitatively different temperature dependences. These differences have led to speculation that the data may include significant surface contributions that have not been characterized, but they have left open the question of the bulk liquid specific heat.

The specific heat of liquid ^{3}He has been remeasured between 12 and 160 mK using a CMN thermometer (see preceding article).

The results are compared with other data in Fig. 2.1. At low temperatures the specific heat is proportional to T as expected for a Fermi

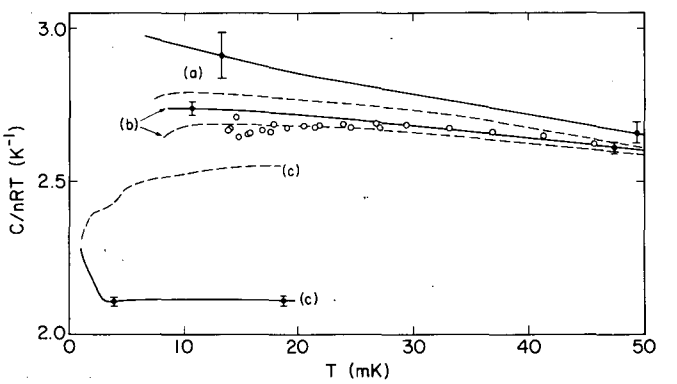

Fig. 2.1. The specific heat of liquid ^{3}He: this work, open circles; data from 3 other laboratories, solid curves (with error bars representing overall scatter); as recalculated on modified temperature scales, dashed curves. (XBL 831-3508)

liquid and gives a new value for the effective mass that will be important in reanalyzing the superfluid properties. The figure also shows that plausible changes in the temperature scales in use in other laboratories reduce the discrepancies to about 5% and suggests that surface effects may not be important. The measurements are being extended to lower temperatures.

* * *

†Brief version of LBL-15646.

3. LOW-TEMPERATURE SPECIFIC HEAT OF POTASSIUM†

John Van Curen, E. W. Hornung, J. C. Lasjaunias, and Norman E. Phillips

A number of unexpected properties of potassium can be understood as charge-density-wave (CDW) effects. Direct proof that potassium, one of the closest approximations to a free-electron metal, has a CDW ground state would have far-reaching implications for the theory of metals. Such proof, in the form of an anomaly in the specific heat, has been reported,[1] but it has been questioned[2] on the basis that the anomaly might arise from temperature scale errors.

The recent work on the laboratory temperature scale ensures its accuracy in the relevant temperature region, and new specific heat measurements were undertaken to provide a more rigorous test of the theoretical prediction.

As shown in Fig. 3.1, the measured heat capacity has the form expected for the usual lattice and electronic contributions. This result shows either that potassium does not have the suggested CDW ground state or that the associated specific heat anomaly is an order of magnitude smaller than predicted. Similar measurements on other alkali metals are planned.

* * *

†Brief version of Phys. Rev. Lett. 49, 1653 (1982); LBL-15126.

1. C. D. Amarasekara and P. H. Keesom, Phys. Rev. Lett. 47, 1311 (1981).
2. Norman E. Phillips, Phys. Rev. Lett. 48, 1504 (1982); A. H. MacDonald and Roger Taylor, ibid., 1505 (1982).

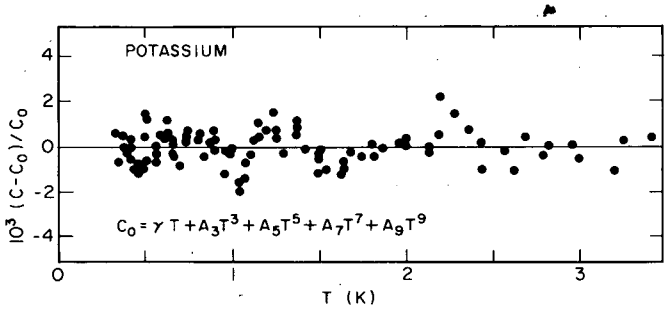

Fig. 3.1. Deviations of the specific heat of potassium from a least squares fit to the usual low-temperature expression. (XBL 831-3506)

4. OBSERVATION OF THE SPIN GLASS-PARAMAGNET PHASE BOUNDARY†

W. E. Fogle, R. A. Fisher, and Norman E. Phillips

The nature of the transition from spin glass to paramagnetic behavior is one of the more interesting and fundamental questions presented by disordered materials. A recent extension of mean field theory to 3-dimensional spins leads to predictions that are qualitatively different from those of earlier theories: The phase boundary in the H-T (field-temperature) plane should have an H^2 dependence, and it should appear as a third order anomaly in the specific heat but not be detectable in the magnetic susceptibility.

Specific heat data on CuMn that had been taken for other purposes were analyzed for evidence of the predicted anomaly.

Although the specific heat effects associated with ordering in spin glasses are much broader in temperature than mean field theory predicts, there is a small anomaly with the predicted field and temperature dependence that is clearly separable from the rest of the specific heat. This result supports the view that there is a real transition in the thermodynamic sense, and constitutes a striking confirmation of the qualitative validity of mean field theory. Similar measurements on other spin glasses that might show a different type of ordering are planned.

* * *

†This result was included in an invited paper presented at the International Conference on Magnetism, Kyoto, Japan, September 1982; to be published in J. Magn. and Mag. Mat., LBL-14845.

1982 PUBLICATIONS AND REPORTS

Refereed Journals

1. W. E. Fogle, E. W. Hornung, M. C. Mayberry, and Norman E. Phillips, "Experiments with Powdered CMN Thermometers Between 10 mK and 4 K, and a Comparison with an NBS SRM 768 Fixed Point Device," Physics 109 & 110B, 2129 (1982); LBL-13790.

2. William E. Fogle, James D. Boyer, Norman E. Phillips, and John Van Curen, "Fogle et al. Respond," Phys. Rev. Lett. 49, 241 (1982); LBL-14741.

3. Norman E. Phillips, "Phason Anomalies in Alkali Metal," Phys. Rev. Lett. 48, 1504 (1982); LBL-13791.

4. John van Curen, E. W. Hornung, J. C. Lasjaunias, and Norman E. Phillips, "Absence of Phason Contribution in the Specific Heat of Potassium," Phys. Rev. Lett. 49, 1653 (1982); LBl-15126.

LBL Reports

1. William E. Fogle, "Some Experiments in Low-Temperature Thermometry," LBl-14399.

Invited Talks

1. G. E. Brodale, R. A. Fisher, W. E. Fogle, N. E. Phillips, and J. Van Curen, "The Effect of Spin-Glass Ordering on the Specific Heat of CuMn," International Conference on Magnetism, Kyoto, Japan, September 1982, LBl-14845.

2. Norman E. Phillips, "Calorimetric Studies of Spin-Glass Ordering in CuMn," Department of Physics, Hokkaido University, Sapporo, Japan, September 16, 1982.

b. Electrochemical Processes*

Charles W. Tobias, Investigator

Introduction. The purpose of this program is to advance scientific methods for the analysis of scale-dependent cell processes and to provide means by which the design and operation of such processes can be optimized with respect to energy efficiency and capital cost. Physical description and quantitative characterization of transport of charged and uncharged species to and from electrode surfaces by convective diffusion are core interests. The analysis of high rate processes, such as electro-machining and electroforming, is undertaken to point the way to new applications in electrometallurgy. A small part of this program is devoted to the exploration of novel electrochemical processes.

1. ANODIC PROCESSES IN PROPYLENE CARBONATE

Karrie Hanson and Charles W. Tobias

The electroreduction of highly active metals at room temperature, of interest both for advanced galvanic cells and industrial electro-winning of metals, has received much attention in this laboratory.[1,2] In particular, the feasibility of potassium deposition from potassium chloroaluminate in propylene carbonate has been demonstrated.[2] Present efforts are directed toward finding a compatible anodic reaction. Criteria for an acceptable anodic process include stability of the solvent in the presence of the electrolysis products, reasonable solubility and conductivity of the salts, and high electrical efficiency for the overall reaction. Based on these objectives, a promising approach is the evolution of the elemental halogens from the potassium salts. These reactions are now being evaluated.

Solvent stability in the presence of bromine was evaluated by using mass spectroscopy to detect halogenated fragments of the propylene carbonate molecule, and light absorption in the visible to observe the change in bromine concentration with time in sealed mixtures of bromine and propylene carbonate. We find that the stability of propylene carbonate in the presence of bromine is highly dependent on the concentration of impurities present--particularly water. Figure 1.1 shows the intensity of the visible absorption of bromine in propylene carbonate as a function of time. When reagent grade bromine is used in the mixtures, the intensity of the signal steadily declines, as shown in curve B. However, when the bromine is dried by distillation, the intensity of the signal remains constant for days (curve A). Mass spectroscopy did not show evidence of the presence of brominated fragments in these solutions.

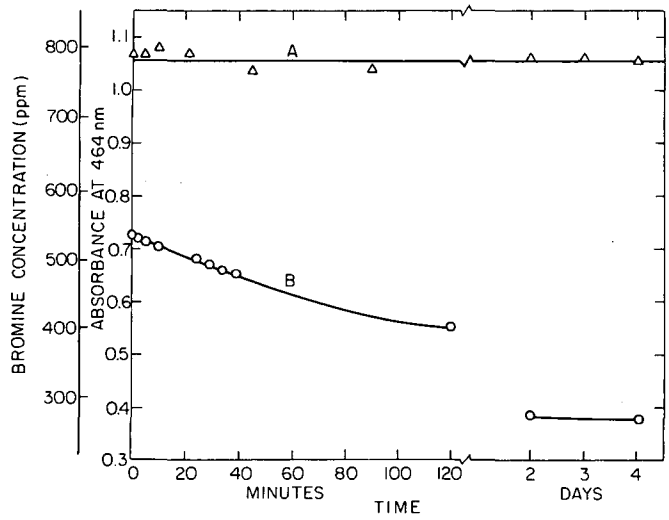

Fig. 1.1. Light absorption of reagent grade (B) and distilled (A) bromine in propylene carbonate. Initial concentrations: B: 500 ppm, A: 833 ppm. Temperature: 22°C. (XBL 831-5145)

Solubility and conductivity studies have been completed for bromide salts. It is shown[2] that because of the diffuse positive charge on the propylene carbonate molecule, small anions are poorly solvated in it, whereas salts with large anions can form saturated solutions in concentration exceeding one molar. Following our work with $KAlCl_4$, the bromide analog, $KAlBr_4$, was synthesized by fusing from KBr and $AlBr_3$. Unlike the chloride counterpart, however, we found that $KAlBr_4$ is not stable in propylene carbonate, rather it disproportionates to form a precipitate of KBr with $AlBr_3$ remaining in solution. A related salt, $KAlBr_3Cl$, was also synthesized and also formed the KBr precipitate in propylene carbonate. Cyclic voltammetry of these solutions showed oxidation of bromide to bromine at approximately 3.25 V (vs a K/K^+ reference electrode) with concomitant potassium deposition at the cathode. No side reactions were noted.

Work is now under way to extend solubility and conductivity studies to determine the concentration dependence of the ionic mobilities of KI and KBr salts in propylene carbonate. A program to characterize the kinetics of the oxidation of bromide and iodide is also in progress.

* * *

*This work was supported by the Director, Office of Energy Research, Office of Basic Energy Sciences, Materials Sciences Division of the U.S. Department of Energy under Contract No. DE-AC03-76SF00098.

1. J. Jorne, "Electrochemical Behavior of the Alkali Metals in Propylene Carbonate," Ph.D. thesis, LBL-1111.
2. H. Law, "Studies on the Electrochemical Behavior of Potassium in Propylene Carbonate," Ph.D. thesis, LBL-9207.

2. WORK IN PROGRESS

(With P. K. Andersen and R. H. Muller)

Boundary layer thinning by means of suspended inert solids in the electrolyte moving past the electrode surface is measured using a rotating disk electrode. Following earlier work on spherical glass beads in this laboratory, optimal particle shapes and sizes are being evaluated for other inert materials. The incremental viscous energy dissipation caused by the presence of suspended particles is also to be determined.

(With D. Fischl and R. H. Muller)

The effect of fixed flow obstacles on enhancing mass transfer rates to and from planar electrodes in a channel is measured by the limiting current method, and results are compared to rates evaluated by the interferometric technique. The incremental power requirement caused by the presence of flow obstacles will be measured and then correlated with the improvement in mass transport rates.

(With D. Barkey and R. H. Muller)

High speed electroforming is investigated as an inverse process to high speed anodic dissolution. Our Hanson Van Winkle Munning ECM apparatus is being modified to accommodate rapid forming of a suitable test shape by deposition of copper. Initial efforts are directed to identifying suitable mass transport conditions to attain high current densities (10-100 A/cm) and to determine possible kinetic limitations of electrocrystallization associated with high deposition rates and their effect on micromorphology and stress in the deposit.

1982 PUBLICATIONS AND REPORTS

Refereed Journals

†1. C. W. Tobias and G. A. Prentice, "A Survey of Numerical Methods and Solutions for Current Distribution Problems," J. Electrochem. Soc. 129, 72 (1982); LBL-12191.

†2. C. W. Tobias and G. A. Prentice, "Simulation of Changing Electrode Profiles," J. Electrochem. Soc. 129, 78 (1982); LBL-12192.

†3. C. W. Tobias and G. A. Prentice, "Deposition and Dissolution on Sinusoidal Electrodes," J. Electrochem. Soc. 129, 316 (1982); LBL-12167.

†4. C. W. Tobias and G. A. Prentice, "Finite Difference Calculation of Current Distributions at Polarized Electrodes," AICHE. 28, 486 (1982); LBL-11058.

‡5. C. W. Tobias and P. C. Foller, "The Anodic Evolution of Ozone," J. Electrochem. Soc. 129, 506 (1982).

‡6. C. W. Tobias and P. C. Foller, "The Mechanism of the Disintegration of Lead Dioxide Anodes under Conditions of Ozone Evolution in Strong Acid Electrolytes," J. Electrochem. Soc. 129, 567 (1982).

7. C. W. Tobias, F. R. McLarnon, and R. H. Muller, "Interferometric Study of Combined Forced and Natural Convection," J. Electrochem. Soc. 129, 2201 (1982); LBL-13032.

8. C. W. Tobias and P. J. Sides, "Resistance of a Planar Array of Spheres, Gas Bubbles on an Electrode," J. Electrochem. Soc. 129, 2715 (1982); LBL-13468.

Other Publications

‡1. C. W. Tobias and P. C. Foller, Inventors, "Electrolytic Process for the Production of Ozone," U. S. Patent No. 4,316,782, February 23, 1982.

2. C. W. Tobias, Chairman, "Assessment of Research Needs for Advanced Battery Systems," Report of the Committee on Battery Materials Technology, National Materials Advisory Board, Commission on Engineering and Technical Systems, National Research Council, Publication NMAB-390, 1982.

†3. C. W. Tobias and A. Kindler, "The Morphology of Electrodeposited Copper," Extended Abstracts, The 161st Meeting of the Electrochemical Society, Montreal, Canada, May 9-14, 1982.

4. C. W. Tobias, R. H. Muller, and D. J. Roha, "Effect of Suspended Particles on the Rate of Mass Transfer to a Rotating Disk Electrode," Extended Abstracts, The 161st Meeting of the Electrochemical Society, Montreal, Canada, May 9-14, 1982.

†5. C. W. Tobias and Dennis Dees, "A Micro-Mosaic Electrode for the Study of Transport Phenomena at Gas Evolving Surfaces," Extended Abstracts No. II-C-19, Vol. I, p. 468, 33rd Meeting of the International Society of Electrochemistry, Lyon, France, September 10-15, 1982.

Invited Talks

1. C. W. Tobias, "Mass Transport and Current Distribution in the Electrodeposition of Metals," IBM Corporation, GTD Laboratory, Endicott, N. J., January 22, 1982.

2. C. W. Tobias, Diamond Shamrock Lectures: "A Perspective of Electrochemical Technology," January 25, 1982; "Current Distribution on Electrode Surfaces," January 27, 1982; "Mass Transport in Electrochemical Cell Processes," January 29, 1982; "Physical Processes in Electrolytic Gas Evolution," February 1, 1982, Case Western University, Cleveland, Ohio.

3. C. W. Tobias, "Advances in Electrochemical Technology," Seminar Lecture given at RCA Sarnoff Research Center, Princeton, N. J., March 9, 1982.

4. C. W. Tobias, "Assessment of the Future Potential of Fuel Cells," Chevron Research Corp., Richmond, CA, April 16, 1982.

5. C. W. Tobias, "Problems in Electrochemical Engineering," Seminar Lecture given at the University of West Virginia, April 19, 1982.

6. C. W. Tobias, R. H. Muller, and D. J. Roha, "Effect of Suspended Particles on the Rate of Mass Transport to a Rotating Disk Electrode," The 161st Meeting of the Electrochemical Society, Montreal, Canada, May 14-19, 1982.

7. C. W. Tobias and A. Kindler, "The Morphology of Electrodeposited Copper," The 161st Meeting of the Electrochemical Society, Montreal, Canada, May 14-19, 1982.

8. C. W. Tobias and Dennis Dees, "A Micro-mosaic Electrode for the Study of Transport Phenomena at Gas Evolving Electrodes," The 33rd Meeting of the International Society of Electrochemistry, Lyon, France, September 6-10, 1982.

9. C. W. Tobias, "Fundamentals of Electrochemical Engineering," Six lectures arranged by the Romande Intercantonal Association of Swiss Universities, Leysin, Switzerland, September 12-16, 1982.

10. C. W. Tobias, "Prospects of Electrochemical Technology," Seminar lecture, Swiss Federal Institute of Technology, Lausanne, Switzerland, September 22, 1982.

11. C. W. Tobias, "A Close Look at Electrolytic Gas Evolution," Seminar lecture, Stanford University, February 24, 1982 and Ecole Nationale Superieure des Industries Chimiques, Nancy, France, October 11, 1982.

12. C. W. Tobias, "Perspectives on Electrochemical Technology," Seminar lecture, De Guigne Technical Center, Stauffer Chemical Co., Richmond, CA and Laboratoire d'Electrochimie Interfaciale du C.N.R.S. Meudon (Bellevue) France, October 14, 1982.

* * *

†Supported by the Division of Electrochemical Systems Research, Office of Conservation and Renewable Energy, U. S. Department of Energy.
‡Supported entirely from University funds.

8. High Temperature and Surface Chemistry

a. High Temperature Thermodynamics*

Leo Brewer, Investigator

Introduction. High temperature chemistry is characterized by the occurrence of unusual species and phases that are often unstable at conventional temperatures. Because of the difficulty of carrying out measurements under conditions where it is often difficult to contain the materials and to avoid contamination, it is important to design experiments to yield information that can be used with predictive models. In this manner, one can often calculate chemical behavior under conditions where measurements have not been made or would not be practical.

In the past, our research has aimed mostly at improving our understanding of the behavior of gases at high temperatures and of refractory containment materials. At present, our main thrust is aimed at improving our understanding of the thermodynamics of metallic alloys. For many alloys, we have a good understanding of the interactions and have quantitative-predictive models which allow prediction of the behavior of unstudied alloys. As an example, we have published a tabulation of the thermodynamic properties and phase diagrams of one hundred binary systems of molybdenum. However, there are some systems for which our understanding is not adequate to allow such quantitative predictions. Our research is aimed at such systems.

Although we will report on other studies, our main thrust at present is to characterize the very stable intermetallic compounds that result from the reaction of transition metals from the left-hand side of the Periodic Table, which do not have enough electrons to use all of their bonding orbitals, with transition metals from the right-hand side, which have so many valence electrons that they are paired in nonbonding orbitals. Our earlier studies have demonstrated the vigor of such reactions and the unusual properties of the resulting phases. It has been difficult to find reliable methods of determining the thermodynamic properties of these phases. Ordinary calorimetric methods are unusable because of the insolubility of the phases. A variety of other techniques have been considered. Each has posed severe experimental problems under the conditions that must be used. The several methods being used will be described below.

*This work was supported by the Director, Office of Energy Research, Office of Basic Energy Sciences, Materials Sciences Division of the U.S. Department of Energy under Contract No. DE-AC03-76SF00098.

1. USE OF GASEOUS-CONDENSED PHASE EQUILIBRATION TO DETERMINE THERMODYNAMIC QUANTITIES FOR VERY STABLE TRANSITION METAL ALLOYS†

Leo Brewer and John Gibson

A transition metal nitride, MN, in equilibrium with a fixed nitrogen pressure, P_N, provides a source of the transition metal at a known thermodynamic activity, a_m. Several of the platinum group metals, P, have been equilibrated with various nitrides of the group IV and V transition metals at temperatures exceeding 2000°C, and the composition of the resulting alloys, M_xP_{1-x}, has been determined by electron microprobe analysis. It has been possible to study a range of alloy compositions for each binary combination by varying P_{N_2} from 0.1 to 11 atm in a graphite tube resistance furnace, but the available compositions have been rather limited because of rapid variations in a_m with x_m for these strongly interacting alloys. The results of these experiments have been checked by a similar method involving equilibration with the corresponding carbide, MC, in the presence of graphite, but only a single a_m and thus a single alloy composition is accessible by this method.

To study a wider range of alloys, the equilibrium vapor pressures of one or both components over alloys of known composition have been determined for several binary combinations. The intensity of atomic effusion from a Knudsen cell is determined by either mass spectrometry or gravimetry, and the effusion rate is converted into the partial pressure of the component(s) monitored. It was hoped to be able to determine the atomic intensity of both constituents in the effusate from the several Nb-Pd alloys studied with a high temperature mass spectrometer made available by Professor Karl Gingerich of Texas A & M University, but even this very sensitive instrument could not accurately measure the pressure of the more refractory component, Nb, of these tightly bound alloys at the highest operating temperature of 2300°C. In the case where one constituent is much more volatile than the other, the weight loss from a Knudsen cell in high vacuum at high temperature may be simply related to the vapor pressure of the more volatile component, and gravimetric experiments have been used to determine the Pd vapor pressure over Zr-Pd, Hf-Pd, Nb-Pd, and Ta-Pd alloys. Preparations are under way to measure the vapor pressure of Ti over Ti-Ir and Ti-Pt alloys using this method.

* * *

†See LBL-13466 and LBL-10633 for details of methods used.

2. HIGH TEMPERATURE EMF MEASUREMENTS†

Leo Brewer and Michael Cima

Wagner solid state cells offer the possibility of determining relative partial molar Gibbs Energies of Engel alloys over a wide composition range. Important systematic errors may result from impurities in the electrolyte, side reactions at the electrode-electrolyte interface, and oxygen transport through pores in the electrolyte. The high stability of yttria-doped thoria reduces the chance of reactions, but it is difficult to produce in high purity, dense ceramic bodies. We have used an oxalate coprecipitation method to make starting material of extremely small particle size. Suitable equipment has been constructed to fire compacts of these powders in the presence of hydrogen at temperatures in excess of 2100°C. The product's pore structure is closed, and can therefore be used in cell construction.

The first alloy to be studied by the EMF technique will be the Nb-Pd system through the cell Pt/Nb-Pd alloy, $NbO_2/ThO_2(YO_{1.5})_{0.15}/NbO_2$, $No_2O_{4.80}$/Pt. Currently, we are preparing electrodes of niobium oxide, the "Lewis acid." They must be well characterized before use in the cell to ensure that they are in equilibrium.

* * *

†See LBL-7691 for discussion of general method.

1982 PUBLICATIONS AND REPORTS

Refereed Journals

1. M. Salmeron, L. Brewer, and G. A. Somorjai, "The Structure and Stability of Surface Platinum Oxide and Oxides of Other Noble Metals," Surf. Sci. 112, 207 (1981); LBL-12411.

†2. L. Peter and B. Meyer, "The Structure of the Dithionite Ion," J. Mol. Struc. 95, 131 (1982); LBL-13783.

†3. B. Meyer and M. Ospina, "Raman Spectrometric Study of the Thermal Decomposition of Aqueous Tri- and Tetrathionate," Phosphorus and Sulfur 14, 23-36 (1982); LBL-14440.

Other Publications

1. L. Brewer, Bibliography on the High-Temperature Chemistry and Physics of Materials, Vol. 26, Part 2, "Gases: (A) Spectroscopy of Interest to High-Temperature Chemistry, and (B) Reactions Between Gases and Condensed Phases," edited by M. G. Hocking and V. Vasantasree, published by IUPAC Commission on High Temperatures and Refractory Materials, London, 1982.

†2. L. Brewer, "Thermodynamic Values for Desulfurization Processes," American Chemical Society Symposium Series, No. 188, Flue Gas Desulfurization, edited by J. L. Hudson and G. T. Rochelle, p. 1-39 (1982); LBL-13846.

†3. G. M. Rosenblatt, "Use of Pitzer's Equations to Estimate Strong-Electrolyte Activity Coefficients in Aqueous Flue Gas Desulfurization Processes," American Chemical Society Symposium Series, No. 188, Flue Gas Desulfurization, edited by J. L. Hudson and G. T. Rochelle, p. 57-73 (1982).

†4. B. Meyer, M. Rigdon, T. Burmer, M. Ospina, K. Ward, and K. Koshlap, "Thermal Decomposition of Sulfite, Bisulfite, and Disulfite Solutions," American Chemical Society Symposium Series No. 188, Flue Gas Desulfurization, edited by J. L. Hudson and G. T. Rochelle, p. 113-125 (1982).

LBL Reports

†1. B. Meyer, K. Koshlap, K. L. Geisling, and R. R. Miksch, "Comparison of Wet and Dry Test Methods for Formaldehyde Emission from UF-Bonded Wood Products," to be published in Forest Products J., LBL-14259.

†2. B. Meyer and N. Carlson, "Formaldehyde Emission from Particleboard Postcurved by Radiofrequency Heating," to be published in Holzforschung, LBL-14286.

†3. B. Meyer, M. Rigdon, and K. Koshlap, "Raman and C-13 NMR Spectrometric Study of the Reaction of Sulfite and Formaldehyde," LBL-12452.

4. L. Brewer, "Systematics of the Properties of the Lanthanides," presented at NATO Advanced Study Institute on the Lanthanides at Braunlage, Germany, July 11-25, 1982, to be published in NATO Proceedings, LBL-14811.

5. L. Brewer, "The Generalized Lewis-Acid-Base Theory: Surprising Recent Developments," presented at American Chemical Society G. N. Lewis Symposium at Las Vegas, NV, March 30, 1982, to be published in ACS Symposium Proceedings, LBL-14867.

6. L. Brewer, "Mathematical Representation of Size and Electronic Factors," presented at Materials Research Society Annual Meeting at Boston, MA, November 2, 1982, to be published in Proceedings, LBL-15220.

7. L. Brewer, "HP-41C Calculator Programs for Fitting of Data by Analytical Functions," LBL-15346.

Invited Talks

1. L. Brewer, "The Relationship Between Thermodynamics and Phase Diagrams," CALPHAD XI Conference, Argonne National Laboratory, May 17, 1982.

2. L. Brewer, "Generalized Lewis Acid-Base Interactions in Metallic Systems," San Francisco Bay Area High Temperature Conference, Stanford University, Stanford, CA, May 19, 1982.

3. L. Brewer, "The Role of Electronic Configurations in Transition Metal Solid-Liquid Equilbria," Workshop on Alloy Theory, Los Alamos National Laboratory, Los Alamos, NM, Sept. 9, 1982.

4. L. Brewer and D. G. Davis, "Predictions of the Engel Theory of Metallic Bonding, Resolution of a Contradiction," Pacific Conference on Chemistry and Spectroscopy, San Francisco, CA, Oct. 27, 1982.

* * *

†This work was supported by the Assistant Secretary for Fossil Energy, Office of Coal Research, Advanced Environmental control Division of the U. S. Department of Energy under Contract No. DE-AC03-76SF00098 through the Morgantown Energy Technology Center, Morgantown, WV.

b. Chemistry and Materials Problems in Energy Production Technologies*

D. R. Olander, Investigator

1. THE UO_2 - ZIRCALOY CHEMICAL INTERACTION†

D. R. Olander

The chemical affinity of UO_2 and zirconium is of practical importance because it affects the integrity of nuclear reactor fuel elements in a severe core damage accident. The laboratory tests reported by Hofmann and Politis[1] revealed the complexity of the UO_2 - Zircaloy interaction, in which three corrosion layers develop between the terminal phases. One of the layers is two-phase, which can only occur in a ternary system.

Existing experimental data on the interaction[1] have been analyzed with a model that accounts for the formation and growth of the three corrosion layers between the oxide and the metal. The diffusion path beginning at UO_2 and ending at pure Zr is shown as the heavy line on the phase diagram of Fig. 1.1. The kinetics of the process are governed by diffusion of oxygen and uranium in the five-zone system with chemical equilibrium at four interfaces. Three of the zones consist of two elements; these are treated by conventional scaling theory. Transport of all three elements (Zr, U, and O) occurs in the remaining two zones, one of which consists of two coexisting phases. Modeling of the system predicts product layer growth rates which are in good agreement with the experimental results at 1500°C, the only temperature at which both kinetic and thermodynamic information is available.

* * *

†Brief version of LBL-14353, to be published in J. Nucl. Mater.

1. P. Hofmann and C. Politis, J. Nucl. Mater. 87, 375 (1979).

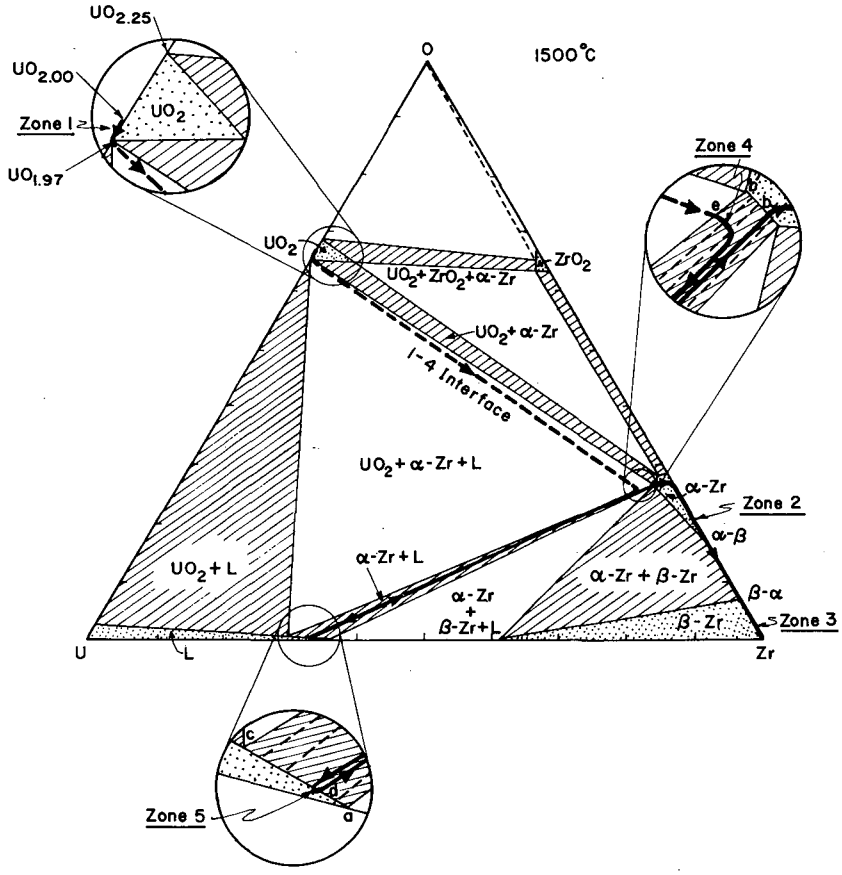

Fig. 1.1. The U-Zr-O phase diagram at 1500° (Ref. 1) showing the diffusion path followed by the corrosion process. (XBL 824-5578)

*This work was supported by the Director, Office of Energy Research, Office of Basic Energy Sciences, Materials Sciences Division of the U.S. Department of Energy under Contract No. DE-AC03-76SF00098.

2. INVESTIGATION OF IRON-CHLORINE REACTION BY MODULATED MOLECULAR BEAM MASS SPECTROMETRY†

M. Balooch, W. J. Siekhaus,‡ and D. R. Olander

Metal-halogen reactions have many technological applications which warrant study of their mechanisms by the techniques of modern surface chemistry. For example, the high volatility of metal halides has long been exploited in halogen lamp design and in production of high purity metals. Similar reactions may play important roles in the water-splitting cycle for hydrogen production.

The reaction of chlorine with polycrystalline iron has been studied by modulated molecular beam-mass spectrometric methods in the temperature range 300 - 1250 K at equivalent chlorine pressures from 2 x 10^{-5} to 3 x 10^{-4} Torr. Volatile $FeCl_2$ is the only detectable reaction product; its production rate increases rapidly with surface temperature and levels off at ~1200 K. A frequency-independent, 45°C reaction-phase lag suggests that a solid-state diffusion process is an integral part of the mechanism. The reaction is shown to be nonlinear with respect to chlorine beam intensity. The maximum in the frequency-phase data and the high frequency drop-off indicate a branch process on the surface for the production of $FeCl_2$. Studies of the chemical state of the surface by laser-simulated desorption and by ESCA revealed the presence of a thin scale of a solid iron chlorine at the spot struck by the modulated beam.

The reaction model involves dissociative chemisorption of chlorine on the surface of a thin scale of FeCl followed by reaction to produce $FeCl_2$ which desorbs. Solution of adsorbed chlorine into the scale and diffusion to the scale-metal interface competes with the surface reaction. The molecular beam date substantiated this model and permitted determination of the rate constants of the elementary steps.

* * *

†To be published in Trans. Faraday Soc.
‡General Chemistry Division, LLNL.

3. A THERMODYNAMIC ASSESSMENT OF IN-REACTOR IODINE SCC OF ZIRCALOY†

D. R. Olander

Recurring failures of the Zircaloy cladding of LWR fuel rods may be because of stress corrosion cracking (SCC) by elemental iodine. However, since the fission yield of cesium exceeds that of iodine, CsI, not I or I_2, is the overwhelmingly favored iodine-containing species. Cesium iodide, however, does not cause SCC of Zircaloy. Possible thermodynamic explanations that could resolve this discrepancy were examined and tested for possible kinetic limitations.

Götzmann[1] has suggested that formation of the ternary cesium-molybdenum-oxygen compound, Cs_2MoO_4, controls the cesium pressure in the fuel-cladding gap. CsI exerts its vapor pressure, and the iodine pressure follows from the law of mass action for the reaction Cs(g) + I(g) = CsI(g). This system supports therefore an iodine pressure of ~10^{-15} atm, still too small to promote SCC.

An SCC model proposed by Peehs[2] envisages that a layer of ZrI(s) forms on the cladding inner surface and establishes an equilibrium pressure of ZrI_4 by the reaction: ZrI(s) + 3I(g) = ZrI_4(g). The pressure of the tetraiodide, ~10^{-10} atm, drives ZrI_4 diffusion down a crack to promote SCC. However, the calculated diffusion flux of ZrI_4 is too small to explain the observed crack propagation rates.

A second thermodynamic model of Zircaloy SCC proposed by Götzmann[1] assumes that the CsI/Cs couple acts to transport iodine from the fuel surface to the crack tip in a manner analogous to the transport of oxygen in the fuel by the CO_2/CO or H_2O/H_2 couples. In this model, iodine is transported as CsI from the outer fuel surface to the tip of a growing crack in the cladding. At the crack tip CsI is decomposed to deliver iodine and the liberated cesium gas diffuses back to the fuel-cladding gap to pick up more iodine from the fuel surface. Iodine supply to the tip allows the crack to advance and continually exposes fresh metal surface that acts as a sink for iodine transported by CsI. But the rate at which this process can supply iodine is too low to sustain a propagating SCC crack. In all cases examined, the great stability of CsI prevents attainment of iodine pressures sufficiently high for the operation of mechanisms which are based on purely thermodynamic grounds. If iodine is responsible for Zircaloy SCC, nonequilibrium mechanisms such as CsI radiolysis, or kinetic limitations to the formation of the equilibrium mixture of the elements present in the fuel-cladding gap, must act to bypass the thermodynamic constraints.

* * *

†Brief version of J. Nucl. Mater. 110, 343 (1982).
1. O. Götzmann, J. Nucl. Mater. 107, 185 (1982).
2. M. Peehs, W. Jung, H. Stehle, and E. Steinberg, in IAEA Specialists Meeting on Pellet-Cladding Interaction in LWRs, Riso, Denmark, September 1980.

4. MULTIPHOTON LASER IONIZATION MASS SPECTROMETRY OF CsI and I†

M. Balooch and D. R. Olander

An important aspect of the behavior of fission products in nuclear reactor fuel elements is the chemistry of cesium and iodine. Although thermodynamics predicts that essentially all of the iodine should be present as CsI, which is nonvolatile and chemically nonaggressive in the fuel, there is indirect evidence that elemental iodine may be released from irradiated fuel.

In the present study the multiphoton ionization technique (MPI) with a tunable dye laser is used as a means of selectively ionizing CsI and I. Figure 4.1 depicts the apparatus. Molecular beams of CsI and I are produced in separate Knudsen

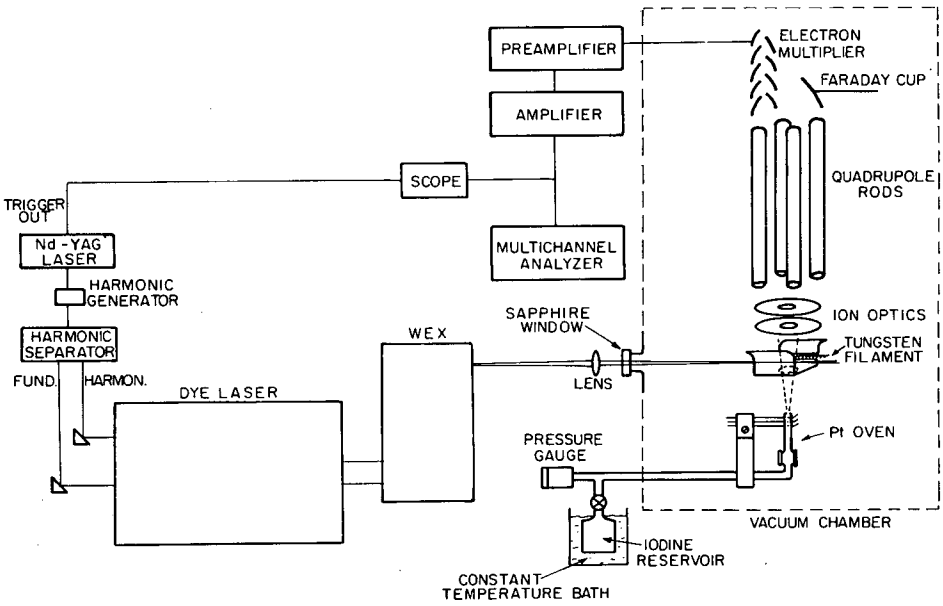

Fig. 4.1. System for molecular beam ionization by laser multiphoton absorption processes. (XBL 828-6353)

cells. The molecular beam is intercepted by a pulse laser with 5 ns width, repetition rate of 10 Hz, and maximum output power of 10 mJ in the wavelength range of interest (~3000 Å). The output of mass spectrometer is processed by a multichannel analyzer.

The results show that when combined with mass analysis, multiphoton ionization has the potential of providing a more highly selective means than electron impact ionization for detecting CsI and I in a mixture of the two vapors. The I atoms can be detected in a mixture with a CsI/I ratio as large as ~10 by operating at a wavelength of 3047 Å. But low repetition rates, short pulse times, and low effective ionization volumes make laser mass spectrometry less effective for measurement of minute quantities than of one species in another.

* * *

†To be published in J. Mass Spect. and Ion Phys.

5. THE KINETICS OF GAS/SOLID/LIQUID REACTIONS BY MODULATED MOLECULAR BEAM MASS SPECTROMETRY

M. Balooch, W. J. Siekhaus,† and D. R. Olander

Over the last decade, understanding of gas-solid reaction processes has been greatly enhanced by utilizing modulated molecular beam techniques in conjunction with AES, LEED, and ESCA. On the other hand, gas-liquid reactions, which are important in photoflash devices, propellant, steelmaking, high temperature flames, transpiration cooling, passivation of liquid metal alloy surfaces, and many other applied areas, are poorly understood.

In the present work, the reactions of molecular chlorine with liquid and solid indium, lead, and tin were studied by modulated molecular beam mass spectrometric methods. InCl, $PbCl_2$ and $SnCl_2$ were the only detectable volatile reaction products. Their production rates increase abruptly at the melting point, the effect being most pronounced for indium. In a separate study using AES, the surface coverage of chlorine was determined as a function of beam intensity and surface temperature.

Molecular beam studies of the In/Cl_2 system show that the reaction probability increases abruptly by an order of magnitude at the melting point of indium. Auger analysis of the surface shows a dramatic drop in chlorine concentration at the same temperature. The apparent reaction probability approaches a limiting value of 0.16 at ~600 K. This behavior indicates that the reaction rate in this temperature region is limited solely by the Cl_2 supply, which is controlled by the sticking probability of molecular chlorine on the surface. The beam intensity variation confirms that the reaction is first order with respect to chlorine beam intensity for both liquid and solid phases of indium.

* * *

†General Chemistry Division, LLNL.

1982 PUBLICATIONS AND REPORTS

Refereed Journals

1. D. R. Olander, A. J. Machiels, M. Balooch, S. K. Yagnik, "Thermal Gradient Migration of Brine Inclusions in Synthetic Alkali Halide Single Crystals," J. Appl. Phys. 53, 669 (1982).

2. D. R. Olander, D. Sherman, and M. Balooch, "Retention and Release of Water by Sintered Uranium Dioxide," J. Nucl. Mater. 107, 31 (1982).

3. D. R. Olander, "A Model of Brine Migration and Water Transport in Rock Salt Supporting a Temperature Gradient," Nucl. Technol. 58, 256 (1982).

4. D. R. Olander, "A Mechanistic Analysis of Ruthenium Transport in UO_2," Nucl. Sci. Eng. 82, 190 (1982).

5. D. R. Olander, "A Thermodynamic Assessment of In-Reactor Iodine SCC of Zircaloy," J. Nucl. Mater. 110, 343 (1982).

6. F. Tehranian and D. R. Olander, "Extrapolation of Low Temperature Vapor Pressure Data of Uranium Carbide to the Liquid Regions," High Temp. Sci. 15, 329 (1982).

7. D. R. Olander, "The Chemical Diffusivity of Oxygen in UO_{2-x}," J. Nucl. Mater. 110, 352 (1982).

LBL Reports

1. C. H. Tsai and D. R. Olander, "Rapid Heating and Vaporization of Binary Solids by Absorbing Radiation--I Numerical Modeling of Heat and Mass Transfer," LBL-15124.

2. M. Balooch and D. R. Olander, "Multiphoton Laser Ionization Mass Spectrometry of Cesium Iodide and Atomic Iodine," LBL-14989.

3. D. R. Olander, "The UO_2 - Zircaloy Interaction," LBL-14353.

4. M. Balooch and D. R. Olander, "Kinetic Study of the Zirconium-Iodine Reaction by Modulated Molecular Beam Mass Spectrometry," LBL-14518.

5. S. H. Shann and D. R. Olander, "Stress Corrosion Cracking of Zircaloy by Cadmium, Iodine, and Metal Iodides," LBL-13855.

6. S. K. Yagnik, "Thermal Gradient Migration of Brine Inclusions in Salt Crystals," LBL-14752.

7. D. Bayen, "Fission Product Release from Irradiated UO_2," LBL-15222.

Invited Talks

1. D. R. Olander, "Analysis of Steam Oxidation of Zircaloy Cladding in High Temperature Nuclear Reactor Transients," Thermal Fuels Behavior Division Seminar, EG&G, Idaho, March 18, 1982.

2. D. R. Olander, "Materials Problems in Nuclear Reactors," Energy & Environment Division, Lawrence Berkeley Laboratory, April 13, 1982.

3. D. R. Olander, "Chemical Aspects of Pellet-Cladding Interaction in Light Water Reactor Fuel Elements," National Meeting, American Nuclear Society, Los Angeles, California, June 8, 1982.

4. D. R. Olander, "Zircaloy Reactions with Steam and with UO_2," Gordon Research Conference on High Temperature Chemistry, Panel on Nuclear Reactor Accident Modeling and High Temperature Chemistry, Tilton, New Hampshire, July 1982.

5. C. H. Tsai, "Laser Vaporization of Uranium Dioxide," Chemical Eng. Div., Argonne National Laboratory, Argonne, Illinois, January 11, 1982.

6. M. Balooch, "Molecular Beam Studies of Metal-Halogen Reactions," Surface Science Seminar, Materials and Molecular Research Division, Lawrence Berkeley Laboratory, April 15, 1982.

7. D. R. Olander, Lecture series on "Nuclear Materials and Uranium Enrichment," Chinese Nuclear Materials Society, Beijing and Chengdu, June - July 1982.

8. D. R. Olander, "The UO_2-Zircaloy Interaction," Pacific Conference on Chemistry and Spectroscopy, San Francisco, California, October 27, 1982.

9. D. R. Olander, "Core Damage and Release of Volatile Fission Products During a Reactor Accident," U.C. Berkeley, Department of Nuclear Engineering Colloquium, September 27, 1982.

c. Plasma Enhanced Deposition of Thin Films*

Dennis W. Hess, Investigator

Introduction. Thin films are used in a wide spectrum of applications, including optical coatings, solar cells, and integrated circuits. Each application requires films with precise properties, tailored for that purpose. Thus, fundamental relationships between film properties and the deposition techniques used for film formation must be established.

Because of the high energy electrons present in an rf glow discharge or plasma, chemical reactions, which normally require elevated temperatures (>500°C) to proceed at a measurable rate, can be carried out at room temperature. Further, because of ion and electron bombardment of film materials during deposition, materials with unique chemical, electrical, and optical properties can be synthesized.

Studies on the plasma-enhanced deposition (PED) of transition metal oxides are described. X-ray diffraction, transmission electron microscopy, and photon-assisted electrolysis are used to investigate materials properties as functions of deposition parameters.

1. PLASMA-DEPOSITED TITANIUM OXIDE PHOTOANODES†

Larry M. Williams‡ and Dennis W. Hess

The current demand for solar energy conversion and storage has kindled an interest in photoelectrochemical systems. Inexpensive materials that display high cell efficiencies and low anode corrosion are needed. Plasma-enhanced deposition is a technique capable of film formation on virtually any substrate material over a wide temperature range.

An rf glow discharge is ignited in a mixture of titanium tetrachloride and oxygen, and titanium oxide films are deposited on titanium substrates. Titanium oxide films are also formed by thermal oxidation of titanium substrates. Comparison of the composition and the photoelectrochemical and structural properties of the films allows the role of the plasma in the establishment of thin film properties to be ascertained.

Plasma-deposited titanium oxide photoanodes have been fabricated with quantum efficiencies higher than the thermally grown anode materials and comparable to those reported for single crystal rutile. The reason for such results appears to be the preferred orientation of the grains observed in plasma deposition. Further, chlorine incorporation from the titanium tetrachloride source gas generates improved short wavelength photoresponse compared to thermally oxidized films. Apparently such improvements result from the reduction of grain boundary and/or surface recombination site densities.

* * *

†Brief version of LBL-14994.
‡Present address: Bell Laboratories, Murray Hill, NJ 07974.

2. STRUCTURE AND PHOTOELECTROCHEMICAL PROPERTIES OF PLASMA-DEPOSITED IRON OXIDE FILMS

Christopher S. Blair and Dennis W. Hess

Iron oxide films have been used widely in the fabrication of electronic devices. The specific applications range from magnetic recording tape, to magnetic bubble memories, to transparent photolithographic masks, to photoanodes for solar energy conversion. Plasma-enhanced deposition offers a method of controlling the structure and properties of iron oxide films, so that particular properties can be obtained by variation of deposition parameters.

Iron oxide films are deposited by igniting a glow discharge in a vapor of iron pentacarbonyl and oxygen. The photoelectrochemical and structural properties of the film are then studied and compared to those of iron oxide films formed by other techniques.

Thus far, plasma-deposited iron oxide films show relatively low photocurrent efficiencies, in agreement with literature reports of other iron oxide photoanodes. Optical absorption measurements on the plasma-deposited films indicate that most of the incident radiation is absorbed within the first 30 nm of the film. Therefore, surface recombination may be the determining factor in the low current efficiencies observed. Iron oxide films deposited in the glow discharge show preferred orientation and much improved photoelectrochemical properties when the deposition temperature reaches 500°C. At this temperature, a balance seems to be reached between ion-bombardment induced defect creation and crystallite orientation effects, leading to improved photoanode efficiencies.

*This work was supported by the Director, Office of Energy Research, Office of Basic Energy Sciences, Materials Sciences Division of the U. S. Department of Energy under Contract No. DE-AC03-76SF00098.

1982 PUBLICATIONS AND REPORTS

Refereed Journals

†1. J. K. Chu, C. C. Tang, and D. W. Hess, "Plasma-Enhanced Chemical Vapor Deposition of Tungsten Films," Appl. Phys. Lett. 41, 75 (1982).

Other Publications

1. D. A. Doane, D. B. Fraser, and D. W. Hess, Eds., Proceedings of the Tutorial Symposium on Semiconductor Technology, The Electrochemical Society, Inc., 1982.

LBL Reports

1. L. M. Williams, "Structure and Photoelectrochemical Properties of Plasma Deposited Titanium Dioxide, LBL-14994.

Invited Talks

1. D. W. Hess, "Plasma-Enhanced Deposition of Silicon and Silicon-Containing Films," ASTM Symposium on Silicon Processing, San Jose, California, January 1982.

* * *

†Supported by the Army Research Office under Contract No. DAAG-29-80-K-0086.

d. Electrochemical Phase Boundaries*

Rolf H. Muller, Investigator

Introduction. The purpose of this work is to advance the understanding of boundary layers and thin films at electrochemical interfaces. New optical techniques are developed and used for the observation of electrode surfaces in liquid media.

Research on high-rate electrodeposition and dissolution, conducted jointly with C. W. Tobias, is described under "Electrochemical Processes." Applied research, "Surface Layers on Battery Materials," supported by the Office of Advanced Conservation Technologies, DOE, is reported under "Electrochemical Energy Storage."

1. NUCLEATION OF Pb ELECTRODEPOSITS ON Ag AND Cu †

Joseph C. Farmer and Rolf H. Muller

An important factor in determining the properties of electrodeposited metals is the nature of the first layer from which the deposit grows. This work was undertaken to determine the micromorphology of the initial stages of Pb deposition on Ag(111) and Cu(111) from the first atomic layer, the underpotential deposit (UPD), to bulk deposits of about 200 Å thickness. Substrates and deposit were chosen because of their ability to form underpotential deposits[1] and their differences in optical properties that make optical detection of small amounts of deposit possible.

Simultaneous cyclic voltammetry, ellipsometry, and light scattering measurements were conducted. The potential was swept from +200 to -800 mV vs Ag/AgCl at rates from 0.1 to 1.5 V/min. The ellipsometer was of the self-nulling type,[2] operated with a Xe arc lamp with a filter for 515 nm. For the light scattering measurements an Ar-ion laser, operated at 515 nm, was used. Optimum values of the deposit properties (UPD thickness and optical constants, bulk deposit thickness and porosity) were determined by minimizing the sum-of-squares errors between ellipsometer measurements and model predictions. The optical constants of bulk Pb and substrates were measured and fall within the range of values found in the literature.

The optical model, which was successful in interpreting the ellipsometer measurements of the underpotential deposit, involves the two-dimensional spreading of metallic islands of monolayer thickness. Coverage of the surface was derived from charge passed. The free energy of adsorption derived for a Langmuir isotherm was found to be 7 ± 1 kcal/mole (95% confidence level) for both substrates. Statistical analysis of the present data does not support a partial charge for the electrosorption bond. In agreement with the formation of a smooth monolayer, no increase in light scattering was observed during formation of the underpotential deposit. The initial stages of bulk deposition occur on top of the underpotential layer. The optical model for the bulk deposit involves a porous layer consisting of metal and electrolyte. The optical properties of this composite layer have been determined by mixing the properties of the two media according to the Bruggeman theory.[3] Upon anodic dissolution, bulk and underpotential deposits are removed sequentially, and the original optical properties of the substrate are restored.

* * *

†Brief version of LBL-15458.

1. D. H. Kolb, in Advances in Electrochemistry and Electrochemical Engineering, Vol. 11, edited by H. Gerischer, Wiley, New York, 1978.
2. H. J. Mathieu, D. E. McClure, and R. H. Muller, Rev. Sci. Instrum. 45, 798 (1974).
3. D. E. Aspnes and J. B. Theeten, Phys. Rev. B 20, 3292 (1979).

2. EFFECT OF RHODAMINE-B ON Pb ELECTRODEPOSITION ON Ag and Cu †

Joseph C. Farmer and Rolf H. Muller

Surface active agents have long been used on an empirical basis to control the surface finish in electrolytic metal deposition.[1] The objectives of this study were to determine coverage and orientation of an adsorbed model substance and its effect on overpotential and micromorphology of a metal deposit, ranging in thickness from atomic coverage to about 1000 Å.

Most of the experiments were conducted with Rhodamine-B chloride as inhibitor, lead as deposit, and copper as electrode substrate. These materials show different optical properties over the visible spectrum. The choice of Rhodamine-B resulted from screening studies with over 15 laser dyes that were investigated because they are strongly light-absorbing and can therefore be detected in small amounts on the surface; they also adsorb strongly, are optically well-characterized, and are available in high purity. Rhodamine-B has been found here to result in a large (150 mV) increase in the overpotential for the Pb bulk deposit. Lead ions are discharged at potentials where neither the specific adsorption of chloride ions nor hydrogen evolution occur. The principal experimental techniques used were cyclic voltammetry and ellipsometry with light of fixed wavelength or spectrally scanned over the visible.

Dye adsorption is found to result in the formation of an incomplete monolayer in underpoten-

*This work was supported by the Director, Office of Energy Research, Office of Basic Energy Sciences, Materials Sciences Division of the U. S. Department of Energy under Contract No. DE-AC03-76SF00098.

tial deposition and a bulk deposit of very low porosity that causes the spectral features of the substrate to disappear while they are still visible with the same amount deposited without the dye (Fig. 2.1). Rhodamine-B, as most inhibitors used in practice, is reduced at the electrode prior to metal deposition, and with the low concentrations used here, its effect therefore disappears after the first potential cycle. Readsorption during a relaxation period at open circuit causes the effects to return. Birefringence of the dye layer indicates that the species responsible for the increase in overpotential has its optical transition moment oriented normal to the surface and is probably bonded as a cation.

* * *

†Brief version of LBL-15459.

1. J. A. Harrison and H. R. Thirsk, in Electroanalytical Chemistry, Vol. 5, edited by A. J. Bard, Dekker, New York, 1971.

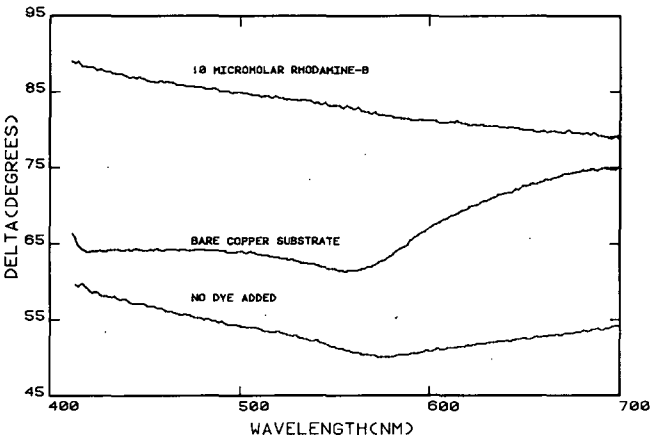

Fig. 2.1. Spectroscopic measurement of the ellipsometer parameter delta for a bare Cu substrate and Pb deposits formed with and without Rhodamine-B. Deposit 33 mC/cm^2, corresponds to 31 nm compact layer. (XBL 828-11272A)

3. SELF-COMPENSATING SPECTROSCROPIC ELLIPSOMETER†

Joseph C. Farmer and Rolf H. Muller

Spectral scanning adds another dimension to the ellipsometry of surfaces and thin films. Extensive modification of a previously built self-compensating instrument[1] has made it possible to combine the advantages of rapid spectral scanning with the inherent accuracy[2] of a compensating ellipsometer operated in the polarizer-compensator-sample-analyzer configuration.

A high-pressure xenon arc lamp serves as a white light source; wavelength can be varied continuously over the visible-uv (370 to 720 nm) at a maximum rate of 114 nm/s by rotating a continuously variable interference filter. A three-reflection Fresnel rhomb with extremely low skew (<0.01 deg) between entrance and exit beams serves as achromatic quarter-wave compensator. The wavelength dependence of the Verdet coefficients for the Faraday-cell glass cores was determined experimentally. A minicomputer (LSI-11/02) is used to collect data from up to 8 channels, average multiple runs, establish difference spectra, and fit model parameters to measurements.

* * *

†Brief version of LBL-15607.

1. H. J. Mathieu, D. E. McClure, and R. H. Muller, Rev. Sci. Instrum. 45, 798 (1974).
2. D. E. Aspnes, Appl. Opt. 14, 1131 (1975).

4. WORK IN PROGRESS

Joseph C. Farmer, Michael Armstrong, J. Richard Gyory, and Rolf H. Muller

Optical models are being developed for the interpretation of ellipsometer measurements of electrochemical submonolayers for which equivalent-film models, which have been used successfully for adsorption from the vapor phase,[1] are not applicable. Anisotropic film models, in which the effect of molecular orientation is considered, are used for determining thickness and orientation of adsorbed dye layers.

Depth-profiling Auger spectroscopy is being combined with ellipsometry to provide additional experimental evidence for the interpretation of thin-film structures and compositions. Lead deposits on copper are investigated in support of studies reported above. Of particular interest is the possible incorporation of the reduced dye in the metal. Vapor-deposited model structures will be used to test optical interpretations.

Some aqueous electrolytes of interest for use in gas electrodes have been found in previous work,[2,3] to form stable liquid films on planar vertical metal surfaces. A study has been initiated to identify the forces responsible for film formation. Present experimental efforts are concerned with the preparation of solutions free of solid particulate impurities.

* * *

1. G. A. Bootsma, Surf. Sci. 14, 52 (1969).
2. J. H. Turney, LBL-171 (1971).
3. H. Gu, LBL-165 (1971).

1982 PUBLICATIONS AND REPORTS

Refereed Journals

1. F. R. McLarnon, R. H. Muller, and C. W. Tobias, "Interferometric Study of Combined Forces and Natural Convection," J. Electrochem. Soc. 129, 2201 (1982); LBL-13032.

2. W. J. Plieth, "Electrochemical Properties of Small Clusters of Metal Atoms and Their Role in Surface-Enhanced Raman Scattering," J. Phys. Chem. 86, 3166 (1982).

LBL Reports

1. C. Coughanowr, "Electrochemical Machining of Cemented Titanium Carbide," M.S. thesis, LBL-13682.

2. Joseph C. Farmer and Rolf H. Muller, "Effect of Rhodamine-B on Pb Electrodeposition on Ag and Cu," LBL-15459 Abstract.

3. Joseph C. Farmer and Rolf H. Muller, "Nucleation of Pb Electrodeposition of Ag and Cu," LBL-15458 Abstract.

Other Publications

1. R. H. Muller, D. J. Roha, and C. W. Tobias, "Effect of Suspended Particles on the Rate of Mass Transfer to a Rotating Disk Electrode," Proceedings of the Symposium on Transport Processes in Electrochemical Systems, Vol. 82-10, Electrochemical Society, 1982.

e. Solid State and Surface Reactions*

Gabor A. Somorjai, Investigator

Introduction. The research program is centered on studies of catalyzed surface reactions and investigations of the atomic structure and chemical composition of solid surfaces and adsorbed monolayers. The kinetics and mechanisms of catalytic surface reactions are studied using well-characterized crystal surfaces at low and high pressures by using a combination of surface science techniques.

The materials that are the focus of our studies are platinum, molybdenum, rhodium, iron and its compounds, alkali metals, and bimetallic alloys. The adsorbates and reactants are mostly hydrocarbons, oxygen, hydrogen and water.

One part of the investigations is directed toward atomic scale understanding of the structure and catalytic behavior of metal surfaces. The other part is aimed at developing new catalysts which substitute for precious metals and exhibit high rates and selectivity.

Surface Structure and Chemisorption by Low Energy Electron Diffraction and Electron Spectroscopy

1. A LEED CRYSTALLOGRAPHY STUDY OF THE (2x2)-C_2H_3 STRUCTURE OBTAINED AFTER ETHYLENE ADSORPTION ON Rh(111)†

R. J. Koestner, M. A. Van Hove, and G. A. Somorjai

The structure of the Rh(111)-(2x2)-C_2H_3 overlayer that was obtained upon the adsorption of ethylene has been determined using a LEED intensity analysis. In agreement with a prior HREELS study, an ethylidyne ($\equiv CCH_3$) species is found to stand perpendicularly above an hcp hollow site with a carbon-carbon distance of 1.45 ± 0.10 Å and a metal-carbon distance of 2.03 ± 0.07 Å. The Zanazzi-Jona and Pendry R-factors for this structure are 0.49 and 0.52, respectively. By comparison with similar organometallic complexes, the relatively short carbon-carbon distance and long metal-carbon distance can be explained by $\sigma - \pi$ hyperconjugation of the surface ethylidyne fragment.

* * *

†Brief version of LBL-13598, LBL-13962, LBL-12803, and LBL-13300.

2. EVIDENCE FOR THE FORMATION OF STABLE ALKYLIDYNE STRUCTURES FROM C_3 AND C_4 UNSATURATED HYDROCARBONS ADSORBED ON THE Pt(111) SINGLE CRYSTAL SURFACE†

R. J. Koestner, J. C. Frost, P. C. Stair, M. A. Van Hove, and G. A. Somorjai

C_3 and C_4 hydrocarbon (methylacetylene, propylene, and the 2-butenes) adsorption on the Pt(111) face was studied by observing the LEED patterns that formed and by measuring the intensity vs voltage spectra for each structure. Two phases exist for each of these molecules adsorbed on the Pt(111) surface. At low temperatures, the unsaturated C-C group forms a di-σ bond to two Pt atoms. Upon warming to about room temperature, and in the presence of hydrogen for the alkynes, a conversion takes place to an alkylidyne species that is bonded to three Pt atoms and has its C-C bond nearest to the metal substrate oriented perpendicularly to the surface. The butylidyne species is shown to order its ethyl group into an (8 x 8) or $(2\sqrt{3} \times 2\sqrt{3})R30^\circ$ superlattice, when the hydrocarbon exposure is increased; this ordering is probably a natural consequence of the steric hindrance among neighboring ethyl groups as the hydrocarbon coverage increases slightly with larger exposures.

* * *

†Brief version of LBL-12780.

3. FORCE-FIELD CALCULATIONS OF THE PACKING ENERGY OF MONOLAYERS OF C_3 AND C_4 HYDROCARBON MOLECULES ADSORBED ON SINGLE CRYSTAL METAL SURFACES†

A. Gavezzotti, M. Simonetta, M. A. Van Hove, and G. A. Somorjai

Force-field calculations have been applied to investigate the packing energy of overlayers of C_3 and C_4 hydrocarbons adsorbed on Pt(111) and Rh(111), in which Van der Waals adsorbate-adsorbate interactions play a significant role. The packing energies were used to compare various adsorbate structures for which Low Energy Electron Diffraction patterns have been obtained and corresponding detailed structures have been proposed. In particular, the conformation of methylacetylene ($HCCCH_3$) in a (2 x 2) arrangement,

*This work was supported by the Director, Office of Energy Research, Office of Basic Energy Sciences, Materials Sciences Division of the U.S. Department of Energy under Contract No. DE-AC03-76SF00098.

and of propylidyne ($\equiv CCH_2CH_3$) and butylidyne ($\equiv CCH_2CH_2CH_3$) in (2 x 2), c(4 x 2) and ($2\sqrt{3}$ x $2\sqrt{3}$)R30° arrangements were considered.

* * *

†Brief version of LBL-14053.

4. VIBRATIONAL STUDIES OF ALKENE DECOMPOSITION ON THE Rh(111) SURFACE

B. E. Koel, J. E. Crowell, M. Mate, and G. A. Somorjai

The identification of the hydrocarbon surface species that can form on the Rh surface as a function of temperature has important mechanistic implications for catalytic methanation and Fischer-Tropsch synthesis reactions. Data are also needed on the bonding and rehybridization of these species to determine the importance of π-d bonding in adsorption and catalytic reactions on group-VIII metals.

High resolution electron energy loss spectroscopy (HREELS) has been used to study the structure of the hydrocarbon monolayers formed under ultrahigh vacuum conditions from the dissociative adsorption of ethylene, propylene, and butenes on the Rh(111) surface above 300 K. The HREELS spectra obtained between 300-430 K indicate the formation of stable alkylidyne species, as suggested by previous LEED studies.

Similarities in the temperature dependence of the sequential dehydrogenation of the surface species can be found. For example, above 430 K only a single high intensity vibrational mode is observed near 780 cm^{-1}, indicating the partially dehydrogenated-surface species is primarily absorbed methylidyne ($CH_{(a)}$) in all cases. Heating to 800 K in UHV is sufficient to remove all surface hydrogen in all cases. The carbonaceous layer formed gives only weak loss peaks and no clearly identifiable Rh-C or C-C vibrational modes.

5. A COVALENT MODEL FOR THE BONDING OF ADSORBED HYDROCARBON FRAGMENTS ON THE (111) FACE OF PLATINUM†

C. Minot, M. A. Van Hove, and G. A. Somorjai

A systematic molecular orbital study of the location of CH_n and $C-CH_n$ (n = 1,2,3) species on a Pt(111) single-crystal surface has been performed by using an Extended Hückel Theory (EHT). These species may be involved in the hydrogenation/dehydrogenation processes of hydrocarbons. The observed dependence of the adsorption site on the number of hydrogens in the CH_n fragments suggests that any CH bond breaking in CH_n species must involve a change of adsorbate bonding site. The carbon is found to be located on the surface in such a way as to complete its tetravalency. Thus, CH occupies a 3-fold coordinated hollow site, CH_2 a 2-fold coordinated bridge site, and CH_3 a 1-fold coordinated top site. $C-CH_3$ is found to be perpendicular to the surface in a 3-fold hollow site in agreement with experimental observations. It is also found that a displacement of $C-CH_2-R$ to a top site makes a C-R cleavage easier.

* * *

†Brief version of LBL-13603.

6. THE ADSORPTION OF BENZENE AND NAPHTHALENE ON THE Rh(111) SURFACE: A LEED, AES, AND TDS STUDY†

R. F. Lin, R. J. Koestner, M. A. Van Hove, and G. A. Somorjai

The adsorption of benzene and naphthalene on the Rh(111) single-crystal surface has been studied by low energy electron diffraction (LEED), Auger electron spectroscopy (AES), and thermal desorption spectroscopy (TDS). Both benzene and naphthalene form two different ordered LEED patterns separated by temperature-induced phase transitions: $\begin{pmatrix} 3 & 1 \\ 1 & 3 \end{pmatrix}$ = c($2\sqrt{3}$ x 4)rect and (3 x 3) for benzene, ($3\sqrt{3}$ x $3\sqrt{3}$)R30°, and (3 x 3) for naphthalene. With increasing temperature, the patterns are found to disorder near or below the first hydrogen TDS peaks. All these phase transitions are irreversible. The ordered structure can be understood in terms of flat-lying or nearly flat-lying intact molecules, and they can be compared with similar structures found on other metal surfaces. Structural models and phase transition mechanisms have been proposed.

* * *

†Brief version of LBL-15820.

7. VIBRATIONAL SPECTROSCOPY USING HREELS OF BENZENE ADSORBED ON THE Rh(111) CRYSTAL SURFACE

B. E. Koel and G. A. Somorjai

High resolution electron energy loss spectroscopy (HREELS) and low energy electron diffraction (LEED) have been used to study the structure of adsorbed benzene (C_6H_6 and C_6D_6) monolayers on the Rh(111) surface at 300 K. Benzene is associatively adsorbed and π-bonded to the surface with the ring plane parallel to the surface plane. The adsorption of benzene on Rh(111) is similar to that on Pt(111) and Ni(111) surfaces, giving rise to similar HREELS spectra, except that only one type of adsorption site is present on Rh(111), indicated by a single symmetric C-H out-of-plane bending vibration.

A C($2\sqrt{3}$ x 4) structure is formed after large exposures. HREELS gives information on the surface bonding geometry that is complementary to the LEED data, providing good description of the adsorbed monolayer. For this ordered structure, the symmetry of the benzene molecules is only weakly distorted from C_{6v} to $C_{3v}(\sigma_d)$ symmetry, and the adsorption site is probably the on-top site with the benzene ring centered over a single Rh atom.

8. THE STRUCTURE OF GRAPHITIC CARBON ON PT(111)

D. F. Ogletree and G. A. Somorjai

When carbon is deposited on the Pt(111) surface by dehydrogenation of hydrocarbons, it forms a disordered overlayer of carbidic carbon. Annealing at 750-800 K produces diffraction rings that correspond to the lattice spacings in the basal plane of bulk graphite. These rings are due to islands of graphite-like carbon at random orientations relative to the platinum substrate. Further annealing at 1050-1100 K causes the graphite diffraction rings to segment into elongated spots. These spots indicate domains of graphite-like carbon rotated by 23 and 37 degrees relative to the platinum substrate. The elongation of the spots in the angular direction, about three times the width in the radial direction, suggests a distribution of four to six degrees in the angular registry between the islands of the incommensurate graphite-like lattice and the substrate lattice.

These elongated spots are seen after annealing for a carbon coverage between 0.1 and 1.0 layers of graphite-like carbon, as determined by Auger spectroscopy and hydrocarbon exposure. Both types of domains have always been observed together. The sharpness of spots is unchanged over this range of coverage. Graphite-like carbon grows by island formation at low pressures on platinum(111).

Above one monolayer additional spots appear at the radius of the graphite rings, and these persist after annealing at 1050-1100K. These additional spots form no obvious pattern and seem to be different each time the structure is formed. This suggests additional graphite-like layers are forming out of registry with the first layer, as in bulk pyrographite. To order pyrographite requires annealing at 2000 - 3000 K, and carbon diffuses into the bulk platinum above 1200 K.

9. THE COADSORPTION OF POTASSIUM AND CO ON THE Pt(111) CRYSTAL SURFACE: A TDS, HREELS, AND UPS STUDY†

J. E. Crowell, E. L. Garfunkel, and G. A. Somorjai

The interaction of CO with a potassium covered Pt(111) surface is investigated using thermal desorption (TDS), high resolution electron energy loss (HREELS), and ultraviolet photoelectron (UPS) spectroscopies. When submonolayer amounts of potassium are preadsorbed, the adsorption energy of CO increases from 25 to 36 kcal/mole, while substantial shifts in the site occupancy from the linear to the bridged site are observed. The CO stretching vibrational frequencies are shown to decrease continuously with either increasing potassium coverage or decreasing CO coverage. A minimum CO stretching frequency of 1400 cm^{-1} is observed, indicative of a CO bond order of 1.5. The work function decreases by up to 4.5 eV at submonolayer potassium coverages, but then increases by 1.5 eV upon CO co-adsorption. The results indicate that the large adsorption energy, vibrational frequency, and work function changes are because of molecular CO adsorption with a substantial charge donation from potassium through the platinum substrate and into the 2 π^* CO orbital.

* * *

†Brief version of LBL-13349 and LBL-14335.

10. THE INTERACTION OF POTASSIUM WITH π-ELECTRON ORBITAL CONTAINING MOLECULES ON Pt(111)†

E. L. Garfunkel, J. J. Maj, M. H. Farias, J. C. Frost, and G. A. Somorjai

The interaction of co-adsorbed potassium with π-orbital containing molecular adsorbates (benzene, PF_3, NO, C_4H_8, and CH_3CN) on the Pt(111) crystal surface was studied by thermal desorption spectroscopy. Co-adsorbed potassium significantly weakened the platinum-benzene bond. Upon heating, more of the benzene desorbed intact when potassium was present, instead of dissociating to yield H_2 and surface carbon. Interestingly, in previous studies we showed that co-adsorbed potassium substantially increased the platinum carbon bond strength for adsorbed CO.

The adsorption of PF_3, CH_3CN, and C_4H_8 was blocked by potassium, and no additional or shifted peaks were observed in the thermal desorption spectra. Adsorbed NO, on the other hand, was found to dissociate in an amount proportional to the K concentration, yielding N_2 and N_2O (as well as NO) in the desorption spectra.

We propose that only adsorbates having molecular orbitals with energy levels located near to E_F can be significantly affected by "electronic promotion" in catalysis.

* * *

†Brief version of LBL-15504.

11. THE CHARACTERIZATION OF Pt/Cu ALLOY AND EPITAXIAL SURFACES

R. Yeates and G. A. Somorjai

Copper deposited on the flat(111) and stepped(553) platinum crystal surfaces was studied with Auger electron spectroscopy (AES), thermal desorption spectroscopy (TDS), and low energy electron diffraction (LEED). AES results indicated that Cu grew on the Pt(111) surface via a layer-by-layer mechanism and via a Volmer-Weber mechanism on the Pt(553) surface. LEED showed that Cu formed islands on the Pt(111) surface and one monolayer of Cu took on the Pt lattice spacing which is 8% larger than the Cu bulk lattice spacing. The bulk Cu lattice spacing was reached after 4 monolayers of Cu. These results indicate a relatively strong Pt-Cu interaction.

TDS of CO from Pt(111)/Cu showed that epitaxial Cu simply blocks adsorption sites of the Pt. The change in the amount of CO desorption from the Pt was directly proportional to the Cu coverage with

no desorption from Pt with $\geq$ 1 monolayer coverage of Cu. No change in desorption energy was observed until high Cu coverages. TDS of CO from the Pt(553)-epitaxial Cu surface showed a preferential adsorption of the Cu away from the CO step adsorption site.

When a Pt crystal with a Cu adlayer was heated, the Cu diffused into the bulk. The activation energy for this process was determined to be 120 KJ/mole. The TDS of CO from the (111) face of these Pt/Cu alloys showed a decrease in the desorption energy of CO. The maximum decrease was 20 KJ/mole for a surface composed of 75% Cu.

12. A NEW MODEL FOR CO ORDERING AT HIGH COVERAGES ON LOW INDEX METAL SURFACES: A CORRELATION BETWEEN LEED, HREELS, AND IRS. CO ADSORBED ON fcc (100) SURFACES†

J. P. Biberian and M. A. Van Hove

We have reexamined the surface structures of CO on (100) surfaces of copper, palladium, nickel, and platinum. We used the types of sites determined by High Resolution Energy Electron Loss Spectroscopy (HREELS), or Infrared Spectroscopy (IRS), to propose new models for the arrangement of CO molecules at coverages exceeding 1/2, i.e., at coverages higher than those corresponding to simple structures c(2 x 2) and p($2\sqrt{2}$ x $\sqrt{2}$)R45°. Laser simulations allowed us to decide the validity of the proposed models. The consequences of these models are the existence of at most two adsorption sites at all coverages, and the existence of antiphase domains separated by walls to form the complex structures. The transition between two consecutive structures because of an increase of coverage is an unidirectional compression, generating more wall regions.

* * *

†Brief version of Surf. Sci. 118, 443 (1982).

13. LEED INTENSITY ANALYSIS OF THE (1 x 5) RECONSTRUCTION OF Ir(100)†

E. Lang,‡ K. Muller,‡ K. Heinz,‡ M. A. Van Hove, R. J. Koestner, and G. A. Somorjai

New experimental LEED data for the reconstructed Ir(100) (1 x 5) surface have been taken with a videocamera coupled to a computer for the generation of I-V curves. Special attention was paid to minimize the effect of uncertainties in the angle of incidence (including those due to residual magnetic fields) and to assure proper background subtraction.

These data have been compared with existing calculated LEED I-V curves to determine the surface structure. An R-factor comparison was made and the basic structural conclusion of the previous study has been confirmed, yielding a quasi-hexagonal reconstructed top layer involving bridge sites with respect to the underlying substrate layer. The top layer may be more buckled than previously thought, but the differences in atomic positions are of the order of the uncertainty of the determination (0.1 Å). A slightly larger contraction of the top layer spacing is found here, which would translate to about 5% bond length contractions between atoms in the top layer and in the next layer. The best structure yields a five-R-factor average of 0.21, a Zanazzi-Jona R-factor 2 x RRZJ of 0.34, and a Pendry R-factor 2 x RPE of 0.45. All other structural models in the long list that were examined can now be rejected.

* * *

†Brief version of LBL-14338.
‡University of Erlangen-Nürnberg, West Germany.

14. THE ADSORPTION AND BINDING OF THIOPHENE, BUTENE, AND H_2S ON THE BASAL PLANE OF MoS_2 SINGLE CRYSTALS†

M. Salmeron and G. A. Somorjai

The adsorption of thiophene, butene, and H_2S has been studied using the basal plane of MoS_2 single crystals in the temperature range of 77-300 K. Only at the lowest temperatures did thiophene adsorb and then desorb intact at 165 K using a partial pressure of 10^{-6} Torr. H_2S and butene behaved similarly and all of the molecules have binding energies in the range of 8-10 kcal/mole.

* * *

†Brief version of LBL-13971.

15. LEED AND AES STUDY OF ZIRCONIUM OVERLAYERS ON THE Pt(100) CRYSTAL FACE

U. Bardi, P. N. Ross, and G. A. Somorjai

Zirconium overlayers were deposited onto Pt(100) surfaces by electron beam evaporation under UHV conditions. A layer-by-layer growth mechanism was observed, which was maintained even when the zirconium was oxidized at low pressure between successive depositions. As-deposited zirconium was highly reactive toward oxygen, carbon monoxide, and hydrocarbons, rapidly forming oxide or carbide, even at submonolayer coverages. Oxide or carbon overlayers were observed to decompose upon UHV annealing at above ca. 700 K. with dissolution of the zirconium into the platinum substrate. The annealed oxide overlayers formed a variety of complex ordered Zr/O/Pt surface structures. Of particular interest was a reversible transformation between an oblique epitaxial structure ($[\frac{21}{11}]$) and the (100)-(1 x 1) Pt structure, produced by oxygen dosing and reversed by 900 K annealing. The epitaxial structure is tentatively identified as a well-ordered $PtZr_xO_y$ surface phase, and the (1 x 1) structure consisted of disordered ZrO_2 islands on top of the (100) surface. The $[\frac{21}{11}]$ surface was unreactive toward carbon monoxide or hydrocarbons, but the (1 x 1) surface chemisorbed carbon monoxide in a manner characteristic of Pt(100).

Studies of Catalyzed Surface Reactions

1. AMMONIA SYNTHESIS CATALYZED BY RHENIUM†

N. D. Spencer and G. A. Somorjai

Polycrystalline rhenium appears to be nearly an order of magnitude more active as an ammonia synthesis catalyst than the most active crystal plane of iron [Fe(111)] at low conversions and in the reactant pressure (20 atm) and temperature (603-713 K) regimes investigated. It displays an activation energy for ammonia synthesis of 16.2 kcal $mole^{-1}$, which is lower than that of Fe(111) (19.4 kcal $mole^{-1}$) under identical experimental conditions. Although rhenium becomes reversibly poisoned at 1-2 Torr of product ammonia, exposure to water or presulfidation has little effect on its catalytic activity. This is in marked contrast to the behavior of iron.

* * *

†Brief version of LBL-14298.

2. INTERACTION OF CO, CO_2, AND D_2 WITH RHODIUM OXIDE: ITS REDUCTION AND CATALYTIC STABILITY

P. R. Watson and G. A. Somorjai

We have investigated the adsorption and interaction of CO, CO_2, and D_2 with $Rh_2O_3 \cdot 5H_2O$ by thermal desorption spectroscopy (TDS). Both CO and D_2 react strongly with the oxide lattice inducing decomposition during the desorption process to yield CO_2 and D_2O. Adsorbed CO_2 desorbs essentially intact. These results are compared with those found on rhodium metal formed by reducing the oxide to the metallic state. On this metallic surface CO_2 dissociates while CO and D_2 desorb without significant reaction. The use of CO_2 to maintain an oxidized metal surface in a reducing atmosphere during a catalytic reaction was investigated.

3. DEUTERIUM ISOTOPE EFFECTS FOR HYDROCARBON REACTIONS CATALYZED OVER PLATINUM SINGLE CRYSTAL SURFACES†

S. M. Davis, W. D. Gillespie, and G. A. Somorjai

The initial rates of hydrocarbon reactions of isobutane, neopentane, cyclohexane, n-hexane, and n-heptane, in the presence of deuterium, were measured over the flat (111), stepped (13,1,1), and kinked (10,8,7) platinum single crystal surfaces in the temperature range 520-650 K and at atmospheric pressures. Inverse isotope effects $[(R_D/R_H) = 1.3\text{-}3.3]$ were detected for a variety of hydrogenolysis, isomerization, and C_5-cyclization reactions. The inverse isotope effects that appear to arise from a combination of kinetic and thermodynamic isotope effects displayed magnitudes that were not much dependent on the platinum surface structure.

* * *

†Brief version of LBL-13363.

4. STUDIES OF SULFUR MONOLAYERS ON Mo(100) AND ITS EFFECTS ON ADSORBATE BINDING

A. Gellman, M. H. Farias, and G. A. Somorjai

The structure and chemical properties of sulfur deposits on a Mo(100) single crystal face were studied. The sulfur deposits exhibit four distinct LEED structures in the range of coverages from one monolayer to the clean surface, the p(2 x 2), c(2 x 4), $\binom{2\bar{1}}{11}$ and c(2 x 2) structures. The p(2 x 1) structure corresponds to one monolayer. The thermal desorption spectrum of sulfur from Mo(100) indicates four distinct binding sites, three at high energies, producing peaks at 1100 K, 1400 K, and 1800 K, and the fourth at 350 K. The low energy peak corresponds to adsorption of sulfur beyond the monolayer.

Thermal desorption studies of the effects of sulfur on various molecules co-adsorbed on the Mo(100) surface were carried out. The molecules studied to this point are D_2, O_2, CO, C_2H_4, n-hexane, and thiophene. The thermal desorption spectra have been studied as a function of sulfur coverage. In all cases the sulfur poisoned the surface by blockage of adsorption sites.

The sulfur covered Mo(100) and the basal plane of MoS_2 were compared. Each has been exposed separately to H_2 and O_2 at pressures of 1 atm and a temperature of 520 K. Under these conditions both surfaces were completely inert to the H_2 atmosphere. In the presence of 1×10^{-7} Torr of O_2 the sulfur on the Mo(100) surface was readily oxidized at temperatures of about 1100 K, and the overlayer was removed as SO and SO_2 upon heating in vacuum. The ordered basal plant of MoS_2 was inert and showed no uptake of oxygen as examined by AES. However, after sputtering with He the MoS_2 showed a marked uptake of oxygen and upon heating evolved SO and SO_2. Sputtering has introduced defects into the surface, destroying the ordered structure seen by LEED, and these defect sites are now vulnerable to attack by O_2.

5. THE EFFECT OF POTASSIUM ON THE CATALYZED REACTIONS OF n-HEXANE OVER Pt(111) AND Pt-[6(111)x(111)] SINGLE CRYSTAL SURFACES

F. Zaera and G. A. Somorjai

The effect of potassium on the n-hexane conversion catalyzed by Pt(111) and Pt[6(111)x(111)] single crystals has been studied near atmospheric pressures. Reaction activity, selectivity, and self-poisoning with time were studied as a function of potassium coverage of the crystal faces. The activity of the catalyst dropped drastically with as little as 2% potassium atoms on the surface, with no improvement in selectivity or stability. The temperature dependence in the range 550-600 K of the reaction rates was not significantly different from the clean platinum case.

The change in the structure of the carbonaceous deposits formed during the reaction has also been studied. The variations with potassium coverage

of the total amount of carbon, the fraction of uncovered platinum, the hydrogen content, and the energetics of dehydrogenation of these deposits were investigated. The inhibition of the dehydrogenation of adsorbed hydrocarbon species in the presence of co-adsorbed potassium on the platinum surface explains the changes of reactivity that are reported.

6. DEHYDROGENATION OF CYCLOHEXANE CATALYZED BY BIMETALLIC Au-Pt SINGLE CRYSTAL SURFACES†

J. W. A. Sachtler and G. A. Somorjai

The cyclohexane dehydrogenation was investigated using two-phase, epitaxial Au on Pt(111) single crystal surfaces and single-phase Au-Pt(111) surface alloys as catalysts, with 20 mbar cyclohexane and 133 mbar H_2 at 573 K. Benzene production was found to be enhanced 4.5-9 fold on surfaces containing about 50 at.% Au. The clean Pt(111) crystal face did not produce detectable amounts of cyclohexene, its formation being completely attributable to the crystal edges. However, the addition of gold to the Pt(111) surface induced production of cyclohexene, surfaces containing about 90 at.% Au being most active. The effects were similar for epitaxial and alloy surfaces, although the latter usually gave higher rates. Cyclohexene hydrogenation and dehydrogenation catalyzed by a Pt(100) single crystal surface, using 13.3 mbar cyclohexene and 13.3 mbar H_2 at 373 K, was only found to be inhibited by an epitaxial Au overlayer. The enhancement by Au of the cyclohexane dehydrogenation to benzene is interpreted as a reduction of the poisoning of Pt sites by benzene and possibly carbonaceous residues at high temperatures. The observation that only Au containing Pt(111) surfaces produced cyclohexene can be explained by ensemble size effects.

* * *

†Brief version of LBL-14406.

7. ENERGY REDISTRIBUTION AMONG INTERNAL STATES OF NITRIC OXIDE MOLECULES UPON SCATTERING FROM Pt(111) CRYSTAL SURFACE†

M. Asscher, W. L. Guthrie, T.-H. Lin, and G. A. Somorjai

The vibrational and rotational states distributions of a supersonic nitric oxide beam, scattered from a Pt(111) single crystal surface, were investigated as a function of crystal temperature and scattering angle. A two-photon ionization technique was applied to monitor the internal energy content of the scattered molecules. The extent of equilibration of the three degrees of freedom of the NO molecule, e.g., translation, rotation, and vibration, as monitored by means of the accommodation coefficient (γ) was found to be $\gamma_{trans} > \gamma_{vib} > \gamma_{rot}$. The small rotational degree of accommodation is proposed to originate from a preferential desorption of rotationally cold NO molecules, as can be rationalized by microscopic reversibility arguments. The cold vibrational distribution, as compared to crystal temperature, is found to be consistent with different desorption kinetics for NO($v" = 0$) and NO($v" = 1$) adsorbed molecules at crystal temperatures between 450-1000 K. At temperatures above 1000 K, a competition between vibrational excitation and molecular desorption is proposed to explain the increased deviation between the observed vibrational distribution and the expected one, if a complete accommodation with the crystal surface occurs.

* * *

†Brief version of LBL-13347 and LBL-15034.

1982 PUBLICATIONS AND REPORTS

Refereed Journals

1. S. Ferrer, J. M. Rojo, M. Salmeron, and G. A. Somorjai, "The Role of Surface Irregularities (Steps, Kinks) and Point Defects on the Chemical Reactivity of Solid Surfaces," Philosophical Magazine 45(2), 261 (1982).

2. S. M. Davis and G. A. Somorjai, "Surface Reactions," Encyclopedia of Materials Science and Engineering, edited by M. B. Bever, Pergamon Press, New York, (1982); LBL-12372.

3. R. J. Koestner, J. C. Frost, P. C. Stair, M. A. Van Hove, and G. A. Somorjai, "Evidence For The Formation of Stable Alkylidyne Structures from C_3 and C_4 Unsaturated Hydrocarbons Adsorbed on the Pt(111) Single Crystal Surface," Surf. Sci. 116, 85 (1982); LBL-12780.

4. M. A. Van Hove and G. A. Somorjai, "Dynamical and Approximate LEED Theories Applied to Layers of Large Molecules," Surf. Sci. 114, 171 (1982); LBL-12803.

5. M. Salmeron and G. A. Somorjai, "The Desorption, Decomposition, and Deuterium Exchange Reactions of Unsaturated Hydrocarbons (Ethylene, Acetylene, Propylene, and Butenes) on the Pt(111) Crystal Face," J. Phys. Chem. 86, 341 (1982); LBL-12857.

6. P. W. Davies, M. Quinlan, and G. A. Somorjai, "The Growth and Chemisorption Properties of Ag and Au Monolayers on Platinum Single Crystal Surfaces: An AES, TDS, and LEED Study," Surf. Sci. 121, 290 (1982); LBL-12946.

7. G. A. Somorjai, "The Surface Science of Heterogeneous Catalysis: Possible Application in Atmospheric Sciences," presented at Atmospheric Chemical Society Conf. on Atmospheric Sciences, Albany, NY; Heterogeneous Atmospheric Chemistry Geophysical Monograph Series 26, 88 (1982); LBL-12986.

8. G. A. Somorjai, "Study of the Structure of Adsorbed Molecules on Solid Surfaces by HREELS and LEED," Proc. 9th Intl. Conf. on Atomic Spectroscopy, XXII CSI, Tokyo, Sept. 1981, Recent Advance in Analytical Spectroscopy, edited by K. Fuwa, Pergamon Press, p. 211 (1982); LBL-12996.

9. W. McLean, C. A. Colmenares, R. L. Smith, and G. A. Somorjai, "Electron Spectroscopy Studies of the Clean Thorium and Uranium Surfaces. The Chemisorption and Initial Stages of Reaction With O_2, CO, and CO_2," Phys. Rev. B 25(1), 8 (1982); UCRL-86167.

10. M. Langell and G. A. Somorjai, "The Composition and Structure of Oxide Films Grown on the (110) Crystal Face of Iron," J. Vac. Sci. Technol. 21, 858, (1982); LBL-13203.

11. E. L. Garfunkel and G. A. Somorjai, "Potassium and Potassium Oxide Monolayers on the Pt(111) and Stepped (755) Crystal Surfaces: A LEED, AES and TDS Study," Surf. Sci. 115, 441 (1982); LBL-13293.

12. N. D. Spencer, R. C. Schoonmaker, G. A. Somorjai, "Iron Single Crystal as Ammonia Synthesis Catalysts: Effect of Surface Structure on Catalyst Activity," J. Catal. 74, 129 (1982); LBL-13294.

13. M. A. Van Hove, R. J. Koestner, and G. A. Somorjai, "The Structures of Small Hydrocarbon Molecules on Rh(111) Studied by Low Energy Electron Diffraction: Acetylene, Ethylene, Methylacetylene, and Propylene," J. Vac. Sci. Technol. 20(3), 886 (1982); LBL-13300.

14. T.-H. Lin, S. T. Ceyer, W. L. Guthrie, and G. A. Somorjai, "The Angular and Velocity Distribution of NO Scattered from the Pt(111) Crystal Surface," J. Chem. Phys. 76, 6398 (1982); LBL-13347.

15. E. L. Garfunkel, J. E. Crowell, and G. A. Somorjai, "The Strong Influence of Potassium on the Adsorption of CO on Platinum Surfaces: A TDS and HREELS Study," J. Phys. Chem. 86, 310 (1982); LBL-13349.

16. J. E. Katz, P. W. Davies, J. E. Crowell, and G. A. Somorjai, "Design and Construction of a High Stability, Low Noise Power Supply for Use with High Resolution Electron Energy Loss Spectrometers," Rev. Sci. Instrum. 53(6), 785 (1982); LBL-13437.

17. F. Zaera and G. A. Somorjai, "Review: Heterogeneous Catalysis on the Molecular Scale," J. Phys. Chem. 86, 3070 (1982); LBL-13551.

18. S. M. Davis, F. Zaera, and G. A. Somorjai, "The Reactivity and Composition of Strongly Adsorbed Carbonaceous Deposits on Platinum. Model of the Working Hydrocarbon Conversion Catalyst," J. Catal. 77, 439 (1982); LBL-13706.

19. M. Salmeron, A. Wold, R. Chianelli, and G. A. Somorjai, "The Adsorption and Binding of Thiophene, Butene and H_2S on the Basal Plane of MoS_2 Single Crystals," Chem. Phys. Lett. 90, 105 (1982); LBL-13971.

20. A. L. Cabrera, N. D. Spencer, E. Kozak, P. W. Davies, and G. A. Somorjai, "Improved Instrumentation to Carry Out Surface Analysis and to Monitor Chemical Surface Reactions In Situ on Small Area Catalysts Over a Wide Pressure Range (10^{-8}–10^5 Torr)," Rev. Sci. Instrum. 53(12), 1888 (1982); LBL-13995.

21. N. D. Spencer and G. A. Somorjai, "Rhenium--An Ammonia Synthesis Catalyst," J. Phys. Chem. Lett. 86, 3493 (1982); LBL-14134.

22. J. P. Biberian and M. A. Van Hove, "A New Model for CO Ordering at High Coverages on Low-Index Metal Surfaces: A Correlation Between LEED, HREELS and IRS. I. CO Adsorbed on fcc(100) Surfaces," Surf. Sci. 118, 443 (1982).

23. R. J. Koestner, M. A. Van Hove, and G. A. Somorjai, "A LEED Crystallography Study of the (2x2)-C_2H_3 Structure Obtained After Ethylene Adsorption on Rh(111), Surf. Sci. 121, 321 (1982); LBL-13598.

24. N. D. Spencer and G. A. Somorjai, "Ammonia Synthesis Catalyzed by Rhenium," J. Catal., 78, 142 (1982); LBL-14298.

LBL Reports

1. S. M. Davis and G. A. Somorjai, "Catalysts by Platinum," submitted to Scientific American, LBL-13163.

2. S. M. Davis, W. D. Gillespie, and G. A. Somorjai, "Deuterium Isotope Effects for Hydrocarbon Reactions Catalyzed over Platinum Single Crystal Surfaces," submitted to J. Phys. Chem., LBL-13363.

3. S. M. Davis, F. Zaera, and G. A. Somorjai, "Surface Structure and Temperature Dependence of Light Alkane Skeletal Rearrangement Reactions Catalyzed Over Platinum Single Crystal Surfaces," submitted to J. Am. Chem. Soc., LBL-13975.

4. C. Minot, M. A. Van Hove, and G. A. Somorjai, "A Covalent Model for the Bonding of Adsorbed Hydrocarbon Fragments On the (111) Face of Platinum," LBL-13603.

5. A. Gavezzotti, M. Simonetta, M. A. Van Hove, and G. A. Somorjai, "Force-Field Calculations of the Packing Energy of Monolayers of C_3 and C_4 Hydrocarbon Molecules Adsorbed on Single Crystal Metal Surfaces," submitted to Surf. Sci., LBL-14053.

6. G. A. Somorjai, "The Surface Science of Heterogeneous Catalysis," to be published in Robert A. Welch Conference Proceedings, LBL-14135.

7. S. M. Davis and G. A. Somorjai, "The Surface Science of Heterogeneous Catalysis," to be published in Chemtech, LBL-14285.

8. R. J. Koestner, M. A. Van Hove, and G. A. Somorjai, "The Structure and Bonding of Hydrocarbons Adsorbed on Metal Surfaces," to be published in Chemtech, April 1982, LBL-13982.

9. J. E. Crowell, E. L. Garfunkel, and G. A. Somorjai, "The Co-adsorption of Potassium and CO on the Pt(111) Crystal Surface: A TDS, HREELS and UPS Study," to be published in Surf. Sci. LBL-14335.

10. E. Lang, K. Muller, K. Heinz, M. A. Van Hove, R. J. Koestner, and G. A. Somorjai, "LEED Intensity Analysis of the (1 x 5) Reconstruction of IR(100)," to be published in Surf. Sci., LBL-14338.

11. J. W. A. Sachtler and G. A. Somorjai, "Influence of Ensemble Size on CO Chemisorption and Catalytic n-Hexane Conversion with Au-Pt(111) Bimetallic Single Crystal Surfaces," to be published in J. Catal., LBL-14406.

12. R. J. Koestner, M. A. Van Hove, and G. A. Somorjai, "The Molecular Structure of Hydrocarbon Monolayers on Metal Surfaces," to be published in J. Phys. Chem., LBL-13962.

13. M. Salmeron, R. Chianelli, and G. A. Somorjai, "A LEED-AES Study of the Structure of Sulfur Monolayers on the Mo(100) Crystal Face," to be published in Surf. Sci., LBL-14551.

14. G. A. Somorjai, "Molecular Ingredients of Heterogeneous Catalysis, International Academy of Quantum Molecular Science, 4th International Congress in Quantum Chemistry," Uppsala, Sweden, June 1982, LBL-14531.

15. B. E. Koel, M. A. Van Hove, and G. A. Somorjai, "LEED and HREELS Studies of Molecular Adsorbates on Model Catalyst Surfaces," Advances in Catalytic Chemistry II Symposium, Salt Lake City, Utah, LBL-14504.

16. M. A. Van Hove, R. J. Koestner, and G. A. Somorjai, "LEED Intensity Analysis of a Surface Structure With Three CO Molecules in the Unit Cell, Rh(111)(2x2)-3CO: Compact Adsorption in Simultaneous Bridge and Non-Symmetric Neat-Top Sites," submitted to Phys. Rev. Lett., LBL-15033.

17. M. Asscher, W. L. Guthrie, T.-H. Lin, and G. A. Somorjai, "Energy Redistribution Among Internal States of Nitric Oxide Molecules Upon Scattering From Pt(111) Crystal Surface," submitted to J. Chem. Phys. LBL-15034.

18. S. T. Ceyer, W. L. Guthrie, and T.-H. Lin, "D_2O Product Angular and Translational Energy Distributions From the Oxidation of Deuterium on Pt(111)," submitted to J. Chem. Phys., LBL-15035.

19. R. Casanova, A. L. Cabrera, H. Heinemann, and G. A. Somorjai, "Calcium Oxide and Potassium Hydroxide Catalyzed Low Temperature Methane Production From Graphite and Water. Comparison of Catalytic Mechanisms," submitted to Fuel, LBL-15067.

20. S. M. Davis, F. Zaera, M. Salmeron, R. Gordon, and G. A. Somorjai, "Energetics and Reversibility of Hydrocarbon Sequential Dehydrogenation on Platinum Single Crystal Surfaces: Thermal Desorption and Carbon-14 Radiotracer Studies," to be published in J. Am. Chem. Soc., LBL-14611.

Invited Talks

1. G. A. Somorjai, "The Structure Sensitivity of Platinum Catalysts for Reforming Reactions as Revealed by Single Crystals Studies," and "The Reactivity of Metal Monolayers on Single Crystal Surfaces of Other Metals: Gold, Silver, Copper and Potassium on Platinum," ACS Meeting, Symposium on "Multimetallic Catalysis," Las Vegas, Nevada, March 19, 1982.

2. G. A. Somorjai, "Studies of Metal and Organic Monolayers by Electron Scattering," The University of Tokyo, Tokyo, Japan, April 5, 1982.

3. G. A. Somorjai, "The Atomic Structures of Surface Monolayers. The Surface Chemical Bond," Fudan University, Shanghai, China, April 8, 1982.

4. G. A. Somorjai, "Catalysis of Hydrocarbon Conversion," Fudan University, Shanghai, China, April 9, 1982.

5. G. A. Somorjai, "The Modern Techniques of Analyzing the Properties of Surfaces," Beijing University, Beijing, China, April 15, 1982.

6. G. A. Somorjai, "The Atomic Structures of Surface Monolayers. The Surface Chemical Bond," Beijing University, Beijing, China, April 17, 1982.

7. G. A. Somorjai, "Principles of Heterogeneous Catalysis. Elementary Surface Reactions," Jilin University, Changchun, China, April 20, 1982.

8. G. A. Somorjai, "Catalysis of Hydrocarbon Conversion," Jilin University, Changchun, China, April 21, 1982.

9. G. A. Somorjai, "Relation Between Surface Science and Catalysis. New Developments," Jilin University, Changchun, China, April 24, 1982.

10. G. A. Somorjai, "ELS and LEED Studies of Catalyst Surfaces," Salt Lake City, Utah, May 19, 1982.

11. G. A. Somorjai, "Molecular Ingredients of Heterogeneous Catalysis," 4th International Congress in Quantum Chemistry, Uppsala, Sweden, June 19, 1982.

12. G. A. Somorjai, "Structure of Atoms and Molecules or Solid Surfaces," American Crystallographic Association Meeting, San Diego, California, August 17, 1982.

13. G. A. Somorjai, "Surface Science of Heterogeneous Catalysis," Philadelphia Catalysis Society, Philadelphia, Pennsylvania, September 8, 1982.

14. G. A. Somorjai, "Surface Science of Heterogeneous Catalysis of Metal Surfaces," Illinois Institute of Technology, Kilpatrick Lecture, Chicago, Illinois, October 14, 1982.

15. G. A. Somorjai, "Toward Energy Independence Through Research in Surface Chemistry and Catalysis;" "The Structure of Adsorbed Monolayers, The Surface Chemical Bond;" and "The Molecular Ingredients of Catalyzed Hydrocarbon Conversion Over Transition Metals," Michigan State University Dow Lectures, Michigan, October 26-28, 1982.

16. G. A. Somorjai, "The Materials Science of Heterogeneous Catalysis," Stanford University, Palo Alto, California, November 2, 1982.

17. G. A. Somorjai, "The Structure and Composition of Solids in the Near Surface Region," U.S. Army Research Office, Metallurgy and Materials Division, Department of the Army, Charleston, South Carolina, December 14, 1982.

18. M. A. Van Hove, "Structural Study of CO Molecules Adsorbed Simultaneously in Linear and Bridge Sites in Rh(111)+(2x2)3CO by LEED Intensity Calculations," American Physical Society Meeting, Dallas, Texas, March 9, 1982.

19. M. A. Van Hove, "What Can Structural Determination by LEED Do?" IBM Research Laboratory, San Jose, California, June 1, 1982.

20. M. A. Van Hove, "LEED Determination of the Structures of Adlayers Containing More Than One Molecule per Unit Cell: CO and Propylidyne on Rh(111), 5th European Conference on Surface Science, Ghent, Belgium, August 25, 1982.

21. M. A. Van Hove, "Structures d'hydrocarbures à périodicité bidimensionnelle par diffraction d'électrons lents," University of Marseille, France, September 3, 1982.

22. M. A. Van Hove, "High-Coverage Structure of CO on Rh(111)," Autonomous University of Madrid, Spain, September 8, 1982.

23. M. A. Van Hove, "Physical Aspects of the Structure and Bonding of CO on Metal Surfaces," Department of Physics, University of California, Berkeley, October 13, 1982.

f. Nuclear Magnetic Resonance*

Alexander Pines, Investigator

Introduction. The primary objectives of this program are to develop new methods in magnetic resonance spectroscopy and to use them to study molecular behavior in condensed phases. This demands an understanding of the interaction of nuclear spins with each other, with other degrees of freedom such as molecular translations, vibrations and rotations, and with external radiation such as light or radiofrequency sources. Recent novel methods developed under the program include multiple quantum spectroscopy, high resolution solid state NMR and magic angle spinning, pulsed optical nuclear double resonance, and nuclear magnetic isotope separation. These methods are being applied to understand structure and dynamics at the molecular level in a number of materials including ferroelectrics, liquid crystals, polymers, organic crystals, and zeolites. Some molecular properties change upon light excitation, and laser magnetic double resonance is being used to examine how these changes dictate the course of photochemical reactions.

1. BROADBAND POPULATION INVERSION†

J. Baum, R. Tycko, J. Murdoch, and A. Pines

The optimal use of power in a spectroscopic experiment demands that power be absorbed as uniformly as possible over a broad band of frequencies. We have developed an approach to the design of phase-shifted, radiofrequency-pulse sequences that have the ability to invert nuclear spin populations over a broad range of resonance frequencies. Previous work in this area has relied upon a pulse-by-pulse analysis of the inverting sequence. Our approach takes as its starting point a particular inverting trajectory for the on-resonance spins. A pulse with a continuously varying phase can be derived from that trajectory. Computer simulations show that, for the proper on-resonance trajectory, the inverting property of the derived pulse holds for off-resonance spins as well. Several mathematical methods for approximating the continuously varying pulse by a sequence of constant phase pulses have been investigated. Applications are also possible in wideband coherent optical excitation with lasers.

* * *

†Abstracted in part from LBL-14206; J. Chem. Phys. 77, 2870 (1982).

2. TIME-RESOLVED OPTICAL NUCLEAR POLARIZATION†

R. Tycko, D. Stehlik,‡ H. Cho, and A. Pines

We have developed a new technique for studying dynamic processes in the excited triplet electronic state of molecular crystals on a microsecond time scale. The technique, called time-resolved optical nuclear polarization, freezes information about the transient excited states in the form of long-lived nuclear magnetization, where it can subsequently be read out by pulsed NMR techniques. The nuclear magnetization is generated by a sequence of precisely timed ultraviolet laser pulses and magnetic field pulses. Measurement of the nuclear magnetization as a function of decay times within the sequence, when interpreted according to the detailed theory of optical nuclear polarization, yields parameters such as the excited state lifetime and excited state spin relaxation times. The utility of the technique has been demonstrated on single-crystal samples of fluorene doped with acridine. The time-resolved technique also shows promise for the generation of large nuclear magnetization in samples or at room temperature where conventional optical nuclear polarization techniques fail.

* * *

†Abstracted in part from LBL-14929; Chem. Phys. Lett. 93, 392 (1982).
‡Department of Physics, Free University of Berlin.

3. ZERO FIELD NMR†

D. Weitekamp,‡ A. Bielecki, D. Zax, and A. Pines

Structural information on molecules in solids must typically be obtained using x-ray diffraction or NMR on single crystals. In powders the spectra are broadened and orientational information is lost. Consider, however, what would happen if the isotropy of space was not broken by some preferred direction, e.g., the beam of x rays or the magnetic field. The spectrum of a powder could then look like that of a single crystal and yield full structural information. This is the basis of zero field NMR, in which the cycling of magnetic fields in a two-dimensional NMR experiment allows us to obtain the dimensional NMR spectrum without any applied external field. Indeed, the powder spectra of solid $Ba(ClO_3)_2 \cdot H_2O$ and $Li_2SO_4 \cdot H_2O$ exhibit well resolved lines yielding structural information without the need for single crystals.

* * *

†Abstracted in part from LBL-10593.
‡Department of Chemistry, University of Groningen, The Netherlands.

*This work was supported by the Director, Office of Energy Research, Office of Basic Energy Sciences, Materials Sciences Division of the U.S. Department of Energy under Contract No. DE-AC03-76SF00098.

4. ANISOTROPIC DIFFUSION IN ORIENTED SYSTEMS†

D. Zax and A. Pines

Molecular diffusion in oriented systems such as polymers and liquid crystals is anisotropic. The degree of anisotropy is an important parameter in understanding the interactions between molecules in these phases. Measurements have been made, using a new multiple quantum spin echo technique developed in our laboratory, on benzene and butyne in Eastman nematic phase 15320. The results show a significant enhancement of diffusion parallel to the director axis and suggest a model in which the shape of the solute molecules determine diffusion effects.

* * *

†Abstracted in part from LBL-14997.

5. HIGH RESOLUTION NMR OF FELDSPARS AND ZEOLITES†

J. M. Millar, J. B. Murdoch, C. Ye, R. Eckman,‡ and A. Pines

Magic-angle spinning (MAS) NMR is an ideal technique for the study of complicated solids: all anisotropic nuclear spin interactions are averaged to zero, leaving a liquid-like spectrum of isotropic chemical shifts. We have obtained high-resolution ^{1}H, ^{2}H, ^{27}Al, and ^{29}Si MAS NMR spectra of a variety of feldspars, zeolites, and other alumino-silicates of importance in catalysis and earth science. Such spectra provide detailed information on coordination numbers and on the nature and extent of silicon-aluminum ordering in these materials. Of particular interest are rapidly quenched feldspar glasses in that their structure may mirror that of the corresponding liquids.

* * *

†Abstracted in part form LBL-15254.
‡Central Research Division, Du Pont.

6. THEORY OF SPIN DIFFUSION IN SOLIDS†

R. Eckman,‡ A. Pines, R. Tycko, and D. P. Weitekamp§

Spin diffusion in solid-state NMR occurs by the exchange of one quantum of energy in flip-flop transitions driven by dipole couplings. It is commonly believed that flip-flop transitions are quenched when the nuclei involved have well-separated resonance frequencies, as is generally the case for inequivalent quadrupolar nuclei. An average Hamiltonian theory of flip-flop transitions reveals that a second order process allows a generalized flip-flop in which nuclei exchange two quanta of energy. We derive a detailed expression for the rate of this double-quantum flip-flop, showing the dependence of the rate on the dipole coupling strength and on the difference in quadrupole splittings for a pair of inequivalent spin-1 nuclei. We expect the double-quantum flip-flop to be the dominant spin diffusion mechanism for quadrupolar nuclei in the absence of interactions with external energy reservoirs.

* * *

†Abstracted in part from LBL-15686.
‡Central Research Division, Du Pont.
§Department of Chemistry, University of Groningen, The Netherlands.

7. TIME-RESOLVED CIDNP AND MAGNETIC ISOTOPE EFFECT†

L. Sterna,‡ J. Baum, and A. Pines

A very important feature of free radical chemistry is the effect of electron spin on chemical bonding. In general, two radicals can bond only if the two unpaired electrons have singlet (S = 0) correlation. The triplet state (S = 1) has repulsive potentials. The electron-nuclear hyperfine coupling causes interconversion of the electron spin states. This can be used to separate nuclear isotopes of different hyperfine coupling into different chemical products (Magnetic Isotope Effect). A crucial factor in the operation of the magnetic isotope effect in a cyclic reaction is that the two radicals of the prepared triplet must stay in the vicinity of one another on a timescale comparable to the inverse hyperfine couplings. In previous reports we have shown that the ^{13}C enrichment in the dibenzylketone reaction exhibits a strong viscosity dependence and goes through a maximum at 10 poise. Current work involves time-resolved CIDNP in cyclic reactions of ketones and long chins to try and enhance the isotope effect. The time resolution is obtained by using a pulsed N_2 laser, with a high power pulsed NMR spectrometer.

* * *

†Abstracted in part from LBL-10594.
‡Shell Development Company, Houston.

8. MOLECULAR CONFORMATION IN LIQUID CRYSTALS†

G. Drobny, B. Oh, H. Fujiwara, and A. Pines

The study of the conformation of aromatic and aliphatic units in liquid crystal molecules is important in understanding the physics and chemistry of their various fascinating phases. This can usually only be accomplished with deuterium isotope substitution and complex analysis of the NMR spectra. However, multiple quantum transitions are extremely sensitive to correlations, both static and dynamic, between the protons of a molecule and are usually resolvable and simple to analyze. We have used this to study the conformations of a number of liquid crystal systems and the relationship of these conformations to the macroscopic phases. For example, in the nematic phase of cyanobiphenyl systems, the conformation of the biphenyl group could be analyzed by fitting the 6- and 7-quantum spectra (the normal 1-quantum spectrum has 1000 lines and can hardly be analyzed) to theoretical models of the order parameters and biphenyl dihedral angle.

Aliphatic chain configurations can also be studied, since the multiple quantum spectra are extremely sensitive to inter-segment dipole-dipole couplings. The best fit is found to be a model with all trans and two conformations with gauche defects.

* * *

†Abstracted in part from LBL-13736.

9. EXCITATION OF HIGH N-QUANTUM TRANSITIONS†

W. S. Warren,‡ D. P. Weitekamp,§ Y. S. Yen, J. R. Garbow, and A. Pines

The question of whether a molecule can be used to absorb and emit photons only in groups of n has been treated further. A number of pulse sequences have been introduced, which in effect induce excitation by only resonant groups of n photons. This causes only n-quantum transitions even when many other transitions might be resonant. The theory explains how this is done by using repeated phase shifts of 2/n in the radiation to build up the selected coherences with all other coherences interfering destructively. The selectivity produces an enormous enhancement of the high n-quantum coherences (or populations) that are normally very weak when governed by an incoherent statistical process. For example, the 12-quantum transition in a many spin crystal can be enhanced by four or five orders of magnitude. Up to 22-quantum excitations have been observed in solid adamantane.

* * *

†Abstracted in part from LBL-15253 and Chem. Phys. Lett. 88, 441 (1982).
‡Department of Chemistry, Princeton University.
§Department of Chemistry, University of Groningen, The Netherlands.

1982 PUBLICATIONS AND REPORTS

Refereed Journals

1. R. Eckman and A. Pines, "High Resolution Proton NMR of Dilute Spins in Solids," J. Chem. Phys. 76, 2767 (1982); LBL-13332.

2. D. P. Weitekamp, J. R. Garbow, and A. Pines, "Search Procedure for Optimizing High Order Multiple Quantum Transition Intensities," J. Magn. Res. 46, 529 (1982); LBL-13557.

3. Y. S. Yen and D. P. Weitekamp, "Indirect Detection of Spin 1 Double Quantum Coherence in Liquids," J. Magn. Res. 47, 476 (1982); LBL-13434.

4. W. S. Warren and A. Pines, "Simple Pulse Sequences for Selective Multiple-Quantum Excitation," Chem. Phys. Lett. 88, 441 (1982); LBL-13006.

5. D. P. Weitekamp, J. R. Garbow, and A. Pines, "Determination of Dipole Coupling Constants Using Heteronuclear Multiple Quantum NMR," J. Chem. Phys. 77, 2870 (1982); LBL-14206.

6. R. Tycko, D. Stehlik, and A. Pines, "Time-Resolved Optical Nuclear Polarization," Chem. Phys. Lett. 93, 392 (1982); LBL-14829.

7. J. R. Garbow, D. P. Weitekamp, and A. Pines, "Bilinear Rotation Decoupling of Homonuclear Scalar Interactions," Chem. Phys. Lett. 93, 504 (1982); LBL-14904.

LBL Reports

1. Y. S. Yen and A. Pines, "Multiple-Quantum NMR in Solids," LBL-14821, J. Chem. Phys., in press.

2. D. Zax and A. Pines, "Study of Anisotropic Diffusion of Oriented Molecules by Multiple Quantum Spin Echoes," LBL-14997.

3. Y. S. Yen, "Multiple Quantum NMR in Solids," Ph.D. thesis, LBL-15253.

4. J. B. Murdoch, "Computer Simulations of Multiple Quantum Spectroscopy," Ph.D. thesis, LBL-15254.

5. R. Eckman, "High Resolution NMR in Solids with Magic Angle Spinning," Ph. D. thesis, LBL-14200.

6. G. Drobny, "NMR Studies of Liquid Crystals and Molecules Dissolved in Liquid Crystals," Ph.D. thesis, LBL-13736.

7. D. P. Weitekamp, "Time Domain Multiple Quantum NMR," Ph.D. thesis, LBL-10593.

8. R. Eckman, R. Tycko, D. Weitekamp, and A. Pines, "Deuterium Spin Diffusion by Double Quantum Flip-Flops," LBL-15686.

Invited Talks

1. A. Pines, "New Angles and Dimensions in NMR," Royal Society of Chemistry, Birmingham, England, March 1982.

2. A. Pines, "New Angles in NMR," The California Catalysis Society Annual Spring Meeting, Pleasanton, California, April 16, 1982.

3. A. Pines, J. R. Garbow, D. P. Weitekamp, and Y. S. Yen, "Free Induction Decay--Where Does It Go?" 23rd Experimental NMR Spectroscopy Conference, Madison, Wisconsin, April 1982.

4. A. Pines, R. Eckman, C. Ye, and J. M. Millar, "Magic Angle Spinning of $^{1}H/^{2}2H$ and Other Nuclei," 23rd Experimental NMR Spectroscopy Conference, Madison, Wisconsin, April 1982.

5. R. Eckman, "High Resolution Proton and Deuterium NMR in Solids," American Chemical Society Middle Atlantic Regional Meeting, University of Delaware, Newark, April 1982.

6. A. Pines, 7th Ampere International Summer School on New Techniques and Applications of Magnetic Resonance, 3 invited lectures, Portoroz, Yugoslavia, June 1982.

7. A. Pines, "Multiple Quantum Spectroscopy," Institute of Experimental Physics, University of Stuttgart, Seminar, Germany, June 21, 1982.

8. A. Pines, "New Angles in Solid State NMR," 24th Rocky Mountains Conference, 4th Vaughan Plenary Lecture, Denver, Colorado, August 1982.

9. A. Pines, Chemistry Department Seminar, Pomona College, Claremont, California, October 1982.

10. A. Pines, Chemistry Department Seminar, University of Arizona, Tuscon, Arizona, October 1982.

11. A. Pines, Chemistry Department Seminar, San Jose State University, San Jose, California, November 1982.

II Chemical Sciences

A. Fundamental Interactions

1. Photochemical and Radiation Sciences

a. Photon-Assisted Surface Reactions, Materials, and Mechanisms*

Gabor A. Somorjai, Investigator

Introduction. This project explores the photocatalyzed dissociation of water (H_2O) at both the solid-liquid and solid-vapor interfaces to produce hydrogen and oxygen gases. The purpose of these studies is to explore the mechanism of the photon-assisted surface reaction, to characterize the semiconductor catalyst, and to establish the optimum conditions (of surface structure, composition, temperature, and electrolyte solution) that maximize the rate of hydrogen and oxygen production and the power conversion efficiency of the process. The materials that are being used include silicon- and magnesium-doped iron oxides and molybdenum and rhenium sulfides.

1. PHOTOCATALYTIC PRODUCTION OF HYDROGEN FROM WATER BY A p- AND n-TYPE POLYCRYSTALLINE IRON OXIDE ASSEMBLY†

C. Leygraf, M. Hendewerk, and G. A. Somorjai

Photodissociation of water using Mg- and Si-doped iron oxides has been accomplished in a p/n diode assembly utilizing only visible light and applying no external bias. While iron oxides have been doped with a wide variety of compounds in the past, this is the first time that p-type photoactivity has been observed for Fe_2O_3. In our experiments new preparation procedures and doping with MgO have produced an iron oxide semiconductor with reproducible p-type photocurrents. This unique p-type material is used in a p/n diode assembly as the cathode to reduce hydrogen while connected to a Si-doped iron oxide which acts as the anode. This is the first successful diode assembly that employs both p- and n-type polycrystalline electrodes to catalytically photodissociate water. The dissociation process results in evolved hydrogen and oxygen gases (at a rate of 2 H_2 molecules per site per min), which are detectable with a gas chromatograph.

With this diode assembly made from cheap and abundant materials (Fe_2O_3, Mg, Si), it may be feasible to extract the hydrogen produced from solar radiation as a storable source of energy, if power conversion efficiency (0.05% at present) can be improved.

Water dissociation experiments have also been carried out in the vapor phase. Samples consisting of p-type Mg-doped and n-type Si-doped iron oxides were pressed together to form a contact junction. The disks were exposed to water vapor in a high pressure cell in an ultrahigh vacuum chamber. Visible light from the solar spectrum was shone on the samples, and oxygen evolution was monitored with a mass spectrometer. Surface analyses of the sample before and after the photodissociation experiments were done with an Auger spectrometer in the UHV chamber to determine whether the oxidation state of the iron was changing during the photodissociation process.

Surface characterization and sample analysis with Auger and x-ray photoelectron spectroscopy as well as detailed studies of the photoactivity of the iron oxide disks are being carried out.

* * *

†Brief version of LBL-14494 and LBL-14560.

2. THE PREPARATION AND SELECTED PROPERTIES OF Mg-DOPED p-TYPE IRON OXIDE AS A PHOTOCATHODE FOR THE PHOTOELECTROLYSIS OF WATER USING VISIBLE LIGHT†

Ch. Leygraf, M. Hendewerk, and G. A. Somorjai

Stable Mg-doped iron oxides that exhibit p-type character have been synthesized. These have been utilized in the form of sintered polycrystalline disks for the photodissociation of water. We report the influence of sintering temperature, surface oxygen deficiency, Mg-doping level, and solution chemistry on the photoactivity of the Mg-doped iron oxide photocathodes.

* * *

†Brief version of LBL-14669 and LBL-15269.

3. WORK IN PROGRESS

Thin film electrodes of the Mg- and Si-doped iron oxides are being prepared in order to improve the power conversion efficiencies of the p/n diode assembly.

An electrochemical cell with two compartments connected by a porous membrane is being constructed. In this system the pH of the electrolyte solution surrounding the p-type cathode and n-type anode can then be varied independently. The

*This work was supported by the Director, Office of Energy Research, Office of Basic Energy Sciences, Chemical Sciences Division of the U.S. Department of Energy under Contract No. DE-AC03-76SF00098.

new cell will interface directly to a UHV chamber for ESCA and other surface analysis measurements. This will permit analysis of the electrode surfaces following an experiment without exposing the samples to the atmosphere.

Capacitance and permittivity measurements are being made to better characterize the p/n diode assembly. Experiments are aimed toward establishing the carrier concentrations, locate the flat band potentials, and determine the permittivity constants of the iron oxides.

In other experiments, Auger spectroscopy is being used to investigate the gradual poisoning of the p-type cathode that occurs in the diode assembly after several hours of operation. Methods of inhibiting the poisoning are also being investigated.

1982 PUBLICATIONS AND REPORTS

Refereed Journals

1. C. Leygraf, M. Hendewerk, and G. A. Somorjai, "Photodissociatioln of Water by p- and n-Type Polycrystalline Iron Oxides by Using Visible Light ($\leq$ 2.7 eV) in the Absence of External Potential," Proc. Natl. Acad. Sci. USA, 79, 5739 (1982); LBL-14494.

2. Ch. Leygraf, M. Hendewerk, and G. A. Somorjai, "Photocatalytic Production of Hydrogen from Water by a p- and n-Type Polycrystalline Iron Oxide Assembly," J. Phy. Chem. 86, 4484 (1982); LBL-14560.

LBL Reports

1. Ch. Leygraf, M. Hendewerk, and G. A. Somorjai, "Mg- and Si-Doped Iron Oxides for the Photocatalyzed Production of Hydrogen From Water by Visible Light (2.2 eV $\leq$ h $\leq$ 2.7 eV)," to be published in J. Catal., LBL-14669.

2. Ch. Leygraf, M. Hendewerk, and G. A. Somorjai, "The Preparation and Selected Properties of Mg-Doped p-Type Iron Oxide as Photocathode for the Photoelectrolysis of Water Using Visible Light," to be published in J. Solid State Chemistry, LBL-15269.

Invited Talks

1. G. A. Somorjai, "Catalyzed Hydrogenation of Graphite and CO. Photocatalyzed Surface Processes," Fudan University, Shanghai, China, April 10, 1982.

2. G. A. Somorjai, "Photocatalyzed Surface Processes," Jilin University, Changchun, China, April 23, 1982.

3. G. A. Somorjai, "Photodissociation of Water Over Fe-Si-O Compound Surfaces," 6th DOE Solar Photochemistry Research Conference, University of Colorado, Boulder, Colorado, June 8, 1982.

4. G. A. Somorjai, "Hydrogen Production by Photocatalyzed Reaction on Fe_2O_3 Surfaces," American Chemical Society, Kansas City, Missouri, September 16, 1982.

5. G. A. Somorjai, "The Surface Science of Heterogeneous Catalysis and Its Application to the Photodissociation of Water," Arizona State University, Tempe, Arizona, November 9, 1982.

b. Photochemistry of Materials in the Stratosphere*

Harold S. Johnston, Investigator

Introduction. The field of stratospheric photochemistry continues to produce new surprises about every two years, and there have been large changes in the predicted effects of nitrogen oxides and of chlorine on stratospheric ozone. During the past year, the calculated effect of chlorine on the stratospheric ozone column has dropped to the lowest value since the effect was postulated ten years ago; and the calculated effect of nitrogen oxides in reducing ozone is about as large as it was at the conclusion of the Climatic Impact Assessment Program (1974). There is no reason to assume that the present results are final, and active work continues on laboratory studies, atmospheric measurements, and model calculations.

1. THE REACTION OF CHLORINE ATOMS WITH NITRIC ACID VAPOR†

W. J. Marinelli and H. S. Johnston

The reaction of chlorine atoms with nitric acid has been presumed to be

$$Cl + HNO_3 \rightarrow HCl + NO_3$$

If fast, this reaction would constitute a strong coupling between chlorine and the oxides of nitrogen in the atmosphere, in that an active form of chlorine (Cl) would be rendered inactive (HCl) and an inert form of nitrogen oxides (HNO_3) would be converted to catalytically active forms (NO_3, NO_2, NO). This reaction had been previously studied in two laboratories,[1,2] but the results at room temperature disagreed by a factor of 300. It was reinvestigated in this laboratory by the method of laser flash photolysis and vacuum ultraviolet resonance fluorescence. Molecular chlorine was photolyzed by a fast (10 ns) laser pulse at 350 nm wavelength, and the disappearance of chlorine atoms was followed by its resonance fluorescence at 138.0 and 139.0 nm. During the course of one run with nitric acid in excess, the chlorine atoms decayed by a pseudo first-order reaction $k_1 = K_2[HNO_3]$. After a series of runs with different nitric acid concentrations, a plot of the pseudo first-order constant against the nitric acid concentration gives the desired second order rate constant, Fig. 1.1. The results found here agreed closely with Ref. 1, but disagreed with Ref. 2. In another experiment the reaction was initiated by passing the laser pulse at 350 nm down a long tube, and an argon-ion excited dye laser at 662 nm was co-axially passed down the same tube in order to measure the build up of the presumed product NO_3. However, no NO_3 was observed under conditions where a large signal would be expected. The conclusion is that NO_3 is not the primary product of the subject reaction and the reaction rate is so slow that it is of no importance in atmospheric chemistry.

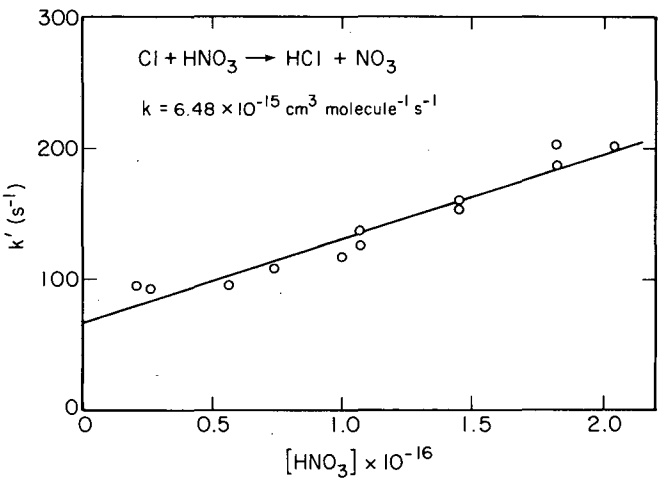

Fig. 1.1. Pseudo first-order rate constants for the reaction of atomic chlorine with nitric acid plotted against the concentration of nitric acid for each run. The slope gives the second order rate constant. Concentrations in units of molecules cm^{-3}. (XBL 8012-12918)

* * *

†Brief version of LBL-13473.

1. M. Leu and W. B. DeMore, Chem. Phys. Lett. 41, 121 (1976).
2. G. Poulet, G. Lebras, and J. Combourieu, J. Chem. Phys. 60, 767 (1978).

2. TEMPERATURE-DEPENDENT ULTRAVIOLET ABSORPTION SPECTRUM OF DI-NITROGEN PENTOXIDE†

Francis Yao, Ivan Wilson, and H. S. Johnston

Vertical profiles and total vertical columns of nitrogen dioxide have been measured at enough latitudes that one can estimate the global distribution of stratospheric nitrogen dioxide.[1] An anomalous effect called the "Noxon Cliff" has been observed,[2] in which the vertical column of nitrogen dioxide decreases dramatically between 45 and 55° latitude in the winter. This sharp decrease of nitrogen dioxide could not be reproduced by recent dynamic and chemical models of the atmosphere. The ultraviolet absorption spectrum of di-nitrogen pentoxide was investigated here between 223 and 300 K and between 200 and 380 nm. These measurements involve simple physics but complicated chemistry. Di-nitrogen pentoxide is thermally unstable and reacts strongly even with bound water on surfaces; and the reaction products, NO_2 and HNO_3, absorb ultraviolet radiation in the same spectral region as N_2O_5. The spectrum was found to be strongly temperature dependent, Fig. 2.1. When this temperature depend-

*This work was supported by the Director, Office of Energy Research, Office of Basic Energy Sciences, Chemical Sciences Division of the U.S. Department of Energy under Contract No. DE-AC03-76SF00098.

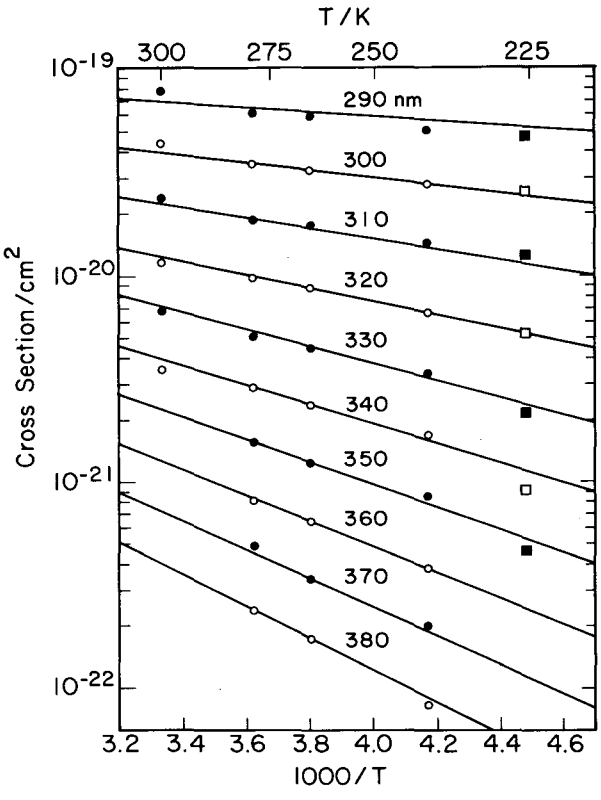

Fig. 2.1. Temperature dependence of the N_2O_5 cross sections at wavelengths between 290 and 380 nm. The temperature dependence is very weak or absent below 280 nm. (XBL 831-7667)

ence is incorporated in the stratospheric models, most of "Noxon's Cliff" is accounted for.[3]

* * *

†Brief version of LBL-14340.

1. S. Solomon, H. S. Johnston, M. Kowalczyk, and I. Wilson, Pure and Applied Geophysics 118, 58 (1980).
2. J. F. Noxon, J. Geophys. Res. 84, 5067 (1979); 85, 4560 (1980).
3. S. Solomon, private communication (1982).

3. WORK IN PROGRESS

A diode laser is being developed to measure free radical intermediates in photochemical reactions at very high resolution in the infrared spectral region. By the method of laser flash photolysis and resonance fluorescence, the primary products of N_2O_5 photolysis are being studied over a wide range of conditions. Also, the fluorescence of the nitrate free radical NO_3 is being investigated in a large cell at low pressure. In this laboratory it has been found that the absorption cross sections of oxygen in the Herzberg continuum has a pronounced temperature dependence.

Future Plans. Experiments are being designed to study the photochemistry of molecular nitrogen in the 6 to 12 eV energy range, with an emphasis on the production of the atomic excited electronic states ^2D and ^2P as well as ground state ^4S and molecular and atomic ions. The Advanced Light Source being planned in the Lawrence Berkeley Laboratory appears to be uniquely suitable for high resolution spectroscopy and cross sections in this spectral region.

1982 PUBLICATIONS AND REPORTS

Refereed Journals

1. W. J. Marinelli, D. M. Swanson, and H. S. Johnston, "Absorption Cross Sections and Line Shape for the NO_3(0-0) Band," J. Chem. Phys. 76, 2864 (1982); LBL-13699.

2. W. J. Marinelli and H. S. Johnston, "Reaction Rates of Hydoxyl Radical with Nitric Acid and with Hydrogen Peroxide," J. Chem. Phys. 77, 1225 (1982); LBL-14293.

3. F. Yao, I. Wilson, and H. S. Johnston, "Temperature-Dependent Ultraviolet Absorption Spectrum for Dinitrogen Pentoxide," J. Phys. Chem. 86, 3611 (1982); LBL-14340.

4. W. J. Marinelli and H. S. Johnston, "Quantum Yield for NO_3 Production from Photolysis of $ClONO_2$," Chem. Phys. Lett. 93, 127 (1982); LBL-14960.

LBL Reports

1. J. R. Podolske and H. S. Johnston, "The Rate of the Resonant Energy-Transfer Reaction Between $O_2(^1\Delta_g)$ and HOO," LBL-14961.

Other Publications

1. H. S. Johnston, "Odd Nitrogen Processes," Chapter 4 in Stratospheric Ozone and Man, Volume I, edited by F. A. Bower and R. B. Ward, CRC Press, Inc., Boca Raton, Florida, 1982, p. 87-140; LBL-10585.

Invited Talks

1. P. S. Connell, F. Magnotta, D. Swanson, and H. S. Johnston, "Product Identification and Quantum Yield Determination in N_2O_5 Photolysis at Several Discrete Wavelengths Between 249 and 300 nm," International Photochemical Symposium, Stanford University, Palo Alto, California, June 1982, Extended Abstract, based on LBL-9034 and LBL-9981.

2. Chemical Physics

a. Energy Transfer and Structural Studies of Molecules on Surfaces*

Charles B. Harris, Investigator

Introduction. A proper description of the ways in which internal excitation energy is transferred between molecules and surfaces through electromagnetic field interactions, particularly at short distances, is crucial to the understanding of a wide variety of molecule-surface interactions. The validity of a classical point dipole model for the transfer of energy between electronically excited molecules and metal surfaces is now generally accepted. The simplicity of this model and the physical insight it provides into the mechanisms of the energy transfer make it attractive for use in many classes of problems. In the past year, the first experiments on a GaAs(110) surface have been completed which demonstrated that the model is also valid to very short (~10 Å) distances above intrinsic semiconductor surfaces. In addition to the work on GaAs, a series of experiments on surface enhanced photochemistry on silver have been initiated. The observations can be interpreted as enhanced multiphoton absorption by adsorbed molecules because of the enhanced electromagnetic laser fields at the surface, followed by fragmentation of the excited molecules out of photoionized three photon states.

1. ENHANCED PHOTOCHEMISTRY ON METAL SURFACES†

C. B. Harris, G. M. Goncher, and C. A. Parsons

The observation of photochemistry on metal surfaces depends on the relative rates of photoexcitation by the incident radiation and deexcitation by energy transfer to metal and surface modes. Rapid quenching of the lowest excited states is expected on metal surfaces; however, excited electronic states reached by even-multiphoton processes can exhibit much longer lifetimes near a surface than the dipole allowed one-photon transitions. When the multiphoton absorption for molecules near surfaces is enhanced (E^4 for two-photon processes, E^6 for three-photon processes), photoreactions from these states are easily observable with low power lasers (<50 mW/cm^2).

The photochemistry on silver shows a nonlinear dependence on incident intensity, and decreases sharply as the surface plasmon energy is approached.

This is interpreted as enhanced multiphoton absorption by adsorbed molecules because of enhanced surface fields at the silver surface, followed by fragmentation of the excited molecules out of photoionized three-photon states. The enhanced multiphoton absorption is presumably due to Mie resonances associated with silver spheres that form when single crystal Ag(111) and Ag(110) are Ar-ion sputtered under UHV conditions.

* * *

†Brief version of J. Chem. Phys. 77(7), 3767 (1982).

2. ELECTRONIC ENERGY TRANSFER TO SEMICONDUCTOR SURFACES†

C. B. Harris, A. P. Alivisatos, and P. M. Whitmore

The first experimental and theoretical investigation of electronic energy transfer from a molecule to the surface of an intrinsic semiconductor, gallium arsenide (110), was completed.

The system chosen for this initial investigation was triplet $n\pi^*$ or 1,4 diazabenzene on GaAs(110). The molecular emission occurs at 3800 Å (3.3 eV) and coincides with a large absorption in the gallium arsenide because of the Λ_3-Λ_1 interband transition.

Figure 1.1a shows the observed distance dependence of the emission lifetime compared to the predictions of a classical local dielectric response theory. The model reproduces, within experimental error, the functional dependence of the lifetime within the molecule-semiconductor separations shown. The success of the theory suggests that the dominant mechanisms for energy transfer to the GaAs surface are included in the local (optical) dielectric constant. Calculations of the wavevector dependence of the energy transfer rate (i.e., the contribution of each of the different wavevector components of the dipole field to the energy transfer), show (cf. Fig. 1.1b) that almost all of the energy is transferred through the high wavevector components of the dipole near field, generating electron-hole pairs in GaAs via non-vertical transitions.

* * *

†Brief version of LBL-15638.

*This work was supported by the Director, Office of Energy Research, Office of Basic Energy Sciences, Chemical Sciences Division of the U.S. Department of Energy under Contract No. DE-AC03-76SF00098.

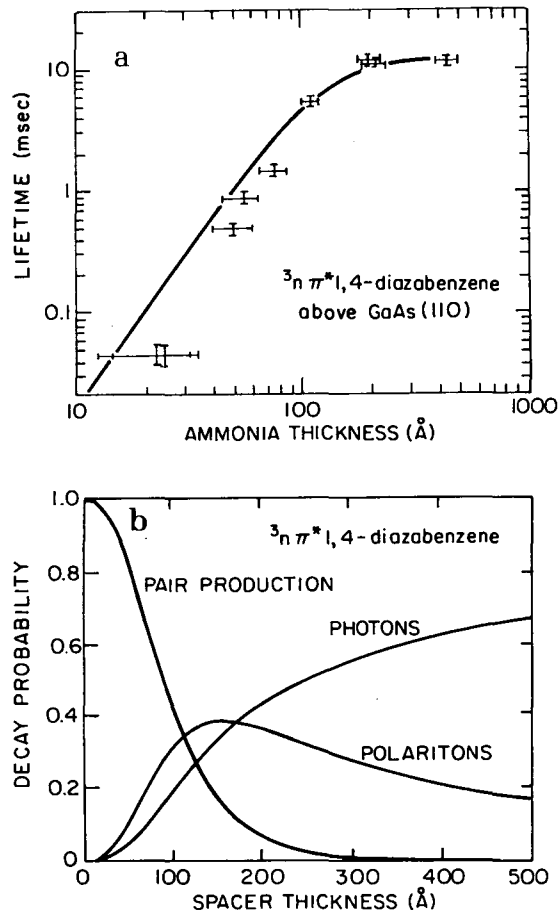

Fig. 1.1. (a) Logarithm plot of the lifetime of the $^3n\pi^*$ state of 1,4-diazabenzene above GaAs(110) vs ammonia spacer thickness. The points are experimental values, and the solid curve is the behavior calculated from a classical dielectric response model for the GaAs surface. (b) Calculated decay probability vs distance for $^3n\pi^*$1,4-diazabenzene on an ammonia spacer over GaAs(110). (XBL 831-5167)

3. VIBRATIONAL COHERENCE AND PICOSECOND STUDIES IN LIQUIDS†‡

C. B. Harris, D. Ben-Amotz, M. Berg, S. M. George, and A. L. Harris

Recently a general theory for transient stimulated Raman scattering, including high laser depletion,[1] has been completed. This theory was motivated by the discovery[2,3] that the assumption of low laser depletion is not justified in coherent picosecond Raman studies of liquids.

Using the effects induced by high laser depletion into a vibrational ensemble and its theoretical understanding, ultrashort vibrational dynamics in liquids can be studied. In particular the attractive and repulsive contributions to vibrational linewidth broadening can be experimentally separated[4] and used to test various theories for liquids.

* * *

†Brief version of References 1-4.

‡This research is not supported by DOE operating funds. However, DOE equipment was used in the experiments.

1. LBL-15640.
2. Picosecond Phenomena III edited by K. B. Eisenthal, R. M. Hochstrasser, W. Kaiser, and A. Laubereau, Springer Series in Chemical Physics 23, 196 (1982).
3. LBL-15639.
4. J. Chem. Phys. 77(9), 4781 (1982).

1982 PUBLICATIONS AND REPORTS

Refereed Journals

1. H. J. Robota, P. M. Whitmore, and C. B. Harris, "Optical Properties of Molecules Chemisorbed on the Ni(111) Surface," J. Chem. Phys. 76(4), 1692 (1982); LBL-11837.

2. P. M. Whitmore, H. J. Robota, and C. B. Harris, "Electronic Energy Transfer from Pyrazine to a Silver(111) Surface Between 10 Å and 400 Å," J. Chem. Phys. Communication 76, 740 (1982); LBL-13031.

†3. S. M. George, A. L. Harris, M. Berg, and C. B. Harris, "The Temperature Dependence of Homogeneous and Inhomogeneous Vibrational Linewidth Broadening Studies Using Coherent Picosecond Stokes Scattering," in Picosecond Phenomena III edited by K. B. Eisenthal, R. M. Hochstrasser, W. Kaiser, and A. Laubereau, Springer Series in Chemical Physics 23, 196 (1982), (Springer-Verlag, Berlin, Heidelberg and New York); LBL-15637.

4. P. M. Whitmore, H. J. Robota, and C. B. Harris, "Mechanisms for Electronic Energy Transfer Between Molecules and Metal Surfaces: A Comparison of Silver and Nickel," J. Chem. Phys. 77(3), 1560 (1982); LBL-13780.

†5. S. M. George and C. B. Harris, "Dependence of Inhomogeneous Vibrational Linewidth Broadening on Attractive Forces from Local Liquid Number Densities," J. Chem. Phys. Notes 77(9), 4781 (1982).

6. G. M. Goncher and C. B. Harris, "Enhanced Photofragmentation on a Silver Surface," J. Chem. Phys. Communication 77(7), 3767 (1982); LBL-14540.

LBL Reports

1. P. M. Whitmore, "Electronic Energy Transfer from Molecules to Metal and Semiconductor Surfaces, and Chemisorption-Induced Changes in Optical Response of the Nickel(111) Surface," Ph.D. thesis, LBL-15092.

2. A. P. Alivisatos and C. B. Harris, "Electronic Energy Transfer to Semiconductor Surfaces: $^3n\pi^*$ Pyrazine/GaAs(110)," LBL-15638.

†3. S. M. George and C. B. Harris, "Theory for Selective Vibrational Dephasing Experiments Using Transient Stimulated Raman Scattering in High Laser Depletion," LBL-15640.

4. D. Ben-Amotz, S. M. George, and C. B. Harris, "Experimental Investigations of High Laser Depletion in Transient Stimulated Raman Scattering," LBL-15639.

5. S. M. George and C. B. Harris, "Picosecond Studies of the Temperature-Dependent Homogeneous and Inhomogeneous Vibrational Linewidth Broadening in Acetonitrile," LBL-15641.

Invited Talks

1. C. B. Harris, "Optical Studies of Chemisorption and Energy Transfer on Metal Surfaces," University of Texas at Austin, April 13, 1982.

2. C. B. Harris, "Optical Studies of Chemisorption and Energy Transfer on Metal Surfaces," Iowa State University, Ames, Iowa, April 15, 1982.

3. C. B. Harris, "Use of Nonlinear Optics on a Picosecond Timescale to Study the Structure and Dynamics of Liquids," Iowa State University, Ames, Iowa, April 16, 1982.

4. C. B. Harris, "The Temperature Dependence of Homogeneous and Inhomogeneous Vibrational Linewidth Broadening Studies Using Coherent Picosecond Scattering," Third Topical Meeting on Picosecond Phenomena, Garmisch, Partenkirchen, W. Germany, June 16-18, 1982.

5. C. B. Harris, "Surface Enhanced Photochemistry," Emil Warburg Symposium on Unconventional Solids, Munich, Germany, June 27 - July 1, 1982.

* * *

†Supported by National Science Foundation.

b. Molecular Beam Spectroscopy*

John S. Winn, Investigator

Introduction. The purpose of this work is to use spectroscopic probes of molecules isolated in a molecular beam environment to elucidate molecular mechanisms of fundamental importance to chemical reaction processes. Often the fate of a complex chemical environment is determined by the elementary steps which initiate a reaction. New understanding of such processes and better control over them are complementary goals of this research.

1. DISSOCIATION MECHANISMS OF METAL CARBONYLS†

John S. Winn,‡ David V. Horák,§ William E. Hollingsworth,¶ and Brian C. Hale‖

Metal carbonyl compounds constitute an attractive class of compounds for the facile transport of chemically reactive metal atoms in the gas phase. Chemically saturated carbonyls are relatively stable and easily prepared compounds characterized by a volatility that is typically fifty orders of magnitude greater than that of the parent bulk metal. Past studies have demonstrated that these compounds can serve as catalysts in many important reactions and that dissociation of the compounds themselves can lead to thin, highly reactive, metal films.

To elucidate the first steps in these processes, the molecular dynamics of the dissociation of isolated carbonyls have been studied using metastable atom impact, electron impact, vacuum ultraviolet photolysis, and near UV photolysis. These sources have enough energy to dissociate carbonyls to the bare metal atom and the stoichiometric number of CO ligands. Atomic fluorescence follows, and the main clue to the mechanism lies in the analysis of this fluorescence.

Each of these energy sources produces dissociation in a similar way. The atomic states indicate that a restricted statistical distribution of energy occurs on dissociation, implying a virtually simultaneous release of all CO ligands. The photolysis and electron impact experiments yield spin-selected atoms, while metastable atom electronic energy transfer experiments show no spin selectivity. One can now predict the dissociation pathways of metal carbonyls under virtually any conditions.

* * *

†Brief version of LBL-14690; J. Phys. Chem. 87, 265 (1983).
‡Present address: Dartmouth College, Hanover, NH 03755.
§Present address: IBM, Burlington, VT.
¶Present address: Columbia University, New York, NY.
‖Present address: Jackson State University, Jackson, MS.

2. SUPERSONIC MOLECULAR BEAM RELAXATION MECHANISMS†‡

John S. Winn,§ Henry S. Luftman,¶ Michael Maier,‖ and Susan A. Sherrow

A gas at equilibrium is well understood to have various modes of internal and translational energy distributed in a simple way characterized by a single parameter, the equilibrium temperature. Radically nonequilibrium flow situations, however, are of great practical importance in devices such as chemical lasers and jet propulsion engines. These situations are sufficiently complex to be incompletely understood at a molecular level.

It has been known for some time that a supersonic molecular beam is characterized by a very narrow translational energy spread about a mean value with internal molecular energies that are highly relaxed. What has not been widely appreciated or recognized is that these flow distributions, translational and internal, are highly coupled. By combining a time-of-flight measurement of the translational energy distribution to a molecular beam electric resonance spectrometer's velocity-selective probe of the rotational energy distribution, one can detect and analyze this coupling.

One finds that molecules moving at a velocity near the median are characterized by a rotational distribution that is more highly relaxed than the distribution characteristic of the velocity averaged ensemble or the molecules moving far from the median velocity. The molecular scattering mechanism that produces such coupled distributions remains to be elucidated.

*This work was supported by the Director, Office of Energy Research, Office of Basic Energy Sciences, Chemical Sciences Division of the U.S. Department of Energy under Contract No. DE-AC03-76SF00098.

* * *

†Brief version of LBL-15091.
‡Supported in part by the National Science Foundation.
§Present address: Dartmouth College, Hanover, NH 03755.
¶Present address: University of Texas, Austin, TX.
‖Present address: IBM, San Jose, CA.

1982 PUBLICATIONS AND REPORTS

LBL Reports

1. J. H. Goble, Jr., "Inversion of the Potential Function of Weakly Bound Diatomic Molecules and Laser-Assisted Excitive Penning Ionization," Ph.D. thesis, LBL-14278.

2. D. V. Horák, "Analysis of Iron Fluorescence from Vacuum Ultraviolet Photolysis of Iron Pentacarbonyl," Ph.D. thesis, LBL-14612.

3. D. V. Horák and J. S. Winn, "Fe* Emission Yield and Photoionization of $Fe(CO)_5$ by VUV Radiation," LBL-14690.

4. H. S. Luftman, "Supersonic Molecular Beam Electric Resonance Spectroscopy and van der Waals Molecules," Ph.D. thesis, LBL-15091.

5. W. E. Hollingsworth, "Metal Atom Fluorescence from the Quenching of Metastable Rare Gases by Metal Carbonyls," Ph.D. thesis, LBL-14917.

c. Selective Photochemistry*

C. Bradley Moore, Investigator

1. ABSOLUTE RATE CONSTANTS FOR THE REMOVAL OF CH_2 ($^1A_1$)†

Andrew O. Langford, Hrvoje Petek, and C. Bradley Moore

Despite the importance of methylene as an intermediate in the oxidation of acetylene and other hydrocarbons, accurate rate constants necessary for modeling studies have been lacking. This state of affairs stems from the existence of two low-lying electronic states that differ significantly in structure and reactivity. Absolute rate constants for the short-lived singlet first excited state ($^1A_1$) are particularly uncertain.

We have recently completed a study of CH_2 ($^1A_1$) removal by a series of collision partners ranging from He to i-C_4H_8 using the technique of laser photolysis/cw laser resonance absorption.[1] Absolute rate constants for CH_2 ($^1A_1$) removal by NO, C_2H_6, C_3H_8, C_2H_4, i-C_4H_8, and CH_2CO were measured for the first time. These processes were found to occur with nearly every collision. Measured rates of CH_2 ($^1A_1$) removal by He, Ar, Kr, N_2, CO and H_2 are in good agreement with other direct measurements recently reported in the literature,[2] but are approximately one order of magnitude faster than rate constant values previously used for modeling.[3] These rates, which include contributions from both reaction and intersystem crossing to the ground state, are shown in Table 1.1.

Absolute rate constants for the removal of vibrationally excited CH_2 ($^1A_1$) by He, Ar, and

Table 1.1. Absolute Rate Constants for CH_2 ($^1A_1$) Removal x 10^{12} (cm^3 $molec^{-1}$ s^{-1}).

	This work	Ref. 2	Ref. 3
He	3.5 ± 0.3	3.1 ± 0.3	0.30 ± 0.07
Ne	-----	4.2 ± 0.6	-----
Ar	5.8 ± 0.5	6.0 ± 0.5	0.67 ± 0.13
Kr	7.9 ± 0.6	7.0 ± 0.6	-----
Xe	-----	16 ± 2	-----
N_2	11 ± 1	8.8 ± 0.3	0.90 ± 0.2
CO	49 ± 4	56 ± 6	-----
O_2	74 ± 5	30 ± 4	-----
NO	160 ± 15	-----	-----
H_2	105 ± 5	130 ± 10	7.0 ± 1.5
CH_4	70 ± 4	73 ± 6	3.5 ± 1.0
C_2H_6	190 ± 20	-----	-----
C_3H_8	240 ± 20	-----	-----
C_2H_4	150 ± 60	-----	-----
i-C_4H_8	225 ± 20	-----	-----
CH_2CO	270 ± 20	-----	-----

*This work was supported by the Director, Office of Energy Research, Office of Basic Energy Sciences, Chemical Sciences Division of the U.S. Department of Energy under Contract No. DE-AC03-76SF00098.

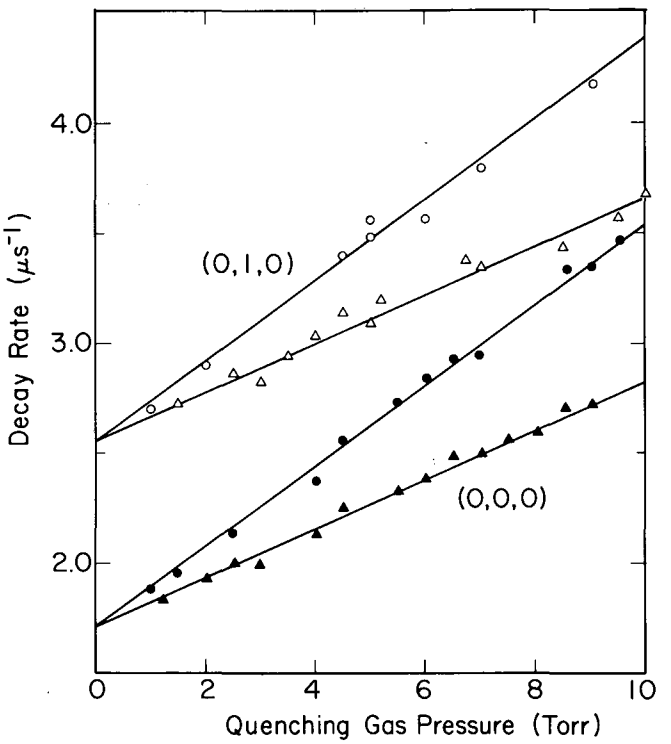

Fig. 1.1. Pseudo-first-order decay rates for the (0,1,0) and (0,0,0) vibrational levels of CH_2 ($^1A_1$) as a function of added He (Δ,▲) and Ar (○,●). The CH_2CO pressures are 0.300 torr for the (0,1,0) decays and 0.200 for the (0,0,0) decays. The solid lines correspond to the (0,0,0) rate constants from Table 1.1. The vibrationally excited molecule undergoes singlet-triplet transfer at the same rate as vibrational ground state. (XBL 832-8066)

CH_2CO have also been measured for the first time. These rates were found to be identical to the ground state rates for both rare gases, where the only channel is intersystem crossing, and for ketene where reaction is the primary channel (Fig. 1.1). The experimental approach is currently being extended to permit studies of ground state CH_2 ($^3B_1$) kinetics in the infrared. The relative importance of reaction and intersystem crossing in the present measurements can then be evaluated.

* * *

†Brief version of LBL-15666, submitted to J. Chem. Phys.

1. A. O. Langford, H. Petek, and C. B. Moore, submitted to J. Chem. Phys.
2. M. N. R. Ashfold, M. A. Fullstone, G. Hancock, and G. W. Ketley, Chem. Phys. 55, 245 (1981).
3. W. Braun, A. M. Bass, and M. J. Pilling, J. Chem. Phys. 52, 5131 (1970).

2. HIGH VIBRATIONAL OVERTONE PHOTOCHEMISTRY

Joseph M. Jasinski, Joan K. Frisoli, and C. Bradley Moore

A better understanding of the behavior of highly vibrationally excited molecules and insight into the requirements for mode selective chemistry can be obtained by studying unimolecular reactions.[1] A cw dye laser was used to induce the isomerizations of cyclobutene and 1-cyclopropylcyclobutene to the corresponding 1,3-butadienes

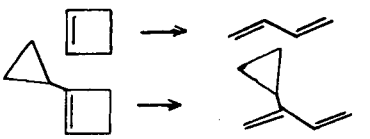

In the vibrational overtone spectra of these molecules (v = 5 and v = 6), inequivalent hydrogens absorb at different frequencies. Visible photons selectively excite the different CH oscillators, thereby depositing a known amount of energy directly into vibrational degrees of freedom of the molecule in its electronic ground state in a single photon absorption. Values of the unimolecular isomerization rate constant, k(E), depend on the total energy and do not show any observable dependence on the type of CH overtone transition excited (Fig. 2.1). These results are consistent with RRKM theory on timescales of several ps and 100 ps for 1-cyclopropylcyclobutene and cyclobutene, respectively, which may imply that either the CH oscillator excited

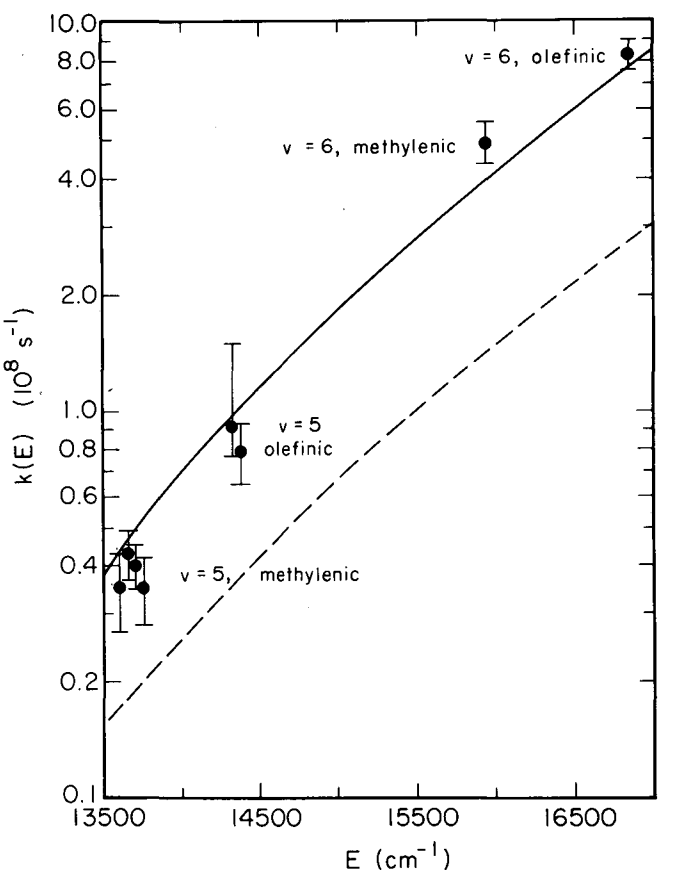

Fig. 2.1. Plot of experimental values of k(E) vs E for cyclobutene. The dotted and solid lines are results of two different RRKM calculations. E has been defined as the photon energy plus the average thermal energy. (XBL 832-8067)

is not strongly coupled to the reaction coordinate, or that energy deposited in a particular bond is randomized on these timescales.

* * *

1. C. B. Moore and I. W. M. Smith, Faraday Discussion, Chem. Soc. 67, 173 (1979).

1982 PUBLICATIONS AND REPORTS

Refereed Journals

1. J. S. Wong, R. A. McPhail, C. B. Moore, and H. L. Strauss, "Local Mode Spectra of Inequivalent C-H Oscillators in Cycloalkanes and Cycloalkenes," J. Chem. Phys. 86, 1478 (1982); LBL-13442.

2. L. Young and C. B. Moore, "Vibrational Relaxation of CH_3F in Inert Gas Matrices," J. Chem. Phys. 79, 5869 (1982); LBL-13871.

3. J. S. Wong and C. B. Moore, "Inequivalent C-H Oscillators of Gaseous Alkanes and Alkenes in Laser Photoacoustic Overtone Spectroscopy," J. Chem. Phys. 77, 603 (1982); LBL-13872.

Invited Talks

1. C. Bradley Moore, "Laser Chemical Kinetics: State Selected and Thermal," University of Colorado, Boulder, Colorado, Department of Chemistry, February 15, 1982.

2. C. Bradley Moore, "Dynamics and Photochemistry of Highly Vibrationally Excited Small Molecules," Pure Chemistry Award Symposium, American Chemical Society National Meeting, Las Vegas, Nevada, March 31, 1982.

3. C. Bradley Moore, "Reaction Rate Measurements by Sensitized Laser Pyrolysis," Avco Everett Research Laboratory, Everett, Massachusetts, May 5, 1982.

4. C. Bradley Moore, "High Overtone Spectroscopy and Vibrational Photochemistry," Los Alamos Scientific Laboratory, Los Alamos, New Mexico, May 13, 1982.

5. C. Bradley Moore, "High Resolution Laser Spectroscopy of Small Molecules," Thirteenth Australian Spectroscopy Conference, Australian Academy of Science, Melbourne, Australia, and La Trobe University, Bundoora, Australia, August 16, 1982.

6. C. Bradley Moore, "Laser Photochemistry," Royal Australian Chemical Institute 7th National Convention of the Physical Chemistry Division, Canberra, Australia, August 26, 1982.

7. C. Bradley Moore, "Vibrational Relaxation of Small Molecules in Solid Rare Gas Matrices," Physical Chemistry Seminar, Department of Chemistry, University of California, Berkeley, September 22, 1982.

8. C. Bradley Moore, "Vibrational Energy Transfer in Matrices: CH_3F, HCN, and NCl (v = 1,2 and 3) in Ar, Kr, and Xe," American Chemical Society National Meeting, Kansas City, Missouri, September 16, 1982.

9. C. Bradley Moore, "Photophysics and Photochemistry of Formaldehyde," Charles F. Hutchison Distinguished Lecturer, Department of Chemistry, University of Rochester, Rochester, New York, November 1, 1982.

10. C. Bradley Moore, "The Chemistry and Spectroscopy of Highly Vibrationally Excited Molecules," Charles F. Hutchison Distinguished Lecturer, Department of Chemistry, University of Rochester, Rochester, New York, November 2, 1982.

11. C. Bradley Moore, "Vibrational Relaxation of Small Molecules in Solid Rare Gas Matrices," Charles F. Hutchison Distinguished Lecturer, Department of Chemistry, University of Rochester, Rochester, New York, November 3, 1982.

12. C. Bradley Moore, "Laser Photochemistry," Department of Chemistry Colloquium, Yale University, New Haven, Connecticut, November 5, 1982.

LBL Reports

1. A. O. Langford, H. Petek, and C. B. Moore, "Collisional Removal of CH_2 ($^1A_1$): Absolute Rate Constants for Atomic and Molecular Collision Partners at 295 K," LBL-15666.

d. Physical Chemistry with Emphasis on Thermodynamic Properties*

Kenneth S. Pitzer, Investigator

Introduction. The general objective is the discovery and development of methods of calculation of thermodynamic and related properties of important chemical systems by use of quantum and statistical mechanics together with experimental measurements for key systems. Recently, an ab initio relativistic quantum mechanical procedure was developed which yields, for molecules containing very heavy atoms, results of comparable accuracy to that attained by others for light molecules. This major advance allows the calculation of energies, bond distances, and other properties of the ground and excited states of molecules, and model surface structures containing very heavy atoms where the conventional nonrelativistic methods are inadequate. Such results are important in understanding surface and catalytic properties and in evaluation of possible laser systems.

Other areas of recent interest include applications of advanced symmetry theory to chemical problems and the statistical mechanics of ionized systems--plasmas as well as electrolyte solutions.

Some related research applying the earlier results of this project to geochemical problems is supported by DOE through the Division of Earth Sciences at LBL and is discussed in Annual Report of that Division.

1. RELATIVISTIC AB INITIO MOLECULAR STRUCTURE CALCULATIONS INCLUDING CONFIGURATION INTERACTION WITH APPLICATION TO SIX STATES OF TlH†

Phillip A. Christiansen,‡ K. Balasubramanian, and Kenneth S. Pitzer

This article represents the first application of a major advance in method of relativistic electron structure calculations that was reported last year. This method makes it feasible to include all relativistic effects in ab initio calculations with the extensive configuration interaction (CI) required to account for electron correlation. TlH was chosen because of the large spin-orbit effect of the 6p orbital of Tl which is important for the bond to H.

Several new computer codes were required but the basic mathematics was available to execute this program in which the spin-orbit operator is obtained from the difference in effective potentials for $j = l + 1/2$ and $j = l - 1/2$ for a given l together with appropriate projection operators. The calculation is initiated in Λ-S coupling at the SCF stage. The spin-orbit terms are introduced at the CI stage along with the electron repulsion integrals. The results are thus valid regardless of the magnitude of the spin-orbit terms.

Calculations were made for five excited states as well as the ground state of TlH. The calculated potential curves agree very well with the experimental curves for both the ground and first excited 0^+ states. The latter has a very peculiar shape that is correctly calculated. There are also a few incompletely interpreted spectral features at higher energy for which a satisfactory explanation is now available from these calculations. Predictions are made concerning several unobserved states. The complete array of potential curves is shown in Fig. 1.1.

* * *

†Brief version of J. Chem. Phys. 76, 5087 (1982); LBL-13799.

‡Present address: Department of Chemistry, Clarkson College of Technology, Potsdam, NY 13676.

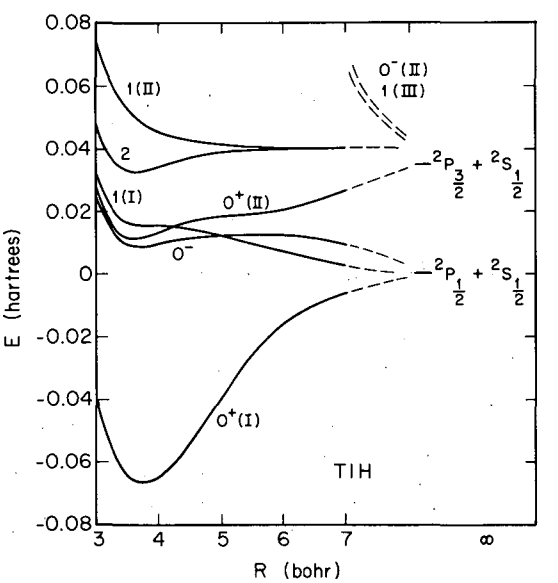

Fig. 1.1. Computed bonding curves for the two lowest 0^+ and 1 states and the lowest 0^- and 2 states of TlH. The dashed curves at large R are estimates. (XBL 831-7976)

2. ELECTRON STRUCTURE CALCULATIONS INCLUDING CI FOR TEN LOW LYING STATES OF Pb_2 and Sn_2. PARTITION FUNCTION AND DISSOCIATION ENERGY OF Sn_2†

K. Balasubramanian and Kenneth S. Pitzer

As a next stage of increased complexity after TlH, the molecules Pb_2 and Sn_2 were selected for relativistic electron structure calculations. These molecules have twice the number of valence

*This work was supported by the Director, Office of Energy Research, Office of Basic Energy Sciences, Chemical Sciences Division of the U.S. Department of Energy under Contract No. DE-AC03-76SF00098.

electrons; they have also received considerable recent attention in experimental spectroscopic investigations.

The calculational method was essentially the same as for the TlH, but with the additional bonding electrons the computational limits would have been exceeded without some further approximations. These approximations were not fundamental, however, and it was possible to show that omitted terms were really unimportant.

A number of very interesting features emerged in this work. The large spin-orbit coupling in Pb_2 yields a pattern of quantum states quite different from that of Sn_2 and the lighter fourth group molecules. Of the ten states calculated, only three had been definitely identified in the experimental spectra of Pb_2 and even less was definitely known for Sn_2. The present results made possible the interpretation of several more experimental spectral features for each molecule and predict uninvestigated spectral regions where bands should be found. For Sn_2 there are several other states within thermal range of the ground state that must be included for accurate interpretation of the mass spectrometric measurements of the dissociation energy. These data were reinterpreted on the basis of the present theoretical results; the revised D_0° is 2.04 ± 0.01 eV.

* * *

†Brief version of J. Phys. Chem. 86, 3068 (1982), LBL-14418; J. Chem. Phys. 78. 321 (1983); LBL-14723.

3. NUCLEAR SPIN STATISTICS OF CUBANE AND ICOSAHEDRAL BOROHYDRIDE IONS†

K. Balasubramanian, Kenneth S. Pitzer, and Herbert L. Strauss

Nuclear spin statistical weights for the rovibronic levels of molecules are of considerable interest since they provide for intensity ratios of rotational lines. The nuclear spin statistical weights of molecules with very high symmetry such as cubane and icosahedral borohydride ions ($B_{12}H_{12}^{-2}$) are neither readily available nor easy to obtain. Recent experimental interest in the vibrational spectra of cubane motivated us to investigate the nuclear spin statistics of these two structures.

We have used the group theoretical-generating-function method and the subsequent computer programs developed in this program as reported last year. These programs need generalized character cycle indices (GCCI's), which can be obtained easily for rigid molecules from their character tables. Several other applications of operator methods and GCCI's can also be found in additional LBL reports.[1]

A comparison between the statistical weights and observed spectra was attempted for the P-branch bands of the 852 cm^{-1} vibration of cubane. The spin weights are 667 for J = 30, 665 for J = 31, 695 for J = 32, 715 for J = 33, etc. These closely spaced numbers do not correspond to the observed spectra. This discrepancy is because of some combination of noise in the spectra, rotational perturbations, and insufficient resolution. Spectra of laser diode resolution should have the predicted intensity ratios. Such an agreement was observed in SF_6.

* * *

†Brief version of J. Mol. Spectr. 93, 447 (1982); LBL-13826.

1. Other reports from this research area: LBL-12644, LBL-12645, LBL-12724, LBL-14437, LBL-14548, and LBL-14598.

1982 PUBLICATIONS AND REPORTS

Refereed Journals

1. Kenneth S. Pitzer, "The Treatment of Ionic Solutions Over the Entire Miscibility Range," Ber. Bunsenges, Phys. Chem. 85, 952 (1982); LBL-12761.

2. K. Balasubramanian, "The Symmetry Groups of Chemical Graphs," Int. J. Quantum Chem. 21, 411 (1982); LBL-12762.

3. K. Balasubramanian, "Spectra of Chemical Trees," Int. J. Quantum Chem. 21, 581 (1982); LBL-13001.

4. K. Balasubramanian, "An Algorithm for the Generation of Nuclear Spin Species and Nuclear Spin Statistical Weights," J. Comput. Chem. 3, 69 (1982); LBL-12644.

5. K. Balasubramanian, "Computer Generation of Nuclear Spin Species and Statistical Weights of Rovibronic Levels," J. Comput. Chem. 3, 75 (1982); LBL-12645.

6. Phillip A. Christiansen and Kenneth S. Pitzer, "Reliable Static Electric Dipole Polarizabilities for Heavy Elements," Chem. Phys. Lett. 85, 434 (1982); LBL-13256.

†7. Pamela S. Z. Rogers, Daniel J. Bradley, and Kenneth S. Pitzer, "Densities of Aqueous Sodium Chloride Solutions from 75 to 200°C at 20 Bar," J. Chem. & Eng. Data 27, 47 (1982); LBL-12407.

8. K. Balasubramanian, Herbert L. Strauss, and Kenneth S. Pitzer, "Nuclear Spin Statistics of Cubane and Icosahedral Borohydride Ions," J. Molec. Spectros. 93, 447 (1982); LBL-13826.

9. Phillip A. Christiansen, K. Balasubramanian, and Kenneth S. Pitzer, "Relativistic Ab Initio Molecular Structure Calculations Including Configuration Interaction with Application to Six States of TlH," J. Chem. Phys. 76, 5087 (1982); LBL-13799.

10. K. Balasubramanian, "Computer Generation of Isomers," Computers & Chemistry 6, 57 (1982); LBL-13692.

11. K. Balasubramanian, "Computer-Assisted Enumeration of NMR Signals," J. Mag. Res. 48, 165 (1982); LBL-13693.

†12. J. Christopher Peiper and Kenneth S. Pitzer, "Thermodynamics of Aqueous Carbonate Solutions Including Mixtures of Sodium Carbonate, Bicarbonate, and Chloride," J. Chem. Thermodynamics 14, 613 (1982); LBL-12725.

13. P. S. Z. Rogers and Kenneth S. Pitzer, "Volumetric Properties of Aqueous Sodium Chloride Solutions," J. of Phys. and Chem. Ref. Data, 11, 15 (1982); LBL-12414.

14. Kenneth S. Pitzer and K. Balasubramanian, "Properties of Ten Electronic States of Pb_2 from Relativistic Quantum Calculations," J. Phys. Chem. 86, 3068 (1982); LBL-14418.

15. K. Balasubramanian, "Method for Constructing Isomerization Reactions," Int. J. Quantum Chem. 22, 385 (1982); LBL-12809.

16. K. Balasubramanian and M. Randić, "Characteristic Polynomials of Structures with Pending Bonds," Theor. Chim. Acta, 61, 307 (1982); LBL-13694.

17. K. Balasubramanian, "Topological and Group Theoretical Analysis in Dynamic NMR Spectroscopy," J. Phys. Chem. 86, 4668 (1982); LBL-14437.

18. K. Balasubramanian, "Symmetry Operators of Generalized Wreath Products and Their Applications to Chemical Physics," Int. J. Quantum Chem. 22, 1013 (1982); LBL-12724.

†19. Kenneth S. Pitzer and John S. Murdzek, "Thermodynamics of Aqueous Sodium Sulfate," J. Solution Chem. 11, 409 (1982); LBL-14522.

†20. Kenneth S. Pitzer, "Self-Ionization of Water at High Temperature and the Thermodynamic Properties of the Ions," J. Phys. Chem. 86, 4704 (1982); LBL-14493.

LBL Reports

1. Kenneth S. Pitzer, "Relativistic Calculations of Dissociation Energies and Related Properties, LBL-14705.

2. K. Balasubramanian, "Operator and Algebraic Methods in NMR Spectroscopy. I. Generation of Spin Species," LBL-14548/1.

3. K. Balasubramanian, "Operator and Algebraic Methods in NMR Spectroscopy. II. Projection Operators and Spin Functions," LBL-14548/2.

4. K. Balasubramanian, "Non-Rigid Molecular Group Theory and Its Applications," LBL-14598.

5. K. Balasubramanian and Kenneth S. Pitzer, "Electron Structure Calculations Including CI for Ten Low Lying States of Pb_2 and Sn_2. Partition Function and Dissociation Energy of Sn_2," LBL-14723.

†6. Kenneth S. Pitzer, "The Thermodynamics of Sodium Chloride Solutions in Steam," LBL-14886.

7. Kenneth S. Pitzer, "The Thermodynamics of Unsymmetrical Electrolyte Mixtures: Enthalpy and Heat Capacity," LBL-15318.

†8. M. Conceição P. de Lima and Kenneth S. Pitzer, "Thermodynamics of Saturated Aqueous Solutions Including Mixtures of NaCl, KCl, and CsCl," LBL-15301.

†9. Rabindra N. Roy, James J. Gibbons, J. C. Peiper, and Kenneth S. Pitzer, "Thermodynamics of the Unsymmetrical Mixed Electrolytes HCl-$LaCl_3$," LBL-15319.

†10. R. C. Phutela and Kenneth S. Pitzer, "Thermodynamics of Aqueous Calcium Chloride, LBL-15322.

†11. M. Conceição P. de Lima and Kenneth S. Pitzer, "Thermodynamics of Saturated Electrolyte Mixtures of NaCl with Na_2SO_4 and with $MgCl_2$, LBL-15323.

12. K. Balasubramanian, "Computer Generation of the Symmetry Elements of Non-Rigid Molecules," LBL-15455.

13. Kenneth S. Pitzer, "Gilbert N. Lewis and the Thermodynamics of Strong Electrolytes," LBL-14214.

Other Publications

1. Kenneth S. Pitzer, "Characteristics of Very Concentrated Aqueous Solutions," in Chemistry and Geochemistry of Solutions at High Temperatures and Pressures, edited by David Rickard and Frans E. Wickman, Pergamon Press, New York, 1982, p. 249.

2. Kenneth S. Pitzer, "Thermodynamics of Electrolyte Solutions Over the Entire Miscibility Range," Chapter 26 Chemical Engineering Thermodynamics, edited by S. F. Newman, Ann Arbor Science, Michigan, 1982.

Invited Talks

1. Kenneth S. Pitzer, "Relativistic Calculations of Dissociation Energies and Related Properties," Lecture at Symposium on Relativistic Effects in Quantum Chemistry at Abô Akademi, Finland, June 21-23, 1982.

2. K. Balasubramanian, "Group Theory of Non-Rigid Molecules and Its Applications," International Symposium on Symmetries and Properties of Non-Rigid Molecules, Ecole Normale Superieure de Jeunes Filles, Montrouge, Paris, France, July 1982.

* * *

†This work was supported by the Director, Office of Energy Research, Office of Basic Energy Sciences, Division of Engineering, Mathematics, and Geosciences of the U.S. Department of Energy under Contract No. DE-AC03-76SF00098.

e. Molecular Interactions*

William A. Lester, Jr., Investigator

1. THEORETICAL STUDY OF ELEMENTARY REACTIONS IN COMBUSTION PROCESSES†

M. Dupuis, W. A. Lester, Jr., T. Takada, and J. J. Wendoloski

The reaction of oxygen atoms with olefins plays an important role in combustion processes and photochemical oxidation. Although global reaction rates have been measured for many of these processes, very little is known about the elementary steps and the free radical intermediates formed in these important reactions.

The mechanism originally proposed by Cvetanović[1] involves the formation of a short-lived diradical CH_2CH_2O from the addition of $O(^3P)$ to the double bond. The diradical undergoes subsequent unimolecular reactions such as formation of "hot" epoxide, hydrogen atom migration to form "hot" acetaldehyde, and other pressure independent fragmentations (I):

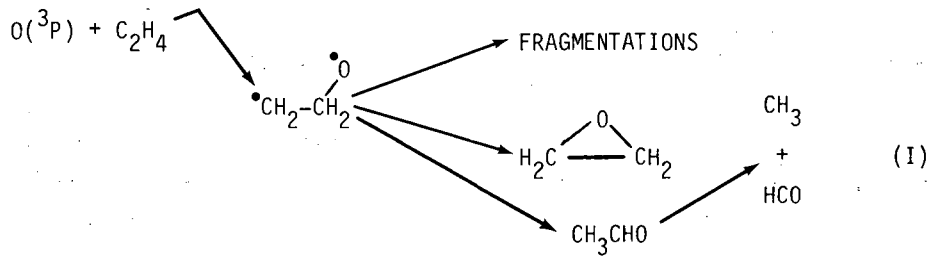

(I)

Direct observation of CH_3, HCO (95%), and CH_2CO (4%) by Kanofsky and Gutman[2] was interpreted as a verification of Cvetanović's mechanism. However, several recent experiments by Lee[3] and by others[4–6] challenge this mechanism and suggest that the vinoxy radical CH_2CHO is a primary product of the $O + C_2H_4$ reaction (II):

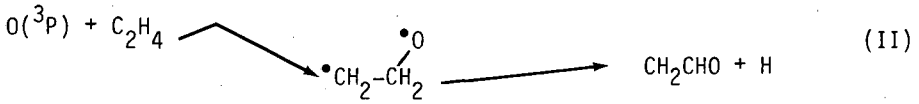

(II)

We used ab initio quantum mechanical methods to study the elementary reactions outlined above. In many bond-breaking and bond-formation processes, the Hartree-Fock (HF) model breaks down. In such cases a multiconfiguration Hartree-Fock (MCHF) wavefunction can provide a qualitatively correct description of the reaction mechanism. Extended configuration interaction (CI) calculations are necessary for quantitatively accurate reaction energies.

The following MCHF and CI results were obtained: (1) the transition state in the addition reaction of $O(^3P)$ to C_2H_4 to form CH_2CH_2O has C_s symmetry, not C_{2v} symmetry as might be expected; (2) the hydrogen atom migration $CH_2CH_2O(^{1,3}A_1) \rightarrow CH_3CHO(^{1,3}A_1)$ has a small energy barrier (<10 kcal/mole) on the singlet surface, but a larger barrier (~50 kcal/mole) on the triplet surface; (3) the has hydrogen atom elimination reaction $CH_2CH_2O \rightarrow H+CH_2CHO$ has a small energy barrier (<5 kcal/mole); and (4) the vinoxy radical CH_2CHO has a near-infrared electronic transition $X^2\bar{A}'' \rightarrow {}^2A'$, recently confirmed by experiment.

These results support the mechanism proposed by Lee and co-workers. There are two triplet surfaces of $O(^3P) + C_2H_4$ that lead to two nearly degenerate states of the diradical CH_2CH_2O. Hy-

*This work was supported by the Director, Office of Energy Research, Office of Basic Energy Sciences, Chemical Sciences Division and the Lawrence Berkeley Laboratory Director's Program Development Funds both of which are under the auspices of the U. S. Department of Energy under Contract No. DE-AC03-76SF00098. Equipment was purchased by the National Science Foundation.

drogen elimination to form H + CH_2CHO ($X\ ^2A''$) is an energetically accessible pathway in the molecular beam experiment. There is insufficient energy, however, for formation of H + $CH_2CHO(A\ ^2A')$. The diradical can undergo collision-induced intersystem crossing which leads to vibrationally hot acetaldehyde that unimolecularly decomposes to form CH_3 + HCO. The energy correlation diagram is shown in Fig. 1.1. The electronic states of CH_2CHO are depicted in Fig. 1.2.

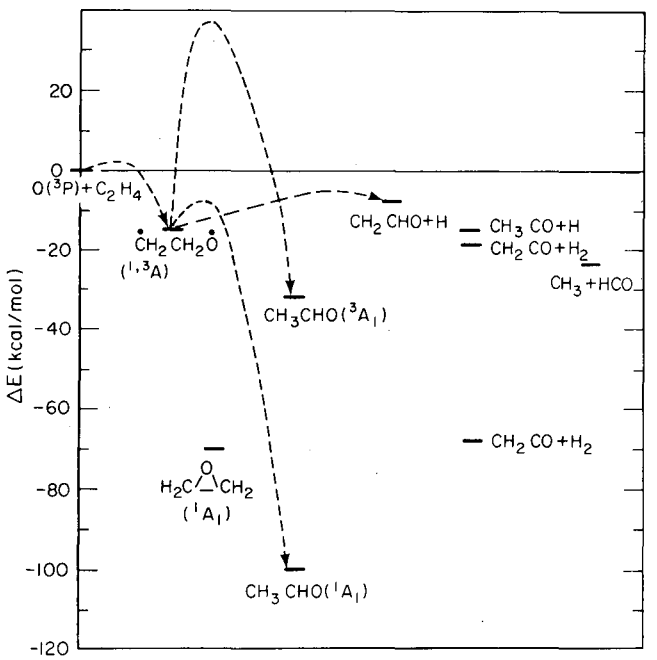

Fig. 1.1. Energy correlation diagram for the O + C_2H_4 system. (XBL 816-2323)

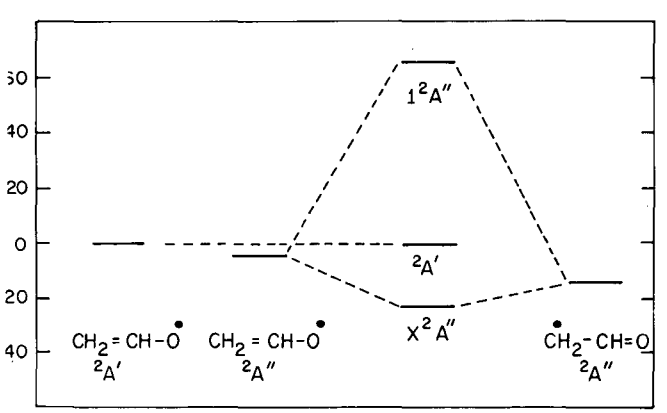

Fig. 1.2. Electronic state correlation diagram for CH_2CHO. (XBL 816-2324)

* * *

†Brief version of J. Chem. Phys. 76, 481 (1982), LBL-12756; J. Chem. Phys. 76, 488 (1982), LBL-12815; Frontiers of Chemistry, Pergamon Press, 1982, p. 156; LBL-12534.

1. R. J. Cvetanović, Adv. Photochem. 1, 115 (1953).
2. J. R. Kanofsky and D. Gutman, Chem. Phys. Lett. 15, 236 (1982).
3. R. J. Buss, R. J. Baseman, G. He, and Y. T. Lee, J. Photochem. 17, 389 (1981).
4. G. Inoue and M. Akimoto, J. Chem. Phys. 74, 425 (1980).
5. H. R. Wendt, H. Kneppe, and H. E. Hunziker, J. Photochem. 17, 377 (1981).
6. K. Kleinermanns and A. C. Luntz, J. Phys. Chem. 85, 1966 (1981).

2. THEORY OF POLYATOMIC PHOTODISSOCIATION†

V. Z. Kresin and W. A. Lester, Jr.

The photodissociation of a polyatomic molecule can be treated as a quantum transition from the ground state (direct photodissociation) or a quasidiscrete intermediate state (indirect photodissociation) to a final dissociative state of photofragments. The Born-Oppenheimer approximation (BOA) enables the problem to be reduced to one of nuclear dynamics only. Indirect photodissociation is caused by deviations from the BOA, i.e., by non-adiabatic interactions. The final dissociative state wavefunction is characterized by both internal and relative translational motion, and thus includes discrete as well as continuous factors.

We have developed an adiabatic approach solely within the framework of the nuclear problem. It describes the dissociative state dependence on interfragment interaction by vibrational frequencies that are functions of the interfragment distance and by translational functions determined by an effective potential energy that includes the vibrational energy. Our choice of zeroth-order approximation results in a small effect of the translational-vibrational interaction, i.e., final-state interaction, on the final dissociative state.

Recent experimental investigations of the photodissociation of CS_2 and NO_2 have yielded nonstatistical distributions of the fragments. Based on our quantum theory of polyatomic photodissociation, one can prove that an inverse distribution of fragments is caused by features of the matrix element that describes the transition to the dissociative state.

* * *

†Brief version of J. Phys. Chem. 86, 2182 (1982) and Chem. Phys. Lett. 87, 392 (1982).

3. FIXED-NODE QUANTUM MONTE CARLO FOR MOLECULES†

P. J. Reynolds, D. M. Ceperley,‡ B. J. Alder,‡ and W. A. Lester, Jr.

This Quantum Monte Carlo (QMC) method joins together two seemingly different research areas, namely, quantum chemistry and statistical mechanics. The hybrid discussed here is a considerable refinement of a technique that has had a long history in theoretical nuclear and condensed matter physics. Unlike many other QMC methods which simply use Monte Carlo to evaluate expectation values using a particular trial wavefunction, the approach we present is a stochastic solution to the Schrödinger equation directly.

The basis of the method is to cast the Schrödinger equation into the form of a diffusion equation, which is then solved stochastically. To reduce the statistical error associated with such a calculation, we use importance sampling. This procedure is incorporated into the technique through an importance function Ψ_T. This function guides the diffusion process into regions of space where Ψ_T is large. Thus, the closer Ψ_T approximates the actual wavefunction of the system, the more quickly diffusion increases the probability density in the appropriate regions of space. Into this method we have incorporated the "fixed-node" approximation which enables treatment of Fermi systems such as atoms and molecules.

We have applied this technique to the computation of the ground-state energies of H_2, LiH, Li_2, and H_2O. Our results in every case exceed the accuracy of the best configuration interaction calculations. We obtain presently between 80 and 100% of the correlation energy of these molecules with a statistical error of about 2% of the correlation energy.

* * *

†Brief version of LBL-13356; J. Chem. Phys. 77, 5593 (1982).
‡Lawrence Livermore National Laboratory.

4. WORK IN PROGRESS

Reaction of $O(^3P)$ with Formaldehyde

The reaction

$$O(^3P) + H_2CO \longrightarrow \text{products} \qquad (1)$$

is important in the oxidation of methane, and thus is of interest in combustion and in atmospheric chemistry. It has long been assumed to proceed via hydrogen abstraction

$$O(^3P) + H_2CO \longrightarrow HCO + OH \qquad (2)$$

Recently, Chang and Barker[1] reported the measurement of a substantial yield (~30%) of a primary product of mass 44, suggesting that the addition reaction is an important channel, i.e.,

$$O(^3P) + H_2CO \longrightarrow H_2COO \qquad (3)$$

The radical H_2COO subsequently isomerizes or dissociates. Our previous study of $O(^3P)$ + C_2H_4 showed that hydrogen atom migration on the triplet surface has a high barrier. This finding suggests that H migration may not be an accessible pathway for O + H_2CO. Instead, H atom elimination would occur to form HCO_2:

$$H_2COO \longrightarrow H + HCO_2 \qquad (4)$$

We have undertaken an ab initio study of the $O(^3P)$ + H_2CO aimed at establishing the reaction pathways for this system.

Adiabatic Approach to Direct Photodissociation and Chemical Reactions

The adiabatic approach applied to indirect photodissociation described in article 2 is being applied to the study of direct photodissociation. We shall also investigate the effect of initial vibrational excitation on photodissociation dynamics. The extension of the adiabatic method for nuclear dynamics to chemical reactions is under way. A chemical reaction can be treated as a quantum transition from a bound-continuous state of reactants to a bound-continuous state of products. Each of these states is analogous to a dissociative state.

Quantum Monte Carlo Method

The QMC method described in article 3 has thus far been restricted to ground-state properties. In order to determine the feasibility and accuracy of the method for excited-state molecules, we have begun work on the $^1A_1$ state of methylene. By also performing additional calculations on the $^3B_1$ ground state, we hope to obtain an independent theoretical estimate of the controversial $^3B_1$–$^1A_1$ energy splitting. We are also embarking on a study of the energy barrier to the H + H_2 exchange reaction. This work will shed light on nodal structure complexity and its implications for the fixed-node approach.

1982 PUBLICATIONS AND REPORTS

Refereed Journals

1. M. Dupuis, J. J. Wendoloski, T. Takada, and W. A. Lester, Jr., "Theoretical Study of Electrophilic Addition: $O(^3P)$ + C_2H_4," J. Chem. Phys. 76, 481 (1982); LBL-12756.

2. M. Dupuis, J. J. Wendoloski, and W. A. Lester, Jr., "Electronic Structure of Vinoxy Radical CH_2CHO," J. Chem. Phys. 76, 488 (1982); LBL-12815.

3. M. Dupuis and J. Pacansky, "Theoretical Study of Cyclopropane and Cyclopropyl Radical: Structure and Vibrational Analysis," J. Chem. Phys. 76, 2511 (1982); LBL-12608.

4. V. Z. Kresin and W. A. Lester, Jr., "Theory of Polyatomic Photodissociation. Adiabatic Description of the Dissociative State and the Translation-Vibration Interaction," J. Phys. Chem. 86, 2182 (1982); LBL-12861.

5. V. Z. Kresin and W. A. Lester, Jr., "Inverse Vibrational Distribution of Photofragments," Chem. Phys. Lett. 87, 392 (1982); LBL-12607.

6. V. Z. Kresin, "Collective Excitations in π-Electron Systems," J. Phys. Chem. 86, 2187 (1982); LBL-12576.

7. A. S. Dickinson, M. S. Lee, and W. A. Lester, Jr., "Close-Coupling Calculations of Li^+-H_2 Diffusion Cross Sections," J. Phys. B 15, 1371 (1982); LBL-13983.

8. P. J. Reynolds, D. M. Ceperley, B. J. Alder, and W. A. Lester, Jr., J. Chem. Phys. 77, 5593 (1983); LBL-13356.

LBL Reports

1. T. Takada, M. Dupuis, and J. F. King, "Molecular Symmetry IV: The Coupled Perturbed Hartree-Fock Method," LBL-14470.

2. T. Takada and M. Dupuis, "On the Electronic Structure of Cubene C_8H_6," LBL-14584.

3. T. Takada and M. Dupuis, "Theoretical Study of the Allyl Radical: Structure and Vibrational Analysis," LBL-14314.

4. M. Dupuis and J. J. Wendoloski, "Theoretical Study of the Vinyl Radical: Structure and Vibrational Analysis," LBL-14872.

5. N. Abusalbi, R. A. Eades, T. Nam, D. Thirumalai, D. Dixon, D. G. Truhlar, and M. Dupuis, "Electron Scattering by Methane: Elastic Scattering and Rotational Excitation Cross Sections Calculated with Ab Initio Interaction Potentials," LBL-14871.

Other Publications

1. W. A. Lester, Jr., M. Dupuis, T. J. O'Donnell, and A. J. Olson, "Some Computational Trends in Theoretical Chemistry," in IUPAC Frontiers of Chemistry, edited by K. J. Laidler, Pergamon, Oxford, 1982, p. 159-167.

Invited Talks

1. W. A. Lester, Jr., "Introduction to the Calculation of Potential Energy Surfaces," Workshop on the Dynamics of the Photodissociation of Simple Molecules, University of Paris-South, Orsay, France, September 1, 1982.

2. W. A. Lester, Jr., "Adiabatic Approach to the Dynamics of Photodissociation," Workshop on the Dynamics of the Photodissociation of Simple Molecules, University of Paris-South, Orsay, France, September 6, 1982.

3. M. Dupuis, "Electronic Structure Aspects of Photodissociation," Symposium on Electron Correlation in Molecules, American Chemical Society Meeting, Las Vegas, Nevada, March 28-April 2, 1982.

4. M. Dupuis, "Ab Initio Characterization of the $H_2CO \rightarrow H_2CO$ Potential Energy Surface," IBM Research Laboratory, San Jose, California, November 18, 1982.

5. M. Dupuis, "MCHF-CI Study of the $H_2CO \rightarrow H_2+CO$ Potential Energy Surface," International Discussion Meeting on State Specific Photodissociation: Formaldehyde," Berkeley, California, November 11-13, 1982.

6. M. Dupuis, "Some Aspects of Electronic Structure Calculations for Polyatomic Systems," State University of New York at Buffalo, New York, August 2, 1982.

7. V. Z. Kresin, "Size Quantization of Thin Films, University of Southern California, Los Angeles, California, April 1982.

8. V. Z. Kresin, "Polyatomic Photodissociation," Howard University, Washington, D.C., July 12, 1982.

f. Theory of Atomic and Molecular Collision Processes*

William H. Miller, Investigator

1. DYNAMICAL MODELS FOR POLYATOMIC REACTION DYNAMICS†‡

B. A. Waite, S. Schwartz, and W. H. Miller

A reliable quantum mechanical description of reactive scattering would clearly be an important tool for application in many areas of chemistry. At present, rigorous treatments are possible for only the simplest reactions, e.g., $H + H_2 \rightarrow H_2 + H$, both because of the limitations of accuracy in determining the potential energy surface and because of the difficulty of quantum reactive scattering calculations. The difficulties become even more pronounced when one wishes to treat systems involving polyatomic molecular systems.

Approximate treatments are thus of considerable interest, and much progress has been made recently utilizing the reaction path Hamiltonian of Miller et al.[1] Specifically, a semiclassical multichannel branching model has been developed for describing a variety of aspects of polyatomic dynamics: state-specific unimolecular decay rates, the tunneling splitting in multidimensional double-well potentials, and resonances in reactive scattering. Numerical calculations based on this model show it to give a quantitatively useful description of these phenomena.

Another approximate model based on the reaction path Hamiltonian exploits the fact that chemical reactions are usually local phenomena; i.e., even in a large molecular system, the reaction typically involves only a few degrees of freedom in an intimate way. It is therefore natural to separate the complete polyatomic system into a "system," the reaction coordinate and the few degrees of freedom that are strongly coupled to it, and a "bath," the remaining (perhaps many) degrees of freedom that are only weakly coupled to the reaction. This "system-bath" decomposition of the reaction path Hamiltonian has been carried out, and it provides a framework for utilizing an accurate dynamical treatment of a few degrees of freedom (the "system") together with an approximate treatment of the much larger number of degrees of freedom (the "bath") that exist but which are not strongly involved in the progress.

Considerable progress has thus been made in the ability to describe the dynamics of polyatomic systems. These techniques should find many applications in the theoretical modeling of chemical processes at the molecular level.

* * *

†Abstracted from J. Chem. Phys. 76, 2412 (1982) and J. Chem. Phys. 77, 2378 (1982).
‡All calculations involved in this work were carried out on a Harris 800 minicomputer supported by National Science Foundation Grant CHE-79-20181.

1. W. H. Miller, N. C. Handy, and J. E. Adams, J. Chem. Phys. 72, 99 (1980).

2. DYNAMICAL EFFECTS OF REACTION PATH SYMMETRY; MODE-SPECIFICITY IN THE UNIMOLECULAR DISSOCIATION OF FORMALDEHYDE†‡

B. A. Waite, S. K. Gray, and W. H. Miller

The photodissociation of formaldehyde

$$H_2CO + h\nu \rightarrow H_2 + CO \qquad (1)$$

has attracted considerable experimental and theoretical attention as a prototype for reaction dynamics in a small polyatomic molecule. (See related work in MMRD by Moore[1] and Schaefer.[2]) The particular aspect of interest here is the question of mode-specificity in the unimolecular dissociation, i.e., the question of whether or not the rate of dissociation depends only on the total excitation energy of the molecule or also on the particular modes of the molecule that are excited.

The path for reaction (1) has been shown from quantum chemistry calculations[2] to be planar, i.e., C_s symmetry. From this fact it has been pointed out that the reaction will at least show mode-specificity between the states of different irreducible representations of C_s symmetry, i.e., A' and A" states. Calculations based on a "symmetry adapted transition state theory"--i.e., the assumption that the dynamics is as statistical as it can be within symmetry restrictions--are shown in Fig. 2.1. The energy region relevant to the experiments[2] is ~5 kcal/mole below the classical threshold, and one sees that rates for the two symmetries differ by a factor of ~20 at the same energy. Symmetry-adapted transition state theory is shown to be a general concept, applying to any reaction for which the transition state has (or almost has) some geometrical symmetry.

Actual dynamical calculations of the state-specific unimolecular rate constants are shown in Fig. 2.2 and one sees here that there is a significant degree of "dynamical" mode-specificity in addition to that demanded by symmetry.

*This work was supported by the Director, Office of Energy Research, Office of Basic Energy Sciences, Chemical Sciences Division of the U. S. Department of Energy under Contract No. DE-AC03-76SF00098.

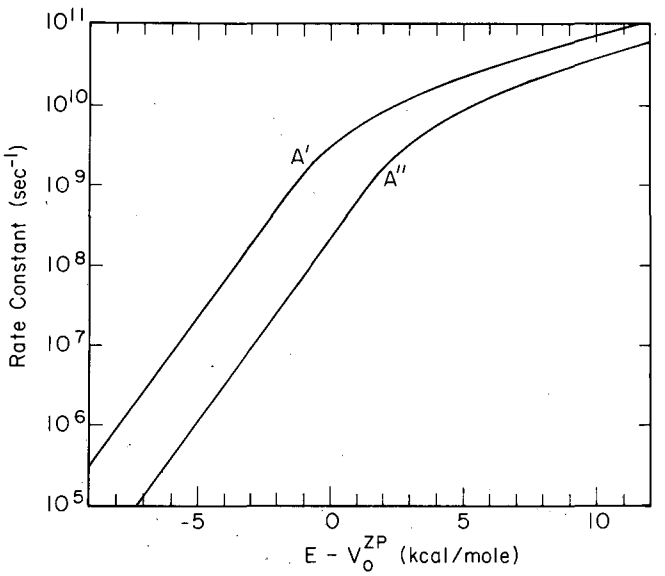

Fig. 2.1. Microcanonical rate constant for the reaction $H_2CO \rightarrow H_2 + CO$ (for total angular momentum $J = 0$) for the symmetries A' and A", as a function of total energy E relative to V_0^{ZP} (the barrier height plus zero point energy of the transition state). (XBL 825-10146)

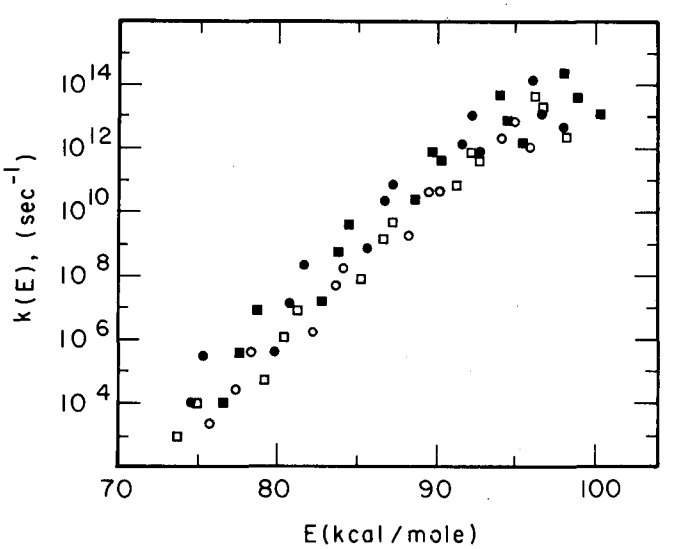

Fig. 2.2. State-specific unimolecular decay rates for the two-mode model reaction $H_2CO \rightarrow H_2 + CO$. Each point corresponds to a complex eigenvalue $E_n - i\Gamma_n/2$; the energy of the metastable state is E_n and its unimolecular decay rate $k_N = \Gamma_n/\hbar$. The solid squares and circles are states of A_1 and B_1 symmetry, respectively, and open squares are A_2 and B_2 states. (XBL 828-11179)

* * *

†Abstracted from J. Am. Chem. Soc. 105, 216 (1983); J. Chem. Phys. 78, 259 (1982); and LBL-15443, J. Phys. Chem., in press.

‡All calculations involved in this work were carried out on a Harris 800 minicomputer supported by National Science Foundation Grant CHE-79-20181.

1. C. B. Moore and Associates, this Annual Report.
2. H. F. Schaefer and Associates, this Annual Report.

1982 PUBLICATIONS AND REPORTS

Refereed Journals

1. C. J. Cerjan, S.-h. Shi, and W. H. Miller, "Applications of a Simple Dynamical Model to the Reaction Path Hamiltonian: Tunneling Corrections to Rate Constants, Product State Distributions, Line Widths of Local Mode Overtones, and Mode-Specificity in Unimolecular Decomposition," J. Phys. Chem. 86, 2244 (1982); LBL-12842.

2. B. A. Waite and W. H. Miller, "A Semiclassical Multichannel Branching Model for Describing State-Specific Unimolecular Decomposition and Other Dynamical Processes in Polyatomic Molecular Systems," J. Chem. Phys. 76, 2412 (1982); LBL-13433.

3. W. H. Miller, "Effect of Reaction Path Curvature and Dimensionality on the Accuracy of Classical Transition State Theory," J. Chem. Phys. 76, 4904 (1982); LBL-13627.

4. P. S. Dardi and S. K. Gray, "Classical and Quantum Mechanical Studies of HF in an Intense Laser Field," J. Chem. Phys. 77, 1345 (1982); LBL-14060.

5. W. H. Miller and S. Schwartz, "System-Bath Decomposition of the Reaction Path Hamiltonian for Polyatomic Scattering; Quantum Perturbative Treatment," J. Chem. Phys. 77, 2378 (1982); LBL-14205.

Other Publications

1. W. H. Miller, Chemical Dynamics, McGraw-Hill Encyclopedia of Science and Technology, 5th Edition, McGraw-Hill, New York, 1982, p. 50.

LBL Reports

1. W. H. Miller, "Dynamical Effects of Symmetry along a Reaction Path; Mode-Specificity in the Unimolecular Dissociation of Formaldehyde," LBL-14300.

2. S. K. Gray, "Classical Aspects of the Laser Excitation of a Morse Oscillator," LBL-14717.

3. S. K. Gray and W. H. Miller, "Classical Model for Electronic Degrees of Freedom: Charge Transfer in Na + I Collisions," LBL-14808.

4. B. A. Waite, S. K. Gray, and W. H. Miller, "Mode-Specificity in the Unimolecular Dissociation of Formaldehyde ($H_2CO \rightarrow H_2 + CO$), a Two-Mode Model," LBL-14855.

5. L. M. Hubbard and W. H. Miller, "Application of the Semiclassical Perturbation (SCP) Approximation to Diffraction and Rotationally Inelastic Scattering of Atoms and Molecules from Surfaces," LBL-15068.

6. J. Bicerano, H. F. Schaefer, and W. H. Miller, "Structure and Tunneling Dynamics of Malonaldehyde, a Theoretical Study," LBL-15155.

7. W. H. Miller, "Symmetry-Adapted Transition State Theory and a Unified Treatment of Multiple Transition States," LBL-15069.

8. L. M. Hubbard, S.-h. Shi, and W. H. Miller, "Multi-Channel Distorted Wave Born Approximation for Reactive Scattering," LBL-15226.

9. D. P. Ali and W. H. Miller, "Effect of Electronic Transition Dynamics on Iodine Recombination in Liquids," LBL-15329.

10. W. H. Miller, "Symmetry-Adapted Transition State Theory: Non-Zero Total Angular Momentum," LBL-15443.

11. W. H. Miller, "On the Question of Mode-Specificity in Unimolecular Reaction Dynamics," LBL-15463.

12. S. Schwartz and W. H. Miller, "System-Bath Decomposition of the Reaction Path Hamiltonian II. Rotationally Inelastic Transition in the 3-d $H + H_2$ Reaction," LBL-15464.

Invited Talks

1. W. H. Miller, "On the Relation of Quasiperiodic on Chaotic Classical Mechanics to Semiclassical Eigenvalues of Polyatomic Molecules and to Mode-Specificity in Unimolecular Reaction Dynamics," Austrian Workshop for Theoretical Chemistry, Mariapfarr, Austria, February 16-19, 1982.

2. W. H. Miller, "Dynamical Effect of Reaction Path Symmetry," ACS National Meeting, Kansas City, Missouri, September 12-17, 1982.

g. Photoelectron Spectroscopy*

David A. Shirley, Investigator

Introduction. This project is dedicated to studying new phenomena by the use of photoelectron spectroscopy and related phenomena.

A major breakthrough was achieved in 1982: the discovery of angle-resolved photoemission extended fine structure (ARPEFS) for surface structure determinations (articles 1 and 2). Normal photoelectron diffraction was applied to oxygen on copper to solve that controversial structure (article 3). Angle-resolved photoemission was used to study the two-dimensional band structure of silver on a copper substrate (article 4) and to follow the evolution of three-dimensional structure (article 5). High-resolution spectra of Ag(111) were also obtained (article 6). A high-resolution, energy-loss spectrometer was finished and tested (article 7).

Gas-phase studies included extension of photoemission spectroscopy using synchrotron radiation into a totally new energy regime--up to 3300 eV (article 8). Photoelectron angular distributions from a 4f shell were measured for the first time (article 9), and a definitive study was carried out on the helium n = 2 satellite problem (article 10). Photoelectron angular distributions were measured from N_2O (article 11) and H_2 (article 12). Finally, rotational relaxation in H_2 was studied (article 13), establishing the nonexistence of a rotational temperature.

1. DIRECT SURFACE STRUCTURE DETERMINATION WITH PHOTOELECTRON DIFFRACTION†

J. J. Barton, C. C. Bahr, Z. Hussain,‡ S. W. Robey, J. G. Tobin, L. E. Klebanoff, and D. A. Shirley

Our development of energy-dependent photoelectron diffraction as a surface structure tool advanced dramatically in 1982. We now have a new theoretical basis and a new data analysis that provide the surface structure information directly. We call this new approach angle-resolved photoemission extended fine structure (ARPEFS).

The new theoretical advance gives an analytic single-scattering formula incorporating approximations valid for our measurements. The formula contains one cosine term for each nearby substrate atom. The frequency of the cosine depends on the substrate-atom and detector positions; the cosine amplitude depends on the substrate-atom and polarization directions.

This leads to the new data analysis. By removing the atomic cross section and expressing the modulations as a function of electron momentum, the experimental data can be analyzed if we adopt high resolution Fourier methods (following article 2). Application of this new approach to our measurements of S(1s) photoemission from c(2x2)S/Ni(001) and p(2x2)S/Cu(001) is shown in Fig. 1.1. The four nearest substrate atoms appear as the first three peaks: the peak near 2 Å corresponds to the atom closest to the detector, the next peak (~3.5 Å) represents two atoms, and the peak at 4.4 Å corresponds to the fourth neighbor which sits behind the S from the detector. The intensity of the third peak is the largest because backscattering is favorable; the first peak is much larger for S/Cu than for S/Ni because the polarization vector was pointed more toward this atom for the Cu measurements. By combining the ARPEFS peak position and intensity information,

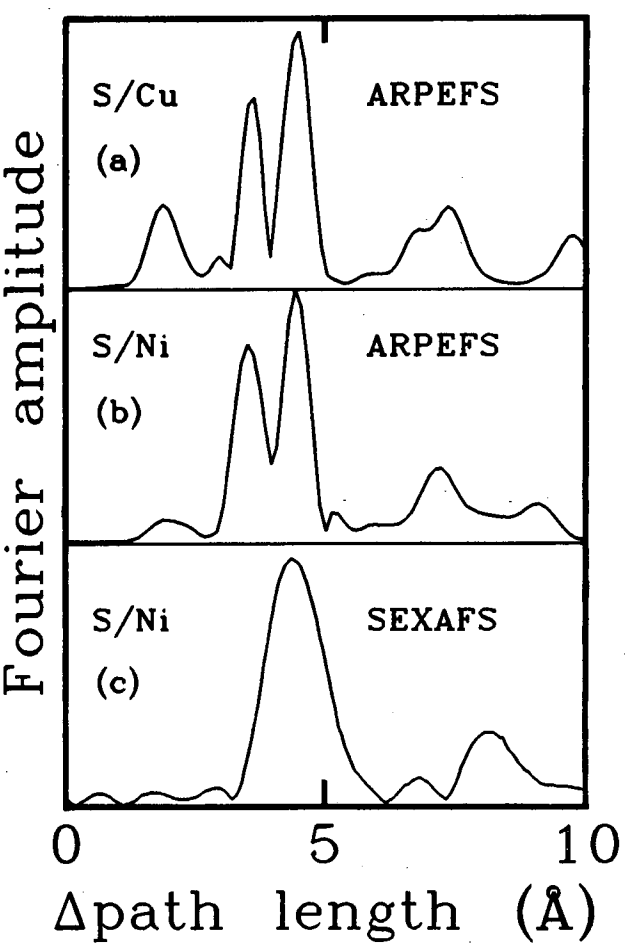

Fig. 1.1. Comparison of Fourier transform amplitudes for (a) ARPEFS from p(2x2)S/Cu(001), (b) ARPEFS from c(2x2)S/Ni(001), and (c) SEXAFS from C(2x2)S/Ni(001)(Ref. 1). The ARPEFS range in k-space was extended using the auto-regressive estimation method prior to Fourier transformation. (XBL 8212-11283)

*This work was supported by the Director, Office of Energy Research, Office of Basic Energy Sciences, Chemical Sciences Division of the U.S. Department of Energy under Contract No. DE-AC03-76SF00098. It was performed at the Stanford Synchrotron Radiation Laboratory, which is supported by the NSF through the Division of Materials Research.

we can directly verify the surface structure for S/Ni and report that S occupies the four-fold hollow site on Cu(001) at a bond length of 2.28 Å.

* * *

†Brief version of LBL-14645.
‡University of Petroleum and Minerals, Dhahran, Saudi Arabia.
1. S. Brennan, J. Stoehr, R. Jaeger, Phys. Rev. B 24, 4871 (1981).

2. HIGH RESOLUTION FOURIER ANALYSIS WITH AUTO-REGRESSIVE LINEAR PREDICTION†

J. J. Barton and D. A. Shirley

Fourier analysis of a sequence containing sinusoidal signals usually proceeds by multiplying the sequence by a window function and applying a fast Fourier transform. The ability to resolve two similar frequencies is then determined by the length of the sequence and is independent of the data's signal-to-noise power ratio. This creates a serious problem for physical measurements that are restricted in their range: no matter how carefully the measurement is made, no improvement in resolution can be obtained. Fortunately, engineers interested in acoustic and seismic Fourier analysis have developed an auto-regressive linear prediction for extrapolating a sequence assuming only that it always has the same average frequency content. Figure 1.1b (see preceding article 1) shows the auto-regressive Fourier amplitude for ARPEFS of S/Ni(001). For comparison Fig. 1.1c shows the normal Fourier analysis of the SEXAFS curve.[1] By comparing the largest peaks in these curves, we see that the auto-regressive method doubles Fourier resolution.

* * *

†Brief version of LBL-14758.
1. S. Brennan, J. Stoehr, and R. Jaeger, Phys. Rev. B 24, 4871 (1981).

3. NORMAL PHOTOELECTRON DIFFRACTION OF O/Cu(001): A SURFACE STRUCTURAL DETERMINATION†

J. G. Tobin, L. E. Klebanoff, D. H. Rosenblatt,‡ R. F. Davis,§ E. Umbach,¶ A. G. Baca, D. A. Shirley, Y. Huang,‖ W. M. Kang,‖ and S. Y. Tong‖

In the normal photoelectron diffraction (NPD) technique, the photoemission intensity of an adsorbate core level is measured normal to the surface as a function of photon (and thus kinetic) energy. An intensity-kinetic energy curve similar to a low energy electron diffraction (LEED) I-V curve is generated which, when compared to theoretical curves, may yield a surface structure.

Oxygen adsorbs on Cu(001) with difficulty, producing a c(2x2) structure at low exposures and a ($\sqrt{2}$ x $2\sqrt{2}$) R45° structure at higher exposures. The two systems were studied at the Stanford Synchrotron Radiation Laboratory on Beam Line I-1. In the c(2x2) structure, oxygen occupies the four-fold hollow site, with $d_\perp$ = 0.80(5) Å (Fig. 3.1).

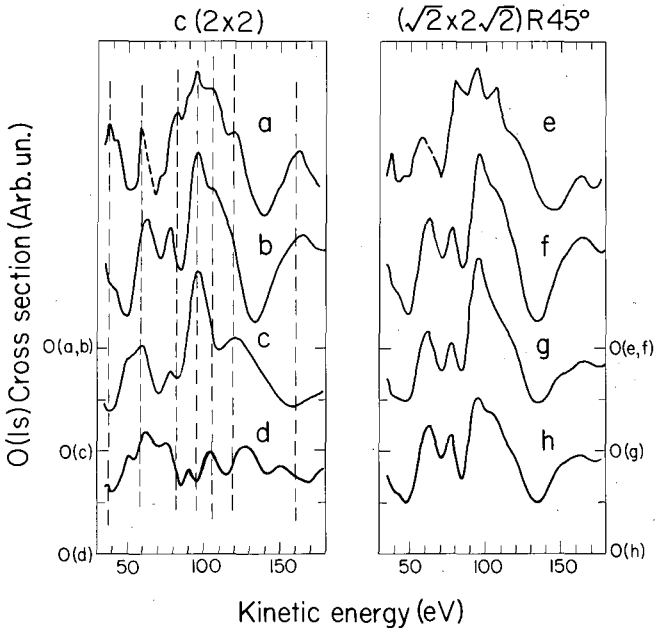

Fig. 3.1. NPD experiment and theory for c(2x2)O/Cu(001): (a) experiment; (b) theory, $d_\perp$ = 0.8 Å, hollow; (c) theory, $d_\perp$ = 0.1 Å, hollow; and (d) theory, $d_\perp$ = 1.4 Å, bridge, V_0 = 10 eV. NPD experiment and theory for ($\sqrt{2}$ x $2\sqrt{2}$) R45° O/Cu(001): (e) experiment; (f) theory, $d_\perp$ = 0.8 Å, hollow for c(2x2); (g) theory, 1:1/2 weighted sum of 0.8 Å hollow and 0.1 Å hollow, c(2x2) calculations; and (h) theory, 1:1/2 weighted sum of 0.8 Å hollow and 1.4 Å bridge, c(2x2) calculations, V_0 = 10 eV. (XBL 827-10738A)

The $\sqrt{2}$ x $2\sqrt{2}$ structure has a similar NPD curve, indicating the same local site geometry for the c(2x2) sublattice. The site of the additional oxygen is unknown, as suggested by Fig. 3.1.

* * *

†Brief version of LBL-14188; Phys. Rev. B 26, 7076 (1982).
‡Watkins-Johnson Company, Palo Alto, CA 94304.
§Research Laboratories, Polaroid Corporation, Waltham, MA 02154.
¶Physik-Department, Technische Universität, München, W. Germany.
‖Department of Physics, University of Wisconsin-Milwaukee, Milwaukee, WI 53201.

4. THE TWO-DIMENSIONAL VALENCE ELECTRONIC STRUCTURE OF A MONOLAYER OF Ag ON Cu(001)†

J. G. Tobin, S. W. Robey, and D. A. Shirley

The electronic structure of the valence bands of bulk three-dimensional metals has been a subject of great experimental and theoretical interest. Included in this have been a number of investigations into the nature of states localized in the topmost layer of single crystal surfaces and theoretical calculations of electronic behavior in monolayer metal slabs.

Here, we present the first complete angle resolved photoemission (ARP) investigation into the valence band structure of a single layer of a metal deposited upon a different metal single crystal. Using ARP excited by polarized vacuum ultraviolet radiation of 21.2 eV (HeI) and 16.8 eV (NeI), the valence bands of the Ag monolayer were mapped vs the parallel component of the crystal momentum of the outgoing electron.

By using two different photon energies, the dependencies of the band binding energies upon the perpendicular component of the crystal momentum could be tested. It was found that, while the bands disperse as functions of the parallel momentum, they are independent of the perpendicular component (Fig. 4.1). This is conclusive evidence of two-dimensional metallic behavior in a monolayer of c(10x2)Ag/Cu(001). Also, using group theoretical selection rules, all of the Ag features have been assigned upon the basis of the polarization dependencies of the features.

* * *

†Brief version of LBL-15133.

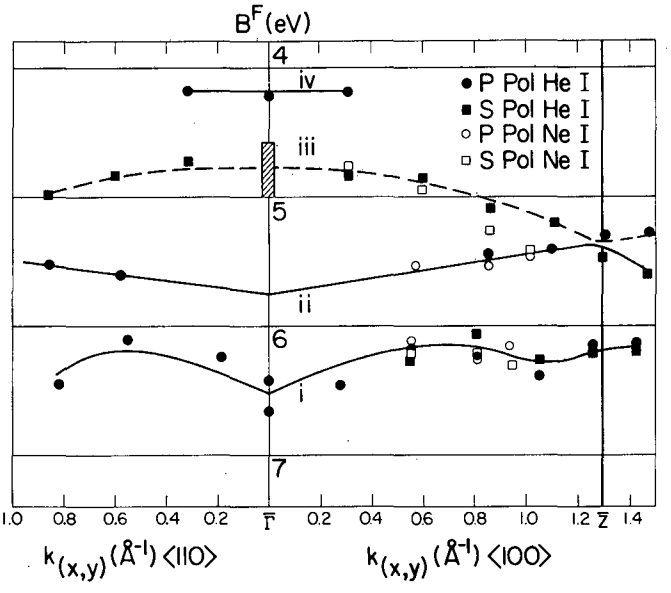

Fig. 4.1. Plot of Ag valence band binding energy vs $k_{\parallel}$ in two directions across the Surface Brillouin Zone of c(10x2)Ag/Cu(001). (XBL 832-1272)

5. THE EVOLUTION TO THREE-DIMENSIONAL VALENCE BAND STRUCTURE IN Ag OVERLAYERS ON Cu(001)†

J. G. Tobin, S. W. Robey, L. E. Klebanoff, and D. A. Shirley

There has been an immense amount of work done investigating the three-dimensional electronic structure of bulk metals. More recently, interest has centered upon elucidation of two-dimensional behavior such as surface states. Experimentation has also extended into the realm of observing the development from atomic to three-dimensional electronic structure in metal clusters[1] and the layer-by-layer band structure of physisorbed Xe.[2] In this article we report the first complete experimental observation of the transition from two-dimensional to three-dimensional valence electronic structure in metal overlayers.

Angle resolved photoelectron spectroscopy is the method of choice, since it allows a direct measurement of the dispersion relations of the metal valence bands and differentiates between 2-D and 3-D dependences.

By measuring the dependences of the binding energies of the states observed in a Ag overlayer upon the momentum parallel to the direction of growth of the overlayer, the evolution to 3-D behavior was observed at exposures of less than or equal to 5 monolayers of Ag. Accompanying these band mapping results, cross section (Fig. 5.1) and final state effects were also seen that suggest convergence to a structure very similar to bulk single crystal Ag(111).

* * *

†Brief version of LBL-15134.

1. S.-T. Lee, G. Apai, M. G. Mason, R. Benbow, and Z. Hurych, Phys. Rev. B 23, 505 (1981).
2. T. Mandel, G. Kaindl, W. D. Schneider, and W. Fischer, submitted to Phys. Rev. Lett.

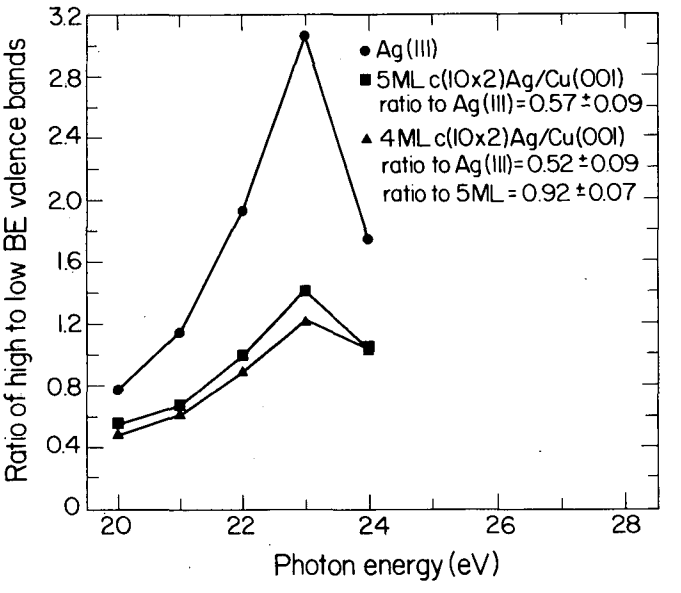

Fig. 5.1. The ratio of the intensity of the high binding energy half of the silver valence bands to the intensity of the low binding energy half of the silver valence bands is plotted as a function of photon energy for the samples Ag(111) and 4 and 5 monolayers of c(10x2)Ag/Cu(001).
(XBL 832-1278A)

6. HIGH RESOLUTION ANGLE-RESOLVED PHOTOEMISSION STUDY OF THE VALENCE BAND STRUCTURE OF Ag(111)†

J. G. Tobin, S. W. Robey, D. A. Shirley, W. J. Gignac,‡ J. G. Nelson,‡ and R. S. Williams‡

The electronic structure of three-dimensional bulk crystals continues to be of great interest in condensed phase material science. Advances in photon sources, such as improvements in synchrotron radiation storage rings, and accompanying advances in spectrometer design have allowed increasingly improved resolution to be achieved in angle-resolved photoemission.

Angle-resolved photoemission is a technique that can be used as a direct probe of the dispersion relations of the valence bands, i.e., the dependence of the binding energies upon crystal momentum.

Here, results are presented that are an extension and improvement upon an earlier experiment.[1] Included are higher resolution data collected at normal emission along the Γ to L line (Fig. 6.1) in the three-dimensional Brillouin Zone ($h\nu$ = 6-32 eV) and off-normal data collected by $h\nu$ = 14 and 21 eV. Presently, data analysis is being pursued, including an attempt to extract lifetimes from peak widths.

* * *

†Brief version of LBL-15135.

‡Department of Chemistry, University of California, Los Angeles, CA 90024.

1. P.S. Wehner, R. S. Williams, S. D. Kevan, D. Denley, and D. A. Shirley, Phys. Rev. B 19, 6164 (1979).

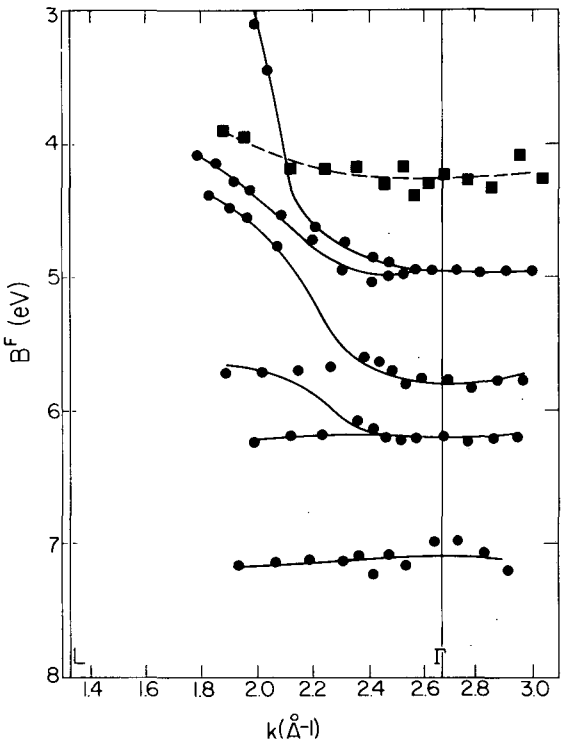

Fig. 6.1. Plot of binding energy vs crystal momentum along the Γ-line in the 3-D Brillouin Zone. (XBL 832-1279A)

7. CONSTRUCTION OF A HIGH RESOLUTION ELECTRON ENERGY LOSS SPECTROMETER

D. H. Rosenblatt,† A. G. Baca, and D. A. Shirley

We have completed construction of a high resolution electron energy loss spectrometer (EELS) for the study of vibrations at surfaces. A monoenergetic beam of electrons is produced by a double-pass electron monochromator based on hemispherical sectors. The single pass analyzer can be rotated in two independent directions. The spectrometer is in a UHV chamber with LEED, Auger, and ion sputtering capabilities. A resolution of 32-40 cm^{-1} is obtained.

We have carried out a coverage dependent study of the system O_2 + Cu(001). Previously, Sexton has studied this system at coverages of 50L and 5000L,[1] while Lehwald and Ibach have studied the similar system O_2 + Ni(001).[2] As can be seen in Fig. 7.1, there is a low coverage O-Cu stretch at 350 cm^{-1}, which shifts to 290 cm^{-1} at high cover-

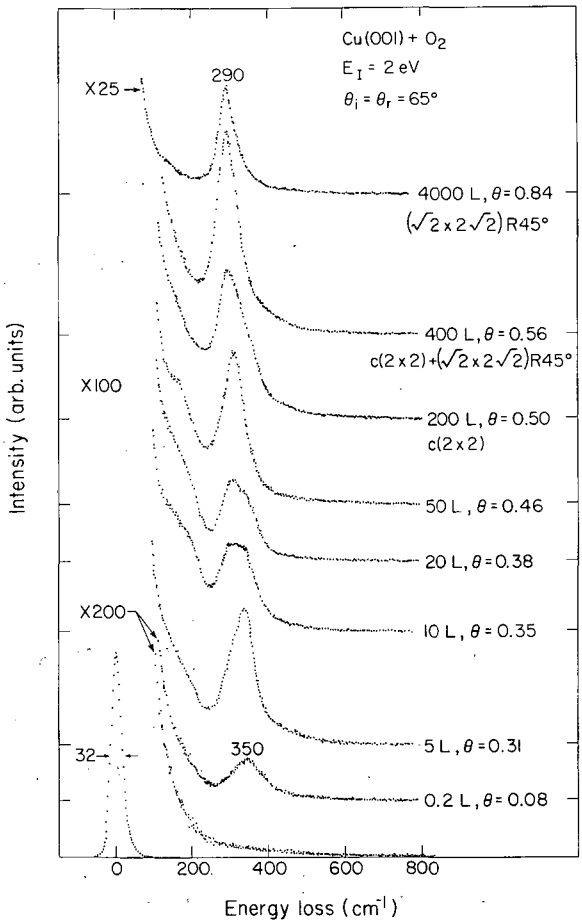

Fig. 7.1. EELS spectra of O-Cu(001) as a function of O_2 exposure, taken in the specular direction with both an angle of incidence (θ_i) and an angle of reflection (θ_r of 65°), and an impact energy of 2 eV. The spectra were taken at 300 K after a brief annealing to 475 K. The magnitude of the exposure, observed LEED pattern [if different from (1x1)], and a rough estimate of fractional oxygen coverage are given for each spectrum. (XBL 8210-4773)

ages. At intermediate coverages the spectra are a superposition of the low and high coverage spectra, similar to what occurs on Ni(001), although the 60 cm^{-1} shift is smaller than the 120 cm^{-1} shift observed in Ni(001).

* * *

†Watkins-Johnson Company, Palo Alto, CA 94304.

1. B. A. Sexton, Surf. Sci. 88, 299 (1979).
2. S. Lehwald and H. Ibach, in Vibrations at Surfaces, edited by R. Caudano, J. M. Gilles, and A. A. Lucas, Plenum, New York, 1982, p. 137.

8. THRESHOLD MEASUREMENTS OF THE K-SHELL PHOTOELECTRON SATELLITES IN Ne AND Ar†

P. H. Kobrin, S. Southworth,‡ C. M. Truesdale, D. W. Lindle, U. Becker,§ and D. A. Shirley

Photoelectron spectra of closed-shell atoms typically show an intense peak at the binding energy of each electronic subshell and weaker satellite peaks at high binding energies. The satellites arise via photoionization to higher energy states of the ion that are approximately described by configurations formed by the removal of a core electron and the promotion of a valence electron to a higher subshell. The study of these satellites is important for an understanding of the many-particle nature of photoionization, which can in turn yield insight into the details of electron correlation in the atom.

The feasibility of studying core-level photoemission satellites in gases at high photon energies (up to 3430 eV) has been proved with the use of synchrotron radiation and time-of-flight detection. K-shell satellites in neon were studied near threshold, in the adiabatic limit, for which the relative intensities were 20-40% lower than in the high-energy limit. The "conjugate shake-up" state was not observed, in contrast to predictions of many-body perturbation theory.[1] In argon, a K-shell satellite was observed, confirming a calculation[2] using shake-up theory. Tentative evidence was obtained that the satellite intensity increases with energy.

* * *

†Brief version of LBL-15042.

‡National Bureau of Standards, Washington, D.C. 20234.
§Institut für Strahlungs- und Kernphysik, Technische Universität Berlin, 1000 Berlin 37, W. Germany.

1. T. Ishihara, J. Mizuno, and T. Watanabe, Phys. Rev. A 22, 1552 (1980).
2. K. G. Dyall, private communication.

9. PHOTOELECTRON MEASUREMENTS OF THE MERCURY 4f, 5p, and 5d SUBSHELLS†

P. H. Kobrin, P. A. Heimann, H. G. Kerkhoff, D. W. Lindle, C. M. Truesdale, T. A. Ferrett, U. Becker,‡ and D. A. Shirley

Mercury is the heaviest stable element with both closed electronic shells and an appreciable vapor pressure at low temperatures. Relativistic effects in photoionization are thus readily studied in mercury.

We have measured photoelectron spectra using the double-angle, time-of-flight (DATOF) method,[1] in which the pulsed time structure of synchrotron radiation from the SPEAR storage ring is used to measure the time-of-flight electrons ejected at two angles. This method enables us to measure simultaneously the relative cross sections, subshell branching ratios, and angular distribution asymmetry parameters of each subshell. Using photons in the energy range 50 to 270 eV, ionization of the 4f, 5p, and 5d subshells was observed (see Fig. 9.1).

In this energy range, the 5p and 5d ionizations both go through Cooper minima, and the 4f ionization exhibits a delayed onset because of a large centrifugal barrier in the 4f → εg channel. These effects manifest themselves in each of the observable parameters. Several theoretical techniques have been applied to mercury photoionization,

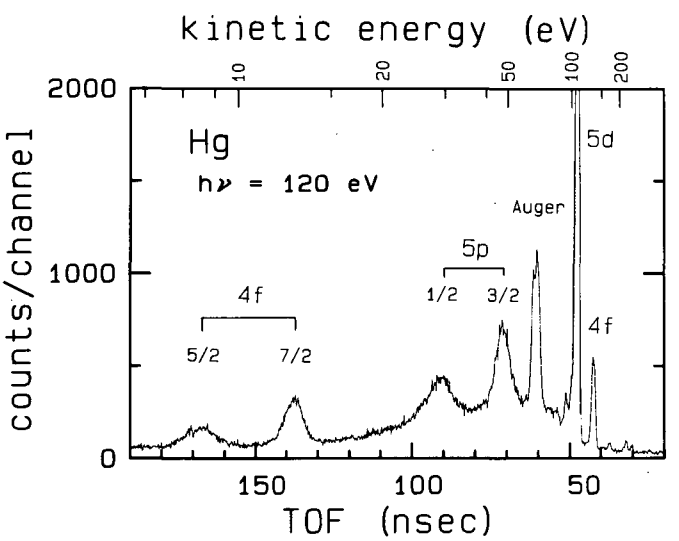

Fig. 9.1. A TOF spectrum of Hg vapor. The 4f peak at 131 eV is due to second-order light. (XBL 8210-2998)

among them the relativistic random-phase approximation with exchange[2] and the Dirac-Slater method.[3] Comparisons are made with these and other theories.

* * *

†Brief version of LBL-14759.
‡Institut für Strahlungs-und Kernphysik, Technische Universität Berlin, 1000 Berlin 37, W. Germany.

1. S. Southworth, C. M. Truesdale, P. H. Kobrin, D. W. Lindle, W. D. Brewer, and D. A. Shirley, J. Chem. Phys. 76, 143 (1982).
2. V. Radojevic and W. R. Johnson, Phys. Lett. 92A, 75 (1982).
3. B. R. Tambe and S. T. Manson, private communication.

10. PHOTOIONIZATION OF HELIUM TO $He^+(n=2)$: AUTOIONIZATION AND FINAL-STATE SYMMETRY†

D. W. Lindle, T. A. Ferrett, U. Becker,‡ P. H. Kobrin, C. M. Truesdale, H. G. Kerkhoff, and D. A. Shirley

The energy dependences of the partial cross section and asymmetry parameter for simultaneous photoionization and photoexcitation to the $He^+(n=2)$ ionic state have been measured for photon energies between 67.4 and 90 eV. Below the $He^+(n=3)$ threshold at 73 eV, a series of Rydberg states leading to this threshold can be excited, with subsequent autoionization to either the ground ionic state, $He^+(n=1)$, or the first excited ionic state, $He^+(n=2)$. Our measurements of the partial cross sections and the asymmetry parameters for production of these two ionic states in the neighborhood of the autoionizing resonances allow the determination of the parameters describing these Fano-type resonances. In addition, the simplicity of the He system allows the calculation of individual dipole and Coulomb matrix elements between the ground, excited, and continuum levels involved in the autoionization process.

The nonresonant data, taken at both higher and lower photon energies than the resonance region, yield information about the symmetry of the $He^+(n=2)$ final state. This symmetry is defined in terms of the ratio, R, of the relative populations of the $He^+(2p)$ and $He^+(2s)$ states, which are effectively degenerate in a photoemission experiment. The ratio R can be obtained from the measured asymmetry parameter for the $He^+(n=2)$ final state.[1] Previous calculations of R have disagreed significantly,[2,3] especially just above the $He^+(n=2)$ threshold. Our measurements support the results of Jacobs and Burke, as well as a new calculation by Berrington et al.,[4] which fits the present data extremely well.

* * *

†Brief version of LBL-15094.
‡Institut für Strahlungs-und Kernphysik, Technische Universität Berlin, 1000 Berlin 37, W. Germany.

1. J. M. Bizau, F. Wuilleumier, P. Dhez, D. L. Ederer, T. N. Chang, S. Krummacher, and V. Schmidt, Phys. Rev. Lett., 48, 588 (1982).
2. V. L. Jacobs and P. G. Burke, J. Phys. B 5, L67 (1972).
3. T. N. Chang, J. Phys. B 13, L551 (1980).
4. K. A. Berrington, P. G. Burke, W. C. Fon, and K. T. Taylor, J. Phys. B 15, L603 (1982).

11. PHOTOELECTRON ANGULAR DISTRIBUTIONS OF THE N_2O OUTER VALENCE ORBITALS IN THE 19-31 eV PHOTON ENERGY RANGE†

C. M. Truesdale, S. Southworth,‡ P. H. Kobrin, D. W. Lindle, and D. A. Shirley

The N_2O molecule has the ground state valence electronic configuration $(6\sigma)^2(1\pi)^4(7\sigma)^2(2\pi)^4$. As part of a continuing program to study photoemission from triatomic molecules, we have measured the vibrationally averaged partial cross sections and asymmetry parameters for the first four ionic states (X,A,B, and C) of N_2O^+ formed by ionization of these orbitals at photon energies of 19-31 eV, using VUV radiation at the Stanford Synchrotron Radiation Laboratory. Vibrationally resolved results for the A and C states were also obtained. Two time-of-flight detectors, at 0° and 54.7° relative to the photon polarization axis, were used to detect electrons ejected from the ionized sample.[1] As an example, the results for the $X^2\Pi 2\overline{\pi}$ state are shown in Fig. 11.1. Of special interest is the similarity of the β parameter of the N_2O^+ X state and that of the X state in CO_2^+, also shown in the figure.

* * *

†Brief version of LBL-15287.
‡National Bureau of Standards, Washington, D.C. 20234.

1. S. Southworth, C. M. Truesdale, P. H. Kobrin, D. W. Lindle, W. D. Brewer, and D. A. Shirley, J. Chem. Phys. 76, 143 (1982).
2. C. E. Brion and K. H. Tan, J. Electron Spectrosc. Relat. Phenom. 15, 241 (1979).
3. T. A. Carlson, P. R. Keller, J. W. Taylor, T. A. Whitley, and F. A. Grimm, to be published.

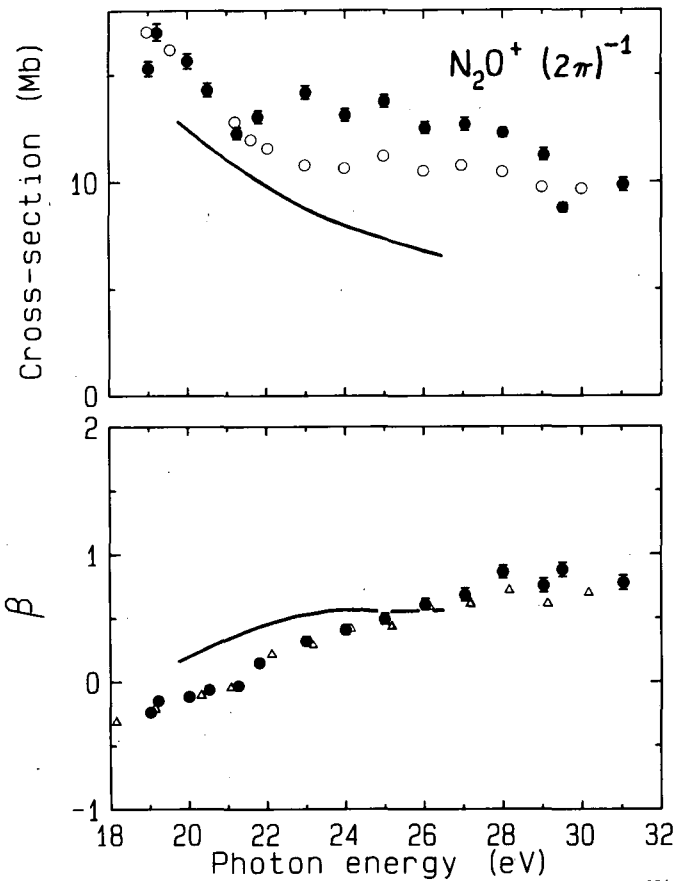

Fig. 11.1. Upper panel: Cross section for the N_2O^+ X state. The present results are shown by filled circles, an (e,2e) study by Brion and Tan[2] by open circles, and the Multiple Scattering Model calculations (MSMXα) of Whitley and Grimm[3] by solid curves. Lower panel: Filled circles are our β(ε) results for the N_2O^+ X state, and triangles show our results for β(ε) of the $X^2\Pi_g 1\pi_g$ state of CO_2^+, which is plotted to show the similarity between π molecular ionization for the two molecules. (XBL 8212-12254)

12. ROTATIONALLY RESOLVED PHOTOELECTRON ANGULAR DISTRIBUTIONS FOR H_2^+ (v'=0) AT λ = 584 Å AND 736 Å†

J. E. Pollard,‡ D. J. Trevor,§ J. E. Reutt, Y. T. Lee, and D. A. Shirley

The measurement of photoelectron angular distributions for selected rotational transitions of molecules is in principle a valuable probe of the dynamics of the photoionization process as well as a very sensitive test of the theoretical description of the behavior of photoelectrons in the continuum. We have measured the photoelectron asymmetry parameter for H_2^+ (v'=0) for the S rotational branch at λ = 584 Å and 736 Å, using a supersonic beam of n-H_2 and a high resolution photoelectron spectrometer.

The rotational selection rules for the process

$$H_2\ (\tilde{X}^1\Sigma_g^+, v'', J'') + h\nu \rightarrow H_2^+\ (\tilde{X}^2\Sigma_g^+, v', J') + e\text{-}(E_k, \ell)$$

have been shown to be J' = J" (Q branch) and J' = J" ± 2 (S and O branches).[1-3] Theoretical calculations of the photoelectron asymmetry parameter indicated that β_Q (J' = J") had a value close to 2.0 and was insensitive to the theoretical method employed and that β_S (J' = J" ± 2) had a value much less than 2.0 and depended strongly on the method of coupling between the p and f partial waves.[3-8] Our values for β_S at 584 Å and 736 Å for H_2^+ (v' = 0), 0.87 ± 0.19 and 0.08 ± 0.15, respectively, illustrate the increased coupling between the p and f photoelectron waves with increased photon energy.

* * *

†Brief version of LBL-13998.
‡The Aerospace Corporation, Los Angeles, CA 90009.
§EXXON Research and Engineering Co., Linden, NJ 07036.

1. J. M. Sichel, Mol. Phys. 18, 95 (1970).
2. R. N. Dixon, G. Duxbury, M. Horani, and J. Rostas, Mol. Phys. 22, 977 (1971).
3. D. Dill, Phys. Rev. A 6, 160 (1972).
4. B. Ritchie and B. R. Tambe, J. Chem. Phys. 68, 755 (1978).
5. N. Chandra, in Abstracts of Papers, 10th Intern. Conf. Phys. Electron Atom. Coll., Commisariat a l'Energie Atomique, Paris, 1977, p. 1210.
6. Y. Itikawa, Chem. Phys. 28, 461 (1978).
7. Y. Itikawa, Chem. Phys. 30, 109 (1978).
8. Y. Itikawa, Chem. Phys. 37. 401 (1979).

13. ROTATIONAL RELAXATION IN SUPERSONIC BEAMS OF HYDROGEN BY HIGH RESOLUTION PHOTOELECTRON SPECTROSCOPY†

J. E. Pollard,‡ D. J. Trevor,§ J. E. Reutt, Y. T. Lee, and D. A. Shirley

The rotational relaxation of n-H_2, p-H_2, D_2, and HD was studied by means of rotationally resolved photoelectron spectroscopy using a collimated supersonic molecular beam.[1] The free jet expansion provides a system in which the internal degrees of freedom of the molecules are initially in contact with a rapidly cooling translation bath. During the early (collisional) part of the expansion, the internal modes can relax by transferring energy into translation. In the later stages, the rotational and translational modes lose contact with one another. Since there is no mechanism for internal equilibrium among rotational modes, the "rotational temperature" is then meaningless. One motivation for this work was to ascertain the (non-thermal) distribution of rotational excitation. The details of the relaxation process can be elucidated by measuring the rotational and vibrational state distributions of the molecules as functions of the stagnation conditions.

Rotational state distributions of hydrogen were determined from the relative intensities of

the Q branch rotational components for a wide range of stagnation pressures with nozzle temperatures from 300-700 K. Significant deviations from a Boltzmann distribution were observed for those cases in which the degree of rotational relaxation was substantial. HD was found to relax after undergoing only one tenth of the number of collisions required to relax H_2 or D_2, presumably because the unsymmetrical HD molecule alone can relax via $\Delta J = \pm 1$ transitions. The state-to-state rate constants method of Rabitz and Lam[2] was used to model the relaxation of p-H_2 and was confirmed to be quite effective in accounting for their experimentally observed population distributions.

* * *

†Brief version of LBL-14279.
‡The Aerospace Corporation, Los Angeles, CA 90009.
§EXXON Research and Engineering Co., Linden, NJ 07036.

1. J. E. Pollard, D. J. Trevor, Y. T. Lee, and D. A. Shirley, J. Chem. Phys. 77, 4818 (1982).
2. H. Rabitz and S.-H. Lam, J. Chem. Phys. 76, 273 (1982).

1982 PUBLICATIONS AND REPORTS

Refereed Journals

1. S. H. Southworth, C. M. Truesdale, P. H. Kobrin, D. W. Lindle, W. D. Brewer, and D. A. Shirley, "Photoionization Cross Sections and Photoelectron Asymmetries of the Valence Orbitals of No," J. Chem. Phys. 76, 143 (1982); LBL-12907.

2. C. M. Truesdale, S. Southworth, P. H. Kobrin, D. W. Lindle, G. Thornton, and D. A. Shirley, "Photoelectron Angular Distributions of H_2O," J. Chem. Phys. 76, 860 (1982); LBL-11822.

3. S. Southworth, W. D. Brewer, C. M. Truesdale, P. H. Kobrin, D. W. Lindle, and D. A. Shirley, "Photoelectron Angular Distributions from H_2 and D_2," J. Elect. Spectros. and Rel. Phen. 26, 43 (1982); LBL-12922.

4. J. W. Hepburn, D. J. Trevor, J. E. Pollard, D. A. Shirley, and Y. T. Lee, "Multiphoton Ionization Photoelectron Spectroscopy of CCl_2F_2 and CCl_3F," J. Chem. Phys. 76, 4287 (1982); LBL-13752.

5. Z. Hussain, E. Umbach, J. J. Barton, J. G. Tobin, and D. A. Shirley, "Angle-resolved Photoemission Study of the Valence Bands of W(011) in the Photon Energy Range 1100-1250 eV: Observation of Strong Direct Transitions and Phonon Effects," Phys. Rev. B 25, 672 (1982); LBL-12672.

6. J. E. Pollard, D. J. Trevor, J. E. Reutt, Y. T. Lee, and D. A. Shirley, "Rotationally Resolved Photoelectron Angular Distributions for H_2^+ ($v' = 0$) at $\lambda = 584$ and 736 Å," Chem. Phys. Lett. 88, 434 (1982); LBL-13998.

7. D. A. Shirley, "Surface and Adsorbate Structural Studies by Photoemission in the $h\nu = 50$- to 500-eV Range," CR in Solid State Materials Science 10, 373 (1982), LBL-9596.

8. J. E. Pollard, D. J. Trevor, J. E. Reutt, Y. T. Lee, and D. A. Shirley, "Rotationally Resolved Photoelectron Spectroscopy of n-H_2, p-H_2, HD, and D_2," J. Chem. Phys. 77, 34 (1982); LBL-13696.

9. Z. Hussain, E. Umbach, D. A. Shirley, J. Stöhr, and J. Feldhaus, "Performance and Application of a Double Crystal Monochromator in the Energy Region $800 \leq h\nu \leq 4500$ eV," Nucl. Instrum. Meth. 195, 115 (1982); LBL-12729.

10. P. H. Kobrin, U. Becker, S. Southworth, C. M. Truesdale, D. W. Lindle, and D. A. Shirley, "Autoionizing Resonance Profiles in the Photoelectron Spectra of Atomic Cadmium," Phys. Rev. A 26, 842 (1982); LBL-13304.

11. D. H. Rosenblatt, S. D. Kevan, J. G. Tobin, R. F. Davis, M. G. Mason, D. R. Denley, D. A. Shirley, Y. Huang, and S. Y. Tong, "Normal Photoelectron Diffraction Studies of Selenium and Sulfur Overlayers on Ni(011) and Ni(111)," Phys. Rev. B 26, 1812 (1982); LBL-13410.

12. D. H. Rosenblatt, S. D. Kevan, J. G. Tobin, R. F. Davis, M. G. Mason, D. A. Shirley, J. C. Tang, and S. Y. Tong, "Off-normal Photoelectron Diffraction Study of the c(2x2) Selenium Overlayer on Ni(001)," Phys. Rev. B 26, 3181 (1982); LBL-13268.

13. J. E. Pollard, D. J. Trevor, Y. T. Lee, and D. A. Shirley, "Rotational Relaxation in Supersonic Beams of Hydrogen by High Resolution Photoelectron Spectroscopy," J. Chem. Phys. 77, 4818 (1982); LBL-14279.

14. J. G. Tobin, L. E. Klebanoff, D. H. Rosenblatt, R. F. Davis, E. Umbach, A. G. Baca, D. A. Shirley, Y. Huang, W. M. Kang, S. Y. Tong, "Normal Photoelectron Diffraction of O/Cu(001): A Surface Structural Determination," Phys. Rev. B 26, 7076 (1982); LBL-14188.

LBL Reports

1. C. M. Truesdale, S. Southworth, P. H. Kobrin, U. Becker, D. W. Lindle, and D. A. Shirley, "K-Shell Auger and Photoelectron Angular Distribution of CO," LBL-12873.

2. S. Southworth, U. Becker, C. M. Truesdale, P. H. Kobrin, D. W. Lindle, S. Owaki, and D. A. Shirley, "Electron Spectroscopy Study of Inner-Shell Photoexcitation and Ionization of Xe," LBL-13697.

3. J. E. Pollard, "Photoelectron Spectroscopy of Supersonic Molecular Beams," Ph.D. thesis, LBL-14285.

4. J. J. Barton, C. C. Bahr, Z. Hussain, S. W. Robey, J. G. Tobin, L. E. Klebanoff, and D. A. Shirley, "Direct Surface Structure Determination with Photoelectron Diffraction," LBL-14645.

5. J. J. Barton and D. A. Shirley, "High Resolution Fourier Analysis with Autoregressive Linear Prediction," LBL-14758.

6. P. H. Kobrin, P. A. Heimann, H. G. Kerkhoff, D. W. Lindle, C. M. Truesdale, T. A. Ferrett, U. Becker, and D. A. Shirley, "Photoelectron Measurements of the Mercury 4f, 5p and 5d Subshells," LBL-14759.

7. D. H. Rosenblatt, "High Resolution Electron Energy Loss Spectroscopy and Photoelectron Diffraction Studies of the Geometric Structure of Adsorbates on Single Crystal Metal Surfaces," Ph.D. thesis, LBL-14774.

8. D. A. Shirley, P. H. Kobrin, D. W. Lindle, C. M. Truesdale, S. Southworth, U. Becker, and H. G. Kerkhoff, "Resonance and Threshold Effects in Photoemission Up to 3500 eV," LBL-14857.

9. D. A. Shirley, "Recent Advances in the Study of Band Structures in Solids by Photoelectron Spectroscopy," LBL-15040.

10. P. H. Kobrin, S. Southworth, C. M. Truesdale, D. W. Lindle, U. Becker, and D. A. Shirley, "Threshold Measurements of the K-Shell Photoelectron Satellites in Ne and Ar," LBL-15042.

11. J. G. Tobin, S. W. Robey, and D. A. Shirley, "The Two-Dimensional Valence Electronic Structure of a Monolayer of Ag on Cu(001)," LBL-15133.

12. J. G. Tobin, S. W. Robey, L. E. Klebanoff, and D. A. Shirley, "The Evolution to Three-Dimensional Valence Band Structure in Ag Overlayers on Cu(001)," LBL-15134.

13. S. Y. Tong, W. M. Kang, D. H. Rosenblatt, J. G. Tobin, and D. A. Shirley, "Photoelectron Diffraction Analysis of the Structure of c(2x2)O on Ni(001)," LBL-15152.

14. J. G. Nelson, W. J. Gignac, R. S. Williams, S. W. Robey, J. G. Tobin, and D. A. Shirley, "ARPES Investigation of Intrinsic Surface States on the Ge (001) 2x1 Reconstructed Surface," LBL-15250.

15. C. M. Truesdale, S. Southworth, P. H. Kobrin, D. W. Lindle, and D. A. Shirley, "Photoelectron Angular Distributions of the N_2O Outer Valence Orbitals in the 19-31 eV Photon Energy Range," LBL-15287.

Invited Talks

1. D. A. Shirley, "Photoelectron Spectroscopy: The Electron's View of Matter," Chemistry Department, University of Hawaii, Manoa, May 5, 1982.

2. D. A. Shirley, "Angle-Resolved and Resonant Photoemission with Synchrotron Radiation," Physics Department, University of Hawaii, Manoa, May 6, 1982.

3. D. A. Shirley, "New Photoemission Results: Shape Resonances and Photoelectron Diffraction," Chemistry Department, University of Hawaii, Manoa, May 7, 1982.

4. D. A. Shirley, "New Interference Phenomena Observed with Photoelectrons," Physical Chemistry Seminar, University of California, Berkeley, California, October 12, 1982.

5. D. A. Shirley, "Angle-Resolved Photoemission: Extended Fine Structure," Bay Area Surface/Interface Technical Meeting, SRI International, Menlo Park, California, December 9, 1982.

6. D. Trevor, "Multiphoton Ionization Photoelectron Spectroscopy," 1982 March Meeting of the American Physical Society, Dallas, Texas, March 8-12, 1982.

7. J. G. Tobin, "Photoemission of Ag Overlayer on Cu (001); the Observation of the Transition from 2-3 Dimensionality," Solid State Physics Seminar, Department of Physics, University of California, Davis, California, October 7, 1982.

8. C. C. Bahr, "Fourier Analysis of Photoelectron Diffraction Data to Determine Adsorbate Structures: c(2x2)S/Ni(100) and p(2x2)S/Cu(100)," Western Regional Meeting of the American Chemical Society, San Francisco, California, October 27-29, 1982.

9. John J. Barton, "Angle-Resolved Photoemission Extended Fine Structure," Ninth Annual Stanford Synchrotron Radiation Laboratory User Group Meeting, Stanford, California, October 22, 1982.

10. P. H. Kobrin, "Atomic Photoelectron Spectroscopy with Synchrotron Radiation," Atomic Physics Seminar, University of Virginia, Charlottesville, Virginia, June 22, 1982.

11. P. H. Kobrin, "Photoelectron Spectroscopy of Gases Using Synchrotron Radiation," Sandia Technical Seminar, Sandia National Laboratory, Livermore, California, December 8, 1982.

h. Crossed Molecular Beams*

Yuan T. Lee, Investigator

Introduction. The major thrust of this research project is to unravel the complex dynamical processes occurring in chemical reactions. Molecular beams of reactants are used to study individual reactive encounters between molecules or to monitor photodissociation events in a collision free environment.

From measurements of the energy and angular distributions of the product fragments, a detailed picture of the reaction mechanism, including preferred orientations of reactants, competition between alternative pathways and partitioning of energy in the products can be obtained.

1. $O(^1D)$ + HD REACTIVE SCATTERING†

A. Wodtke, R. J. Baseman, and Y. T. Lee

The ^1D state of atomic oxygen is a highly reactive entity which readily inserts in C-H bonds and quenches easily to the ground ^3p state. The reaction with H_2 occurs with large cross section, and one of the surfaces of approach correlates with ground state H_2O. Schinke and Lester[1] have calculated an ab initio surface for the reaction and performed trajectory studies on the surface. They identify two mechanisms, insertion of the oxygen into the H-H bond followed by H elimination and collinear attack with rebound of the OH. The insertion pathway has no potential barrier while a small (~3 kcal/mole) barrier exists for collinear approach.

Earlier work in this laboratory with $O(^1D)$ + H_2 has shown that insertion is the major reactive channel at low collision energies. These studies have now been extended to $O(^1D)$ + HD in which the presence of two channels, forming OH or OD provides a more sensitive test of the dynamical behavior of the system. The reactive scattering was measured with the high resolution, universal cross-molecular beam machine, with a supersonic jet of $O(^1D)$ produced in a plasma discharge and a jet of HD from a tungsten oven. Angular and velocity distributions of OH and OD product were measured and these were deconvoluted to produce product energy and center-of-mass angular distributions.

Both OH and OD product were found to be backscattered, pointing to the abstraction mechanism as a significant contribution to the overall reaction. The ratio of OH to OD product agreed well with statistical predictions and the expected isotope effect. The translational energy distribution of both products also agreed with statistical calculations.

This study shows that the abstraction channel begins to compete significantly with the insertion channel at higher collision energies. The oxygen which does insert forms a highly excited complex that lives only one rotational period before dissociation.

* * *

†Brief version of LBL-15259.

1. R. Schinke and W. A. Lester, Jr., J. Chem. Phys. 72, 3754 (1980).

2. PHOTOEXCITATION STUDIES OF SUBSTITUTED CYCLOHEPTATRIENES

R. J. Brudzynski, P. Felder, R. J. Buss, and Y. T. Lee

An important aspect of unimolecular reactions is the collisional energy transfer to and from the excited molecule. The absence of detailed information about these processes has necessitated crude assumptions in theoretical treatments of the effect these processes have on unimolecular reaction rates. We would like to investigate energy transfer in single collisions with a highly vibrationally excited molecule, and a promising candidate is the substituted cycloheptatriene (R-CHT). These molecules absorb near uv radiation, being excited to the S_1 state and promptly undergo internal conversion to high vibrational levels of the ground state. Preparatory to energy transfer studies we have investigated unimolecular decomposition of excited CHT and isopropyl substituted CHT.

A supersonic jet of the R-CHT was crossed with a Nd:YAG laser, and photofragments were detected at several angles. The laser/beam interaction region could be translated upstream from the detector viewing region. The behavior of the product signal as a function of laser position can be used to determine the lifetime of the excited species. The method is most sensitive to lifetimes in the range 2.0 to 200 μsec. Both CHT and isopropyl-CHT were found to have lifetimes less than 2 μsec.

The CHT, which is known to isomerize to toluene, was found to decay by two channels, yielding H + benzyl and CH_3 + phenyl. The angular distributions of product are shown in Fig. 2.1 together with the statistical calculations, which are found to fit reasonably well.

The isopropyl-CHT can isomerize to give either methyl-isopropyl-benzene, or isobutyl-benzene. Two product channels were observed which we attribute to formation of CH_3 + CH_3-C_6H_4-$CHCH_3$ and $CH(CH_3)_2$ + benzyl.

*This work was supported by the Director, Office of Energy Research, Office of Basic Energy Sciences, Chemical Sciences Division of the U. S. Department of Energy under Contract No. DE-AC03-76SF00098.

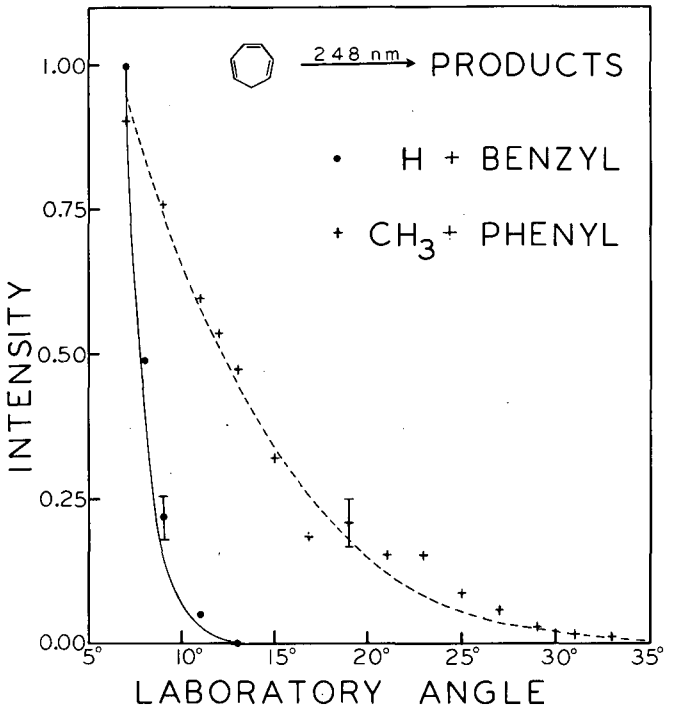

Fig. 2.1. Angular distribution of products from KrF excitation of cycloheptatriene. Lines are statistical calculations. Error bars are 1σ.
(XBL 824-9135)

3. PHOTOCHEMISTRY OF GLYOXAL†

J. W. Hepburn, R. J. Buss, L. J. Butler, and Y. T. Lee

Glyoxal is a model system for studying molecular photophysics and photochemistry. The first excited singlet state has been the subject of many studies, but the photochemistry remains only poorly known. In recent ab initio work by Osamura et al.[1] it has been proposed that one mechanism for decay of S_1 glyoxal is the three body decomposition to give $2CO + H_2$ in a concerted fashion from a near planar transition state. Stimulated by this interesting theoretical work, we have used the method of molecular beam photofragment translational spectroscopy to measure products of the unimolecular decay of glyoxal after laser excitation to the S_1 state.

A supersonic jet of glyoxal in a helium seed gas was excited with a Nd:YAG pumped dye laser at 4398 Å, which is resonant with the band origin of the 8_0^1 band of the S_1 state. The photofragments were measured with the rotatable mass spectrometer at several angles. In Fig. 3.1 are shown the time-of-flight data measured at three masses, 10° from the glyoxal beam.

Our experimental results show that three distinct channels are occurring in this system. From the mass 30 and mass 29 spectra, it is seen that two reaction paths are present, which we attribute to formation of $CO + H_2CO$ and $CO + HCOH$. The latter channel is only slightly exoergic at these excitation energies according to the calculations

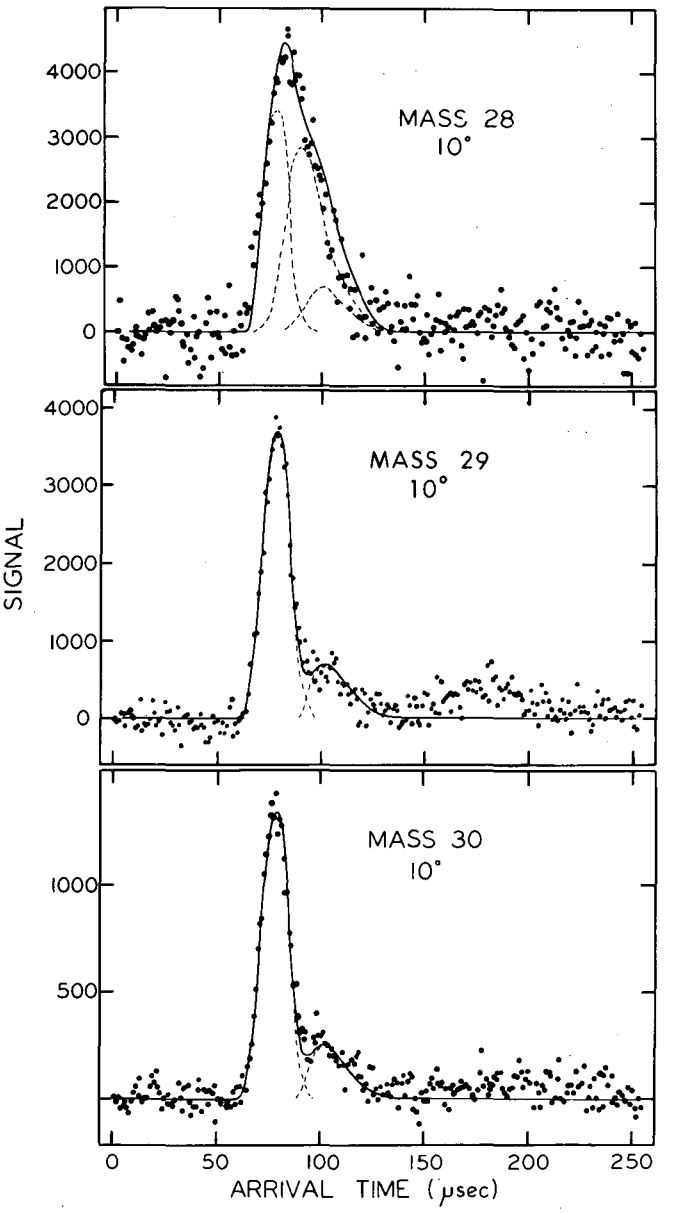

Fig. 3.1. Time-of-flight spectra taken with detector 10° from the molecular beam. Solid lines are calculated fits to the data. Contributions from each channel are shown as dotted lines.
(XBL 826-10473)

of Osamura et al. In the mass-28 spectra a third feature appears as a shoulder on the larger peak, and this can only arise from the formation of $2CO + H_2$.

This study has shown unambiguously that the S_1 state of glyoxal does undergo predissociation in a collision-free environment. We have found evidence for the occurrence of the three body decomposition and for the heretofore unidentified hydroxymethylene molecule.

* * *

†Brief version of LBL-15467.

1. Y. Osamura, H. F. Schaefer, M. Dupuis, and W. A. Lester, Jr., J. Chem. Phys. 75, 5828 (1981).

4. ELASTIC SCATTERING OF ArXe AND KrXe†

R. T. Pack,‡ J. J. Valentini,‡ C. H. Becker, R. J. Buss, and Y. T. Lee

In a collaborative study with the Los Alamos group, we have obtained elastic differential cross sections for scattering of Ar and Kr by Xe. These have been combined with accurate viscosity measurements[1] and second virial coefficient data[2] in order to obtain very accurate interaction potentials. The three properties used in the fitting are complementary for this purpose because the differential cross section at this collision energy (1.5 kcal/mole) is most sensitive to the attractive well part of the potential while the viscosity and virial coefficients are most sensitive to the location and shape of the repulsive wall.

The differential cross sections were obtained with the universal cross-molecular beam machine in a scattering experiment with supersonic beams of the two rare gases. The interatomic potential is an M3SV generalized Morse-spline-van der Waals form.

The experimental differential cross section for the Kr-Xe system is shown in (Fig. 4.1) with the solid line showing the calculated fit. The derived potential gives an excellent fit except for minor disagreement in the region of the rainbow angle. This study is the first reported derivation of a multiproperty empirical interatomic potential for ArXe and KrXe.

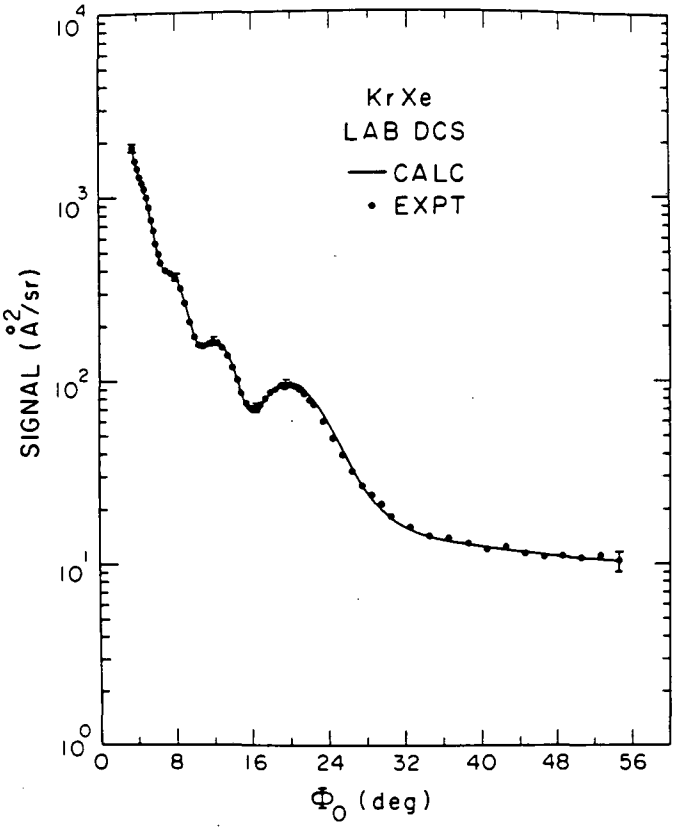

Fig. 4.1. KrXe laboratory differential scattering. The solid line is the calculated result; the points are from the present experiment. Uncertainties of a few representative points are shown. The arbitrary units here are chosen to correspond to square angstroms per steradian.
(XBL 8212-12538)

* * *

†Brief version of LBL-14952.
‡Permanent address: Los Alamos National Laboratory, Los Alamos, NM 87545.

1. J. Kestin, H. E. Khalifa, and W. A. Wakeham, Physica (Utrecht) 90, 215 (1978).
2. J. Brewer, Tech. Rept AD663448, AFOSR Contract No. AF49(638)-1620 (1967), available from the Clearinghouse for Federal Scientific and Technical Information; H. P. Rentschler and B. Schramm, Ber. Bunsenges Phys. Chem. 81, 319 (1977).

5. PHOTODISSOCIATION OF LARGE WATER CLUSTERS†

M. F. Vernon, R. Page, and Y. T. Lee

As part of a continuing study of the decomposition of vibrationally excited water clusters, new measurements have been made of the lifetime, frequency dependence, and cluster size dependence for clusters containing 13-25 water molecules. The reason for the study was to see if the cluster size could become large enough so that the "heat capacity" would enable the cluster to exist vibrationally excited for many microseconds. This idea was stimulated by our previous results which suggested that the geometry for the clusters to predissociate when excited with 10 kcal/mole of energy was far removed from their equilibrium configuration. The energy was then thought to be well distributed among the cluster. By making the cluster larger, the average energy in any one of the hydrogen bonds would be smaller than the bond energy, hence its lifetime would be lengthened. The results of the current study showed that even for clusters containing 25 water molecules, the lifetime is less than 1 microsecond, the minimum time resolution of our apparatus.

* * *

†Brief version of LBL-11970.

6. INFRARED MULTIPHOTON DISSOCIATION OF C_2F_5CL AND C_2F_5Br†

D. Krajnovich, A. Giardini-Guidoni, P. Schulz, Aa. Sudbo, F. Huisken, Z.Zhang, Y. R. Shen, and Y. T. Lee

Preliminary results of experiments on the infrared multiphoton dissociation of C_2F_5Cl were presented in an earlier Annual Report.[1] A few years ago more detailed measurements on C_2F_5Cl were made using a high repetition rate CO_2 laser. C_2F_5Br was also studied for comparison purposes. The analysis of the new data has now been completed. In the case of C_2F_5Cl, competition is observed between the two lowest energy dissociation channels: C-Cl and C-C bond fission. The higher energy C-C channel accounts for approxi-

mately 20% of the dissociation yield at an energy fluence of 0.6 J/cm^2, increasing to 60% at 10 J/cm^2. Our earlier conclusion[1] concerning the presence of a small exit barrier for the C-C fission reaction appears to be incorrect because of a background modulation effect in the data measured at small angles. In the case of C_2F_5Br, the only primary reaction observed is Br atom elimination, in agreement with statistical expectations for this molecule. For both C_2F_5Cl and C_2F_5Br, secondary dissociation of C_2F_5 primary product to CF_3 + CF_2 during the CO_2 laser pulse is observed at high energy fluences. In the case of the Cl- and Br-atom elimination reactions of C_2F_5Cl and C_2F_5Br, deviations from simple RRKM translational energy distributions are observed at low recoil energies ($\leq$0.15 kcal/mole). These deviations result from the requirement to conserve angular momentum during the dissociation.

* * *

†Brief version of LBL-15354.
1. MMRD Annual Report 1978, LBL-10000, pp. 473-477.

7. MOLECULAR BEAM STUDIES OF VIBRATIONAL PREDISSOCIATION OF $(C_2H_4)_2$ AND $(NH_3)_2$ USING A PULSED CO_2 LASER†

D. Krajnovich, P. Schulz, Aa. Sudbo, Y. R. Shen, and Y. T. Lee

In April 1979 we carried out some experiments on the vibrational predissociation of $(C_2H_4)_2$ and $(NH_3)_2$ using a high repetition rate CO_2 laser. In both cases efficient vibrational predissociation is observed between 930-980 cm^{-1}. The lineshapes for the predissociation yield measured at a laser energy fluence of 0.6 J/cm^2 are not symmetrical. The products of the $(C_2H_4)_2$ and $(NH_3)_2$ predissociation reactions are formed with a mean recoil energy of 0.25 and 0.23 kcal/mole, respectively. The distribution of product recoil energies is roughly exponential in both cases. For both reactions the predissociation yield exhibits a very weak dependence on the laser power over a 100-fold range. Complete saturation of the predissociation yield is not achieved at our highest energy fluences of ~2 J/cm^2. These results suggest that: (i) only one photon (~2.7 kcal/mole) is involved in the predissociation reaction for $(NH_3)_2$ as well as $(C_2H_4)_2$; (ii) the predissociation yield lineshape is inhomogeneously broadened; (iii) power broadening of the initial levels is very important in the initial absorption. In the case of $(C_2H_4)_2$, these conclusions disagree with those obtained by other workers[1] using a CW CO_2 laser.

* * *

†Brief version of LBL-15354.
1. M. P. Casassa, O. S. Bomse, and K. C. Janda, J. Chem. Phys. 74, 5044 (1981).

1982 PUBLICATIONS AND REPORTS

Refereed Journals

†‡1. Carl C. Hayden, Daniel M. Neumark, Kosuke Shobatake, Randal K. Sparks, and Y. T. Lee, "Methylene Singlet-Triplet Energy Splitting by Molecular Beam Photodissociation of Ketene," J. Chem. Phys. 76, 3607 (1982).

‡§2. Pauline Ho, Douglas J. Bamford, Richard J. Buss, Yuan T. Lee, and C. Bradley Moore, "Photodissociation of Formaldehyde in a Molecular Beam," J. Chem. Phys. 76, 3630 (1982); LBL-13438.

‡3. J. W. Hepburn, D. J. Trevor, J. E. Pollard, D. A. Shirley, and Y. T. Lee, "Multiphoton Ionization Photoelectron Spectroscopy of CCl_2F_2 and CCl_3F," J. Chem. Phys. 76, 4287 (1982); LBL-13752.

4. Yuan T. Lee, "Molecular Beam Studies of Bimolecular Reactions: F + H_2 and Li + HF," Ber. Bunsenges. Phys. Chem. 86, 378 (1982); LBL-13712.

5. J. E. Pollard, D. J. Trevor, J. E. Reutt, Yuan T. Lee, and D. A. Shirley, "Rotationally Resolved Photoelectron Angular Distributions for H_2^+ (v'=0) at λ = 584 and 736 Å," Chem. Phys. Lett. 88, 434 (1982); LBL-13998.

6. J. E. Pollard, D. J. Trevor, Y. T. Lee, and D. A. Shirley, "Rotationally Resolved Photoelectron Spectroscopy of n-H_2, p-H_2, HD, and D_2," J. Chem. Phys. 77, 34 (1982); LBL-13696.

§7. M. F. Vernon, D. J. Krajnovich, H. S. Kwok, J. M. Lisy, Y. R. Shen, and Y. T. Lee, "Infrared Vibrational Predissociation Spectroscopy of Water Clusters by the Crossed Laser-Molecular Beam Technique," J. Chem. Phys. 77, 47 (1982); LBL-11970.

8. F. A. Houle, S. L. Anderson, D. Gerlich, T. Turner, and Y. T. Lee, "Nonadiabaticity in Ion-Molecule Reactions: Coupling of Proton and Charge Transfer in the H_2^+ and D_2^+ + Ar System," J. Chem. Phys. 77, 1842 (1982); LBL-13638.

9. S. L. Anderson, T. Turner, B. H. Mahan and Y. T. Lee, "The Effects of Collision Energy and Ion Vibrational Excitation on Photon and Charge Transfer in H_2^+ + N_2, CO, O_2," J. Chem. Phys. 77, 1842 (1982); LBL-13556.

10. Piergiorgio Casavecchia, Guozhong He, Randal K. Sparks, and Yuan T. Lee, "Rare Gas-Halogen Atom Interaction Potentials from Crossed Molecular Beams Experiments: I($^2P_{3/2}$) + Kr, Xe($^1S_0$)," J. Chem. Phys. 77, 1878 (1982); LBL-14261.

11. Guozhong He, R. J. Buss, R. J. Baseman, R. Tse, and Y. T. Lee, "Crossed Molecular Beams Studies of the Reaction of O(^3P) with C_2H_3Br," J. Phys. Chem. 86, 3547 (1982); LBL-14322.

§12. M. F. Vernon, J. M. Lisy, D. J. Krajnovich, A. Tramer, H. S. Kwok, Y. R. Shen, and Y. T. Lee, "Vibrational Predissociation Spectra and Dynamics

of Small Molecular Clusters of H_2O and HF," Faraday Discussion No. 73, Van der Waals Molecules, St. Catherine's College, Oxford, England, April 5-7, 1982, to be published; LBL-13740.

13. J. E. Pollard, D. J. Trevor, Y. T. Lee, and D. A. Shirley, "Rotational Relaxation in Supersonic Beams of Hydrogen by High Resolution Photoelectron Spectroscopy," J. Chem. Phys. 77, 4818 (1982); LBL-14279.

14. R. T. Pack, J. J. Valentini, C. H. Becker, R. J. Buss, and Y. T. Lee, "Multiproperty Empirical Interatomic Potentials for ArXe and KrXe," J. Chem. Phys. 77, 5475 (1982); LBL-14952.

15. D., Krajnovich, F. Huisken, Z. Zhang, Y. R. Shen, and Y. T. Lee, "Competition Between Atomic and Molecular Chlorine Elimination in the Infrared Multiphoton Dissociation of CF_2Cl_2," J. Chem. Phys. 77, 5977 (1982); LBL-14478.

16. F. Huisken, D. Krajnovich, Z. Zhang, Y. R. Shen, and Y. T. Lee, "Competing Dissociation Channels in the Infrared Multiphoton Decomposition of Ethyl Vinyl Ether," J. Chem. Phys., submitted July 1982.

LBL Reports

1. Carl Clay Hayden, "Molecular Beams Studies of the Energetics and Dynamics of Elementary Chemical Reactions," Ph.D. thesis, LBL-13660.

2. Robert J. Baseman, "Crossed Molecular Beams Reactive Scattering of Oxygen Atoms, Ph.D. thesis, LBL-15259.

Invited Talks

1. Yuan T. Lee, "Molecular Beam Chemistry," Chinese Institute of Engineers Annual Meeting, San Francisco, California, January 30, 1982.

2. Yuan T. Lee, "Dynamic Resonance Phenomena on Reactive Scattering," Department of Chemistry, University of California, Irvine, California, March 8, 1982.

3. Yuan T. Lee, "Vibrational and Translational Energy Dependence in Reactions of H_2^+," American Chemical Society Meeting, Las Vegas, Nevada, March 30-April 1, 1982.

4. R. J. Buss, "$O(^3P)$ Reactions with Unsaturated Hydrocarbons, Mechanism and Dynamics," American Chemical Society Symposium, Chemical Kinetics of Combustion, Las Vegas, Nevada, March 28-April 1, 1982.

5. Yuan T. Lee, "Molecular Beam Studies of Reaction Dynamics," Department of Chemistry, University of Indiana, Indianapolis, Indiana, April 22, 1982.

6. Yuan T. Lee, "Molecular Beam Studies of Reaction Mechanism and Photochemical Processes," Department of Chemistry, University of Pittsburgh, Pittsburgh, Pennsylvania, May 19, 1982.

7. Yuan T. Lee, "Reaction of Oxygen Atoms with Unsaturated Hydrocarbons," International Symposium on Chemical Kinetics Related to Atmospheric Chemistry, Tsubuka Science Center, Tsubuka, Japan, June 6-10, 1982.

8. Yuan T. Lee, "Molecular Beam Studies on Elementary Reactions and Photochemical Processes," Symposium on Reaction Dynamics, Institute for Molecular Sciences, Okazaki, Japan, June 12, 1982.

9. Yuan T. Lee, "Molecular Beam Research at Berkeley," Institute for Molecular Sciences, Okazaki, Japan, June 14, 1982.

10. Yuan T. Lee, "Recent Advances in Reaction Dynamics," Institute of Chemistry, Beijing, China, June 22, 1982.

11. Yuan T. Lee, "Primary Photochemical Processes," Institute of Chemistry, Beijing, China, June 23, 1982.

12. Yuan T. Lee, "Molecular Beam Studies of Reaction Dynamics," Institute of Chemical Physics, Dalien, China, June 25, 1982.

13. R. J. Buss, "Molecular Beam Study of Glyoxal Predissociation From the S_1 State," 15th Informal Conference on Photochemistry, Stanford University, Stanford, California, June 27-July 1, 1982.

14. Yuan T. Lee, "Molecular Beam Investigation on Laser Chemistry," Department of Chemistry, Fudan University, Shanghai, China, June 28, 1982.

15. Yuan T. Lee, "The Use of Vacuum UV Photons in the Investigation of Energetics and Dynamics of Elementary Reactions," University of Taiwan, Taiwan, July 14-30, 1982.

16. Carl C. Hayden, "F + H_2 Reactive Scattering Experimental Results," Gordon Research Conference on Atomic and Molecular Interactions, New London, New Hamsphire, July 25-30, 1982.

17. R. J. Buss, "The Study of High Energy Collisions in Molecular Beams," 11th International Hot Atom Chemistry Symposium, University of California, Davis, California, August 16-21, 1982.

18. Yuan T. Lee, "Molecular Beam Studies on Reaction Dynamics," XI International Chemical Kinetics Symposium, Göttingen, West Germany, August 22-27, 1982.

19. Yuan T. Lee, "Molecular Beam Studies of Primary Photochemical Processes of Organic Molecules," Department of Chemistry, Harvard University, Cambridge, Massachusetts, September 29, 1982.

20. Yuan T. Lee, "Molecular Beam Photofragmentation Studies of Simple Polyatomic Molecules," Wayne State University, October 11, 1982.

21. Yuan T. Lee, "Primary Photochemical Processes of Polyatomic Molecules," Annual Meeting of Canadian Physicists Association, Division of Atomic

and Molecular Physics, University of Alberta, Alberta, Canada, October 22-23, 1982.

22. Yuan T. Lee, "Molecular Beam Studies of Primary Photochemical Processes of Organic Molecules," Department of Chemistry, University TC :IμK/ 3μEI hμUL u+ Cν Utah, December 7, 1982.

23. Yuan T. Lee, "Molecular Beam Chemical Kinetics," Golden Jubilee of Chinese Chemical Society, Taipei, Taiwan, China, December 12, 1982.

* * *

†Partially supported by the Office of Naval Research under Contract No. N00014-75-C0671.

‡Partially supported by the National Science Foundation.

§Partially supported by the Assistant Secretary for Nuclear Energy, Office of Advanced Systems and Nuclear Projects, Advanced Isotope Separation Division, U. S. Department of Energy under Contract No. DE-AC03-76SF00098.

i. Potential Energy Surfaces for Chemical Reactions*

Henry F. Schaefer III, Investigator

Introduction. This research program has two goals--related yet distinct. The first goal is the development of new theoretical and/or computational methods for the description of "what electrons are doing in molecules," to use the words of Robert S. Mulliken. Specifically, the single outstanding problem in the field is the correlation problem, that of formulating models for going beyond the single-particle or Hartree-Fock approximation. The second goal of our research is to apply these theoretical methods to significant problems of broad chemical interest. Currently two areas are of special concern: (1) model theoretical studies of chemisorption, metal clusters, and organometallic species and (2) potential energy surfaces that govern gas-phase chemical reactions. Research in the former area is ultimately aimed at a truly molecular understanding of catalysis, a subject pertinent to future energy requirements, but sometimes approached by trial and error methods. In the latter area our research sometimes tends toward molecules potentially important in interstellar space, atmospheric chemistry, and the development of high power laser systems. It is to be emphasized that in recent years theoretical chemistry has become a significant source not only of broad generalities, but also of specific predictions concerning molecular systems that may be very important but inaccessible to experiment.

1. TERMINAL VS BRIDGE BONDING OF METHYLENE TO METAL SYSTEMS, Al_2CH_2 AS A MODEL SYSTEM†

Douglas J. Fox and Henry F.Schaefer III

The first mononuclear transition metal methylene complex, $Cp_2TaCh_3CH_2$, was synthesized by Schrock in 1975. However, during the intervening seven years, only one other terminally bonded neutral methylene complex, the $Cp_2Zr(PPh_2Me)CH_2$ molecule of Schwartz, has been reported. The very first transition metal methylene complex reported in the literature was not a terminal structure at all but rather the bridged molecule $[CpMn(CO)_2)_2]_2CH_2$ of Herrmann. Moreover, since 1975 quite a number of additional neutral bridging CH_2 organometallics have been synthesized.

The weight of the evidence would appear to suggest that bridging transition metal methylene complexes are going to be far more prevalent than the analogous terminally bound species. The goal of LBL theoretical studies in this area was to understand why the bridging methylene is apparently favored over the terminal structure.

The metal dimer-methylene system M_2CH_2 is the simplest that can in principle display both terminal M-M-CH_2 and bridging

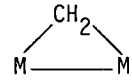

geometrical structures. Having previously studied the terminal Al-CH, Al-CH_2, and Al-CH_3 metal-organic fragment species, the Al_2CH_2 system was chosen to allow a competition between the terminal and bridged structures. Nonempirical molecular electronic structure theory was used, with double zeta (DZ) and DZ + polarization basis sets in conjunction with both self-consistent-field (SCF) and configuration interaction (CI) methods. Among structures considered (see Fig. 1.1), the bridging arrangement, with the

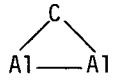

and CH_2 planes perpendicular to each other, lies lowest energetically. For this structure the Al-Al distance is 3.61 Å, the Al-C distance 2.00 Å, and the methylene bond angle 105.5°. The completely planar structure, found by twisting the methylene group 90°, is predicted to lie 31 kcal higher, but has a much shorter Al-Al distance, 3.03 Å. The terminal structure lies 46 kcal above the absolute minimum on the energy surface and has r_e(Al-Al) = 2.87 Å, r_e(Al-C) = 1.81 Å, and a methylene bond angle of 112.2°. All of the above structures are closed-shell singlets in their lowest electronic states, but the energies of several triplet species are also discussed. The Al-C bond energy for the terminal structure is 81 kcal, in good agreement with that predicted (77 kcal) earlier by comparable methods for $AlCH_2$. However, for the bridging Al_2CH_2, the $Al_2...CH_2$ dissociation energy is much larger, 127 kcal. Vibrational frequencies for the bridging and terminal Al_2CH_2 species presented and discussed.

* * *

†Brief version of LBL-14339; J. Chem. Phys., in press.

*This work was supported by the Director, Office of Energy Research, Office of Basic Energy Sciences, Chemical Sciences Division of the U.S. Department of Energy under Contract No. DE-AC03-76SF00098.

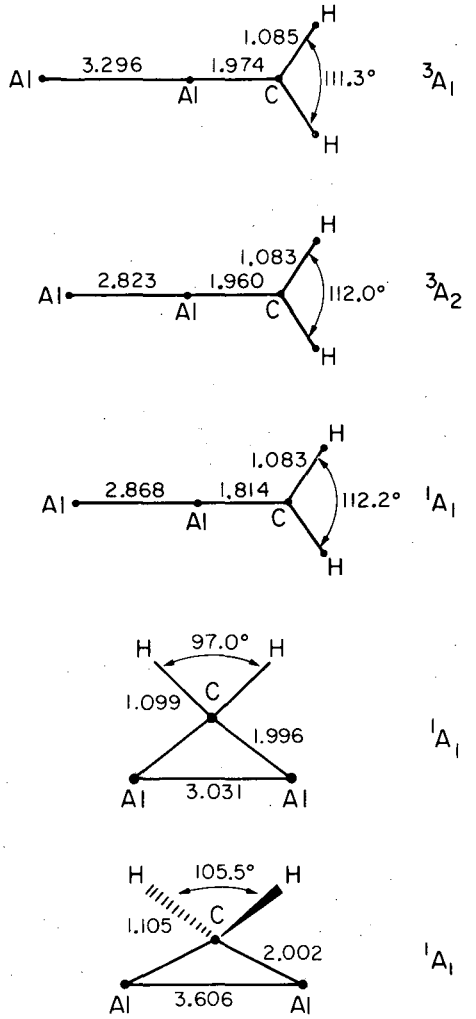

Fig. 1.1. Theoretical molecular structures for various conformations and electronic states of Al_2Ch_2. (XBL 821-3545A)

2. THE WEAKLY EXOTHERMIC REARRANGEMENT OF METHOXY RADICAL ($CH_3O^\bullet$) TO THE HYDROXYMETHYL RADICAL ($CH_2OH^\bullet$) †

Svein Saebo,‡ Leo Radom,‡ and Henry F. Schaefer III

Although the $CH_3O^\bullet$ and $CH_2OH^\bullet$ radicals have long been considered critical intermediates in combustion and atmospheric processes, only very recently has the potential significance of the isomerization $CH_3O^\bullet \rightarrow CH_2OH^\bullet$ been appreciated. This isomerization and related aspects of the $CH_3O^\bullet/CH_2OH^\bullet$ potential surface have been studied using ab initio molecular electronic structure theory with moderately large basis sets and with incorporation of electron correlation. The vibrational frequencies of $CH_3O^\bullet$, $CH_2OH^\bullet$, and seven other stationary points on the potential energy hypersurface have been predicted, both to compare with results from spectroscopy and to provide estimates of zero-point vibrational corrections. In general, there is reasonable agreement with those vibrational frequencies of $CH_3O^\bullet$ and $CH_2OH^\bullet$ which are known from experiment. Our theoretical methods predict that $CH_3O^\bullet$ lies 4.9 kcal mol^{-1} higher in energy than $CH_2OH^\bullet$ with a barrier to rearrangement to $CH_2OH^\bullet$ of 36.9 kcal mol^{-1}. Rearrangement of $CH_3OH^\bullet$ to $CH_2OH^\bullet$ via a dissociation-recombination mechanism is energetically more costly (by 6.1 kcal mol^{-1}). The Jahn-Teller distortion of $CH_3O^\bullet$ from point group C_{3v} is described in some detail. Barriers to inversion and rotation in $CH_2OH^\bullet$ are predicted and compared with the results of ESR experiments. Finally the dissociation of $CH_3O^\bullet$ and $CH_2OH^\bullet$ to yield formaldehyde plus $H^\bullet$ are each predicted to involve modest reverse activation energies.

* * *

†Brief version of LBL-15495; J. Chem. Phys., in press.

‡Present address: Research School of Chemistry, Australian National University, Canberra, Australia.

3. CYCLIC D_{6h} HEXAAZABENZENE--A RELATIVE MINIMUM ON THE N_6 POTENTIAL ENERGY HYPERSURFACE? †

Paul Saxe and Henry F. Schaefer III

The well-known German physical organic chemist Vogler has recently reported laboratory evidence for the formation of hexaazabenzene from photochemical elimination in cis-diazidobis (triphenylphosphorane) platinum(II). As evidenced by the news article in the May 24, 1982 edition of Chemical and Engineering News, this finding has attracted widespread attention. Previous theoretical studies have suggested that the D_{6h} benzene-like structure is not a minimum on the N_6 potential energy hypersurface. Here the N_6 problem has been addressed at the self-consistent-field (SCF) level of theory using double zeta (DZ) and double zeta plus polarization (DZ+P) basis sets. The smaller set yields the prediction that the D_{6h} structure is a transition state connecting two equivalent bond alternant N_6 equilibrium geometries. A second transition state for dissociation to three nitrogen molecules (which are energetically much lower than N_6) was also located. Contrary to previous theoretical work hexaazabenzene is found to be a minimum at the highest completely consistent level of theory. The equilibrium geometry occurs for $r_e(N\text{-}N)$ = 1.288 Å, a bond distance suggesting that N_6 is a classic aromatic molecule. The transition state to $3N_2$ lies 10.3 kcal higher and has the planar bond alternant structure $r_1(N\text{-}N)$ = 1.178 Å, $r_2(N\text{-}N)$ = 1.551 Å. Harmonic vibrational frequencies for hexaazabenzene are predicted with both theoretical methods and demonstrate that the energy surface is very flat with respect to bond alternating B_{2u} displacements. The inclusion of correlation effects lowers the barrier to N_6 dissociation when geometrical structures obtained at the SCF level of theory are assumed. Figure 3.1 summarizes the theoretical predictions.

* * *

†Brief version of LBL-15156; J. Am. Chem. Soc., in press.

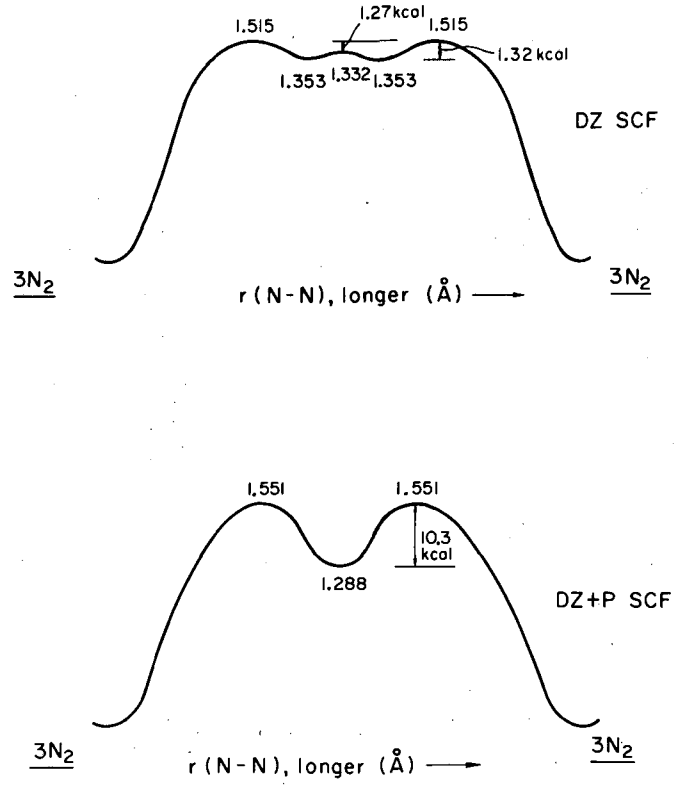

Fig. 3.1. Qualitative sketches of the potential energy surface connecting D_{6h} hexaazabenzene with three infinitely separated N_2 molecules. As a one-dimensional reaction coordinate, the longer of the two distinct N-N distances in $D_{3h}N_6$ was chosen. Of course, the two N-N distances coalesce as one passes from D_{3h} to D_{6h} point group.
(XBL 826-3914)

1982 PUBLICATIONS AND REPORTS

Refereed Journals

1. M. A. Vincent and H.F. Schaefer, "Isomeric Structures of CH_2LiF, the Prototype Carbenoid," J. Chem. Phys. 77, 6103 (1982); LBL-13785.

2. Y. Osamura, Y. Yamaguchi, P. Saxe, M. A. Vincent, J. F. Gaw, and H. F. Schaefer, "United Theoretical Treatment of Analytic First and Second Energy Derivatives in Open-Shell Hartree-Fock Theory," Chemical Physics 72, 131 (1982); LBL-15165.

3. H. F. Schaefer, "The Silicon-Carbon Double Bond: A Healthy Rivalry Between Theory and Experiment," Accounts of Chem. Res. 15, 283 (1982); LBL-14276.

4. M. A. Vincent, Y. Yoshioka, and H. F. Schaefer, "High Spin Electronic States of the Experimentally Observed Molecular Ions $MnCH_2^+$ and $CrCH_2^+$," J. Phys. Chem. 86, 3905 (1982); LBL-14287.

5. P. Saxe, D. J. Fox, H. F. Schaefer, and N. C. Handy, "The Shape-Driven Graphical Unitary Group Approach to the Electron Correlation Problem. Application to the Ethylene Molecule," J. Chem. Phys. 77, 5584 (1982); LBL-14093.

6. P. Saxe, Y. Yamaguchi, and H. F. Schaefer, "Analytic Second Derivatives in Restricted Hartree-Fock Theory: A Method for High-Spin Open-Shell Molecular Wave Functions," J. Chem. Phys. 77, 5647 (1982); LBL-14408.

Other Publications

1. H. F. Schaefer, "Quantum Chemistry," Encyclopedia of Science and Technology, 5th edition, McGraw-Hill, New York, 1982, p. 164.

LBL Reports

1. D. J. Fox and H. F. Schaefer, "Terminal vs. Bridge Bonding of Methylene to Metal Systems. Al_2CH_2 as a Model System," LBL-14339.

2. G. Fitzgerald, P. Saxe, and H. F. Schaefer, "Singlet Cyclobutyne: A Relative Minimum on the C_4H_4 Potential Energy Hypersurface?" LBL-14622.

3. P. Saxe and H. F. Schaefer, "Cyclic D_{6h} Hexaazabenzene--A Relative Minimum on the N_6 Potential Energy Hypersurface?" LBL-15156.

4. W. D. Laidig and H. F. Schaefer, "Electronic Symmetry Breaking in Polyatomic Molecules. Multiconfiguration Self-Consistent-Field Study of the Cyclopropenyl Radical, C_3H_3," LBL-14092.

5. Y. Yamaguchi, J. F. Gaw, and H. F. Schaefer, "Molecular Clustering About A Positive Ion. Structures, Energetics, and Vibrational Frequencies of the Protonated Hydrogen Clusters H_3^+, H_5^+, H_7^+, and H_9^+," LBL-15154.

6. S. Saebo, L. Radom, and H. F. Schaefer, "The Weakly Exothermic Rearrangement of Methoxy Radical (CH_3O) to the Hydroxymethyl Radical (CH_2OH)," LBL-15495.

7. M. R. Hoffmann, Y. Yoshioka, and H. F. Schaefer, "Vibrational Frequencies for Silacetylene and Its Silylidene and Vinylidene Isomers," LBl-14312.

8. J. Bicerano, H. F. Schaefer, and W. H. Miller, "Structure and Tunneling Dynamics of Malonaldehyde, A Theoretical Study," LBL-15155.

9. P. S. Bagus, H. F. Schaefer, and C. W. Bauschlicher, "The Convergence of the Cluster Model for the Study of Chemisorption: $Be_{36}H$, LBL-15496.

10. W. D. Laidig and H. F. Schaefer, "Where to Look for the Electronic Spectrum of Hydrogen Isocyanide, HNC," LBL-14203.

11. K. S. Kim, H. F. Schaefer, L. Radom, J. A. Pople, and J. S. Binkley, "Vibrational Frequencies of the HCCN Molecule. A Near Degeneracy Between Bent Cyanocarbene and Linear Allene-Related Geometries," LBL-15166.

12. G. Fitzgerald and H. F. Schaefer, "Structures, Energetics, and Vibrational Frequencies of Cyclopropyne," LBL-15888.

13. M. A. Vincent, H. F. Schaefer, A. Schier, and H. Schmidbauer, "The Molecular and Electronic Structure of Phosphonium Cyclopropylide $H_3P = C(CH_2)_2$: A Theoretical Study," LBL-15399.

Invited Talks

1. H. F. Schaefer, "The Third Age of Quantum Chemistry," presented at the following places:
Symposium on Theoretical Organic Chemistry/ Computational Quantum Chemistry, Canberra, Australia, February 12, 1982.
Research School of Chemistry, Australian National University, March 1982.
Department of Theoretical Chemistry, University of Sydney, Australia, March 1982.
Department of Chemistry, University of Nevada, Reno, Nevada, April 30, 1982.
Department of Chemistry, University of California, Irvine, May 3, 1982.
Department of Chemistry, Harvard University, Cambridge, Massachusetts, May 17, 1982.
Lester P. Kuhn Memorial Lecturer, Department of Chemistry, Johns Hopkins University, Baltimore, Maryland, May 18, 1982.
Chemistry Division, Argonne National Laboratory, Argonne, Illinois, May 19, 1982.
Department of Chemistry, Ohio State University, Columbus, Ohio, May 20, 1982.
Department of Chemistry, California Institute of Technology, Pasadena, California, May 25, 1982.
Gordon Research Conference on High Temperature Chemistry, Tilton, New Hampshire, July 29, 1982.

2. P. Saxe, "Capabilities of the Shape-Driven Graphical Unitary Group Approach," Theoretical Chemistry Group, Los Alamos Scientific Laboratory, Los Alamos, New Mexico, August 1982.

3. H. F. Schaefer, "Analytic Energy Second Derivatives in Molecular Electronic Structure Theory," Symposium on Transition States in Chemistry, American Chemical Society, Kansas City, Missouri, September 15, 1982 and Department of Chemistry, University of Hawaii, Honolulu, Hawaii, December 17, 1982.

3. Atomic Physics

a. Atomic Physics*

Richard Marrus, Investigator

1. PARITY VIOLATION IN ATOMS†

E. Commins and P. Drell

During the past year we completed construction of the apparatus and carried out a careful theoretical and experimental study of possible sources of systematic error in parity measurements. We have found, and dealt with, the two main sources of trouble. These are:

(a) Misaligned magnetic field combined with small residual nonreversing components of electric field. By carrying out parity measurements with the magnetic field deliberately misaligned by a large amount, we have demonstrated that this effect is small and can be corrected for adequately.

(b) Electric field sign-dependent background that varies with linear polarization of laser light. This is a subtle effect that we discovered the explanation only after many weeks of difficult investigation. It arises because of photoelectron ejection from tantalum electrodes in the cell by scattered laser light. These electrons are accelerated in the electric field and excited thallium atoms to fluoresce. The small background thus created depends on the sign of the electric field and the light polarization, and can thus create a false parity effect. The solution to this problem is to replace the tantalum electrodes with new electrodes (nickel) with a short wavelength photoelectric threshold $\lambda_0 < \lambda$, where λ is our laser wavelength. This is now being done. Meanwhile, we have made numerous improvements in apparatus sensitivity and have also isolated and treated various other small sources of systematic error. We remain confident that a precise measurement can be carried out in the very near future.

* * *

†Brief version of LBL-15510.

2. ONE PERCENT MEASUREMENT OF THE LIFETIME OF THE 2 $^2S_{1/2}$ STATE OF HYDROGENLIKE ARGON (Z = 18)†

Harvey Gould and Richard Marrus

The 2 $^2S_{1/2}$ state is the only metastable state in the hydrogen isoelectronic sequence. It decays by simultaneous emission of two electric dipole photons (2E1) and by single-photon relativistic magnetic dipole decay (M1). Because exact calculations can be performed for one-electron atoms, the measurement of the lifetime of the 2 $^2S_{1/2}$ state is a very rigorous test of the theory of these decays.

Figure 2.1 shows the theoretical[1-3] and experimental[4-9] decay rates scaled by Z^{-6} of the 2 $^2S_{1/2}$ state of the hydrogen isoelectronic sequence. The decrease in the 2E1 rate shown in Fig. 2.1 is because of relativistic corrections, which at Z = 18 are 1.1%. The upper curve shows the contribution of the M1 rate. Our measurement of the 2 $^2S_{1/2}$ lifetime in hydrogenlike argon of 3.487 (0.036) ns, in agreement with the theoretical value of 3.497 ns, is the first experiment to see the presence of the M1 component. It is marginally sensitive to the relativistic correction to the 2E1 rate.

The lifetime of the 2 $^2S_{1/2}$ state was measured by the beam-foil time-of-flight technique. The extremely small error is a reflection of our understanding of the systematic effects in this experiment, including cascades from higher excited states, interference from the spectra of helium-like ions, collisions in the residual gas, and the effects of spectator electrons.

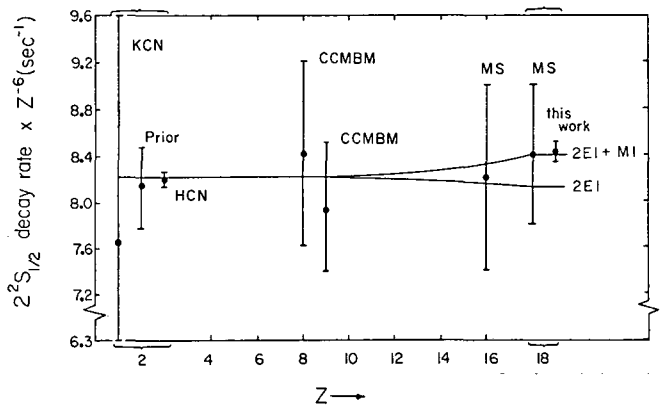

Fig. 2.1. Comparison of experimental and theoretical 2 $^2S_{1/2}$ decay rates of hydrogenlike atoms. All decay rates have been divided by Z^6. Theory is from Ref. 4, and the experimental points are MS, Ref. 5; CCMBM, Ref. 6; HCN, Ref. 7; Prior, Ref. 8; and KCN, Ref. 9. (XBL 832-8350)

*This work was supported by the Director, Office of Energy Research, Office of Basic Energy Sciences, Chemical Sciences Division of the U.S. Department of Energy under Contract No. DE-AC03-76SF00098.

* * *

†Brief version of LBL-15649.

1. S. P. Goldman and G. W. F. Drake, Phys. Rev. A 24, 183 (1981).
2. W. R. Johnson, Phys. Rev. Lett. 29, 1123 (1972).
3. F. A. Parpia and W. R. Johnson, Phys. Rev. A 26, 1142 (1982).
4. S. Klarsfeld, Phys. Lett. 30A, 382 (1969).
5. R. Marrus and R. W. Schmieder, Phys. Rev. A 5, 11670 (1972).
6. C. L. Cocke, B. Curnutte, J. R. Macdonald, J. A. Bednar, and R. Marrus, Phys. Rev. A 9, 2242 (1974).
7. E. A. Hinds, J. E. Clendenin, and R. Novick, Phys. Rev. A 17, 670 (1978).
8. M. H. Prior, Phys. Rev. Lett. 29, 611 (1972).
9. C. A. Kocher, J. E. Clendenin, and R. Novick, Phys. Rev. Lett. 29, 615 (1972).

3. ELECTRON CAPTURE BY LOW-ENERGY MULTICHARGED NEON IONS†

Richard Marrus, Michael Prior, and C. R. Vane

Capture of electrons by multicharged ions at thermal and subthermal energies is an important process in fusion devices and the interstellar medium. In fusion devices, it can lead to serious energy losses resulting from electron capture and subsequent radiation. As a result, many studies of this process have been carried out with ions in the energy range $\geq$ 100 q/eV, where q is the charge. These studies have employed a variety of ion sources, notably EBIS devices and ECR sources. The results at these energies yield cross sections which vary slowly with energy and are mainly monotonic in q.

In order to extend these measurements to lower energies, we have employed as an ion source the recoil ions produced when a fast beam from an accelerator traverses a low-density gas. The energies of these recoil ions is quite low, typically about 1-2xq eV. These ions are then confined in an electrostatic ion trap where they can undergo charge capture collisions with the neutral atoms present in the gas. Detection of the ions is done with a commercial quadrupole mass analyzer and a channeltron detector. By monitoring the ion density as a function of time after the accelerator pulses, the exponential decay that results from electron capture is observed. From this decay a decay constant γ is obtained, which can be written in the form $\gamma = \langle\sigma v\rangle n + \gamma_0$, where $\langle\sigma v\rangle$ is the velocity-averaged capture cross section, n is the gas density, and γ_0 is the loss rate resulting from processes independent of gas density. The quantity $\langle\sigma v\rangle$ can be extracted from the measured rate constants by making a linear plot of γ vs n and taking the slope. An effective cross section is obtained by dividing $\langle\sigma v\rangle$ by the root-mean-square velocity of the ions in the trap. This is possible because the virial theorem for the logarithmic potential present in a cylindrical trap shows V_{rms} to be independent of the ion orbit.

Results for the effective cross section shows that at fixed velocity there are very strong oscillations with the ion charge q. This is indicative of a resonance capture process where electron transfer can take place only if the binding energy in the state in which capture occurs equals the ionization potential. An unusual feature of our data is that some of the charge states exhibit very strong velocity dependences while, for the same velocity range, cross sections for other charge states are velocity insensitive. This differs from data taken by other experiments at higher energies.

* * *

†Brief version of LBL-15720.

1982 PUBLICATIONS AND REPORTS

Refereed Journals

1. R. Mann, C. L. Cocke, A. S. Schlachter, M. Prior, and R. Marrus, "Selective Final State Population in Electron Capture by Low-Energy, Highly Charged Projectiles Studied by Electron-Gain Spectroscopy." Phys. Rev. Lett. 49, 1329 (1982).

2. H. Gould and J. Alonso, "Charge, Changing Cross Sections for Pb and Xe Ions at Velocities Up to 4 x 10^9 cm/sec," Phys. Rev. A 26, 1134 (1982).

3. R. Marrus, M. Prior, and C. R. Vane, "Electron Capture by Trapped Low-Energy Multicharged Neon Ions," Nucl. Instrum. Meth. 202, 171 (1982).

4. L. Hunter, E. Cummins, and L. Roesch, "Measurements of Spontaneous-Emission Rates in Atomic Thallium," Phys. Rev. A 25, 885 (1982).

4. Chemical Energy

a. Formation of Oxyacids of Sulfur from SO_2*

Robert E. Connick, Investigator

Introduction. The primary goal of the research is to investigate the fundamental chemistry of sulfur dioxide, as well as species formed from it, in aqueous solution. There is strong interest currently in this chemistry because of the pernicious effects of acid rain, formed when sulfur containing fuels, such as coal, are burned and the gaseous products are allowed to escape into the atmosphere, with the ultimate formation of sulfuric acid. Initially combustion forms sulfur dioxide. The best way currently to control acid rain is to remove the sulfur dioxide from the stack gases of coal-burning power plants with aqueous scrubbers. Thus, the chemistry of sulfur dioxide and the species formed from it at low acidity is vital to the understanding and design of these massive installations. In addition the aqueous chemistry of sulfur dioxide is important when it escapes into the atmosphere, as it is believed that the oxidation to sulfuric acid occurs in water films on suspended dust particles.

A secondary and not closely related goal is to determine the factors controlling the rate of substitution reactions in the first coordination sphere of metal ions. These reactions are important in almost all processes involving metal ions in solution. This includes metal ion complex formation, some oxidation-reduction reactions, as well as many biological processes involving metal ions.

1. THE RATE AND MECHANISM OF EXCHANGE OF OXYGENS BETWEEN BISULFITE ION AND WATER

Robert E. Connick and David A. Horner

Work in progress. When sulfur dioxide dissolves in water, it retains its molecular structure as SO_2, rather than hydrating to H_2SO_3. On ionization to bisulfite ion and hydrogen ion, it must react with a water molecule. The forward and reverse of the ionization reaction lead to exchange of the oxygens of bisulfite ion and water. It is believed that this is the dominant mechanism for oxygen exchange. The two studies reported in the literature are in strong disagreement as to the rate.

In the present study the nuclear magnetic resonance signal of oxygen-17 is being used to measure the exchange rate. The results so far are in agreement with one of the earlier studies as to rate, but appear to be yielding further insights on the reaction. In the pH region around 4, two oxygen-17 signals are observed arising from HSO_3^-, one corresponding to ca. 20% and the other ca. 80%. It seems likely that these two signals correspond to the two isomers of bilsulfite ion: one with the proton bonded to the sulfur and the other with the proton bonded to an oxygen. While the existence of the two isomers has been postulated for some time and Raman evidence has been obtained for their presence in solution, this would be the first time that such direct evidence was found and a measure of their abundance obtained. Experiments are under way to try to detect the proton resonance of the less labile species, which presumably is the one with the proton attached to the sulfur.

2. RATES OF SUBSTITUTION REACTIONS ON METAL IONS

Robert E. Connick and Michael R. Wagner

Work in progress. Rates at which substitution takes place of ligands coordinated to metal ions have yielded a wealth of information on the mechanisms of such reactions, particularly in recent years. Yet the factors controlling the lability of such ligands are still incompletely understood. The present work is aimed at trying to resolve the relative importance of ionic, electronic, and steric effects using a single metal ion, Ni^{2+}, partially complexed by a variety of ligands, and by measuring the exchange rate of the attached water molecules. A comparison of iminodiacetate with methyl iminodiacetate is under way.

Computer simulation of an exchange reaction on a metal ion is being written for publication with Dr. Berni Alder.

1982 PUBLICATIONS AND REPORTS

Refereed Journals

1. R. E. Connick, T. M. Tam, and E. von Deuster, "Equilibrium Constant for the Dimerization of Bisulfite Ion to Form $S_2O_5^{2-}$," Inorg. Chem. 21, 103 (1982); LBL-12272.

2. I. Nagypál, I. Fábián, and R. E. Connick, "NMR Relaxation Studies in Solution of Transition Metal Complexes, VII: Protonation of the Vanadyl Ion in Aqueous Solution," Acta. Chimica Academiae Scientiarum Hungaricae 110(4), 447 (1982).

3. R. E. Connick and T. G. Braga, "Kinetics of the Oxidation of Bisulfite Ion by Oxygen," ACS Symposium Series, No. 188, edited by J. L. Hudson and G. T. Rochell, 1982, p. 153-171; LBL-13259.

Invited Talks

1. Robert E. Connick, "Computer Modeling of Solvent Exchange in the First Coordination Sphere of Metal Ions," Stanford University, Palo Alto, Chemistry Department Seminar, January 12, 1982.

*This work is supported by the Director, Office of Energy Research, Office of Basic Energy Sciences, Chemical Sciences Division of the U.S. Department of Energy under Contract No. DE-AC03-76SF00098.

b. Catalytic Hyrogenation of CO: Catalysis on Well-Characterized Surfaces*

Gabor A. Somorjai, Investigator

and

Catalysis by Supported Metals*

Alexis T. Bell, Investigator

Introduction. The purpose of this program is to develop an understanding of the fundamental processes involved in catalytic conversion of carbon monoxide and hydrogen to gaseous and liquid fuels. Attention is focused on defining the factors that limit catalyst activity, selectivity, and resistance to poisoning, and the relationship between catalyst composition/structure and performance. To meet these objectives, a variety of surface diagnostic techniques (LEED, AES, XPS, EELS, IRS, TPD) are used to characterize supported and unsupported catalysts before, during, and after reaction. The information thus obtained is combined with detailed studies of reaction kinetics to elucidate reaction mechanisms and the influence of modifications in catalyst composition and/or structure on the elementary reactions involved in carbon-monoxide hydrogenation.

1. THE HYDROGENATION OF CO OVER RHODIUM FOIL, AND RHODIUM COMPOUNDS, $FeRhO_3$ and Na_2RhO_3

M. Logan and G. A. Somorjai

The hydrogenation of carbon monoxide has been studied over rhodium foil and rhodium-containing refractory oxides. We have determined product distributions, turnover frequencies, and activation energies for the reaction. We have found an inverse deuterium effect on the rhodium foil, like that found on ruthenium by Kellner and Bell[1] with $Rate(D_2)/Rate(H_2) \approx 1.4$. The partial pressure dependence of the reaction rate has also been determined. For a rate law of the form $Rate = kP_{CO}^{x}P_{H_2}^{y}$, the values $x = -1$ and $y = +1$ were obtained. The activation energy does not depend on the total pressure of the reactant gases, but it changes with the CO to H_2 partial pressure ratio. This change in activation energy implies a change in the rate-determining step of the reaction.

Preliminary studies of rhodium oxides have been performed on Na_2RhO_3 and $FeRhO_3$. The Na_2RhO_3 was found to produce mainly alkanes and some alkenes and oxygenated molecules while $FeRhO_3$ formed methane and alkenes (mainly ethene and propene) almost exclusively.

*This work was supported by the Director, Office of Energy Research, Office of Basic Energy Sciences, Chemical Sciences Division of the U.S. Department of Energy under Contract No. DE-AC03-76SF00098.

* * *

1. C. S. Kellner and A. T. Bell, J. Catal. 67, 175 (1981).

2. THE EFFECTS OF ADDITIVES ON THE Fe AND Re CATALYZED CO HYDROGENATION REACTIONS

E. L. Garfunkel, J. Parmeter, and G. A. Somorjai

Rhenium and iron foils have been studied as model Fischer-Tropsch catalysts in a high pressure/low pressure apparatus. In addition to the clean metal surfaces, the effects of K, Na, and O "promoters" and C and S "poisons" were examined to learn more about the role of surface additives.

Using a 4:1 ratio of H_2:CO at 2 atm total pressure, activation energies for the production of methane were found to be 24 (Fe) and 28 (Re) kcal/mol. At 520 K, clean rhenium produced ~95% methane and ~5% C_2^+ (ethylene, ethane, propylene...), while clean iron produced ~80% methane and ~20% C_2^+. On rhenium, submonolayers of Na lowered the methanation rate and changed the selectivity to ~80% methane and ~20% C_2^+. On iron the presence of alkali (Na or K) decreased the overall rate. The changes in selectivity varied according to the degree of oxidation of the substrate and alkali overlayer, usually favoring C_2^+ with alkali present.

Oxidation of the rhenium surface, on the other hand, increased both the total rate of reaction and the selectivity toward methane (~98%). The same effect was observed on iron surfaces. The increased methanation rate upon oxidation was mainly because of an increased surface area as monitored from CO thermal desorption peak area. The activation energies for the production of ethylene were lower than those for methanation on both surfaces.

The cause for catalyst poisoning on both Fe and Re surfaces was found to be the irreversible build up of a "graphitic" carbon overlayer. Sulfur was also a poison, and it enhanced the rate of carbon build up during the reaction. Auger and thermal desorption spectroscopies were used to analyze the surfaces before and after reactions.

3. THE PRODUCTION OF METHANOL FROM CO AND H_2 OVER THORIUM OXIDE CATALYST SURFACES

J. Maj, C. Colmenares, and G. A. Somorjai

These studies are being carried out in the Lawrence Livermore Laboratory where there are extensive facilities for handling actinide elements and their compounds that include thorium oxide. High surface area oxide was synthesized by precipitating thorium carbonate and then heating slowly up to 400°C. CO_2 and H_2O are driven off and the oxide with about 10 m^2/gm area is produced.

Using a microreactor in the flow-mode, the CO/H_2 reaction is carried out at 50 atm total pressure and in 1:2 and 2:1 gas ratios. Under these conditions methanol is produced almost exclusively in the temperature range 250-350°C, with an optimum turnover frequency at 325°C. Above 400°C the catalyst slowly deactivates.

4. CHARACTERIZATION OF CARBON DEPOSITS FORMED DURING CO HYDROGENATION OVER RUTHENIUM

P. Winslow and A. T. Bell

Transient response mass spectrometry and Fourier-Transform infrared spectroscopy were used to study the nature of carbon species present on the surface of a silica supported ruthenium catalyst during Fischer-Tropsch synthesis. Carbon was found to exist on the catalyst surface as linearly adsorbed CO and two forms of nonoxygenated carbon. The integrated absorption coefficient of the linear adsorbed CO was determined by isotope displacement and found to be nonlinear with coverage. The two forms of nonoxygenated carbon, α and β, were distinguished by their relative reaction rates during titration of the catalyst surface with deuterium. The α-carbon was found to be very reactive and appears to be the primary form involved in Fischer-Tropsch synthesis. The β-carbon is much less reactive than the α-carbon. It was established that under helium flush, the β-carbon is gradually converted to the α-carbon.

The influence of reaction conditions on the amounts of each carbon species was studied at 473 K; the surface coverage by CO was independent of either CO or H_2 partial pressure and corresponded to about 0.98 of a Ru monolayer. The α-carbon coverage did not exceed 0.02 of a monolayer, was independent of time for a given set of conditions, and increased with increasing D_2 pressure or decreasing CO pressure. By contrast, the β-carbon coverage increased monotonically in time, growing to about 0.10 of a monolayer after 5 hr. The accumulation of β-carbon accelerates with increasing CO partial pressure.

5. THE INFLUENCE OF METAL-SUPPORT INTERACTIONS ON THE SYNTHESIS OF METHANOL OVER PALLADIUM

R. F. Hicks and A. T. Bell

In a previous investigation, it was shown that metal-support interactions strongly influence the activity and selectivity of Pd for the synthesis of methanol from CO and H_2. The present study was undertaken to elucidate the manner in which a support influences Pd catalysts. To date, the work has focused on determining the kinetics of methanol and methane synthesis over a series of silica and lanthanum oxide-supported Pd catalysts. For a given set of reaction conditions, Pd/La_2O_3 catalysts exhibit methanol turnover frequencies ten to twenty times greater than those observed for Pd/SiO_2 catalysts. Quite surprisingly, the kinetics of methanol synthesis are virtually the same for silica and lanthanum oxide-supported Pd. This equivalence is expressed by the close similarity of the activation energies and the power law dependencies on H_2 and CO partial pressures. Substantial differences occur, though, in the kinetics of methane synthesis on the two types of catalyst. The effects of metal dispersion on the specific activities for methanol synthesis are also different on the two supports. On silica, the specific activity is nearly independent of dispersion, whereas on lanthanum oxide the specific activity increases with increasing dispersion. For both supports, the specific activity for methane synthesis increases monotonically with decreasing dispersion.

The physical characteristics of Pd/SiO_2 and Pd/La_2O_3 are being determined through the use of XPS, infrared spectroscopy of adsorbed CO, and TPD spectroscopy of adsorbed H_2 and CO. Infrared spectra of adsorbed CO indicate that the principal planes exposed by supported Pd are 100 and 111. For Pd/La_2O_3, CO adsorption is observed on both 100 and 111 planes, the proportion depending on the dispersion of Pd. For Pd/SiO_2, CO adsorption occurs primarily on 100 planes. Correlation of the observed rate data with the infrared observations for Pd/La_2O_3 suggests that the 111 planes of Pd are a factor of two less active than the 100 planes.

1982 PUBLICATIONS AND REPORTS

Refereed Journals

1. E. L. Garfunkel, J. E. Crowell, and G. A. Somorjai, "The Strong Influence of Potassium on the adsorption of CO on Platinum Surfaces: A TDS and HREELS Study," J. Chem. Phys. 86, 310 (1982); LBL-13349.

2. M. Langell and G. A. Somorjai, "The Composition and Structure of Oxide Films Grown on the (110) Crystal Face of Iron," J. Vac. Sci. Technol. 21, 858 (1982); LBL-13203.

3. W. McLean, C. A. Colmenares, R. L. Smith, and G. A. Somorjai, "Electron Spectroscopy Studies of the Clean Thorium and Uranium Surfaces. The Chemisorption and Initial Stages of Reaction with O_2, CO, and CO_2," Phys. Rev. B 25(1), 8 (1982); UCRL-86167.

4. P. R. Watson and G. A. Somorjai, "The Formation of Oxygen-Containing Organic Molecules by the Hydrogenation of Carbon Monoxide Using a Lanthanum Rhodate Catalyst," J. Catal. 74, 282 (1982); LBL-12969.

5. P. R. Watson and G. A. Somorjai, "The Interactions of CO, CO_2, and D_2 with Rhodium Oxide ($RH_2O_3 \cdot 5H_2O$): Its Reduction and Catalytic Stability," J. Phys. Chem. 86, 3993 (1982); LBL-13524.

6. N. W. Cant and A. T. Bell, "Studies of Carbon Monoxide Hydrogenation Over Ruthenium Using Transient Response Techniques," J. Catal. 73, 257 (1982); LBL-12598.

7. C. S. Kellner and A. T. Bell, "Effects of Dispersion on the Activity and Selectivity of Alumina-Supported Ruthenium Catalysts for the Hydrogenation of Carbon Monoxide," J. Catal. 75, 251 (1982); LBL-12429.

8. J. A. Baker and A. T. Bell, "Hydrogenation of Carbon Monoxide Over Ruthenium. Detection of Surface Species by Reactive Scavenging," J. Catal. 78, 165 (1982); LBL-13773.

LBL Reports

1. A. T. Bell, "The Role of CH_x(x = 1-3) Species in Fischer-Tropsch Synthesis," LBL-14503.

Other Publications

1. A. T. Bell and L. L. Hegedus, "Catalysis Under Transient Conditions," ACS Symposium Series 178, Am. Chem. Soc., Washington, D.C., 1982.

Invited Talks

1. G. A. Somorjai, "Catalyzed Hydrogenation of Graphite and CO. Photocatalyzed Surface Processes," Fudan University, Shanghai, China, April 1982.

2. G. A. Somorjai, "Catalyzed Hydrogenation of Carbon Monoxide," Jilin University, Changchun, China, April 1982.

3. A. T. Bell, "Fischer-Tropsch Synthesis Over Ruthenium. A Case Study in the Analysis of Reaction Mechanisms," Research Division, W. R. Grace & Co., Columbia, Maryland, January 1982.

4. A. T. Bell, "Fischer-Tropsch Synthesis Over Ruthenium Catalysts," Tarrytown Technical Center, Union Carbide Corp., Tarrytown, New York, March 1982.

5. A. T. Bell, "Studies of the Mechanism and Kinetics of Hydrocarbon Formation During Fischer-Tropsch Synthesis Over Ruthenium," Sohio Research Center, Cleveland, Ohio, March 1982.

6. A. T. Bell, "Synthesis of Oxygenated Compounds from CO and H_2," Sohio Research Center, Cleveland, Ohio, March 1982.

7. A. T. Bell, "Fischer-Tropsch Synthesis Over Ruthenium. Studies of Reaction Mechanism, Kinetics, and Effects of Metal Dispersion," Central Research & Development Department, E. I. duPont de Nemours & Co., Wilmington, Delaware, April 1982.

8. A. T. Bell, "The Role of CH_x(x = 1-3) Species in Fischer-Tropsch Synthesis," Symposium on Advances in Catalytic Chemistry II, Salt Lake City, Utah, May 1982.

9. A. T. Bell, "Studies of the Mechanism of CO Hydrogenation," First International Summer School on Advanced Coal Technologies, Cosenza, Italy, July 1982.

10. A. T. Bell, "Mechanism and Kinetics of Fischer-Tropsch Synthesis Over Ruthenium Catalysts," Engler-Bunte Institut, Universität Karlsruhe, Karlsruhe, Germany, July 1982.

11. A. T. Bell, "Mechanism and Kintics of Fischer-Tropsch Synthesis Over Ruthenium Catalysts," Institut für Physikalische Chemie, Universität München, München, Germany, July 1982.

12. A. T. Bell, "Applications of Fourier-Transform Infrared Spectroscopy to Studies of Adsorbed Species," Gordon Conference on Vibrational Spectroscopy, Wolfboro, New Hampshire, August 1982.

13. A. T. Bell, "Effects of Metal-Support Interactions on the Synthesis of Methanol over Palladium," China-Japan-USA Symposium on Heterogeneous Catalysis, Dalian, People's Republic of China, September 1982.

14. A. T. Bell, "Studies of CO Hydrogenation over Supported Metal Catalysts," Department of Chemistry, Nanjing University, People's Republic of China, September 1982.

15. A. T. Bell, "Temperature Programmed Desorption of H_2 and NO from a Rh/SiO_2 Catalyst. Determination of Rate Parameters," 184th National Meeting of the ACS, Kansas City, Missouri, September 1982.

16. A. T. Bell, "Synthesis of Hydrocarbons and Oxygenated Products Over Ruthenium and Palladium," Department of Chemical Engineering, University of Minnesota, Minneapolis, Minnesota, October 1982.

17. A. T. Bell, "Studies of Surface Reactions Under Transient Conditions Using Fourier-Transform Spectroscopy," Annual AIChE Meeting, Los Angeles, California, November 1982.

c. Organometallic Chemistry of Coal Conversion*

K. Peter Vollhardt, Investigator

Introduction. The purpose of this work is to develop organic and organometallic methodology concerned with furthering the understanding of basic processes in coal conversion and related catalytic reactions. These include studies on the mechanism of the Fischer-Tropsch and other C-C bond forming reactions, the synthesis of homogeneous analogs of surface intermediates in the reduction of carbon monoxide, the organometallic activation of thiophene with respect to sulfur extrusion, and the construction of novel binuclear transition metal complexes in order to establish their potential catalytic and stoichiometric chemistry.

1. BISCARBYNE CLUSTERS AS HOMOGENEOUS ANALOGS OF FISCHER-TROPSCH INTERMEDIATES ON SURFACES†

Neal T. Allison,‡ John R. Fritch,§ David E. Van Horn,¶ K. Peter C. Vollhardt, and Eric C. Walborsky

Biscarbyne clusters are being investigated as potential mimics of surface species thought to be intermediates in Fischer-Tropsch reactions and the skeletal rearrangement of hydrocarbons as observed in platforming. This work should lead to a better understanding of catalysis on surfaces, the design of better catalysts, and the discovery of new catalytic reactions.

The approach used relies on the ready synthetic accessibility of trinuclear cobalt biscarbyne clusters reported by the Principal Investigator in 1980. Work has been completed concerning the potential nucleophilic character of these systems, which has led to the discovery of novel chemistry at the apical carbon, including hydrogen-deuterium exchange reactions that can be considered as models for such exchange processes on surfaces.

The x-ray crystallographic analysis of the parent compound reveals a crystallographic C_3h symmetry in the solid state with both $\mu_3\eta^1$-bonded carbyne ligands lying on the threefold axis and the three cobalt atoms in the mirror plane. The C-H bonds are oriented perpendicular to the trinuclear cobalt core. This is an important result because surface carbyne species have been postulated to be able to adopt a bent configuration with respect to the surface metal atoms.

While exploring the chemistry of the double deck cluster 1, an unprecedented rearrangement was uncovered involving the simultaneous coupling and decoupling of carbyne fragments (1 --> 2).

This reaction constitutes a new homogeneous model for C-C bond-forming and bond-breaking on surfaces.

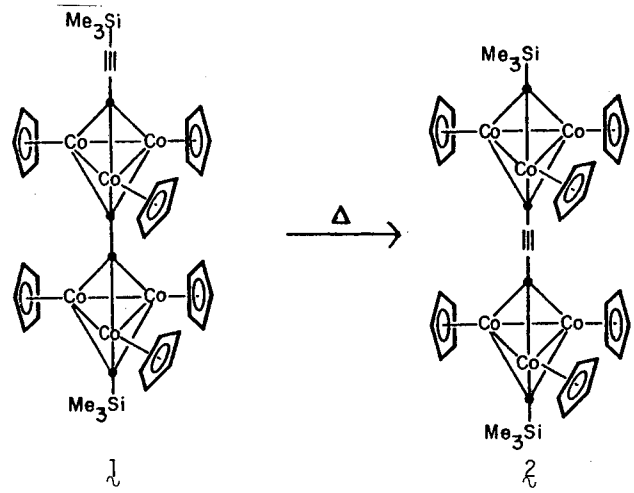

1 2

* * *

†Brief version of J. Chem. Soc., Chem. Comm., 203 (1982), LBL-13759, and of LBL-15413 and LBL-15414.
‡Present address: Dept. of Chemistry, University of Arkansas.
§Present address: Celanese Corporation, Corpus Christi, TX.
¶Present address: Dept. of Chemistry, Texas A & M University, College Station, TX.

2. TRANSITION METAL MEDIATED THERMAL EXTRUSION OF SULFUR DIOXIDE FROM THIOPHENE-1,1 DIOXIDES†

James S. Drage and K. Peter C. Vollhardt

CpCo-η^4-2,5-dimethylthiophene-1,1-dioxide 3 was prepared by irradiation of the free heterocycle in the presence of $CpCo(CO)_2$. Flash vacuum pyrolysis leads solely to CpCo-η^4-1,2,-dimethylcyclobutadiene 4 by SO_2 extrusion. A crossover experiment has shown that the complexes stay intact during this transformation; ligand exchange cannot be observed. Positional isomerization of the cyclobutadiene ligand (as reported earlier) occurs at higher temperatures than those required to eject SO_2 from its precursor. Pyrolysis of either of the diastereomers of CpCo-η^4-(2-methyl-5-sec-butyl)thiophene-1,1-diox-ide gave completely diastereoisomerized CpCo-cyclobutadienes, but only partially equilibrated starting materials. The observed data suggest as a reasonable mechanism metal insertion into the thiophene ring followed by SO_2 extrusion involving a deinsertion pathway.

*This work was supported by the Director, Office of Energy Research, Office of Basic Energy Sciences, Chemical Sciences Division of the U.S. Department of Energy under Contract No. DE-AC03-76SF00098.

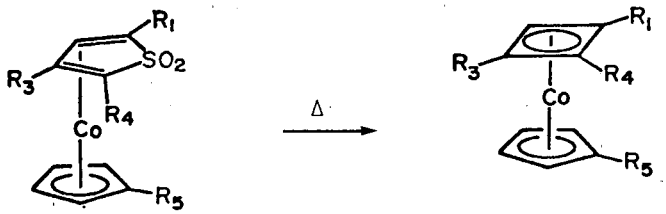

3 4

* * *

†Brief version of Organometallics 1, 1545 (1982), LBL-14977.

3. WORK IN PROGRESS

The scope and limitations of the reaction of trinuclear cobalt biscarbyne clusters with sulfur that leads to cluster degradation and the formation of metalladithiolanes are being explored. Crossover-labeling experiments have shown that this reaction involves intramolecular carbyne-carbyne coupling.

A facile entry into fulvalene dinuclear metal complexes has been found. Several complexes have been analyzed by x-ray crystallography. Preliminary investigations have led to the discovery of new organometallic transformations. Fulvalenediruthenium tetracarbonyl has been shown to undergo a photolytic (sunlight) isomerization to a new dinuclear cluster in which both the sp_2-sp_2 bonds of the fulvalene ligand as well as the metal-metal bond have been cleaved. This process has been shown to be thermally reversible, thus constituting a novel potential photochemical storage cycle.

The chemistry of fulvalenedimolybdenum hexacarbonyl is being investigated.

Exploratory work is concerned with synthetic approaches to bisvinylidene complexes.

1982 PUBLICATIONS AND REPORTS

Refereed Journals

1. K. P. C. Vollhardt, "Cobalt Mediated Bond Forming and Bond Breaking Reactions: Synthetic and Mechanistic Perambulations," Chem. Aust. 49, 3 (1982); LBL-13997.

2. D. E. Van Horn and K. P. C. Vollhardt, "Some Remarkable Reactions of the Biscarbyne Clusters $[\mu_3\eta^1\text{-}CR_1]$ $[\mu_3\eta^1\text{-}CR_2][\eta^5\text{-}C_5H_5)Co]_3$ With Electrophiles," J. Chem. Soc., Chem. Commun. 203 (1982); LBL-13759.

†3. D. J. Brien, A. Naiman, and K. P. C. Vollhardt, "Catalytic Co-Cyclisation of α,ω-Cyanoalkynes With Alkynes: A Versatile Chemo- and Regioselective Synthesis of 2,3-Substituted 5,6,7,8-Tetrahydroquinolines and Other Cycloalka[1,2-b]pyridines," J. Chem. Soc., Chem. Commun. 133 (1982).

†4. B. C. Berris and K. P. C. Vollhardt, "An Approach to Tricyclo[8.4.0.$0^{4,7}$]-tetradecahepta-1,3,5,7,9,11, 13-ene (benzo[1,2-a]cyclobuta[1,2-e]cyclooctatetra-ene): Unusual Thermal Rearrangements in the $C_{14}H_{10}$-Manifold," Tetrahedron 38, 2911 (1982).

‡5. R. A. Earl and K. P. C. Vollhardt, "On the Synthetic Utility of Thermally Generated Imines: The Retro-ene Imino Diels-Alder Reaction," Heterocycles 19, 265 (1982).

†6. E. D. Sternberg and K. P. C. Vollhardt, "Cobalt-Mediated [2+2+2]Cycloadditions En Route to Natural Products: A Novel Total Synthesis of Steroids Via the One-Step Construction of the B,C,D-Framework from an A-Ring Precursor," J. Org. Chem. 47, 3447 (1982).

†7. W. V. Dower and K. P. C. Vollhardt, "The Thermal Conversion of 1,5,9-Triynes to Aromatic Compounds: [2+2+2]Cycloadditions or Sigmatropic Rearrangements?" Angew. Chem. 94, 712 (1982); Angew. Chem., Int. Ed. Engl. 21, 685 (1982); Angew. Chem. Suppl., 1545 (1982).

8. J. S. Drage, R. A. Earl, and K. P. C. Vollhardt, "Deoxygenation of Allylic Carbinolamides and Related Alcohols by Acidic Sodium Cyanoborohydride: Scope and Limitations," J. Heterocyclic Chem. 19, 701 (1982).

†9. J. P. Tane and K. P. C. Vollhardt, "Cyclopentadienone Complexes as Synthons: Ring- and Regiospecific Nucleophilic Additions to Cobaltocinium Salts. Synthesis of Substituted Cyclopentadienes and Cyclopentenones," Angew. Chem. 94, 642 (1982); Angew. Chem., Int. Ed. Engl. 21, 617 (1982); Angew. Chem. Suppl., 1360 (1982).

†10. B. C. Berris, Y.-H. Lai, and K. P. C. Vollhardt, "A Cobalt Catalyzed Biphenylene Synthesis," J. Chem. Soc., Chem. Commun., 953 (1982).

11. J. S. Drage and K. P. C. Vollhardt, "Thermal Extrusion of Sulfur Dioxide from $(\eta^5\text{-}C_5H_5)Co\text{-}\eta^4$-thiophene-1,1-dioxides: A New Organometallic Reaction," Organometallics 1, 1545 (1982); LBL-14977.

†12. W. V. Dower and K. P. C. Vollhardt, "Mechanism of the Isomerization of 1,5,9-Cyclododecatriyne to Hexaradialene: 1,2:3,4:5,6-Tricyclobutabenzene Is Not an Intermediate," J. Am. Chem. Soc. 104, 6878 (1982).

LBL Reports

1. V. W. Day, D. E. Horn, and K. P. C. Vollhardt, "The Structure of $[\mu_3\eta^1\text{-}CH]_2[\eta^5\text{-}C_5H_5Co]_3$, a Biscarbyne Cluster Derived by the Triple Bond Cleavage of Ethyne," LBL-15413.

2. N. T. Allison, J. R. Fritch, K. P. C. Vollhardt, and E. C. Walborsky, "An Unprecedented Biscarbyne Cluster Rearrangement Involving Simultaneous Coupling and Decoupling of Carbyne Fragments: A New Homogeneous Model for C-C Bond-Forming and Bond-Breaking on Surfaces," LBL-15414.

Invited Talks

1. K. P. C. Vollhardt, "Transition Metal Mediated [2+2+2]Cycloadditions: A Better Version of the Diels-Alder Reaction?" University of Minnesota, Minneapolis, St. Paul, Minnesota, January 13, 1982.

2. K. P. C. Vollhardt, "Transition Metal Mediated Carbon-Carbon Bond Formation," Iowa State University, Ames, Iowa, January 14, 1982.

3. K. P. C. Vollhardt, "Mechanistic Investigations in Cobalt Mediated Carbon-Carbon Bond-Making and Bond-Breaking Reactions," Hoffmann-LaRoche Incorporated, Nutley, New Jersey, January 25, 1982.

4. K. P. C. Vollhardt, "Transition Metal Catalyzed Routes to Natural Products," North Jersey ACS Organic Chemistry Section, New Jersey, January 25, 1982.

5. K. P. C. Vollhardt, "Enyne Cyclizations in Organic Synthesis," UC Irvine, Irvine, California, February 8, 1982.

6. K. P. C. Vollhardt, "Cobalt Mediated Cyclizations in Organic Synthesis," University of West Virginia, Morgantown, West Virginia, March 23, 1982.

7. K. P. C. Vollhardt, "Cobalt Mediated Cyclizations in Organic Synthesis," Bucknell University, Lewisburg, Pennsylvania, March 24, 1982.

8. K. P. C. Vollhardt, "Transition Metal Mediated [2+2+2] Cycloadditions," Pennsylvania State University, University Park, Pennsylvania, March 25, 1982.

9. K. P. C. Vollhardt, "Remarkable Bond-Making and Bond-Breaking in the Coordination Sphere of Transition Metals," ACS Midland Section, Midland, Michigan, April 13, 1982.

10. K. P. C. Vollhardt, "Transition Metals in Total Synthesis," Pfizer Incorporated, Groton, Connecticut, April 15, 1982.

11. K. P. C. Vollhardt, "Transition Metal Mediated [2+2+2] Cycloadditions: A Better Version of the Diels-Alder Reaction?" DuPont Central Research, Wilmington, Delaware, April 16, 1982.

12. K. P. C. Vollhardt, "Remarkable Rearrangements in the Coordination Sphere of Transition Metals," University of Nice, Nice, France, June 1, 1982.

13. K. P. C. Vollhardt, "Total Synthesis of Natural Products Using Transition Metal Catalysts and Reagents," Plenary Lecturer, Groupe d'Etudes de Chimie Organometallique, Ile des Embiez, France, May 31-June 4, 1982.

14. K. P. C. Vollhardt, "Biscarbyne Clusters as Potential Homogeneous Models of Surface Species," Invited Lecturer, Second Homogeneous Catalysis Research Conference, Department of Energy, University of Wisconsin, Madison, Wisconsin, June 7-9, 1982.

15. K. P. C. Vollhardt, "Transition Metals in Organic Synthesis," Plenary Lecturer, Second China-Japan-USA Organometallic and Inorganic Chemistry Seminar, Shanghai, China, June 14-18, 1982.

16. K. P. C. Vollhardt, "Transition Metal Mediated Routes to Natural Products," Université Louis Pasteur, Strasbourg, France, September 6, 1982.

17. K. P. C. Vollhardt, Invited Lecturer (five lectures), Utah Organometallic Chemistry Workshop, Department of Chemistry, University of Utah, Salt Lake City, Utah, September 20-24, 1982.

18. K. P. C. Vollhardt, "Transition Metals in the Total Synthesis of Natural and Unnatural Products," Indiana University, Bloomington, Indiana, October 20, 1982.

19. K. P. C. Vollhardt, "Remarkable Rearrangements in the Coordination Sphere of Transition Metals," Indiana University, Bloomington, Indiana, October 21, 1982.

20. K. P. C. Vollhardt, "Transition Metal Catalyzed Routes to Natural and Unnatural Products," Technische Hochschule Darmstadt, Darmstadt, West Germany, December 16, 1982.

21. K. P. C. Vollhardt, "Transition Metal Catalysis in Organic Synthesis," University of Marburg, Marburg, West Germany, December 17, 1982.

* * *

†Supported in part by NIH.
‡Supported in part by NSF.

d. Synthetic and Physical Chemistry*

William L. Jolly, Investigator

Introduction. The purpose of this project is to use photoelectron spectroscopy to determine the nature of the bonding in significant inorganic and organometallic compounds. By measuring core electron binding energies of appropriate transition metal compounds, it is possible to study the interaction of metal d electrons with various ligands and to identify various modes of ligand-metal bonding that have analogs in the intermediates of catalyzed organic reactions. Core binding energies can also be used, in conjunction with valence shell ionization potentials, to quantify the bonding or antibonding character of molecular orbitals.

1. AN X-RAY PHOTOELECTRON SPECTROSCOPIC STUDY OF THE σ- AND π-ALLYL GROUPS†

A. J. Ricco, A. A. Bakke, and W. L. Jolly

From a comparison of the atomic core binding energies of $CH_3Mn(CO)_5$, $(n\text{-}C_3H_7)Mn(CO)_5$, $(\sigma\text{-}C_3H_5)Mn(CO)_5$, and $Mn_2(CO)_{10}$, we conclude that the methyl, propyl, and σ-allyl groups in the first three compounds are negatively charged. Both the carbon 1s binding energies and theoretical considerations indicate an unusually large relaxation energy associated with the ionization of the terminal carbon atom of the σ-allyl group. The $\pi\text{-}C_3H_5$ group in $(\pi\text{-}C_3H_5Mn(CO)_5$ has a relatively low electron density, undoubtedly because it is a formal 3-electron donor group. The carbon 1s data indicate that the C_5H_5 group in $(\eta^5C_5H_5)Mn(CO)_5$ is probably positively charged.

* * *

†Brief version of Organometallics 1, 94 (1982); LBL-12912.

2. AN X-RAY PHOTOELECTRON SPECTROSCOPIC STUDY OF THE BONDING IN (ALKYLIDYNE)TRICOBALT NONACARBONYL COMPLEXES AND RELATED COMPOUNDS†

S. F. Xiang, A. A. Bakke, H. W. Chen, C. J. Eyermann, J. L. Hoskins, T. H. Lee, D. Seyferth, H. P. Withers, Jr., and W. L. Jolly

The core electron binding energy of the methylidyne carbon atom in $RC[Co(CO)_3]_3$ compounds is a function of the electronegativity of the R group. The core binding energies of the $[Co(CO)_3]_3$ cluster generally change similarly, but to a smaller extent, with changing R group. However, for R = OCH_3 and R = $N(CH_3)_2$, the core binding energies of the $[Co(CO)_3]_3$ cluster are significantly lower than expected. These data, and a combination of UPS and XPS data for the chloro and bromo compounds, indicate that groups such OCH_3, $N(CH_3)_2$, Cl, and Br act as π donors toward the $C[Co(CO)_3]_3$ system. Binding-energy data indicate that the CH groups of $HC[Co(CO)_3]_3$ and $(HC)_2[Co(CO)_3]_2$ are negatively charged, with the CH group of $HC[Co(CO)_3]_3$ more negative than those of $(HC)_2[Co(CO)_3]_2$. The significantly lower binding energies of $[Co(CO)_3]_4$ reflect the fact that three of the carbonyl groups in this compound are bridging.

* * *

†Brief version of Organometallics 1, 699 (1982); LBL-13320.

3. AN X-RAY PHOTOELECTRON SPECTROSCOPY STUDY OF TRANSITION METAL μ-METHYLENE COMPLEXES AND RELATED COMPOUNDS†

S. F. Xiang, H. W. Chen, C. J. Eyermann, W. L. Jolly, S. P. Smit, K. H. Theopold, R. G. Bergman, W. A. Herrmann, and R. Pettit

Gas-phase core electron binding energies have been determined for $[Fe(CO)_4]_2CH_2$, $[CpMn(CO)_2]_2CH_2$, $(CpCoCO)_2CH_2$, $(CpRhCO)_2CH_2$, and several structurally related compounds. The binding-energy data indicate that the CH_2 groups in the $\mu\text{-}CH_2$ complexes are highly negatively charged, especially in the manganese, cobalt, and rhodium compounds. Data for $Fe(CO)_4C_2H_4$ indicate that the CH_2 groups in this compound are negatively charged but less so than in the $\mu\text{-}CH_2$ compounds. Data for $Fe_3(CO)_{12}$ suggest the presence of both terminal and bridging carbonyl groups.

* * *

†Brief version of Organometallics 1, 1200 (1982); LBL-14069.

4. JUSTIFICATION OF THE APPROXIMATION THAT SHIFTS IN NONBONDING VALENCE ORBITAL IONIZATION POTENTIAL ARE EIGHT-TENTHS OF SHIFTS IN CORE BINDING ENERGY†

W. L. Jolly and C. J. Eyermann

Empirical and theoretical data are cited to support the approximation that shifts in strictly nonbonding valence orbital ionization potential are eight-tenths of corresponding shifts in core binding energy. This approximation is shown to be useful in the quantification of the bonding and antibonding character of molecular orbitals.

* * *

†Brief version of J. Phys. Chem. 86, 4834 (1982); LBL-14532.

*This work was supported by the Director, Office of Energy Research, Office of Basic Energy Sciences, Chemical Sciences Division of the U.S. Department of Energy under Contract No. DE-AC03-76SF00098.

5. WORK IN PROGRESS

We have just completed an XPS study of volatile iron cluster compounds and a combined XPS/UPS study of the manganese pentacarbonyl halides. We are investigating the nature of the interactions of ethylene with the d orbitals of the iron atom in the complex $Fe(CO)_4C_2H_4$.

1982 PUBLICATIONS AND REPORTS

Refereed Journals

1. A. J. Ricco, A. A. Bakke, and W. L. Jolly, "An X-Ray Photoelectron Spectroscopic Study of the σ- and π-Allyl Groups," Organometallics 1, 94 (1982); LBL-12912.

2. S. F. Xiang, A. A. Bakke, H. W. Chen, C. J. Eyermann, J. L. Hoskins, T. H. Lee, D. Seyferth, H. P. Withers, Jr., and W. L. Jolly, "An XPS Study of the Bonding in Alkylidynetricobalt Nonacarbonyl Complexes and Related Compounds," Organometallics 1, 699 (1982); LBL-13320.

3. S. F. Xiang, H. W. Chen, C. J. Eyermann, W. L. Jolly, S. P. Smit, K. H. Theopold, R. G. Bergman, W. A. Herrmann, and R. Pettit, "An XPS Study of Transition Metal μ-Methylene Complexes and Related Compounds," Organometallics 1, 1200 (1982); LBL-14069.

4. W. L. Joly and C. J. Eyermann, "Justification of the Approximation that Shifts in Nonbonding Valence Orbital Ionization Potential are Eight-Tenths of Shifts in Core Binding Energy," J. Phys. Chem. 86, 4834 (1982); LBL-14532.

LBL Reports

1. W. L. Jolly, "The Use of Core Binding Energies in the Assignment of the Ultraviolet Photoelectron Spectra of the Manganese Pentacarbonyl Halides," LBL-15161.

2. D. B. Beach, J. L. Hoskins, W. L. Jolly, S. P. Smit, and S. F. Xiang, "A Gas-Phase XPS Study of Iron Cluster Compounds," LBL-14798.

Invited Talks

1. W. L. Jolly, "The Study of Organometallic Compounds by X-Ray Photoelectron Spectroscopy," Second Homogeneous Catalysis Research Conference, Madison, Wisconsin, June 7-9, 1982.

2. W. L. Jolly, "Photoelectron Spectroscopy and Inorganic Chemistry," Seminar at San Francisco State University, Chemistry Department, November 5, 1982.

3. W. L. Jolly, "Core Binding Energies Aid the Interpretation of Valence Photoelectron Spectra," Symposium at American Chemical Society Meeting, El Paso, Texas, December 1-3, 1982.

e. Chemistry and Morphology of Coal Liquefaction*

Heinz Heinemann, Investigator, with Alexis T. Bell, James W. Evans, Richard H. Fish, Alan V. Levy, Eugene E. Petersen, Gabor A. Somorjai, Theodore Vermeulen, and K. Peter Vollhardt, Investigators

(See Fossil Energy Section)

f. Electrochemical Systems*

John Newman, Investigator

1. MATHEMATICAL MODELING AND OPTIMIZATION OF LIQUID-JUNCTION PHOTOVOLTAIC CELLS†

Mark E. Orazem and John Newman

The liquid-junction photovoltaic cell is an electrochemical system with semiconducting electrodes. This system has been extensively studied as a means of converting solar energy to electrical and chemical energy.

A mathematical model of the liquid-junction photovoltaic cell was coupled with primary resistance calculations to predict the optimal performance of a photoelectrochemical cell with a slotted-semiconductor electrode. The cell resistance is a function of three geometric ratios, chosen to be t/G, h/G, and L_{AB}/h (see Fig. 1.1),

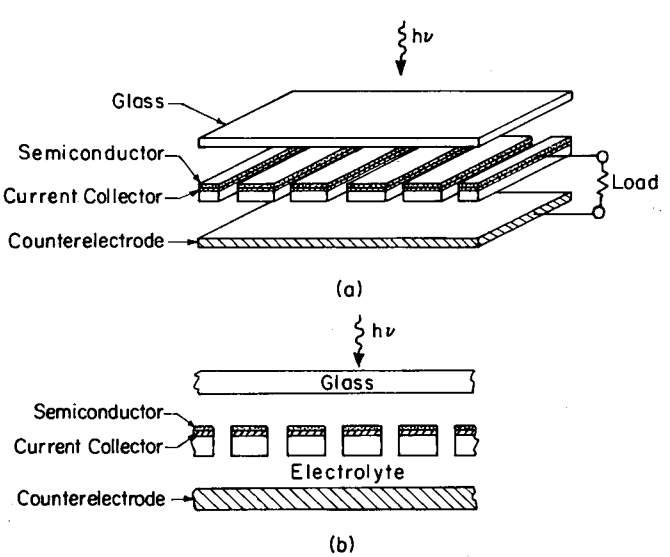

Fig. 1.1. Schematic diagram of the slotted-electrode photovoltaic cell. (XBL 831-7974)

where L_{AB} is the length of the protruding electrode assembly, t is the thickness of the protruding electrode assembly, G is the halfwidth of the slot in the semiconductor assembly, and h is the separation between the electrode and the upper insulating wall.

The mathematical model was used to calculate the effect of cell design on the performance of an n-type GaAs semiconducting anode in contact with an 0.8 M K_2Se, 0.1 M K_2Se_2, 1.0 M KOH electrolytic solution. The maximum power density of the slotted-electrode cell is presented in Fig. 1.2 as a function of L_{AB}/h. The optimal value for L_{AB}/h was 4, the maximum power density was 47.8 W/m^2, and the maximum power efficiency was 5.4%. At maximum power the current density was 15 mA/cm^2 delivered at 477.6 mV.

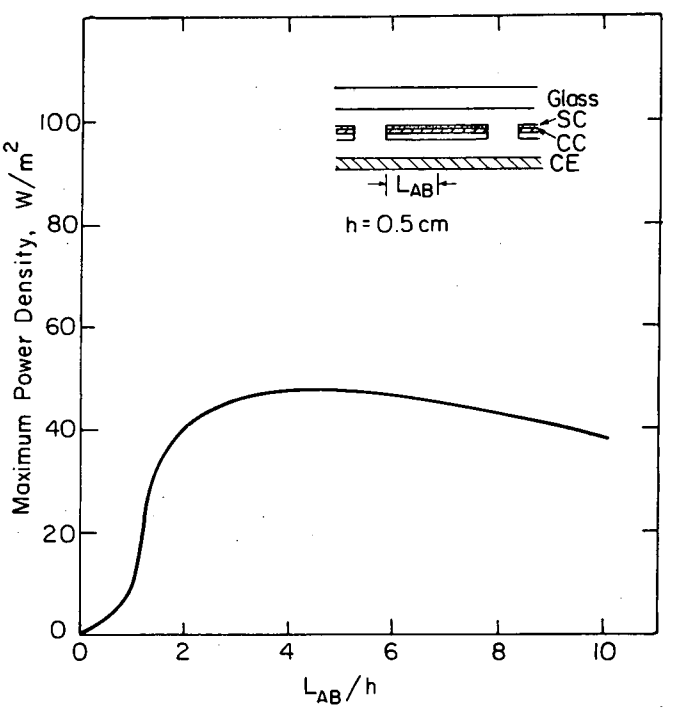

Fig. 1.2. Maximum power density as a function of L_{AB}/h for the slotted-electrode photovoltaic cell (t = 0.1 cm, h = 0.5 cm, and G = 1.0 cm). (XBL 831-7975)

*This work was supported by the Director, Office of Energy Research, Office of Basic Energy Sciences, Chemical Sciences Division of the U.S. Department of Energy under Contract No. DE-AC03-76SF00098.

* * *

†Brief version of LBL-15494.

2. ELECTROCHEMICAL REMOVAL OF MERCURY FROM CONTAMINATED BRINE SOLUTIONS†

Michael Matlosz and John Newman

Aqueous solutions contaminated with heavy-metal ions may present serious toxic health hazards. The use of high-surface-area electrochemical reactors, such as flow-through porous electrodes, shows promise for the effective treatment of these solutions.

A flow-through porous electrode consists of a support material (such as carbon), which is permeable and electrically conducting. A solution, contaminated with a heavy-metal ion (mercuric ion, in this case), flows through the bed, while a small electric current is drawn through the support material. The heavy-metal ions are removed from the solution by electrodeposition (electroplating) onto the packing material.

The experimental porous electrode used in this study is 3 in. in diameter and 6 in. in height, and consists of a cylindrical bed of carbon flakes and chips. Typically, mercury concentrations can be reduced by a factor of ten thousand in a single pass through the reactor at flow rates as high as ten bed volumes per hour. The results are very encouraging, and the system appears attractive as a potential treatment method.

* * *

†Brief version of LBL-14708.

1982 PUBLICATIONS AND REPORTS

LBL Reports

1. Michael Matlosz and John Newman, "Use of a Flow-through Porous Electrode for Removal of Mercury from Contaminated Brine Solutions," presented at the Electrochemical Society Conference, Montreal, Quebec, Canada, May 10, 1982, LBL-14708.

2. Mark E. Orazem and John Newman, "Primary Current Distribution and Resistance of a Slotted Electrode Cell," LBL-15494.

Invited Talks

1. W. H. Smyrl, "Metal Displacement Reactions," Electrochemical Society Conference, Montreal, Quebec, Canada, May 12, 1982.

g. Surface Chemistry—Application of Coordination Principles*

Earl L. Muetterties, Investigator

The establishment of coordination principles for the chemisorption of hydrocarbons and their derivatives on nickel and platinum surfaces represents the primary objective of this research. Carbon-hydrogen and carbon-carbon bond scission reactions are common reactions that ensue after molecular chemisorption, and an understanding of these procedures is being sought through isotopic labeling techniques. A complementary study of metal cluster reactions is in progress using a metal isotopic labeling technique.

Earlier, the topographical dependence of the nickel and platinum surface dehydrogenation of cyclohexene and cyclohexadienes to benzene was established by displacement reactions. Also, a stereochemical model was generated for the molecular details of this dehydrogenation reaction. The model has now been extended to cycloalkenes in general and has provided, through recent experiments, insights into this area of hydrocarbon surface chemistry.[1]

Thermal desorption and isotopic labeling studies have indicated that cycloheptatriene after chemisorption on atomically flat nickel and platinum surfaces is dehydrogenated below ~90°C to yield a C_7H_7 species. On Ni(100), a substantial fraction of the implicated C_7H_7 surface species is converted to benzene at temperatures of about 100°C. The isomeric molecule, norbornadiene, is also partially converted to benzene at 225-250°C on Pt(111) and Pt(100). Labeling studies established that the carbon atom lost in the benzene formation is the CH_2 carbon atom. Cyclooctene and cyclooctadienes were partially converted to cyclooctatetraene on Pt(111) at elevated temperatures.

The postulated surface reaction of $\underline{c}\text{-}C_nH_{2n-2m}$ + M(surface)$\longrightarrow$M(surf)-$\underline{c}$-C_nH_n + M(surf)-H_{n-2m} appears to have some general applications within the metal surface chemistry of cyclic olefins and polyenes. The studies are being extended to other cycloalkenes and cyclopolyenes such as cyclobutene and cyclononene.

The absence of metal-metal bond scission in the course of $Re_2(CO)_{10}$ ligand substitution reactions has been definitively established.[2] Samples of pure $^{185}Re_2(CO)_{10}$ and $^{187}Re_2(CO)_{10}$ were prepared from the isotopically pure metals. Ligand substitution reactions with CO and with triphenylphosphine were effected at 150°C with a mixture of $^{185}Re_2(CO)_{10}$ and $^{187}Re_2(CO)_{10}$, and the products were analyzed by mass spectrometry. No cross labeled ($^{185}Re^{187}Re$) product was detected. Ligand substitution in $Re_2(CO)_{10}$ under thermal initiation proceeds by the reaction sequence: $Re_2(CO)_{10} \rightleftharpoons[(-CO)] Re_2(CO)_9 \xrightarrow{L}$ product. In contrast, ligand substitution in $Re_2(CO)_{10}$ with photochemical initiation proceeded with Re-Re bond scission as established by the labeling technique.

* * *

1. M.-C. Tsai, J. Stein, C. M. Friend, and E. L. Muetterties, J. Am. Chem. Soc. 104, 3533 (1982).
2. A. M. Stolzenberg and E. L. Muetterties, J. Am. Chem. Soc. 105, 0000 (1983).

1982 PUBLICATIONS AND REPORTS

Refereed Journals

1. R. R. Burch, E. L. Muetterties, and V. W. Day, "Dehydrogenation of 1,3-Cyclohexadiene by {HRh[P(O-i-C_3H_7)$_3$]$_2$}$_2$: Preparation, Dynamic NMR and X-Ray Crystal Structure of [η^3-$CH_2C_6(CH_3)_5$]-Rh[P(O-i-C_3H_7)$_3$]$_2$," Organometallics 1, 188 (1982).

2. H. W. Choi and E. L. Muetterties, "The Synthesis and Chemistry of Binary Zerovalent Transition Metal Phosphite Complexes," J. Am. Chem. Soc. 104, 153 (1982).

3. V. W. Day, I. Tavanaiepour, S. S. Abdel-Meguid, J. F. Kirner, L.-Y. Goh, and E. L. Muetterties, "Modes of Phosphite Reactions with Transition-Metal Complexes. Crystal Structures of (η^5-C_5H_5)Cr[P(O)(OCH$_3$)$_2$](CO)$_2$[P(OCH$_3$)$_3$] and {[(CH$_3$HO)$_2$PMo[P(COH$_3$)$_3$]$_5^+$}(PF$_6^-$)," Inorg. Chem. 21, 657 (1982).

4. R. M. Wexler, M.-C. Tsai, C. M. Friend and E. L. Muetterties, "Pyridine Coordination Chemistry of Nickel and Platinum Surfaces," J. Am. Chem. Soc. 104, 2034 (1982).

†5. M.-C. Tsai and E. L. Muetterties, "Platinum Metal Surface Chemistry of Benzene and Toluene," J. Am. Chem. Soc. 104, 2534 (1982); LBL-13628.

†6. M.-C. Tsai, C. M. Friend, and E. L. Muetterties, "Dehydrogenation on Nickel and Platinum Surfaces. Conversion of Cyclohexane, Cyclohexene and Cyclohexadiene to Benzene," J. Am. Chem. Soc. 104, 2539 (1982); LBL-13629.

7. E.-B. Meier, R. R. Burch, E. L. Muetterties and V. W. Day, "A Dinuclear Rhodium Complex with an Octahedral Rhodium(III) and a Square Planar Rhodium(I) Center," J. Am. Chem. Soc. 104, 2661 (1982).

8. E. L. Muetterties, J. R. Bleeke, Z.-Y. Yang, and V. W. Day, "Complexity in the Reductive Reaction of $CoCl_2$ in the Presence of Phosphites. Isolation of Stable, Noninterconvertible Co[P(OCH$_3$)$_3$]$_4$ and Co$_2$[P(OCH$_3$)$_3$]$_8$ Molecules," J. Am. Chem. Soc. 104, 2940 (1982).

*This work was supported by the Director, Office of Energy Research, Office of Basic Energy Sciences, Chemical Sciences Division of the U.S. Department of Energy under Contract No. DE-AC03-76SF00098.

†9. M.-C. Tsai, J. Stein, C. M. Friend, and E. L. Muetterties, "Chemistry of Cyclic Olefins and Polyenes on Nickel and Platinum Surfaces," J. Am. Chem. Soc. 104, 3533 (1982); LBL-14860.

10. R. R. Burch, E. L. Muetterties, R. G. Teller, and J. M. Williams, "Selective Formation of Trans-Olefins by a Catalytic Hydrogenation of Alkynes Mediated at Two Adjacent Metal Centers," J. Am. Chem. Soc. 104, 4257 (1982).

11. E. L. Muetterties, "The Organometallic Chemistry of Metal Surfaces," Proceedings of the Xth International Conference on Organometallic Chemistry, 9-14 August, 1981, Pure and Applied Chemistry 54, 83 (1982).

†12. M.-C. Tsai, C. M. Friend, and E. L. Muetterties, "Dehydrogenation of Cyclohexane, Cyclohexene and Cyclohexadienes to Benzene on Nickel and and Platinum Surfaces," J. Va. Sci. Technol. 20, 533 (1982); LBL-13450.

13. E. L. Muetterties, "Metal Clusters," C&E News 60, No. 35, 28 (1982).

Other Publications

1. E. L. Muetterties, R. R. Burch, and A. M. Stolzenberg, "Molecular Features of Metal Cluster Reactions," Ann. Rev. Phys. Chem. 33, 89 (1982).

Invited Talks

1. E. L. Muetterties, "Hydrocarbon Reactions at Metal Centers," Centenary Lecture of the Royal Chemical Society, London, May 13, 1982.

2. E. L. Muetterties, "Cluster Chemistry," Stanford Research Institute, June 1982.

3. E. L. Muetterties, "Metal Surface Chemistry," American Vacuum Society Meeting, IBM Research Laboratories, June 1982.

4. E. L. Muetterties, "Cluster Chemistry," Stanford University, February 1982.

5. E. L. Muetterties, Plenary Lecturer, International Conference on Inorganic Stereochemistry, University of Reading, England, 1982.

* * *

†This work was supported by the Director, Office of Energy Research, Office of Basic Energy Sciences, Chemical Sciences Division of the U. S. Department of Energy under Contract No. DE-AC03-76SF00098.

All other publications were funded by the National Science Foundation under grants Nos. CHE-79-03933 and CHE-8000038.

h. High-Energy Oxiders and Delocalized-Electron Solids*

Neil Bartlett, Investigator

Introduction. This research group is concerned with the electron oxidation of aromatic molecules and other electron-delocalized materials. A major interest is graphite intercalation.[1] The factors that are important in bringing about intercalation are being assessed as are the changes in the properties (particularly the electrical conductivity) which accompany the intercalation. Since bands of the carbon-atom layers serve as the source (valence band) of electrons or sink (conduction band) for electrons, and substantial electron-oxidation or reduction can occur without disruption of the graphite-sheet structure, graphite intercalation compounds offer the prospect of appreciable electrochemical oxidation (or reduction) without catastrophic structural change.

For a clear understanding of intercalation, and its scope, it is essential to know the nature of the guest species (especially their charge), their concentration and, if possible, their disposition with respect to the carbon atoms of the infinite graphite sheet galleries within which they are contained. The mobility of the species within the graphite galleries is also of interest. Efforts are being made to determine how quickly and reversibly electrochemical oxidation and reduction of the graphite salts can be carried out. How far the graphite can be oxidized before structurally destructive and irreversible changes occur is also being investigated.

* * *

1. For recent review see LBL-13751.

1. AN ELECTROCHEMICALLY REVERSIBLE INTERCALATION OF GRAPHITE BY FLUORINE IN THE PRESENCE OF HYDROGEN FLUORIDE†

Tom Mallouk and Neil Bartlett

XPS spectra, of representative samples of the new graphite fluoride C_xF ($5 > x > 2$) reported last year, have been obtained in collaborative studies with Dr. K. O. Bomben and Professor W. L. Jolly. The spectra show that the carbon, even in the fluorine rich material of composition $C_2{\cdot}_5F$, is graphite-like. The F 1s binding energies show, however, that the fluorine is more negatively charged than in Teflon or carbon monofluoride, although less so than the fluorine in LiF. ^{13}C NMR studies, in collaboration with the Colorado State University NMR Regional Center, also show that much of the carbon of C_xF remains graphite-like, and that the remaining carbon (presumably that bound to F) is chemically shifted beyond carbon in KelF, thus also indicating that the F in C_xF is highly negative. These findings and the apparent preservation of the planarity of the carbon atom sheets (remarked upon in the previous report) indicate that the F atoms in C_xF may be linked to the C atoms two at a time, one F atom above and one below the C atom in a carbon-atom sheet. The bonding orbital in such a three-center four-electron F-C-F bond has the symmetry appropriate for π bonding to its graphite environment. Thus the remarkable constancy of the in-plane C-C distance over the entire C_xF composition range (see Table 1.1) is accounted for. Also the occupied nonbonding orbital has no carbon-orbital component and thus should bestow high negative charge on the F ligands. This model accounts for all of the observed properties, but it remains to be established. (Attempts to obtain J-resolved ^{13}C NMR spectra that are in progress may provide the proof.)

Another indicator of unusual bonding of fluorine to carbon comes from the finding that the intercalation of graphite by fluorine in the presence of HF is reversible. The intercalation can be reversed chemically or electrochemically, when x in C_xF exceeds 2.3. By using a large excess of graphite as the reducing agent, a high-stage graphite hydrofluoride is obtained but electrochemical reduction provides for complete conversion back to graphite:

$$C_xF + e^- \rightarrow xC + F^-$$

Material of composition C_xF may also be synthesized electrochemically to $x \approx 2.6$ (below which value of x the C_x F becomes highly resistive).

Table 1.1. Some Physical Properties of C_xF.

C/F ratio	a_o (Å)	c_o (Å)	ρ (Ω - cm)
5.22(5)[a]	2.456(3)[a]	5.22(2)[a]	$>8 \times 10^{-3}$
3.67	2.459	5.36	8×10^{-1}
3.20	2.456	5.45	3×10^{0}
2.70	2.460	5.71	2×10^{1}
2.42	2.459	6.02	1×10^{3}
2.15	2.468	6.22	1×10^{7}
1.94	2.464	6.45	2×10^{7}

[a]Numerals in parentheses are estimated standard deviations for the last place quoted. The e.s.d. for each set of numbers in a vertical column is approximately constant.

*This work was supported by the Director, Office of Energy Research, Office of Basic Energy Sciences, Chemical Sciences Division of the U.S. Department of Energy under Contract No. DE-AC03-76SF00098.

Such syntheses have used lead difluoride (which is a good F^- ion conductor) as the source of F^- and HF/NaF solution as electrolyte. Hence, the system $C_xF|HF\text{-}NaF|M$, where M is a metal not oxidized by H^+ (e.g., Pb, Ag, Cu, Hg), affords a secondary battery. Open circuit voltages of C_xF against $Pb|PbF_2$ have been determined (x in parentheses): (3.7), 2.03; (2.7), 2.20; (2.5), 2.38 volts.

Thus, C_xF promises to exhibit novel F bonding to carbon (with perhaps five coordinate carbon) and also is a highly reversible and powerful oxidizing electrode material.

* * *

†Based on LBL-13815 and LBL-15173.

2. A THERMODYNAMIC THRESHOLD FOR THE INTERCALATION OF GRAPHITE BY HEXAFLUOROSPECIES MF_6^-†

Guy L. Rosenthal and Neil Bartlett

Previous work in these laboratories[1,2] had indicated that the intercalation of graphite by hexafluorides required an oxidizing potential greater than that afforded by ReF_6 but less than that of hexafluorides such as OsF_6, IrF_6, and PtF_6. The electron affinity threshold appeared to be close to 120 kcal $mole^{-1}$, but that this was a thermodynamic threshold and not a kinetic one was not determined. Studies of the hexafluoroarsenate and hexafluorophosphate salts of graphite have now established such a thermodynamic threshold.

The finding[3] that graphite intercalation by arsenic pentafluoride is associated with electron-oxidation of the graphite according to the half reaction:

$$3\ AsF_5 + 2e^- \rightarrow 2\ AsF_6^- + AsF_3 \qquad (1)$$

and that graphite was not similarly intercalated by phosphorus pentafluoride, which is physically similar to AsF_5, suggested that graphite intercalation by such fluorides depended primarily on the oxidizing potential of the fluoride. Indeed earlier studies[2] in these laboratories had established the synthesis of graphite hexafluorophosphates $C_x^+PF_6^-$ by exploiting the very favorable energy of formation of PF_6^- via the reaction:

$$PF_{5(g)} + 1/2\ F_{2(g)} + e^- \rightarrow PF_6^-{}_{(g)} \quad . \qquad (2)$$

In the present work second and higher stage $C_x^+PF_6^-$ salts have been reduced to graphite by phosphorus trifluoride:

$$PF_{3(g)} + 2\ PF_6^-{}_{(g)} \rightarrow 3\ PF_{5(g)} + 2e^- \quad . \qquad (3)$$

These reductions proceed spontaneously at 20°C and x-ray powder photographs of the reduced product are indistinguishable in d spacings, and almost as sharp as the photographs of the starting graphite. Clearly the phosphorus equivalent of reaction (1) does not occur because the free-energy change for PF_6^- and PF_3 formation is much less favorable than for arsenic species.

Since some AsF_5 can be retrieved [although always accompanied by AsF_3, formed according to (1)] from first stage compounds made from graphite and AsF_5, it appears that the conversion according to (1) is not complete in the first stage material. It is therefore probable that the electron affinity of AsF_5 [according to half reaction (1)] is close to threshold. Clearly the corresponding electron affinity for the phosphorus analogue must lie below such a threshold. These electron affinities have been evaluated. The threshold electron affinity for graphite intercalation by species similar in size and charge to PF_6^- must be greater than 86 kcal $mole^{-1}$ and perhaps close to the value of 121 kcal $mole^{-1}$ observed for the AsF_6^- case.

* * *

†Based on LBL-15499.

1. B. W. McQuillan, Ph. D. thesis, University of California, Berkeley, 1980.
2. B. W. McQuillan and Neil Bartlett, "Graphite Chemistry," in Intercalation Chemistry, edited by M. Stanley Whittingham and Allan J. Jacobson, Academic Press, New York, June 1982, p. 19-53.
3. N. Bartlett, R. N. Baigioni, B. W. McQuillan, A. S. Robertson and A. C. Thompson, J. C. S. Chem. Comm., p. 200 (1978).

3. INTERCALATION OF GRAPHITE BY SILICON TETRAFLUORIDE AND FLUORINE TO YIELD A SECOND-STAGE SALT $C_{24}SiF_5$†

G. L. Rosenthal, T. E. Mallouk, and Neil Bartlett

Assessment of the fluoride ion affinity of SiF_4 by Beauchamp and Murphy[1] places this affinity as slightly inferior to that of BF_3. Since the latter is intercalated readily by graphite in the presence of fluorine, it appeared probable on thermodynamic grounds that SiF_4 would be similarly intercalated in the presence of elemental fluorine. Such intercalation does occur at ~40°C with 1:1 $SiF_4|F_2$ mixture (~50 atm) to yield a second-stage compound [a_o = 2.46(1), c_o = 11.29(1) Å] of composition $C_{\sim 24}SiF_5$. This product interacts with excess PF_5, with quantitative displacement of SiF_4, to yield a first-stage fluorophosphate [a_o = 2.46(1), c_o = 7.65(1) Å] according to the equation:

$$C_{24}SiF_5 + 2\ PF_5 \rightarrow C_{24}PF_6 \cdot PF_5 + SiF_4 \qquad (1)$$

This first-stage fluorophosphate falls to a second-stage salt [a_o = 2.46(1), c_o = 10.87(1) Å] under vacuum:

$$C_{24}PF_6 \cdot PF_5 \xrightarrow{20°C} C_{24}PF_6 + PF_5 \qquad (2)$$

The second stage fluorophosphate can be prepared directly, but it is harder to obtain a pure second-stage material than via the $C_{24}SiF_5$ salt. $C_{24}SiF_5$, like $C_{24}PF_6$ [see Eq. (2)] is reduced to graphite by PF_3, at 20°C, thus indicating that the original $C_{24}SiF_5$ synthesis does not involve extensive C-F bond formation.

The ease of displacement of SiF_4 by superior or less volatile fluoroacids makes $C_{24}SiF_5$ a valuable reagent for the production of graphite salts, some of which are not otherwise accessible. Thus, the fluorophosphorane $C_6F_5PF_4$ cannot be directly intercalated by graphite in the presence of fluorine because it is fluorinated by elemental fluorine to yield PF_5 and C_6F_6. When added to $C_{24}SiF_5$, only SiF_4 is observed as a volatile and the fluorophosphorane is intercalated:

$$SiF_5^- + C_6F_5PF_4 \rightarrow C_6F_5PF_5^- + SiF_4$$

Thus, $C_{24}SiF_5$ acts as a mildly oxidizing fluoride source and should find wider application in graphite salt synthesis.

* * *

†Based on LBL-15457.

1. M. K. Murphy and J. L. Beauchamp, J. Am. Chem. Soc. 99, 4992 (1977).

1982 PUBLICATIONS AND REPORTS

LBL Reports

1. G. L. Rosenthal, T. E. Mallouk, and Neil Bartlett, "Intercalation of Graphite by Silicon Tetrafluoride and Fluorine to Yield a Second-Stage Salt $C_{24}SiF_5$," LBL-15457.

2. Thomas Mallouk and Neil Bartlett, "Reversible Intercalation of Graphite by Fluorine: A New Bifluoride, $C_{12}HF_2$, and Graphite Fluorides C_xF $(5 > x > 2)$," LBL-13815.

Other Publications

1. B. W. McQuillan and Neil Bartlett, "Graphite Chemistry" in Intercalation Chemistry, edited by M. Stanley Whittingham and Allan J. Jacobson, Academic Press, New York, 1982, p. 19-53; LBL-13751.

2. Neil Bartlett, "Electron-Oxidation of Aromatic Molecules, Layer-Form Boron Nitride and Graphite," in The Chemical Industry, edited by D. H. Sharp and T. F. West, Ellis Harwood Ltd., Chichester, England, 1982, p. 292-305; LBL-12475.

3. Neil Bartlett, "Rado," in Enciclopedia della Chimica, Vol. IX, 1982, p. 312-314, USES Edizioni Scientifiche, Firenze, Italy.

Invited Talks

1. Neil Bartlett, "Electron Oxidation of Aromatic Molecules and Other Electron Delocalized Systems," Dalton Division, Annual Chemical Congress, Royal Society of Chemistry, University of Aston, Birmingham, England, March 31, 1982.

2. Neil Bartlett, "Stabilizing High Oxidation States," National Main-Group Chemistry Workshop, Keystone, Colorado, June 1, 1982.

3. Neil Bartlett, "Heats of Formation of Fluoro-Anions and Their Relationship to Graphite Intercalation," 183rd American Chemical Society National Meeting, Kansas City, Missouri, September 12-17, 1982.

4. Neil Bartlett, "Stabilizing High-Oxidation State Cations," 10th International Symposium on Fluorine Chemistry, University of British Columbia, Vancouver, Canada, August 1-6, 1982.

5. Neil Bartlett, "Graphite Intercalation by Fluorides and Fluorine," Max-Planck-Institut für Festkörperforschung, Giessen, Germany, October 29, 1982.

i. Transition Metal Catalyzed Conversion of CO, NO, H_2, and Organic Molecules to Fuels and Petrochemicals*

Robert G. Bergman, Investigator

Introduction. The focus of current work on this project is the elucidation of the mechanisms by which metals induce the formation and cleavage of carbon-hydrogen (C-H) bonds. In one group of studies, a new set of C-H bond forming processes involving two metals has been found; some of this work was summarized last year. More recently, the remarkable discovery of an organometallic system in which the metal inserts into the C-H bonds of completely saturated hydrocarbons, leading directly to hydridometal alkyl complexes, has been made. Despite much investigation, this is the first such system to be reported, and current efforts are directed at exploration of the detailed chemical properties of this system and elucidation of the factors which make it work.

1. ACTIVATION OF C-H BONDS IN SATURATED HYDROCARBONS ON PHOTOLYSIS OF $(\eta^5\text{-}C_5Me_5)(PMe_3)IrH_2$. RELATIVE RATES OF REACTION OF THE INTERMEDIATE WITH DIFFERENT TYPES OF C-H BONDS, AND FUNCTIONALIZATION OF THE METAL-BOUND ALKYL GROUPS†

Andrew H. Janowicz and Robert G. Bergman

Irradiation of iridium dihydride 1 in hydrocarbon solvents neopentane and cyclohexane gives[1] the corresponding hydridoalkyl complexes 3. These are apparently formed by photochemical extrusion of H_2, producing reactive iridium intermediate 2; this complex then undergoes oxidative addition into the C-H bond in the hydrocarbon, leading to stable products 3a and 3b (see Scheme 1).

Recent results have (a) shown that intermediate 2 has astonishingly wide C-H insertion reactivity, (b) provided information about the mechanism of the reaction, (c) uncovered a thermal method for carrying out the C-H activation reaction, (d) provided information about the relative rates of reaction of 2 with different types of hydrocarbons, and (e) allowed development of a method for functionalization of the hydridoalkyl complexes 3.

The breadth of reactivity of this system has been demonstrated by carrying out the irradiation of 1 in a wide range of solvents. So far, every solvent investigated has proven to be reactive. Not all of these have been studied in detail, but competition experiments with several have allowed measurement of the relative rates at which the intermediate 2 reacts with different types of C-H bonds. Relative to cyclohexane (1.0), these are: benzene (4.0), cyclopropane (2.65), cyclopentane (1.6), neopentane (1.14), cyclodecane (0.23), cyclooctane (0.09). Intramolecular relative reactivity studies have also been carried out; for example, the aromatic hydrogens in p-xylene (1,4-dimethylbenzene) react 3.7 times faster than the methyl hydrogens. This type of experiment has provided evidence against a radical mechanism for the reaction, which should favor attack at the methyl group, generating the more stable benzylic radical. This mechanistic conclusion is reinforced by experiments using isotopically labeled solvents, and crossover experiments which demonstrate that the hydrogen and alkyl group found on

Scheme I

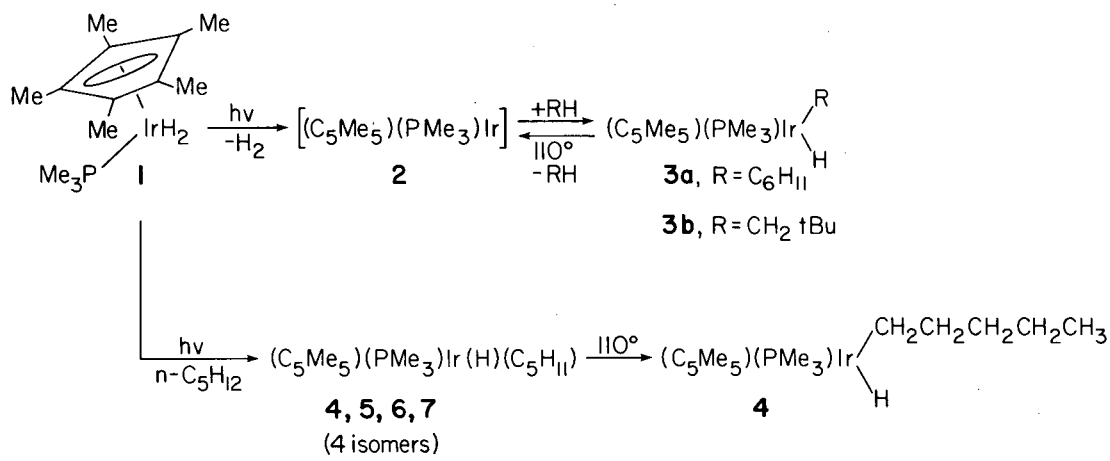

*This work was supported by the Director, Office of Energy Research, Office of Basic Energy Sciences, Chemical Sciences Division of the U. S. Department of Energy under Contract No. DE-AC03-76SF00098.

each molecule of product 3 were associated with one another in the starting hydrocarbon. A radical mechanism seems especially unlikely in view of the reactivity of the C-H bonds in cyclopropane, which have very high bond energy (106 kcal/mole).

The dihydride 1 is quite stable thermally. However, heating a given hydridoalkyl complex 3 to 110° causes reductive elimination of hydrocarbon, regenerating 2 which is then able to insert into the C-H bond of other hydrocarbons. In this way, the hydridoalkyl complexes may be used as starting materials for thermal C-H activation reactions. This thermal reaction has also allowed us to investigate the differences between kinetic and thermodynamic products formed in these reactions. For example, as shown in Scheme 1 irradiation of 1 in n-pentane at 0° gives four products (4-7), derived from insertion of 2 into each of the different types of C-H bonds in the hydrocarbon (two diastereomers are formed on insertion into the C-H bonds at C-2). Heating this mixture to 110°, where reversible elimination and C-H readdition occur, results in conversion to the thermodynamic product, which is solely the primary hydridoalkyl complex 4. Thus, quite selective activation of a primary C-H bond in a linear hydrocarbon can be achieved.

Functionalization of the alkyl group of complexes 3 has been carried out using the multistep sequence illustrated in Scheme 2. Conversion of 3 to the corresponding bromoalkyl complexes 8 is effected smoothly using $CHBr_3$. Treatment of this material with $HgCl_2$ results in transfer of the alkyl group to mercury; halogenation of the resulting alkylmercurial 9 delivers the corresponding alkyl halide 10 in good yield. This sequence therefore provides an overall method for stoichiometric conversion of a hydrocarbon into an alkyl halide, using a method which avoids free radical intermediates.

Scheme 2

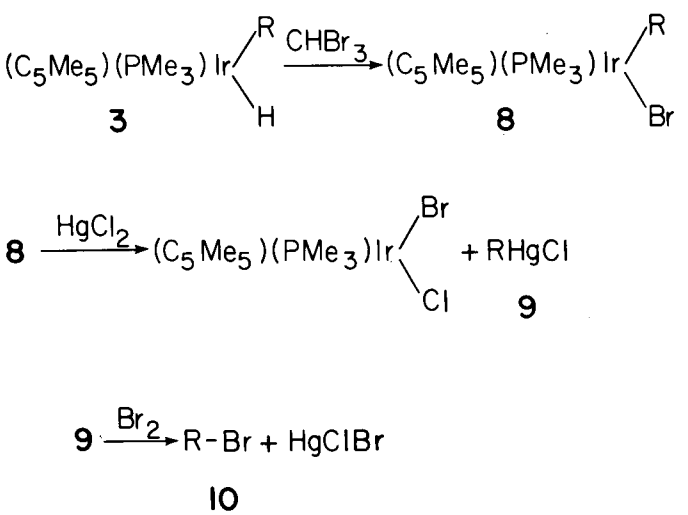

* * *

†Brief version of LBL-14421 and LBL-15145.

1. A. H. Janowicz and R. G. Bergman, J. Am. Chem. Soc. 104, 352 (1982).

2. WORK IN PROGRESS

On the iridium system summarized above, research continues aimed at understanding the factors which make the system uniquely reactive toward intermolecular attack on saturated hydrocarbons. Investigation of the reactions of intermediate 2 with a wider range of organic substrates is being explored, and special attention is being paid to those (e.g., methanol and certain dienes) which seem to give unusual products. Analogs of 1 which contain phosphine ligands other than PMe_3 have been synthesized, and their hydrocarbon activation reactions are being studied. Some of these ligands have electronic properties very different from those of PMe_3 and PPh_3. In others longer alkyl chains, capable of both inter- and intramolecular reaction, are present. Finally, a successful method for preparing the corresponding rhodium dihydride $(\eta^5\text{-}C_5Me_5)(PMe_3)RhH_2$ has been developed. It, too, effects C-H activation reactions of completely saturated hydrocarbons, although in this case the products are stable only at low temperatures. This system is now being explored in detail.

1982 PUBLICATIONS AND REPORTS

Refereed Journals

1. A. H. Janowicz and R. G. Bergman, "C-H Activation in Completely Saturated Hydrocarbons: Direct Observation of M + R-H → M(R)(H)," J. Am. Chem. Soc. 104, 352 (1982); LBL-13402.

†2. K. H. Theopold, W. H. Hersh, and R. G. Bergman, "Binuclear Metallacycles: Organometallic Ring Systems Containing Two Metal Centers," Isr. J. Chem. 22, 27 (1982).

†3. K. H. Theopold and R. G. Bergman, "Carbon-to-Carbon Migration of the Dimetallic Group in Dinuclear Cobalt Alkylidene Complexes," Organometallics 1, 219 (1982).

‡4. K. H. Theopold, P. N. Becker, and R. G. Bergman, "Asymmetric Induction in Reactions Employing Enolates Generated from Cyclic Organotransition-Metal Acyl Complexes," J. Am. Chem. Soc. 104, 5250 (1982).

‡5. K. H. Theopold and R.G. Bergman, "Synthesis, Crystal and Molecular Structure, and Chemistry of (μ-Trimethylene)bis(η-cyclopentadienyl)bis-(μ-carbonyl)dicobalt, a Five-Membered Dicobaltacycle," Organometallics 1, 1571 (1982).

LBL Reports

1. A. H. Janowicz, Ph. D. Thesis, "A Mechanistic Study of the Formation and Cleavage of C-H Bonds: Hydrogenolysis of M-C Bonds/C-H Bond Activation of Saturated Hydrocarbons," LBL-14421.

2. A. H. Janowicz and R. G. Bergman, "Activation of C-H Bonds in Saturated Hydrocarbons on Photolysis of $(\eta^5\text{-}C_5Me_5)(PMe_3)IrH_2$. Relative Rates of Reaction of the Intermediate with Different Types of C-H Bonds, and Functionalization of the Metal-Bound Alkyl Groups," LBL-15145.

Invited Talks

1. R. G. Bergman, "Formation of New Bonds to Carbon Using Organotransition Metal Complexes," Department of Chemistry, University of North Carolina, January 14, 1982; Department of Chemistry, University of Arizona, Tucson, Arizona, March 15, 1982; Department of Chemistry, University of Wisconsin at Madison, April 2, 1982; and Department of Chemistry, University of California, Riverside, October 13, 1982.

2. R. G. Bergman, "Homogeneous Intermolecular Oxidative Addition of Iridium to Single C-H Bonds in Completely Saturated Hydrocarbons," Shell Development Company Westhollow Research Center, Houston, Texas, March 24, 1982; 65th Chemical Institute of Canada Conference, Toronto, Canada, June 1, 1982; 28th Stanford University Industrial Affiliates Symposium on Homogeneous Catalysis, Stanford University, California, July 1, 1982, and Microsymposium on Kinetics and Mechanism, 3rd International Symposium on Homogeneous Catalysis, Milan, Italy, September 1, 1982.

3. R. G. Bergman, "C-H Activation," Catalytica Associates Inc., Santa Clara, California, April 19, 1982.

4. R. G. Bergman, general lectures on Reaction Mechanisms, A. C. S. Intensive Refresher Course in Organic Chemistry, University of Wisconsin, Madison, Wisconsin, June 23-25, 1982.

5. R. G. Bergman, "Asymmetric Induction in Carbon-Carbon Bond Forming Reactions Using Cobalt Metallacycles," Gordon Research Conference on Stereochemistry, Plymouth State College--North, Plymouth, New Hampshire, June 29, 1982.

6. R. G. Bergman, lectures on: (a) Migratory Insertion Reactions, (b) The Oxidative Addition Reaction, and (c) Metallacycles, University of Utah, Organometallic Chemistry Workshop, Salt Lake City, September 21-24, 1982.

7. R. G. Bergman, "Transformations of Organic Compounds Induced by Transition Metal Complexes," Department of Chemistry, Oberlin College, Oberlin, Ohio, November 8, 1982.

8. R. G. Bergman, "The Use of Organotransition Metal Complexes in the Formation of Carbon-Nitrogen Bonds," Dyson Perrins Laboratory, University of Oxford, England, November 29, 1982.

9. R. G. Bergman, "C-H Activation of Saturated Hydrocarbons Using Soluble Iridium Complexes," Meeting of the Royal Society of Chemistry--Dalton Division, London, England, November 30, 1982 and Institut de Chemie des Substances Naturelles, Centre National de la Recherche Scientifique, Gif-sur-Yvette, France, December 1, 1982.

10. R. G. Bergman, "Intermolecular Activation of C-H Bonds in Saturated Hydrocarbons Using Soluble Iridium Complexes," Table Ronde Roussel Uclaf, Direction des Relations Scientifiques, Paris, France, December 2-3, 1982.

11. R. G. Bergman, "Activation of C-H Bonds in Completely Saturated Hydrocarbons Using Soluble Iridium Complexes," Institut de Chimie, Université Louis Pasteur de Strasbourg, France, December 6, 1982 and Laboratoire de Chimie de Coordination Organique, Université de Rennes, France, December 8, 1982.

* * *

†Supported by the National Science Foundation (Grant No. CHE79-26291).

‡Supported by the National Institutes of Health (Grant No. GM-25459).

5. Chemical Engineering Sciences

a. High-Pressure Phase Equilibria in Hydrocarbon-Water (Brine) Systems*

John M. Prausnitz, Investigator

Introduction. The need for new sources of energy has produced interest in recovery of natural gas from aquifers in Louisiana, Texas, and the Gulf of Mexico Region. These aquifers contain large amounts of natural gas (mostly methane) in contact with water or brine. It is estimated that at least a 50-year supply of natural gas is recoverable at current annual U.S. consumption rates of natural gas.[1]

Pressures in the aquifers may be as high as 1500 bar. Temperatures may be as high as 270°C. At present, it is not economic to mine these reservoirs but, in view of the large deposits, there is much incentive to make such mining attractive. The purpose of this project is to obtain some of the fundamental physicochemical information needed to design such mining operations. For efficient recovery of natural gas from aquifers, high-pressure, vapor-liquid equilibrium data are required. In addition, these data are useful for estimating how much natural gas is present in the aquifers. Our goals are twofold: First, we seek to study experimental high-pressure, vapor-liquid equilibria pertinent to natural-gas aquifers. Second, we want to represent the phase equilibria with a molecular-thermodynamic model.

* * *

1. R. A. Kerr, Science 207, 1455 (1980).

1. EXPERIMENTAL HIGH-PRESSURE VAPOR-LIQUID EQUILIBRIUM

Jack Wong, Gabriele Di Giacomo, Eldon R. Larsen, Georg Roessling, and John M. Prausnitz

Experimental high-pressure, phase-equilibrium data for natural-gas/brine mixtures are scarce. We have designed and built a high-pressure equilibrium cell for pressures to 2000 bar and temperatures to 400°C. The cell is fabricated of INCONEL (a high-strength, corrosion- resistant, nickel-chromium alloy); all other wetted components are cold-worked 316-stainless steel. At present, we are studying the methane/water system. The methane/water mixture is stirred with a chromium-plated, cylindrical, magnetically driven mixer. The cell and related tubing are enclosed in a constant-temperature air bath. After equilibration, small samples of each phase (less than 100 μl each) are removed from the 165-ml cell under carefully controlled conditions to avoid changes in composition. Samples of the vapor and liquid phases are taken at separate times to disturb the equilibrated phases as little as possible during sampling. The sample of the liquid phase is flashed completely to form a vapor. The high-pressure, vapor-phase sample is expanded to low pressure. The pressure on each sample after these operations is in the range 10-40 psia. Subsequent to the expansion-flash step, the samples are analyzed using a gas chromatograph equipped with a gas-sample valve.

We have measured high-pressure solubilities of methane in water at 140 and 160°C and found the data to agree with those of Sultanov et al.[1] Experimental work continues for the methane/water system, toward extension to the methane/water/salt system.

* * *

1. R. G. Sultanov, V. G. Skripka, and A. Yu. Namiot, Gazov. Prom. 17, 6 (1972).

2. MODELING OF HIGH-PRESSURE PHASE EQUILIBRIA

Eldon R. Larsen and John M. Prausnitz

For low-molecular-weight, nonpolar fluids (e.g., light hydrocarbons), simple equations of state correlate vapor pressure and some volumetric properties reasonably well. Polar fluids (notably water) cannot be treated so easily. For mixtures, the equation of state must be written as a (non-obvious) function of composition.

We use a method that allows superposition of the residual thermodynamic properties of pure methane and of pure water. This method employs the theorem of corresponding states with molecular shape factors. These shape factors are constants for simple fluids, but for polyatomic fluids, they may be functions of temperature and/or density. We apply reasonable mixing rules to the superimposed properties to obtain residual properties for the mixture. From these properties, we calculate phase equilibria.

The shape factors for methane are constants. For water, one of the shape factors is constant, one varies with temperature, and one varies with temperature and density. Using reasonable mixing rules, we are able to model well phase equilibria for the water/methane system to high pressures and temperatures. This suggests that a useful, first basis is now available for calculating phase equilibria for natural-gas aquifers.

*This work was supported by the Director, Office of Energy Research, Office of Basic Energy Sciences, Chemical Sciences Division of the U.S. Department of Energy under Contract No. DE-AC03-76SF00098.

1982 PUBLICATIONS AND REPORTS

Refereed Journals

1. W. B. Whiting and J. M. Prausnitz, "Equations of State for Strongly Nonideal Fluid Mixtures: Application of Local Compositions Toward Density-Dependent Mixing Rules," Fluid Phase Equilibria 9, 119 (1982); LBL-14012 and LBL-14013).

†2. G. M. Lobien and J. M. Prausnitz, "Infinite-Dilution Activity Coefficients From Differential Ebulliometry," Ind. Eng. Chem. Fund. 21, 109 (1982).

†3. G. M. Lobien and J. M. Prausnitz, "Correlation for the Ratio of Limiting Activity Coefficients for Binary Liquid Mixtures," Fluid Phase Equilibria 8, 149 (1982).

4. V. Brandani and J. M. Prausnitz, "Two-Fluid Theory and Thermodynamic Properties of Liquid Mixtures: General Theory," Proc. Natl. Acad. Sci. (USA) 79(14), 4506 (1982).

5. V. Brandani and J. M. Prausnitz, "Two-Fluid Theory and Thermodynamic Properties of Liquid Mixtures: Application to Hard Sphere Mixtures," Proc. Natl. Acad. Sci. (USA) 79(16), 5103 (1982).

6. V. Brandani and J. M. Prausnitz, "Two-Fluid Theory and Thermodynamic Properties of Liquid Mixtures: Application Simple Mixtures of Non-electrolytes," Proc. Natl. Acad. Sci. (USA) 79(18), 5729 (1982).

‡7. E. M. Pawlikowski, J. Newman, and J. M. Prausnitz, "Phase Equilibria for Aqueous Solutions of Ammonia and Carbon Dioxide," IEC Proc. Des. Dev. 21, 764 (1982).

§8. R. Rittman, H. Knapp, and J. M. Prausnitz, "Enthalpy and Dew-Point Calculations for Aqueous Gas Mixtures Produced in Coal Gasification and Similar Processes," IEC Proc. Des. Dev. 21, 695 (1982).

¶9. E. C. Bishop, W. Popendorf, D. Hanson, and J. M. Prausnitz, "Predicting Relative Vapor Ratios for Organic Solvent Mixtures," Am. Ind. Hyg. Assoc. J. 43(9), 656 (1982).

Other Publications

‡1. E. M. Pawlikowski, J. Newman, and J. M. Prausnitz, "Vapor-Liquid Equilibrium Calculations for Aqueous Mixtures of Volatile, Weak Electrolytes and Other Gases for Coal Gasification Processes," Chem. Eng. Thermodynamics 1982, edited by Stephen A. Newman, Ann Arbor Science Publishers.

2. H. Knapp, R. Doering, L. Oellrich, U. Ploecker, and J. M. Prausnitz, "Vapor-Liquid Equilibria for Mixtures of Low Boiling Substances," DECHEMA Chemistry Data Series, Vol. VI, 1982.

Invited Talks

1. D. Dimitrelis, and J. M. Prausnitz, "Thermodynamic Properties of Strongly Nonideal Fluid Mixtures From an Extended Quasi-Chemical Theory," Annual Meeting of American Institute of Chemical Engineering, Los Angeles, California, November 1982.

2. D. Dimitrelis, R. J. Topliss, and J. M. Prausnitz, "High-Pressure Vapor-Liquid Equilibria in Ternary Systems Containing Two Miscible Liquids and One Supercritical Gas," Industrial Physical Chemistry Group Meeting of the Royal Society of Chemistry, Faraday Division, Cambridge, United Kingdom, September 1982.

3. E. R. Larsen, "Molecular Thermodynamics of High-Pressure Phase Equilibria for the Methane/Water System," Department of Chemical Engineering Colloquium, University of California, Berkeley, California, June 1982.

4. E. R. Larsen, "High-Pressure Phase Equilibria for the Methane/Water System," Shell Research Co., Houston, Texas, March 1982; Exxon Production Research Co., Houston, Texas, March 1982; Union Carbide Corp., Charleston, West Virginia, March 1982; and CONOCO, Ponca City, Oklahoma, June 1982.

5. J. M. Prausnitz, "Molecular Thermodynamics for Chemical Process Design," Chemical Engineering Department, Cornell University, Ithaca, New York, December 1982; Chemical Engineering Department, State University of New York, Buffalo, New York, April 1982 (Union Carbide Lecture); and Chemical Engineering Department, University of Texas, Austin, Texas, April 1982 (van Winkle Lecture).

6. J. M. Prausnitz, "Recent Developments in Phase Equilibria for Petroleum Process Applications," Chemical Engineering Department, Shell Development Co., Houston, Texas, December 1982; and Chemical Engineering Department, Texaco Research Co., Houston, Texas, December 1982.

7. J. M. Prausnitz, "The Generalized van der Waals Model for Dense Fluids and Fluid Mixtures," Joint US and Chinese Meeting of American Institute of Chemical Engineering, Beijing, People's Republic of China, September 1982.

8. S. I. Sandler and J. M. Prausnitz, "The Generalized van der Waals Theory," Annual Meeting of American Institute of Chemical Engineering, Los Angeles, California, November 1982.

9. G. T. Caneba, D. S. Soong, and J. M. Prausnitz, "Diffusion and Sorption of Organic Volatiles in SBS Block Copolymers and SBR Random Copolymers," Annual Meeting of American Institute of Chemical Engineering, Los Angeles, California, November 1982.

10. J. M. Prausnitz, "Generalized van der Waals Theory as a Basis for Phase-Equilibrium Calculations in Chemical Engineering," American Society for Engineering Education, Santa Barbara, California, August 1982.

* * *

†This work supported by a grant from the National Science Foundation.
‡This work supported by a grant from the National Science Foundation and a Hertz Fellowship.
§This work supported by the Humboldt Foundation.
¶This work supported by a grant from the Operational Safety and Health Administration.

III Nuclear Sciences

A. Low-Energy Nuclear Science

1. Heavy Element Chemistry

a. Actinide Chemistry*

Norman M. Edelstein, Richard A. Andersen, Neil Bartlett, John G. Conway, Kenneth N. Raymond, Glenn T. Seaborg, Andrew Streitwieser, Jr., David H. Templeton, and Alan Zalkin, Investigators

Introduction. The central purpose of the project in heavy element chemistry is to study lanthanide and actinide materials in order to provide the basic knowledge necessary for their safe and economic use in present and future technology. The work encompasses related applied problems in actinide chemistry.

The program includes the preparation of new gaseous, liquid, and solid phases and studies of their physical and chemical properties. Techniques for characterization include x-ray diffraction, optical and vibrational spectroscopy, magnetic resonance, and magnetic susceptibility. Equilibrium and kinetic data for complex formation are measured. From these complementary studies, new insights into the structural and chemical principles of actinide compounds are obtained with which to design new synthetic schemes to produce new materials.

Specific sequestering agents for the actinides continue to be developed and tested. Similarities in the coordination chemistry, biological transport, and in vivo distribution properties of Fe(III) and Pu(IV), coupled with the observation that microbes produce specific and highly effective sequestering agents for Fe(III), have led to the preparation and characterization of a number of synthetic, biomimetic sequestering agents that specifically complex Pu(IV) and other actinide(IV) ions.

The fundamental chemistry of organoactinide, and related organolanthanide compounds, their reactions, structures and bonding, are being explored with the development of new materials, catalysts and reagents as the objective. Detailed spectroscopic studies are continuing on these new materials, on actinide ions diluted in host single crystals, and on the free atoms and free ions of the actinide series in order to understand their electronic structure and to compare the properties of the f transition series with the more thoroughly studied d transition series.

*This work was supported by the Director, Office of Energy Research, Office of Basic Energy Sciences, Chemical Sciences Division of the U. S. Department of Energy under Contract No. DE-AC03-76SF00098.

Specific Sequestering Agents for the Actinides

1. LIPOPHILIC ENTEROBACTIN ANALOGUES. TERMINALLY N-ALKYLATED SPERMINE/SPERMIDINE CATECHOLCARBOXAMIDES†‡

F.T. Weitl, K. N. Raymond, and P. W. Durbin

Linear polycatecholcarboxamide (LICAM) ligands and their sulfonated (LICAMS) or carboxylated (LICAMC) derivatives are very effective in removing Pu(IV) from mice, when administered intravenously or intraperitoneally. In order to increase the lipophilicity of such compounds and thus alter their distribution in vivo, a number of N-alkylated LICAM derivatives have been prepared.

The selective alkylation of the terminal nitrogen of spermine and spermidine have been accomplished by reaction of the amine with an appropriate aldehyde or ketone to form a Schiff base. The latter was catalytically reduced with hydrogen. Reaction of the resulting alkylated amine with 2,3-dimethoxybenzoyl chloride and subsequent deprotection was carried out using previously reported procedures (Fig. 1.1).

The effects of these bulky groups on the kinetics and thermodynamics of complex formation, in vivo organ distribution, and toxicity are currently under investigation. A significant preliminary result is that the N-alkylated LICAM derivations are primarily cleared via a hepatic pathway, in contrast to the renal clearance of more polar chelating agents.

* * *

†Brief version of LBL-12140; J. Org. Chem. 46, 5234 (1981).

‡This work was partially supported by the National Institutes of Health.

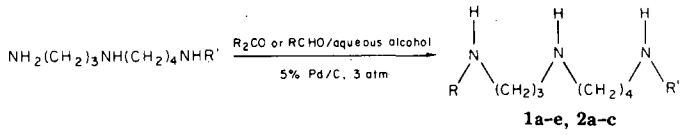

1a-e, 2a-c

no.	R	R'
1a	$(CH_3)_2CH$	$(CH_3)_2CH$
1b	$CH_3(CH_2)_9$	$CH_3(CH_2)_9$
1c	$C_6H_5CH_2$	$C_6H_5CH_2$
1d	C_6H_{11}	C_6H_{11}
1e	$CH_3(CH_2)_7$	$CH_3(CH_2)_7$
2a	$(CH_3)_2CH$	$(CH_2)_3NHCH(CH_3)_2$
2b	$CH_3(CH_2)_9$	$(CH_2)_3NH(CH_2)_9CH_3$
2c	C_6H_{11}	$(CH_2)_3NHC_6H_{11}$

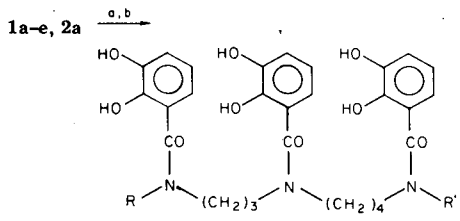

3a, R = R' = $(CH_3)_2CH$
3b, R = R' = $CH_3(CH_2)_9$
3c, R = R' = $C_6H_5CH_2$
3d, R = R' = C_6H_{11}
3e, R = R' = $CH_3(CH_2)_7$
4a, R = $(CH_3)_2CH$; R' = $(CH_2)_3N(CO-$ 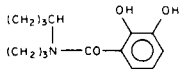

[a] (a) 3 (or 4) equiv of DMBCl followed by 6 (or 8) equiv of NEt_3/THF. [b] Excess BBr_3/CCl_4 or CH_2Cl_2 followed by hydrolysis.

Fig. 1.1. Preparation of N-alkylated spermine/spermidine catecholcarboxamides. (XBL 831-7601)

2. FERRIC ION SEQUESTERING AGENTS. SELECTIVITY OF SULFONATED POLY(CATECHOYLAMIDES) FOR FERRIC ION†‡

M. J. Kappel and K. N. Raymond

Although the synthetic chelating agents EDTA and DTPA effectively remove toxic metals from the body, they also bind divalent calcium and zinc and must be administered as the calcium or zinc salts to avoid depletion of these elements. Even then, toxicity results when these ligands are administered to test animals over prolonged periods. Thus, there is a need for development of chelating agents that are capable of selectively chelating the toxic metal without removing biologically significant divalent metal ions. For catechoylamide ligands to be considered as possible alternatives to chelating agents presently in use, the evaluation of their selectivity for ferric ion or Pu(IV) is important.

Potentiometric titrations were used to determine the stabilities of Ca(II), Mg(II), Cu(II), Zn(II), Ni(II), and Co(II) with several sulfonated catechoylamide ligands: a bis(catechoylamide), 1,6-bis(2,3-dihydroxy-5-sulfobenzoyl)-1,6-diazahexane (4-LICAMS); a tris(catechoylamide), 1,3,5-tris(2,3-dihydroxy-5-sulfobenzoyl)tris(aminomethyl) benzene (MECAMS); a tetrakis(catechoylamide), 1,5,10,14-tetrakis(2,3-dihydroxy-5-sulfobenzoyl)-1,5,10,14-tetraazatetradecane (3,4,3-LICAMS). Structural formulas for these ligands are shown in Figure 2.1.

For all ligands studied the titrations demonstrated the following relative stabilities: Fe(III) >> Cu(II) > Zn(II) > Ni(II), Co(II) > Mg(II) > Ca(II). These poly(catechoylamide) ligands possess great selectivity for ions of high charge to ionic radius ratios such as Fe(III) and Pu(IV); their selectivity is similar to that shown by desferrioxamine B, the current chelating agent for ion overload, and is greater than that demonstrated by DTPA, the chelating agent most often used for plutonium and other heavy-metal ion decorporation.

* * *

†Brief version of LBL-14680; Inorg. Chem. 21, 3437 (1982).

‡This work was partially supported by the National Institutes of Health.

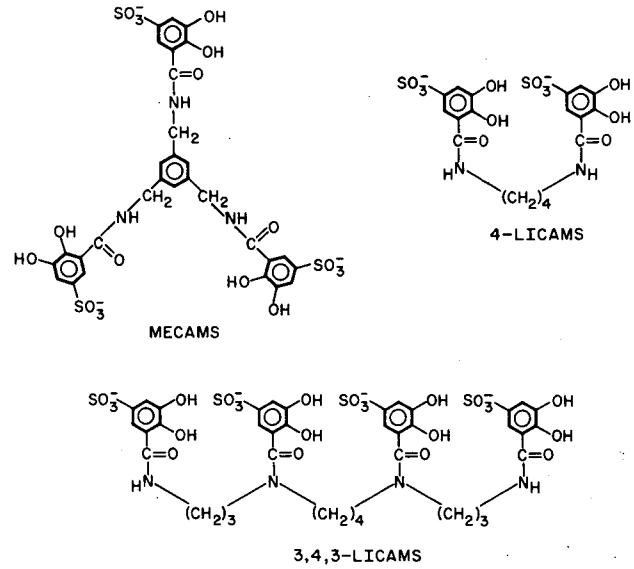

Fig. 2.1. Structural formulas of sulfonated catechoylamide ligands. (XBL 8010-12608)

3. GALLIUM AND INDIUM IMAGING AGENTS†‡

S. M. Moerlein,§ M. J. Welch,§ V. L. Pecoraro, G. B. Wong, and K. N. Raymond

^{67}Ga and ^{111}In have been used extensively as tumor imaging agents. Because these are group IIIB elements with charges and coordination chemistry similar to Fe(III), the catecholamide sequestering agents developed for that ion [and Pu(IV)] have also been investigated as Ga- and In-binding radiopharmaceuticals.

The solution equilibria for the reactions of Ga(III) and In(III) with the hexadentate ligands N,N',N"-tris(2,3-dihydroxy-5-sulfonatobenzyol)-1,3,5-tris(aminomethyl)benzene (MECAMS) and N,N',N"-tris-(2,3-dihydroxy-5-sulfonatobenzoyl)-1,5,10-triazadecane (3,4-LICAMS), and the bidentate catechol N,N-dimethyl-2,3-dihydroxy-5-sulfonatobenzamide (DMBS) have been determined by spectrophotometric and potentiometric titrations. The effect of 3,4-LICAM-C (see Fig. 3.1) on the biodistribution and clearance of ^{67}Ga was determined in Sprague-Dawley rats.

Both Ga(III) and In(III) are coordinated by three catecholate groups at high pH and have formation constants of the order $\beta_{110} = 10^{38} M^{-1}$. As the acidity of the medium is increased, the metal complexes of the hexadentate sequestering agents undergo protonation reactions. In contrast, protonation of the $M^{III}(DMBS)_3$ complexes results in dissociation of a catechol moiety to form $M^{III}(DMBS)_2$. LICAM-C complexed ^{67}Ga *in vivo* and hastened the renal clearance of the nuclide. The gallium concentration was decreased in all organs, with exception of the liver and spleen, where we suggest that hydroxide precipitates interfere with gallium sequestration by 3,4-LICAM-C. The gallium in abscess tissue was only slightly affected, giving rise to an increase in the ^{67}Ga abscess-to-soft-tissue concentration ratio when 3,4-LICAM-C is administered. Dosimetry calculations show that the siderophore decreases the radiation burden from ^{67}Ga citrate.

* * *

†Brief version of Nucl. Med. 23, 501 (1982), and Inorg. Chem. 21, 2029 (1982).
‡This work was partially supported by the National Institutes of Health.
§The Edward Mallinckrodt Institute of Radiology, Washington University School of Medicine, St. Louis, MO 63110.

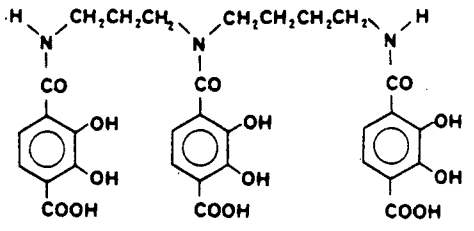

Fig. 3.1. Chemical structure of 3,4-LICAM-C. (XBL 831-7602)

4. SYNTHESIS AND STRUCTURAL CHEMISTRY OF TETRAKIS(THIOHYDROXAMATO)HAFNIUM(IV) IN $Hf(CH_3C_6H_4(S)N(O)CH_3)_4 \cdot C_2H_5OH$†‡

K. Abu-Dari and K. N. Raymond

Determination of the coordination geometry of the unconstrained tetrakis(bidentate)metalate(IV) complexes is a fundamental component in the design of an octadentate chelating agent that incorporates four such functionalities to form an optimum metal coordination environment.

While we have prepared thiohydroxamate complexes of Th(IV), no crystals suitable for structure analysis have been obtained. Instead, we report the synthesis and structural characterization of the hafnium complex, the title compound.

The structure of the compound tetrakis-(N-methyl-p-thiotolylhydroxamato)hafnium(IV) displays a bicapped trigonal prismatic coordination polyhedron, a polyhedron not observed for the catecholato and hydroxamato complexes studied to date (see Fig. 4.1).

* * *

†Brief version of LBL-13173; Inorg. Chem. 21, 1676 (1982).
‡This work was partially supported by the National Institutes of Health.

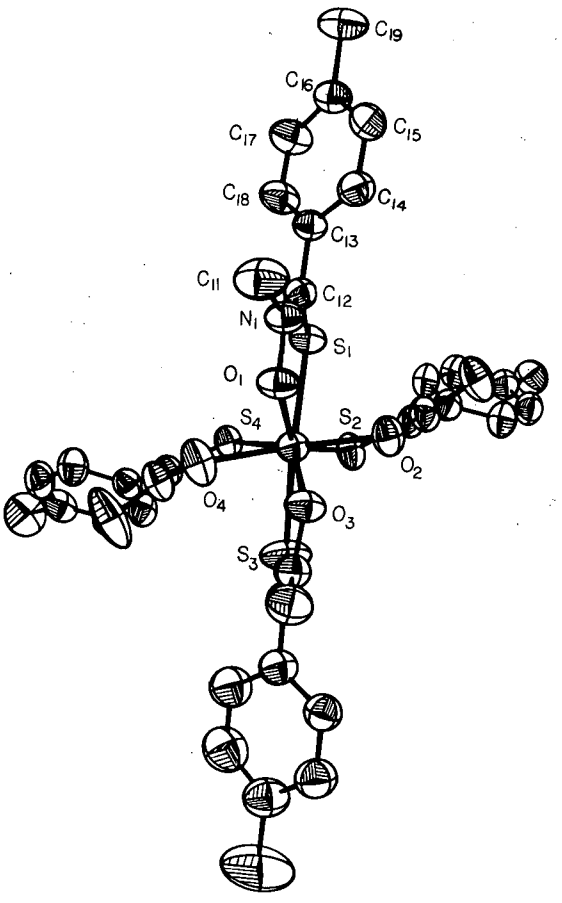

Fig. 4.1. Perspective view and atom numbering scheme for tetrakis(N-methyl-p-thiotolylhydroxamato)hafnium(IV). (XBL 799-11358)

Synthetic and Structure Studies of Actinides and Other Compounds

1. ORGANOURANIUM COMPLEXES OF PYRAZOLE AND PYRAZOLATE. SYNTHESIS AND X-RAY STRUCTURES OF $U(C_5Me_5)_2Cl_2$ ($C_3H_4N_2$), $U(C_5Me_5)_2Cl(C_3H_4N_2)$, AND $U(C_5Me_5)(C_3H_3H_2)_2$†

C. W. Eigenbrot, Jr. and K. N. Raymond

As part of our effort to create, examine and explain structural and magnetic probes of the bonding in organolanthanide and actinide compounds, we have sought the synthesis and magnetic characterization of an appropriate dimeric uranium complex. Our recent report of the synthesis and structure of $UCp_3(pz^-)$ (pz^- = pyrazolate) revealed that our attempt to form a dimer (based on a precedent in titanium chemistry, $[TiCp_2(pz^-)_2]$) resulted instead in the formation of a monomeric species, allowing us to characterize a new mode of pyrazolate bonding. To investigate what role, if any, steric factors played in the formation of the monomeric compound and to learn more about the pyrazolate ion as a ligand, we have adjusted the size and number of the $Cp(C_5H_5)$ ligands. We anticipated that a reduction in the total steric bulk of the other ligands might lead to the formation of one or more dimeric species.

The compound $UCp_2"Cl_2$ (Cp" = C_5Me_5) has proven to be a useful starting material for other studies but does not produce dimers. Instead, the compounds $U(C_5Me_5)_2Cl(pz^-)$ and $U(C_5Me_5)_2(pz^-)_2$ are formed by the reaction between $U(C_5Me_5)_2Cl_2$ and stoichiometric amounts of $Na(pz^-)$. In the course of this study, an adduct of neutral pyrazole, $U(C_5Me_5)_2Cl_2(pz)$ (pz = pyrazole) was also characterized (Fig. 1.1).

The ^1H NMR, spectrum of $UCp_2"Cl_2(pz)$ reveals a fluxionality of the pyrazole ligand. The magnetic behavior of both $UCp_2"Cl_2(pz)$ and $UCp_2"(pz^-)$ is as one expects for U^{4+} ions. However, $UCp_2"(pz^-)_2$ does not exhibit similar magnetic behavior. Instead of decreasing with increasing temperature from an initial high value as the others, the susceptibility of $UCp_2"(pz^-)_2$ has its minimum at low temperature and increases as the temperature increases, until it becomes relatively invariant with temperature. The crystal structures are illustrated in Fig. 1.1.

* * *

†Brief version of LBL-13073; Inorg. Chem. 21, 2653 (1983).

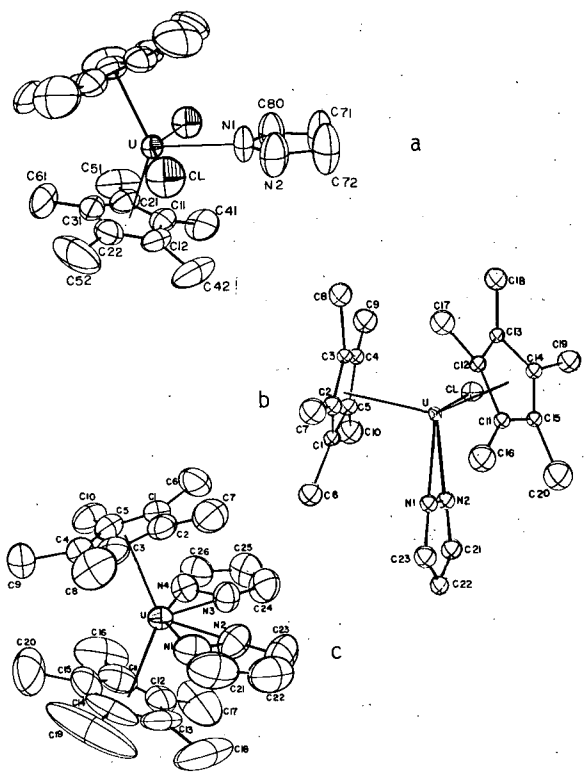

Fig. 1.1. ORTEP drawing of the molecular unit of: a) $UCp_2"Cl_2(pz)$; b) $UCp_2"Cl(pz^-)$; and c) $UCp_2"(pz^-)_2$. (XBL 831-7603)

2. SYNTHESIS AND CRYSTAL STRUCTURES OF THE TETRAKIS(METHYL-TRIHYDROBORATO) COMPOUNDS OF ZIRCONIUM(IV), THORIUM (IV), URANIUM(IV) AND NEPTUNIUM(IV)†

R. Shinomoto, E. Gamp, N. M. Edelstein, D. H. Templeton, and A. Zalkin

Actinide(IV) borohydrides are of considerable interest because of their high volatilities which could prove useful for the separation of various elements or for the separation of isotopes of the same element. These compounds exhibit two structural types. The first type, $M(BH_4)_4$ where M = Th, Pa, U, is a polymeric solid at room temperature with markedly different volatilities for various M, i.e., $(U(BH_4)_4$ readily sublimes under vacuum at 25°C vs ~150°C for $Th(BH_4)_4$. The second type of compound, where M = Np, Pu, is a volatile, chemically unstable liquid at room temperature, and a monomeric solid at ~10°C. In the second type the local symmetry about the metal

ion is tetrahedral and is like that found in the Zr and Hf borohydrides; however, the Np and Pu compounds crystallize in a different space group than the Zr and Hf compounds.[1] Schlesinger, et al. have reported the synthesis and isolation of two methyl derivatives of uranium borohydride, the mono and tetra(methylborohydride) derivatives, $U(BH_4)_3(BH_3CH_3)$ and $U(BH_3CH_3)_4$.[2] The mono(methyl borohydride) derivative and the tetra(methylborohydride) derivative were expected to be monomeric and of interest for spectroscopic and magnetic measurements. We have prepared and investigated the properties of some methylated borohydrides and report in this article the synthesis and crystal structure of $M(BH_3CH_3)_4$, M = Zr, Th, U, and Np.

The following synthesis gave satisfactory yields.

$$MCl_4 + 4LiBH_3CH_3 \xrightarrow{\text{chlorobenzene}} M(BH_3CH_3)_4 + 4LiCl.$$

The reaction described above was also carried out in ether and THF. These solvents were satisfac tory for $Zr(BH_3CH_3)_4$; but for $U(BH_3CH_3)_4$ and $Th(BH_3CH_3)_4$, adducts with the solvent were formed. Pure $U(BH_3CH_3)_4$ prepared in ether could be sublimed from its adduct, but $Th(BH_3CH_3)_4$ could not be sublimed adduct-free. Use of chlorobenzene as a solvent eliminated this problem. $Np(BH_3CH_3)_4$ was prepared only in chlorobenzene.

$Zr(BH_3CH_3)_4$, $Np(BH_3CH_3)_4$, $Th(BH_3CH_3)_4$, and $U(BH_3CH_3)_4$ are monomolecular in the crystalline state. The metal atom is tetrahedrally coordinated to the four methylborohydride groups of the molecule. Twelve hydrogen atoms from the BH_3 entities are in close contact to the metal atom, see Fig. 2.1. The $Zr(BH_3CH_3)_4$ and $Np(BH_3CH_3)_4$ structures consist of a body-centered packing of molecules. The coordination in these two compounds is similar to that found in their borohydrides. The Zr-B distances in $Zr(BH_3CH_3)_4$ and $Zr(BH_4)_4$ are 2.335(3) and 2.34(3) Å, respectively; the Np-B distances in $Np(BH_3CH_3)_4$ and $Np(BH_4)_4$ are 2.487(6) and 2.46(3) Å, respectively. The Th and U complexes are very near to being crystallographically isomorphous. The uranium compound is in a monoclinic space group, but in the Th compound the b axis is inclined to the a c plane by about 2°, which results in a triclinic space group. Whereas in the uranium compound the unit cell contains two crystallographically different but chemically identical molecules; the thorium compound contains four. Within these structures the M-B bond lengths deviate less than 2σ (for U) and 3σ (for Th) from their respective average, and the B-M-B angles in both structures are all within 3σ of being tetrahedral.

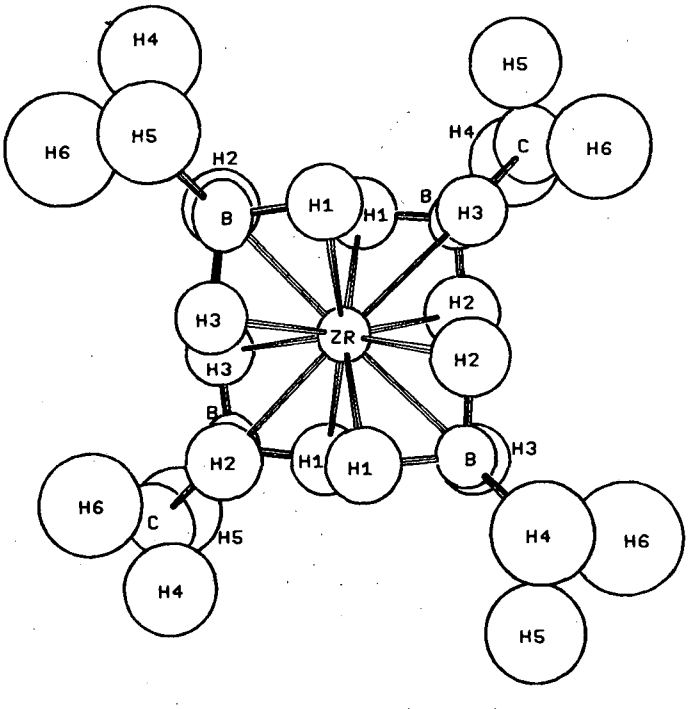

Fig. 2.1. ORTEP drawing of $Zr(BH_3CH_3)_4$. (XBL 812-8217)

The $(BH_3CH_3)_4$ sublimes easily under vacuum at ~40°C which makes it the most volatile compound of thorium known to date.

* * *

†Brief version of LBL-15090.

1. R. H. Banks, N. M. Edelstein, B. Spencer, D. H. Templeton, and A. Zalkin, J. Am. Chem. Soc., 102, 620 (1980).
2. H. I. Schlesinger, H. C. Brown, L. Horvitz, A. C. Bond, L. D. Tuck, and A. O. Walker, J. Am. Chem. Soc., 75, 222 (1953).

3. TERTIARY PHOSPHINE COMPLEXES OF THE f-BLOCK METALS; PREPARATION OF PENTAMETHYLCYCLOPENTADIENYL-TERTIARY PHOSPHINE COMPLEXES OF YTTERBIUM (II AND III) AND EUROPIUM (II). THE CRYSTAL STRUCTURE OF $Yb(Me_5C_5)_2Cl(Me_2PCH_2PMe_2)$†

T. D. Tilley, R. A. Andersen, and A. Zalkin

As a continuation of our synthetic studies on the phosphine complexes of the f-block metals, we have studied the reaction of bidentate phosphines with the divalent metallocenes, $M(Me_5C_5)_2(OEt_2)$ where M is Eu or Yb. These studies were undertaken with the view toward studying Lewis acid-base equilibria in these f-metal systems to provide a sound experimental basis for understanding the bonding. This is of considerable interest since tertiary phosphines were previously thought to be unable to form bonds to the f-elements.

The metallocenes $M(Me_5C_5)_2(OEt_2)$ react with $Me_2PCH_2CH_2PMe_2$ to give hydrocarbon insoluble $M(Me_5C_5)_2(Me_2PCH_2CH_2PMe_2)$, M = Eu or Yb. These complexes are sparingly soluble in Et_2O, but dissolve in tetrahydrofuran (THF) with displacement of the phosphine giving $M(Me_5C_5)_2(thf)$. The insoluble nature of the phosphine complexes suggests that they are polymeric, the phosphine acting as a bidentate, bridging ligand rather than as chelating ligand. Consistent with this hypothesis, reaction of $M(Me_5C_5)_2(OEt_2)$ with $Me_2PCH_2PMe_2$ gives the hydrocarbon soluble complexes $M(Me_5C_5)_2(Me_2PCH_2PMe_2)$. The Yb complex may be oxidized by $YbCl_3$ giving the trivalent complex, $Yb(Me_5C_5)_2Cl(Me_2PCH_2PMe_2)$. The crystal structure (Fig. 3.1) shows that the phosphine is

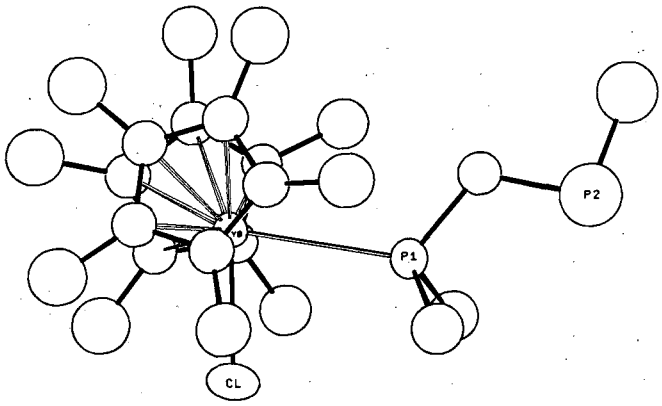

Fig. 3.1. ORTEP view down the centroids of the Cp rings. (XBL 823-8224)

acting as a monodentate ligand, with Yb-P, Yb-Cl, and Yb-C (ave.) bond distances of 2.94, 2.53, and 2.65 ± 0.03 Å, respectively.

It is of interest to note that $Me_2PCH_2PMe_2$ is displaced by diethyl ether in the divalent complexes showing that the coordinative affinity of the divalent lanthanides toward phosphine is rather poor relative to diethyl ether. This is in contrast to the observations in tetravalent uranium in which the phosphines are not displaced by oxygen or nitrogen donors.

* * *

†Brief version of LBL-14367.

4. PREPARATION AND CRYSTAL STRUCTURE OF BIS-[BIS(PENTAMETHYLCYCLOPENTADIENYL)YTTERBRIUM(III)]UNDECACARBONYLFERRATE, $[(Me_5C_5)_2Yb]_2[Fe_3(CO)_{11}]$: A COMPOUND WITH FOUR ISOCARBONYL (Fe-CO-Yb) INTERACTIONS†

T. D. Tilley and R. A. Andersen

We have continued our synthetic and bonding studies on $Yb(Me_5C_5)_2(OEt_2)$ to act as a single electron-transfer reagent toward organometallic compounds. These studies are aimed at activating coordinated carbon monoxide by coordination of the Lewis acid, $Yb(Me_5C_5)_2$, to the oxygen atom of carbon monoxide followed by electron transfer to the lowest unoccupied molecular orbital of carbon monoxide. These two processes will lengthen and weaken the carbon-oxygen triple bond and activate the ligand for further reaction with reagents, such as, hydrogen. These studies will provide data that might be useful for modeling the heteronuclear activation of carbon monoxide.

The cluster compound, $Fe_3(CO)_{12}$, reacts with $Yb(Me_5C_5)_2(OEt_2)$ to give the paramagnetic species (μ = 3.91 B.M. per Yb (III)), $[Yb(Me_5C_5)_2]_2[Fe_3(CO)_{11}]$ which has CO stretching frequencies in the infrared that are significantly lower in energy than found in the parent $Fe_3(CO)_{12}$. This fact suggests that coordination and electron transfer weakens the carbon-oxygen bond in the complex. The crystal structure of the complex (Fig. 4.1) shows that it contains four bridging Yb-OC-Fe groups. The averaged Yb-C and Yb-O distances are 2.57(1) and 2.243(3) Å, respectively. The carbon-oxygen bond lengths in the Yb-OC-Fe unit are lengthened by ca. 0.05 Å relative to

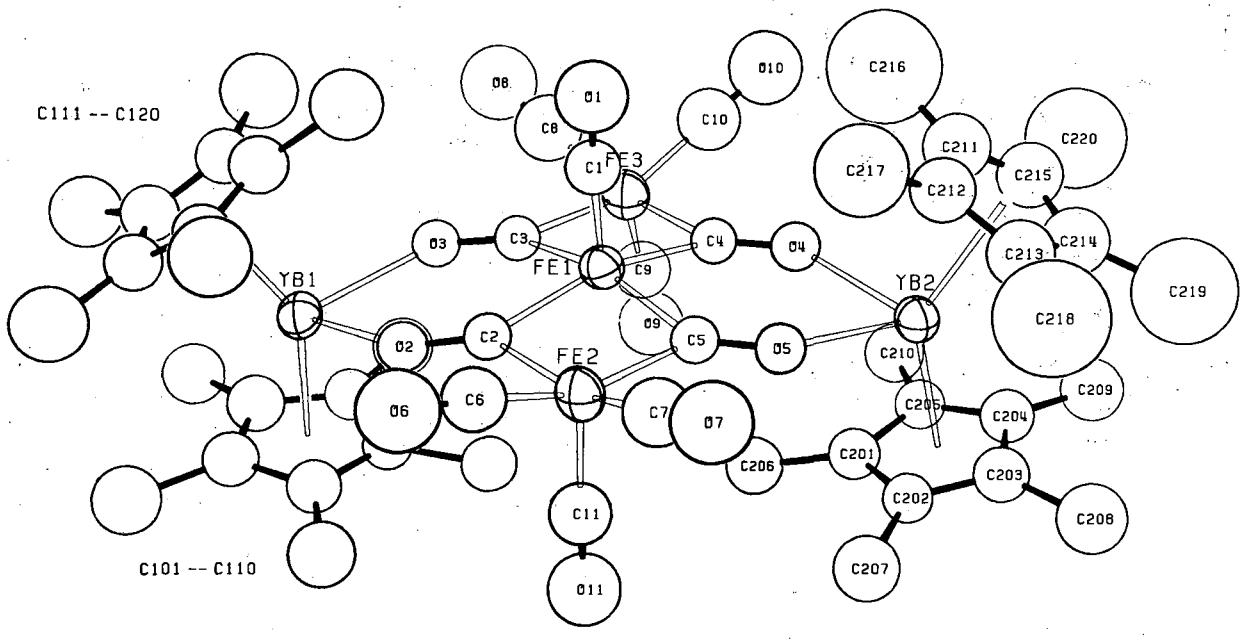

Fig. 4.1. An ORTEP drawing of $[Me_5C_5)_2Yb]_2[Fe_3(CO)_7(\mu\text{-}CO)_4]$. (XBL 815-9793)

normal bridging carbon-oxygen bond lengths, as expected on the basis of the infrared data.

* * *

†Brief version of LBL-13612.

5. TERTIARY PHOSPHINE COMPLEXES OF THE f-BLOCK METALS: CRYSTAL STRUCTURE OF $Yb[N(SiMe_3)_2]_2[Me_2PCH_2CH_2PMe_2]$: EVIDENCE FOR A YTTERBIUM-γ-CARBON INTERACTION†

T. D. Tilley, R. A. Andersen, and A. Zalkin

We have extended the study of phosphine coordination complexes to the divalent silylamide complexes, $M[N(SiMe_3)_2]_2$, where M is Eu or Yb, in order to probe the effect of the nature of the anionic ligand relative to their ability to change the electron density on the metal atom. Since the Me_5C_5 ligands are more electron-donating relative to silylamide ligands, the former should afford more electron rich compounds. Thus, silylamide compounds should form thermodynamically stronger bonds to phosphine donor ligands.

The phosphine, $Me_2PCH_2CH_2PMe_2$, reacts with $NaM[N(SiMe_3)_2]_3$ where M is Eu or Yb, or $Yb[N(SiMe_3)_2]_2(OEt_2)_2$ to give $Yb[N(SiMe_3)_2]_2$-$(Me_2PCH_2CH_2PMe_2)$ or $Eu[N(SiMe_3)_2]_2(Me_2PCH_2CH_2PMe_2)_{1.5}$. The coordinated phosphine cannot be displaced by diethyl ether, but the phosphine can be displaced by the stronger base, tetrahydrofuran. The crystal structure (Fig 5.1) of the ytterbium complex shows that the Yb-P and Yb-B distances are 3.012(4) and 2.331(13) Å, respectively. More significantly, a γ-carbon atom of the Me_3Si groups on each $(Me_3Si)_2N$-ligand is closer to the ytterbium atom (3.04 Å) than the sum of the van der Waals distance of Yb (II) and a methyl group (3.7 Å). As a consequence of this interaction, the three hydrogen atoms on the γ-carbon atom are locked in position and they were located in the x-ray study. The hydrogen atoms are pointing away from the ytterbium atom, precluding any substantial Yb...H interaction. The close Yb...C approach could be because of a direct Yb...C interaction, an unprecedented event, or because of an interaction of the ytterbium atom with the electron pair in the C-H bond. In order to describe the bonding in a more precise fashion, a neutron diffraction study is planned so that the hydrogen atoms may be located with high accuracy. Nevertheless, the C-H bond activation observed is a useful model for the intramolecular activation of C-H bonds.

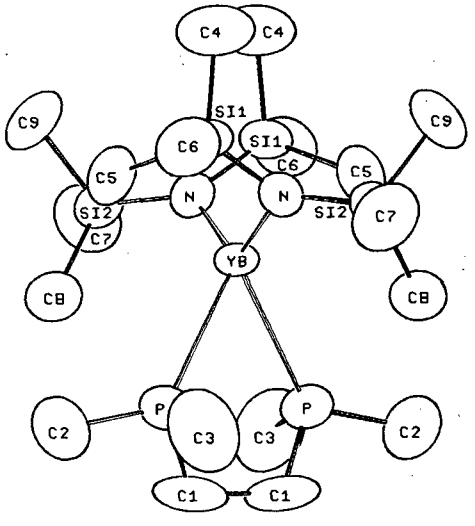

Fig. 5.1. An ORTEP diagram of $Yb[N(SiMe_3)_2]_2$ (dmpe). (XBL 8110-7070)

* * *

†Brief version of LBL-14025.

6. STEREOCHEMISTRY OF BIS(CARBOXYLATO)BIS(CHLORO)BIS(TERTIARY PHOSPHINE) DIMOLYBDENUM COMPLEXES; CRYSTAL AND MOLECULAR STRUCTURE OF TWO ISOMERS OF $(Me_3CCO_2)_2Cl_2(PEt_3)_2Mo_2$†

John D. Arenivar, Vera V. Mainz, Helena Ruben, Richard A. Andersen, and Allan Zalkin

Compounds of the type $Mo_2X_2(PR_3)_2(O_2CR)_2$ provide a potentially rich area for investigating stereochemical phenomena in these quadruply bonded, binuclear molecules since a variety of isomers are possible. Tetrachlorotetra(triethylphosphine)dimolybdenum reacts with two molar equivalents of pivalic acid, Me_3CCO_2H, to give air-stable dichlorobis(triethylphosphine)-bis(pivalato)dimolybdenum (A). In contrast, reaction of tetra(pivalato)dimolybdenum with trimethyl chlorosilane and triethylphosphine gives an air-stable compound (B) of the same empirical formula as (A) but it is a different geometrical isomer (Fig. 6.1). The crystal structures of both isomers have been determined by conventional x-ray diffraction methods. The isolation of two isomers, beginning from different starting materials, has not been observed in quadruply bonded molybdenum systems.

An interesting feature of isomer A is that the two oxygen atoms of each of the carboxylate groups are trans to two different ligands. This type of stereochemistry allows a comparison of the molybdenum-oxygen bond lengths as a function of the

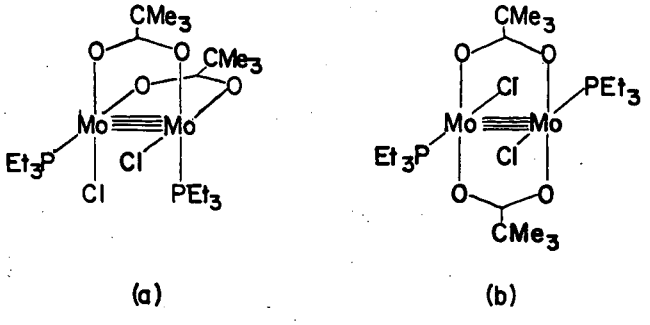

Fig. 6.1. Structural formulas for isomers A and B. (XBL 831-7557)

trans-ligands within the same molecule. The average molybdenum-oxygen bond distance trans to chloride is 0.07 Å (8σ) shorter than the average molybdenum-oxygen bond trans to phosphine. This difference indicates that phosphine lies higher than chloride in a trans-influence series in Mo(III) chemistry. A structural comparison between the two isomers is revealing since isomer A has chloride ligands trans to a carboxylate group whereas isomer B has chloride ligands trans to triethylphosphine. The average molybdenum-chloride bond length in isomer A is 0.02 Å (4σ) shorter than the average molybdenum-chloride distance in isomer B. This suggests that phosphine lies higher on a trans-influence series than a carboxylate group. Combining this result with the one developed above, two inequalities may be written: $Et_3P > Me_3CCO_2$ and $Et_3P > Cl$. In a similar fashion, comparison of molybdenum-oxygen bond lengths between the two isomers yields the inequality $Me_3CCO_2 \geq Cl$. Thus a trans-series, based upon bond length changes in the two isomers, may be written $Et_3P > Me_3CO_2 \geq Cl$.

* * *

†Brief version of LBL-13381.

7. ANOMALOUS SCATTERING BY PRASEODYMIUM, SAMARIUM AND GADOLINIUM AND STRUCTURES OF ETHYLENEDIAMINETETRAACETATE SALTS†

Lieselotte K. Templeton, David H. Templeton, Allan Zalkin, and Helena W. Ruben

To measure anomalous scattering of x-rays by rare earth elements in experiments with synchrotron radiation,[1,2] we needed the crystal structure parameters for sodium praseodymium ethylenediaminetetraacetate octahydrate and the isomorphous samarium and gadolinium salts. These salts and several others crystallize according to the orthorhombic space group Fdd2.[3] This samarium salt was used by Koetzle and Hamilton[4] to measure anomalous neutron scattering. We repeated the determination of Sm using x-rays so that the synchrotron experiments could be analyzed with atomic form factors identical (apart from anomalous scattering terms) with those used in the structure determination. Crystals that we have tested of the dysprosium compound, and also the holmium one, are monoclinic, but with a structure very nearly the same as the orthorhombic one. The rare earth oxide was dissolved in HCl and mixed with a hot solution of the edta salt and crystals were grown by slow cooling or slow evaporation. The x-ray diffraction data for the three compounds were measured using MoKα x-rays. Crystal data and other details are listed in Table 7.1.

The trial structures for refinement were derived directly or indirectly from Koetzle's[5] coordinates for the Sm salt, but modified by various transformations of setting. With R value in the range 0.024 to 0.037 this work achieved its primary objectives of obtaining parameters which fit x-ray diffraction intensities accurately enough to be used to analyze our synchrotron radiation experiments cited above. A second result is the experimental values of f'' for these three rare earth elements for MoKα radiation (Table 7.1). Like our earlier results for Cs (Ref. 6) and Co and Cl (Ref. 7) the agreement is excellent with the values calculated by Cromer and Liberman[8] for this wavelength remote from the absorption edges. This is in contrast to huge

Table 7.1. Crystal and Diffraction Data, $NaLn(edta)\cdot 8H_2O$.

Ln	Pr	Sm	Gd
a(Å)	19.589(3)	19.503(11)	19.409(3)
b(Å)	35.763(5)	35.596(17)	35.477(4)
c(Å)	12.121(2)	12.119(5)	12.119(1)
U(Å^3)	8491.5	8413.4	8344.8
D_x(Mg m^{-3})	1.865	1.913	1.950
μ, MoKα (mm^{-1})	2.38	2.90	3.29
unique reflections, $F^2 > \sigma$	3449	3368	3386
$R = \Sigma\|\Delta\|/\Sigma\|F_o\|$	0.037	0.030	0.024
f'', exper.	2.87(11)	3.64(10)	3.91(9)
f'', calc.	2.82[a]	3.442[b]	3.904[b]

[a]Cromer and Liberman (1981).
[b]Cromer and Liberman (1970).

differences observed in the immediate regions of absorption edges. The crystal structure itself, which has already been described by earlier authors cited above, needs little comment here. The principal differences among these isomorphous crystals are the results of the different sizes of the lanthanide ions. Corresponding distances for our three structures tend downward consistently with increasing atomic number, with an average decrease of 0.061 Å from Pr to Gd; the ionic radii calculated from oxide and chloride structures[9] decrease 0.075 Å in the same interval. There is nothing novel about the bond structure of the edta moiety, but the redundancy of these three determinations permits averaging of from 3 to 12 independent measurements to get accurate average values for each chemical type of bond distance and angle. These averages are shown in Fig. 7.1.

* * *

†Brief version of LBL-13866.

1. L. K. Templeton, D. H. Templeton, and R. P. Phizackerley, J. Am. Chem. Soc. 102 1185 (1980).
2. L. K. Templeton, D. H. Templeton, R. P. Phizackerley, and K. O. Hodgson, Acta. Cryst. A38, 74 (1982); T. Ueki, A. Zalkin, and D. H. Templeton, Act Cryst. 20, 436 (1966).
3. J. L. Hoard, B. Lee, and M. D. Lind, J. Am. Chem. Soc. 87, 1612 (1965).
4. T. F. Koetzle and W. C. Hamilton, Anomalous Scattering, edited by S. Ramaseshan and S. C. Abrahams, Munksgaard, Copenhagen, (1975), p. 498.
5. T. F. Koetzle, private communication (1978).
6. L. K. Templeton and D. H. Templeton, Acta Cryst. A34, 368 (1978).
7. D. H. Templeton, A. Zalkin, H. W. Ruben, and L. K. Templeton, Acta Cryst. B35, 1608 (1979).
8. D. T. Cromer and D. Liberman, J. Chem. Phys. 53, 1891 (1970); D. T. Cromer and D. Liberman, Acta Cryst. A37, 267 (1981).
D. H. Templeton and C. H. Dauben, J. Am. Chem. Soc. 76, 5237 (1954).

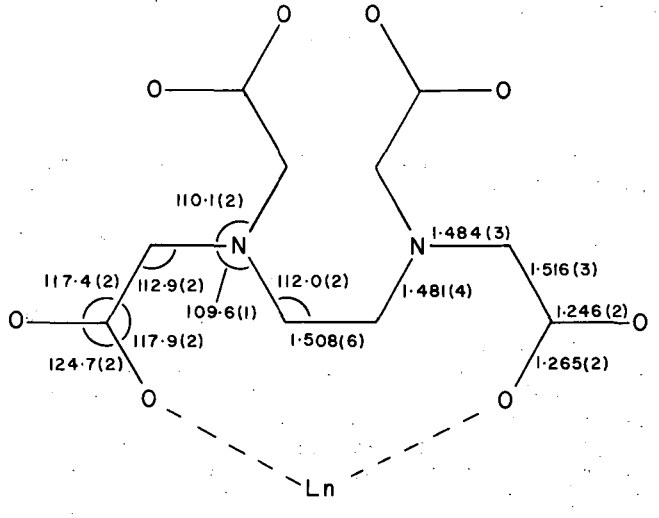

Fig. 7.1. Bond distances (Å) and angles (deg) in the edta moiety, averaged for the 3 to 12 chemically equivalent bonds in the Pr, Sm, and Gd salts. (XBL 8112-13065)

8. DIPOTASSIUMO BIS-([8]ANNULENE)YTTERBIUM(II) AND BIS-([8]ANNULENE)-CALCIUM†

S. A. Kinsley and A. Streitwieser, Jr.

The nature of the carbon-metal bonding in organolanthanide compounds remains a matter of continuing interest. Lanthanides generally have a stable +3 oxidation state, but several (e.g., europium and ytterbium) also form divalent compounds. The comparison of such compounds with those of the alkaline earth elements (e.g., calcium) is of especial interest because of the high ionic character of these systems.

Many di-[8]annulene compounds are known for +3 lanthanides, but only a single such compound has been reported for the +2 state.[1] We have now prepared and compared $K_2[Yb(C_8H_8)_2]$ and $K_2[C_8H_8)_2]$.

Both compounds have identical IR spectra and similar x-ray power patterns. The infrared spectra strongly suggest a sandwich structure. Consequently, both compounds probably have identical crystal structures and bond character. These results further emphasize the lack of importance of the 4f orbitals in ytterbium(II) chemistry, e.g., the ring-metal interaction in these compounds is undoubtedly wholly ionic.

* * *

†Brief version of LBL-15018.

1. A. Greco, S. Cesca, and G. Bertolini, J. Organometal. Chem. 113, 321 (1976).

Physical and Spectroscopic Properties

1. OPTICAL SPECTROSCOPY AND ELECTRON PARAMAGNETIC RESONANCE OF Pa^{4+} IN $ThBr_4$ AND $ThCl_4$ CRYSTALS†

J. C. Krupa, S. Hubert, M. Foyentin, E. Gamp, and N. Edelstein

Thorium tetrabromide and thorium tetrachloride are new host lattices for spectroscopic studies of tetravalent actinide ions, and in some cases trivalent lanthanide ions. At room temperature both crystals have a D_{4h}^{19} tetragonal structure isostructural with UCl_4. In this structure, the Th^{4+} ions are at a site of D_{2d} symmetry and other tetravalent actinide ions can substitute into this site. Single crystal neutron diffraction experiments on $ThBr_4$ revealed that the low temperature structure is incommensurate with a modulation along the four-fold axis.[1] Below the transition temperature, the sinusoidal distortion which modulates the Br ion positions reduces the actinide ion site symmetry from D_{2d} to D_2. However, it has been shown from spectral singularities of U^{4+}:$ThBr_4$ by absorption spectroscopy that some of the impurity ions pin the phase of the modulation and are in D_{2d} sites. Studies of Pa^{4+} in $ThBr_4$ by optical spectroscopy have been undertaken to further study the crystal field effects of the incommensurate structure on the $5f^1$ configuration and to compare the derived parameters

with earlier work on Pa^{4+} in $ThCl_4$.[2] Electron paramagnetic resonance (EPR) studies described in this article provide information about the ground state of Pa^{4+} diluted in $ThCl_4$ and $ThBr_4$. The results of these measurements will be presented.

The absorption and emission spectra of Pa^{4+}:$ThBr_4$ closely resembled the spectra previously reported for Pa^{4+}:$ThCl_4$.[2] At 77 K, four absorption bands were observed between 1480 nm and 1870 nm for Pa^{4+}:$ThCl_4$ and between 1540 nm and 1870 nm for Pa^{4+}:$ThBr_4$. The peculiar line shapes observed for the zero-phonon transitions can be explained by the incommensurate structure of the host crystal, $ThBr_4$, below 95 K. In the pure material, the sinusoidal modulation of the Br ion positions along the four-fold high symmetry axis reduces the metal ion site symmetry from D_{2d} to D_2. In the diluted crystal, the Pa^{4+} impurity forces the local symmetry (at some Pa^{4+} sites) to remain D_{2d}. Therefore the symmetry at the Pa^{4+} sites varies from D_{2d} at one extreme to the maximum D_2 distortion at the other. The line shape then follows a continuous variation which reflects the shift of the energy levels as the symmetry changes. This variation which is shown in Fig. 1.1 for the π spectra ($E \parallel C$), can be described as a continuum of absorption lines between two sharp edges. Similar peak shapes were obtained for Pa^{4+}:$ThCl_4$ which confirms the postulated modulated structure for this host material as determined by nuclear quadrupole resonance spectroscopy.[3]

The EPR spectra of powders of Pa^{4+}:$ThBr_4$ (Fig. 1.2) and Pa^{4+}:$ThCl_4$ are almost identical and clearly show that the g and A tensors are almost isotropic. Relatively narrow line widths are

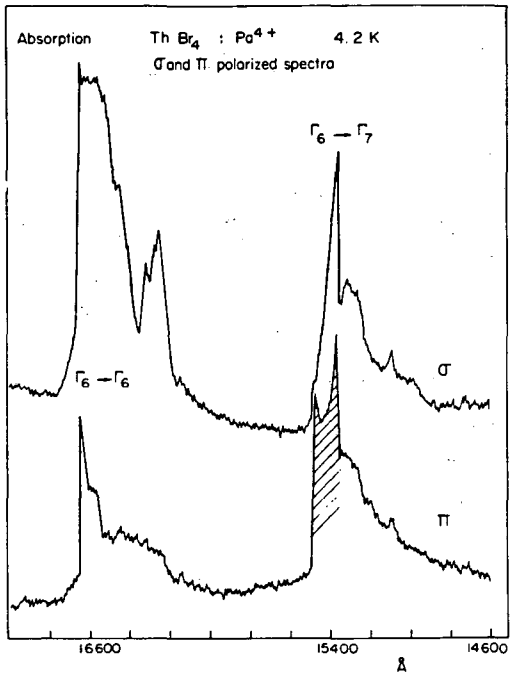

Fig. 1.1. Influence of the incommensurate structure of $ThBr_4$ on the Pa^{4+} absorption band shapes at 4.2K. The shaded peak is typical.
(XBL 831-7599)

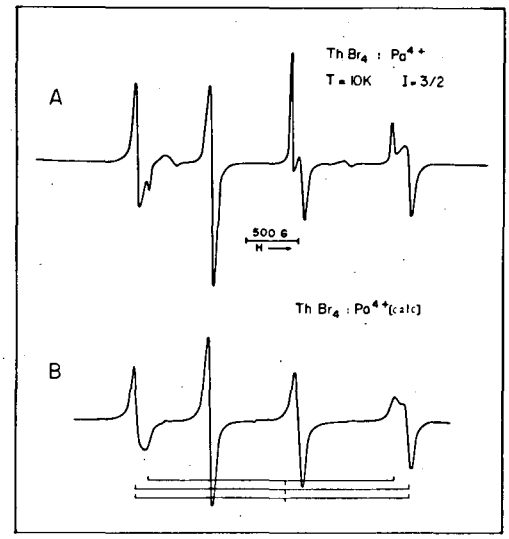

Fig. 1.2. (A) Experimental EPR spectrum for Pa^{4+}:$ThBr_4$. (B) Calculated EPR spectrum for Pa^{4+}:$ThBr_4$. (XBL 831-7600)

found for these samples which suggest that the deviations from D_{2d} symmetry do not greatly affect the magnetic properties of the ground state. Nevertheless, the experimental spectra, especially Pa^{4+}:$ThCl_4$, show a marked anisotropy of the line width which increased when the magnetic field is perpendicular to the highest symmetry axis. The increase in line width in this plane could be because of the decrease in symmetry from D_{2d} to D_2 for the modulated structure which should split $g_\perp$ into g_x and g_y. Single crystal EPR data for the x,y-plane are necessary to confirm the above hypothesis.

* * *

†Brief version of LBL-15084.

1. L. Bernard, R. Currat, P. Delamoye, C. Zeyen, S. Hubert, and R. de Kouchkovsky, J. of Physics C, in press.
2. J. C. Krupa, M. Hussonnois, M. Genet, and R. Guillaumont, J. Chem. Phys. 77, 154 (1982).
3. C. Khan Malek, A. Peneau, L. Guebe, P. Delamoye, and M. Hussonnois, J. Molec. Struc., in press.

2. FOURIER TRANSFORM SPECTROMETRY OBSERVATIONS OF THE ACTINIDES

J. G. Conway, E. F. Worden, J. Brault, R. Hubbard, and J. Wagner

As part of a continuing national effort on the classification of the free ion spectra of the actinide elements, the spectrum of uranium in the wavelength region of 2 to 5 μ in a water-cooled hollow cathode source has been analyzed. Over 5000 lines have been assigned to transitions between known energy levels of U I and U II. The tolerance between the observed and calculated levels is 0.005 cm^{-1}. About 4000 lines remain unassigned. Uranium has also been observed in the wavelength region from 2500 Å to 2 μ in the same source.

The spectra of ^{240}Pu, ^{241}Am, ^{242m}Am, and ^{244}Cm have also been measured in the wavelength region of 1 μ to 2500 Å using an electrodeless discharge lamp. The spectrum of ^{243}Am has already been measured by Frank Tomkins of Argonne National Laboratory and is available for analysis.

All measurements were obtained on the Kitt Peak National Observatory Fourier transform optical spectrometer using a variety of beam splitters. The intensity response of the spectrometer was determined with standard radiance lamps and calibrated argon miniarcs.

1982 PUBLICATIONS AND REPORTS

Refereed Journals

1. T. D. Tilley and R. A Andersen, "Preparation and Crystal Structure of Bis[bis(pentamethylcyclopentadienyl)ytterbium(III)] Undecacarbonyltriferrate, $[(Me_5C_5)_2Yb]_2[Fe_3(CO)_{11}]$; A Compound with Four Isocarbonyl (Fe-CO-Yb) Interactions," J. Am. Chem. Soc. 104, 1772 (1982); LBL-13612.

2. T. D. Tilley, R. A. Andersen, and A. Zalkin, "Tertiary Phosphine Complexes of the f-Block Metals; Crystal Structure of $Yb[N(SiMe_3)_2]_2$-$[Me_2PCH_2CH_2PMe_2]$: Evidence for a Ytterbium-γ-Carbon Interaction," J. Am. Chem. Soc. 104, 3725 (1982); LBL-14025.

3. A. Zalkin, D. H. Templeton, W. D. Luke, and A. Streitwieser, Jr., "Synthesis and Structure of Dicyclopentanouranocene, $U[C_8H_6(CH_2)_3]_2$," Organometallics 1, 618 (1982); LBL-13216.

4. D. L. Perry, A. Zalkin, H. Ruben, and D. H. Templeton, "Synthesis, Characterization, and Structure of a Uranyl Complex with a Disulfide Ligand, Bis(di-n-propylammonium)adisulfidobis (di-n-propylmonothiocarbamato)Dioxouranate(VI)," Inorg. Chem. 21, 237 (1982); LBL-10654.

5. A. Zalkin, H. Ruben, and D. H. Templeton, "The Structure of Nickel Uranyl Acetate Hexahydrate," Acta Cryst. B38, 610 (1982); LBL-12551.

6. J. D. Arenivar, V. V. Mainz, H. Ruben, R. A. Andersen, and A. Zalkin, "Stereochemistry of Bis(carboxylato)Bis(chloro)Bis(tertiary phosphine) Dimolybdenum Complexes; Crystal and Molecular Structures of Two Isomers of $(Me_3CCO_2)_2(PEt_3)_2Mo_2$," Inorg. Chem. 21, 2649 (1982); LBL-13381.

7. T. Hayhurst, G. Shalimoff, J. G. Conway, N. Edelstein, L. A. Boatner, and M. M. Abraham, "Optical Spectra and Zeeman Effect for Pr^{3+} and Nd^{3+} in $LuPO_4$ and YPO_4," J. Chem. Phys. 76, 3960 (1982); LBL-13388.

8. L. K. Templeton, D. H. Templeton, A. Zalkin, and H. Ruben, "Anomalous Scattering by Praesodymium, Samarium and Gadolinium, and Structure of Ethyldiamminetetraacetate Salts," Acta Cryst. B38, 2155 (1982); LBL-13866.

†9. D. H. Templeton and L. K. Templeton, "X-Ray Dichroism and Polarized Anomalous Scattering of the Uranyl Ion," Acta Cryst. A38, 62 (1982); LBL-12477.

†10. L. K. Templeton, D. H. Templeton, R. P. Phizackerley, and K. O. Hodgson, "L_3-Edge Anomalous Scattering by Gadolinium and Samarium Measured at High Resolution with Synchrotron Radiation," Acta Cryst. A38, 74 (1982): LBL-12825.

11. T. D. Tilley, R. A. Andersen, A. Zalkin, and D. H. Templeton, "Bis(pentamethylcyclopentadienyl)carboxylato and Dithiocarbamato Derivatives of Neodymium(III) and Ytterbium (III). Crystal Structure of Bis(pentamethylcyclopentadienyl)-Diethyldithiocarbamato Ytterbium(III)," Inorg. Chem. 21, 2644 (1982).

12. T. D. Tilley, R. A. Andersen, B. Spencer, and A. Zalkin, "Crystal Structure of Bis(pentamethylcyclopentadienyl) Bis(Pyridine)-Ytterbium(II)," Inorg. Chem. 21, 2647 (1982).

13. J. L. Robbins, N. Edelstein, B. Spencer, and J. C. Smart, "The Synthesis and Electronic Structures of Decamethylmetallocenes," J. Am. Chem. Soc. 104, 1882 (1982).

14. K. Abu-Dari and K. N. Raymond, "Specific Sequestering Agents for the Actinides. 8. Synthesis and Structural Chemistry of Tetrakis(thiohydroxamato)hafnium(IV) in $Hf(CH_3C_6H_4(S)N(O)CH_3)_4$-$C_2H_5OH$," Inorg. Chem. 21, 1676 (1982); LBL-13173.

‡15. V. L. Pecoraro, G. B. Wong, and K. N. Raymond, "Gallium and Indium Imaging Agents. 2. Complexes of Sulfonated Catechoylamide Sequestering Agents," Inorg. Chem. 21, 2209 (1982).

‡16. C. W. Eigenbrot, Jr. and K. N. Raymond, "Organouranium Complexes of Pyrazole and Pyrazolate. Synthesis and X-Ray Structures of $U(C_5Me_5)_2Cl_2(C_3H_4N_2)$, $U(C_5Me_5)_2Cl(C_3H_4N_2)$, and $U(C_5Me_5)$-$(C_3H_3N_2)_2$," Inorg. Chem. 21, 2653 (1982); LBL-13073.

17. C. W. Eigenbrot, Jr. and K. N. Raymond, "Crystal and Molecular Structure of $[Nd(tren)_2(CH_3CN)](ClO_4)_3$," Inorg. Chem. 21, 2867 (1982); LBL-13075.

‡18. S. M. Moerlein, M. J. Welch, and K. N. Raymond, "Use of Tricatecholamide Ligands to Alter the Biodistribution of Gallium-67: Concise Communication," J. Nucl. Med. 23, 501 (1982).

‡19. M. J. Kappel and K. N. Raymond, "Ferric Ion Sequestering Agents. 10. Selectivity of Sulfonated Poly(catechoylamides) for Ferric Ion," Inorg. Chem. 21, 3437 (1982); LBL-14680.

‡20. S. R. Cooper, Y. B. Koh, and K. N. Raymond, "Synthetic, Structural, and Physical Studies of Bis(triethylammonium) Tris(catecholato)vanadate(IV), Potassium Bis(catecholato)oxovanadate(IV), and Potassium Tris(catecholato)-vanadate(III)," J. Am. Chem. Soc. 104, 5092 (1982).

LBL Reports

1. R. Shinomoto, E. Gamp, N. Edelstein, D. H. Templeton, and A. Zalkin, "Synthesis and Crystal Structures of the Tetrakis(methyltrihydroborato) Compounds of Zirconium(IV), Thorium(IV), Uranium(IV) and Neptunium(IV)," submitted to Inorg. Chem., LBL-15090.

2. T. D. Tilley, R. A. Andersen, and A. Zalkin, "Tertiary Phosphine Complexes of the f-Block Metals; Preparation of Pentamethylcyclopentadienyl-Tertiary Phosphine Complexes of Yb(II and III) and Eu(II). The Crystal Structure of $Yb(Me_5C_5)_2Cl(Me_2PCH_2PMe_2)$," submitted to Inorg. Chem., LBL-14367.

3. S. A. Kinsley and A. Streitwieser, Jr., "Dipotassium Bis-([8]Annulene)-Ytterbium(II) and Bis-([8]Annulene) Calcium, LBL-15018.

4. R. P. Planalp, R. A. Andersen, and A. Zalkin, "Dialkyl Bis[Bis(Trimethylsilylamideo] Group IV A Metal Complexes; Preparation of Bridging Carbene Complexes by γ-Elimination of Alkane. Crystal Structure of $\{ZrCHSi(Me)_2NSiMe_3\text{-}[N(SiMe_3)_2]_2\}_2$," LBL-14754.

5. N. M. Edelstein and J. Goffart, "Magnetic Properties of the Actinides," to be published in The Chemistry of the Actinide Elements, J. J. Katz, G. T. Seaborg, and L. R. Morss, Eds., Chapman and Hall Ltd., London, LBL-14195.

Other Publications

1. Actinides in Perspective, N. M. Edelstein, Ed., Pergamon Press, Oxford, 1982.

2. K. N. Raymond and T. P. Tufano, "Coordination Chemistry of the Siderophores and Recent Studies of Synthetic Analogues," in The Biological Chemistry of Iron, H. B. Dunford, D. Dolphin, K. N. Raymond, and L. Seiker, Eds., D. Reidel Publishing Company, Dordrecht, Holland, 1982, pp. 85-105.

3. K. N. Raymond, M. J. Kappel, V. L. Pecoraro, W. R. Harris, C. J. Carrano, F. L. Weitl, and R. W. Durbin, "Specific Sequestering Agents for Actinide Ions," in Actinides in Perspective, N. M. Edelstein, Ed., Pergamon Press, Oxford and New York, 1982, pp. 491-507.

4. K. N. Raymond, V. L. Pecoraro, W. R. Harris, and C. J. Carrano, "Actinide Coordination and Discrimination by Human Transferrin," in Environmental Migration of Long-Lived Radionuclides, International Atomic Energy Agency, Vienna, 1982, pp. 571-577.

5. G. T. Seaborg, "The Plutonium Story," in Actinides in Perspective, N. M. Edelstein, Ed., Pergamon Press, 1982.

Invited Talks

1. R. A. Andersen, "Electron Transfer Properties of Lanthanide(II) Complexes," 2nd Homogeneous Catalysis Research Conference (DOE), Madison, Wisconsin, June 7-9, 1982.

2. R. A. Andersen, "Phosphine Complexes of the Actinide Metals," University of California, Davis, California, October 17, 1982.

3. D. H. Templeton, "Anomalous X-Ray Scattering," a series of six lectures, University of Lausanne, Switzerland, October 27-December 1, 1982.

4. D. H. Templeton, "Anomalous Scattering of Synchrotron Radiation," University of Paris, France, October 5, 1982; University of Berne, Switzerland, November 19, 1982; University of Neuchatel, Switzerland, November 29, 1982; and Federal Technical University, Zurich, Switzerland, December 9, 1982.

5. N. M. Edelstein, "Measurement of Formation Constants and Solubilities of Actinide Ions in Neutral Solution," Institute for Inorganic Chemistry, Free University, Berlin, W. Germany, June 3, 1982.

6. N. M. Edelstein, "Synthetic and Spectroscopic Studies on Actinide Halides and Borohydrides," Centre Études Nucléaires, Saclay, France, June 30, 1982.

7. J. G. Conway, "Atomic Spectroscopy of Actinide Elements," Institute of Atomic Energy, Beijing, China, April 6, 1982; Institute of Modern Physics, Lanzhou, China, April 12, 1982; and Institute of Nuclear Research, Shanghai, China, April 16, 1982.

8. J. G. Conway, "Laser Spectroscopy of Rare Earths and Actinides," Institute of Atomic Energy, Beijing, China, April 7, 1982.

9. J. G. Conway, "Absorption Spectra of Actinide Ions in Crystals," Institute of Atomic Energy, Beijing, China, April 7, 1982.

10. J. G. Conway, "Spectroscopy in China," Northern California Section, Society for Applied Spectroscopy, University of California, Berkeley, September 16, 1982.

11. A. Streitwieser, Jr., "New Developments in Uranocene Chemistry," University of Wisconsin, Sprague Lectures, Madison, Wisconsin, May 7, 1982; Tel Aviv University, Tel Aviv, Israel, Sackler Lectures in Chemistry, October 26, 1982; and Ben Gurion University of Negev, Beersheva, Israel, October 27, 1982.

12. K. N. Raymond, "The Coordination Site and Fe(III) Exchange Processes for Transferrin and Siderophores," 65th Canadian Chemical Conference and Exhibition, Toronto, Canada, May 30-June 2, 1982.

13. K. N. Raymond, "Synthesis and Properties of Iron(III) and Actinide(IV) Specific Sequestering Agents," 37th Annual Northwest Regional Meeting of the American Chemical Society, Eugene, Oregon, June 17-18, 1982.

14. K. N. Raymond, "The Iron Coordination Site and Metal Ion Exchange Kinetics of Transferrin and Lactoferrin," ACS Pacific Conference on Chem-

istry and Spectroscopy, San Francisco, California, October 27-29, 1982.

15. K. N. Raymond, "Coordination Chemistry of Biological Iron Transport Compounds," Oregon Graduate Center, Beaverton, Oregon, February 1, 1982; University of Texas, Austin, Texas, April 22, 1982; University of Houston, Houston, Texas, April 23, 1982; Princeton University, Princeton, New Jersey, April 28, 1982; Columbia University, New York, New York, April 29, 1982; Yale University, New Haven, Connecticut, April 30, 1982; Harvard University, Cambridge, Massachusetts, May 3, 1982; and Polaroid Corporation, Cambridge, Massachusetts, May 4, 1982.

16. K. N. Raymond, "Microbial Iron Chelating Agents--Their Recognition and Transport," University of Southern California, Los Angeles, California, October 5, 1982.

17. G. T. Seaborg, "40 Years of Plutonium Chemistry: The Beginnings," Meeting of the American Chemical Society, Kansas City, Missouri, September 13, 1982.

18. G. T. Seaborg, "The Transuranium Elements," Symposium on 50th Anniversary of the Discovery of the Neutron, Cambridge University, Cambridge, England, September 16, 1982.

* * *

†Partially supported by the National Science Foundation.
‡Partially supported by the National Institutes of Health.


IV
Fossil Energy

Fossil Energy

a. Electrode Surface Chemistry*

Phillip N. Ross, Jr., Investigator

Introduction. Commercialization of phosphoric acid fuel cell technology requires a capital cost reduction and an extension of power plant life compared to currently available technology. Significant capital cost reduction can be achieved if an oxygen reduction catalyst that is catalytically more active than platinum can be developed. The objective of the present research is to develop the physical and chemical understanding of the oxygen-platinum surface interactions necessary for the rational selection of alloying ligands that modify the basic catalytic properties of platinum. It is felt that the platinum-oxygen bond energy will be changed when ligands are bonded to the surface platinum atoms and that, by the use of appropriate ligands, an optimal bond energy will result in enhanced catalytic activity relative to the pure platinum surface.

Previous work in this program has shown that supported bimetallic catalysts employing Ti, Zr or Ta in addition to Pt produced enhanced activity for oxygen reduction. It was not clear in that work how the Pt and the base metal were associated on the support, although there was some evidence by x-ray diffraction of alloy formation. The focus of the present research is to determine the manner in which the base metal modifies the catalytic properties of Pt by the use of ordered (single crystal) intermetallic solid electrodes well-characterized by the techniques of contemporary surface science (LEED, AES, XPS).

1. HIGH COVERAGE STATES OF OXYGEN ON Pt(001) AND (111)†

G. Derry and P. N. Ross, Jr.

Oxygen chemisorption on the Pt(111) and Pt(001) surfaces was studied for various surface temperatures and oxygen pressures. These studies were carried out in an ultrahigh vacuum chamber with capability for x-ray and uv photoelectron spectroscopy, and thermal desorption spectroscopy. The electron spectrometer is of the angle-resolving hemispherical type, allowing variable surface sensitivity by varying the take-off angle.

Thermal desorption results for several typical exposures are presented in Fig. 1.1. If the oxygen pressure is ~10^{-5} Pa and the surface temperature near ambient (≲370 K), a dissociated adsorbed species forms on both the Pt(111) and Pt(100) crystal faces. Saturation coverage on Pt(111) was ~0.25 ML, somewhat greater than for Pt(100) (~0.2 ML). The thermal desorption of the low temperature species on both surfaces can be represented by second order Arrhenius kinetics. Exposure at elevated surface temperature (~570 K) and higher oxygen pressure (~10^{-3} Pa) resulted in the formation of higher coverage states (both conditions are necessary). The saturation coverage on Pt(111) increased by about a factor of 2, and the desorption lineshape developed an asymmetry on the low temperature side. For Pt(100), the saturation coverage increased by a factor of 4-5 and the desorption lineshape developed a complex structure. Arrhenius kinetics no longer describe these thermal desorption spectra. XPS indicated the binding energy of the O1s core level was 0.4 eV lower for the higher coverage

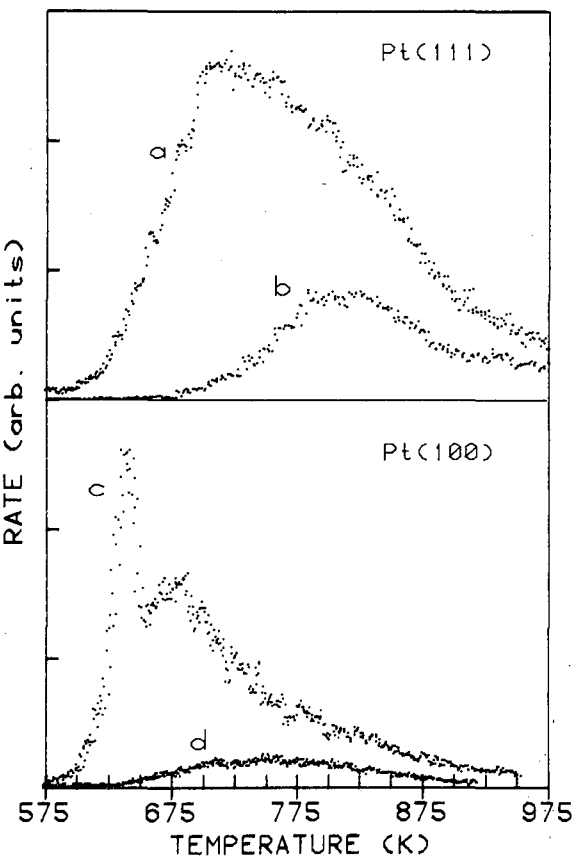

Fig. 1.1. Thermal desorption spectra for Pt(111) and Pt(100) after: (a) high pressure, high temperature dosing; (b) room temperature dosing. Scale for (100) reduced by a factor of 2.
(XBL 831-7641)

*This work was supported by the Assistant Secretary for Fossil Energy, Office of Coal Fuel Cells, Advanced Concepts Division of the U.S. Department of Energy under Contract No. DE-AC03-76SF00098 through the Fuel Cell Project Office, NASA Lewis Research Center, Cleveland, Ohio.

state on Pt(100) than for the low coverage state. For oxygen on Pt(111), the O1s binding energy was the same for both high and low coverage. UPS from the valence band was consistent with these O1s XPS results. The new features that appear in the Pt valence band upon adsorption of oxygen on Pt(111) differed only in magnitude between the high coverage and low coverage states. The high coverage state on Pt(100), however, produced a new feature in the UPS spectrum just below the Fermi level which was not observed for the low coverage state.

From these data, we deduce that the high coverage state of oxygen on Pt(100) is a new state chemically distinct from the low coverage state. On Pt(111), however, the low coverage and high coverage states are chemically the same. Variable take-off angle O1s spectra indicated that the high coverage states are still on the surface, not below the surface. Our observation of both high and low coverage states forming under different conditions of temperature and pressure reconciles previously contradictory reports in the literature for oxygen adsorption on Pt(100).

* * *

†Brief version of LBL-15231.

2. ADSORPTIVE AND CATALYTIC PROPERTIES OF ZIRCONIUM OVERLAYERS ON Pt(001)†‡

U. Bardi, P. N. Ross, Jr., and G. Somorjai

Metallic zirconium was deposited on a [001] oriented substrate by electron beam evaporation in UHV conditions. LEED and AES were used to characterize the surface structure and composition, thermal desorption was used to obtain information on the adsorbed species, and low pressure ($P = 10^{-5}$, 10^{-6} torr) catalysis experiments were used to characterize the catalytic properties of the surface. The zirconium overlayer was observed to grow on the Pt surface at room temperature by the layer-by-layer mechanism. Zirconium on platinum was found to react readily with oxygen, carbon monoxide, and hydrocarbons forming overlayer oxides on carbides, respectively. Thermal annealing in UHV at $T > 900$ K caused decomposition of these overlayers and dissolution of zirconium into the bulk. A surface that was annealed after metallic zirconium deposition reacted more slowly with oxygen, but eventually equilibrated to form the same surface phase as obtained by annealing the oxide overlayer. Several ordered structures were observed by LEED after annealing, which depended on the amount of zirconium deposited and the oxygen content in the surface. The presence of these ordered structures indicates that the Pt-Zr interaction remains strong even when the zirconium is oxidized, probably indicative of the formation of a Pt-ZrO_x surface compound. The adsorptive properties of these surface compounds were observed using CO and O_2 as "probe" molecules. The TDS results indicated that: (a) the Pt-ZrO_x surface has a Pt enriched top layer with a ZrO_x underlayer; (b) a ligand effect from the Pt-Zr bond reduces the Pt-CO and Pt-O bonding interactions. The behavior of the annealed ZrO_x on Pt surface appears to be analogous to the SMSI effect reported[1] for Pt dispersed on TiO_2.

* * *

†Brief version of LBL-15294.

‡This work was also supported by the Director, Office of Energy Research, Office of Basic Energy Sciences, Materials Sciences Division of the U.S. Department of Energy under Contract No. DE-AC03-76SF00098.

1. S. Tauster and S. Fung, J. Catal. 55, 29 (1978).

3. ADSORPTIVE AND CATALYTIC PROPERTIES OF POLYCRYSTALLINE Pt_3Ti†

U. Bardi, P. N. Ross, Jr., and G. Somorjai

Polycrystalline Pt_3Ti was prepared by arc melting the pure metals in an argon atmosphere. A clean surface, defined by Auger electron spectra (AES) that show only lines characteristic of Pt and Ti, could be produced by ion bombardment and thermal annealing in ultrahigh vacuum. Analysis of AES Pt/Ti peak height ratios indicated that the clean vacuum annealed surface is enriched in Pt. Thermal desorption (TDS) studies of carbon monoxide and hydrogen were conducted on the clean annealed surface, and on the same surface covered by an evaporated Pt overlayer. As shown in Fig. 3.1, the carbon monoxide TDS peak from the Pt_3Ti surface was shifted ca. 60 K lower in temperature, with about 60-70% of the coverage, from the peak for the pure Pt surface. This shift is interpreted as a ligand effect on the Pt because of the strong intermetallic bonding that occurs in this intermetallic compound. Qualitatively similar effects were observed in hydrogen thermal desorption spectra. Essentially no chemisorption of either hydrogen or carbon monoxide was observed when the surface was pre-treated in oxygen at

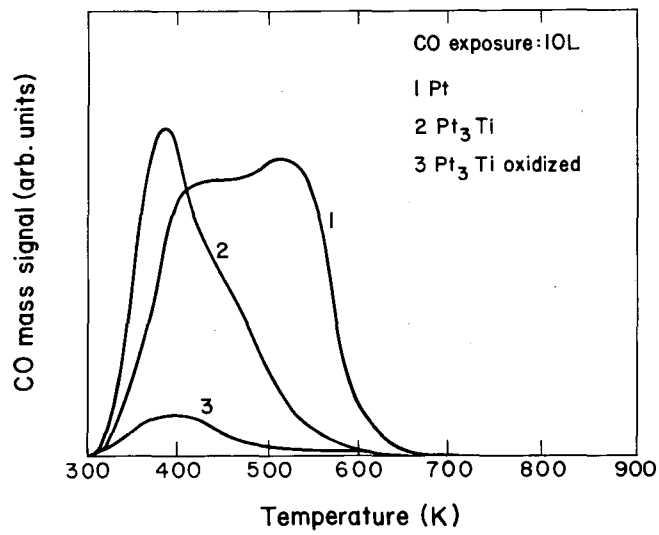

Fig. 3.1. Thermal desorption spectra for CO on polycrystalline Pt_3Ti relative to polycrystalline Pt. (XBL 8211-4657)

elevated temperature. Based on these TDS observations, one would expect dramatically different behavior of Pt_3Ti than for pure Pt in CO/H_2 reactions. In oxidizing environments, however, Pt_3Ti appears to have only negative characteristics relative to pure Pt.

* * *

†This work was also supported by the Director, Office of Energy Research, Office of Basic Energy Sciences, Materials Sciences Division of the U.S. Department of Energy under Contract No. DE-AC03-76SF00098

1982 PUBLICATIONS AND REPORTS

LBL Reports

1. G. Derry and P. N. Ross, Jr., "High Coverage States of Oxygen Adsorbed on Pt(001) and (111) Surfaces," to be published in Surf. Sci., LBL-15231.

2. U. Bardi, P. N. Ross, Jr., and G. Somorjai, "Structure and Composition of Annealed Zirconium Overlayers on Pt(001)," submitted to J. Vac. Sci. Tech., LBL-15294.

3. U. Bardi, P. N. Ross, Jr., and G. Somorjai, "Ligand Effects in CO Chemisorption on Polycrystalline Pt_3Ti," submitted to J. Catal., LBL-15603.

4. U. Bardi, G. Somorjai, and P. N. Ross, Jr., "Adsorption and Catalysis on Zirconium Overlayers on Pt(001) Surfaces," LBL-15604.

Other Publications

1. P. N. Ross, Jr., "Studies of Adsorption at Well-Ordered Electrode Surfaces Using LEED," in Chemistry and Physics of Solid Surfaces IV, edited by R. Vanselow and R. Howe, Springer-Verlag, 1982, p. 173-200.

b. Studies of Materials Erosion/Wear in Coal Conversion Systems*

Alan V. Levy, Investigator

1. THE HIGH TEMPERATURE EROSION OF DUCTILE ALLOYS†

Jennifer Patterson and Alan Levy

Erosion tests were conducted in inert gas atmospheres at elevated temperatures in order to determine the effect of temperature on the erosion process in metals without corrosion also occurring. The interpretation of combined erosion-corrosion data from elevated temperature exposures is aided by the erosion-only data developed in this task.

The materials tested were 304 and 310SS. The materials were eroded by 300 gm of 55 μm silicon carbide particles at a velocity of 30 m/s. Nitrogen was used as the carrier gas. The tests were conducted at 25°C through 900°C and 90° and 30° particle impingement angles.

In Fig. 1.1, the steady state erosion rate is presented as a function of erodent particle weight for 310SS. A roughly parabolic curve is shown for the 30° impingement angle tests with a flat portion of 0.4×10^{-4} g/g occurring up to a temperature of approximately 400°C. A similar result was obtained for 304SS with a minimum occurring at 0.51×10^{-4} g/g. Above 400°C the erosion rate increased rapidly for both alloys. At an impingement angle of 90°, the 310SS curve shows a decrease in the erosion rate with temperature to a minimum at 400°C. The behavior of the alloy at both impingement angles can be explained by the platelet mechanism of erosion. At 800°C, the erosion rate was determined for several velocities and was found to increase with erodent particle velocity.

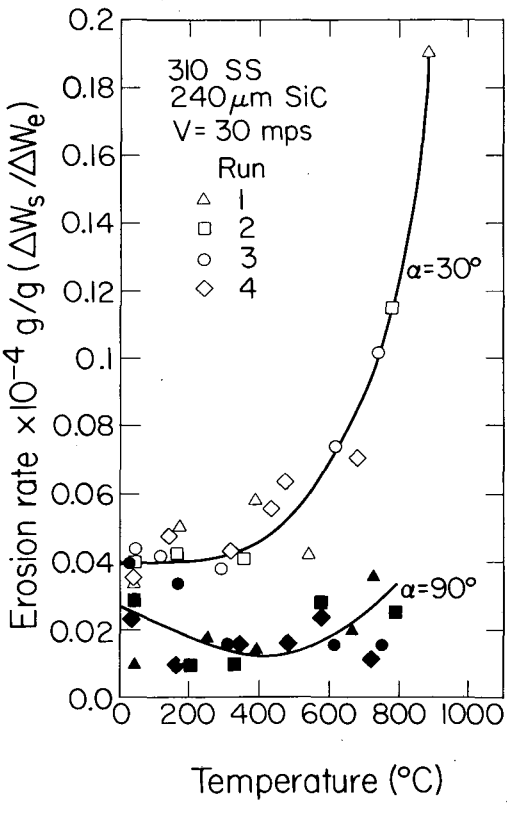

Fig. 1.1. Erosion rates of 310SS at elevated temperatures. (XBL 827-7092)

* * *

†Brief version of LBL-15655.

2. METHODS FOR CHARACTERIZATION OF EROSION BY GAS-ENTRAINED SOLID PARTICLES†

Jennifer Patterson and Alan Levy

The experimental techniques used in the incremental type of erosion testing of ductile metals have been studied in order to optimize them. The areas addressed in this investigation were specimen preparation, erosion testing, and data analysis. Criteria for the preparation of metal specimens used in gas-solid erosion testing were established. The detailed steps in erosion testing were assessed and standardized. The various measurements of solid particle velocity were evaluated. An analysis was made of characteristic errors in erosion rates measurement and methods of reducing these errors were developed.

Identical erosion experiments using two cleaning methods, wiping with a tissue and ultrasonic cleaning in alcohol, resulted in a 38% lower erosion rate using the tissue cleaning method because of residual erodent on the specimen surface that protected it from subsequent erosion exposures.

Because of inherent small errors in measurement of weight differences of <1 mg that occur in incremental erosion testing, a method of handling the data was developed that did not utilize finite difference of before and after weights. A differentiation of the curve of incremental weight of the specimen vs the amount of eroding particles results in incremental erosion rate curves which have markedly less scatter than those generated using the finite difference method.

* * *

†Brief version of LBL-15017.

*Research sponsored by the Department of Energy under DOE/FEAA 15 10 0, Advanced Research and Technical Development, Fossil Energy Materials Program, Work Breakdown Structure Element LBL-3.5 and U.S. Department of Energy under Contract No DE-AC03-76SF00098.

3. EFFECT OF PARTICLE VELOCITY ON THE PLATELET MECHANISM OF EROSION†

Mostafa Aghazadeh and Alan Levy

The erosion of ductile metals in gas-solid particle streams varies exponentially with particle velocity. This effect has been reported in the literature for many years and used in erosion mechanism models. The validity of the platelet mechanism of erosion was determined over a range of velocities.

Increasing the velocity from 30 to 130 m/s was found to increase the size of the craters and resulting platelets formed while the mechanism remained the same. Figure 3.1 shows the cross section of 1020 steel after being eroded at 30 m/s and 130 m/s with silicon carbide particles. Over the relatively large range of test velocities,

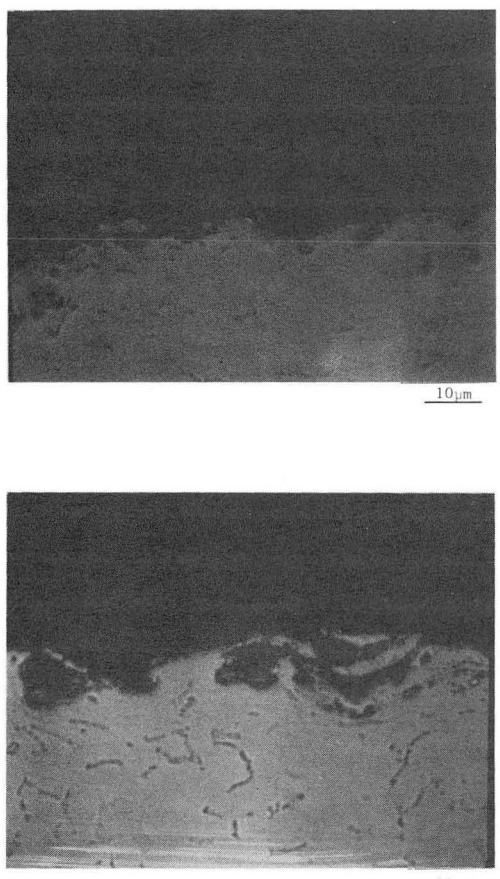

Fig. 3.1. Cross section of eroded 1020 steel surfaces at V = 30 and 130 m/s. (XBB 831-430)

the erosion rate of the 1020 steel increased from 0.2×10^{-5} cc/g to 9.5×10^{-5} cc/g because much larger platelets were formed and removed. A number of steel and aluminum alloys responded similarly to Al_2O_3 and SiC erodent particles. Larger platelets were formed at a 30° impingement angle than at a 90° angle with a corresponding increased erosion rate.

* * *

†Brief version of LBL-15656.

4. EROSION OF BORIDE COATINGS†

Mostafa Aghazadeh and Alan V. Levy

The operation of metal surfaces subjected to severe abrasive or sliding wear has been aided by the application of hard materials to the wear surface. The potential of protection of substrates by hard facing materials in erosive wear was investigated using a family of Ni-Cr-B alloys with large percentages of hard, second-phase boride particles in the nickel matrix.

The erosion of the hard facing alloys was determined as a function of composition, morphology, and method of application on a mild steel substrate. Several important relationships were determined between the material variables and their erosion rates. Unlike abrasive wear where the eroding particles are held in position as they translate across the eroding surface, in gas-solid particle impact erosion, the quantity of boride hardening phase in the alloy (>>40% to 40%) and the resultant hardness have very little effect on the erosion rate. The addition of hard tungsten carbide particles to one of the alloys to further harden it even resulted in a significant increase in the erosion rate.

The erosion rate was determined to increase with increasing random porosity in the coating. Figure 4.1 shows the cross sections of a nickel-boron alloy deposited on the mild steel surface by three different processes. The dense, braze-coat alloy had an erosion rate of 5.37×10^{-6} cc/g. The same alloy in the flame sprayed form had an erosion rate of 6.08×10^{-6} cc/g, while the most porous form of the alloy, the plasma sprayed coating, had an erosion rate of 6.44×10^{-6} cc/g. Much knowledge is being developed by these tests that will aid alloy selection and refinement for service in erosive environments.

* * *

†Brief version of LBL-15293.

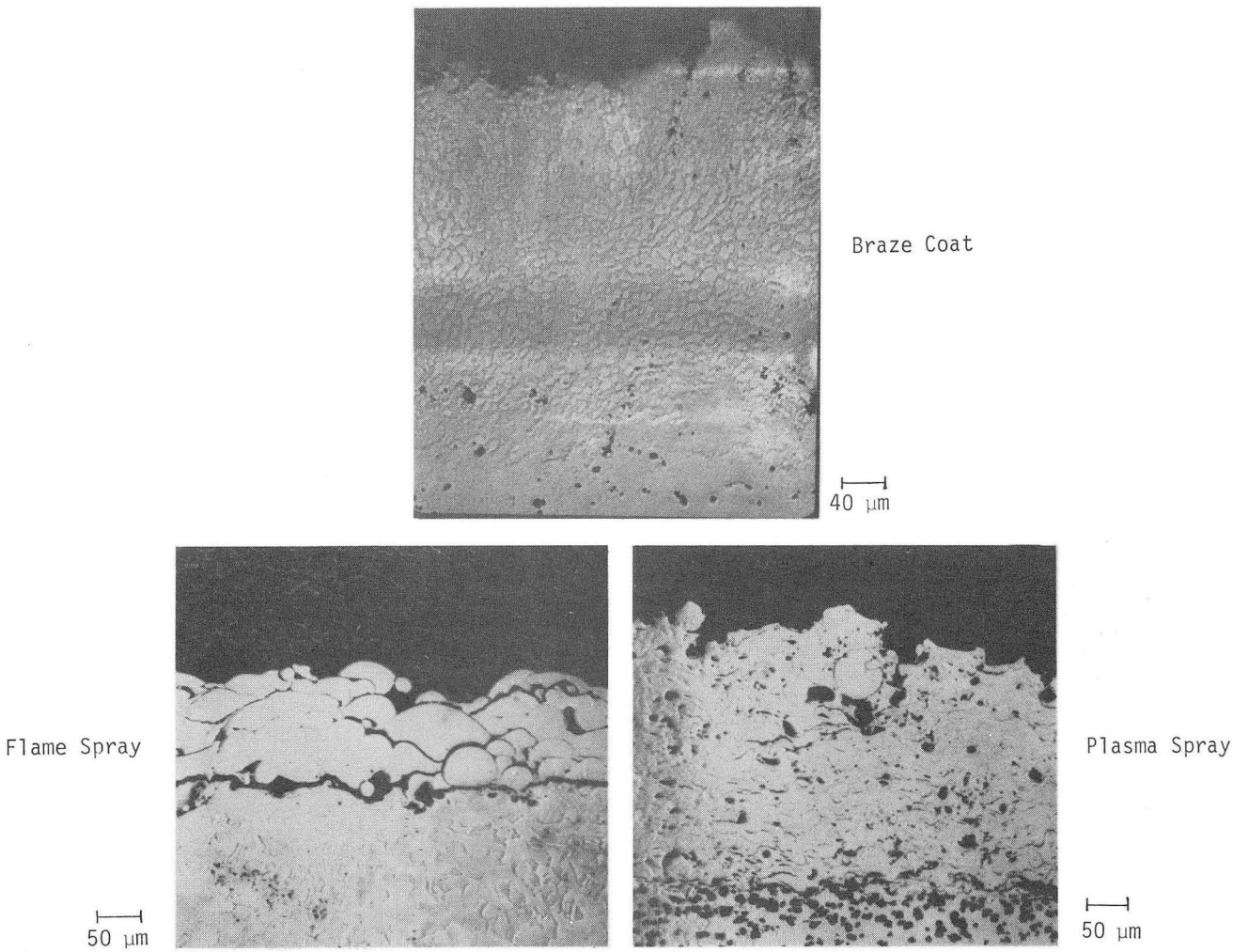

Fig. 4.1. Cross sections of uneroded nickel alloy, AMS 4779 Ni-B. (XBB 827-6203)

5. EROSION-CORROSION OF STEELS IN A BURNER DUCT TEST DEVICE†

Elliot Slamovich and Alan Levy

The combined erosion-corrosion of low alloy and stainless steels in air was determined using the ACES exhaust gas burner facility at the Sandia National Combustion Research Center. The purposes of the project are to: (1) determine the morphology of the eroded-corroded surfaces compared to only corroded and only eroded surfaces, (2) determine the mechanism of simultaneous erosion-corrosion, and (3) examine the conditions under which corrosive or erosive attack on the alloy dominates.

Tests have been run on cubes of several steels ranging in chromium content from 0-18%. They were eroded by 5 μm diameter fly ash at 15 m/s in an oxygen rich, combusted propane-air stream at 700 to 1000°C. The samples were mounted to expose two faces of the test cube to the particle flow and two faces to just the corrosive gases. Thus, corrosion behavior was determined simultaneously with the combined erosion-corrosion behavior in a single specimen. The 410SS specimen (Fig. 5.1) was exposed to the erosive-corrosive environment at 900°C.

At the test conditions used, corrosion was the dominant mechanism. The individual crystals shown in both the corroded and eroded-corroded photos were identified as iron oxide by Raman spectroscopy. The great difference in the morphologies of the two sides is indicative of the complexity of the combined erosion-corrosion mechanism. The enhancement of crystal growth as the result of a selective removal of the iron oxide crystals by the erosion process is clearly seen as is the erosion of the tops of the crystals to form a point. The same effect was also observed in the other chromium bearing alloys tested. The ability of the brittle iron oxide crystals to resist being completely removed by the impact of the eroding particles and to grow to such a large size compared to the corroded-only side crystals indicates that new mechanisms of erosion of brittle scales must be considered.

* * *

†Brief version of LBL-15657.

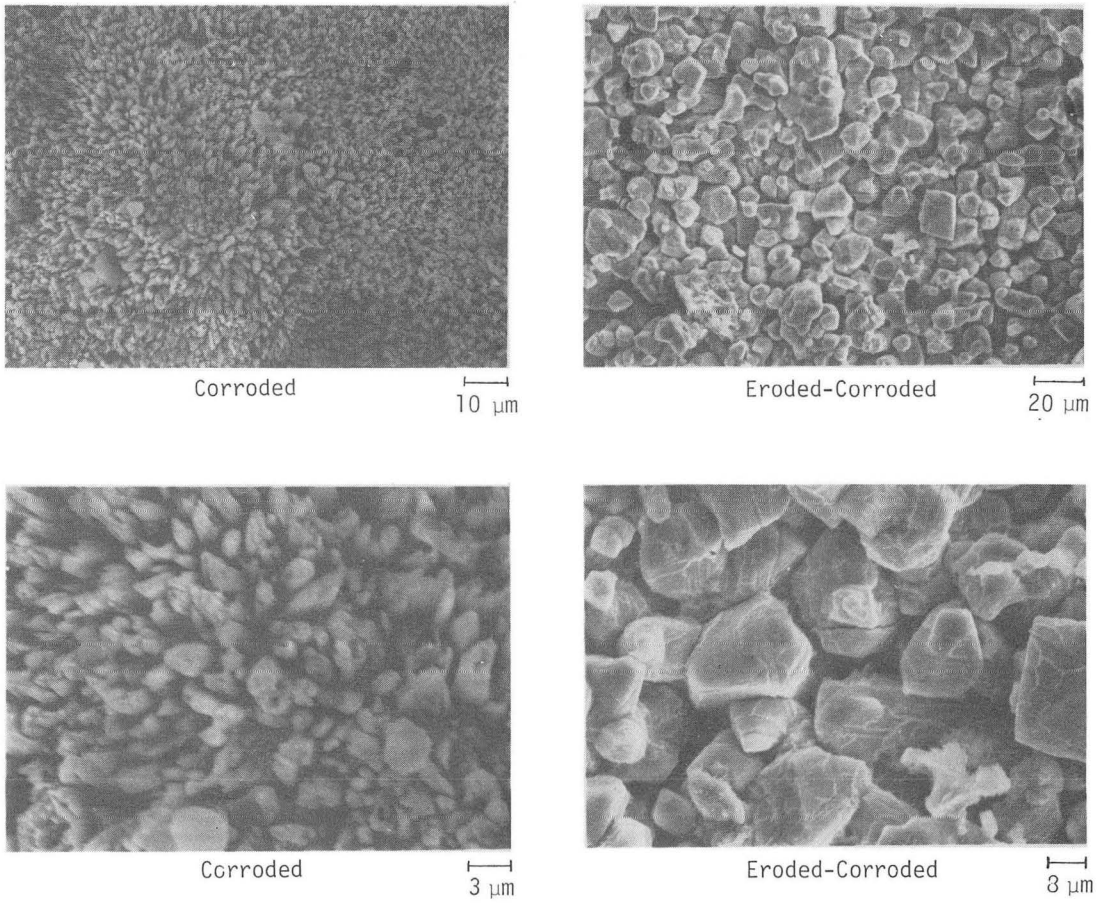

Fig. 5.1. Surface of corroded and eroded-corroded 410SS. (XBB 8210-9325)

6. EROSION OF METALS IN LIQUID SLURRIES†

Paul Yau and Alan Levy

The erosion of low alloy steels was determined at 25°C over a range of velocities and impingement angles using 30 wt.% -200 mesh coal in kerosene slurries. The slurry and test conditions simulated part of the conditions that exist in the slurry mixing area of a direct coal liquefaction process plant.

4340 steel was tested at 3 heat treat conditions: as-quenched, 200°C temper, and spheroidize annealed. 1018 plain carbon steel was tested in the hot-rolled and spherodize-annealed conditions. It was determined that, in general, the greater the ductility of the heat treated alloy, the lower the erosion rate. The 4340 in the as-quenched condition with an elongation of 8% eroded 3 to 4 times as much as 4340 in the spheroidize-annealed condition with an elongation of 25%, depending on the impingement angle. The effect of velocity on the erosion rate of hot-rolled 1018 steel was determined for a range of velocities from 10 to 30 m/s. The velocity exponents varied from 2.0 at a 20° impingement angle to 1.6 at a 90° impingement angle.

Figure 6.1 shows the effect of impingement angle on erosion for spheroidized 4340 and 1020 steels. The 4340 has a tensile strength of 100 ksi and an elongation of 25% while the 1020 steel has a lower tensile strength of 57 ksi and a higher elongation of 36%. Both steels eroded similarly at the higher impact angles while the less ductile 4340 eroded somewhat more at the lower impact angles. The reason for the difference in the relative amount of erosion between the alloys at lower and higher impingement angles was related to the lubricating nature of the non-aqueous fluids in the slurries.

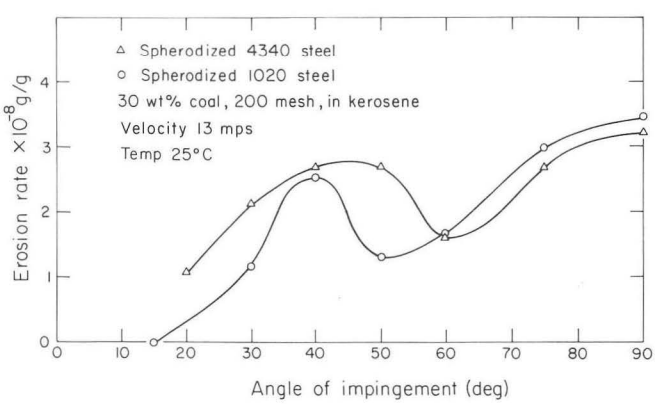

Fig. 6.1. Erosion rate of spheroidized 4340 and 1020 steel in coal-kerosene slurry. (XBL 8211-7300)

* * *

†Brief version of LBL-15658.

7. CORROSION OF METALS IN OIL SHALE RETORTS†

Elliott Slamovich and Alan Levy

An investigation of metallic corrosion in the oxidizing and sulfidizing environments of oil shale retorts has been completed. Both the corrosion environments of underground in-situ and above-ground retorts were investigated. Test samples were exposed in large retorts of both types. The effect of chromium content in commercial steel alloys exposed to in-situ retorting environments was determined using a small laboratory crucible containing Green River shale at a test temperature of 980°C.

It was determined that different patterns of corrosion, external and internal, occurred for each alloy exposed to the same test conditions. Higher chromium content alloys had lower external corrosion. However, the presence of chromium promoted internal corrosion. The chromium free, 1018-mild steel had extensive external corrosion but no internal corrosion. The 2 1/4Cr and 5Cr containing steels formed internal iron sulfides while the 9Cr and austenitic stainless steels were internally oxidized. The occurrence of the oxides and sulfides on each alloy was explained reasonably well, using the appropriate thermodynamic equilibrium stability diagrams.

Tests were performed on alloys containing 0-25% Cr to determine the nature of the corrosion problem in above-ground retorts that were retorting Green River shale where the operating temperatures are typically 500-550°C. Only the 1018 plain carbon steel showed mild corrosion (20 mil/year) after 400 hours of exposure. These results indicate that there will be little or no corrosion problem in such retorts as long as temperatures remain in the 500 - 550°C range.

* * *

†Brief version of LBL-13809.

1982 PUBLICATIONS AND REPORTS

Other Publications

1. A. Levy, "Metal Corrosion in Oil Shale Retorts," Proceedings of Conference on Corrosion-Erosion-Wear of Materials in Emerging Energy Systems, NACE, Berkeley, California, January 1982.

2. A. Levy, "Erosion of Ductile and Brittle Materials," Proceedings of Conference on Corrosion-Erosion-Wear of Materials in Emerging Energy Systems, NACE, Berkeley, California, January 1982.

3. A. Levy and G. Hickey, "Surface Degradation of Metals in Simulated Synthetic Fuels Plant Environments," Paper no. 154, NACE Corrosion 82, Houston, Texas, March 1982.

4. M. Landkof, D. Boone, D. Whittle, and A. Levy, "Protective Coating Systems for Use in Combustion Gases," Paper no. 287, NACE Corrosion 82, Houston, Texas, March 1982.

5. A. Levy and E. Slamovich, "Elevated Temperature Corrosion of Steel Alloys in Oil Shale Retorting Environments," Proceedings of Electrochemical Society Conference on Corrosion/Energy Technology, Paper no. 113, ECS Annual Fall Meeting, Detroit, Michigan, October 1982.

LBL Reports

1. J. Patterson and A. Levy, "Elevated Temperature Erosion of Alloys," LBL-15655.

2. J. Patterson and A. Levy, "Methods for Characterization of Erosion of Gas-Entrained Solid Particles," LBL-15017.

3. M. Aghazadeh and A. Levy, "The Effect of Particle Velocity on the Platelet Mechanism of Erosion," LBL-15656.

4. A. Levy, T. Bakker, E. Sholz, M. Aghazadeh, "Erosion of Hard Metal Coatings," LBL-15293.

5. E. Slamovich and A. Levy, "Erosion-Corrosion of Steels in a Burner Duct Test Device," LBL-15657.

6. A. Levy, P. Tom, and P. Yau, "Erosion Mechanism of Steels in Liquid Slurries," LBL-15658.

7. A. Levy and E. Slamovich, "Erosion of Metals in Oil Shale Retorts--Final Report," LBL-13809.

Invited Talks

1. A. Levy, "Erosion-Corrosion Behavior of Materials in Synthetic Fuels Processes," ASME Energy Technology Conference, New Orleans, Louisiana, March 1982.

2. A. Levy and J. Patterson, "Elevated Temperature Erosion of Ductile Alloys in Neutral Gases," AIME-TMS Meeting, St. Louis, Missouri, October 1982.

3. A. Levy and P. Tom, "Mechanism of Erosion of Steels in Non-Aqueous Liquid Slurries," AIME-TMS Meeting, St. Louis, Missouri, October 1982.

4. A. Levy, "Slurry Erosion of Alloy Steels at Elevated Temperatures," AIME-TMS Meeting, St. Louis, Missouri, October 1982.

5. A. Levy, "Erosion Testing Using a Jet Nozzle Test Device," ASTM G2 Workshop, Williamsburg, Virginia, December 1982.

c. Chemistry and Morphology of Coal Liquefaction*

Heinz Heinemann, Investigator, with Alexis T. Bell, James W. Evans, Richard H. Fish, Alan V. Levy, Eugene E. Petersen, Gabor A. Sormorjai, Theodore Vermeulen, and K. Peter Vollhardt, Investigators

Introduction. This program is concerned with a basic understanding of the chemistry and physics of coal liquefaction and with coal gasification as a preliminary step to liquefaction. It has brought together a team of organic, physical, and organometallic chemists, chemical engineers, and materials scientists, some of whom have had extensive industrial experience. Accomplishments of the past year are presented in the reports of the six tasks involved.

Task 1: SELECTIVE SYNTHESIS OF GASOLINE RANGE COMPONENTS FROM SYNTHESIS GAS†

A. T. Bell, Investigator with R. Dictor and J. Canella

The research carried out during the past year has been aimed at three principal objectives. The first was to develop a capability for complete on-line analysis of the products produced during Fischer-Tropsch synthesis. The second objective was to determine the influence of reaction conditions on the synthesis of hydrocarbons and oxygenated products over an iron catalyst contained in a well-stirred slurry. The third objective was to establish whether olefins, produced as a primary product of Fischer-Tropsch synthesis, undergo significant further chain growth and whether the recycle of olefins can be used to obtain non-Schulz-Flory product distributions.

Proper analysis of reaction products is essential to understanding the effects of catalysis composition and reaction conditions on the kinetics of Fischer-Tropsch synthesis. For the purposes of the present task, a gas chromatographic system was developed that permits a complete on-line analysis of all products to be performed in about an hour. A 1/8 in. x 9 ft stainless steel column packed with Chromsorb 106 is used to separate CO, CO_2, C_1 through C_5 hydrocarbons, as well as acetaldehyde and acetone; C_4 through C_{30} hydrocarbons and oxygenates are separated on a 50 m glass capillary column coated with OV 101. The identity of the major and many of the minor products have been established by GC/MS.

The synthesis of hydrocarbons over a fused Fe catalyst, promoted with potassium, has been studied in a well-stirred autoclave. The product distribution changes with time and approaches a Schulz-Flory distribution asymptotically. Each product approaches the steady-state distribution with a time constant that depends on the molecular weight and Henry's Law constant of the product in the paraffin wax used to suspend the catalysts. A mathematical model of the evolution of the product distribution was found to describe the observed results very successfully and to explain many anomalies in the published literature.

The dependence of the synthesis rates on H_2 and CO partial pressures, and temperature has been determined. The H_2 dependence is unity for all products. The CO dependence is -0.42 for methane and increases to zero for C_4. This suggests that the formation of light hydrocarbons can be reduced at low H_2/CO ratios and high total pressures. The activation energies for all products were nearly the same, lying between 26 and 29 kcal/mole. At low conversions the primary C_{2+} hydrocarbons are α-olefins, and the primary oxygenates are C_{2+} aldehydes. As conversion increases, the olefin to paraffin ratio decreases slightly, and the aldehydes are converted increasingly to alcohols. Very little methanol is produced at any conversion level.

Experiments were conducted to test whether the feedback of olefins could be used to alter the product distribution. For these runs, a fixed bed reactor was operated at 305°C and 5 atm, using a H_2O/CO of 2 in the feed gas. To simulate olefin feedback, 5% off ethylene, propylene, or cis-2-butene was added to the synthesis gas feed. It should be noted that the concentration of added olefin is much greater than that present due to synthesis alone. The addition of ethylene causes a 60% increase in the production of propylene and no more than a 10% increase in the production of butenes. The balance of the product is unaffected by ethylene addition. The addition of propylene causes a 15% increase in the formation of butenes and a slight increase in the formation of ethylene, but has no other effect. The only effects of cis-2-butene addition are a 40% increase in propylene formation and a slight increase in ethylene formation. In each of the cases examined, the proportion of the added olefin converted to products of greater chain length is only a few percent. From these results, it is concluded that small olefins do not enter into the chain growth process very efficiently, and in fact may undergo hydrogenolysis to produce lower molecular weight products.

* * *

*This work was jointly supported by the Director, Office of Energy Research, Office of Basic Energy Sciences, Chemical Sciences Division and the Assistant Secretary for Fossil Energy, Office of Coal Research, Liquefaction Division of the U.S. Department of Energy under Contract No. DE-AC03-76SF00098 through the University Contracts Management Division of the Pittsburgh Energy Technology Center, Pittsburgh, Pennsylvania.

†Partially covered by LBL-14964.

Task 2: ELECTRON MICROSCOPE STUDIES†

J. W. Evans, Investigator, with D. J. Coates

Controlled atmosphere electron microscopy (CAEM) has been used to examine high density pyrolytic graphite during the course of reaction with water vapor in argon, catalyzed by potassium and sodium hydroxide. Thin specimens of highly oriented pyrolytic graphite were mounted on grids and dipped into 0.38 M potassium hydroxide solution. After drying, the specimens were mounted on a heating stage and placed into a Gatan "environmental cell" within a Hitachi 650 keV transmission electron microscope. Argon, at approximately 1 atm pressure was bubbled through water at room temperature, giving an Ar/H_2O ratio of about 40/1, and then introduced into the environmental cell to give a pressure of 50 Torr. The specimens were heated in the flowing gas mixture and periodically observed. At 500°C the potassium hydroxide was dispersed as particles 0.1 0.5 μm in diameter on the surface of the graphite. With increasing exposure time, gasification was evident as the particles at the edges of the graphite crystals began moving toward the crystal centers leaving channels in their wake.

Figure 2.1 shows two micrographs recorded 11 min apart taken from a sequence showing the channel growth at 500°C. Channels are evident in two adjacent graphite crystals emanating from the edges of the crystals, each channel with a particle at its head. The interface between the particles in the channels and the graphite shows a hexagonal, faceted morphology. As the reaction continues the particles move and the length of the channels increase, as can be seen by the particles arrowed. The channels remain roughly parallel-sided, indicating that there is little effect of uncatalyzed reaction at the channel edges or of wetting of the channel sides by catalytic material. Initially particles lying on the surface of the graphite crystals do not contribute to the catalytic gasification of the carbon. At a later stage, however, faceted pits in the graphite are evident at the former positions of these particles. The catalyst particles are present within, and at one edge of, the pits. In some cases channeling by these particles away from the original pits is evident.

Similar observations have been noted at 600°C. At this temperature, however, no "incubation" period was noted for the catalytic reaction involving the particles dispersed on the surfaces of the graphite crystals and widespread channeling due to gasification was observed from outset.

These studies show that potassium hydroxide is effective in catalyzing the steam gasification of graphite and that the mode of the catalyzed attack is a channeling one with each channel being headed by a particle of potassium compound. Similar observations of the catalysis by sodium and calcium compounds have been made in the Berkeley microscope.

* * *

†Partially covered by LBL-14463; Journal of Catalysis, in press.

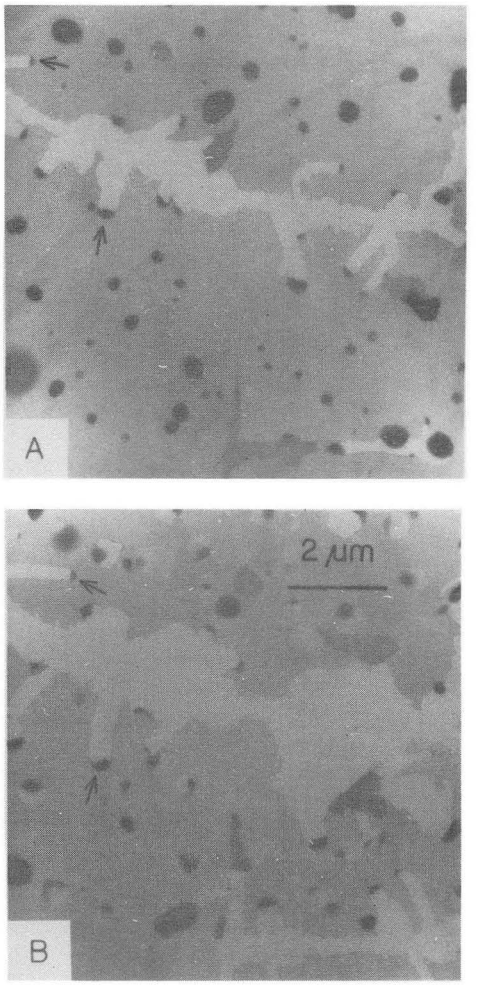

Fig. 2.1. (XBB 824-3397)

Task 3: CATALYZED LOW TEMPERATURE HYDROGENATION OF COAL†

G. A. Somorjai, Investigator, with A. Cabrera and R. Casanova

The purpose of these studies is to produce high molecular weight hydrocarbons by the catalyzed depolymerization and hydrogenation of carbonaceous solids (graphite, char, etc.).

a. Methane Production From the Alkali Hydroxide Catalyzed Reaction of Graphite with Water Vapor at Low Temperatures (500-600 K)

A. Cabrera

The production of gaseous CH_4 and CO_2 (or CH_4 and CO) from graphite occurs rapidly in the temperature range 500-650 K with low activation energy (10 ± 3 kcal) in the presence of alkali compounds. KOH, K_2CO_3, LiOH, CsOH, and NaOH all appear to catalyze both the reduction of C to CH_4 and its oxidation to CO_2 or CO.

b. Calcium Oxide Catalyzed Low Temperature Methane Production From Graphite

R. Casanova

Calcium oxide catalyzes the transformation of graphitic carbon to an active form of carbon in the presence of water vapor:

$$\text{(graphite)} \xrightarrow{CaO,\ H_2O} C_{(active)}.$$

This transformation could be monitored by x-ray photoelectron spectroscopy, and its activation energy is 16.3 kcal/mole. Methane formation only occurs in the presence of hydrogen as the active carbon is gasified with an activation energy of 25.5 kcal/mole:

$$C_{(active)} + 2H_2 \xrightarrow{CaO} CH_4.$$

c. Study of Potassium Intercalated Graphite

Potassium-intercalated graphites C_8K and $C_{24}K$ have been employed for our reaction studies using water vapor. The rate of methane production is much lower for the intercalated samples than when KOH was on the external surface of the pure graphite sample. It appears that alkali catalyst intercalation plays no important role during gasification.

d. Reaction Rate Studies of the Structure Sensitivity of Graphite Gasification

Reaction rate studies were carried out using different surface area and thickness graphite samples. While increasing the basal plane area of graphite did not increase the reaction rate, increasing the thickness (edge area) increased the methane production rate in proportion.

* * *

†Partially covered by LBL-15067.

Task 4: SELECTIVE HYDROGENATION, HYDROGENOLYSIS, AND ALKYLATION OF COAL AND COAL RELATED LIQUIDS BY ORGANOMETALLIC SYSTEMS†

K. P. C. Vollhardt, Investigator

a. Finalizing Studies on the Reaction of Benzene with Aluminum Chloride

Y.-H. Lai and L. S. Benner

The reaction of benzene with aluminum trichloride has been studied under many different conditions, and generally a complex mixture of hydrocarbons is obtained. However, the nature of the major products reported varied greatly in the early experiments, and the accuracy of the structure assignments might be held in doubt because of insufficient separation and characterization of the product mixtures. A detailed analysis of the volatile components of the reaction has never been performed.

Heating benzene and $AlCl_3$ in a glass pressure vessel under various conditions furnished alkybenzenes in addition to a variety of other products. Application of pressure, however, reduced the number of products (resulting in cleaner GC traces) and their overall yield.

A typical GC trace of the reaction of benzene with $AlCl_3$ shows the four major products being toluene, ethylbenzene, tetralin, and biphenyl.

The reaction always yields some polymeric materials, believed to contain polyphenyls. The monitored reaction also shows an initial build-up of polynuclear aromatic hydrocarbons such as methylphenanthrenes, methylanthracenes, and phenylnaphthalenes which are known to undergo Scholl-type polycondensation reactions in the presence of $AlCl_3$.

In order to minimize polymerization and condensation reactions, several experiments were carried out under hydrogen in the presence of a catalytic amount of PtO_2. Hydrogen consumption was fairly rapid, and as expected, the reaction was much cleaner.

Several labeling experiments were performed. Reaction of C_6D_6 gave completely labeled products. Not unexpectedly, a 1:1 mixture of C_6H_6 and D_6D_6 gave complete scrambling. Therefore, an equimolar mixture of C_6H_6 and $^{13}C_6H_6$ (90% enriched) was exposed to $AlCl_3$ [N_2 (1 atm), 160°C, 48 hr]. Surprisingly, ^{13}C–^{12}C exchange (ca. 5%) was observed in recovered "unreacted" benzene and additional scrambling in all other volatile products as analyzed by GC/MS. The mass spectral peak patterns indicate substantially intact incorporation of alkyl chains derived from the original benzene ring. Thus, the connectivity of the initial carbon arrays is extensively preserved in the alkybenzenes (including annulated and cycloalkylbenzenes) formed. The mechanism by which label exchange occurs is not understood at present.

An extension of our investigation involved the $AlCl_3$-induced cracking of some cycloalkanes and polynuclear aromatic hydrocarbons under hydrogenation conditions as models for the hydroliquefaction of coal and/or heavy petroleum hydrocarbons. The results are summarized in the schemes below. In these reactions there was insubstantial polymer formation, in contrast to the other studies. The reaction of larger cycloalkanes gives mainly ring contraction products.

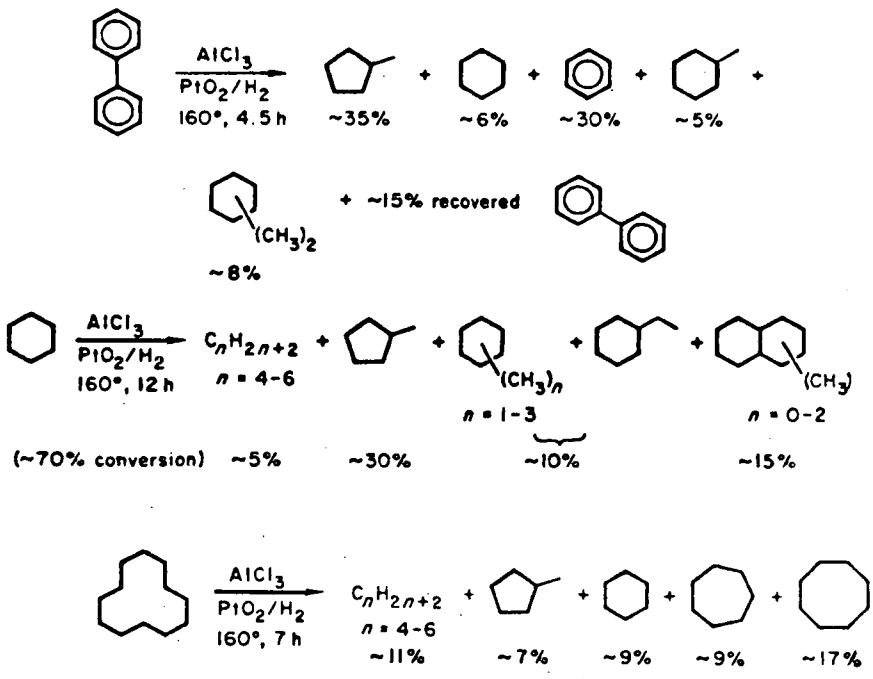

It is clear that many of the reactions described will play a significant role in any process that attempts to liquefy coal or heavy petroleum hydrocarbons in the presence of Lewis acids. It appears that the use of Lewis acid alone leads to polymerization and subsequent catalyst deactivation. On the other hand, simultaneous application of a platinum hydrogenation catalyst and hydrogen, although successfully minimizing polymerization, results in secondary reactions, such as premature hydrogenation competing favorably with the cracking of hydrocarbons. A successful method for hydroliquefaction of coal would seem to depend on the search for a bifunctional catalyst having complementary properties of Lewis acid and hydrogenation activity.

b. Diene Cobalt Complexes as Models for Hydrogenolysis of and Hydrogenshifts in Coal Unsaturates

We have postulated the theoretical feasibility of aromatic hydrocarbon hydrogenolysis by a route involving an initial arene--dihydroarene step followed by a metal promoted ring opening to a complexed oligoene:

Proposal (1)

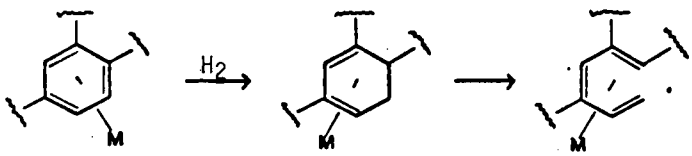

If successful, this could provide a long sought and unique method for coal hydrogenolysis. This proposal has prompted an investigation of the thermal and photolytic chemistry of transition metal diene and triene complexes, models for the last two species in (1).

We have found that CpCo-η^4-cyclohexa-1,3-diene (Cp = η^5-C_5H_5) is remarkably stable thermally with respect to ring opening, but that it undergoes relatively rapid intramolecular hydrogen shifts via intermediate metal hydrides. Moreover, on laser irradiation one can observe the desired ring opening to CpCo-η^4-1,3,5-hexatriene, albeit with low quantum efficiency.

To probe the potentially adverse thermodynamics of the postulated ring opening, it was planned to test the thermal behavior of CpCo-η^4-cis-1,3,5-hexatriene. For this purpose the complexation chemistry of the ligand under irradiative conditions was subjected to detailed scrutiny. A range of products was observed, including some of the desired cis-complex, but also a substantial amount of the trans-isomer. The latter is the major compound on prolonged irradiation. We have established the mechanism of this isomerization through the investigation of labeled butadiene-CpCo.

The reactions uncovered in this work constituted novel potential pathways by which hydrocarbons may transform on surfaces and in homogeneous catalytic hydrogenative and reforming systems. They also provide useful models for the possible chemistry of coal liquids when exposed to transition metal catalysts for the purposes of hydrogenation, desulfurization, and rearrangement.

* * *

†Brief version of LBL-15606, in press.

Task 5: CHEMISTRY OF COAL SOLUBILIZATION†

R. H. Fish and T. Vermeulen, Investigators, with A. D. Thormodsen

We have demonstrated with model coal compounds, which include polynuclear aromatic and polynuclear heteroaromatic nitrogen compounds, that transition metal carbonyl hydrides, generated catalytically under a wide variety of conditions, selectively reduce the nitrogen heterocyclic ring in polynuclear heteroaromatic nitrogen compounds. Moreover, we discovered that $(\phi_3P)_3RhCl$ or Wilkinson's catalyst will also selectively reduce the nitrogen containing ring in polynuclear nitrogen heterocyclic compounds under extremely mild conditions (80°C, 300 psi H_2, for 2 hr).

With the latter catalyst $(\phi_3P)_3RhCl$, we also found a dehydrogenation reaction with a saturated nitrogen heterocyclic compound, 9-10-dihydrophenanthridine, which provided the first example of a transfer hydrogenation using quinoline as the acceptor molecule.

The use of deuterium gas (D_2) in place of H_2 has given important insights into the hydrogenation reaction with phenanthridine and quinoline as substrates. The position alpha to the nitrogen in both dihydrophenanthridine (C_9) and quinoline (C_2) were deuterated. Additionally, exchange of an aromatic hydrogen for deuterium implicates cyclometallation reactions in both cases (Schemes 1 and 2).

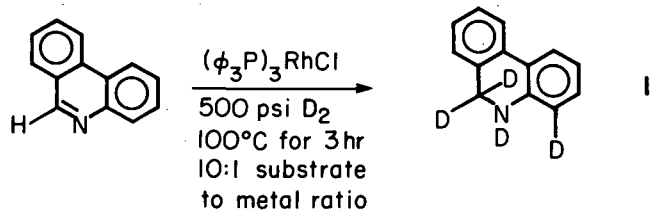

1

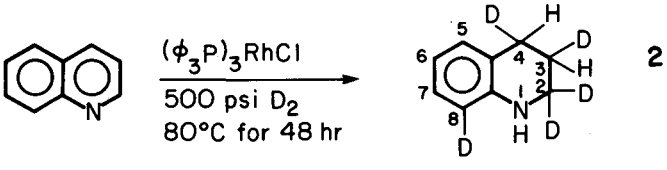

2

Initial competition experiments under hydrogenation conditions revealed several interesting facts: Quinoline in the presence of thiophene, with $(\phi_3P)_3RhCl$ as catalyst, provided tetrahydroquinoline with no apparent inhibition by thiophene. However, quinoline in the presence of pyridine was not hydrogenated implicating basicity as a criterion for reactions to occur. Possibly, pyridine acts, as CO did, by binding to rhodium and preventing quinoline from coordinating to the metal center.

* * *

†Partially covered by LBL-13735.

Task 6: COAL CONVERSION CATALYSTS: DEACTIVATION STUDIES†

A. V. Levy and E. E. Petersen, Investigators, with M. West and M. C. Smith

Catalysts used to hydrodesulfurize coal-derived liquids and petroleum residua are deactivated by the trace metals these liquids contain. The titanium in coal liquids and the vanadium in residua deposit on the external and internal surfaces of the catalyst, thus both blocking access to the interior of the catalyst and covering active surface sites. Our objective is to examine this metal deposition process and how it affects desulfurization activity. We have approached the problem three different ways: we have measured local metal deposition rates under realistic but experimentally manageable conditions; we have developed an extensive computer model describing the deactivation of a single catalyst pellet by metal deposits, and we have developed a technique to measure directly the decreased diffusivity of a catalyst containing metal deposits.

A comprehensive set of experiments using vanadium naphthenates as a model compound and a sour gas oil as a model liquid was completed during the past year. Stirred autoclave runs were made from 325° to 400°C at vanadium levels of 100 to 400 ppm under 800 psig hydrogen and up to 48 hr in length. Catalysts samples were withdrawn periodically and analyzed for local metal concentration with KEVEX x-ray microanalyzer across a polished cross section. Radial concentration profiles of vanadium in catalysts samples taken at 8, 24, 32, and 48 hr are shown in Fig. 6.1.

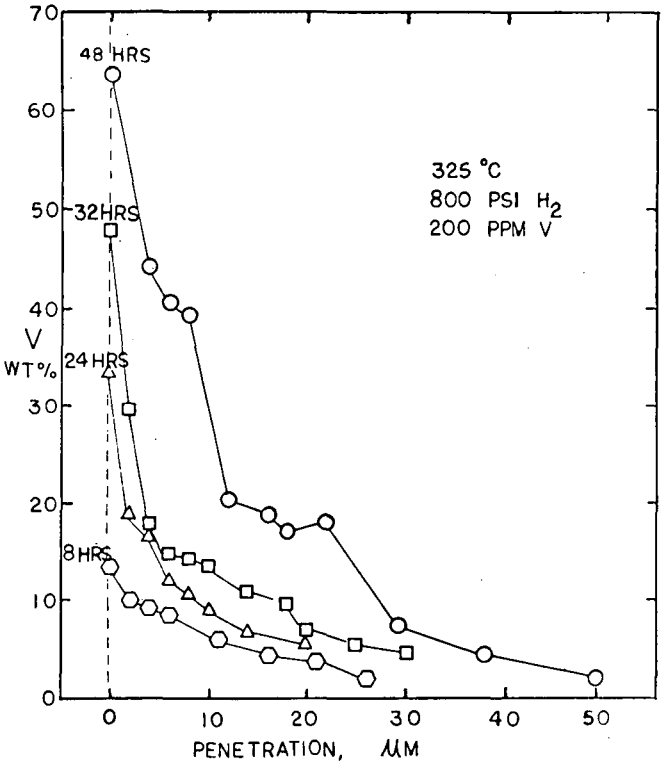

Fig. 6.1. (XBB 831-7572)

The temperature was 325°C and the vanadium concentration 200 ppm as naphthenate. Increased exposure time increases the amount of metal deposited and increased the deposit penetration. These profiles are indicative of a diffusion-controlled reaction. Deposition continues long after a monolayer of vanadium sulfide is deposited demonstrating that vanadium sulfide is itself an active catalyst for demetallation.

Because of diffusion limitations, vanadium deposits preferentially at the outside of the catalyst eventually building up a monolayer or more of sulfide and covering the active molybdenum-cobalt sulfide surface. This layer of vanadium sulfide is still active toward demetallation so deposition continues but at a slower rate than fresh catalyst.

Figure 6.2 shows smoothed radial concentration profiles of vanadium from catalysts run at four different temperatures and otherwise similar conditions. As expected for a diffusion-controlled reaction the apparent effectiveness factor decreases with increasing temperature, i.e., the profiles penetrate less deeply. However, the maximum demetallation rate at the outside edge where diffusion is not important decreases with increasing temperature instead of increasing as expected. The most plausible explanation for this phenomenon is that homogeneous demetallation in the bulk liquid produces vanadium sulfide particles which reduces the concentration of vanadium naphthenate in the bulk solution, and the net result is a decreased overall demetallation rate on the catalyst. Homogeneous demetallation is minimal at 325°C, but is extensive at 400°C and

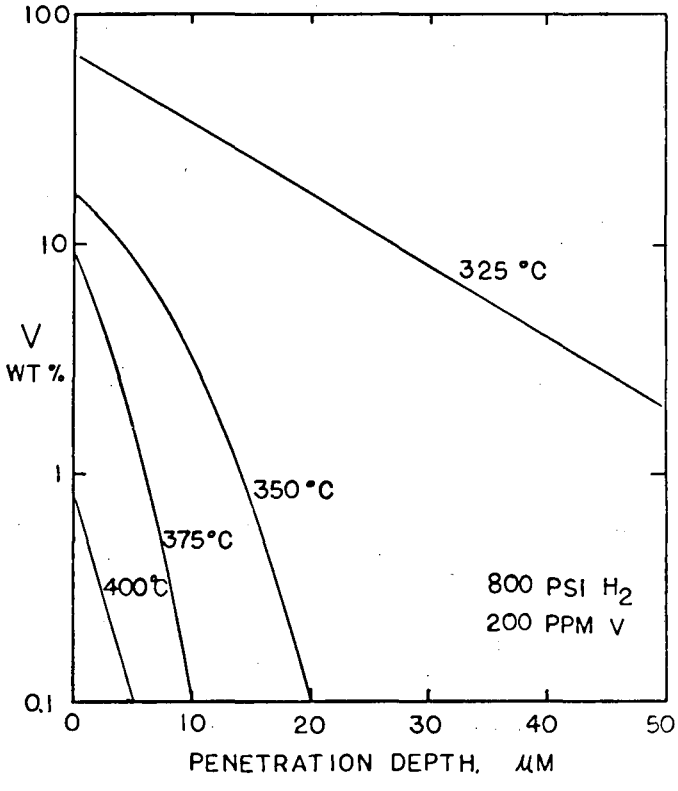

Fig. 6.2. (XBB 831-7570)

is evidenced by the vanadium-rich sludge that settles out of diluted gas oil samples.

A model has been developed to simulate the deactivation of a catalyst pellet during the desulfurization and demetallation of a heavy oil. The objective of the modeling is to examine the resistance of different pore size distributions to deactivation so that catalyst improvements can be identified.

The model is based on the solution of the differential equations for diffusion and reaction in a catalyst pellet. The main feature of the model is the calculation of the model parameters from the pore size distribution of the catalyst as the pore sizes are altered during the lifetime of the catalyst.

* * *

†Brief version of LBL-15432.

1982 PUBLICATIONS AND REPORTS

Refereed Journals

1. A. L. Cabrera, Heinz Heinemann, and G. A. Somorjai, "Methane Production from the Catalyzed Reaction of Graphite and Water Vapor at Low Temperatures," J. Catalysis 75, 7 (1982).

2. Richard H. Fish, A. D. Thormodsen, and G. A. Cremer, "Homogeneous Catalytic Hydrogenation I," J. Am. Chem. Soc. 104, 5234 (1982).

LBL Reports

1. A. T. Bell and R. A. Dictor, "An Explanation for Deviation of Fischer-Tropsch Products from a Schulz-Flory Distribution," submitted to I & EC Process Design and Development, LBL-14964.

2. R. Casanova, A. L. Cabrera, H. Heinemann, and G. A. Somorjai, "Calcium Oxide and Potassium Hydroxide Catalysed Low Temperature Methane Production from Graphite and Water. Comparison of Catalytic Mechanisms," submitted to Fuel, LBL-15067.

3. Richard H. Fish and A. D. Thormodsen, "Selective Catalytic Reductions of Polynuclear Heteroaromatic Nitrogen Compounds, Using Both Homogeneous and Heterogenized Forms of Chorotris (Triphenylphosphine) Rhodium I," LBL-14958.

4. M. West, M. C. Smith, E. E. Petersen, A. V. Levy, and H. Heinemann, "Hydrodemetallation of Model Compounds of a Cobalt-Molybdenum Catalyst," LBL-15432.

Other Publications

1. D. J. Coates, J. W. Evans, A. L. Cabrera, G. A. Somorjai, and Heinz Heinemann, "An Electron Microscopy Study of the Low Temperature Catalyzed Steam Gasification of Graphite," J. Catalysis, in press.

2. Y.-H. Lai, L. S. Benner, and K. P. C. Vollhardt, "Studies on the Reaction of Benzene and Other Hydrocarbons with Aluminum Chloride. The Effect of Catalytically Activated Hydrogen," Fuel, in press.

Invited Talks

1. Heinz Heinemann, "Alkali Catalyzed Low Temperature Gasification of Graphite," Kurt Wohl Memorial Lecture, University of Delaware, April 15, 1982.

2. Heinz Heinemann, "Heat and Mass Transfer Phenomena in Fischer-Tropsch Slurry Reactors," International Coal Conversion Conference, Pretoria, South Africa, August 1982.

3. Heinz Heinemann, "The Past 40 Years of Chemical Industry," 5th Roermond Conference on Catalysis, Roermond, Netherlands, July 1982.

4. R. H. Fish, "Selective Catalytic Reductions of Polynuclear Heteroatomic Nitrogen Compounds," N. Y. Academy of Science Conference on Catalytic Transition Metal Hydrides, New York, November 1982.

5. K. P. C. Vollhardt, "Remarkable Bond-Making and Bond-Breaking in the Coordination Sphere of Transition Metals," ACS Midland Section, Midland, Michigan, April 13, 19821.

6. K. P. C. Vollhardt, "Remarkable Rearrangements in the Coordination Sphere of Transition Metals," University of Nice, Nice, France, June 1, 1982.

7. K. P. C. Vollhardt, "Remarkable Rearrangements in the Coordination Sphere of Transition Metals," Indiana University, Bloomington, Indiana, October 21, 1982.

d. Materials Characterization in Fossil Fuel Combustion Products*

Donald Boone and Alan V. Levy, Investigators

Introduction. The purpose of this study is to develop an understanding of materials behavior in combustion zone environments by evaluating the behavior of specific material systems in engine tests and in appropriate laboratory simulations. Development of a basic understanding of the cause and effect relationship between material performance and the processing techniques used in their fabrication is an additional goal of this program. Particular interest has been focused on the diesel engine and the combustion of lower grade fuels, alternate fuels, and the direct combustion of coal. As a consequence, material performances have been determined by erosion, wear, hot corrosion, oxidation and thermal fatigue resistance testing.

An additional aspect of this program has been the correlation of national coating deposition research efforts, mainly in the area of high temperature erosion resistant systems and ceramic thermal barrier systems, with laboratory and field testing both in diesel and gas turbine engines.

1. EROSION OF SiC HARD COATING MATERIALS†

Eric Scholz, Donald Boone, and Alan Levy

Silicon carbide is known to be an excellent combustion engine component protective coating because of its extreme hardness and very low wear rate and its resistance to high temperature corrosion. In 1981 several of the most promising refractory hard metal coatings and monolithic bodies commercially available or in development were erosion tested. A type of chemical vapor deposition (CVD) silicon carbide, called Controlled Nucleation Thermochemical Deposition (CNTD) SiC, showed the best performance. This year the CNTD SiC was examined more closely to determine the reasons for its superiority by relating the erosion behavior to the properties and morphology of variations of the coating and to the effects of its manufacturing variables.

The variables considered were the hardness, which is determined primarily by the level of free silicon in the coating and coating thickness. CNTD coating samples of five hardnesses, ranging from 2400 to 4000 VHN, with thicknesses ranging from 80 to 210 μm were tested as well as a standard CVD SiC coating for comparison. The erosion testing was performed at room temperature using 200 μm SiC particles in a solid particle-airstream at 30 m/s at impingement angles of 30° and 90°. All of the coatings were brittle with a high erosion peak occurring at the start of each test with a subsequent drop to a relatively low steady state erosion rate, which was much greater at 90° than at 30°. Coatings with a thickness <90 μm failed almost immediately. Above a hardness of 3000 VHN, hardness did not affect the erosion rate. Below 3000 VHN the erosion rate increased significantly with decreased hardness. The CNTD SiC coating was superior to the standard CVD SiC coating, especially at 90° where the standard CVD SiC failed immediately.

The key to the erosion resistance of the CNTD SiC is the extremely fine grain size deposited by the continual renucleation of the grains as they are formed. The oriented, columnar growth of standard CVD SiC is replaced with uniform, essentially equi-axed, extremely small grains in the CNTD SiC, on the order of 1000 Å or less (standard CVD coating grain sizes can approach a millimeter diameter with large L/D ratios). The result is an erosion mechanism of very fine cracking and chipping of material around small surface craters. The lower erosion rates are due to the very small chips of material that are removed from the surface.

* * *

†Brief version of LBL-15293.

2. EROSION OF CERAMIC THERMAL BARRIER COATINGS†

A. Davis, D. Boone, and A. Levy

The use of ceramic thermal barrier coatings in a number of combustion engine types is often limited by their inadequate resistance to thermal fatigue, coating cracking, and spallation. Performance has been significantly improved in these areas by the introduction of controlled microporosity and/or microcracking in the ceramic structure, usually a stabilized or yttria partially stabilized zirconia. The purpose of this project was to determine the solid particle impact erosion resistance of the microporous and cracked coatings to determine their use potential in engines burning degraded fuels.

The erosion tests were carried out at room temperature using 60-100 μm SiO_2 erodent particles with 30 m/s velocity at 90° and 30° impingement angles. Weight loss per unit of erodent was measured, and the structures of the eroded surfaces were studied. Significant differences in erosion behavior were found between different ceramic coating structures, the processes used to produce them, and the compositions of the ceramic. For plasma-spray-deposited ceramics, structures with higher levels of microporosity and microcracking induced to provide acceptable thermal fatigue resistance exhibited reduced resistance to particulate erosion. However, a microstructurally segmented-ceramic structure aligned per-

*This work was supported by the Assistant Secretary for Fossil Energy, Office of Coal Research, Heat Engines and Heat Recovery Division of the U.S. Department of Energy under Contract No. DE-AC03-76SF00098 through the Battelle Memorial Institute, Pacific Northwest Laboratories, Richland, Washington.

pendicular to the substrate that was produced by electron beam physical vapor deposition techniques showed comparable erosion resistance to some of the more dense plasma spray coatings and better thermal fatigue behavior.

* * *

†Brief version of LBL-15667.

1982 PUBLICATIONS AND REPORTS

Other Publications

1. E. Demeray, J. Fairbanks, and D. Boone, "Physical Vapor Deposition of Ceramic Coatings for Gas Turbine Engines,"Proceedings of the 1982 ASME Gas Turbine Conference, Paper no. 82-GT-265, London, England, April 1982.

2. D. Boone, "Ceramics Coatings for Advanced Energy Technologies," Proceedings of Ceramics in Advanced Energy Technologies Colloquium, The Petten Establishment, The Netherlands, September 1982.

3. D. Boone, et al.,"The Structure and Performance of Electrophoretically Applied Aluminide Coatings," Proceedings of International Conference on Metallurgical Coatings, Thin Solid Films AVS, San Diego, California, April 1982.

4. D. Boone, M. Edwards, G. Newberry, "Low Temperature (704°C) Hot Corrosion of Nickel-Based Superalloys, "Proceedings of Electrochemical Society Conference on Corrosion/Energy Technology, Paper no. 128, ECS Annual Fall Meeting, Detroit, Michigan, October 1982.

LBL Reports

1. A. Davis, D. Boone, and A. Levy, "Erosion of Ceramic Thermal Barrier Coatings," LBL-15667.

2. A. Levy, T. Bakker, E. Sholz, and M. Azabadeh, "Erosion of Hard Metal Coatings," LBL-15293.

Invited Talks

1. D. Boone, "Substrate and Processing Effects on Carbon-Carbon Coating Systems," Composite Materials Conference, 6th Annual Conference of the Ceramic-Metal Systems Division, American Ceramic Society, Cocoa Beach, Florida, January 1982.

2. D. Boone and J. Exell, "The Substrate HF Effect in Aluminide Coatings," AIME-TMS Fall Meeting, St. Louis, Missouri, October 1982.

3. D. Boone and R. Lambertson, "The Effect of Aluminide Processing Variables on Oxide Structure, AIME-TMS Fall Meeting, St. Louis, Missouri, October 1982.

4. D. Boone and B. Rose, "Low Temperature (700°C) Corrosion Testing of Modified Aluminide Coatings," AIME-TMS Fall Meeting, St. Louis, Missouri, October 1982.

5. D. Boone, R. Lambertson, and M. Barber, "Protective Oxide Characterization of Mn Modified Aluminide Coatings," AIME-TMS Fall Meeting, St. Louis, Missouri, October 1982.

e. Solution Thermodynamics of Sulfites and Sulfite Oxidation Mechanisms*

Leo Brewer and Robert E. Connick, Investigators

Introduction. Acid rain is formed primarily by the oxidation of sulfur dioxide to sulfuric acid when the former is released into the atmosphere through combustion of sulfur-containing coal. Release of sulfur dioxide can be prevented by passing the stack gases through aqueous scrubbers of low acidity where the sulfur dioxide is converted to bisulfite ion. The present project is concerned with obtaining reliable thermodynamic and kinetic data to support improvements in the complex chemical processes that occur in flue gas desulfurization and to provide data for modeling these systems.

1. THE MECHANISM OF OXIDATION BISULFITE ION BY OXYGEN

Robert E. Connick and Paul Chieng

Work in Progress. An important reaction in flue gas desulfurization processes is the oxidation of bisulfite ion by oxygen to form sulfate ion. In some processes oxidation is desired and in others avoided, so that control of the rate is of general importance. Study of the reaction is difficult because it is a chain reaction and therefore highly subject to catalysis and inhibition by a great variety of chemicals. Results are extremely difficult to reproduce. During the year attention was focused primarily on the detection of an intermediate in the reaction that has been tentatively identified as a peroxy sulfite species. Knowledge of its existence seriously limits the number of possible mechanisms that can be proposed for any given rate law. Present research is being directed toward identifying the chain initiation step.

1982 PUBLICATIONS AND REPORTS

See section on "Formation of Oxyacids of Sulfur from SO_2" for R. E. Connick and section on "High Temperature Thermodynamics" for L. Brewer.

*This work was supported by the Assistant Secretary for Fossil Energy, Office of Coal Research, Advanced Environmental Control Division of the U.S. Department of Energy under Contract No. DE-AC03-76SF00098 through the Morgantown Energy Technology Center, Morgantown, West Virginia.

f. Process Chemicals Parameters in Aqueous Sulfur Dioxide Removal by Lime/Limestone Scrubbers*

C. Beat Meyer and Robert E. Connick, Investigators

Introduction. In flue gas desulfurization processes for removing sulfur dioxide from stack gases of coal burning power plants, the sulfur dioxide is absorbed into an aqueous solution where it may undergo a wide variety of reactions, depending on the particular process employed. The present work is aimed at investigating the basic chemistry of a number of species that can be formed in solutions under conditions similar to those in FGD processes.

1. THE THERMAL DECOMPOSITION OF AQUEOUS TRI- AND TETRATHIONATE†‡

C. B. Meyer, M. Ospina, K. Koshlap, A. Tini, and K. Ward

The polythionates constitute an important but complex group of sulfur compounds formed in the acid decomposition of thiosulfate ion and in most systems containing any of the 13 oxyacids of sulfur currently known. While a great deal of research has been done on these species, the data have been extremely difficult to interpret, because there are usually a number of species present simultaneously and the analytical methods are cumbersome and imprecise. It was hoped that the application of modern techniques would lead to a clearer understanding of their chemistry and therefore greater control of their effects in FGD processes.

Raman spectroscopy is an excellent tool for detecting individual species since the Raman lines of two species usually do not overlap, at least for all lines. Thus, it is usually possible to identify a particular species even in a mixture of several. The method suffers from lack of great sensitivity so that solutions of greater than ~0.03 M are needed unless resonance Raman can be used. In addition it is not simple to get quantitative measurements of concentration, although this difficulty can be mostly avoided by using an internal standard.

Raman studies have been made of the rate of decomposition of 0.25 M trithionate and 0.5 M tetrathionate ions at 20, 35, 50 and 70°C. During the reactions tri- and tetrathionate interconvert. Thiosulfate is a prominent intermediate. The end products are elemental sulfur, sulfate, disulfite, and bisulfite. The decomposition of trithionate initially follows a first order rate law with a rate constant of 0.14 hr^{-1} at 70°C. In the case of tetrathionate the reaction is preceded by an induction period.

---

*This work was supported by the Assistant Secretary for Fossil Energy, Office of Coal Research, Advanced Environmental Control Division of the U. S. Department of Energy under Contract No. DE-AC03-76SF00098 through the Morgantown Energy Technology Center, Morgantown, West Virginia.

* * *

†Work supported in part by the Department of Chemistry, University of Washington, Seattle, Washington.
‡Brief version of Phosphorus and Sulfur 14, 23 (1982).

2. THE STRUCTURE OF DITHIONITE ION†‡

L. Peter§ and C. B. Meyer

Dithionite ion, $S_2O_4^{2-}$, is a highly active and widely used reducing agent whose structure in solids and aqueous solution has been a matter of controversy. The x-ray investigation of Dunitz showed the structure to be C_{2v} in solid $Na_2S_2O_4 \cdot 2H_2O$. On the other hand, Simon and Kuchler concluded from Raman spectra in solution that the ion was D_{2h}.

Raman spectroscopy was used once again to investigate the structure of the ion in solution. Modern Raman equipment with lasers and photon counting should yield more reliable results than the older apparatus that depended on photographic recording.

The Raman spectrum of the aqueous ion differs considerably from that of $Na_2S_2O_4 \cdot 2H_2O$. The spectrum found differed from the solution spectrum of Simon and Küchler in that two additional weak bands were detected and one reported by the earlier authors could not be found. The spectrum was compared to other X_2Y_4 type molecules and found to resemble that of P_2F_4 most closely. It is concluded that the symmetry is C_{2h}. It is also proposed that the S-S bond length is considerably shorter in the aqueous ion than in solid $Na_2S_2O_4 \cdot 2H_2O$ and that the configuration of the ion is strongly susceptible to environmental effects.

* * *

†Work supported in part by the Department of Chemistry, University of Washington, Seattle, Washington.
‡Brief version of J. Molec. Struc. 95, 131 (1982).
§Present address: Chemistry Department, Seattle Pacific University, Seattle, Washington 98119.

1982 PUBLICATIONS AND REPORTS

Refereed Journals

1. B. Meyer and M. Ospina, "Raman Spectrometric Study of the Thermal Decomposition of Aqueous Tri- and Tetrathionate," Phosphorus and Sulfur 14, 23 (1982).

2. L. Peter and B. Meyer, "The Structure of Dithionite Ion," J. Molec. Struct. 95, 131 (1982).

For publications by R. E. Connick, see section on "Formation of Oxyacids of Sulfur from SO_2."

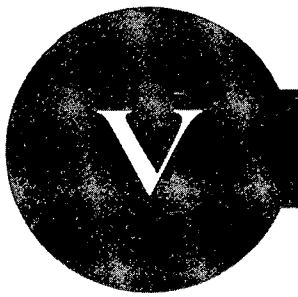

V Advanced Isotope Separation Technology

Advanced Isotope Separation Technology

A. Applications and Assessments of Advanced Techniques

a. Isotope Separation by Laser Photochemistry*

C. Bradley Moore, Investigator

1. DETERMINATION OF ARRHENIUS PARAMETERS FOR UNIMOLECULAR REACTIONS OF CHLOROALKANES BY IR LASER PYROLYSIS†

Hai-Lung Dai, Eliot Specht, Michael R. Berman, and C. Bradley Moore‡

In photochemical isotope separation schemes an accurate knowledge of unimolecular reaction energy barriers and rate constants is often required for modeling an enrichment process. Reaction rates as a function of total photon energy absorbed by a molecule and thermal reaction rates in ambient and laser-heated gases must be known. Traditional methods measure rates on longer timescales than appropriate for most laser enrichment (LIS) processes. Many literature data are in error due to unsuspected reactions on vessel walls or free radical chain reactions.

A simple and reliable method is elaborated for accurate measurements of thermal rate constants of homogeneous gas phase unimolecular reactions. A pulse of CO_2 laser radiation was used to multiphoton excite SiF_4 sensitizer molecules and consequently produce temperatures in the range 1100–1400 K. Expansion of the heated gas column quenches pyrolysis reactions on a 10 μs timescale, Fig. 1.1. There are no hot surfaces to induce chemistry. HCl elimination from C_1H_5Cl, E_a = 57.4 kcal/mol and log $A(s^{-1})$ = 13.8 was used as an internal temperature standard. For the molecular elimination $CCl_3CH_3 \rightarrow HCl + CCl_2CH_2$, E_a = 49.5 ± 1.3 kcal/mol and log $A(s^{-1})$ = 13.1 ± 0.3 were determined. In these experiments the major decomposition products of $CHCl_2CH_2Cl$ are HCl and cis- or trans-CHClCHCl with E_a = 58.5 ± 2, log A = 14.1 ± 0.4 and E_a = 59.5 ± 2, log A = 13.9 ± 0.4, respectively (Fig. 1.2 and Table 1.1).

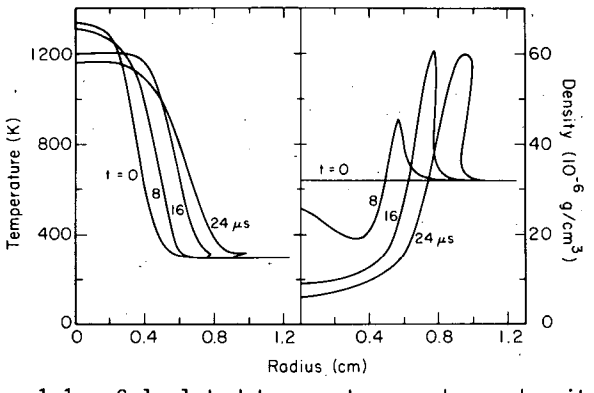

Fig. 1.1. Calculated temperature and gas density profiles at times following absorption of 0.044 J laser energy at 5.6 torr. The initial centerline temperature is 1334 K. (XBL 831-7981)

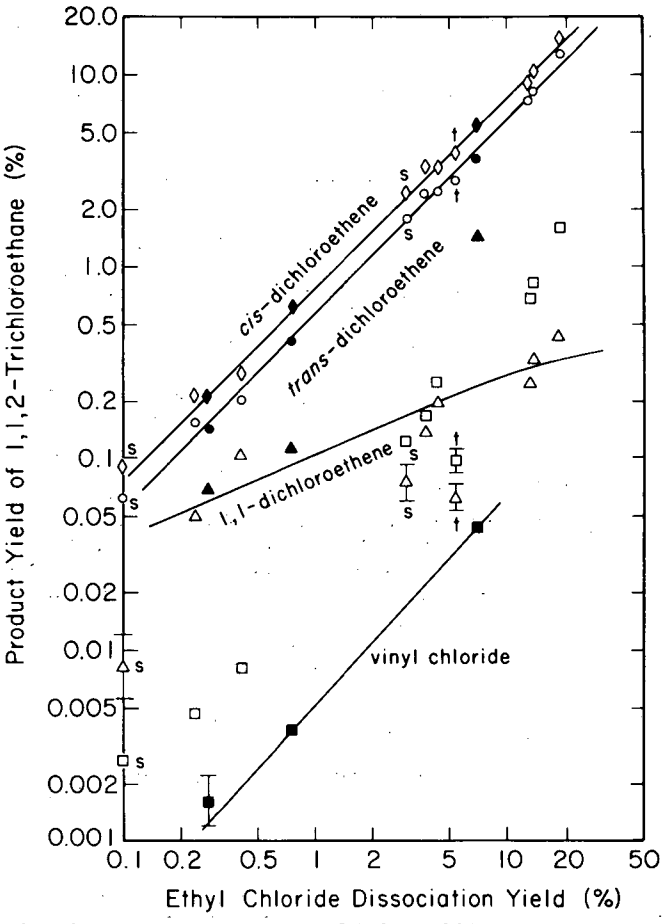

Fig. 1.2. The product yield from 112-TCE dissociation vs EtCl dissociation yield. Blank points (◇) are results from pyrolyses with the 3.8-cm-long cell. Filled points (◆) denote the pyrolyses without ethyl chloride. (s) denotes the short (0.9 cm) cell pyrolyses at the same pressure and (t) the pyrolysis with toluene in the mixture. The curves are the best fits from the gas dynamic model calculation with E_a and A shown in Table 1.1 (for CCl_2CH_2, E_a = 27 kcal/mole and log A = 6.9 since most 1,1-dichloroethene is formed by radical chain reaction. (XBL 831-7980)

*This work was supported by the Assistant Secretary for Nuclear Energy, Office of Advanced Systems and Nuclear Projects, Advanced Isotope Separation Technology Division of the U.S. Department of Energy under Contract No. DE-AC03-76SF00098.

Table 1.1. Rate Constants for Unimolecular Decomposition of $CHCl_2CH_2Cl$.

Method	Temperature Range (K)	E_a (kcal/mole), log[A(s^{-1})]			
		cis-$C_2H_2Cl_2$[a]	trans-$C_2H_2Cl_2$[a]	CCl_2CH_2[a]	$CHClCH_2Cl$[b]
Sensitized Laser Pyrolysis	1150 - 1400	58.5 ± 2 14.1 ± 0.4	59.5 ± 2 13.9 ± 0.4	>60 <13.2	64 ± 4 12.8 ± 0.8
Chemical Activation	~90 kcal/mole[c]	59 - 60 ---	59 - 60 ---	57 ---	--- ---
Flow Pyrolysis	620 - 770	--- ---	--- ---	38 9.7[d]	--- ---
Flow Pyrolysis	640 - 800	--- ---	--- ---	34 9.9[d]	--- ---

[a]Values are for the HCl molecular elimination reaction.

[b]Determined from the yield of vinyl chloride.

[c]Initial energy constant.

[d]Determined from the total HCl production rate. CCl_2CH_2 was the major product and is primarily derived from radical chain reaction.

HCl elimination to give CCl_2CH_2 and C - Cl bond breaking to $CHClCH_2Cl$ radical have higher activation energies. The method is generally useful for kinetics at high temperature, and especially useful for LIS conditions.

* * *

†Brief version of LBL-15665; J. Chem. Phys. 77, 4494 (1982).
‡Joint Institute for Laboratory Astrophysics Visiting Fellow.

1982 PUBLICATIONS AND REPORTS

Refereed Journals

1. H.-L. Dai, E. Specht, M. R. Berman, and C. Bradley Moore, "Determination of Arrhenius Parameters for Unimolecular Reactions of Chloroalkanes by IR Laser Pyrolysis," J. Chem. Phys. 77, 4494 (1982); LBL-15665.

Invited Talks

1. C. Bradley Moore, "Laser Isotope Separation and Photochemistry," Colorado School of Mines, Physics Department, Golden, Colorado, March 2, 1982.

VI Energy Storage

Energy Storage

Electrochemical Energy Storage*

James W. Evans, Rolf H. Muller, John Newman, Philip N. Ross, and Charles W. Tobias, Investigators

Introduction. The overall aim of this program is to improve the energy efficiency, lower the capital cost, and increase the materials yield of electrochemical processes employed in the conversion and storage of energy in electrolytic and galvanic cells.

a. Surface Morphology of Metals in Electrodeposition*

Charles W. Tobias, Investigator

Introduction. The objective of this project is to develop a pragmatic understanding of the partial processes governing the macrocrystallization of metals. This understanding is necessary for the design and optimization of metal deposition processes, including those in rechargeable galvanic cells. Current projects include: (1) The effect of hydrodynamic flow on the surface morphology of zinc, (2) dynamic modeling of surface profiles in electrodeposition and dissolution, and (3) mass transport effects in the deposition of alloys.

1. LIMITING CURRENTS AND THE EFFECT OF HYDRODYNAMIC FLOW ON THE MORPHOLOGY OF ZINC DEPOSITS†

J. Faltemier, D. Rajhenbah, and C. W. Tobias

The macromorphology of zinc obtained by electrodeposition from acidic zinc salt solutions is studied under a wide range of process conditions and electrolyte properties. The influences of current density, pH, hydrodynamic conditions, time of deposition, and zinc salt composition are investigated to evaluate the importance of each one's contribution to the nature and quality of the deposit. Under certain conditions the morphology of the deposit reflects the fluid motion over the surface of the electrode. Zinc has a tendency to form grooved deposits in both laminar and turbulent flow and under conditions when mass-transfer is not controlling, i.e., well below the limiting current.

To verify the transport conditions, mass transfer limiting currents of zinc deposition in acidic $ZnCl_2$ and $ZnSO_4$ solutions have been determined by potential sweep voltammetry using a rotating disk electrode. Various zinc concentrations, rotational speeds, and potential sweep rates were used in obtaining the cathodic polarization curves. High sweep rates (100, 200 mV/s) and low concentrations (0.05 M, 0.10 M) of zinc in well-supported electrolyte solutions give distinct limiting current plateaus for all rotational speeds (Fig. 1.1). In 0.05 M $ZnCl_2$ + M KCl solution, only the 200 mV/s sweep rate and the lower rotational speeds (200, 400 rpm) give limiting current plateaus.

Zinc diffusion coefficients obtained from the limiting currents are: 0.98×10^{-5} cm^2/s in 0.05 M $ZnCl_2$ + M KCl and 0.78×10^{-5} cm^2/s in 0.05 M $ZnSo_4$ + M Na_2SO_4, in reasonable agreement with literature values.[1,2] The zinc surface area increases too rapidly at slower potential sweep rates, and also at higher zinc concentration, to permit the development of distinct limiting current plateaus.

The morphology of electrodeposited zinc is investigated under galvanostatic conditions in a channel flow cell with a Pt cathode and Zn anodes, in situ, using time-lapse motion picture photography. In the absence of mass-transfer control, zinc forms grooved deposits in a certain current

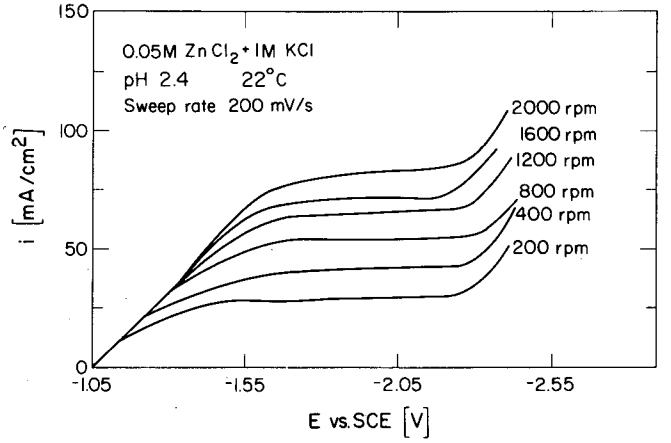

Fig. 1.1. Cathodic polarization of Zn reduction in 0.05 M $ZnCl_2$ + 1 M KCl solution on a rotating disk electrode at various rotational speeds. Sweep rate 200 mV/s. (XBL 831-15)

*This work was supported by the Assistant Secretary for Conservation and Renewable Energy, Office of Energy Systems Research, Energy Storage Division of the U.S. Department of Energy under Contract No. DE-AC03-76SF00098.

density range (5-80 mA/cm^2) reflecting the fluid motion in both laminar and turbulent flow situations (Re 1600-9000); smooth deposits develop at higher current densities, most likely because of higher nucleation rates. Time-lapse motion picture experiments enable further study of the sequence of events occurring in the development of zinc deposit morphology.[3,4]

Within a few seconds after the start of Zn deposition, the Pt substrate is fully covered. At low current densities (hence, low overpotentials) the deposit contains a large range of growing, protruding crystals. Because of ohmic advantage and also because of improved mass transfer, the large protrusions tend to grow faster than smaller ones. Better mixing in the wake of large protrusions tends to cause rapid nucleation and formation of ridges. Eventually the secondary flow patterns stabilize, resulting in the formation of well-defined, quite evenly spaced ridges in the metal deposit. At high current densities the nucleation is more dense, the size distribution of crystallites is narrow, therefore protrusions, and hence striations do not form.

* * *

†Brief version of LBL-15338.

1. J. T. Kim and J. Jorne, JES, 127, 8 (1980).
2. J. Albright and D. Miller, J. Solution Chem. 4, 809 (1975).
3. T. Tsuda and C. W. Tobias, M.S. thesis by Tsuda, LBL-13056.
4. MMRD 1981 Annual Report, LBL-12838.

2. MODELING OF CURRENT DISTRIBUTION WITH ACTIVE-PASSIVE KINETICS

J. Dukovic and C. W. Tobias

Quantitative knowledge of the distribution of current is important to many electrochemical systems: batteries, electroplating, corrosion control, electroforming, etc. Numerical modeling has been successfully applied to a broad range of current-distribution problems, including systems with irregular and moving electrode profiles.[1]

The present work is designed to extend the scope of current distribution modeling to encompass systems that involve active-passive kinetics. A case of special interest is the coexistence of distinct active and passive regions side by side on the same electrode. A finite-element model has been developed for cells that exhibit this phenomenon. As in previous models, the potential obeys Laplace's equation, but in this case the boundary condition at the anodes comprises an idealized active-passive, current-voltage characteristic.

For experimental verification of the model, a rotating-cylinder cell was designed and built. The highly asymmetric electrode arrangement promotes the coexistence of separate active and passive regions on an anode that is segmented to allow determination of currents by weight loss. Typical results for the dissolution of a Ni 200 anode in 2.0 M H_2SO_4 + 1.0 M $NiSO_4$ electrolyte are shown in Fig. 2.1. The location of the active-passive boundary was found to be stable, and the character of the current distribution followed expectations.

The prediction from the model, using kinetic-overpotential data and conductivities appropriate to the experimental system, is shown and compared to the experimental current distribution in Fig. 2.1. The agreement between experiment and theory is good.

* * *

1. G. A. Prentice, "Modeling of Changing Electrode Profiles," Ph.D. thesis, LBL-11694.

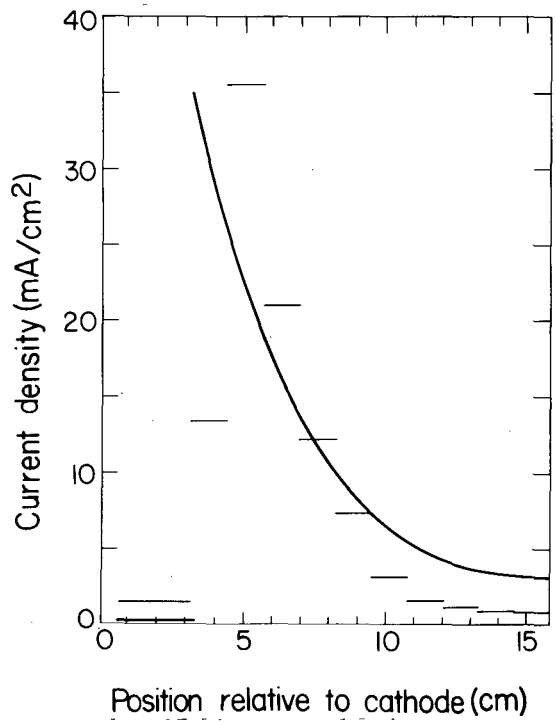

Fig. 2.1. Current distribution as obtained by experiment (horizontal dashes) and as predicted by the model (heavy line). (XBL 832-1187)

b. Metal Couples in Nonaqueous Electrolytes

Charles W. Tobias, Investigator

Introduction. The objective of this project is to develop practical alternatives to aqueous or high temperature molten salt systems for the efficient electrochemical reduction and oxidation of reactive metals. Past accomplishments include development of a process for recovery of alkali metals from their simple salts dissolved in propylene carbonate solvent. Current work is aimed at improving solvent preparation techniques, increasing solvent stability, and identifying the mechanisms by which co-solvents improve solubility and conductivity. A related project under the direction of R. H. Muller concerns the chemical nature of surface films on alkali metals in propylene carbonate electrolytes.

1. SOLUBILITY OF POTASSIUM SALTS IN SELECTED ORGANIC SOLVENTS

P. H. Johnson and C. W. Tobias

Knowledge of the solubility of inorganic salts in organic solvents is needed to gain better understanding of solvation in organic media and to guide the development of organic electrolyte solutions for electrochemical applications. In contrast to the relative abundance of data on other properties of these solute-solvent systems (e.g., conductivity, heats of solution, transport numbers), there is a paucity of data on solubility.

The solubilities and solution densities of five potassium salts (KCl, KBr, KI, KSCN, $KClO_4$) is under study in five aprotic organic solvents: ethylene carbonate, propylene carbonate, butyrolactone, dimethylformamide, dimethoxyethane, and mixtures of these solvents (Table 1.1).

The solvents and salts used were commercially available, reagent-grade. Solvents were dried with molecular sieves (Linde 4A), and the salts stored under vacuum over P_2O_5. Saturated solutions were prepared by adding an excess of the dried salt to the dried solvents in a capped vial. The vials were stored in a dessicator for at least a week and briefly shaken daily. The ethylene carbonate solutions were stored at 40°C. The other solutions were stored at room temperature (22-24°C). Solubility was determined by atomic absorption spectrometry.

The results obtained in this work compare favorably with literature values. The K_{sp} of KBr in DMF calculated from the solubility obtained in this work is 2.37. A value of 2.4 is reported by Parker.[1] The solubilities of several potassium salts reported by Harris[2] are up to 40% higher than those obtained in this work. Because Harris determined solubility by solvent evaporation, incomplete removal of the solvent could be responsible for the high solubility values.

Table 1.1. Solubilities of Potassium Salts in Selected Organic Solvents.

Salt	Solvent	Molar Solubility	Molal Solubility	Density	ID No.
KCl	BL	7.49×10^{-4}	6.73×10^{-4}	1.1129	1[a]
	DMF	1.99×10^{-3}	2.12×10^{-3}	0.9386	2
	DME	5.82×10^{-6}	6.61×10^{-6}	0.8813	3
	EC	3.03×10^{-3}	2.25×10^{-3}	1.3498	4
	PC	2.76×10^{-4}	2.34×10^{-4}	1.1817	5[a]
KBr	BL	9.59×10^{-3}	8.57×10^{-3}	1.1194	6
	DMF	6.52×10^{-2}	6.90×10^{-2}	0.9476	7
	DME	2.56×10^{-4}	2.90×10^{-4}	0.8826	8[a]
	EC	3.11×10^{-2}	2.31×10^{-2}	1.3484	9
	PC	4.81×10^{-3}	4.04×10^{-3}	1.1906	10
KI	BL	0.755	0.641	1.2062	11
	DMF	1.66	1.51	1.1644	12
	DME	8.65×10^{-3}	9.62×10^{-3}	0.8824	13
	EC	0.891	0.630	1.4489	14
	PC	0.251	0.225	1.2148	15[a]
KSCN	BL	2.62	2.33	1.2283	16
	DMF	1.87	1.96	1.0298	17
	DME	2.05	2.26	0.9904	18[a]
	EC	1.64	1.22	1.4055	19
	PC	1.57	1.32	1.2479	20
$KClO_4$	BL	0.103	9.23×10^{-2}	1.1201	21
	DMF	0.971	0.985	1.0247	22[a]
	DME	8.86×10^{-4}	1.01×10^{-4}	0.8800	23
	EC	0.694	0.519	1.3646	24
	PC	4.43×10^{-2}	3.73×10^{-2}	1.1888	25

[a]High experimental uncertainty in solubility value.
BL = butyrolactone
DMF = dimethylformamide
DME = dimethoxyethane
EC = ethylene carbonate
PC = propylene carbonate

* * *

1. Parker, JACS 89, 3703 (1967).
2. Harris, Ph.D. thesis, UCRL-8381.

c. Engineering Analysis of Electrolytic Gas Evolution

Charles W. Tobias, Investigator

Introduction. Electrolytic gas evolution is among the most common reactions in electrolysis and in advanced rechargeable batteries. This project is directed toward the quantitative description of partial processes involved in the nucleation, growth, coalescence, and the detachment of gas bubbles. Of special interest are the effects of moving individual bubbles and of gas-electrolyte emulsions on ohmic cell resistance and on mass transport of charged and uncharged species to and from electrode surfaces. A thorough understanding of the physical processes, involved in the liberation and movement of gases at electrodes and in the electrolyte, should lead to improved energy efficiency and lower capital costs in process and device technology.

1. STUDIES OF BUBBLE DYNAMICS WITH THE MOSAIC ELECTRODE AND AN IMPROVED DATA ACQUISITION SYSTEM

D. Dees and C. W. Tobias

At a gas evolving electrode, surface molecules are produced and diffuse into the electrolyte, forming a supersaturated layer near the electrode. Bubbles are then nucleated and grow through coalescence and diffusion until they disengage from the surface and rise, causing a microscopic flow of electrolyte, thereby enhancing the transport of reacting ions and product species. A micromosaic electrode capable of generating individual bubbles and measuring their effect on transport processes has been developed in this laboratory.[1]

The utility of the device to record changes in the rate of mass transfer during a single bubble disengagement has already been demonstrated.[2] However, the micromosaic electrode has been found to be susceptible to mechanical degradation and chemical corrosion, despite the special protective safeguards designed into the device. The degradation of the electrode, which is quite apparent from an examination with an optical microscope, severely limits the useful lifetime of an electrode and makes it necessary to acquire the maximum amount of information from each experiment. To make this possible, a data acquisition system has been designed and built, and a program developed, in-house, for the on-line control of the mosaic electrode. The system is capable of monitoring the current to each of the segments for a period of up to a few minutes and can make as many as 100 current measurements to each segment per second. Faster or longer time studies can be made on fewer segments. The computer not only controls the input/output of data, it also has the capability of monitoring and controlling the growth of bubbles during experiments. Data acquisition can be triggered manually or automatically by the computer.

The micromosaic electrode coupled to the data acquisition system was used to obtain more detailed information[2] on changes in mass transfer rates resulting from a single bubble disengagement event. Indicative of the capability of this device to resolve mass transfer events on a scale of 100 μ are the three types of rate changes observed at various distances from a disengaging bubble (Fig. 1.1).

* * *

1. Dennis Dees and Charles W. Tobias, "Studies of Bubble Dynamics on a Mosaic Electrode," MMRD 1981 Annual Report, LBL-13840.

2. Dennis W. Dees and Charles W. Tobias, "A Micro-Mosaic Electrode for the Study of Transport Phenomena at Gas Evolving Surfaces," Extended Abstracts, 33rd Meeting of the International Society of Electrochemistry, Lyon, France, September 5-10, 1982, p. 456-458.

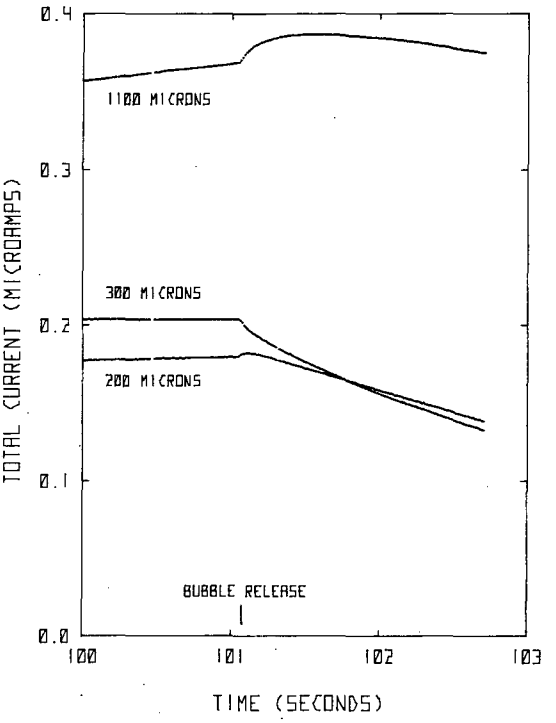

Fig. 1.1. Limiting currents for the reduction of Fe^{3+} to Fe^{2+} to segments located at various distances from a disengaging 1530-μ-diam hydrogen bubble. (XBL 833-89)

1982 PUBLICATIONS AND REPORTS

Refereed Journals

1. C. W. Tobias and G. A. Prentice, "A Survey of Numerical Methods and Solutions for Current Distribution Problems," J. Electrochem. Soc. 129, 72 (1982); LBL-12191.

2. C. W. Tobias and G. A. Prentice, "Simulation of Changing Electrode Profiles," J. Electrochem. Soc. 129, 78 (1982); LBL-12192.

3. C. W. Tobias and G. A. Prentice, "Deposition and Dissolution on Sinusoidal Electrodes," J. Electrochem. Soc. 129, 316 (1982); LBL-12167.

4. C. W. Tobias and G. A. Prentice, "Finite Difference Calculation of Current Distributions at Polarized Electrodes," AICHE. 28, 486 (1982); LBL-11058.

†5. C. W. Tobias and P. C. Foller, "The Anodic Evolution of Ozone," J. Electrochem. Soc. 129, 506 (1982).

†6. C. W. Tobias and P. C. Foller, "The Mechanism of the Disintegration of Lead Dioxide Anodes under Conditions of Ozone Evolution in Strong Acid Electrolytes," J. Electrochem. Soc. 129, 567 (1982).

‡7. C. W. Tobias, F. R. McLarnon, and R. H. Muller, "Interferometric Study of Combined Forced and Natural Convection," J. Electrochem. Soc. 129, 2201 (1982); LBL-13032.

‡8. C. W. Tobias and P. J. Sides, "Resistance of a Planar Array of Spheres, Gas Bubbles on an Electrode," J. Electrochem. Soc. 129, 2715 (1982); LBL-13468.

Other Publications

†1. C. W. Tobias and P. C. Foller, Inventors, "Electrolytic Process for the Production of Ozone," U. S. Patent No. 4,316,782, February 23, 1982.

2. C. W. Tobias, Chairman, "Assessment of Research Needs for Advanced Battery Systems," Report of the Committee on Battery Materials Technology, National Materials Advisory Board, Commission on Engineering and Technical Systems, National Research Council, Publication NMAB-390, 1982.

3. C. W. Tobias and A. Kindler, "The Morphology of Electrodeposited Copper," Extended Abstracts, The 161st Meeting of the Electrochemical Society, Montreal, Canada, May 9-14, 1982.

‡4. C. W. Tobias, R. H. Muller, and D. J. Roha, "Effect of Suspended Particles on the Rate of Mass Transfer to a Rotating Disk Electrode," Extended Abstracts, The 161st Meeting of the Electrochemical Society, Montreal, Canada, May 9-14, 1982.

5. C. W. Tobias and Dennis Dees, "A Micro-Mosaic Electrode for the Study of Transport Phenomena at Gas Evolving Surfaces," Extended Abstracts No. II-C-19, Vol. I, p. 468, 33rd Meeting of the International Society of Electrochemistry, Lyon, France, September 10-15, 1982.

Invited Talks

1. C. W. Tobias, "Mass Transport and Current Distribution in the Electrodeposition of Metals," IBM Corporation, GTD Laboratory, Endicott, N. J., January 22, 1982.

2. C. W. Tobias, Diamond Shamrock Lectures: "A Perspective of Electrochemical Technology," January 25, 1982; "Current Distribution on Electrode Surfaces," January 27, 1982; "Mass Transport in Electrochemical Cell Processes," January 29, 1982; "Physical Processes in Electrolytic Gas Evolution," February 1, 1982, Case Western University, Cleveland, Ohio.

3. C. W. Tobias, "Advances in Electrochemical Technology," Seminar Lecture given at RCA Sarnoff Research Center, Princeton, N. J., March 9, 1982.

4. C. W. Tobias, "Assessment of the Future Potential of Fuel Cells," Chevron Research Corp., Richmond, CA, April 16, 1982.

5. C. W. Tobias, "Problems in Electrochemical Engineering," Seminar Lecture given at the University of West Virginia, April 19, 1982.

‡6. C. W. Tobias, R. H. Muller, and D. J. Roha, "Effect of Suspended Particles on the Rate of Mass Transport to a Rotating Disk Electrode," The 161st Meeting of the Electrochemical Society, Montreal, Canada, May 14-19, 1982.

7. C. W. Tobias and A. Kindler, "The Morphology of Electrodeposited Copper," The 161st Meeting of the Electrochemical Society, Montreal, Canada, May 14-19, 1982.

8. C. W. Tobias and Dennis Dees, "A Micro-Mosaic Electrode for the Study of Transport Phenomena at Gas Evolving Electrodes," The 33rd Meeting of the International Society of Electrochemistry, Lyon, France, September 6-10, 1982.

9. C. W. Tobias, "Fundamentals of Electrochemical Engineering," Six lectures arranged by the Romande Intercantonal Association of Swiss Universities, Leysin, Switzerland, September 12-16, 1982.

10. C. W. Tobias, "Prospects of Electrochemical Technology," Seminar lecture, Swiss Federal Institute of Technology, Lausanne, Switzerland, September 22, 1982.

11. C. W. Tobias, "A Close Look at Electrolytic Gas Evolution," Seminar lecture, Stanford University, February 24, 1982 and Ecole Nationale Superieure des Industries Chimiques, Nancy, France, October 11, 1982.

12. C. W. Tobias, "Perspectives on Electrochemical Technology," Seminar lecture, De Guigne Technical Center, Stauffer Chemical Co., Richmond, CA and Laboratoire d'Electrochimie Interfaciale du C.N.R.S. Meudon (Bellevue) France, October 14, 1982.

* * *

†Supported entirely from University funds.
‡Supported by the Director, Office of Energy Research, Office of Basic Energy Sciences, Materials Sciences Division of the U.S. Department of Energy.

d. Surface Layers on Battery Materials*

Rolf H. Muller, Investigator

Introduction. The purpose of this work is to provide direct experimental information about formation and properties of surface layers on battery electrode materials. Present studies are concerned with lithium in nonaqueous solutions. A more broadly based research program, supported by the Office of Basic Energy Sciences, Division of Materials Sciences, DOE, is described in the sections "Electrochemical Phase Boundaries," R. H. Muller, Investigator, and "Electrochemical Processes," C. W. Tobias, Investigator.

1. IMPEDANCE AND ELLIPSOMETER MEASUREMENTS OF SURFACE LAYERS ON LITHIUM†

Felix Schwager and Rolf H. Muller

Lithium is an attractive battery material because of its high potential and low equivalent weight. Lithium can be used in different ambient-temperature nonaqueous electrolytes primarily because of the formation of surface layers which prevent the spontaneous reaction of the metal with solvents and solutes. However, these surface layers hinder the efficient metal deposition from solution during recharge. The present measurements were conducted in order to determine film properties not affected by damage possibly inflicted in previous pulse measurements,[1] to investigate an approach to improve film conductivity, and to clarify discrepancies between ellipsometrically and electrochemically determined film thicknesses. Lithium nitride was investigated as a protective surface layer because of reported high ionic conductivity.[2]

Simultaneous ac-impedance and ellipsometer measurements were conducted. Real and imaginary parts of the complex impedance were derived from Lissajous figures of current and potential displayed on an oscilloscope. The ellipsometer was of the self-compensating type in the polarizer-quarter wave plate-sample-analyzer configuration with a mercury arc (546 nm) or argon ion laser (514 nm) light source. Nitride films were formed by different exposures to gaseous nitrogen.

Film resistances derived from the low-frequency intercepts of complex impedance plots are in good agreement with pulse measurements. The previous interpretation of differences in film thickness between optical and electrical measurements as being caused by inhomogeneous film structure therefore remains valid. The highest film resistance was obtained for films formed in $LiClO_4$ solutions of propylene carbonate (PC), the lowest in pure solvent. Nitride layers showed intermediate film resistances. The protective properties of these layers were still evident after 250 h exposure to 1 M $LiClO_4$ at open circuit. The formation of the nitride layer was found to be strongly inhibited by trace amounts of oxide. Ellipsometer measurements during polarization of lithium in 1 M $LiClO_4$/PC showed a large difference between anodic and cathodic processes: metal dissolution appears to occur through the oxide layer with roughening of the substrate, but metal deposition occurs primarily on top of the oxide in the form of islands.

* * *

†Brief version of Extended Abstract, LBL-13618.

1. Y. Geronov, F. Schwager, and R. H. Muller, J. Electrochem. Soc. 129, 1422 (1982).
2. R. A. Huggins, Electrochim. Acta 22, 773 (1976).

2. WORK IN PROGRESS

Gholambbas Nazri and Rolf H. Muller

Surface layers of improved ionic conductivity are necessary for the deposition of lithium from nonaqueous solutions in rechargeable batteries. To identify such surface layers, which also should be self-healing and inhibit corrosion reactions, two approaches are being taken: control of composition and microstructure. To those ends, improved means to form lithium nitride films and disordered oxygen and hydrogen-doped nitrides are under study.

To further investigate the validity of the conclusion[1] that the protective surface layer formed on lithium in propylene carbonate-lithium perchlorate electrolyte was an oxide that resulted from reaction with residual water rather than lithium carbonate, as conventionally accepted,[2] two experimental approaches are being taken: electrolyte of extremely low water content, prepared by treatment with lithium amalgam, is being used, and freshly cut lithium electrodes are brought in contact with a very small volume of electrolyte in a new thin-layer cell. Infrared spectroscopy has shown (Fig. 2.1) that the precipitate formed on lithium amalgam is not lithium carbonate but probably a polymerization product of the solvent.

* * *

1. Y. Geronov, F. Schwager, and R. H. Muller, J. Electrochem. Soc. 129, 1422 (1982).
2. F. P. Dousek, J. Jansta, and J. Riha, J. Electroanal. Chem. 46, 281 (1973).

*This work was supported by the Assistant Secretary for Conservation and Renewable Energy, Office of Energy Systems Research, Energy Storage Division of the U. S. Department of Energy under Contract No. DE-AC03-76SF00098.

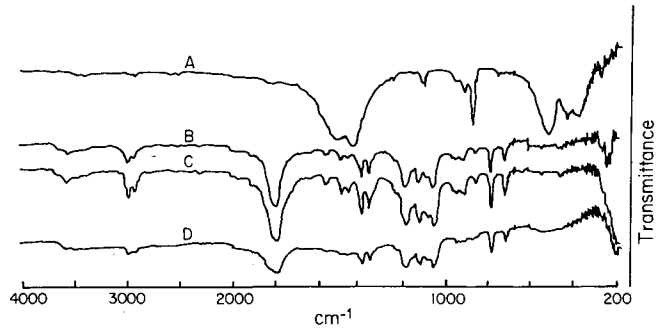

Fig. 2.1. Infrared spectra of (A) Li_2CO_3, (B) propylene carbonate, (C) liquid phase, and (D) precipitate at lithium amalgam-propylene carbonate interface. (XBL 831-7554)

1982 PUBLICATIONS AND REPORTS

Refereed Journals

1. Y. Geronov, F. Schwager, and R. H. Muller, "Electrochemical Studies of the Film Formation on Lithium in Propylene Carbonate Solutions under Open-Circuit Conditions," J. Electrochem. Soc. 129, 1422 (1982); LBL-12102 Rev. 2.

Other Publications

1. F. J. Schwager and R. H. Muller, "Impedance and Ellipsometer Measurements of Lithium Electrodes in Propylene Carbonate Solutions," Extended Abstract No. 295, Electrochemical Society, Detroit, Michigan, October 17-21, 1982; LBL-13618.

e. Electrode Kinetics and Electrocatalysis*

Phillip N. Ross, Jr., Investigator

Introduction. Complex electrochemical reactions in which chemical bonds are broken and/or formed are invariably catalytic, with electrode kinetics varying by many orders of magnitude for different electrode materials. Catalytic electrode materials are essential to technologies like fuel cells, metal-air batteries, electrolyzers, and in electro-organic synthesis. Metal-metal ion (Me/Me^{Z+}) couples form the largest class of negative electrode types for batteries. Two general distinctions of Me/Me^{Z+} couples can be made: those where the ionic state (or discharged state) is insoluble (e.g., a metal/metal oxide couple), and those where the ionic state is solvated (e.g., Zn/Zn^{2+} in acid). The kinetics of Me/Me^{Z+} couples are relatively rapid, but are not usually controlled by only a charge transfer step. These reactions are often quasi-reversible, in the sense that they proceed at high rate and small overpotential, but they do not follow simple charge transfer rate expressions. Phenomena frequently cited as contributing to the finite overpotential in Me/Me^{Z+} systems are critical nucleation, intermediate or precursor formation, and impurity adsorption. In a mechanistic sense and at the atomic level, several technologically important Me/Me^{Z+} systems are still not well understood.

1. LOW ENERGY ELECTRON DIFFRACTION (LEED) CHARACTERIZATION OF METAL ELECTRODE SURFACES†

F. T. Wagner and P. N. Ross, Jr.

To understand what happens at Me/Me^{Z+} electrodes at the atomic level requires a method of following the changes in the atomic structure of the electrode surface. Low energy electron diffraction (LEED) provides a sensitive probe of the atomic-scale structure of solid surfaces. Although early LEED theory was restricted to the treatment of perfect low index surfaces or surfaces with perfectly ordered arrays of steps, the technique has been advanced to deal with a statistical distribution of steps and other forms of surface defects. Improvements in both theory and experimental technique are now allowing the type, size distribution, and density of imperfections to be identified. It should be possible to make definitive structure determination of electrode surfaces by ex situ LEED analysis, thereby considerably advancing the state of understanding the transformations occurring at electrode surfaces.

Two electrode systems are currently under investigation, zinc deposition on copper and gold single crystal substrates and the formation of platinum oxide on platinum single crystal surfaces, both in acid fluoride electrolyte. The former is an example of an Me/Me^{Z+} electrode and the latter an Me/MeO_x electrode. The platinum/platinum oxide system is of special fundamental importance at present because of persistent speculation in the literature that cycling platinum electrodes through metal-oxide transformation disorders the metallic state[1,2] and creates an "activated" state of platinum.[3,4]

Figure 1.1a shows the LEED pattern for a UHV prepared Pt(100) surface that was contacted with 0.3 M HF at 0.4 V RHE, swept ten times at 100 mV/s between 0.02 and 0.82 V RHE and separated from the electrolyte while potentiostated at 0.4 V. No significant differences were observed by LEED between this LEED pattern and the one for the surface exposed only to the argon backfill gas (at any incident beam energy 50-175 eV). Exposure of the UHV surface to the backfill gas caused a transformation from the so-called (5 x 20) reconstructed surface to the (100)-(1x1) surface structure. Thus, contact with electrolyte and potentiodynamic cycling within the metallic potential region causes no discernible change in the structure of the surface.

Figure 1.1b shows the effect of cycling into the oxide formation potential region on the LEED pattern at the beam energy of 134 eV. At 134 eV, the (10) and (20) spots were sharp while the (11) spots are broadened. There was a characteristic alternate spot broadening as a function of energy, e.g., at 178 eV and 114 eV the (11) spots are sharp while the (10) and (20) were diffuse. The fact that every LEED beam is sharp at some energies indicates that most surface atoms are still in positions of the three-dimensional crystal lattice. Surface defects can introduce new periodicities with dimensions close to the incident electron wavelength to produce new spots or changes in spot shapes. The diffraction effects of periodic steps along the [010] and [011] directions at a fcc (100) crystal surface were computed by the Ewald construction method. Given diffraction data from a staircase stepped surface, one can determine the terrace width from the angular splitting of the spots and the step height from the incident energies at which the beams are sharp. If the steps are randomly up and down, the diffraction peaks become diffuse rather than split at characteristic energies, but the mean terrace width can be determined from the angular dispersion at the characteristic energies. Comparison of the Ewald construction with the energies at which the observed (11) and (10) LEED spots were sharp are in exact agreement for randomly up and down monatomic steps, and from the analysis spot broadening the mean terrace width is calculated to be about 5 atoms or about 15 Å.

It was concluded from the detailed analysis of LEED patterns that a Pt(100) surface cycled 10 times through the surface oxide phase has a ver-

*This work was supported by the Assistant Secretary for Conservation and Renewable Energy, Office of Energy Systems Research, Energy Storage Division of the U.S. Department of Energy under Contract No. DE-AC03-76SF00098.

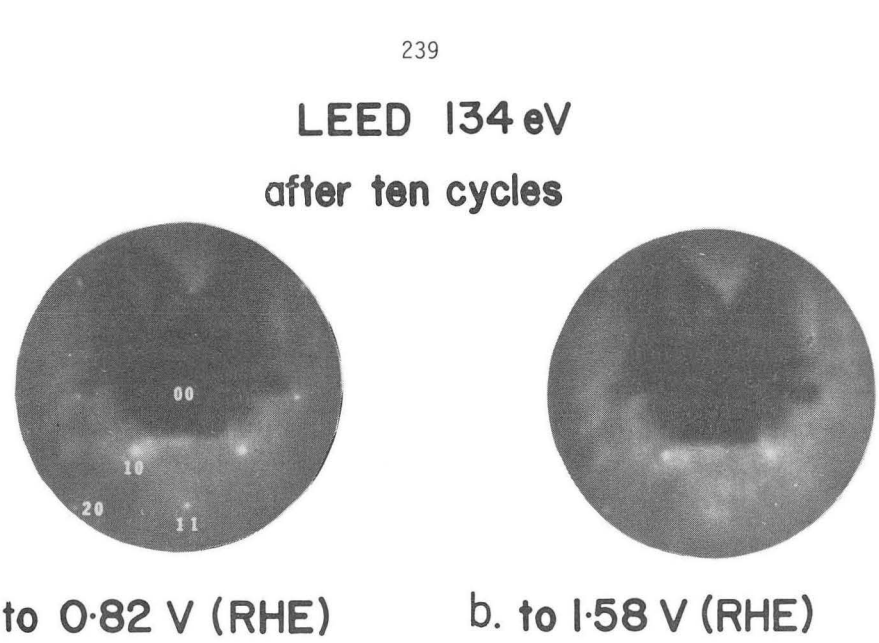

Fig. 1.1. (a) LEED pattern for Pt(100) cycled within metallic potential region; (b) LEED pattern for cycling into surface oxide formation. (XBB 824-4022B)

tically dislocated terrace structure with a mean terrace width of 15 Å. The step dislocation density is ca. 3×10^{14} sites/cm^2 and the ordered (100) site density is 12×10^{14} sites/cm^2, i.e., about one atom in every four is associated with a dislocation. A Pt(100) surface cycled only within the metallic potential region has a longer range order, with a dislocation density less than 5×10^{13} sites/cm^2, or only one atom in twenty is associated with a dislocation. Cycling through the oxide phase does introduce a significant concentration of high coordination sites into a low index surface, and would "activate" the surface for structure sensitive reactions. However, oxygen reduction is not a structure sensitive reaction,[5] and cycling the Pt(100) does not "active" the surface for this reaction.

* * *

†Brief version of LBL-15461.

1. J. Clavilier, J. Electroanal. Chem. 107, 211 (1980).
2. R. Parsons, J. Electrochem. Soc. 127, 176C (1980).
3. J. Hoare, Extended Abstracts Volume 82-1, The Electrochem. Soc., Princeton, NJ, 1982, p. 571.
4. A. J. Appleby, J. Electrochem. Soc. 117, 642 (1970).
5. P. Ross, J. Electrochem. Soc., 126, 69 (1979).

2. DIFFUSION CONTROLLED MULTI-SWEEP CYCLIC VOLTAMMETRY FOR A REVERSIBLE DEPOSITION REACTION OCCURRING ON ROTATING DISK AND STATIONARY ELECTRODES†

P. C. Andricacos and P. N. Ross, Jr.

An analysis is presented of the behavior of a diffusion controlled reversible deposition reaction with constant deposit activity occurring on rotating disk (RDE) or stationary planar (SPE) electrodes. The potential is swept linearly between two values, the more anodic of which is the reaction equilibrium potential, calculated from the Nernst equation on the basis of c^b, the bulk concentration of the depositing ion. The Nernst-Siver approximation[1,2] is used for the RDE, whereas semi-infinite linear diffusion is assumed for the SPE. In both cases, capacitance and natural convection-effects are not taken into consideration.

In the case of a RDE, a periodic [in the sense that the response to the $(n + 1)$st sweep is indistinguishible from that for the nth sweep] state is obtained immediately after the first cathodic sweep, provided that the reversal time, θ, is equal to or greater than the RDE characteristic time δ^2/D (or $\theta' = D\theta/\delta^2 \geq 1$), where δ is the thickness of the Levich diffusion layer. In terms of a dimensionless sweep rate,[2] σ, defined as

$$\sigma = mFv\delta^2/RTD, \quad v \equiv \text{dimensional sweet rate},$$

the periodic cathodic current maximum appears for $\sigma \gtrsim 3$ (Fig. 2.1). Compared to the linear sweep voltammetry (LSV) maximum,[2] it is lower in height and shifted in the cathodic direction. A net cathodic charge is obtained during each complete cycle indicating the formation of a net deposit on the electrode surface.

In the case of an SPE, it is shown that current transients (Fig. 2.2) are bounded from above by the LSV current and from below by the hypothetical periodic current obtained by reversing at infinite overpotential. Another hypothetical periodic state that is obtained by infinite cycling at finite reversal overpotentials follows the same rule. For the SPE, the true periodic state requires either infinite reversal overpotential or infinite sweeps. For practical purposes, it is more convenient to define a quasi-periodic state. It was found that the higher the reversal

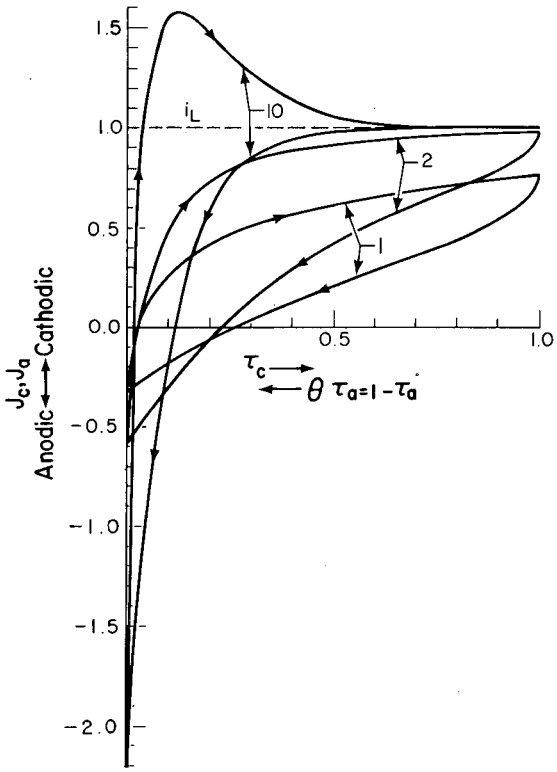

Fig. 2.1. Periodic RDE current density functions for σ = 1,2, and 10. $J = i/i_L$, where i is the current density during a potential sweep, and i_L is the RDE diffusion limiting current density. J_c and J_a are current functions during cathodic and anodic sweeps, respectively. $\tau_c = Dt_c/\delta^2$ is dimensionless time into a cathodic sweep. For $\sigma<3$, J_c is a monotonic function of τ_c; for higher σ values a maximum, $J_{c,max}$, appears in both LSV and periodic current functions. For the LSV function, $J^0_{c,max} = 0.61\sigma^{1/2}$, $\sigma \geq 4$ (Ref. 2), whereas for the periodic function, $J_{c,max} = -0.88\sigma^{0.25}$, $\sigma \geq 9$. (XBL 825-620)

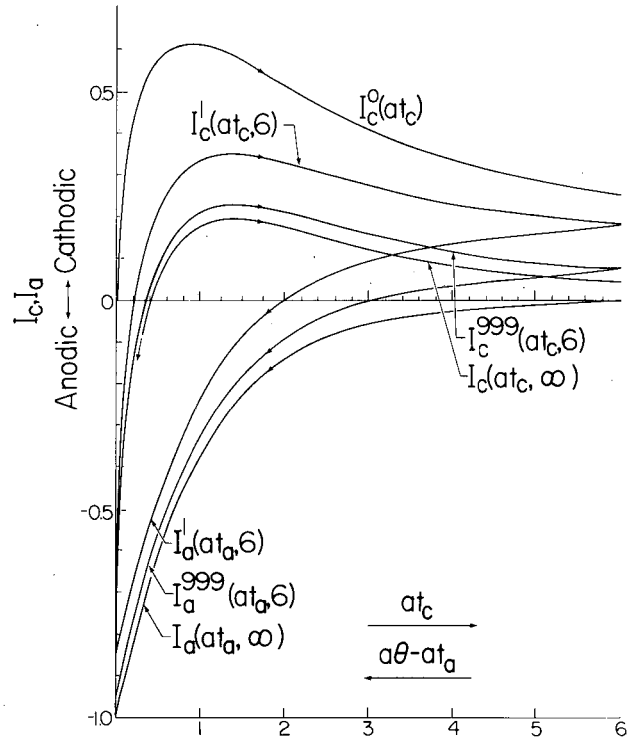

Fig. 2.2. SPE current density functions for different values of the number of already applied cycles and a reversal overpotential of 6RT/nF. $I^{\ell} = i^{\ell}/(nFD^{1/2}a^{1/2}c^b)$, where i^{ℓ} is the current density during the $(\ell + 1)$th sweep, and $a = nFV/RT$. The at_c is overpotential in RT/nF units into a cathodic sweep. Cathodic current maxima are bounded from above by the LSV transient,[3] $I^0_{c,max} = 0.61$, and from below by the periodic state at infinite reversal overpotential, $I_{c,max} = 0.19$. (XBL 825-619)

overpotential, the smaller the number of cycles necessary to achieve quasi-periodicity. Multiple sweeping changes the linear dependence of the cathodic current maximum on the square root of the sweep rate observed in LSV (Ref. 3) with generally smaller slopes that depend on the number of cycles in addition to the usual parameters.[3] Net cathodic charges are obtained after each complete cycle.

The theoretical expectations are being compared to experimental observations for the electrodeposition of Ag from nitrate solution. Preliminary results suggest excellent agreement with the predicted behavior.

* * *

†Brief version of LBL-14524 and LBL-14525.

1. Yu. G. Siver, Russ. J. Phys. Chem. 33, 533 (1959); 34, 273 (1960).
2. P. C. Andricacos and H. Y. Cheh, J. Electrochem. Soc. 127, 2153 (1980).
3. T. Berzins and P. Delahay, J. Am. Chem. Soc. 75, 555 (1953).

1982 PUBLICATIONS AND REPORTS

Refereed Journals

1. F. T. Wagner and P. N. Ross, Jr., "LEED Analysis of Electrode Surfaces: Structural Effects of Potentiodynamic Cycling on Pt Single Crystals," J. Electroanal. Chem., in press (1982); LBL-14761.

2. P. N. Ross, Jr. and K. A. Gaugler, "The Observation of Surface Sensitive $M_{2,3}$ Absorption Edge Shifts by Reflected Electron Energy Loss Spectroscopy (REELS); "Surf. Sci.

Other Publications

1. A. J. Appleby and P. N. Ross, Jr., "Fuel Cell Systems for Electric Vehicles: An Overview," Power Sources for Electric Vehicles, edited by B. McNicol and D. Rand, Elsevier Scientific, 1982, in press.

LBL Reports

1. P. N. Ross, Jr. and F. T. Wagner, "Prospects for the Development of Non-Noble Metal Catalysts for Hydrogen-air Fuel Cells," LBL-14192.

2. P. Adnricacos and P. N. Ross, Jr., "Diffusion Controlled Multi-Sweep Cyclic Voltammetry: I. Reversible Deposition on a Rotating Disc Electrode," to be published in J. Electrochem. Soc., LBL-14524.

3. P. Andricacos and P. N. Ross., Jr., "Diffusion Controlled Multi-Sweep Cyclic Voltammetry: II. Reversible Deposition on a Stationary Planar Electrode," to be published in J. Electrochem. Soc., LBL-14525.

4. P. N. Ross, Jr., "Engineering Analysis of an NH_3-Air Alkaline Fuel Cell System for Vehicular Applications," LBL-14578.

Invited Talks

1. P. N. Ross, Jr., "The Effect of Impurities and Potentiodynamic Cycling on Hydrogen Adsorption on Pt Single Crystal Electrodes," 161st Meeting of the Electrochemical Society, Montreal, Canada, May 1982.

2. P. N. Ross, Jr., "Engineering Analysis of an NH_3-Air Alkaline Fuel Cell System for Vehicles," Workshop on Renewable Fuels and Advanced Power Sources for Transportation, Boulder, Colorado, June 1982.

3. P. N. Ross, Jr., "Catalytic Properties of Pt-Group IV and V Intermetallic Compounds," Gordon Research Conference on Catalysis, New London, New Hampshire, June 1982.

4. P. N. Ross, Jr., "Structural Analysis of Electrode Surfaces by Low Energy Electron Diffraction (LEED)," International Conference on Electronic and Molecular Structure of the Electrode-Electrolyte Interface, Logan, Utah, July 1982.

f. Electrical and Electrochemical Behavior of Particulate Electrodes *

James W. Evans, Investigator

Introduction. The purpose of this work is to investigate particulate electrodes in metal-air batteries. The acceptance of electric vehicles for public use depends on the development of a high-efficiency, low-cost battery. The metal-air battery offers a prospect of meeting these requirements if one or both of the electrodes are in the particulate form. Particle-to-particle electronic conduction is essential for a particulate electrode to function and has a significant effect on electrode performance; such conduction is poorly understood, although there is evidence that conductivity decreases as the particle volume fraction drops. This group's previous investigation, mathematical modeling of aluminum reduction cells, was closed out late in the year and is reported below.

1. DEVELOPMENT AND TESTING OF THE MATHEMATICAL MODEL FOR THE HALL-HÉROULT CELL†

Steve Lympany,‡ Huai-Chuan Lee, and James W. Evans

The major consumer of energy in the production of aluminum is the Hall-Héroult cell wherein electrical energy is used to electrolytically reduce aluminum oxide to metal. A mathematical model for the cell has been developed. Two performance parameters of interest, from an energy consumption viewpoint, are the current efficiency of the cell and the flatness of the interface between the two liquid layers in the cell (molten aluminum and the molten salt electrolyte). The former variable has an obvious connection with the energy consumed per unit mass of product; the latter is important because "bowing" of this interface prevents the reduction of the anode-interface distance (resistive losses in the electrolyte).

Both the current efficiency and flatness of the interface are primarily dependent on electromagnetic forces that arise within the cell from the interaction of cell currents with magnetic fields. The magnetic fields arise from current flow within the cell, surrounding conductors ("bus bars") and surrounding cells. The current efficiency is less than 100% because aluminum has a slight solubility in the electrolyte, and dissolved aluminum is transported to the anode where it reoxidizes. This transport of aluminum is because of turbulent convection in the electrolyte, and is, therefore, a function of the electrolyte flow, a flow which is driven by the electromagnetic forces. The model computes the current distribution in the cell, the magnetic field, the electromagnetic stirring forces, the velocity field of the electrolyte and aluminum, the bowing of the interface, and the current efficiency.

Figure 1.1 depicts the conductors in and around six 185 kA cells forming part of two adjacent rows of cells (three cells shown in each row). The computed current efficiency for one of the cells is also given in the figure. The computed interface shape for the cell shown arrowed in Fig. 1.1 is depicted in Fig 1.2. The computed current efficiency and interface trough to peak distance are consistent with observations on actual cells.

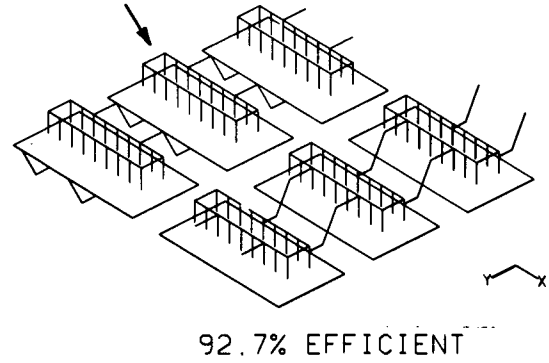

Fig. 1.1. Six 18 kA quarter riser cells in two potlines. Only the anode and cathode bus, risers, and anode rods for each cell are shown. Subsequent calculations are for the cell marked with an arrow and take account of the currents in all the conductors shown. (XBL 831-7977)

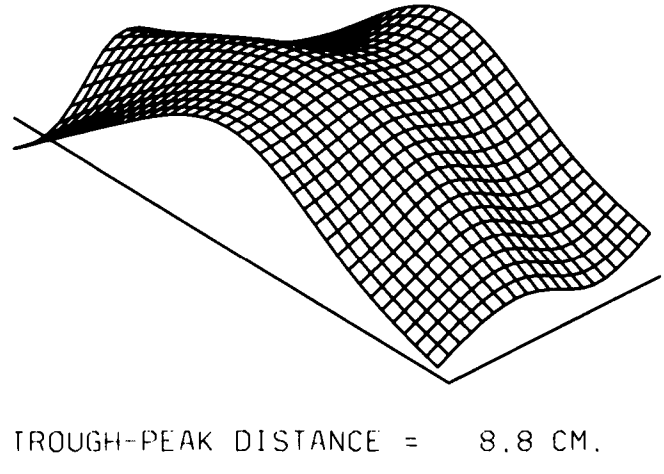

Fig. 1.2. The interface between aluminum and cryolite computed for the cell indicated in Fig 1.1. Straight lines indicate a horizontal plane. The vertical scale is exaggerated by a factor of 40. Current flow in the potline is from upper right to lower left. (XBL 831-7978)

*This work was supported by the Assistant Secretary for Conservation and Renewable Energy, Office of Energy Systems Research, Energy Storage Division of the U. S. Department of Energy under Contract No. DE-AC03-76SF00098.

During FY 1982 the mathematical model was used to predict the effect of design changes on cell performance. It was predicted that separating the rows of cells by a greater distance would be beneficial, but that increasing the separation between cells in a row would have little effect. The model successfully predicted the well-known inferior performance of cells at the end of rows. An interesting prediction was that the electrolyte/aluminum interface could be flattened considerably in a design in which current is removed through the bottom of the cell, rather than the sides (which is the present practice). Bowing of the interface is reduced by a factor of five for a cell of this nature.

Details of the mathematical model and the computer programs have been requested by three aluminum companies (Alcoa, Reynolds, and Martin Marietta) and have been transferred to them.

* * *

†Brief version of LBL-14386, to be published in Metallurgical Transactions.
‡Present address: Dames & Moore, Golden, CO 80401.

2. WORK IN PROGRESS

The mathematical modeling of aluminum cells has been discontinued (at the request of DOE) in favor of an experimental investigation of the behavior of particulate electrodes. Such electrodes may find application in energy storage (e.g., the zinc-air battery), but little is known about their behavior. Of particular interest are conduction mechanisms within the electrode (particle-to-particle charge transport) and the transient behavior of the particle potentials. An apparatus is under construction in which these two phenomena can be studied.

1982 PUBLICATIONS AND REPORTS

Refereed Journals

†1. I. Masterson and J. W. Evans, "Fluidized Bed Electrowinning of Copper; Experiments Using 150 Amp and 1,000 Amp Cells and Some Mathematical Modelling," Met. Trans. 13B, 3 (1982).

‡2. M. Dubrovsky and J. W. Evans, "An Investigation of Fluidized Bed Electrowinning of Cobalt Using 50 and 1,000 Amp Cells," Met. Trans. 13B, 293 (1982).

§3. M. H. Abbasi and J. W. Evans, "Monte Carlo Simulation of Radiant Transport through an Adiabatic Packed Bed or Porous Solid," AIChE J. 28, 853 (1982).

¶4. J. N. Barbier, P. Cremer, J. W. Evans, and Y. R. Fautrelle, "Simulation Numérique des Fours Chauffés par Induction," J. de Mécanique, Théorique et Appliquée 1, 533 (1982).

5. D. J. Coates, J. W. Evans, and S. S. Pollack, "Identification of the Origin of TiO_2 Deposits on a Hydrodesulfurisation Catalyst," Fuel 61, 1245 (1982); LBL-13244.

6. D. J. Coates, J. W. Evans, and K. H. Westmacott, "Defects in Antiferromagnetic Nickel Oxide," J. Mat. Sci. 17, 3281 (1982).

Other Publications

1. J. W. Evans, "Physical Chemistry of High Temperature Technology," AIChE J. 28, 868 (1982), book review.

LBL Reports

1. S. D. Lympany and J. W. Evans, "The Hall-Héroult Cell: Some Design Alternatives Examined by a Mathematical Model," Met. Trans. in press, LBL-14386.

2. S. D. Lympany and J. W. Evans, "An Improved Mathematical Model for Melt Flow in Induction Furnaces and Comparison with Experimental Data," Met. Trans. in press, LBL-15170.

3. D. J. Coates, A. L. Cabrera, J. W. Evans, H. Heinemann, and G. A. Somorjai, "An Electron Microscopy Study of the Low Temperature Catalysed Steam Gasification of Graphite," J. of Catalysis in press, LBL-14463.

Invited Talks

1. D. J. Coates, K. H. Westmacott, and J. W. Evans, "The Effect of Microstructure on the Reduction of Nickel Oxide," AIME Annual Meeting, Las Vegas, Nevada, February 1982.

2. M. Dubrovsky, J. W. Evans, and T. Huh, "Fluidized Bed Electrowinning of Metals at Moderate Electrical Energy Consumption Rates," AIME Annual Meeting, Las Vegas, Nevada, February 1982.

3. Y. Nakano, M. Abbasi, and J. W. Evans, "A New Predictive Technique for the Diffusion of Gases in Porous Solid," International Symposium on the Physical Chemistry of Iron and Steelmaking," Conference of Metallurgists, Toronto, Canada, August 1982.

4. S. D. Lympany, R. Moreau, and J. W. Evans, "Magnetohydrodynamic Effects in Aluminum Reduction Cells," Proc. Int. Union of Theoretical and Applied Mechanics Symp., Cambridge, England, September 1982.

5. S. D. Lympany, D. Ziegler, and J. W. Evans, "Simulation of Electrolyte Flows and Mass Transport in Electrometallurgy," AIChE Annual Meeting, Los Angeles, November 1982.

* * *

†Supported by the Office of Surface Mining, Department of the Interior.
‡Supported by National Science Foundation.
§Supported by intramural funds, University of California.
¶Supported by the Institut de Mécanique, Grenoble, France.

g. Electrochemical Properties of Solid Electrolytes*

Lutgard C. De Jonghe, Investigator

When sodium beta aluminas are in prolonged contact with molton sodium at elevated temperatures, the sodium beta alumina is partially reduced.[1] This leads to an electrolyte that contains a gradient in the electronic/ionic transport number ratio. Theoretical considerations, based on thermodynamic calculations, indicated that if current is passed through such an electrolyte, the possibility exists of internal deposition of sodium.[2] Under normal circumstances, the cell operating conditions are such that internal sodium deposition does not occur. However, the presence of impurities may depress the applied voltage at which such degradation may be initiated.

* * *

1. L. C. De Jonghe and A. Buechele, J. Mat. Sci. 17, 885 (1982).
2. L. C. De Jonghe, J. Electrochem. Soc. 129, 752 (1982).

1. IMPURITIES AND SOLID ELECTROLYTE FAILURE†

Lutgard C. De Jonghe

A thermodynamically based model is used to assess the effects of the formation of a layer of lowered ionic conductivity and increased electronic conductivity on the applied voltage at which solid electrolyte failure is to be expected. Such a layer can result from electrolyte contamination with electrode impurities. It is found that when a significant increase in electrolyte resistivity is produced, electrolyte failure can be initiated by deposition of sodium internally in the solid electrolyte. The results stress the necessity of operating solid electrolyte cells, such as Na/S, in a manner that minimizes electrode contamination.

* * *

†Brief version of Solid State Ionics 7, 61 (1982).

2. GRAIN BOUNDARIES AND SOLID ELECTROLYTE DEGRADATION†

Lutgard C. De Jonghe, A. Buechele, and A. H. Yoon

Sodium beta" alumina solid electrolytes containing some very large grains were subjected to a unidirectional sodium ion current. The exit surface of the sodium ions was then examined, and it was found that degradation has been initiated at the boundaries of very large grains (Fig. 2.1).

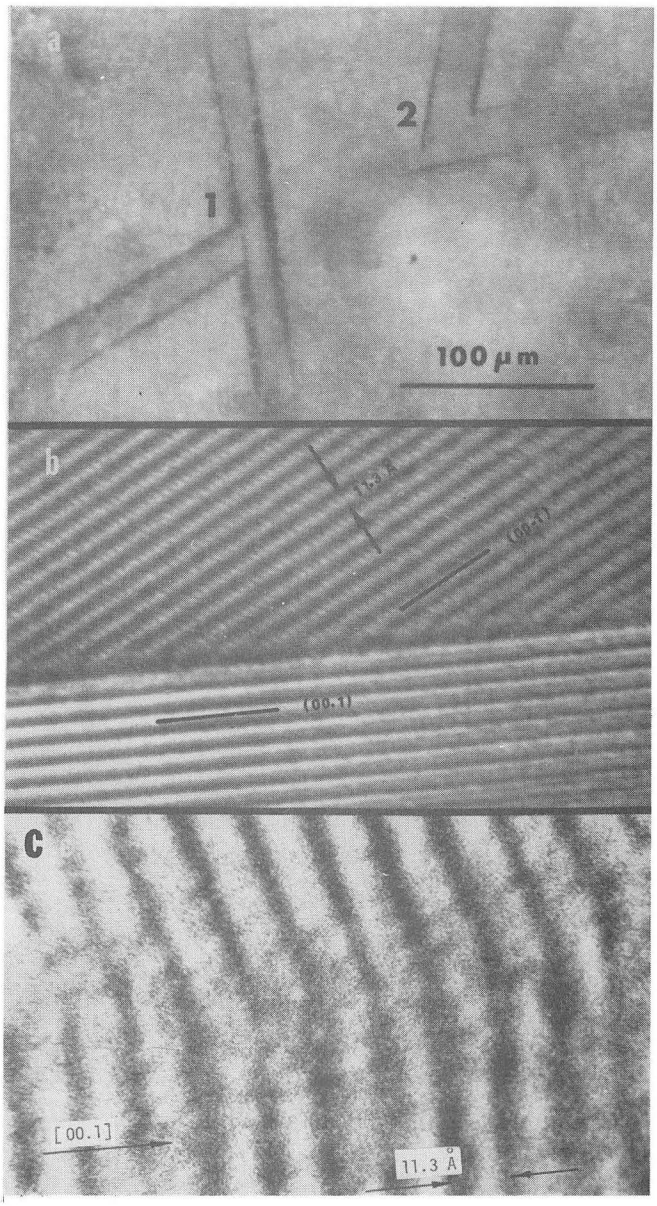

Fig. 2.1. (a) Optical micrograph of silver-stained sodium exit surface for electrolyte subjected to unidirectional current flow of 50 mA/cm^2, in a Na/Na cell, at 300°C. The two configurations of Mode I initiation have been labeled. (b) Lattice image of a grain boundary structure corresponding to 1 in (a). (c) Lattice image of a grain boundary structure corresponding to 2 in (a). (XBB 823-2763A)

The grain junctions are marked at 1 and 2. There is degradation at the junction of the two grains at 1, but none at the junction of the grains at 2; they are two different types of boundaries [Fig. 2.1(b) and (c)]. This observation suggests that the long, faceted sides of the large grains are mechanically weak. These facets correspond

*This work was supported by the Assistant Secretary for Conservation and Renewable Energy, Office of Energy Systems Research, Electrochemical Systems Research Division of the U. S. Department of Energy under Contract No. DE-AC03-76SF00098.

to 00.1 planes. Further evidence of the low bonding strength along 00.1 faceted grain boundaries can be seen in Fig. 2.2, which shows a fracture along a partial 00.1 faceted grain boundary. In the region where the grain boundary deviated from an exact 00.1 facet, the spinel-spinel block bonding, arrowed in Fig. 2.2, survived. The fractured path shows directly that grain boundary strength depends on grain boundary structure.

* * *

†Brief version of LBL-14150.

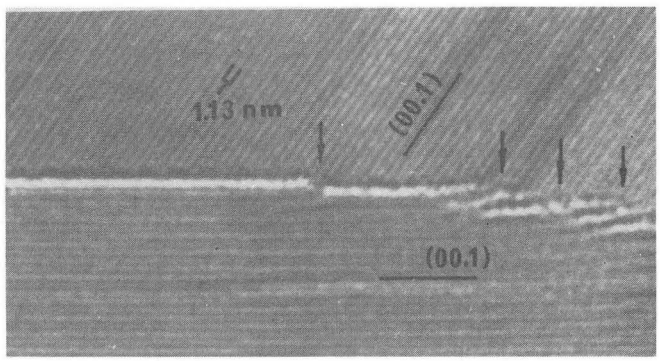

Fig. 2.2. Fracture at a grain boundary partially faceted along 00.1 planes. Where the grain boundary deviates from an exact 00.1 facet, as in Fig. 2.1(c) direct spinel-spinel block bonds (arrowed) have survived. This demonstrates directly that the grain boundary strength depends on its structure. (XBB 823-2134)

1982 PUBLICATIONS AND REPORTS

Refereed Journals

1. L. C. De Jonghe, "Impurities and Solid Electrolyte Failure," Solid State Ionics 7, 61 (1982).

†2. L. C. De Jonghe, "Transport Number Gradients and Solid Electrolyte Degradation," J. Electrochem. Soc. 129, 752 (1982).

†3. L. Feldman and L. C. De Jonghe, "Initiation of Mode I Degradation in Sodium-Beta Alumina Electrolytes," J. Mat. Sci. 17, 517 (1982).

†4. L. C. De Jonghe and A. Buechele, "Chemical Coloration of Sodium Beta Aluminas," J. Mat. Sci. 17, 885 (1982).

†5. L. C. De Jonghe, L. Feldman, and A. Buechele, "Failure Modes of Na-Beta Alumina," Solid State Ionics 5, 267 (1981).

LBL Reports

†1. L. C. De Jonghe, "Degradation Mechanisms of Sodium Beta Aluminas," LBL-14365.

†2. A. Buechele, L. C. De Jonghe, and D. Hitchcock, "Degradation of Sodium Beta" Alumina: Effect of Microstructure," LBL-13188.

†3. L. C. De Jonghe, A. Buechele, and K. H. Yoon, "Grain Boundaries and Solid Electrolyte Degradation," LBL-14150.

Invited Talks

1. Lutgard C. De Jonghe, "Solid State Electrochemistry and Batteries," Institute of Physics and Chemistry, University of Sao Paulo, Sao Carlos, Brazil, August 1982 (15 talks).

2. Lutgard C. De Jonghe, "Materials Problems in Energy Storage," Department of Materials Science, Federal University of Sao Carlos, Brazil, August 1982.

3. Lutgard C. De Jonghe, "Solid Electrolyte Properties," Institute of Physics, Federal University of Minas Gerais, Belo Horizonte, Brazil, September 1982.

4. Lutgard C. De Jonghe, "Solid Electrolyte Batteries," Institute of Nuclear Energy Research, University of Sao Paulo, Sao Paulo, Brazil, September 1982.

5. Lutgard C. De Jonghe, "Electrochemical Energy Storage," Energy Company of Sao Paulo (CESP), Sao Paulo, Brazil, September 1982.

6. Lutgard C. De Jonghe, "Microstructure and Properties of Sodium Beta Aluminas," RUCA, Antwerp, Belgium, June 1982.

* * *

†Support was also provided by the Electric Power Research Institute.

h. Analysis and Simulation of Electrochemical Systems*

John Newman, Investigator

Introduction. This program includes the investigation of efficient and economical methods for electrical energy conversion and storage, and development of mathematical models to predict the behavior of electrochemical systems and to identify important process parameters. Experiments are used to verify the completeness and accuracy of the models.

1. WORK IN PROGRESS

Experiments have been conducted to study the passivation behavior of iron electrodes in aqueous acidic media. The experimental results obtained with a rotating-disk electrode revealed an anodic limiting current. In an electrolytic solution of a given composition, the limiting current was found to be proportional to the square root of the disk rotation speed. For a given rotation speed, the limiting-current decreased with increasing electrolyte pH. Current oscillations have been observed within certain potential ranges on the limiting-current plateau. The frequency of these oscillations has been found to be proportional to the square root of the disk rotation speed. Subharmonic current oscillations have also been observed under certain voltage and rotation speed conditions.

Work is currently under way to develop a model describing the oscillatory phenomena. Physical phenomena judged to be important include iron dissolution kinetics, salt film formation and dissolution, potential distribution, concentration profiles in the electrolyte, hydrodynamics, and the dependence of the passivation potential on surface conditions. The model will include a stability analysis using techniques involving limit cycles and bifurcation analysis.

An alternating current impedance method is being used to study the anodic electrodissolution of a rotating zinc disk in an acidic chloride medium. Initially, the corrosion process must be characterized by establishing the dc polarization behavior. A model has been developed to analyze experimentally obtained kinetic data. The model also determines the corrosion potential and current for a wide range of electrolyte compositions. Finally, the ac behavior must be studied. An ac impedance experimental procedure, applicable over a wide frequency domain, is currently being developed. Information about the capacitive double-layer, along with the faradaic electron-transfer reaction will be obtained and analyzed.

Quantitative design and scale-up criteria are needed for battery systems. Presently, parametric or empirical studies are done to determine the effect of design variables on battery performance. A computer model that utilizes fundamental small cell data (or micromodeling data) is being developed that predicts the energy and power performance of a scaled-up battery. The model is general and may be applied to many types of battery systems. The battery can be optimized for maximum energy or power, or a compromise design may be selected. Inherent limitations of battery performance or specific areas of development requiring attention can be identified. In general, voltage and weight penalties of the current collectors, interconnecting bus and post, electrolyte, positive and negative active material, and cell container are taken into account. Subject to variation or prediction are the number of positive electrodes per cell, length of the bus and post, area of electrodes, current collector weight, and total delivered capacity. These results are based on a correlation of dimensionless resistance vs plate area. This figure is curve fit and is used to generate the combined resistance of the electrochemical cell and current collecting grids as a function of depth of discharge. Accuracy to within 3 to 5% of a more sophisticated method is typically obtained.

An improved method for approximating the conductivity of heterogeneous porous electrodes is being developed. The method currently used in the mathematical model of the lithium-aluminum/iron sulfide cell overestimates electrode conductivity. An extension of the classical result of Maxwell was applied and resulted in effective conductivities as much as an order of magnitude smaller than those obtained by the previous method. This method will later be extended to develop a mathematical model of the lithium-silicon/iron disulfide cell.

Channel flow between two plane parallel electrodes is used in many industrial electrochemical processes, such as metal refining, energy storage, and electro-organic synthesis. A mathematical model is being developed to predict the current and potential distribution in a channel flow cell with an interelectrode gap on the order of, or thinner than, the diffusion layer thickness. That is, a product from one electrode reaches and reacts at the other electrode. One of the preliminary results of the model was a criterion to determine whether or not the thin-diffusion-layer approximation may be applied to a given channel flow cell. The model can take into account an arbitrary number of species and multiple reactions at the electrodes.

An experimental research program is under way to develop a fundamental understanding of the precipitation of nickel hydroxide by the electrochemical reduction of nitrate ions, which changes the pH. This electrode occurs as the positive in a number of practical or promising

*This work was supported by the Assistant Secretary for Conservation and Renewable Energy, Office of Energy Systems Research, Energy Storage Division of the U.S. Department of Energy under Contract No. DE-AC03-76SF00098.

systems (those with negative electrodes of hydrogen, zinc, iron, and cadmium). Polarization characteristics of some nickel nitrate solutions were determined with a rotating-disk-electrode apparatus. Ring/disk electrode experiments indicate the irreversibility of the electrode processes.

The performance of sodium-sulfur secondary cells is strongly influenced by the diffusion of anions and cations through the polysulfide melt. Thus, optimal design of sulfur electrodes will depend upon the availability and accuracy of diffusion coefficient data for polysulfide melts. An experimental apparatus has been built to measure the diffusion coefficient of sodium ions in melts of sodium polysulfides, using the method of restricted diffusion. Some preliminary experiments have been performed with this apparatus, and work is currently under way to perfect the design of the apparatus. In addition, binary interaction parameters for sodium polysulfide melts, assuming a "pseudo-binary" melt, have been calculated using transport data obtained from the open literature.

1982 PUBLICATIONS AND REPORTS

Refereed Journals

1. Peter S. Fedkiw and John Newman, "Mass-Transfer Coefficients in Packed Beds at Very Low Reynolds Numbers," Intern. J. Heat Mass Transfer 25, 935-943 (1982).

Invited Talks

1. John Newman, "Electrochemical Systems Modeling," Applied Battery and Electrochemical Research Program, Lawrence Berkeley Laboratory, Review of the Technology Base Research Project, June 2, 1982.

2. John Newman, "Mathematical Model of the Li-Al/FeS Molten Salt Battery," Sandia National Laboratories, Albuquerque, New Mexico, Materials Science Seminar, June 18, 1982.

3. L. Redey, "Electrochemical Characterization of Li-Al/FeS Cells," Detroit Meeting of the Electrochemical Society, October 17-22, 1982.

VII Magnetic Fusion Energy

Magnetic Fusion Energy

a. Structural Materials and Weldments for High Field Superconducting Magnets*

John W. Morris, Jr., Investigator

Introduction. Large, high field superconducting magnets are essential components in all current designs for fusion energy systems. The selection of suitable materials for the structures of these magnets poses unique problems. The magnet case must withstand the high structural loads imposed by the Lorentz force in the winding, and it sustains these loads at cryogenic temperature (4 K) in the presence of high magnetic fields. The effect of low temperature on the mechanical properties of structural alloys is only partly understood, and the influence of high magnetic fields is virtually unknown. The combined requirements of high structural strength, high fracture toughness, and fatigue resistance in the superconducting magnet environment make it probable that new structural alloys will be needed for the construction of commercial fusion energy devices. The present project is intended to contribute to the development of these new alloys by clarifying the behavior of structural materials in the magnet environment and by designing, identifying, and testing new alloys and weldments that promise superior structural performance.

1. THE MAGNETO-MECHANICAL CRYOGENIC RESEARCH FACILITY (MMCR)

B. Fultz, R. Kopa, and J. W. Morris, Jr.

Research on the mechanical properties of materials in an environment resembling that of a high field superconducting magnet requires a versatile facility capable of cryogenic tensile, fracture toughness, and fatigue crack growth measurements in the presence of high, steady magnetic fields. Standard fatigue and toughness tests require large specimens and therefore a large bore magnet.

Such a system has been installed in MMRD (Fig. 1.1). The central element of the system is a large bore, NbTi superconducting solenoid that can achieve a field above 8.6 T. The test specimen is contained in a variable temperature anticryostat that has a cylindrical 101 mm diameter tail section within the solenoid. The cryostat and magnet sit in a 244 kN Instron 1332 servohydraulic load frame with the actuator assembly mounted on its upper crosshead.

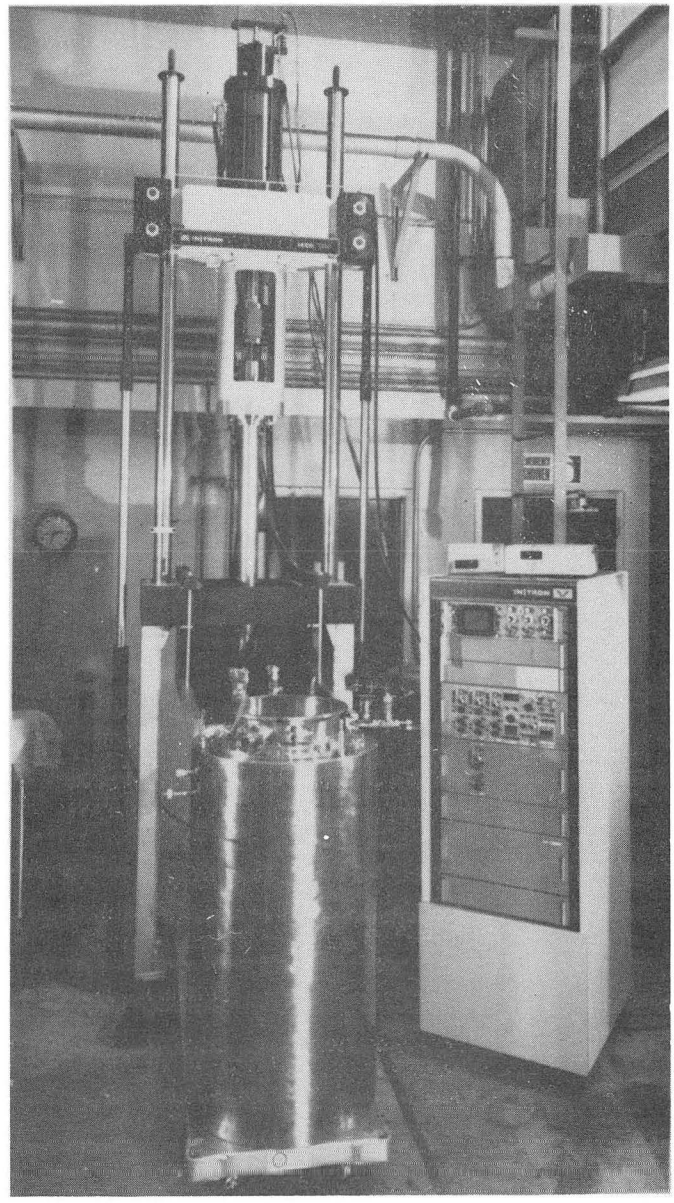

Fig. 1.1. The MMCR facility. (CBB 824-4162)

This device is capable of performing standard laboratory tensile, toughness, and fatigue tests on full sized specimens at selected temperature down to 4 K and magnetic field up to 8.6 T.

*This work was supported by the Director, Office of Energy Research, Office of Fusion Energy Development and Technology Division of the U.S. Department of Energy under Contract No. DE-AC03-76SF00098.

2. MAGNETIC FIELD EFFECTS ON MECHANICAL PROPERTIES OF STAINLESS STEELS

B. Fultz, R. Kopa, G. M. Chang, and J. W. Morris, Jr.

The stainless steels that are now commonly specified for the structures of high field superconducting magnets are 304 and 316 in the L and LN grades. These steels are in an austenite phase that is metastable at cryogenic temperature. They undergo a martensitic transformation under strain that may be promoted by a high magnetic field. It is hence important to characterize their mechanical properties in the presence of high magnetic fields. It is expected that the largest field effect will appear in fatigue tests, but it is first necessary to study tensile behavior.

Preliminary tensile tests have been conducted on both 304L and 304LN alloys in various processing conditions. These tests reveal systematic changes in the tensile properties at 77 K in an 8 T field. The flow stress increases, the ultimate tensile strength increases, and the elongation drops. The effect increases with the amount of prior deformation on the sample. The increase in flow stress is approximately 8% in cold worked 304LN.

3. AUSTENITIC Fe-Mn CRYOGENIC STEELS

R. Ogawa and J. W. Morris, Jr.

Nonmagnetic steels from the Fe-Mn system are potential structural alloys for the cryogenic cases of high field superconducting magnets. Alloys from this class offer excellent strength and toughness at 4 K, are nonmagnetic even under large strains, and are inexpensive relative to the conventional stainless steels.

Recent research under this project[1] concentrated on the role of the interstitial content in cryogenic mechanical behavior of Fe-Mn-Ni-Cr alloys. This investigation led to the selection of the composition Fe-18Mn-5Ni-16Cr-0.024C-0.22N. This alloy was made and tested at 4 K. Both its strength-toughness combination and its fatigue properties equal or exceed those of 304LN. Its strength-toughness characteristic is compared to the trend line for conventional stainless steels in Fig. 3.1. Its properties exceed those of the stainless steels and approach the "JAERI envelope," the target range of properties set by the Japanese fusion program.

* * *

1. R. Ogawa and J. W. Morris, Jr., Proceedings of the International Cryogenic Materials Conference, Kobe, Japan, edited by K. Tachikawa and A. Clark, Butterworths, London, England, 1982, p. 124.

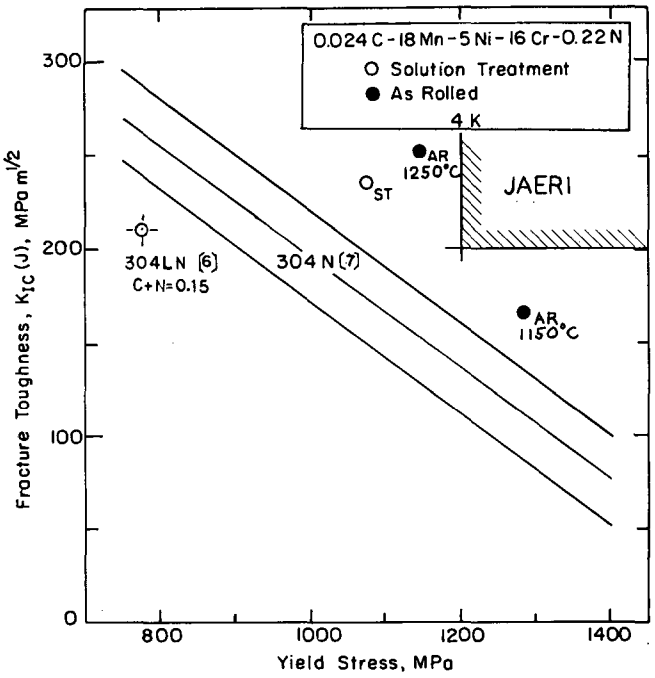

Fig. 3.1. The strength and toughness of three Fe-Mn research alloys at 4 K are compared to the trend line for conventional stainless steels and to the "JAERI envelope," the target values for magnet case materials for the Japanese fusion program. (XBL 824-5496)

1982 PUBLICATIONS AND REPORTS

Other Publications

1. J. W. Morris, Jr. and B. Fultz, "Effects of Magnetic Fields on Martensitic Transformations and Mechanical Properties in Stainless Steels at Low Temperature," Proceedings of the International Cryogenic Materials Conference, Kobe, Japan, edited by K. Tachikawa and A. Clark, Butterworths, London, England, 1982, p. 343.

2. R. Ogawa and J. W. Morris, Jr., "The Influence of Nitride and Carbonitride Precipitation on the Cryogenic Mechanical Properties of High Manganese Austenitic Steels," Proceedings of the International Cryogenic Materials Conference, Kobe, Japan, edited by K. Tachikawa and A. Clark, Butterworths, London, England, 1982, p. 124.

LBL Reports

1. H. J. Kim and J. W. Morris, Jr., "The Development of a Ferritic Consumable Welding Grain-Refined Fe-12Ni-0.25Ti to Retain Toughness at 4.2 K," Welding J., in press, LBL-13046.

2. B. Fultz, G. M. Chang, and J. W. Morris, Jr., "Effects of Magnetic Fields on Martensite Transformations and Mechanical Properties of Steels at Low Temperatures," in press, LBL-15518.


VIII
Nuclear Waste Management

Nuclear Waste Management

a. Thermodynamic Properties of Chemical Species in Nuclear Waste*

Norman M. Edelstein, Investigator

Introduction. The purpose of this program is to investigate the thermodynamic properties of anticipated actinide and fission product ions and the compounds they may form in geologic environments, so that their chemical behavior and potential migration in a nuclear waste setting can be assessed with improved capability.

A number of laboratory studies are being undertaken to obtain data concerning species, oxidation states, effect of complexing ligands, and other related information. Such data will contribute to a better understanding of the chemical systems that may be involved in various geologic media and will furnish more reliable parameters for radionuclide migration modeling studies.

1. VOLTAMMETRIC STUDIES OF THE NpO_2^+ CARBONATE SYSTEMS†

H. Nitsche and N. M. Edelstein

The lack of accurate thermodynamic data for actinide species in aqueous solution prevents a realistic assessment of the amounts and rates of release of radionuclides from an underground waste repository.[1,2] One of the more important actinide nuclides for which little accurate data is available is neptunium, which can exist in the +5 state under environmental conditions.[3]

We have studied the complexation of NpO_2^+ ($c = 5.9 \times 10^{-5}$ M) at a pH of 8.33 by carbonate ion in $NaClO_4$ solutions ($I = 0.05$ M) by computer controlled voltammetry.[4] The data have been analyzed by use of the Lingane equation.[5] Figure 1.1 shows the differential pulse voltammograms of the quasi-reversible NpO_2^+ oxidation with increasing carbonate concentrations and the subsequent negative potential shift.

From an analysis of this data and assuming the most stable complex for the oxidized species is the 1:3 complex $NpO_2(CO_3)_3^{4-}$, we find

$$\log\left(\frac{\beta_{NpO_2(CO_3)_3^{4-}}}{\beta_{NpO_2(CO_3)_2^{3-}}}\right) = 10.2 \quad .$$

*This work was supported by the Assistant Secretary of Nuclear Energy, Office of Commercial Nuclear Waste Management, Commercial Waste Management Program Division of the U.S. Department of Energy under Contract No. DE-AC03-76SF00098 through the Battelle Memorial Institute, Office of Nuclear Waste Isolation (ONWI), Columbus, Ohio, under MPO No. E511-05100.

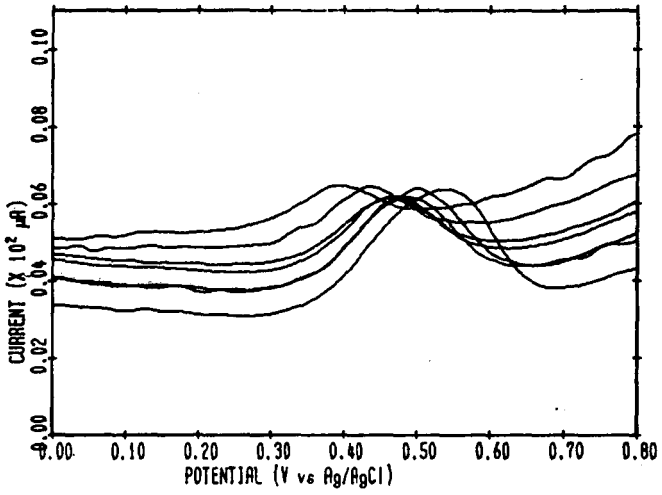

Fig. 1.1. Potential shift of Np V/VI oxidation ($c = 5.86 \times 10^{-5}$ M) with addition of $NaHCO_3$ at pH 8.33 in 0.05 M $NaClO_4$. (XBL 833-8701)

Since there is no information available on the formation constant for the 1:3 complex of $NpO_2(CO_3)_3^{4-}$, we have used the value of $\log \beta_{130} = 21.4$ for the corresponding $UO_2(CO_3)_3^{4-}$ (Ref. 6) and obtain the stability constant for $NpO_2(CO_3)_2^{3-}$ of $\log \beta_{120} = 11.2 \pm 1$. Verification of this result is under way by spectrophotometric methods.

* * *

1. J. M. Cleveland, in Chemical Modeling in Aqueous Systems, edited by E. A. Jenne, ACS Symposium Series 93, Washington, D.C., 1979, p. 16.
2. B. Allard, "Solubilities of Actinides in Neutral or Basic Solutions," in Proceedings of the Actinides-1981 Conference, edited by N. Edelstein, Pergamon Press, Oxford, 1982, p. 553.
3. J. B. Moody, Technical Status Report, OWNI-321 (1981).
4. S. D. Brown and B. R. Kowalski, Anal. Chim. Acta 107, 13 (1979).
5. J. J. Lingane, Chem. Rev. 20, 1 (1941).
6. S. L. Phillips, LBL-14313, 1982.

2. THE SOLUBILITIES OF CRYSTALLINE NEODYMIUM AND AMERICIUM TRIHYDROXIDE

R. J. Silva

One of the hazardous actinides in nuclear waste from a long-term point of view is ameri-

cium.[1] If trivalent Am behaves like the trivalent lanthanides, and there is good reason to expect that it will,[2] Am would be expected to form an insoluble hydroxide under environmental conditions. Unfortunately, there has been no systematic investigation of the solubility of well-characterized $Am(OH)_3$ reported in the literature. The objective of this work was: (1) to measure the solubility of well-characterized, crystalline $Am(OH)_3$ as a function of pH and obtain a value for the solubility product constant, and (2) to measure the solubility of well-characterized crystalline $Nd(OH)_3$ as a function of pH and, by comparing the results with (1) above, determine if it is a good analog compound for $Am(OH)_3$.

Pure crystalline $Nd(OH)_3$ and $Am(OH)_3$ were prepared and characterized through the measurement of their x-ray powder patterns. Portions of the solid materials were placed separately in contact with aqueous solutions of 0.1 M $NaClO_4$ of different pH values at 25 ± 1°C. The solubilities of the two materials were determined from measurements of the solution concentrations of Nd and Am as a function of time. The open points in Figs. 2.1 and 2.2 are the results of the experimental measurements for Nd and Am, respectively.

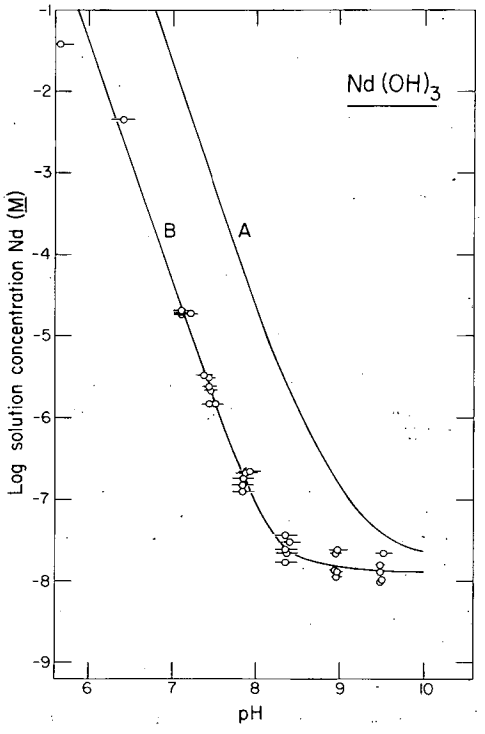

Fig. 2.1. Plot of the logarithm of the solution concentration of Nd in aqueous 0.1 M $NaClO_4$ solutions as a function of pH at 25°C.

(XBL 8210-1200)

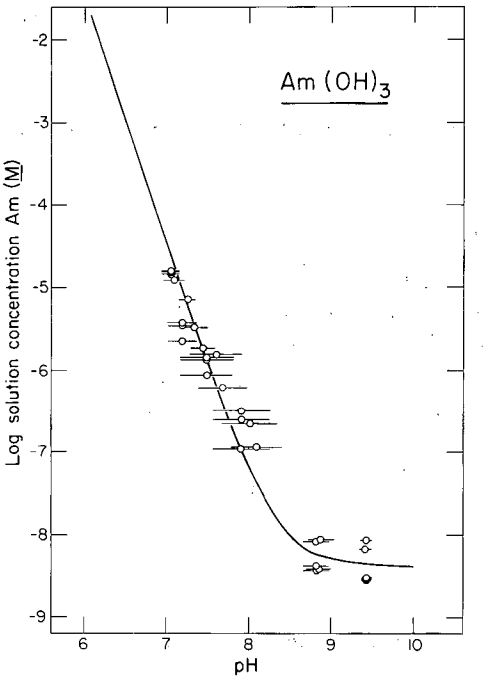

Fig. 2.2. Plot of the logarithm of the solution concentration of Am in aqueous 0.1 M $NaClO_4$ solutions as a function of pH at 25°C.

(XBL 8210-1201)

The results of the experimental measurements were analyzed in terms of the solubility product and hydrolysis reactions given in Table 2.1. Also presented in Table 2.1 are the thermodynamic constants for the reactions for Nd given by Baes and Mesmer.[3] Since the analysis involves the solution of a number of coupled equations simultaneously, the calculations of the concentrations of solution species and solubilities from the thermodynamic constants were made using a computer code called MINEQL.[4]

The solid curve labeled (A) in Fig. 2.1 resulted from calculations using the constants of Baes and Mesmer.[3] Clearly, the predicted solubility of $Nd(OH)_3$ was considerably higher than that measured in these experiments. Analysis of the data involved systematically varying the values of the constants for reactions (1), (3), (4), and (5), and comparing the resulting calculated curves with the experimental points in Figs. 2.1 and 2.2. The solid curve labeled (B) in Fig. 2.1 and the solid curve in Fig. 2.2 represent the best fits to the experimental data. The values of the solubility product and hydrolysis constants used to obtain the best fits are given in Table 2.1 for both Nd and Am. The solubilities and speciation of Nd and Am as a function of pH are quite similar, and $Nd(OH)_3$ should be a good analog compound for $Am(OH)_3$.

Table 2.1. Solubility Product and Hydrolysis Constants of Nd^{3+} and Am^{3+} for 25°C and Corrected to Zero Ionic Strength.

Reaction	Log K Nd (Ref. 3)	Nd (This work)	Am (This work)
(1) $M(OH)_3(S) + 3H^+ = M^{3+} + 3H_2O$; K_{s10}	18.6	16.0 ± 0.2	15.9 ± 0.4
(2) $M^{3+} + H_2O = M(OH)^{2+} + H^+$; K_{11}	-8.0	-7.7 + 0.3	-7.7 ± 0.3
(3) $M^{3+} + 2H_2O = M(OH)_2^+ + 2H^+$; K_{12}	-16.9[a]	-15.8 ± 0.5	-16.0 ± 0.7
(4) $M^{3+} + 3H_2O = M(OH)_3^0 + 3H^+$; K_{13}	-26.5[a]	-23.9 ± 0.2	-24.3 ± 0.3
(5) $M^{3+} + 4H_2O = M(OH)_4^- + 4H^+$; K_{14}	-37.1	<34	<34.5

[a]Predictions.

* * *

1. J. B. Moody, Radionuclide Migration/ Retardation: Research and Development Technology Status Report, Office of Nuclear Waste Isolation, Battelle Memorial Institute report ONWI-321, 1982, p. 6.
2. C. F. Baes, Jr., and R. E. Mesmer, The Hydrolysis of Cations, Wiley and Sons, N.Y., 1976, p. 191.
3. Ibid, p. 137.
4. J. C. Westall, J. C. Zachary, and F. M. M. Morel, "MINEQL, A Computer Program for the Calculation of Chemical Equilibrium Composition of Aqueous Systems," Dept. Civil Eng., Massachusetts Institute of Technology, Cambridge, MA, Technical Note 18, 1976.
5. N. Edelstein, J. Bucher, R. Silva, and H. Nitsche, "Thermodynamic Properties of Chemical Species in Nuclear Waste: Topical Report," ONWI/LBL-14325.

3. HYDROLYSIS AND HYDROLYTIC PRECIPITATION REACTIONS FOR NpO_2^+, Nd^{3+}, and Cm^{3+}

J. J. Bucher and N. Edelstein

A number of long-lived actinides are present in spent nuclear fuels and high level processed waste in sufficient quantities to remain a radiological hazard, even after 1000 years, if placed in an underground repository. If these materials interact with groundwater, a number of insoluble compounds and solution species can be formed. In order to determine what species can be formed with various anionic species, reliable thermodynamic data must be available for hydrolysis reactions and for the solubilities of the metal hydroxides. We have studied these reactions for the univalent species NpO_2^+ and for two trivalent ions Cm^{3+} and Nd^{3+}, by a potentiometric titration method using a computer-controlled automatic titrator and the program STBLTY for data analysis.[1]

The hydrolysis and precipitation reactions for the metal ions under study are given in Table 3.1 along with the results of an earlier study[2] for NpO_2^+ and the best values for Nd^{3+} as determined by Baes and Mesmer in their critical review.[3] Our experimental values are also listed in Table 3.1. For NpO_2^+ our value of log K_{10-1} and log K_{s10-1} confirm the results of the earlier study.[2] The values found for the first hydrolysis quotient of Nd^{3+} and Cm^{3+} are approximately the same and agree well with the Nd^{3+} value chosen by Baes and Mesmer.[3] We found no strong evidence for the formation of dimers or higher polymeric species; our data could equally well be explained by colloid formation before the hydroxide precipitates. Our value for the $Nd(OH)_3$ solubility, log K_{s10-3} = 15.8, is in reasonable agreement with the value for $Cm(OH)_3$ solubility, but disagrees by approximately three orders of magnitude with the literature value, log K_{s10-3} = 18.6. It is, however, in excellent agreement with recent measurements of the solubility of $Nd(OH)_3$ and $Am(OH)_3$ determined by radiochemical techniques.[4] Finally, it is important to note that the hydrolytic behavior of Nd^{3+} and Cm^{3+} is similar as expected from the systematics of the chemistry of the trivalent ions of the lanthanide and actinide series.

* * *

1. A. Avdeff, and J. J. Bucher, Anal. Chem. 50, 2137 (1978).
2. K. A. Kraus, and F. Nelson, U.S.A.E.C. Report AECD-1864, 1948, Oak Ridge, TN.
3. C. F. Baes, and R. E. Mesmer, The Hydrolysis of Cations, Wiley-Interscience, N.Y., 1976, p. 129.
4. R. J. Silva, Lawrence Berkeley Laboratory Report LBL-15055, 1982.

Table 3.1. Hydrolysis Quotients and Solubility Product of NpO_2^+, Nd^{3+} and Cm^{3+} in Approximately 0.1 M KCL.

Reaction[a]	Log Q Literature	This Work
1) $NpO_2^+ + HOH = NpO_2(OH)_{aq.} + H^+$; K_{10-1}	-8.85[b]	-9.05 ± 0.05
2) $NpO_2(OH)_{solid} + H^+ = NpO_2^+ + HOH$; K_{s10-1}	4.8[b]	5.3 ± 0.1
3) $M^{3+} + HOH = M(OH)^{2+} + H^+$; K_{10-1}	-8.0[c]	-7.7 ± 0.3
4) $2M^{3+} + 2HOH = M_2(OH)_2^{4+} + 2H^+$; K_{20-2}	-13.86[c]	-
5) $3M^{3+} + 5HOH = M_3(OH)_5^{4+} + 5H^+$; K_{30-5}	<-28.5[c]	-
6) $M(OH)_3$ solid $+ 3H^+ = M^{3+} + 3HOH$; K_{s10-3}	18.6[c]	15.8 ± 0.2

[a] $M^{3+} = Nd^{3+}$ or Cm^{3+}.

[b] Ref. 2.

[c] For Nd^{3+} from Ref. 3.

1982 PUBLICATIONS AND REPORTS

LBL Reports

1. N. Edelstein, J. Bucher, R. Silva, and H. Nitsche, "Thermodynamic Properties of Chemical Species in Nuclear Waste: Topical Report," ONWI/LBL-14325.

2. R. J. Silva, "Thermodynamic Properties of Chemical Species in Nuclear Waste: Topical Report. The Solubilities of Crystalline Neodymium and Americium Trihydroxides," ONWI/LBL-15055.

3. H. Nitsche and N. Edelstein, "Thermodynamic Properties of Chemical Species in Nuclear Waste: I. Carbonate Complexation of Np(V) in Near Neutral and Basic Solutions: Topical Report," ONWI/LBL-14935.

4. J. J. Toman, "Convolution Techniques in Analytical Electrochemistry," Ph.D. thesis, LBL-14429.


IX
Work for Others

Work for Others

1. National Aeronautics and Space Administration (NASA)

a. Theoretical Studies of Formyl Radical Formation in Selected Combustion Reactions*

William A. Lester, Jr., Investigator†

1. WORK IN PROGRESS

Ab initio Hartree-Fock, multiconfiguration Hartree-Fock, and configuration interaction methods are being applied to important problems of combustion chemistry, with particular emphasis on emission processes in flames. An important intermediate that contributes to flame spectra is the formyl (HCO) radical which has a low-lying electronically excited state ($A^2\Pi$) that lies ~27 kcal/mole above the ground ($X\ ^2A'$) state. It is important to know the fraction of HCO formed directly in the A state.

The most relevant reaction is

$$H_2CO + OH \longrightarrow HCO + H_2O \quad . \qquad (1)$$

Its energy correlation diagram is shown in Fig. 1.1. The minimum energy pathway and the transition state structure for the ground state $^2A'$ surface maintains a plane of symmetry. The calculated transition-state structure shows that the attacking O atom is nearly collinear with the attacked CH bond. Large basis sets and CI methods must be used for quantitative accuracy.

The excited state surface corresponds to the second state of singlet spin. Special techniques and methods are required to treat excited states. Determination of the transition state is in progress.

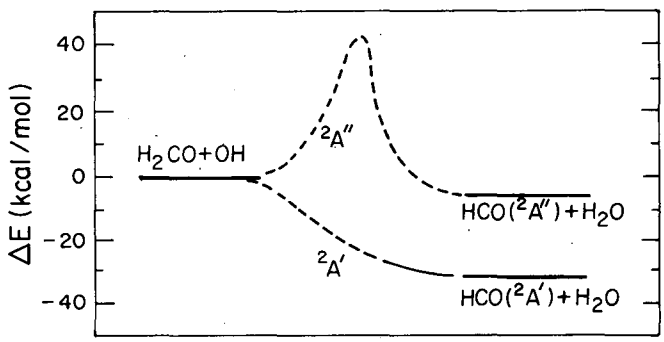

Fig. 1.1. Energy correlation diagram for $H_2CO + OH \rightarrow HCO + H_2O$. (XBL 816-2351)

Another reaction relevant to $HCO(A^2\Pi)$ formation is

$$CH_2 + O \longrightarrow H + HCO \quad . \qquad (2)$$

Formaldehyde (H_2CO) in its ground and excited electronic state is a stable intermediate in this reaction. $HCO(A^2\Pi)$ originates from H_2CO ($^1n\rightarrow\pi^*$), $H_2CO(^1\pi\rightarrow\pi^*)$, and $H_2CO(^3\pi\rightarrow\pi^*)$. Calculations are under way to determine the transition-state structure for the various elementary steps, as well as the transition state structure and energy barrier for

$$CH_2 + O \longrightarrow H_2CO \quad .$$

*This work was supported by the Ames Research Center, NASA, under Contract No. A 86130B (LML). Equipment was purchased through the National Science Foundation.

†Scientific Staff member at LBL operating under Contract No. DE-AC03-76SF00098.

2. Office of Naval Research

a. Structure and Performance of Al_2O_3*

Donald H. Boone and Alan V. Levy, Investigators†

Introduction. The protection of structural materials in high temperature oxidizing and hot corrosion conditions that occur in the combustion zones of gas turbines and diesel engines is provided by the formation of a protective oxide. In many cases the requirements of increased efficiencies and higher operation temperatures have resulted in a decrease in the lifetimes of an engine and its components. For this and other reasons much effort has been directed toward the use of thin protective coatings which are designed to be compatible with higher strength substrates and to form a protective oxide. One such system is the so-called diffusion aluminide coating applied to both nickel and cobalt base superalloys. Protection is provided by the formation of an Al_2O_3 rich layer and degradation occurs by oxide spallation and/or fluxing in cyclic oxidation and hot corrosion.

The addition of noble metals to these coatings has been reported to increase their protection in both oxidation and hot corrosion environments. Little is understood of the reason for these reported improvements and of the interactions between the noble metal, often platinum, the aluminide, the substrate, and the protective oxide. A research effort was initiated to establish the structural features of noble metal enhanced aluminide coatings. Also being investigated are coating formation characteristics, mechanism of interdiffusion, degradation modes and behavior under a variety of elevated-temperature, simulated-combustion environments.

1. PLATINUM MODIFIED ALUMINIA COATINGS‡

Lori Purvis and Donald Boone

Although limited documentation of the structure and phases of platinum modified aluminides exist in the literature, the implication of earlier studies has been that the platinum containing coatings have a standard structure and excellent protection in a variety of environments. Preliminary evaluation of a number of experimental and commercially available coatings, however, has indicated the existence of a wide range of structures. These vary from an essentially single-phase, high-platinum content outer zone through a two-phase structure to a single-phase NiAl-Pt phase coating.

In all cases, a zone of Pt enrichment was found at the surface, extending varying distances into the coating even though these coatings are produced by the same initial deposition of a Pt layer (8 μm) followed by an aluminizing treatment. This suggests essentially inward aluminum diffusion through the initial Pt-rich phase found on the surface.

Hot corrosion tests confirmed a strong effect of the test conditions on the protection provided by the addition of Pt, as well as an effect of the specific coating structure present. While a large beneficial effect of Pt was found in furnace hot corrosion testing at 900°C, little if any improvement was found at 700°C. The single phase high Pt-Al content surface phase structure was found to be more corrosion resistant, particularly at 900°C. Indications of a strong substrate alloy composition effect were also seen, with the coatings on some alloys showing a much stronger "Pt effect" than on others.

These and other tests indicate the probable effect of the Pt in limiting the concentration of certain elements at the surface and the subsequent effects of these elements on the structure, compositions, and protection of the oxide that forms. Previous studies have reported a possible effect of the Pt to be the formation of a higher purity Al_2O_3 protective oxide. Since Al_2O_3 has been found to offer little resistance to basic fluxing in low temperature corrosion, a limited Pt effect would be expected.

These hypotheses are being explored in a study of both the mechanism of formation using controlled pre-aluminizing diffusion treatments and the specific activity of aluminizing coating cycles. Substrates with controlled addition of potentially critical elements such as Ti and Hf are also being studied.

* * *

‡Brief version of LBL-15668.

*This work was supported by the Office of Naval Research, Department of Defense under Government Order No. N 00014-82-F-0055.

†Scientific Staff members at LBL operating under Contract No. DE-AC03-76SF00098.

b. Electron-Phonon Coupling and the Properties of Thin Films and Inhomogeneous Superconductors*

Vladimir Z. Kresin, Investigator †

Introduction. This research is concerned with the study of several interconnected problems. Contacts, containing superconducting and normal films, have been studied. It is particularly interesting to consider the proximity systems superconductor-semiconductor (S-SC) and superconductor-semimetal (S-SM) because, in this way, it is possible to induce the superconducting state in new materials. Josephson tunneling into a proximity system is another example of an interesting phenomenon. The properties of such systems are very sensitive to the strength of the electron-phonon interaction, and this interaction should be included directly in the theory.

1. SYSTEMS CONTAINING THIN FILMS‡

A. Critical temperature

A theory of the proximity effect can be developed on the basis of the method of the thermodynamic Green function. The electron-phonon interaction can be included directly. As a result one can get the following expression for T_c of the proximity system $S_\alpha - M_\beta$:

$$T_c = T_c^S \left[\frac{\pi T_c^S}{2\langle u \rangle \gamma} \right]^\rho , \qquad (1)$$

where T_c^S is the critical temperature in the absence of the proximity effect, $\gamma \approx 1.78$, $\rho = (\nu_\beta/\nu_\alpha)(L_\beta/L_\alpha)$, L_α and L_β are the thicknesses of the films, ν_α and ν_β are the densities of the states, $u(\omega) = \Gamma^{1-\delta}\omega^\delta\delta = \Gamma^2/(\omega^2+\Gamma^2)$, $\Gamma = \pi\tilde{T}^2 S(\nu_\alpha L_\alpha + \nu_\beta L_\beta)$, $\tilde{T}$ is the tunneling matrix element, S is the area of the contract, ω is the phonon frequency, and $\langle \cdots \rangle$ means average over the phonon spectrum. If the β film is a semiconductor, then T_c can vary as a function of the electron concentration.

B. Size quantization

If the semiconductor (or semimetal) film is size-quantizing, the density of states oscillates as a function of L_β and according to Eq. (1), T_c becomes a non-monotonic function of L_β.

A perfectly realistic situation is one in which only the lowest energy level is filled (e.g., in Bi films up to $L_\beta \approx 5 \times 10^2$ Å). Then the geometry of the Fermi line results in the appearance of peculiar charge density waves, lattice instability, and structural transitions.

* * *

‡A brief version of LBL-12699; Phys. Rev. B 25, 157 (1982).

2. JOSEPHSON TUNNELING AND PROXIMITY EFFECT‡

The structures S_α-M_β-I-S_γ containing the proximity system, for example, Nb-I-Al-Pb have attracted a lot of interest particularly in connection with the investigation of new systems with artificial barriers. The thickness and temperature dependences of the maximum Josephson current I_M have been investigated. It turns out that I_M decreases with increasing L_β and that the sharpness of this decrease depends strongly on the ratio of the energy gaps $\Delta_\alpha/\Delta_\gamma$ and on the strength of the electron-phonon interaction. If M_β is a superconductor ($T_c^\alpha > T_c^\beta$), then I_M depends on the electron-phonon coupling λ_β even if $T > T_c^\beta$. The typical temperature dependence is shown in Fig. 2.1.

* * *

‡A brief version of LBL-15647, IEEE Transactions Electron Devices (1983).

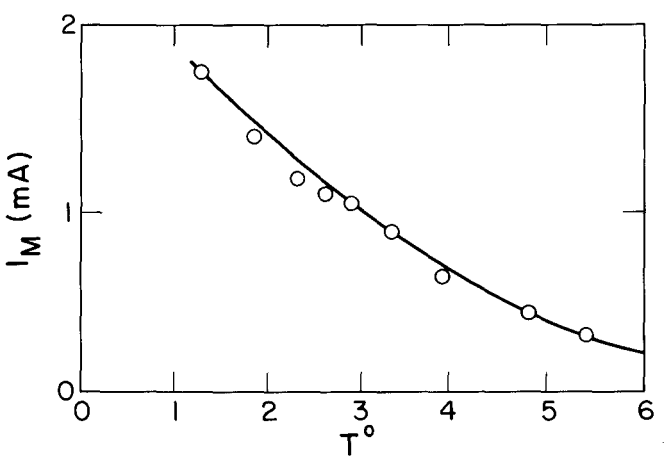

Fig. 2.1. The dependence $I_M(T)$ for the Pb-Cu-PbO-Pb system; solid line is the theoretical curve, open points the experimental data (S. Greenspoon and H. Smith).

*This work was supported by the Office of Naval Research under Contract No. N00014-82-F-0103.

†Scientific Staff member at LBL operating under Contract No. DE-AC03-76SF00098.

3. WORK IN PROGRESS

The critical temperature of the transition to the superconducting state can be increased in several ways. The softening of the phonon spectrum is one of the main mechanisms, and we are going to investigate this mechanism in detail. A particularly interesting case is connected with the contribution of low modes $\omega \lesssim T_c$. It turns out that the dependence of T_c on the position and intensity of the low peak is non-trivial. This problem is interesting also from the point of view of the search for non-phonon mechanisms of superconductivity.

1982 PUBLICATIONS AND REPORTS

Refereed Journals

1. V. Z. Kresin, "Influence of Electron-Phonon Coupling on Superconducting Contacts and the Properties of Superconductor-Semimetal (or Semiconductor) Systems," Phys. Rev. B 25, 157 (1982); LBL-12699.

LBL Reports

1. V. Z. Kresin, "Josephson Current in Proximity Junction," submitted to IEEE Transactions Electron Devices," LBL-15647.

Invited Talks

1. V. Z. Kresin, "Critical Temperature of Proximity System," Bell Laboratories, Murray Hill, New Jersey, July 15, 1982.

3. Electric Power Research Institute (EPRI)

a. Phase Equilibria for Fixed Bed Gasification Products, Byproducts, and Water*

John M. Prausnitz, Investigator

Introduction. Many coal-gasification processes include a quench step where the hot effluent gas from the gasifier is cooled quickly by water. This quench step is necessary to strip heavy tar components and entrained ash from the gas prior to further processing. Current designs for quench steps operate at temperatures near or below 250°C. Either three or four phases may be present in the quench vessel: a vapor phase, a light hydrocarbon or oil phase, an aqueous liquid phase, and a heavy hydrocarbon or tar phase. To design the quench operation and subsequent separation steps, phase equilibria must be available. These equilibria must be correlated by some molecular model so that limited mutual solubility data may be used to predict solubilities at other temperatures, pressures, and compositions.

Molecular-thermodynamic models, capable of representing complex phase equilibria, contain parameters that are related to the energies of interaction and to the sizes of the various molecules in the mixture. These parameters must be obtained by fitting the model to vapor-liquid-liquid or mutual-solubility data. A literature search for such data has been completed; we have found that very few fundamental data have been published. Therefore, we have initiated an experimental program.

1. MEASUREMENT OF PHASE EQUILIBRIA

Frank E. Anderson, Dorothea M. Luedecke, and John M. Prausnitz

To measure liquid-liquid equilibria for binary aqueous-organic mixtures, we have constructed a stirred quartz equilibrium cell from which we can remove samples at pressures to 150 bar and temperatures to 250°C. Samples are analyzed using gas-liquid chromatography. We are currently measuring liquid-liquid equilibria for the benzene-water system, because a large body of experimental results already exists for this system; therefore, our results can be compared to those from other sources.

We charge the apparatus with the mixture of interest, set the temperature, measure the composition of each liquid phase, and measure the total pressure of the mixture. The apparatus serves three functions: equilibration, sampling, and analysis.

The equilibration section of the apparatus is composed of an equilibrium cell enclosed in a heated air bath. The quartz equilibrium cell has a MONEL flange clamped on each end. The glass construction allows viewing the cell contents at experimental conditions.

In the sampling section, samples of each phase are withdrawn from the cell, using commercially available pressure generators. Samples are flashed completely to form vapor phases. Liquid samples (300 μl) are transmitted to vaporization vessels (1 liter) through high-pressure, 6-port chromatographic valves.

Our preliminary experimental results for lutidine/water and for benzene/water are in good agreement with previously published data.

2. THEORETICAL METHODS FOR CORRELATION OF PHASE EQUILIBRIA

Frank E. Anderson, Edmundo G. Azevedo, Dorothea Luedecke, and John M. Prausnitz

There are two thermodynamic procedures for the correlation of phase-equilibrium data. The first uses liquid-phase activity coefficients and vapor-phase fugacity coefficients; we calculate vapor-phase and liquid-phase properties by two different models. For the vapor, we use a modified version of the Redlich-Kwong equation of state suitable for the vapor phase alone. For the liquid phases, we calculate activity coefficients by some liquid-mixture model such as UNIFAC.

In the UNIFAC method, we divide each molecule into functional groups. We relate the activity coefficient of a component to the sum of the functional-group interactions. We account for the size of the functional groups through group-volume parameters, available from crystallographic measurements. The activity coefficient calculated by UNIFAC depends on composition and temperature. The UNIFAC interaction-energy parameters must be obtained from fitting the UNIFAC model to experimental data. This procedure works well over a limited temperature range.

The second procedure calculates fugacity coefficients for each component in each of the three or four phases present. All fugacity coefficients are calculated from the same equation

*This work was supported by the Electric Power Research Institute (EPRI) under Contract No. RP 1901-1 through an agreement with the Director, Office of Energy Research, U.S. Department of Energy under Contract No. DE-AC03-76SF00098.

of state; we use an equation of the van der Waals form. For the repulsive part, we use an expression of the Carnahan and Starling type for hard bodies. For the attractive part, we use a simple form similar to that used in the Redlich-Kwong equation. Our model also accounts for dimerization of hydrogen-bonding species (e.g., water, phenolics, pyridines) through superposition of chemical equilibria on the equation of state.

1982 PUBLICATIONS AND REPORTS

For publications see section on "High-Pressure Phase Equilibria in Hydrocarbon-Water (Brine) Systems."

b. Inhibitive Salts for Reducing High Temperature Oxidation and Spallation*

David P. Whittle, Investigator†

Introduction. It has been known for many years that the addition of small amounts of reactive elements to heat resistant alloys produces a marked improvement in the alloy's behavior under cyclic oxidation conditions. More recently, it has been shown that fine dispersions of a wide range of stable oxides in the alloy have essentially the same effect. Metallic additions affect the growth rate and the possible mechanism of scale development and result in increased adhesion. However, oxide dispersions also affect the initial transient stage of oxidation, making it possible to develop a continuous protective scale (namely, Cr_2O_3 or Al_2O_3) at alloy Cr and Al levels below those required in the absence of a dispersed oxide. Thus, in general, oxide dispersions are better than metallic additions, although they are not as conveniently produced, requiring either a powder-metallurgy route or an impractical internal oxidation treatment.

An alternative approach is to deposit the active element oxide as a surface coating, since it is probable that, even in true dispersion containing alloys, it is only the surface concentration that is important. A surface coating technique also possesses the obvious advantage that it can be applied to large, complex or inaccessible assemblies or components already in service.

The idea of surface coatings of this type is not new; indeed it was included in the original patents of the rare-earth effects,[1,2] although it does not appear to have been investigated since that date. What is new, however, is a more complete understanding of the rare-earth effect, which makes it very appropriate to examine the feasibility of using surface coatings of stable oxides as a means of improving resistance to scale spallation and oxidation.

1. OXIDATION OF Ni-Cr AND Co-Cr ALLOYS COATED WITH REACTIVE ELEMENT SALTS

Stephen Smith, Ajaya K. Misra, and
David P. Whittle

The object of this program is to introduce various reactive specimens to the surface of high temperature alloys and to study the effect on subsequent oxidation.

The techniques used for surface application were either hot dipping the alloy into the nitrate solution of the reactive species or anodically depositing a coating from the same solution. Decomposition of the resultant coating to oxide, at 400°C, was followed by oxidation at 1000°C in static air.

Initial results indicate that there is a beneficial effect afforded by selected reactive element oxides such as La and Y, when applied to alloys that are established Cr_2O_3 formers. Ni-25% Cr coated with the La salt was oxidized under cycling conditions--20 hr cycles--at 1000°C. After 300 hr total exposure, a very thin Cr_2O_3 scale was observed. In contrast, an uncoated alloy of this composition, oxidized for 100 hr at 1000°C, developed a much thicker Cr_2O_3 scale.

* * *

1. L. B. Pfeil, U. K. Patent No. 459848 (1937).
2. L. B. Pfeil, U. K. Patent No. 574088 (1945).

*This work was supported by the Electric Power Research Institute (EPRI) under Contract Number RP 2261-1, through an agreement with the Director, Office of Energy Research, U.S. Department of Energy under Contract No. DE-AC03-76SF00098.

†Dr. Whittle died in July 1982. This report has been prepared by Dr. Stephen Smith. Since Dr. Whittle's death, Dr. J. Stringer of the Electric Power Research Institute has been acting as technical advisor, pending the appointment of a full-time successor.

c. Investigate New Fuel Cell Electrolyte and Electrode Concepts*

Philip N. Ross, Investigator

Introduction. Phosphoric acid is the electrolyte currently in use for commercial hydrogen-air cells. It is a relatively weak acid (pK = 2.1), and there is specific adsorption of phosphoric acid anions on Pt surfaces that probably interfere negatively with the oxygen reduction reaction at Pt electrodes. Trifluoromethane sulfonic acid (TFMSA) is a very strong acid, and specific adsorption of the anion on Pt in 0.1 M TFMSA appears to be minimal as determined by recent measurements. Therefore, it is expected that oxygen reduction on Pt electrocatalysts in TFMSA would proceed at higher rates than in phosphoric acid. Technologically, the problem with TFMSA as a fuel cell electrolyte is that in the concentrated form needed in practice, the acid wets the polytetrafluoroethylene (PTFE) hydrophobic bonding agent used in gas diffusion electrodes causing a collapse of the three-phase interfacial structure. It is hypothesized that this wetting is because of the CF_3- functional group and that multibasic homologs of this acid, e.g., tetrafluorethane -1,2- disulfonic acid (TFEDSA), would not wet PTFE. Another technological problem with TFMSA is its relatively high volatility at practical operating temperatures (>100°C). It is felt that higher homologs of TFMSA would have a lower vapor pressure, so that multibasic higher homologs of TFMSA may have all the advantageous properties of this acid but with low volatility and with the desired wetting properties. The object of this program is to study oxygen reduction on the family of perfluoroalkylsulfonic acids to determine whether or not the desirable characteristics of TFMSA are intrinsic to this class of organic compounds.

1. THE EFFECT OF $H_2PO_4^-$ ANION OF THE KINETICS OF OXYGEN REDUCTION ON Pt†

P. C. Andricacos and P. N. Ross, Jr.

In view of the existing evidence in favor of non-adsorbing nature of TFMSA on Pt,[1] we have chosen this acid as the baseline from which the effect of adsorbing anions on the O_2 reduction kinetics can be observed. For this purpose, mM concentrations of H_3PO_4 were added to a 0.1 M TFMSA solution (pH = 1), and the O_2 reduction kinetics were measured with the rotating disk electrode (RDE) method. Since H_3PO_4 is a weak acid, ($K_1 = 7.6 \times 10^{-3}$) mM addition to a strong acid solution does not affect the pH significantly. The O_2 reduction kinetics were also determined in a 0.7 M H_3PO_4 solution that has the same pH (=1) as 0.1 M TFMSA. RDE data in the 100-900 rpm range were analyzed with the i^{-1} vs $\omega^{-1/2}$ correlation to verify the first order dependence of the reaction kinetics on the O_2 surface concentration. Since the H_3PO_4 additions did not affect the well-defined diffusion limiting currents (i_L) in the 0.1 M TFMSA solution, the measured value of i_L was used to determine the diffusion-free kinetic current, i_K. A summary of mass transport and kinetic data appears in Tables 1.1 and 1.2, respectively.

Experimental findings and their analysis have indicated that (a) O_2 reduction is first order with respect to the surface concentration of O_2 in all solutions; (b) the diffusion limiting current, i_L, is lower by ~15% in the 0.7 M H_3PO_4 solution than in the 0.1 M H_3PO_4 solution than in the 0.1 TFMSA solution; (c) i_L in the 0.1 M TFMSA solution is not affected by H_3PO_4 additions (up to 11.4 mM); (d) O_2 reduction kinetics in 0.7 M H_3PO_4 are slower than in 0.1 M TFMSA by a factor of approximately 15; (e) additions of H_3HP_4 in the mM range to a 0.1 M TFMSA solution significantly lower the reaction rate; and (f) Tafel slopes are not significantly affected by additions of H_3PO_4 to the 0.1 M TFMSA solution.

A thorough quantitative analysis of the poisoning effect of $H_2PO_4^-$ is prevented by the lack of anion coverage data for the $H_2PO_4^-$ concentrations used in the present study. However,

Table 1.1. Values of the B Coefficient for O_2 Reduction in TFMSA, H_3PO_4, and Their Mixtures.

	B/mA·cm^{-2} sec$^{1/2}$	
Electrolyte	I[a]	II[b]
0.1 M TFMSA	0.459	0.499
0.1 M TFMSA + 0.38 mM H_3PO_4	0.459	0.505
0.1 M TFMSA + 11.4 mM H_3PO_4	0.459	0.496
0.7 M H_3PO_4	0.382	0.423

[a]Slope of i_L vs $\omega^{1/2}$.

[b]Slope of i^{-1} vs $\omega^{-1/2}$ where i_L is the diffusion limiting current density and i is the measured current under mixed diffusion-kinetic control.

$B = 0.62nFc^bD^{2/3}\nu^{-1/6}$, where n = 4 for the 4-electron reduction of O_2 to H_2O, c^b is the bulk concentration of O_2, D is its diffusion coefficient, and ν is the electrolyte kinematic viscosity.

*This work was supported by the Electric Power Research Institute (EPRI) under Contract No. RP-1676-2 through an agreement with the Assistant Secretary for Conservation and Renewable Energy, U.S. Department of Energy under Contract No. DE-AC03-76SF00098.

Table 1.2. Kinetic Parameters of O_2 Reduction on Pt in TFMSA, H_3PO_4, and Their Mixtures.

Electrolyte	$[H_2PO_4^-]$ mol·dm^{-3}	i_K/mA·cm^{-2} E/V			Tafel slope/V·dec^{-1} E/V	
		0.700	0.800	0.900	>0.800	0.700–0.800
0.1 M TFMSA	–	52	9.4	1	0.85	0.117–0.135
0.1 M TFMSA + 0.38 mM H_3PO_4	2.9×10^{-5}	22	4.2	0.4	N.D.	0.114–0.140
0.1 M TFMSA + 11.4 mM H_3PO_4	8.7×10^{-4}	10	1.8	0.2	N.D.	0.127–0.137
0.7 M H_3PO_4	7.3×10^{-2}	5	0.7	0.06	N.D.	0.113–0.135

NOTE: N.D. is not a well-defined Tafel slope in this region.

extrapolations from the literature values[2] for the 2.9×10^{-5} M $H_2PO_4^-$ (Table 1.2) anion concentration yield a surface coverage of 25%, assuming that three Pt sites are blocked by each anion. The observed factor of 2.5 in the decrease in O_2 reduction kinetics for this $H_2PO_4^-$ concentration cannot then be explained on the grounds of site blocking only.

It was concluded that a combination of site blocking of Pt by $H_2PO_4^-$ and activation energy changes in the adsorption of O_2H in the presence of $H_2PO_4^-$ account qualitatively for the significant decrease in O_2 reduction kinetics observed when very small amounts of H_3PO_4 are added to a 0.1 M TFMSA solution (pH = 1).

* * *

†Brief version of LBL-15266.

1. O. Petrii, S. Vasina, and L. Lukyanycheva, Soviet Electrochem. 17, 1144 (1982).
2. G. Horanyi, E. Rizmayer, and G. Inzelt, J. Electroanal. Chem. 93, 183 (1978).

1982 PUBLICATIONS AND REPORTS

LBL Reports

1. P. N. Ross, Jr. and P. Andricacos, "The Effect of $H_2PO_4^-$ anion on the Kinetic of Oxygen Reduction on Pt," to be published in J. Electroanal. Chem., LBL-15266.

2. P. N. Ross, Jr., "Evaluation of Tetrafluoroethane -1,2- Disulfonic Acid as a Fuel Cell Electrolyte," to be published in J. Electrochem. Soc., LBL-14762.

d. Improved Beta-Alumina Electrolytes for Advanced Storage Batteries*

Lutgard C. De Jonghe, Investigator

Introduction. When sodium beta or beta" alumina solid electrolytes are subjected to ionic charge transfer in sodium/sodium or in sodium/sulfur cells, degradation of the electrolytes may occur. The electrochemical degradation may take different forms, as was recently discussed in Ref. 1. Mode I degradation involves the cathodic plating of sodium into a pre-existing surface flaw on the sodium side of the electrolyte, causing crack extension above some critical value of the electrode current density. Mode II involves a possible internal deposition of metallic sodium during charge transfer through an inhomogeneous solid electrolyte.[2]

A sensitive method for detecting the initiation of crack propagation, acoustic emission monitoring, was used in the present investigation.

* * *

1. L. C. De Jonghe, L. Feldman, and A. Buechele, J. Mat. Sci. 16, 780 (1981).
2. L. C. De Jonghe, J. Electrochem. Soc. 129, 752 (1982).

1. DEGRADATION OF SODIUM BETA"-ALUMINA: EFFECT OF MICROSTRUCTURE†

A. C. Buechele, Lutgard C. De Jonghe, and David Hitchcock

Acoustic emission detection was used for the study of failure initiation of Na beta"-alumina electrolytes in sodium/sodium cells. The two different microstructures examined, A and B, are shown in Fig. 1.1.

The observed critical current density for initial crack propagation was related to the distribution of pre-existing active flaws in the surface of the electrolyte in contact with the negative sodium electrode and to the current distribution on the electrode. The statistical nature of the active flaw distribution led to a corresponding Weibull distribution of the current densities necessary to initiate Mode I degradation. The average critical current densities for the two specimen types were 145 mA/cm^2 for microstructure B and 640 mA/cm^2 for microstructure A. The electrolyte with smaller grain size has a

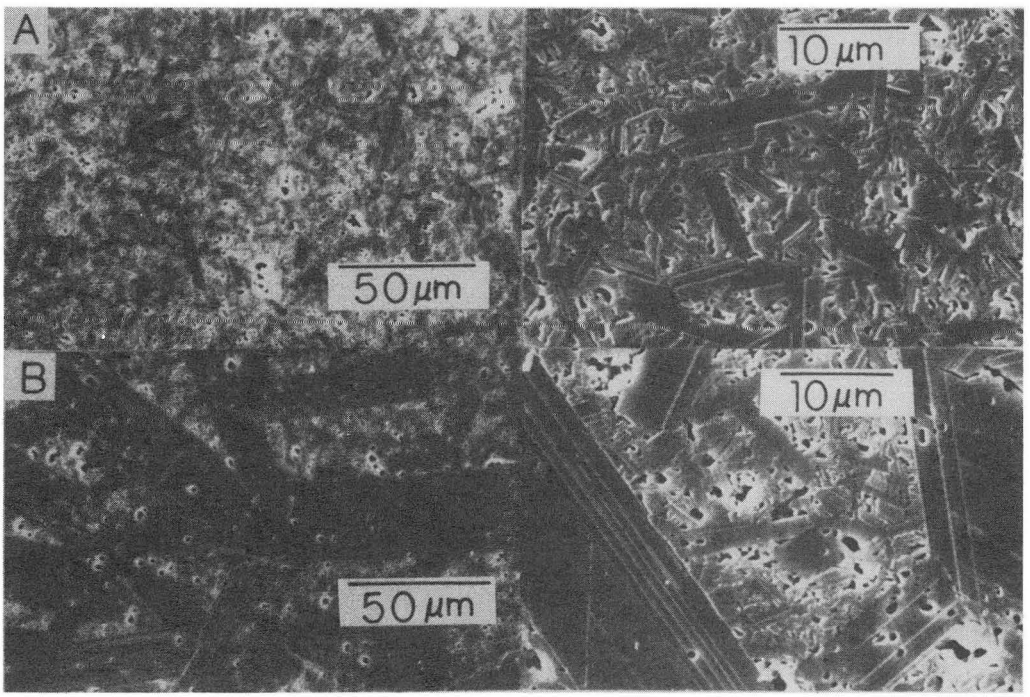

Fig. 1.1. Comparison of the electrolyte microstructures. Scanning electron micrograph of electrolyte etched in H_3PO_4. (XBB 815-4088)

*This work was supported by the Electric Power Research Institute (EPRI) under Contract No. RP 252-3, through an agreement with the Assistant Secretary for Conservation and Renewable Energy, U.S. Department of Energy under Contract No. DE-AC03-76SF00098.

significantly higher threshold for failure initiation. Corrections for the non-uniformity of the current distribution were calculated and led to average failure current densities at 240 and 700 mA/cm^2. The ratio of the average critical current density is comparable to that of the average grain size or the average length of the fraction with large grains.

* * *

†Brief version of LBL-13188 Rev.

1982 PUBLICATIONS AND REPORTS

Refereed Journals

1. L. C. De Jonghe, "Transport Number Gradients and Solid Electrolyte Degradation," J. Electrochem. Soc. 129, 752 (1982).

2. L. Feldman and L. C. De Jonghe, "Initiation of Mode I Degradation in Sodium Beta Alumina Electrolytes," J. Mat. Sci. 14, 885 (1982).

3. L. C. De Jonghe and A. Buechele, "Chemical Coloration of Sodium Beta Aluminas," J. Mat. Sci. 17, 885 (1982).

LBL Reports

1. L. C. De Jonghe, "Degradation Mechanisms of Sodium Beta Aluminas," LBL-14365.

2. A. Buechele, L. C. De Jonghe, and D. Hitchcock, "Degradation of Sodium Beta" Alumina: Effect of Microstructure," LBL-13188 Rev.

3. L. C. De Jonghe, A Buechele, and K. H. Yoon, "Grain Boundaries and Solid Electrolyte Degradation," LBL-14150.

Invited Talks

1. L. C. De Jonghe, "Degradation Phenomena in Sodium Beta" Solid Electrolytes," Compagnie Générale d' Electricité, Maroussis, France, June 1982.

2. L. C. De Jonghe, "Performance of Sodium Beta" Alumina in Na/Na and Na/S Cells," Dow Chemical, Walnut Creek, California, September 1982.

3. L. C. De Jonghe, "Solid Electrolytes for the Na/S Storage Battery, Electric Power Research Institute, Palo Alto, California, June 1982.


X
Appendices

Appendix A

Materials and Molecular Research Division Personnel

Scientific Staff

1982 Investigators	Postdoctoral and Other Scientists	Graduate Students
Neil Bartlett	R. Brusasco B. Desbat M. Dove C. Platte T. Richardson A. Tressaud W. Totsch J. Verniolle A. Waterfeld	T. Mallouk B. McQuillan J. Nitschke F. Okino G. Rosenthal
Alexis Bell		J. Baker R. Dictor T. Frederick R. Hicks D. Jordan M. Reichmann J. Rieck R. Underwood P. Winslow
Robert Bergman	W. Hersh M. Matturro	P. Becker T. Bischoff J. Bonfiglio H. Bryndza J. Buchanan P. Comita T. Gilbert N. Jacobson A. Janowicz L. Newman C. Nitsche R. Periana-Pillai M. Seidler P. Seidler K. Theopold M. Wax W. Weiner G. Yang
Robert Bragg		D. Baker L. Henry J. Hoyt J. Johnson B. Mehrotra A. Pearson
Leo Brewer	D. Davis C.B. Meyer G. Rosenblatt K.Ward	J. Bularzik E. Faizi S. Hahn J. Gibson

1982 Investigators	Postdoctoral and Other Scientists	Graduate Students
Brewer (cont'd)		R. McCurdy R. Stimach
John Clarke	M. Devoret	C. Hilbert R. Koch H. Mamin J. Martinis P. Maxton R. Miracky J. Pelz D. Seligson F. Wellstood
Marvin Cohen	S. Froyen S. Louie D. Vanderbilt	C.T. Chan K.J. Chang M-Y. Chou M. Hybertsen P. Lam Z. Levine J. Northrup
Robert Connick	C. Chieng K. Krushwitz W. Tini K. Ward	D. Horner M. Wagner
Lutgard De Jonghe	M. Armand M. Chang H. Schmid K-H. Yoon	C. Balfe A. Buechele C. Cameron M. Chang J-C. Chen M. Herrara D. Hitchcock B-H.Hwang S. Kikugawa Y. Kim C. Mailhe R. McClelland G. Raj M. Weiser S. Wu
Didier de Fontaine	J-P. Simon W. Teitler	E. Colas H-M. Jang K. Krishnan J. Kulic R. Pro H-C. Tsai
Norman Edelstein N. Bartlett S. Brown J. Conway K. Raymond G. Seaborg	K. Abu-Dari R. Andersen S. Bachrach J. Bucher S. Davis P. Edwards	J. Arenivar S. Barclay P. Becker J. Boncella B. Borgias J. Brennan

1982 Investigators	Postdoctoral and Other Scientists	Graduate Students
Edelstein (cont'd)		
A. Streitwieser	T. Hayhurst	T. Chung
D. Templeton	D. Kagan	M. Derzon
A. Zalkin	R. Klutz	S. Fletcher
	J.C. Krupa	G. Freeman
	W. Muller	B. Gilbert
	C. Orvig	G. Girolami
	K. Rajnak	M. Halpern
	G. Shalimoff	S. Kinsley
	L. Templeton	L. Loomis
	H-K. Wang	M. Lyttle
	G. Wong	R. Moore
	D. Zhang	D. O'Donovan
	D. Zhu	V. Pecoraro
		R. Planalp
		R. Scarrow
		R. Shinomoto
		K. Smith
		J. Toman
		T. Tufano
		S. Un
		G. Williams
Anthony Evans	B. Dalgleish	W. Blumenthal
	W. Kriven	L. Cheng
	J. Lamon	S. Chiang
	D. Marshall	H.S. Choy
	M. Omori	G. Crumley
	T. Uchiyama	T. Dabbs
		M. Drory
		K. Faber
		Y. Fu
		C-H. Hsueh
		S. Johnson
		J. Low
		M-C. Lu
		J. Maasberg
		J. Marion
		C. Ostertag
		C. Rossington
		W. Shubin
		M. Thouless
		H-C. Tsai
James Evans	D. Coates	M. Abbasi
	S. Lympany	M. Hall
	R. Moreau	T. Huh
	Y. Nakano	H-C. Lee
	D. Rieck	C. Palmer
		M. Rau
		K. Spring
Leo Falicov		R. Osario
		M. Robbins
		J. Tersoff
		R.H. Victora
Iain Finnie	A. Misra	S. Chavez
		A. McGee
		S. Soemantri

1982 Investigators	Postdoctoral and Other Scientists	Graduate Students
Andreas Glaeser		J-C. Chen
Ron Gronsky	E. Boden A. Goldberg J. Penisson P. Rez J. Steeds L. Tanner	L. Andersen C. Clark P. DeRoo S. Cheruvu J. Howe E. Kamenetzky R. Kilaas J. Mazur M. McCormack J. Rose G. Tamayo E. Thomann
Eugen Haller	S. Pearton	
Charles Harris		M. Alivasatos M. Berg J. Brown S. George G. Goncher A. Harris C. Parsons P. Whitmore
Heinz Heinemann Bell Bergman J.Evans Levy Somorjai Vollhardt		
Dennis Hess		C. Blair A. Wakita L. Williams
Carson Jeffries		P. Bryant J. Culbertson B. Furman G. Held E. Pakulis J. Perez J. Testa
Harold Johnston	R. Carlson P. Estacio	J. Hebel S. Solomon D. Swanson
William Jolly	K. Bomben C. Eyermann	M. Ajmani D. Beach

1982 Investigators	Postdoctoral and Other Scientists	Graduate Students
Yuan Lee	R. Buss O. Dutuit P. Felder J. Hepburn J. O'Brien H. Schmidt J. Van Den Biesen	R. Baseman R. Brudzynski S. Bustamente L. Butler M. Covinsky J. Frey C. Hayden S. Huang D. Krajnovich T. Minton D. Neumark M. Okumura R. Page J. Reutt G. Robinson P. Schulz M. Valentine M. Vernon P. Weiss A. Wodtke L. Yeh
William Lester	L. Johnson K. Jolls P. Reynolds	R. Barnett C. Dateo R. Grimes L. Johnson
Alan Levy	W. Coons I. Finnie T. Foley R. Glardon M. Holt J. Humphrey F. Pourahmadi P. Tom P. Turi W. Worrell	M. Arnal E. Ettehadieh H. Frank K. Johnson I. Kliafas F. Pourahmadi H-L. Tsai
S. Louie	S. Froyen	C-T. Chan J-Q. Wang J. Willick
Bruce Mahan		T. Turner
Richard Marrus	J-P. Briand A. Chetioui E. Commins H. Gould J. Leavitt M. Mittleman M. Prior H. Shugart	P. Drell C. Munger C. Tanner
William Miller	C. Cerjan L. Hubbard	D. Ali T. Carrington

1982 Investigators	Postdoctoral and Other Scientists	Graduate Students
Miller (cont'd)		
	S. Shi	P. Dardi
		S. Gray
		S. Schwartz
		B. Waite
C. Bradley Moore	L. Aljibury	A. Abbate
	C. Chi-Ke	D. Bamford
	J. Jasinski	J. Frisoli
	A. Kung	F. Hovis
	D. Nesbitt	A. Langford
	P. Ogilby	W. Natzle
		H. Petek
		J. Wong
		L. Young
John W. Morris, Jr.	M. Hong	G-M. Chang
	G-X. Hu	D. Dietderich
	R. Kopa	D. Fior
	H.J. Lee	D. Frear
	L-S. Li	B. Fultz
	R. Ogawa	M. Hong
	D. Powell	D.Johnson-Walls
	J. Sanchez	H-J. Kim
	M-C. Shin	Y-H. Kim
	Y. Tomota	E. Kostlan
		H. Lee
		H-L. Lin
		T. Mohri
		K. Sakai
		J. Sanchez
		S. Shaffer
		Y-C. Shih
		H-K. Shin
		M. Strum
		L. Summers
		I-W. Wu
		K. Xue
Earl Muetterties	R. Feltham	J. Bleeke
	D. Heinekey	R. Burch
	J. Kouba	H. Choi
	J. Stein	W. Cwirla
	M. Tachikawa	T.M. Gentle
		V. Grassian
		D. Klarup
		Y. Otonari
		G. Schmidt
		K. Shanahan
		S. Slater
		M. Tsai
		R. Wexler
Rolf Muller	W. Giba	D. Barkey
	G. Nazri	C. Coughanowr
		J. Farmer
		D. Fischl
		R. Gyory

1982 Investigators	Postdoctoral and Other Scientists	Graduate Students
John Newman	E. Pawlikowski	M. Berg D. Bernardi V. Edwards A. Hauser N. Matlosz M. Orazem P. Pierini T. Risch P. Russell G. Trost
Donald Olander	M. Balooch R. Kohli A. Machiels N. Ohashi S. Zhou	M. Derzon D. Dooley M. Farnaam P. Goubeault K. Kim G. Mitchem D. Sherman F. Tehranian S. Yagnik
Joseph Pask	P. Spencer A. Tomsia F. Zhang	K. Wada
Norman Phillips	J. Flouquet E. Hornung J. Lasjaunias K. Matho	W. Fogle C. Lisse M. Mayberry J. Van Curen
Alexander Pines	R. Goldberg H. Fujiwara U. Nitsan H. Zimmermann	A. Bielecki J. Baum H. Cho G. Drobny R. Eckman J. Garbow J. Millar B. Oh E. Schneider A. Thayer R. Tycko Y-S. Yen D. Zax
Kenneth Pitzer	K. Balasubramanian S-W. Wang	
John Prausnitz		F. Anderson M. Gibson E. Larsen S. Sepahban W. Whiting J.O. Wong

1982 Investigators	Postdoctoral and Other Scientists	Graduate Students
Paul Richards	H. Levinson A. Smith	J. Bonomo W. Challener S. Chiang M. Engelhardt M. Hueschen S. McBride W. McGrath G. Tobin
Robert Ritchie	N.H. Croft D. Sarma S. Suresh	V. Dutta T. George S. Ivy K. Johnston T. Lin R. Pendse J-L. Tzou E. Zaiken
Philip Ross	P. Andricacos U. Bardi G. Derry F. Wagner J. Willsau	A. Cabrera
Richard Saykally		
Henry Schaefer III	J. Bicerano J. Breulet J. Goddard R. Pitzer A. Schier H. Sokol M. Vincent Y. Yamaguchi	M. Colvin G. Fitzgerald D. Fox J. Gaw R. Grev M. Hoffman T.J. Lee G. Raine P. Saxe
Alan Searcy	D. Beruto D. Chung S. Louie D. Meschi Z. Munir E. Thomsen	J. Farnsworth A. Hegedus M.G. Kim T. Reis
Y. Ron Shen	C. Chen T. Rasing S. Shen L. Shi P. Ye H. Zhu	G. Boyd M-m. Cheung S. Durbin T. Heinz H. Hsiung R. Pecyner H. Tom X-D. Zhu
David Shirley	U. Becker P. Dabbousi	A. Baca C. Bahr

1982 Investigators	Postdoctoral and Other Scientists	Graduate Students
Shirley (cont'd)	W. Heppler	J. Barton
	Z. Hussain	R. Davis
	G. Kaindl	T. Ferrett
	G. Lui	W. Glad
	D. Trevor	P. Heimann
		L. Klebanoff
		P. Kobrin
		D. Lindle
		C. Parks
		J. Pollard
		S. Robey
		D. Rosenblatt
		A. Schach von Wittenau
		M. Schulz
		J. Tobin
		C. Truesdale
Gabor Somorjai	M. Asscher	B. Bent
	R. Casanova	E. Benjamin
	P. Davies	J. Crowell
	F. Delannay	R. Fox
	G. Ertl	C. Galik
	M. Farias	E. Garfunkel
	S. Ferrer	A. Gellman
	M. Kudo	W. Guthrie
	M. Langell	M. Hendewerk
	C. Leygraf	B. Koel
	R-F. Lin	R. Koestner
	W. McLean	M. Levin
	M. Salmeron	G. Lewis
	N. Spencer	T. Lin
	J. Turner	M. Logan
	W. Tysoe	C. Mate
		B. Naasz
		D. Ogletree
		M. Quinlan
		J. Twiford
		R. Yeates
		G. Yee
		F. Zaera
Gareth Thomas	J. Davey	J. Ahn
	M. Hall	R-S. Caron
	T. Harvey	L. Chan
	R. Hoel	T. Dinger
	N. Kim	J-S. Gau
	J. Koo	A. Jhingan
	C. Kung	K. Krishnan
	J. Leteurtre	C. Kwok
	X. Meng	I-N. Lin
	R. Mishra	A. Nakagawa
	G. Monks	S. Ong
	J. Penisson	L. Rabenberg
	J. Rayment	J. Ruchlewicz
	W. Salesky	M. Sung
	M. Sarikaya	H. Tokushige
	J. Steeds	J. Wasynczuk
	G. VanTendeloo	X-F. Wu
	M. von Heimendahl	Y-S. Yoon
	J. Yan	
	A-J. Yang	

1982 Investigators	Postdoctoral and Other Scientists	Graduate Students
Charles Tobias	P. Cettou D-S. Doh D. Rajhenbah	P. Andersen R. Anderson D. Dees J. Dukovic J. Faltemier K. Hanson W. Hui R. Hyman P. Johnson T. Tsuda M. Verbrugge G. Whitney
K. Peter Vollhardt	Y-H. Lai D. Van Horn	R. Colborn J. Drage J. King J. Tane M. Tilset E. Walborsky T. Weidman
Jack Washburn	R. Hagstrom G. Hirsch C. Lampert D. Sadana Y. Wang	R.S. Caron C. Jou P. Ling W-L. Lo T. Mowles T. Sands D. Sipes T-H. Wei N-R. Wu Y-J. Wu T. Zee
Kenneth Westmacott	U. Dahmen J. Davey P. Ferguson M. Hall J. Leteurtre G. Monks J. Pennison J. Steeds R. Schonbucher G. Szaloky M. Von Heimendahl	J-M. Lang A. Pelton S. Puranikmath L. Wu
David Whittle	D. Boone I. Cornet H. Hindam A. Misra S. Smith R. Streiff M. Yee	H. Akuezue S. Berggren S-H. Choi P. Hou J-Y. Lee R. Pendse F. Yang
John Winn	M. Maier	B. Hale W. Hollingsworth D. Horak

1982 Investigators	Postdoctoral and Other Scientists	Graduate Students
Winn (cont'd)		H. Luftman S. Sherrow
Peter Yu		C. Collins J. Weiner

Support Staff

Division Administrative Staff

C. Peterson - Assistant Division Head, Administration
K. McArthur - Assistant Division Administrator

Administration	Personnel	Purchasing
M. Janzen	S. Quarello	S. Stewart
L. Irvin	P. Paladini	C. Sterling
M. Bowman	I. Gosiengfiao	
S. Muir		
S. Shirey		

Technical Editing	Special Projects
J. Knight	E. Skrydlinski

Administrative/Secretarial Staff

N. Alpaugh	S. Gangwer	B. Nagaue
R. Arcol	M. Gill	V. Narasimhan
M. Atkinson	C. Gliebe	E. Nilson
K. Becky	C. Gloria	M. Noyd
H. Benson	C. Hacker	A. Ozturkmen
M. Besser	J. Hoagfelt	M. Penton
C. Bilorusky	D. Israel	L. Pham
G. Brazil	D. Johanson	M. Rector
K. Brusse	H. Johnson	J. Shull
D. Carmichael	P. Johnson	J. Smith
B. Carter	R. Jones	S. Thur
N. Charpentier	S. Kaul	A. Weightman
K. Denison	T. Learned	S. Wilde
J. Denney	S. Macahilig	L. Yanac
L. Franson	D. Merrill	C. Yoder
S. Ewing	M. Moore	S. Young
M. Gabbay	B. Moriguchi	B. Zambrano

Technical Staff

W. Toutolmin - Technical Coordinator

D. Ackland	K. Franck	J. Holthuis	R. McCurdy	S. Smit
G. Baum	L. Galovich	J. Jacobsen	W. Murrell	H. Sokol
E. Benjamine	K. Gaugler	L. Johnson	B. Neilson	V. Stumpf
G. Blowers	W. Giba	P. Johnson	J. Patterson	C. Thom
E. Boden	C. Gibson	D. Jurica	A. Pentecost	P. Tom
H. Bowman, Jr.	J. Glazer	B. Kan	L. Purvis	G. Tong
H. Brendel	R. Gray	K. Koshlap	H. Riebe	P. Turi
R. Brusasco	A. Gronsky	E. Kostlan	P. Ruegg	K. Wada
C. Carter	W. Goward	D. Krieger	E. Scherr	R. Wagner
B. Chandler	H. Harrell	M. Kujala	E. Scholz	M. Wall
M. Cima	W. Heppler	D. MacDonald	S. Shaffer	H. Weeks
A. Davis	C. Hickeyr	V. Mantyd	J. Severns	W. Wong
D. Dietderich	G. Hirsch	J. Martinis	E. Slamovich	N. Yates
E. Fong				P. Yau

Appendix B

Materials and Molecular Research Division Committees

DIVISIONAL COUNCIL

M. Cohen
N. Edelstein
H. Heinemann
H. Johnston
J. Morris, Jr.

BUILDING AND SPACE COMMITTEE
(Includes Buildings 50D, 62, 70A, 72, and the Chemical and Materials Sciences Laboratory)

R. Gronsky
D. Meschi
R. Muller*
A. Zalkin

DIVISIONAL RESEARCH STAFF COMMITTEE

N. Edelstein
L. Falicov
R. Muller*
K. Westmacott

ELECTRON MICROSCOPE USERS COMMITTEE

R. Gronsky
J. Morris, Jr.
P. Ross*
K. Westmacott

EQUIPMENT REVIEW COMMITTEE

J. Clarke
A. Evans
C. B. Moore
R. Muller*

SAFETY AND LABORATORY STANDARDS COMMITTEE

D. Ackland
G. Baum
T. Britt
D. Davis
E. Fong
K. Franck
B. Fultz
T. Gentle
W. Giba
W. Hemphill
T. Hickcock
H. Hindam
J. Holthuis
L. Irvin
L. Johnson
D. Krieger
K. McArthur
D. Meschi*
R. Muller
S. Ozturkmen
C. Peterson
H. Rieber
J. Severns
E. Slamovich
S. Smith
C. Sterling
S. Stewart
L. Summers
W. Toutolmin
W. Wong

TECHNICAL STAFF AND SHARED FACILITIES COMMITTEE

L. De Jonghe*
R. Gronsky
J. Morris, Jr.
P. Ross
G. Somorjai
D. Whittle

MMRD Building 62 Building Manager: D. Meschi
(Alternate: C. Peterson)

MMRD Building 72 Building Manager: K. Westmacott
(Alternate: D. Ackland)

* Chairman

Appendix C

List of Seminars

Surface Science and Catalysis Science

Date	Speaker and Affiliation	Seminar Title
1-7-82	Prof. L. Schmidt University of Minnesota	Reactions of NO on Pt at Low and High Pressures
1-14-82	Prof. G. Ertl University of Munich	Scattering and Deexcitation of Metastable Noble Gas Atoms at Surfaces
*1-18-82	Dr. W. F. Egelhoff National Bureau of Standards	Surface Core Level Shifts in Binary Alloys: ΔH of Surface Segregation and Chemisorption
1-21-82	Prof. E. L. Park University of Maryland	Critical Phenomena in Chemisorbed Layers
*1-22-82	Prof. H. Siegmann ETH-Zurich and IBM	Surface Magnetism and Chemisorption
*1-26-82	Dr. P. Eisenberger Exxon Research	X-Ray Scattering Studies of Surfaces: Structure and Melting Phenomena
1-28-82	Prof. H. Gerischer Fritz-Haber-Institut Berlin	Photoelectrochemical Studies of Semiconductors with Layer Structures
*2-1-82	Dr. J. Rowe Bell Telephone Laboratories	Recent Structural Studies of Surfaces Using EXAFS
2-4-82	Dr. R. L. Hartgerink Exxon Research	Catalytic Coal Gasification: Mechanisms and Process Development
2-11-82	Dr. J. Chadi Xerox PARC	Why Do Semiconductor Surfaces Reconstruct?
*2-12-82	Prof. W. Brenig Technical University Munich	Kinetic Processes at Solid Surfaces: Theory and Some Typical Experimental Results
2-18-82	Prof. W. E. Spicer Stanford University	Study of Alloy Surfaces (CuNi, PdAu, PtCu) Adsorbate Site and Geometric Effects and Examples of Relations Between UHV and Atmospheric Pressure Reactions
2-25-82	Dr. G. Kokatailo Mobil Research	Zeolite Structure and Catalysis
3-4-82	Dr. T. E. Felter Sandia, Livermore	Recent Studies of the Adsorption and Oxidation of Small Molecules Over Single Crystal Surfaces of Transition Metals Using Photoelectron Spectroscopy
3-4-82	Dr. V. Udaya S. Rao DOE-Pittsburgh Energy Technology Center	Indirect Liquefaction Using Metal-Zeolite Catalysts
3-11-82	Dr. J. Shinn Chevron Research	A Model of the Chemical Structure and Liquefaction Behavior of Bituminous Coal
3-18-82	Dr. F. Herman IBM, San Jose	Recent Developments in the Physics and Chemistry of Semiconductor Interfaces
3-23-82	Drs. Y. Huang and J. C. Tang University of Wisconsin	Determination of Surface Structure by Photoelectron Diffraction

*Special Seminar

Surface Science and Catalysis Science (continued)

Date	Speaker and Affiliation	Seminar Title
3-25-82	Dr. J. Horsley Exxon Research	X-Ray Absorption Edge Resonances as Probes of Catalyst Electronic Structure
3-26-82	Dr. G. B. Fisher General Motors	The Role of Mechanistic and Kinetic Factors in the Water Formation Reaction on Platinum
4-8-82	Dr. S. Weller SUNY, Buffalo	Efficient Catalysts for Coal Liquefaction
4-14-82	Dr. H. Shulz Tech. University-Karlsruhe	Initial Selectivity of Fischer-Tropsch CO Hydrogenation
4-15-82	Dr. M. Balooch UCB/LBL	Molecular Beam Study of Metal Halogen Reactions
4-22-82	Dr. R. J. Behm IBM, San Jose	Hydrogen on Fe(110): Ordered Phases and Temperature/Coverage Dependence
4-29-82	Prof. M. Simonetta University of Milan	Force Field Calculations for Crystallography
5-6-82	Dr. R. M. Laine Stanford Research International	Homogeneous Catalytic Formation of C-N Bonds: Fischer-Tropsch-Like Reactions of Amines With Synthesis Gas
5-13-82	Dr. E. Wymore Dow Chemical	Balance in Industrial Research
5-20-82	Prof. E. W. Plummer University of Pennsylvania	Mysteries of Hydrogen Adsorption (NEW)
5-26-82	Dr. Kenzi Tamaru University of Tokyo	Selectivity and Mechanisms of COH_2 Reaction on Transition Metals
5-27-82	Prof. C. J. Radke University of California Berkeley	Adsorbed Configurations of Colloidal Molecules at Charged Aqueous-Solid Interfaces
6-3-82	Dr. R. L. Schwoebel Sandia Laboratories	Hydrogen Trapping in Metals
6-10-82	Prof. S. Y. Tong University of Wisconsin	The Role of Surface Image Potential in Elastic and Inelastic Electron Scattering from Surface
6-16-82	Prof. G. Blyholder University of Arkansas	Matrix Spectroscopy Applied to Surface Chemistry
6-29-82	Professor J. Oudar Ecole Nationale Superieure de Chimie-Paris	Sulfur Adsorption and Poisoning of Metals
7-15-82	Dr. P. A. Thiel Sandia-Livermore	The Mechanism of an Adsorbate-Induced Surface Reconstruction: CO on Pt(100)
7-19-82	Dr. K. Tanaka Rikagaku Kenkyusho Japan	Photocatalytic Oxidation and Reduction of Organic Compounds over Metal/TiO_2 Powders
8-6-82	Prof. J. B. Pendry Imperial College London	X-Ray Absorption Near-Edge Fine Structure: The Inside Story
8-12-82	Dr. J. P. Biberian University of Marseille France	Adsorption of Cl on Si(III): Etching of Si by Cl

Surface Science and Catalysis Science (continued)

Date	Speaker and Affiliation	Seminar Title
8-19-82	Dr. J. C. Frost Heriot-Watt University Edinburgh	The Application of Mössbauer Spectroscopy to the Study of Surfaces
8-27-82	Prof. N. Sheppard Dr. M. A. Chesters University of East Anglia England	Professor N. Sheppard - Some Correlations Between Vibrational Spectra of Hydrocarbons Adsorbed on Finely Divided Metals and Single Crystals Metal Surfaces Dr. M. A. Chesters - Some Application of Auger Electron Spectroscopy and Reflection-Absorption Infrared Spectroscopy to the Characterization of Adsorbed Species on Single Crystal Metal Surfaces
8-30-82	Dr. P. A. Thiry University of Namur Belgium	HREELS Study of Gas-Metal Interactions: Oxygen on CuZn, Oxygen on Magnesium and Formic Acid on Gold
8-31-82	Dr. S. L. Bernasek Princeton University	Directed Energy Production of Novel Metallic Surfaces
8-31-82	Dr. L. H. Dubois Bell Laboratories	Fundamental Studies of the Strong Metal-Support Interactions: Chemisorption and Catalysis on Nickel Silicides
9-2-82	Prof. A. Meisel Karl-Marx Universitat	X-Ray Spectroscopic and Photoelectron Spectroscopic Investigation of the Electronic Structure of Matter
9-21-82	Prof. C. Aharoni University of Pennsylvania	Effect of Surface Diffusion in the Kinetics of Chemisorption
9-22-82	Dr. J. Klinowski University of Cambridge	Electron Diffraction and NMR Studies of Zeolite Structure and Function
9-28-82	Dr. K. Wandelt University of Munich	"Local Surface Dipole Probing Characterization of Atomic-Scale Surface Roughness"
9-30-82	Professor M. B. Maple University of California San Diego	"Metallic Oxydation: Its Role in the Oscillatory Reaction of Co and O_2 Over Transition Metal Catalysts"
10-7-82	Dr. J. R. Katzer Mobil Research and Development	"Selectivity to Alcohols in CO Hydrogenation Over Supported Rhodium
10-14-82	Prof. S. W. Benson University of Southern California	Entropy Structure and the Transition State: A Thermochemical View of Catalysis
10-21-82	Professor W. Maier University of California Berkeley	Hydro-Denitrogenation Studies
10-22-82	Dr. E. Bertel University of Innsbruck Austria	Oxydation of Rare Earths (Er, Yb) and Transition Metals (Ti): A Case Study of Three Different Mechanisms
10-28-82	Prof. J. Shabtai University of Utah	Stereochemical and Kinetic Aspects of Hydrogenation and Hydrodenitrification Reactions Over Sulfided Catalysts
11-4-82	Prof. E. Solomon Stanford University	Photo Electron Spectroscopic Studies of the Interaction of CO with ZnO Surfaces
11-5-82	Prof. G. Doyen University of Munich	Quantum Theory of Rotational Excitations in Molecule/Surface Scattering

Surface Science and Catalysis Science (continued)

Date	Speaker and Affiliation	Seminar Title
11-11-82	Dr. F. Mares Allied Chemical Corp.	Metal Nitrosyl Complexes as Oxygen Transfer Agents in the Specific Oxidation of Organic Substrates
11-12-82	Dr. M. Gorbaty Exxon Research and Engineering	Chemical and Physical Structure of Coal
11-16-82	Dr. A. Gavezzotti University of Milan	Quantum Chemical and Force-Field Calculations on Chemisorption
11-17-82	Dr. V. W. Weekman Mobil-Tyco Company	Catalyzing the Conversion of Photons to Electrons-Photo Voltaics
12-2-82	Dr. R. A. Van Santen Shell Development Company	Chemical Bonding to Transition Metal Surfaces
Reaction Dynamics		
4-5-82	Dr. K. Bergmann Universitat Kaiserlautern West Germany	Rotational Rainbow Structure in the Na_2-Rare Gas Scattering Cross Sections
6-21-82	Prof. J. P. Simons Department of Chemistry University of Nottingham England	Photochemical Reaction Dynamics, Supersonic Beam Studies and Product Rotational Alignment
6-23-82	Prof. A. E. W. Knight Griffith University Brisbane, Australia	Collisional Energy Transfer in the Ground Electronic State of Large Polyatomics: State Selection by Stimulated Emission Pumping
11-1-82	Prof. H. Nakamura Institute for Molecular Science Oakazaki, 444 Japan	Semiclassical Theory of Rotationally Induced Non-Adiabatic Transitions in Atomic Collisions
11-2-82	Prof. F. Gianturco Institute of Chemical Physics University of Rome, Italy	Proton-Molecule Inelastic Collisions as Precursors of Chemical Reactions
Electron Microscopy of Materials		
1-19-82	Dr. D. Smith University of Cambridge Cambridge, England	Recent Applications of the Cambridge 600kV High Resolution Electron Microscope
4-23-82	Dr. B. Jouffrey Laboratoire d'Optique Electronique Centre National de la Recherche Scientifique Toulouse, France	On Some Recent Applications of Chemical Analysis by Using Characteristic Energy Losses
5-7-82	Dr. R. Taylor Dept. of Metallurgy and Science of Materials University of Oxford	A Study of Magnetisation Processes in Imperfect Crystals by High Voltage Electron Microscopy
6-16-82	Dr. P. Régnier Centre d'Etudes Nucléaires de Saclay Saclay, France	Microstructure Evolution in Pt-C During Electron Irradiation in HVEM
Other Seminars Hosted		
1-29-82	Dr. H. Gerischer Fritz Haber Institute Max Plank Gesellschaft, Berlin	Photocurrent-Voltage Curves of Semiconductors Dependence on Surface Reaction Kinetics and Resistance

Other Seminars Hosted (continued)

Date	Speaker and Affiliation	Seminar Title
2-16-82	Prof. J. Halpern University of Chicago	Mechanisms and Stereochemistry of Asymetric Catalysis
3-82	Prof. J. Gaube Chemical Engineering Department Technical University of Darmstadt W. Germany	Simultaneous Determination of Vapor-Liquid and Liquid-Liquid Equilibria
3-82	Prof. O'Donnell Chemical Engineering Department University College Dublin, Ireland	Distillation of Spirits
5-13-82	Dr. C. W. Bauschlicher Polyatomics Research Institute Mountain View, California	Transition Metal Hydrides
6-82	Prof. K. Gubbins Chemical Engineering Department Cornell University Ithaca, New York	Perturbation Theories of Fluids and Fluid Mixtures
*6-2-82	Dr. E. R. Davidson Department of Chemistry University of Washington Seattle, Washington	Theoretical Studies of Triplet State Radiative Lifetimes: Formaldehyde, Methylene, and Sulfur Dioxide
6-16-82	Prof. J. Gerratt University of Bristol England	R-Mattix Studies of Molecular Collision Processes
6-23-82	Prof. C. M. Van Baal Technical University Delft, Netherlands	Kinetics of Ising Alloys
7-8-82	Dr. P. Taylor Division of Chemical Physics Commonwealth Scientific and Industrial Research Organization Melbourne, Australia	The Complete Active Space SCF Method
9-12--16-82	Prof. N. Watanabe Department of Industrial Chemistry Sakyo-ku, Kyoto University, Japan	Electrochemical Application of Graphite Intercalation Compounds Containing Fluorine
9-17-82	Dr. T. Sandstrom Chalmers University of Technology Gothenburg, Sweden	The Comparison Ellipsometer, a New Optical Method for the Measurement of Thin Surface Films
9-24-82	Prof. J. B. Cohen Northwestern University Evanston, Illinois	The Effect of the Shape of the Phonon Dispersion Curve on Precipitation Reactions in Alloys
9-28-82	Prof. D. P. Craig Research School of Chemistry Australian National University Canberra, Australia	Dynamic Topochemistry: A Theoretical View of Chemistry in Flexible Cages
10-82	Ms. S. Roadcap Chevron Research Co. Richmond, California	Process Simulation at Chevron
10-21-82	Dr. R. Bellows Exxon Research and Engineering Linden, New Jersey	The Exxon Zinc-Bromine Battery

*Special Seminar

Other Seminars Hosted (continued)

Date	Speaker and Affiliation	Seminar Title
11-82	Dr. H. Kistenmacher Research Laboratories Linde Co. Hoellriegelskreuth, W. Germany	Physical Property Routines in Multicomponent Multiphase Systems
11-1-82	Dr. R. J. Charles G.E. Research and Development	Phase Equilibria in the SiO_2–Al_2O_3 System
11-2-82	Prof. F. Gianturco Institute of Chemical Physics University of Rome, Italy	Proton–Molecule Inelastic Collisions as Precursors of Chemical Reactions
11-9-82	Dr. E. Hodge ASEA Pressure Systems	Why HIP (Hot Isostatic Processing)?
11-17-82	Dr. E. Evleth Centre de Mécanique Ondulatoire Appliquée Paris, France	Rationalization of the Structures of Rydberg Molecules
11-19-82	Dr. M. Datta Federal Institute of Technology Lausanne, Switzerland	Transpassive Dissolution of Metals

Appendix D

Index of Investigators

Andersen, Richard A. 195

Bartlett, Neil 185, 195
Bell, Alexis T. 173, 217
Bergman, Robert G. 188
Boone, Donald H. 224, 256
Bragg, Robert H. 56
Brewer, Leo 103, 226

Clarke, John 87
Cohen, Marvin L. 94
Connick, Robert E. 172, 226, 227
Conway, John G. 195

de Fontaine, Didier 25
De Jonghe, Lutgard C. 53, 244, 264

Edelstein, Norman M. 195, 251
Evans, Anthony G. 70
Evans, James W. 22, 217, 242

Falicov, Leo M. 91
Finnie, Iain 66
Fish, Richard H. 217

Glaeser, Andreas M. 64
Gronsky, Ronald 1, 14

Harris, Charles B. 133
Heinemann, Heinz 217
Hess, Dennis W. 110

Jeffries, Carson D. 82
Jolly, William L. 179
Johnston, Harold S. 131

Kresin, Vladimir Z. 257

Lee, Yuan T. 160
Lester, William A., Jr. 144, 255
Levy, Alan V. 68, 212, 217, 224, 256

Marrus, Richard 170
Meyer, C. Beat 227
Miller, William H. 148
Moore, C. Bradley 138, 229
Morris, John W., Jr. 27, 249
Muetterties, Earl L. 183
Muller, Rolf H. 112, 236

Newman, John 181, 246

Olander, D. R. 106

Pask, Joseph A. 43
Petersen, Eugene E. 217
Phillips, Norman E. 97
Pines, Alexander 124
Pitzer, Kenneth S. 141
Prausnitz, John M. 191, 259

Raymond, Kenneth N. 195
Richards, Paul L. 73
Ritchie, Robert O. 39
Ross, Phillip N., Jr. 209, 238, 262

Schaefer, Henry F., III 166
Seaborg, Glenn T. 195
Searcy, Alan W. 45
Shen, Yuen-Ron 77
Shirley, David A. 151
Somorjai, Gabor A. 115, 129, 173, 217
Streitwieser, Andrew, Jr. 195

Templeton, David H. 195
Thomas, Gareth 4, 14
Tobias, Charles W. 100, 231, 233, 234

Vermeulen, Theodore 217
Vollhardt, K. Peter 176, 217

Washburn, Jack 49
Westmacott, Kenneth H. 11, 14, 22
Whittle, David P. 58, 72, 261
Winn, John S. 136

Yu, Peter Y. 85

Zalkin, Alan 195

GPO 687-118/8

This report was done with support from the Department of Energy. Any conclusions or opinions expressed in this report represent solely those of the author(s) and not necessarily those of The Regents of the University of California, the Lawrence Berkeley Laboratory or the Department of Energy.

Reference to a company or product name does not imply approval or recommendation of the product by the University of California or the U.S. Department of Energy to the exclusion of others that may be suitable.

TECHNICAL INFORMATION DEPARTMENT
LAWRENCE BERKELEY LABORATORY
UNIVERSITY OF CALIFORNIA
BERKELEY, CALIFORNIA 94720